THE ROLE OF IRON IN BACTERIAL PATHOGENESIS

EDITED BY: Susu M. Zughaier and Pierre Cornelis
PUBLISHED IN: Frontiers in Cellular and Infection Microbiology

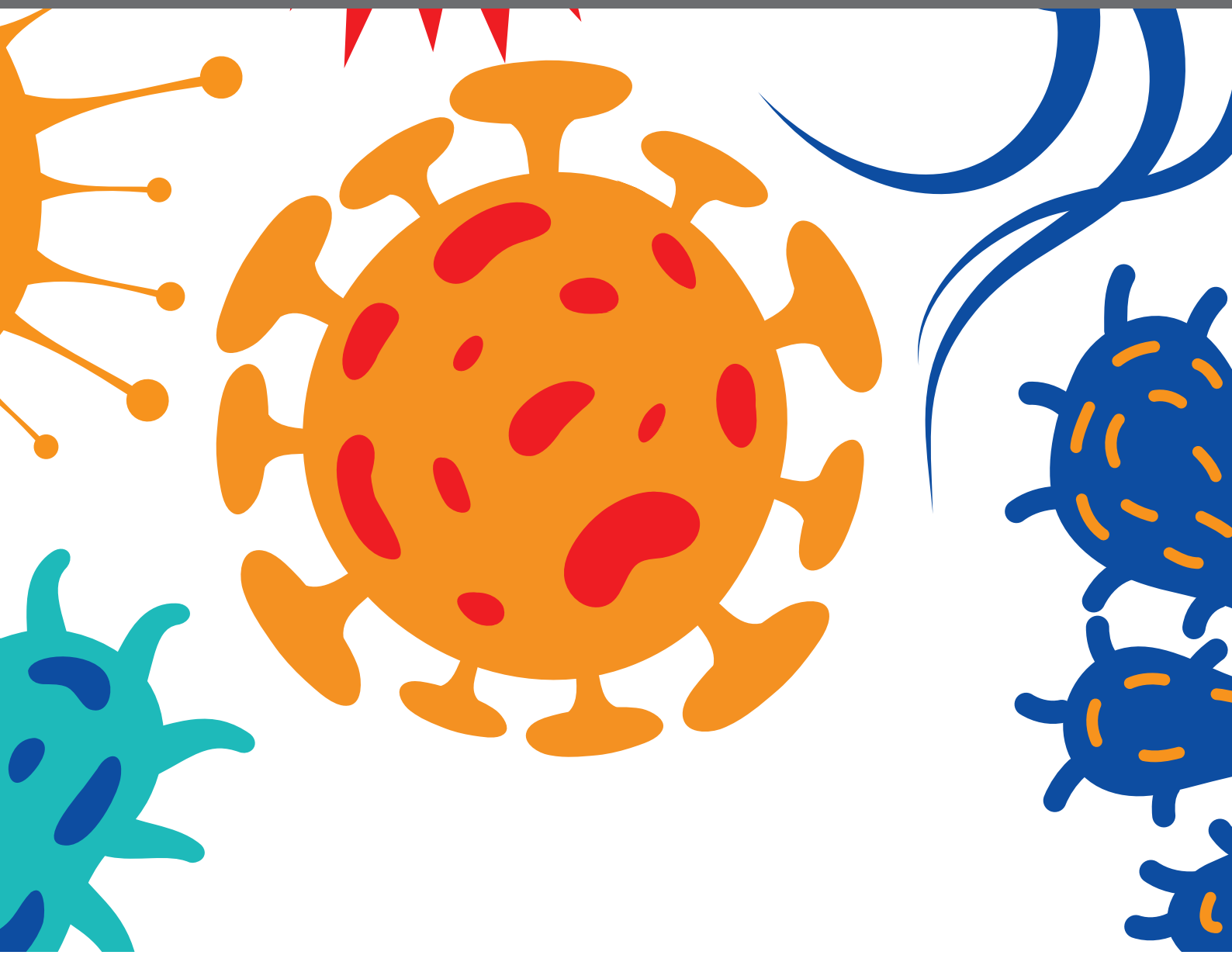

frontiers Research Topics

frontiers

ISSN 1664-8714
ISBN 978-2-88945-662-8
DOI 10.3389/978-2-88945-662-8

About Frontiers

Frontiers is more than just an open-access publisher of scholarly articles: it is a pioneering approach to the world of academia, radically improving the way scholarly research is managed. The grand vision of Frontiers is a world where all people have an equal opportunity to seek, share and generate knowledge. Frontiers provides immediate and permanent online open access to all its publications, but this alone is not enough to realize our grand goals.

Frontiers Journal Series

The Frontiers Journal Series is a multi-tier and interdisciplinary set of open-access, online journals, promising a paradigm shift from the current review, selection and dissemination processes in academic publishing. All Frontiers journals are driven by researchers for researchers; therefore, they constitute a service to the scholarly community. At the same time, the Frontiers Journal Series operates on a revolutionary invention, the tiered publishing system, initially addressing specific communities of scholars, and gradually climbing up to broader public understanding, thus serving the interests of the lay society, too.

Dedication to Quality

Each Frontiers article is a landmark of the highest quality, thanks to genuinely collaborative interactions between authors and review editors, who include some of the world's best academicians. Research must be certified by peers before entering a stream of knowledge that may eventually reach the public - and shape society; therefore, Frontiers only applies the most rigorous and unbiased reviews.
Frontiers revolutionizes research publishing by freely delivering the most outstanding research, evaluated with no bias from both the academic and social point of view. By applying the most advanced information technologies, Frontiers is catapulting scholarly publishing into a new generation.

What are Frontiers Research Topics?

Frontiers Research Topics are very popular trademarks of the Frontiers Journals Series: they are collections of at least ten articles, all centered on a particular subject. With their unique mix of varied contributions from Original Research to Review Articles, Frontiers Research Topics unify the most influential researchers, the latest key findings and historical advances in a hot research area! Find out more on how to host your own Frontiers Research Topic or contribute to one as an author by contacting the Frontiers Editorial Office: researchtopics@frontiersin.org

THE ROLE OF IRON IN BACTERIAL PATHOGENESIS

Topic Editors:
Susu M. Zughaier, Qatar University, Qatar
Pierre Cornelis, Vrije Universiteit Brussel, Belgium

The collection of articles published in this eBook represent different facets of the interactions between pathogens and their host concerning the battle for iron. Pathogens have developed different strategies to acquire iron from their host. These include the production of siderophores, heme acquisition and ferrous iron uptake.

Citation: Zughaier, S. M., Cornelis, P., eds. (2018). The Role of Iron in Bacterial Pathogenesis. Lausanne: Frontiers Media. doi: 10.3389/978-2-88945-662-8

Table of Contents

frontiers in Cellular and Infection Microbiology

EDITORIAL
published: 16 October 2018
doi: 10.3389/fcimb.2018.00344

Editorial: Role of Iron in Bacterial Pathogenesis

Susu M. Zughaier[1]* *and Pierre Cornelis*[2]*

[1] Department of Basic Medical Sciences, College of Medicine, Qatar University, Doha, Qatar, [2] Microbiology Unit, Department of Bioengineering Sciences, Vrije Universiteit Brussel and VIB Department of Structural Biology, Brussels, Belgium

Keywords: iron depletion, virulence factors, host defense against pathogenic bacteria, iron-regulated genes, siderophore

Editorial on the Research Topic

Role of Iron in Bacterial Pathogenesis

Iron is the fourth-most abundant element on the earth, and it is needed by most organisms, including bacteria. It exists in two oxidation states, Fe^{2+} and Fe^{3+}, and is involved in many oxido-reduction reactions (Andrews et al., 2013). Ferric iron (Fe^{3+}) is the dominant form in oxygenated environments and has a very low solubility, which presents a problem for microorganisms with an aerobic lifestyle (Andrews et al., 2013). Conversely, in anaerobic environments or in microaerobic conditions at low pH, the soluble ferrous iron (Fe^{2+}) is the most abundant form (Andrews et al., 2003). Bacterial pathogens face a problem because free iron is not available since it is bound to heme or by circulating proteins such as transferrin or lactoferrin (Finkelstein et al., 1983; Cornelissen and Sparling, 1994). Pathogens use different strategies to obtain iron from the host, via the production of extracellular Fe^{3+}-chelating molecules termed siderophores (either their own or produced by other microorganisms), the uptake of heme, and the uptake of Fe^{2+} (Feo system) (Andrews et al., 2013). A single pathogen can adapt its iron-uptake strategy in response to the type of infection (acute or chronic) and the availability or lack of ferrous iron (Cornelis and Dingemans, 2013). In this issue, several authors present several facets around iron uptake in different bacterial pathogens. *Yersinia pestis* produces the yersiniabactin siderophore under aerobic conditions and the Feo Fe^{2+} uptake system under microaerobic conditions (Fetherston et al., 2012). The *feo* operon of *Y. pestis* is peculiar since it is repressed by Fe via the Fur repressor only under microaerobic, but not under aerobic conditions, unless the promotor region is truncated. The other facet of the host-pathogen battle for iron is the host response to the bacterial pathogen. As shown, again for *Y. pestis*, a live vaccine induces an iron nutritional immunity via the production of hemopexin and transferrin iron-binding proteins.

Some pathogenic bacteria infect fish, such as *Vibrio anguillarum* and *Photobacterium damselae*, both belonging to the Vibrionaceae. Citrate is probably the simplest siderophore and is produced by the citrate synthase and excreted by *P. damselae* strains unable to produce the vibrioferrin siderophore, thus establishing a link between the cellular metabolism and iron uptake. In their review article, Li and Ma describe the ways by which different *V. anguillarum* pathogenic strains take up iron either via the production of siderophores (anguibactin, vanchrobactin), uptake of xenosiderophores enterobactin or ferrichrome, or uptake of heme or ferrous iron. *Burkholderia* represents a genus of β-proteobacteria with 90 species, including the *B. cepacia* complex (BCC), which cause infections in the lungs of patients with cystic fibrosis and *B. pseudomallei*, which causes meloidiosis. Butt and Thomas reviewed the different iron-uptake strategies of these highly adaptable bacteria, including the production of siderophores (ornibactins, cepaciachelin, pyochelin, malleobactin), the uptake of heme and of ferrous iron. *Francisella tularensis* is the causative agent of tularemia and able to replicate in macrophages. *F. tularensis* can take up the siderophore

Edited by:
John S. Gunn,
The Ohio State University,
United States

Reviewed by:
Kevin Mason,
The Ohio State University,
United States

***Correspondence:**
Susu M. Zughaier
szughaier@qu.edu.qa
Pierre Cornelis
pcornel@vub.ac.be

Specialty section:
This article was submitted to Molecular Bacterial Pathogenesis, a section of the journal Frontiers in Cellular and Infection Microbiology

Received: *22 August 2018*
Accepted: *11 September 2018*
Published: *16 October 2018*

Citation:
Zughaier SM and Cornelis P (2018) Editorial: Role of Iron in Bacterial Pathogenesis. Front. Cell. Infect. Microbiol. 8:344. doi: 10.3389/fcimb.2018.00344

rhizoferrin, but relies on the Feo system for the uptake of ferrous iron. The uptake of rhizoferrin does, however, not need the TonB protein as in other bacteria, while the uptake of Fe^{2+} involves an outer membrane protein termed FupA, which is also unusual. Inhibition of the uptake of iron by bacteria involves, among other approaches, the use of gallium–protoporphyrin IX as shown in the case of *Pseudomonas aeruginosa*. The GaPPX is a heme analog that can be taken up via outer membrane heme receptors, inhibiting the growth of *P. aeruginosa* under conditions of iron limitation. Once in the cell, GaPPX was shown to target the aerobic respiration.

Bacterial pathogens sense iron-limiting conditions and respond accordingly by upregulating iron-acquisition mechanisms and virulence genes (Zughaier et al., 2014). Mouméne et al. report that the intracellular bacteria *Ehrlichia ruminantium* upregulates the type 4 secretion system (T4SS) and virulence genes under iron depletion via the newly identified master regulatory protein ExrR. Ferric uptake regulator (Fur) is a transcription factor that upregulates virulence factors in bacteria during iron depletion. Guo et al. used an unmarked gene deletion system to investigate the role of Fur in the virulence of *Riemerella anatipestifer*, an avian pathogen. Using RNA-seq analysis, they determined fur-regulated genes and identified putative fur-binding sequences. Their study further demonstrated that deleting the *fur* gene led to a reduction of virulence *in vivo*. In response to infection, the host limits the bioavailability of iron by upregulating expression of hepcidin, the master iron-regulating hormone, which limits iron uptake from the gut and retains iron in macrophages. Nairz et al. investigated the role of dietary iron enrichment in host-pathogen interactions during *Salmonella typhimurium* infection in mice with hereditary hemochromatosis (genetic *Hfe*-deficiency) compared to wild type. They observed that *Salmonella* infection induced hepcidin and hypoferremia in an Hfe-independent manner. However, iron overload increased the bacterial load in mice. Further, *Salmonella* infection in mice responded to iron-depleting conditions in the host by upregulated iron-acquisition genes.

Malhotra et al. report that *Mycobacterium tuberculosis (M. tb)* utilizes its highly conserved glycolytic enzyme GAPDH to acquire iron from the host by binding to lactoferrin with high affinity. *M. tb* sequesters iron from lactoferrin bound to GAPDH on the surface of bacteria. Sharma and Bisht provide a perspective on the role of iron-storing proteins in the emergence of antibiotic resistance. Based on their previous observation that iron-storing proteins, bacterioferritin (Rv1876) and ferritin (Rv3841), were overexpressed in aminoglycosides-resistant isolates of *M. tb*, they used a computational approach (STRING analysis) to predict protein partners that interact with bacterioferritin and ferritin. Among the identified partners is the hypothetical transmembrane protein Rv1877, which is predicted to be involved in drug resistance; therefore, Rv1877 may be a potential drug discovery target.

AUTHOR CONTRIBUTIONS

All authors listed have made a substantial, direct and intellectual contribution to the work, and approved it for publication.

REFERENCES

Andrews, S., Norton, I., Salunkhe, A. S., Goodluck, H., Aly, W. S., Mourad-Agha, H., et al. (2013). Control of iron metabolism in bacteria. *Metal Ions Life Sci.* 12, 203–239. doi: 10.1007/978-94-007-5561-1_7

Andrews, S. C., Robinson, A. K., and Rodriguez-Quinones, F. (2003). Bacterial iron homeostasis. *FEMS Microbiol. Rev.* 27, 215–237

Cornelis, P., and Dingemans, J. (2013). *Pseudomonas aeruginosa* adapts its iron uptake strategies in function of the type of infections. *Front. Cell. Infect. Microbiol.* 3:75. doi: 10.3389/fcimb.2013.00075

Cornelissen, C. N., and Sparling, P. F. (1994). Iron piracy: acquisition of transferrin-bound iron by bacterial pathogens. *Mol. Microbiol.* 14, 843–850.

Fetherston, J. D., Mier, I. Jr., Truszczynska, H., and Perry, R. D. (2012). The Yfe and Feo transporters are involved in microaerobic growth and the virulence of *Yersinia pestis* in bubonic plague. *Infect. Immun.* 11, 3880–3891. doi: 10.1128/IAI.00086-12

Finkelstein, R. A., Sciortino, C. V., and McIntosh, M. A. (1983). Role of iron in microbe-host interactions. *Rev. Infect. Dis.* 5(Suppl. 4), S759–S777.

Zughaier, S. M., Kandler, J. L., and Shafer, W. M. (2014). *Neisseria gonorrhoeae* modulates iron-limiting innate immune defenses in macrophages. *PLoS ONE* 9:e87688. doi: 10.1371/journal.pone.0087688

Conflict of Interest Statement: The authors declare that the research was conducted in the absence of any commercial or financial relationships that could be construed as a potential conflict of interest.

frontiers in Cellular and Infection Microbiology

ORIGINAL RESEARCH
published: 21 July 2017
doi: 10.3389/fcimb.2017.00331

The *feoABC* Locus of *Yersinia pestis* Likely Has Two Promoters Causing Unique Iron Regulation

*Lauren O'Connor †, Jacqueline D. Fetherston and Robert D. Perry **

Department of Microbiology, Immunology, and Molecular Genetics, University of Kentucky, Lexington, KY, United States

The FeoABC ferrous transporter is a wide-spread bacterial system. While the *feoABC* locus is regulated by a number of factors in the bacteria studied, we have previously found that regulation of *feoABC* in *Yersinia pestis* appears to be unique. None of the non-iron responsive transcriptional regulators that control expression of *feoABC* in other bacteria do so in *Y. pestis.* Another unique factor is the iron and Fur regulation of the *Y. pestis feoABC* locus occurs during microaerobic but not aerobic growth. Here we show that this unique iron-regulation is not due to a unique aspect of the *Y. pestis* Fur protein but to DNA sequences that regulate transcription. We have used truncations, alterations, and deletions of the *feoA::lacZ* reporter to assess the mechanism behind the failure of iron to repress transcription under aerobic conditions. These studies plus EMSAs and DNA sequence analysis have led to our proposal that the *feoABC* locus has two promoters: an upstream P1 promoter whose expression is relatively iron-independent but repressed under microaerobic conditions and the known downstream Fur-regulated P2 promoter. In addition, we have identified two regions that bind *Y. pestis* protein(s), although we have not identified these protein(s) or their function. Finally we used iron uptake assays to demonstrate that both FeoABC and YfeABCD transport ferrous iron in an energy-dependent manner and also use ferric iron as a substrate for uptake.

Keywords: ferrous transport, plague, iron regulation, ferric uptake, promoter structure

OPEN ACCESS

Edited by:
Pierre Cornelis,
Vrije Universiteit Brussel, Belgium

Reviewed by:
Gregory Plano,
University of Miami, United States
Deborah Anderson,
University of Missouri, United States
Simon Colin Andrews,
University of Reading, United Kingdom

****Correspondence:***
Robert D. Perry
rperry@uky.edu

† ***Present Address:***
Lauren O'Connor,
Department of Human Genetics,
University of Michigan Medical School, Ann Arbor, MI, United States

Received: *04 April 2017*
Accepted: *05 July 2017*
Published: *21 July 2017*

Citation:
O'Connor L, Fetherston JD and Perry RD (2017) The feoABC Locus of Yersinia pestis Likely Has Two Promoters Causing Unique Iron Regulation. Front. Cell. Infect. Microbiol. 7:331. doi: 10.3389/fcimb.2017.00331

INTRODUCTION

Iron is an essential nutrient and plays an important role in the pathogenesis of many organisms. Mammals chelate inorganic iron and heme using ferritin and hemoglobin in intracellular environments while transferrin, lactoferrin, heme- and hemoglobin-binding proteins sequester it in extracellular environments. Successful pathogens are able to acquire iron from these sources using a number of mechanisms: (1) secreted siderophores (2) heme transporters (3) ferric and ferrous transporters, as well as (4) transferrin and lactoferrin binding proteins to acquire iron from the host (Skaar, 2010).

Iron acquisition is crucial for the pathogenesis of *Yersinia pestis*, the causative agent of bubonic, pneumonic, and septicemic plague (Perry and Fetherston, 1997). Although, *Y. pestis* has multiple uptake systems for acquiring iron, relatively few have been shown to play a role in virulence in mammals (Kirillina et al., 2004; Perry, 2004; Forman et al., 2010). The yersiniabactin (Ybt) siderophore system is one of the most important for obtaining ferric iron (Kirillina et al., 2006; Perry and Fetherston, 2011) and is critical for virulence during pneumonic and the early stages of bubonic plague (Bearden et al., 1997; Fetherston et al., 1999, 2010). Ybt is encoded on the

chromosomal *pgm* locus, a 102 kb region that can be spontaneously deleted. Recently, Bobrov et al. showed that components of the Ybt system are also involved in zinc uptake (Bobrov et al., 2014). The functions of 4 loci within the *pgm* locus have been determined: (1) *ybt* which encodes genes for the biosynthesis, regulation, and transport of the Ybt siderophore, (2) *fet-flp*, which encodes a ferrous iron transport system, (3) *hms*, which encodes components for biofilm development and (4) *rip*, which is involved in intracellular survival in phagocytic cells (Jarrett et al., 2004; Kirillina et al., 2004; Pujol et al., 2009; Forman et al., 2010).

The Yfe, Yfu, Yiu, and Hmu systems are ABC transporters involved in iron or heme uptake (Perry et al., 1990; Darby et al., 2002; Kirillina et al., 2004; Forman et al., 2010). The Hmu system is functional *in vitro* and is essential for the use of heme, but it does not play a role in the progression of bubonic or pneumonic plague (Thompson et al., 1999; Forman et al., 2010). The Yfu and Yiu transporters are functional *in vitro*; however, they are not important for the disease progression of bubonic plague (Gong et al., 2001; Kirillina et al., 2006). The Yfe system is an ABC transporter that transports iron and manganese. YfeA is a periplasmic binding protein that can bind Fe, Mn, and Zn, however, only Fe and Mn can be transported into the cytoplasm through the inner membrane permeases, YfeC and YfeD, with the help of the ATPase, YfeB (Bearden and Perry, 1999; Perry et al., 2012). Bearden et al. demonstrated that in an Ybt$^-$ background, a *ΔyfeAB* mutant had ∼2.5- fold decrease in its ability to transport iron (Bearden and Perry, 1999). In 2012, Fetherston et al. showed that in a Ybt$^-$ background, a *ΔyfeAB ΔfeoB* mutant was completely defective in transporting ferrous iron (Fetherston et al., 2012). The Yfe and Feo systems appear to play somewhat of a redundant role *in vitro*, and play a role in the virulence of bubonic, but not pneumonic plague (Bearden and Perry, 1999; Fetherston et al., 2012).

The FeoABC system is comprised of three proteins. FeoB is an 85 kDa permease, which transports iron from the periplasm into the cytoplasm. FeoA is a small, 8.5 kDa protein that is predicted to interact with FeoB and stimulate GTPase activity. FeoC is a small, 9 kDa protein of unknown function. Due to its winged-helix motif, it has been predicted to play a role in regulation in *Escherichia coli* (Kammler et al., 1993; Lau et al., 2013). FeoA$_{YP}$ and FeoB$_{YP}$ have 77 and 74% identity to FeoA$_{EC}$ and FeoB$_{EC}$ respectively, whereas FeoC$_{YP}$ only has 57% identity to FeoC$_{EC}$ (Altschul et al., 1997). Guo et al. provided indirect evidence that FeoC is a negative regulator of the *feoABC* operon in *Y. pestis* (Gao et al., 2008). However, in our hands, a *ΔfeoC* mutant did not affect transcription from the *feo* promoter under aerobic or microaerobic conditions (Fetherston et al., 2012). Due to our data, and the lack of homology between FeoC in *Y. pestis* and *E. coli*, we do not believe FeoC is a transcriptional repressor of the *feoABC* operon in *Y. pestis*. FeoC has been shown to contain an oxygen sensitive 4Fe-4S cluster and to bind to FeoB preventing its proteolytic degration by FtsH in *Klebsiella pneumoniae* (Hung et al., 2012; Hsueh et al., 2013; Kim et al., 2013). However, a similar role in *Y. pestis* is uncertain since the Feo system is functional in a *ΔfeoC* mutant (Fetherston et al., 2012).

Iron is an essential element for the growth and pathogenesis of *Y. pestis*. However, excess iron in the presence of oxygen can lead to damaging reactive oxygen radicals. Therefore, iron transport into the cell is a very tightly regulated process. All of the tested ferrous and ferric iron uptake systems in *Y. pestis* are repressed by Fe-Fur under aerobic conditions, except for the FeoABC system. However, the *feoABC* locus is repressed by Fe under microaerobic conditions (Forman et al., 2010; Fetherston et al., 2012).

The *feoA* promoter in *Y. pestis* contains putative Fnr- and ArcA-binding sites (Gao et al., 2008). Previously, we have shown that *Δfnr, ΔarcA,* and *ΔrstAB* mutations do not affect *feoB* transcription (Fetherston et al., 2012), even though Fnr positively regulates the *feo* operon of *E. coli* and *Shigella*, and ArcA and RstA are positive regulators of the operons in *Shigella* and *Salmonella*, respectively (Kammler et al., 1993; Boulette and Payne, 2007; Jeon et al., 2008).

In this study, we examined the transcriptional regulation of the *feoABC* operon. Our results suggest that a unique feature of the *feo* promoter region in *Y. pestis* prevents Fe-Fur repression aerobically but not microaerobically. We also demonstrate that the Yfe and Feo systems function in iron uptake under both reducing and non-reducing conditions.

MATERIALS AND METHODS

Bacterial Strains and Growth Conditions

Y. pestis KIM6+ and derivatives of this strain (Table S1) were inoculated from −80°C glycerol stocks onto Congo Red plates. Plates were incubated at 30°C for ∼48 h. Individual colonies were inoculated onto Tryptose Blood Agar Base (TBA) slants with the appropriate antibiotic, and incubated at 30°C overnight. *E. coli* strains were inoculated from −80°C glycerol stocks onto TBA slants with appropriate antibiotics and incubated at 30°C overnight. For transformants, *E. coli* cells were grown in Luria broth (LB) or on LB agar plates.

Plasmid Construction

5′-Truncations of the *Y. pestis* KIM6+ *feo* Promoter Region

Promoter truncations were constructed by PCR amplification using the primer pairs listed in Table S2. PCR products were digested with *Pme*I and *Asc*I and and cloned into the same sites of pWSK*feoA*::*lacZ* (Fetherston et al., 2012; Table S1). The resulting plasmids with the correct inserts were verified by sequencing and were electroporated into *Y. pestis* strains.

Construction of an *E. coli feoA* Promoter Reporter

Primer pair Ecfeo-5′ and Ecfeo-3′ was used to amplify an ∼329 bp fragment from DH5α. The 3′ end of this fragment corresponds to the equivalent of nucleotide 1 in **Figure 1** (just prior to the predicted ATG start at 0 to −2). The PCR fragment was digested with *Pme*I and *Asc*I and cloned into the same sites of pWSK*feoA*::*lacZ*. Clones containing the correct insert were identified using Ecfeo-5′ and the universal −40 primer, verified by sequencing, and one clone (pWSK*feoA*$_{E.coli}$::*lacZ*) was electroporated into KIM6+ and KIM6-2030.

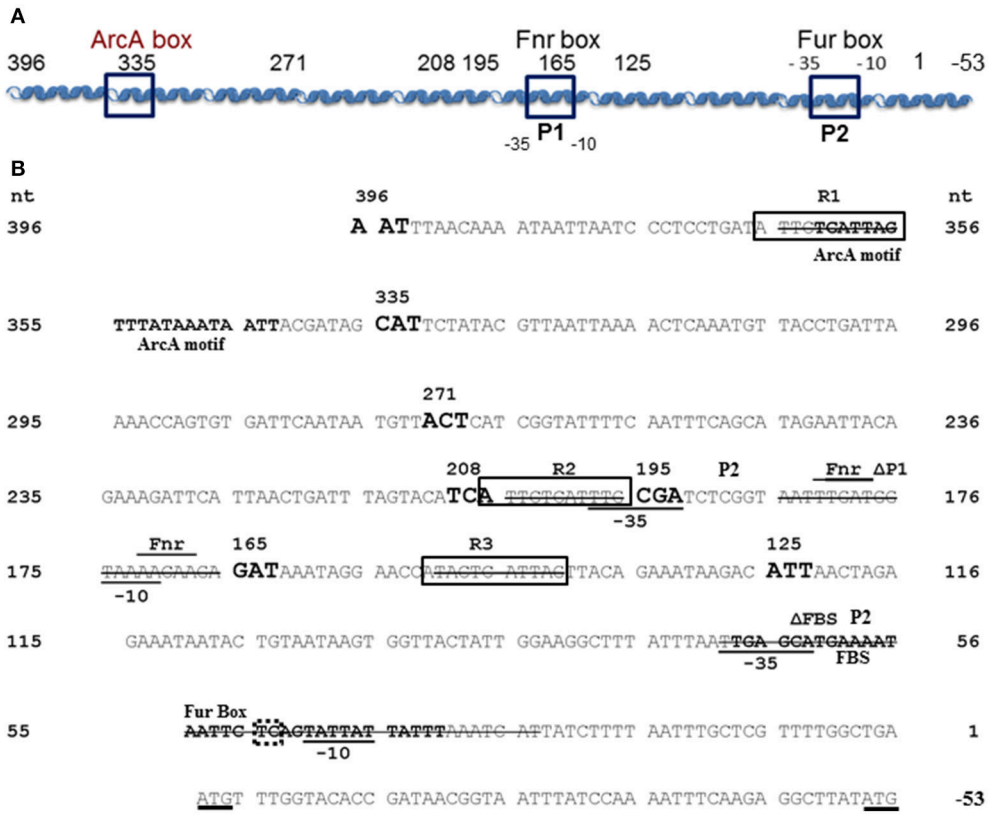

FIGURE 1 | *Y. pestis feoABC* promoter region. **(A)** A diagram of the cloned *feoABC* promoter region showing two −10 −35 regions (P1 and P2 promoters), the proven Fur binding site (FBS) and regions with the best match to Fnr and ArcA motifs. The size and locations of 5′-truncations cloned into *lacZ* reporters are numbered and all except a 447 bp promoter fragment have 3′ ends at nucleotide (nt) 1; the *feoA*447 promoter fragment spans nt 396 to −53. **(B)** The sequence of the cloned region is shown with nt 1 corresponding to the first nt upstream of the original annotated translational start for *feoA*. A transcriptional stop is upstream of nt 396 and nt −51 to −50 corresponds to an updated annotated translational start for *feoA*. −35 and −10 regions are underlined as are the two different annotated ATG starts. Three repeats (R1–R3) are boxed as is the FBS. Various deletions in reporters have a line through the deleted nucleotide sequences. The FBS and the best match to a predicted ArcA motif in *Shigella* (Boulette and Payne, 2007) are labeled and in bold font. The over lined and labeled residues indicate the best match for a putative Fnr binding site consensus. The various 5′-truncations cloned into *lacZ* reporters are numbered and shown in increased, bold font. With one exception, the promoter regions for all reporter constructions end with nt 1. The dotted box around TC residues of the Fur-repressible P2 promoter element indicate the −13 and −14 residues indicative of a σ^S-dependent promoter.

Construction of the Integration Vector pUC18R6K-lac-Gm

To construct a pUC18R6K-mini-Tn*7*T-Gm integration vector containing *lacZ* and a multi-cloning site (MCS), we first moved the *lacZ* gene with the *feo* promoter from pBSfeoPlacZΔRs (Fetherston et al., 2012) into pWSK129. The plasmid, pBSfeoPlacZΔRs, was digested with *Eag*I and filled in with Klenow. The ∼3.8 Kb fragment containing *lacZ* and the *feo* promoter was cloned into the *Eco*RV site of pWSK129 to generate pWSKfeoPlacZΔRs. This plasmid was digested with *Pme*I and *Asc*I to remove the *feo* promoter and a multiple cloning site (MCS) was inserted in its place. The MCS was isolated from a PCR reaction containing pNEB193 as a template with the universal −40 and reverse universal primers. The PCR product was digested with *Pme*I and *Asc*I and cloned into the *Pme*I/*Asc*I sites of pWSKfeoPlacZΔRs to generate pWSKlacMCS. The presence of the MCS was confirmed by sequencing. An ∼3.5 Kb *Xho*I/*Xma*I fragment containing the *lacZ* gene with the MCS was isolated from pWSKlacMCS and cloned into the *Xho*I and *Xma*I sites of pUC18R6K-mini-Tn*7*T-Gm (Choi et al., 2005) to generate the integration vector, pUC18R6K-lac-Gm. A clone containing the correct insertion was identified by PCR with the universal −40 primer and integvec-up.

Cloning *feoA, feoA165, feoA208,* and *feoA447* Promoters into pUC18R6K-lac-Gm

A *Pme*I/*Xho*I fragment containing *lacZ* with the respective *feo* promoter was isolated from pWSKfeoPlacZΔRs, pWSKfeoA165::lacZ as well as pWSKfeoA208::lacZ and ligated to the 3.4 Kb *Pme*I/*Xho*I fragment of pUC18R6K-lac-Gm to yield pUCR6KfeoA-lac-Gm, pUCfeoA165-lac-Gm and pUCR6Kfeo208-lac-Gm. Plasmids with the correct configuration were identified by PCR using primers Feo-Pro2 and integvec-up as well as by restriction enzyme digests. Following electroporation into KIM6+ along with pTNS2, strains containing the appropriate sequences integrated at the

Tn*7* insertion site were identified by PCR with primer pair Feo-Pro2 and attTn*7*Yp-fwd and designated KIM6-2203+ (*att*Tn*7*:: *feoA::lacZ*), KIM6-2204+ (*att*Tn*7*:: *feoA165::lacZ*) and KIM6-2205+ (*att*Tn*7*:: *feoA208::lacZ*).

The *feo*A447 promoter fragment (spanning nucleotides 396 to −50 in **Figure 1**) was isolated from a PCR reaction containing pWSKfeo (Fetherston et al., 2012) as a template with primers Feo-Pro1 and FeoP-4. The PCR products were eluted from Zymo columns, digested with *Pme*I and *Asc*I, and ligated into the same sites in pNEB193. A plasmid containing the *feo*A447 fragment was identified by sequence analysis and termed pNEBfeoP447. The *Pme*I/*Asc*I promoter fragment from pNEBfeoP447 was then ligated into the *Pme*I/*Asc*I sites of pUCR6K-lac-Gm. The resulting clones were screened using primers FeoP-4 and integvec-up as well as by restriction enzyme digests to identify a pUCR6K derivative carrying *lac*Z with the *feo*A447 promoter. This plasmid (pUCR6KfeoP447-lac-Gm) was introduced into KIM6+ along with pTNS2 and screened for integration by PCR with Feo-Pro2 and attTn*7*Yp-fwd primers. A strain containing the proper integrated reported was designated KIM6-2206+ (*att*Tn*7*:: *feoA447::lacZ*).

Deletion of Specific Sequences within the *feo* Promoter of *Y. pestis*

Twenty base pairs encompassing the putative upstream (P1) promoter region of the *feo* operon were deleted using primer pair dfeoP1-5 and dfeoP1-3 in an overlapping PCR reaction with pNEBfeoP DNA as a template and Phusion (NEB). The PCR products were cleaned through Zymo columns, digested with *Dpn*I, and transformed into DH5α. Plasmids containing the deletion were detected by PCR using primers pfeo2 and pfeo-R6. The products were analyzed on 5% polyacrylamide gels to detect the 20 bp deletion which was confirmed by sequencing. A *Pme*I/*Asc*I fragment was isolated from one of the clones (designated pNEBΔfeoP1) that contained the correct sequence and inserted into the corresponding sites of pUCR6K-lac-Gm. The ligation reactions were transformed into DH5α (λ pir) and plated on LB agar with 100 μg of ampicillin/ml. Plasmids containing an insert were identified by PCR using primers Feo-Pro2 and integvec-up. One of these, designated pUCR6K-ΔfeoP1-lac-Gm, was electroporated along with pTNS2 into KIM6+, incubated for 1 h at 30°C and plated on TBA containing 10 μg of gentamicin/ml. A strain in which the *feo lac* construct was integrated into the Tn*7* insertion site was identified by PCR using primers Feo-Pro2 and attTn*7*Yp-fwd and designated KIM6-2207+ (*att*Tn*7*:: *feoA*Δ*feoP1::lacZ*).

The same basic procedure was used to delete the P2 promoter region [41 bps which include the Fur binding site (FBS), −10 and −35 regions; Gao et al., 2008] and three repeated sequences within the *feo* promoter region (R1-3; **Figure 1**). Primers dfeoFBS-3 and dfeoFBS-5 were used to delete the P2 promoter region. Initial clones (pNEBΔfeoFBS) were screened with primer pair Feo-Pro2 and feoΔ20-5. Plasmids containing an insert in pUCR6K-lac-Gm were identified using integvec-up and the universal −40 primer and designated pUCR6K-ΔfeoFBS-lac-Gm.

Primer pairs FeoR1d-5 and FeoR1d-3, FeoR2d-5 and FeoR2d-3, and FeoΔR3-5 with FeoΔR3-3 were used to delete 10 bp that included repeated sequences R1, R2, and R3 (**Figure 1**) in separate PCR reactions. The pNEB clones with deletions of R2 and R3, designated pNEBfeoΔR2 and pNEBfeoΔR3 respectively, were initially identified by PCR with primer pair pfeo2 and pfeo-R6. Clones with deletions of R1, termed pNEBfeoΔR1, were screened with primers Feo-Pro1 and FeoR2d-5. The final constructs in the integration vector were named pUCR6KfeoΔR1, pUCR6KfeoΔR2, and pUCR6KfeoΔR3.

Suicide plasmids with the promoter deletions were separately electroporated along with pTNS2 into KIM6+, incubated for 1 h at 30°C and plated on TBA containing 10 μg of gentamicin/ml. A strain in which the *feo lacZ* reporter deletion was integrated into the Tn*7* insertion site was identified by PCR using primers Feo-Pro2 and attTn*7*Yp-fwd. These strains were designated KIM6-2208+ (*att*Tn*7*:: *feoAΔFBS::lacZ*), KIM6-2209+ (*att*Tn*7*:: *feoAΔR1::lacZ*), KIM6-2210+ (*att*Tn*7*:: *feoAΔR2::lacZ*), and KIM6-2211+ (*att*Tn*7*:: *feoAΔR3::lacZ*).

β-Galactosidase Assays

From TBA slants, *Y. pestis* cells were inoculated to an OD_{620} of 0.1 in chelex 100-treated PMH2 (cPMH2) at a pH of 6.0, 6.5, or 7.5 with or without 10 μM $FeCl_3$ and grown at 37°C at 250 rpm through 2 transfers (6-8 generations). Lysates were assayed for enzymatic activity using ONPG (4-nitrophenyl-β-D-galactopyranoside) as a substrate as previously described (Miller, 1992). The statistical significances of differences were calculated using the 2-tailed student's *t*-test.

Iron Transport Studies

Y. pestis cells were grown in cPMH2 under aerobic conditions for ∼5 generations prior to use in iron transport assays under reducing conditions. Transport was initiated by adding $^{55}FeCl_3$ to a final concentration of 0.2 μCi/ml to cultures containing 5 mM sodium ascorbate. Parallel cultures, preincubated for 10 min with 100 μM carbonyl cyanide *m*-chlorophenylhydrazone (CCCP), were used to demonstrate energy-independent binding. The $^{55}FeCl_3$ used in the transport studies was diluted into PMH2 containing 100 mM sodium ascorbate, incubated for at least 30 min at room temperature, and filtered through a 0.45-μm filter before being added to the cultures. Duplicate samples (0.5 ml) were taken at various time points after the addition of $^{55}FeCl_3$, filtered through 0.45-μm GN-6 nitrocellulose membranes, and rinsed twice with PMH2 medium containing 20 μM $FeCl_3$. The membranes were added to vials containing Bio-Safe II scintillation fluid (Research Products International) and counted in a Beckman LS3801 liquid scintillation counter. Unfiltered samples were used to determine the total amount of radioactivity in each culture. The results are expressed as percent uptake/0.4 OD_{620} to compensate for slight increases in cell density during the course of the assay.

For transport under non-reducing conditions *Y. pestis* cells were grown in cPMH1 for ∼5 generations prior to use in iron transport assays. Transport was initiated by adding filtered $^{55}FeCl_3$ to a final concentration of 0.2 μCi/ml to cultures

containing cold $FeCl_3$. Cultures were processed and analyzed as described above.

Electrophoretic Mobility Shift Assays

Electrophoretic mobility shift assays (EMSAs) were used to demonstrate binding to the *feo* promoter region. Full length and truncated *feo* promoter probes were amplified by PCR using primer pairs pfeoF4 and pfeoR4, pfeoF5 and pfeoR5, or pfeoF6 and pFeoR6 (Table S2). *Y. pestis* KIM6+ or KIM6 *fur::kan-9* (KIM6-2030) were grown with or without added iron in cPMH2 media through 2 passages to an OD_{620} of 0.3–0.4, cells centrifuged and frozen at −80°C. Cell pellets were resuspended in 2 ml of B-PER II reagent, 2 μl of lysozyme (10 mg/μl), 2 μL of DNase I and 4 μL of DNase I buffer and incubated with shaking for 20 min at room temperature. Samples were centrifuged to remove debris and protein content analyzed by the Bradford assay and comparison by SDS-PAGE. Lysates were aliquoted and stored at 4°C. Binding reactions [100 mM Tris, 750 mM KCl, 10 mM dithiothreitol (DTT), 50 mM $MgCl_2$, 12.5% glycerol, 50 mM EDTA [pH 8], 20 fmol biotinylated DNA probe, and *Y. pestis* cell lysates] were incubated at room temperature for 20 min. 5X EMSA loading buffer (50 mM Tris, 250 mM KCl, 5 mM DTT, 37 μM bromophenol blue) was added and the reactions were loaded onto a 6% DNA retardation gel (Invitrogen) with prechilled 0.5X TBE buffer and run at a constant voltage of 120 V for 90 min. After electrophoresis, gels were transferred to a Biodyne B Nylon membrane (Thermo Fisher Scientific) with prechilled 0.5X TBE buffer at a constant voltatge of 120 V for 45 min. Following transfer, the membrane was crosslinked with a UV Stratalinker 2400 (Stratagene, La Jolla, CA) and incubated overnight with 20 mL blocking buffer (Thermo Fisher Scientific). The Chemiluminescent Nucleic Acid Detection Module (Thermo Fisher Scientific) was used according to the manufacturer's protocol. The membrane was visualized on CL-X Posure Film (Thermo Fisher Scientific).

RESULTS

Truncations of the *feoA* Promoter Affect Overall Expression and Repression by Fe-Fur

Although, all other tested promoters controlling expression of iron transport systems in *Y. pestis*, are repressed by iron under aerobic conditions, the *feoA* promoter is repressed only under static (microaerobic) conditions. The other Fe^{2+} transporters (Yfe, Fet-flp, and Efe) are repressed by iron under borth aerobic and microaerobic conditionas and none of the 4 *Y. pestis* Fe^{2+} transporters are repressed by aerobic conditions compared to microaerobic conditions (Perry and Fetherston, 2004; Fetherston et al., 2012; Perry et al., 2012). We hypothesized that some aspect of the *feoA* promoter is preventing Fe-Fur regulation under aerobic conditions. To test this hypothesis we made 5′-truncations of the *feo* promoter region and fused them to a *lacZ* transcriptional reporter (**Figure 1**). KIM6 (*Δpgm* Feo^+) strains carrying the various reporter plasmids were grown in cPMH2 in the presence and absence of iron under aerobic growth conditions at 37°C. When the intergenic region between *y3913* and *feoA* is truncated from 396 to 335 bp, transcriptional activity increased ∼2.5-fold in the presence and absence of iron (**Figure 2**). This activity was further increased to a 4-fold difference, both in the presence and absence of iron when the 396 bp promoter region was truncated to 271 bp. A modest but statistically significant 1.3-fold ron-mediated repression was not observed until the *feoA* promoter region was truncated to 208 bp. This construct still had overall increased transcriptional activity compared to the full-length 396 bp promoter region (**Figure 2**). A further truncation to 195 bp maintained repression in the presence of iron, while the overall transcriptional activity decreased. The 165 and 125 bp promoters, showed stronger iron-mediated repression (2.6- and 3-fold, respectively), and overall transcriptional activity that returned to the 396bp promoter levels (**Figure 2**). Thus, the 396 to 165 bp region somewhat prevents Fe-Fur repression aerobically, while the 396 to 335 bp region somewhat lowers overall transcriptional activity from the *feoA* promoter region.

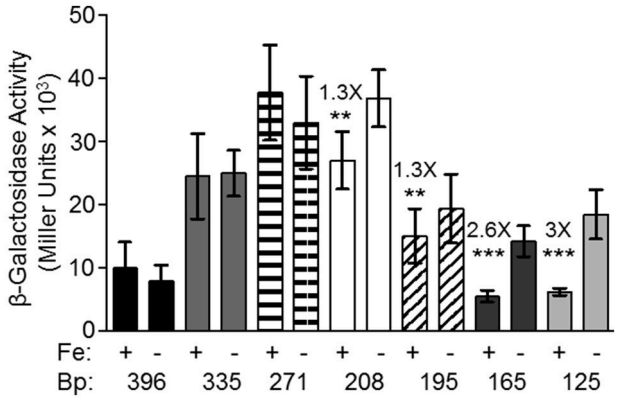

FIGURE 2 | The 396 bp *feoABC* promoter is not repressed by iron under aerobic conditions, while the 165 and 125 bp truncated promoters are repressed by iron. KIM6+ carrying the various reporter plasmids were grown in the presence or absence of 10 μM $FeCl_3$ at 37°C under aerobic conditions in cPMH2. Samples were taken during mid-exponential phase for β-galactosidase assays. Activities are averages of multiple samples from at least two independent experiments expressed in Miller units. Error bars represent standard deviations. Statistically significant fold differences due to iron status are shown (**$P \leq 0.003$, ***$P \leq 0.0002$).

The *feoA* Promoter Is Iron-Repressed Aerobically under Acidic Conditions

In *Salmonella*, RstA activates transcription from the *feo* promoter (Jeon et al., 2008). Previous work showed that a *ΔrstAB* mutation does not affect transcription from the *Y. pestis feoA* promoter (Fetherston et al., 2012). Since the *rstAB* operon is activated by the PhoP/PhoQ two-component regulators, which are activated by acidic pH (Jeon et al., 2008; Choi et al., 2009), we examined whether acidic conditions affected transcription from the *feoA* promoter. *Y. pestis* cells with full-length or truncated promoters were cultured in cPMH2 at pHs of 6.0, 6.5, or 7.5. It should be noted that all of the strains grew very slowly at pH 6.

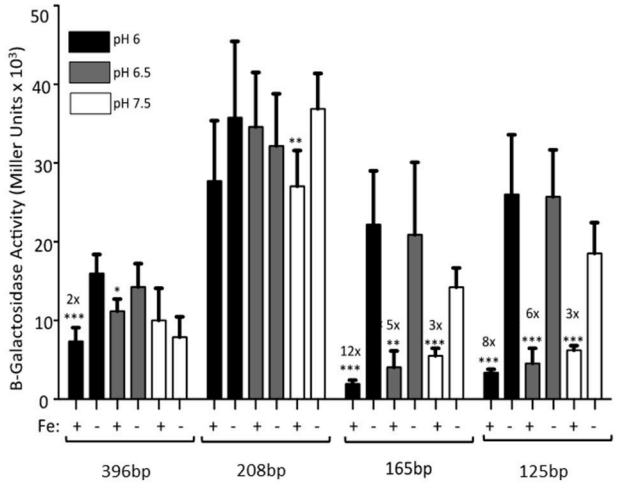

FIGURE 3 | The full-length *feoABC* promoter is repressed aerobically by iron under acidic conditions. KIM6 carrying the various reporter plasmids were grown in the presence or absence of 10 μM $FeCl_3$ at 37°C under aerobic conditions in cPMH2 at pH 6, pH 6.5, or pH 7.5. Samples were taken during mid-exponential phase for β-galactosidase assays. Activities are averages of multiple samples from at least two independent experiments expressed in Miller units. Error bars represent standard deviations. Statistically significant fold differences due to iron status are shown (*$P \leq 0.02$, **$P \leq 0.002$, ***$P \leq 0.0002$).

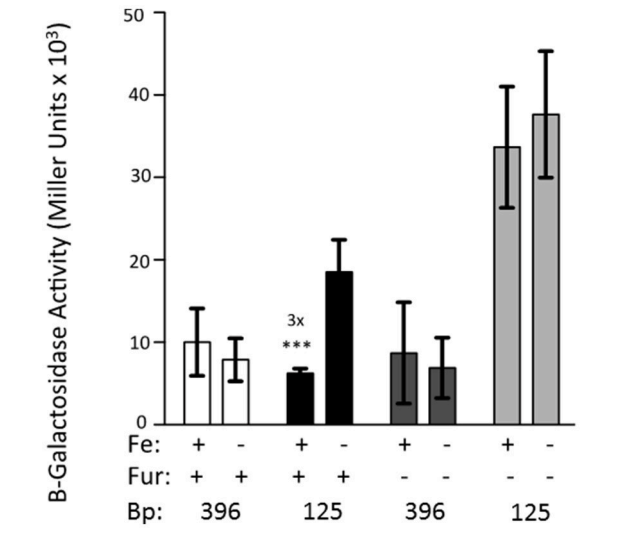

FIGURE 4 | Fur is necessary for the iron-repression of the 125 bp promoter clone. KIM6 (*fur*$^+$) and KIM6-2030 (*fur::kan*), carrying either the 396 or 125 bp reporter plasmids were grown in the presence or absence of 10 μM $FeCl_3$ at 37°C under aerobic conditions in cPMH2. Samples were taken during mid-exponential phase for β-galactosidase assays. Activities are averages of multiple samples from at least two independent experiments expressed in Miller units. Error bars represent standard deviations. The statistically significant fold difference due to iron status is shown (***$P < 0.0002$).

The 396 bp promoter had a 2-fold repression in the presence of iron when the cultures were grown at pH 6. A slight, but not statistically significant repression was seen at pH 6.5. Expression levels at pH 7.5 (from **Figure 2**) are shown for all constructs for reference (**Figure 3**). However, RstAB is not responsible for this effect since KIM6+ (*rstAB*$^+$) and KIM6-2189+ (*ΔrstAB*) had similar levels of activity from the *feoA::lacZ* reporter (Fetherston et al., 2012).

When the promoter was truncated to 208 bp, there was no significant iron repression at any of the tested pH levels (**Figure 3**), perhaps due to the high standard deviations associated with this reporter. While the 165 and 125 bp promoter truncations, showed ∼3-fold iron-mediated repression at pH 7.5, iron repression increased to 5- and 6-fold at pH 6.5, respectively. When the pH was further lowered to 6, the iron repression became even more pronounced—12- and 8-fold respectively. At all pHs, the pattern of increased expression from the 208 bp reporter, compared to the 396, 165, and 125 bp reporters was maintained (**Figure 3**).

Iron Repression of the Truncated *feo* Promoters Is Dependent on Fur

The 396 bp reporter does not exhibit iron repression. However, truncation of the promoter region to 125 bp causes transcriptional repression of the reporter by iron (**Figure 2**). This experiment was repeated using KIM6-2030 (*fur::kan* mutant) carrying the 396 or 125 bp reporter. With this *fur* mutant the 125 bp promoter reporter no longer exhibited iron repression. This indicates that Fur is responsible for the observed repression of the 125 bp reporter (**Figure 4**).

The Lack of Iron-Repression of the *feo* Promoter Is due to the Promoter Sequence, Not a Property of the *Y. pestis* Fur Protein

To determine whether the *feo* promoter itself or a unique aspect of the Fur protein in *Y. pestis* was preventing aerobic iron repression of the *feoA* promoter, we used a *lacZ* transcriptional reporter fused to the *E. coli feo* promoter region. The *E. coli feo::lacZ* reporter showed iron repression under aerobic conditions in *Y. pestis* (Figure S1). This suggests that a unique aspect of the *Y. pestis* Fur protein is not responsible for the lack of iron repression of the *Y. pestis feo* promoter under aerobic conditions. Rather the sequence/structure of the *Y. pestis feoA* promoter region likely prevents iron repression under aerobic, but not microaerobic conditions.

A Protein(s) That Is Not Fur Is Binding to the *feo* Promoter Region

We hypothesized that a repressor binding to the *feo* promoter region between 396 and 208 bp is the reason for increased transcriptional activity in the truncated promoters. Additionally, a second protein binding to the *feoA* promoter may prevent iron-repression under aerobic conditions. To examine these possibilities, an electrophoretic mobility shift assay (EMSA) was performed using whole cell lysates from *Y. pestis* that had been grown aerobically in the presence or absence of iron. Biotinylated probes were generated by PCR using primers that spanned the 396 bp *feoA* promoter, a 251 bp 3′-truncated *feo* promoter fragment, or a 146 bp 5′-truncated *feo* promoter fragment

(**Figure 5A**). A shift was observed using the 396 bp (**Figure 5B**), 251 bp (**Figure 5B**), and 126 bp (**Figure 5C**) probes regardless of growth conditions.

We would not expect to see Fur binding in the EMSAs since Fur needs to be bound to a divalent cation in order to bind DNA (de Lorenzo et al., 1988). Even in the cultures where iron was added, the intracellular iron bound to Fur would likely be converted in the ferric form after cell lysis. Typically $MnCl_2$ is added to cell lysates or purified Fur, when studying Fur binding, since the Mn^{2+} serves as a stable divalent cation under aerobic conditions (Friedman and O'Brian, 2003). However, since there is a Fur-binding site in the *feoA* promoter it was necessary to ensure that Fur was not responsible for this shift. Cell lysates from the *fur* mutant grown with or without iron were also used, and also resulted in a shift with the 396 bp (**Figure 5B**) and 146 bp (**Figure 5C**) probes. The 251 bp probe was not tested. Therefore, this observed shift is not due to Fur binding, but some other *Y. pestis* protein. In order to further identify the region in which the protein(s) is binding, two additional biotinylated probes were generated by PCR, splitting the 251 bp probe into an upstream 126 bp probe and downstream 125 bp probe (**Figure 5A**). Regardless of growth condition, a shift was seen with the upstream 126 bp probe, but not with the 125 bp downstream probe (**Figure 5C**). These data suggest that there are (1) two proteins binding the *feo* promoter: one within the 126 bp probe (396 to 271 bp region in **Figure 1**) and one within the 146 bp probe (146 to 1 bp region in **Figure 1**) or (2) one protein binding to both regions.

The Lack of Aerobic Iron Regulation Is Not due to Titration of a Transcriptional Regulator

Although, the pWSK vectors are considered low-copy number (Wang and Kushner, 1991) which we have used in transcriptional analysis of transcriptional regulation of numerous promoters (Fetherston et al., 1999, 2012; Gong et al., 2001; Kirillina et al., 2006; Forman et al., 2010; Perry et al., 2012), we wanted to ensure that our results were not due to titration of some negative regulatory factor by the *feoA* reporter plasmids. Therefore, we constructed vectors where the reporter gene would integrate into the Tn*7* insertion site of *Y. pestis* using the Tn*7*-based system developed by Choi et al. (2005). We tested integrated reporters with the *feoA* (396 bp), *feoA165*, and *feoA208 lacZ* reporters in KIM6+ grown under static and aerobic conditions in the presence or absence of iron. The integrated reporters behaved in the same fashion as their plasmid counterparts (compare Figure S2 and **Figure 2**) with regard to the overall transcriptional activity and iron regulation. Thus, the *feoA* construct was only repressed by iron in cultures grown under static conditions while *feo*A165 reporter was iron-regulated under both static and aerobic conditions. The activity of the integrated *feo*A208::*lacZ* construct was much higher than the other two *feo* constructs and exhibited the same regulation pattern as its plasmid counterpart (compare Figure S2 and **Figure 2**). The integrated *lac*Z gene without any promoter fragment exhibited very low activity under all conditions (Figure S2).

We also used the integrated reporter system to examine regulation of an extended fragment of the *feoA* promoter region. Subsequent analysis and annotation of the *Y. pestis feoABC* operon predicts the start codon for *feo*A is further downstream than the originally annotated initiating ATG (at 0 to −2) in **Figure 1**. To determine if the additional bp separating the 2 predicted ATG start codons would affect the regulation of the *feo* operon, we made another *feoA*::*lacZ* reporter (pUCR6KfeoP447-lac-Gm) that included these nucleotides and integrated it into the Tn*7* insertion site of KIM6+. The reporter with the extended promoter fragment exhibited the same properties as our original *feoA*::*lacZ* construct (data not shown) indicating that the additional base pairs did not play a role in the regulation of the *feoABC* operon.

The *feoABC* Locus Is Likely Transcribed from Two Independent Promoters

The transcriptional and binding data caused us to re-examine the *feoA* promoter region. Another, putative RNA polymerase (RNAP)—binding site (labeled P1/-10/-35 in **Figure 1**; the putative P1 promoter spans the Fnr binding site) is located upstream of the FBS and the P2 promoter (**Figure 1**). To test this, we deleted 41 bp that encompass the FBS and includes the putative −35 and −10 regions for the downstream P2 promoter. This strain, designated KIM6-2208+ (*att*Tn*7*:: *feoA*Δ*FBS*::*lacZ*) had higher β-galactosidase activity (1.5–2.5X) than the integrated reporter with the original *feoA*::lac*Z* construct (KIM6-2203+; *att*Tn*7*:: *feoA*::*lacZ)* under all conditions (**Figure 6**). Absence of the downstream P1 promoter may allow better read through from transcription initiation at the upstream P2 promoter. Interestingly, the *att*Tn*7*:: *feoA*Δ*FBS*::*lacZ*) reporter was slightly repressed (∼2-fold) by iron under static but not aerobic conditions. Examination of the *feoA* promoter revealed additional potential FBSs with weaker matches to the *Y. pestis* consensus FBS (Zhou et al., 2006), located at bp 262–280 (11/19 bp) and bp 204–222 (12/19). Whether, either of these regions is responsible for the iron repression observed with the *att*Tn*7*:: *feoA*Δ*FBS*::*lacZ* reporter is unknown; however, the observed ∼2-fold iron repression was alleviated in a *Y. pestis fur* mutant (KIM6-2030+; **Figure 6**).

Deletion of 20 bp that would include the putative −10 region of the upstream P1 promoter resulted in an integrated construct (*att*Tn*7*:: *feoA*Δ*feoP1*::*lacZ* in KIM6-2207+) with lower overall β-galactosidase activity than the original *att*Tn*7*:: *feoA*::*lacZ* reporter in KIM6-2203+ under both static and aerobic conditions. However, like the *att*Tn*7*:: *feoA165*::*lacZ* reporter in KIM6-2204+, the *att*Tn*7*:: *feoA*Δ*feoP1*::*lacZ* reporter was repressed by iron under both conditions. This provides additional evidence that the *Y. pestis feo* operon contains 2 promoter regions with the downstream P2 promoter being repressed by iron when cells are grown either statically or aerobically and suggest that the upstream P1 promoter is more active and slightly repressed by iron only under static conditions.

In examining the *Y. pestis feo* promoter region, we noted the presence of 3 nearly identical 11 bp direct repeat sequences, two of them located before the upstream P1 promoter (R1 and R2)

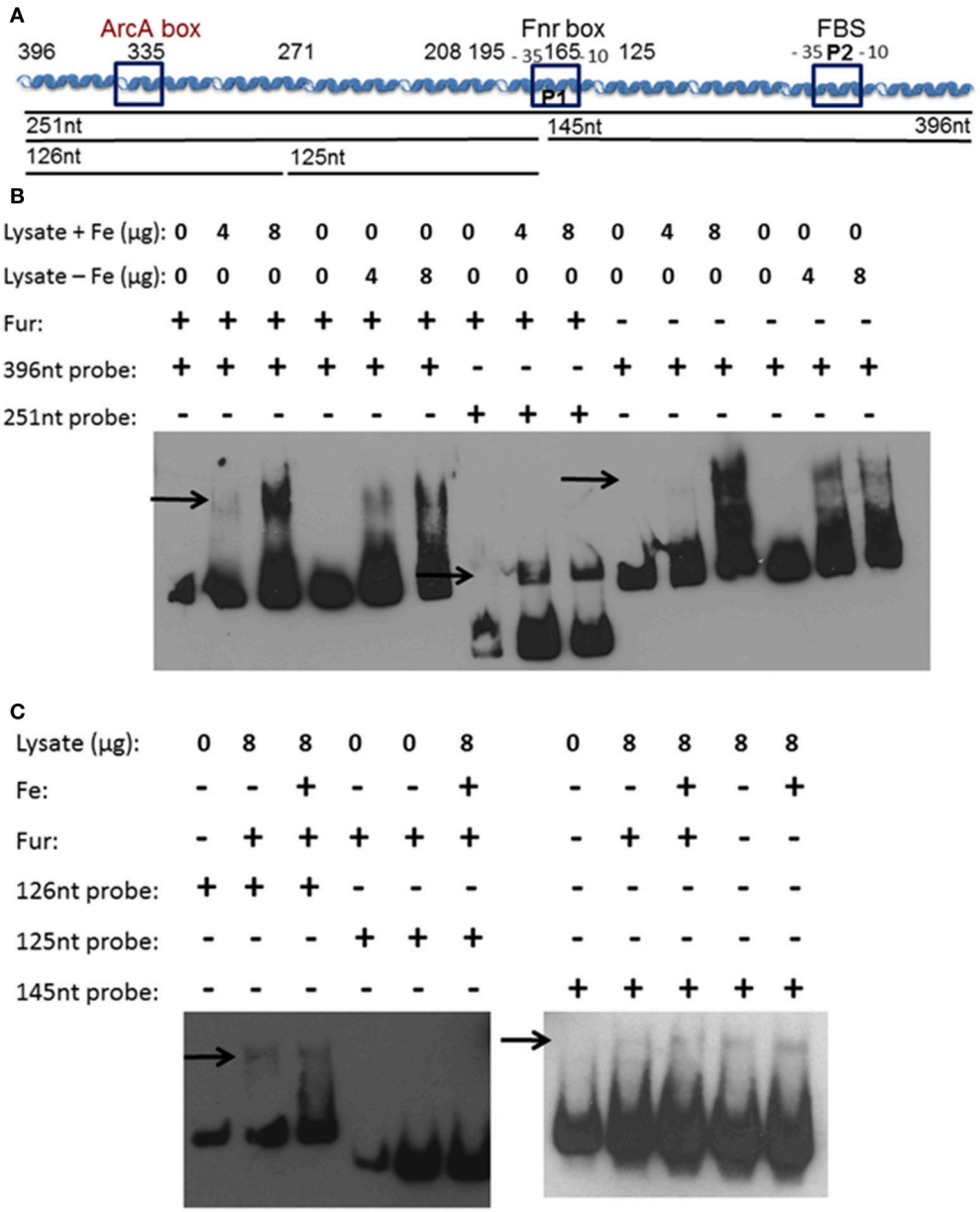

FIGURE 5 | A soluble protein(s) bind(s) the *feoA* promoter in at least two locations. **(A)** A diagram of the cloned *feoABC* promoter region showing two −10 −35 regions (P1 and P2), the proven FBS and regions with the best match to Fnr and ArcA motifs. The size and locations of 5′-truncations cloned into *lacZ* reporters are numbered. The DNA probes used in EMSAs are depicted as black lines with the nucleotide size indicated. **(B)** EMSAs using KIM6+ (*fur*$^{+}$) or KIM6-2030 (*fur::kan*) whole cell lysates with or without added iron and the 396 or 251 bp biotinylated probes. **(C)** EMSAs using KIM6+ or KIM6-2030 whole cell lysates with or without added iron and the 126 bp, 125 bp or 145 biotinylated probes. Representative blots from two or more independent analyses are shown. Arrows indicate mobility-shifted bands.

and one (R3) present between the 2 promoters (**Figure 1** and Table S3). To determine if these regions regulated expression of the *feoABC* operon, we deleted each of them in turn and analyzed the effect on the β -galactosidase activity of strains carrying the respective integrated reporters. An R3 deletion (*att*Tn*7*:: *feoA*Δ*R3*::*lacZ* in KIM6-2211+) had no significant effect on the expression of the *feoA*::*lacZ* reporter under any of the tested conditions. Similarly, deletion of R1, the most distally located repeat, had no effect on regulation in that the reporter construct (*att*Tn*7*:: *feoA*Δ*R1*::*lacZ* in KIM6-2209+) was only repressed by iron in cells grown under static conditions. Under aerobic conditions, the *att*Tn*7*:: *feoA*Δ*R1*::*lacZ* reporter was not repressed by iron but was less active (51–65%) than the *att*Tn*7*:: *feoA165*::*lacZ* reporter. The *att*Tn*7*:: *feoA*Δ*R2*::*lacZ* in KIM6-2211+ reporter in KIM6-2210+ behaved essentially the same as the *att*Tn*7*:: *feoA*Δ*feoP1*::*lacZ* reporter. Expression of the *lacZ*

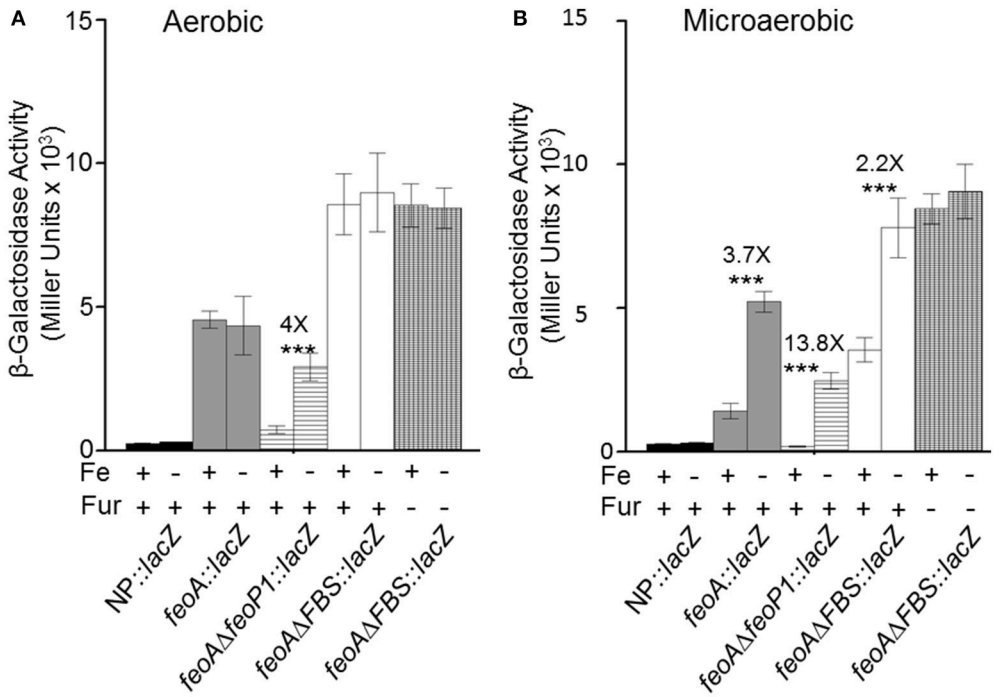

FIGURE 6 | Transcription from integrated *feoA* promoters occurs in the presence and absence of P1 or P2 promoter regions aerobically and microaerobically. Transcription from the *att*Tn*7*::*feoA*::*lacZ* reporter (KIM6-2202+) is compared to transcription from the *attTn7::feoAΔP1::lacZ* (KIM6-2207+) and *attTn7::feoAΔFBS::lacZ* (KIM6-2208+) reporters. The FBS deletion also deletes the −10 and −35 region of the P2 promoter. KIM6-2212+ (*att*Tn*7*::*lacZ*; no promoter region) is used as a negative control. All strains were grown in the presence or absence of 10 μM $FeCl_3$ at 37°C under aerobic or microaerobic conditions in cPMH2. Samples were taken during mid-exponential phase for β-galactosidase assays. Activities are averages of multiple samples from at least two independent experiments expressed in Miller units. Error bars represent standard deviation. The statistically significant fold difference due to iron status is shown (***$P < 0.0002$).

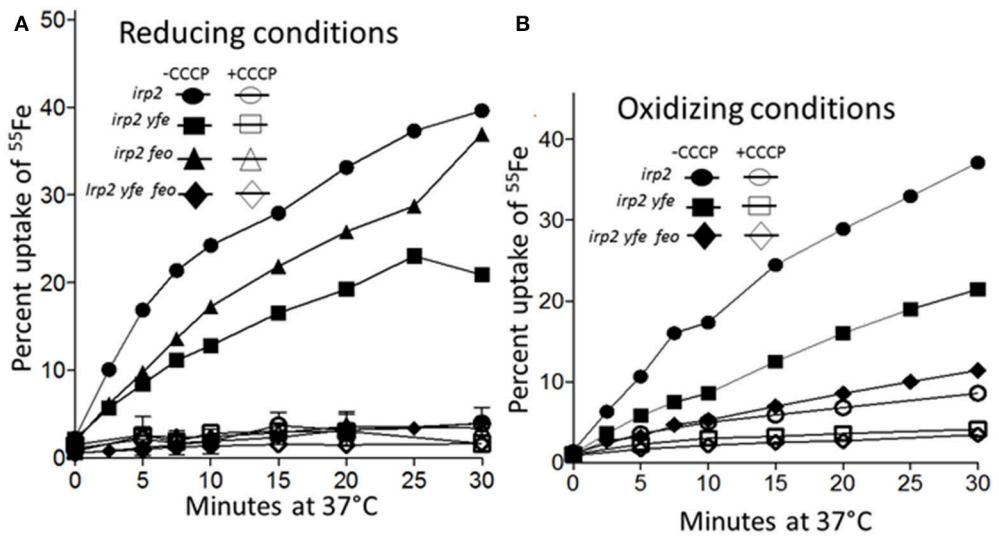

FIGURE 7 | Iron uptake by the Feo and Yfe transporters under reducing **(A)** and non-reducing **(B)** conditions. The uptake of radiolabeled iron (^{55}Fe) by *Y. pestis* strains Irp2$^-$Yfe$^+$ Feo$^+$ [*irp2*; circles], Irp2$^-$ Yfe$^-$ Feo$^+$ [*irp2 yfe*; squares], (Irp2$^-$ Yfe$^+$ Feo$^-$[*irp2 feo*; triangles]), and (Irp2$^-$ Yfe$^-$ Feo$^-$ [*irp2 yfe feo*; diamonds]) incubated at 37°C in the presence **(A)** or absence **(B)** of ascorbate was monitored over time. Cells were poisoned metabolically by incubation for 10 min with 100 μM CCCP before the addition of the isotope (open symbols). The uptake curves are averages of duplicate samples from two or more replicate experiments.

gene was lower relative to the *att*Tn*7*:: *feoA*::*lacZ* reporter but was repressed by iron under both static and aerobic growth conditions (Figure S3). The R2 deletion would remove a potential −35 box for the putative P1 promoter (**Figure 1**) which likely accounts for the results we obtained with this construct.

The *FeoABC* and *YfeABCD* Systems Transport Iron under Both Reducing and Non-reducing Conditions

To demonstrate that the Yfe and Feo systems are involved in active iron transport, transport assays were performed under reducing and non-reducing conditions. Sodium ascorbate was utilized to maintain $^{55}FeCl_3$ in the reduced, ferrous state. An *Δirp2* mutant (unable to make Ybt), transported ∼40% of the ferrous iron under reducing conditions (**Figure 7A**) and ∼35% under non-reducing conditions (**Figure 7B**) by 30 min of incubation at 37°C. The uptake was energy-dependent, since CCCP-poisoned cells showed very little cell-associated iron (**Figures 7A,B**). The *Δirp2 Δyfe* double mutant, transported iron at slightly reduced rates compared to the *Δirp2* mutant, under both reducing (∼3-fold) (**Figure 7A**) and non-reducing (∼2-fold) (**Figure 7B**). The *Δirp2 Δfeo* double mutant had slightly reduced rates of uptake under reducing conditions compared to the *Δirp2* mutant (**Figure 7A**). However, the *Δirp2 Δyfe Δfeo* triple mutant showed very little cell-associated iron, a level comparable to the CCCP-poisoned cells, under both reducing (**Figure 7A**), and non-reducing (**Figure 7B**) conditions. This indicates, that Yfe and Feo have somewhat redundant *in vitro* ferrous uptake functions with one system partially compensating for loss of the other. However, together they are crucial for ferrous iron transport under the short-term *in vitro* uptake conditions used here. In addition, these assays indicate that the Yfe and Feo systems can use ferric iron as well as ferrous.

DISCUSSION

The FeoABC system is widespread in bacteria and transcriptional regulation by Fnr, ArcA, RstAB and Fur has been demonstrated, particularly in *E. coli, Salmonella,* and *Shigella* (Kammler et al., 1993; Boulette and Payne, 2007; Jeon et al., 2008). Although, the *Y. pestis feoA* promoter encodes putative putative Fnr- and ArcA-binding sites (Gao et al., 2008), *Δfnr* and *ΔarcA* mutations do not affect *feoB* transcription. In addition, *oxyR*, *rstA,* or *feoC* mutations failed to affect *feoB* transcription. Finally, the *feoABC* operon is repressed by iron and Fur during microaerobic but not aerobic growth (Forman et al., 2010; Fetherston et al., 2012). Thus, the *Y. pestis feoABC* locus currently has unique regulatory properties.

To assess the mechanism behind the lack of iron and Fur repression during aerobic growth, we assessed the regulation of 5′-truncations of *feoA::lacZ* reporter with a 396 bp intergenic/promoter region. Modest aerobic iron-mediated repression occurred with the 208 bp *feoA::lacZ* and stronger aerobic iron- repression was observed with the 165 and 125 bp promoter truncations (**Figure 2**). This repression was increased when *Y. pestis* cells were grown at acidic pHs (6.0 and 6.5) and even the 396 bp *feoA*::*lacZ* was repressed by iron after growth at pH 6.0 (**Figure 3**). When the *feoA* promoter from *E. coli* linked to *lacZ* was expressed in *Y. pestis*, it was repressed by iron aerobically (Figure S1), confirming that it is a unique aspect of the *Y. pestis feoA* promoter region that is preventing iron-Fur repression aerobically and not an aspect of the *Y. pestis* Fur protein. Thus, we propose that the 396 to 165 bp region somewhat prevents Fe-Fur repression aerobically and that pH has some influence on this.

In addition, when the promoter was truncated from 396 to 335 bp or 271 bp, there was an overall increase in transcriptional activity (**Figure 2**), suggesting that a repressor binds to the 396 to 335 bp region, lowering overall transcription. A series of EMSA experiments found that a *Y. pestis* cytoplasmic protein(s) bound to two regions: 396 to 271 and 145 to 1 bp (**Figure 5**). Although, we have not identified this protein(s) it is not Fur (**Figure 5**).

These results caused us to reexamine the sequence of the region upstream of *feoA*. This led to our hypothesis that a second promoter region (designated P1 in **Figure 1**; 198 to 171 bp which overlaps the putative Fnr-binding site) is upstream of the originally annotated Fur-repressible promoter (69 to 29 bp including the FBS; P2 in **Figure 1**). Note that the defined binding region for the 396 to 271 bp region lies outside of the predicted second promoter region. Significant transcriptional activity from the putative P2 promoter was demonstrated in a construct that deleted the P1 promoter region (*feoAΔFBS*::lacZ). Iron addition showed a modest (∼2-fold) repression of the P1 promoter under static (microaerobic) but not aerobic conditions. Although two weaker potential FBS sites (262–280 and 204–222) are upstream of the P1 promoter, their role in iron regulation has not been examined. We also identified three direct repeats (R1-R3 in **Figure 1**) and tested their role(s) on transcription of the *feoABC* operon. Deletion of R3 (151 to 141 bp region in **Figure 1**) had no effect on expression compared to the *feoA*::*lacZ* reporter, while the R1 (366 to 356 bp region in **Figure 1**) deletion reduced expression under aerobic conditions (51–65%) without altering iron regulation under either aerobic or microaerobic conditions (Figure S3). In contrast, the *feoAΔR2*::*lacZ* had activity essentially the same as the *feoAΔfeoP1*::*lacZ* reporter. Note that the R2 repeat (206 to 196 bp region in **Figure 1**) is not within regions to which protein(s) bind (396 to 271 and 145 to 1 bp; **Figure 5**). Thus, the transcriptional effect observed in the R2 deletion likely occurs because this repeat overlaps the P1 −35 box (**Figure 1** and Figure S3). Thus, there is no evidence that the R1-3 repeats play a direct role in transcriptional regulation from either P1 or P2.

In our current model, truncation of the 297 bp region to 125 or 165 bp, eliminates the upstream P1 promoter, forcing transcription from the second Fur-regulated P1 promoter (**Figure 1**). Although, the 195 and 208 bp promoter truncationss contained both RNAP-binding sites, binding would not be optimal since the RNAP typically spans −55 to +20. Thus, there may have been limited transcription from the upstream P1 promoter with the majority coming from the downstream iron-repressible P2 promoter. The upstream RNAP polymerase binding site may favor an alternative RNAP possibly with a σ^S subunit. In *E. coli*, Becker and Hengge-Aronis found that σ^S-dependent promoters have a tendency to have a "C" at position

−13 and either a "T" or "G" at position −14. Of the promoters they examined, 85% had a "C" at −13, 40% had a "T" at −14, and 40% had a "G" at −14 (Becker and Hengge-Aronis, 2001). The upstream RNA polymerase binding site contains a "C" at position −13 and a "T" at position −14 (**Figure 1**). Activity of σ^SRNAP promoters is not limited to stationary phase—activity is also induced in response to stresses such as osmotic, heat shock, and low pH (Kazmierczak et al., 2005). Whether, the upstream promoter uses an alternative RNAP or simply responds to environmental stresses remains to be determined.

In our model, aerobic conditions, as well as acidic conditions are stresses that lead to transcription from the upstream putative P1 promoter instead of or in addition to the σ^{70}-RNAP, Fe-Fur repressible P2 promoter making iron-regulation negligible under these conditions. However, under microaerobic conditions, transcription from the upstream promoter is repressed. Whether this repression is due to a requirement for a different sigma factor RNAP or a DNA looping mechanism related to the two unidientifed protein binding sites that occludes the upstream promoter is undetermined. However, this leaves the downstream Fur-regulated P2 promoter as the active promoter which can be repressed by iron and Fur. Unlike FeoA, which has high amino acid similarity to FeoA of *E. coli* and *Shigella*, the *feoA* promoter regions of *Y. pestis* and *E. coli* show no significant similarities when compared via a DNA BLAST search (Zhang et al., 2000). Thus, the avoidance of iron-repression aerobically may be unique to *Y. pestis,* at least until the *feoA* promoter regions of other bacteria are assessed under aerobic conditions. Whether this lack of regulation aerobically plays a positive role in *Y. pestis* remains to be determined. One possible role would be that Feo serves to acquire basal levels of iron aerobically even under iron-surplus conditions. *Y. pestis* also appears to be unique in that Fnr, ArcA, RstAB, and FeoC do not regulate the *feoABC* operon (Fetherston et al., 2012) although they are proven regulators of this operon in other enterics (Kammler et al., 1993; Boulette and Payne, 2007; Jeon et al., 2008; Kim et al., 2013).

As expected our transport studies showed that FeoABC and YfeABCD each function to take up iron in an energy-dependent manner under reducing conditions (ferrous) (**Figure 7A**) Together these two system are responsible for nearly all the iron uptake observed. However, the Fet-Flp system and likely the EfeUOB systems also function in iron uptake. Perhaps neither of these systems functioned significantly during the 30-min time frame or conditions of this experiment. Unexpectedly we found that both the FeoABC and YfeABCD systems could use ferric iron as a substrate for uptake over the 30 min period (**Figure 7B**). These experiments did not distinguish between the possibility that both systems transport ferric iron or that ferric iron is reduced to ferrous prior to transport. However, either alternative suggests that the FeoABC and YfeABCD transporters could function aerobically under non-reducing conditions.

AUTHOR CONTRIBUTIONS

LO is the first author. LO and JF contributed experimental work and planning of the research course. RP oversaw the research and contributed to the planning of the research course.

ACKNOWLEDGMENTS

This work was supported by Public Health Services Grant RO1 AI33481 from the US National Institutes of Health.

SUPPLEMENTARY MATERIAL

The Supplementary Material for this article can be found online at: http://journal.frontiersin.org/article/10.3389/fcimb.2017.00331/full#supplementary-material

REFERENCES

Altschul, S. F., Madden, T. L., Schäffer, A. A., Zhang, J., Zhang, Z., Miller, W., et al. (1997). Gapped BLAST and PSI-BLAST: a new generation of protein datatbase search programs. *Nucleic Acids Res.* 25, 3389–3402. doi: 10.1093/nar/25.17.3389

Bearden, S. W., Fetherston, J. D., and Perry, R. D. (1997). Genetic organization of the yersiniabactin biosynthetic region and construction of avirulent mutants in *Yersinia pestis*. *Infect. Immun.* 65, 1659–1668.

Bearden, S. W., and Perry, R. D. (1999). The Yfe system of *Yersinia pestis* transports iron and manganese and is required for full virulence of plague. *Mol. Microbiol.* 32, 403–414. doi: 10.1046/j.1365-2958.1999.01360.x

Becker, G., and Hengge-Aronis, R. (2001). What makes an *Escherichia coli* promoter σS dependent? Role of the −13/−14 nucleotide promoter positions and region 2.5 of σS. *Mol. Microbiol.* 39, 1153–1165. doi: 10.1111/j.1365-2958.2001.02313.x

Bobrov, A., Kirillina, O., Fetherston, J. D., Miller, M. C., Burlison, J. A., and Perry, R. D. (2014). The *Yersinia pestis* siderophore, yersiniabactin, and the ZnuABC system both contribute to zinc acquisition and the development of lethal septicaemic plague in mice. *Mol. Microbiol.* 93, 759–775. doi: 10.1111/mmi.12693

Boulette, M. L., and Payne, S. M. (2007). Anaerobic regulation of *Shigella flexneri* virulence: ArcA regulates *fur* and iron acquistion genes. *J. Bacteriol.* 189, 6957–6967. doi: 10.1128/JB.00621-07

Choi, E., Groisman, E. A., and Shin, D. (2009). Activated by different signals, the PhoP/PhoQ two-component system differentially regulates metal uptake. *J. Bacteriol.* 191, 7174–7181. doi: 10.1128/JB.00958-09

Choi, K.-H., Gaynor, J. B., White, K. G., Lopez, C., Bosio, C. M., Karkhoff-Schweizer, R. R., et al. (2005). A Tn7-based broad-range bacterial cloning and expression system. *Nat. Methods* 2, 443–448. doi: 10.1038/nmeth765

Darby, C., Hsu, J. W., Ghori, N., and Falkow, S. (2002). *Caenorhabditis elegans*: plague bacteria biofilm blocks food intake. *Nature* 417, 243–244. doi: 10.1038/417243a

de Lorenzo, V., Giovannini, F., Herrero, M., and Neilands, J. B. (1988). Metal ion regulation of gene expression: Fur repressor– operator interaction at the promoter region of the aerobactin system of pColV-K30. *Mol. Biol.* 203, 875–884. doi: 10.1016/0022-2836(88)90113-1

Fetherston, J. D., Kirillina, O., Bobrov, A. G., Paulley, J. T., and Perry, R. D. (2010). The yersiniabactin transport system is critical for the pathogenesis of bubonic and pneumonic plague. *Infect. Immun.* 78, 2045–2052. doi: 10.1128/IAI.01236-09

Fetherston, J. D., Mier, I. Jr., Truszczynska, H., and Perry, R. D. (2012). The Yfe and Feo transporters are involved in microaerobic growth and the virulence of *Yersina pestis* in bubonic plague. *Infect. Immun.* 80, 3880–3891. doi: 10.1128/IAI.00086-12

Fetherston, J. D., Bertolino, V. J., and Perry R. D. (1999). YbtP and YbtQ: two ABC transporters required for iron uptake in *Yersinia pestis*. *Mol. Microbiol.* 32, 289–299. doi: 10.1046/j.1365-2958.1999.01348.x

Forman, S., Paulley, J. T., Fetherston, J. D., Cheng, Y. Q., and Perry, R. D. (2010). Yersinia ironomics: comparison of iron transporters among *Yersinia pestis* biotypes and its nearest neighbor, *Yersinia pseudotuberculosis*. *BioMetals* 23, 275–294. doi: 10.1007/s10534-009-9286-4

Friedman, Y. E., and O'Brian, M. R. (2003). A novel DNA-binding site for the ferric uptake regulator (Fur) protein from *Bradyrhizobium japonicum*. *J. Biol. Chem.* 278, 38395–38401. doi: 10.1074/jbc.M306710200

Gao, H., Zhou, D., Li, Y., Guo, Z., Han, Y., Song, Y., et al. (2008). The iron-responsive Fur regulon in *Yersinia pestis*. *J. Bacteriol.* 190, 3063–3075. doi: 10.1128/JB.01910-07

Gong, S., Bearden, S. W., Geoffroy, V. A., Fetherston, J. D., and Perry, R. D. (2001). Characterization of the *Yersinia pestis* Yfu ABC iron transport system. *Infect. Immun.* 69, 2829–2837. doi: 10.1128/IAI.67.5.2829-2837.2001

Hsueh, K.-L., Yu, L.-K., Chen, Y.-H., Cheng, Y.-H., Hsieh, Y.-C., Ke, S.-C., et al. (2013). FeoC from Klebsiella pneumoniae contains a [4Fe-4S] cluster. *J. Bacteriol.* 195, 4726–4734. doi: 10.1128/JB.00687-13

Hung, K.-W., Tsai, J.-Y., Juan, T.-H., Hsu, Y.-L., Hsiao, C.-D., and Huang, T.-H. (2012). Crystal structure of the *Klebsiella pneumoniae* NFeoB/FeoC complex and roles of FeoC in regulation of Fe^{2+} transport by the bacterial Feo system. *J. Bacteriol.* 194, 6518–6526. doi: 10.1128/JB.01228-12

Jarrett, C. O., Deak, E., Isherwood, K. E., Oyston, P. C., Fischer, E. R., Whitney, A. R., et al. (2004). Transmission of *Yersinia pestis* from an infectious biofilm in the flea vector. *J. Infect. Dis.* 190, 783–792. doi: 10.1086/422695

Jeon, J., Kim, H., Yun, J., Ryu, S., Groisman, E. A., and Shin, D. (2008). RstA-promoted expression of the ferrous iron transporter FeoB under iron-replete conditions enhances Fur activity in *Salmonella enterica*. *J. Bacteriol.* 190, 7326–7334. doi: 10.1128/JB.00903-08

Kammler, M., Schon, C., and Hantke, K. (1993). Characterization of the ferrous iron uptake system of *Escherichia coli*. *J. Bacteriol.* 175, 6212–6219. doi: 10.1128/jb.175.19.6212-6219.1993

Kazmierczak, M. J., Wiedmann, M., and Boor, K. J. (2005). Alternative sigma factors and their roles in bacterial virulence. *Microbiol. Mol. Biol. Rev.* 69, 527–543. doi: 10.1128/MMBR.69.4.527-543.2005

Kim, H., Lee, H., and Shin, D. (2013). The FeoC protein leads to high cellular levels of the Fe(II) transporter FeoB by preventing FtsH protease regulation of FeoB in *Salmonella enterica*. *J. Bacteriol.* 195, 3364–33670. doi: 10.1128/JB.00343-13

Kirillina, O., Bobrov, A. G., Fetherston, J. D., and Perry, R. D. (2006). A hierarchy of iron uptake systems: Yfu and Yiu are functional in *Yersinia pestis*. *Infect. Immun.* 74, 6171–6178. doi: 10.1128/IAI.00874-06

Kirillina, O., Fetherston, J. D., Bobrov, A. G., Abney, J., and Perry, R. D. (2004). HmsP, a putative phosphodiesterae, and HmsT, a putative diguanylate cyclase, control Hms-dependent biofilm formation in *Yersinia pestis*. *Mol. Microbiol.* 54, 75–88. doi: 10.1111/j.1365-2958.2004.04253.x

Lau, C. K. Y., Ishida, H., Liu, Z., and Vogel, H. J. (2013). Solution structure of *Escherichia coli* FeoA and its potential role in bacterial ferrous iron transport. *J. Bacteriol.* 195, 46–55. doi: 10.1128/JB.01121-12

Miller, J. H. (1992). *A Short Course in Bacterial Genetics. A Laboratory Manual and Handbook for Escherichia coli and Related Bacteria*. Cold Spring Harbor, NY: Cold Spring Harbor Laboratory Press.

Perry, R. D. (2004). "Yersinia" in *Iron Transport in Bacteria*, eds J. H. Crosa, A. R. Mey, and S. M. Payne (Washington, DC: ASM Press), 219–240.

Perry, R. D., and Fetherston, J. D. (1997). *Yersinia pestis*-etiologic agent of plague. *Clin. Microbiol. Rev.* 10, 35–66.

Perry, R. D., and Fetherston, J. D. (2004). "Iron and heme uptake systems," in *Yersinia Molecular and Cellular Biology,* eds E. Carniel and B. J. Hinnebusch (Norfolk: Horizon Bioscience), 257–283.

Perry, R. D., and Fetherston, J. D. (2011). Yersiniabactin iron uptake: mechanisms and role in *Yersinia pestis* pathogenesis. *Microbes Infect.* 13, 808–817. doi: 10.1016/j.micinf.2011.04.008

Perry, R. D., Bobrov, A. G., Kirillina, O.,Rhodes, E. R., Actis, L. A., and Fetherston, J. D. (2012). *Yersinia pestis* transition metal divalent cation transporters. *Adv. Expt. Biol. Med.* 954, 267–279. doi: 10.1007/978-1-4614-3561-7_34

Perry, R. D., Pendrak, M. L., and Schuetze, P. (1990). Identification and cloning of a hemin storage locus involved in the pigmentation phenotype of *Yersinia pestis*. *J. Bacteriol.* 172, 5929–5937. doi: 10.1128/jb.172.10.5929-5937.1990

Pujol, C., Klein, K. A., Romanov, G. A., Palmer, L. E., Cirota, C., Zhao, Z., et al. (2009). *Yersinia pestis* can reside in autophagosomes and avoid xenophagy in murine macrophages by preventing vacuole acidification. *Infect. Immun.* 77, 2251–2261. doi: 10.1128/IAI.00068-09

Skaar, E. P. (2010). The batte for iron between bacterial pathogens and their vertebrate hosts. *PLoS Pathog.* 6:e1000949. doi: 10.1371/journal.ppat.1000949

Thompson, J. M., Jones, H. A., and Perry, R. D. (1999). Molecular characterization of the hemin uptake locus (*hmu*) from *Yersinia pestis* and analysis of *hmu* mutants for hemin and hemoprotein utilization. *Infect. Immun.* 67, 3879–3892.

Wang, R. F., and Kushner, S. R. (1991). Construction of versatile low-copy-number vectors for cloning, sequencing and gene expression in *Escherichia coli*. *Gene.* 100, 195–199.

Zhang, Z., Schwartz, S., Wagner, L., and Miller, W. (2000). A greedy algorithm for aligning DNA sequences. *J. Comput. Biol.* 7, 203–214. doi: 10.1089/10665270050081478

Zhou, D., Qin, L., Han, Y., Qiu, J., Chen, Z., Li, B., et al. (2006). Global analysis of iron assimilation and fur regulation in *Yersinia pestis*. *FEMS Microbiol. Lett.* 258, 9–17. doi: 10.1111/j.1574-6968.2006.00208.x

Conflict of Interest Statement: The authors declare that the research was conducted in the absence of any commercial or financial relationships that could be construed as a potential conflict of interest.

frontiers in Cellular and Infection Microbiology

ORIGINAL RESEARCH
published: 21 June 2017
doi: 10.3389/fcimb.2017.00277

Host Iron Nutritional Immunity Induced by a Live *Yersinia pestis* Vaccine Strain Is Associated with Immediate Protection against Plague

*Ayelet Zauberman *, Yaron Vagima, Avital Tidhar, Moshe Aftalion, David Gur, Shahar Rotem, Theodor Chitlaru, Yinon Levy and Emanuelle Mamroud **

Department of Biochemistry and Molecular Genetics, Israel Institute for Biological Research, Ness-Ziona, Israel

Prompt and effective elicitation of protective immunity is highly relevant for cases of rapidly deteriorating fatal diseases, such as plague, which is caused by *Yersinia pestis*. Here, we assessed the potential of a live vaccine to induce rapid protection against this infection. We demonstrated that the *Y. pestis* EV76 live vaccine protected mice against an immediate lethal challenge, limiting the multiplication of the virulent pathogen and its dissemination into circulation. *Ex vivo* analysis of *Y. pestis* growth in serum derived from EV76-immunized mice revealed that an antibacterial activity was produced rapidly. This activity was mediated by the host heme- and iron-binding proteins hemopexin and transferrin, and it occurred in strong correlation with the kinetics of hemopexin induction *in vivo*. We suggest a new concept in which a live vaccine is capable of rapidly inducing iron nutritional immunity, thus limiting the propagation of pathogens. This concept could be exploited to design novel therapeutic interventions.

Keywords: *Yersinia pestis*, plague, iron nutritional immunity, hemopexin, live vaccine, EV76, protective immunity, innate immunity

OPEN ACCESS

Edited by:
Pierre Cornelis,
Vrije Universiteit Brussel, Belgium

Reviewed by:
Girija Ramakrishnan,
University of Virginia, United States
Roger Derek Pechous,
University of Arkansas for Medical Sciences, United States

****Correspondence:***
Ayelet Zauberman
ayeletz@iibr.gov.il
Emanuelle Mamroud
emmym@iibr.gov.il

Received: *23 April 2017*
Accepted: *06 June 2017*
Published: *21 June 2017*

Citation:
Zauberman A, Vagima Y, Tidhar A, Aftalion M, Gur D, Rotem S, Chitlaru T, Levy Y and Mamroud E (2017) Host Iron Nutritional Immunity Induced by a Live Yersinia pestis Vaccine Strain Is Associated with Immediate Protection against Plague. Front. Cell. Infect. Microbiol. 7:277. doi: 10.3389/fcimb.2017.00277

INTRODUCTION

Live vaccines are able to elicit extensive humoral immunity against specific antigens as well as inflammatory and cellular protective immune responses. Furthermore, the presentation of antigens to the host immune system in the context of infection can potentiate the amplitude and longevity of the protective response.

While the ability of live vaccines to serve as platforms for the initiation of adaptive protective responses against infections has been well documented (Coward et al., 2014; Minor, 2015), their ability to evoke protective innate immune mechanisms remains largely unknown. The induction of rapid, non-specific protective responses by live vaccines could provide a means to delay the progression of infection during sudden outbreaks, thereby extending the therapeutic window and allowing for the elicitation of the adaptive response, the manifestation of which typically requires more time post-exposure. In addition, the identification of potent innate immune mechanisms could lead to the discovery of novel bacterial or host-borne therapy targets, which are essential countermeasures to antibiotic-resistant pathogens.

Plague, which is caused by *Yersinia pestis*, is a fatal disease that has caused millions of deaths in three world pandemics. Over the last few decades, plague has persisted in Africa, Asia and the Americas, and since the 1990s, it has been categorized as a re-emerging disease (Bertherat, 2016).

At the same time, *Y. pestis* has been recognized as a Tier 1 select biological agent due to its potential use as a bioweapon (Inglesby et al., 2000). The severity of the disease in combination with concerns regarding the existence of antibiotic-resistant *Y. pestis* strains has prompted efforts to develop safe live vaccines (Titball and Williamson, 2004; Feodorova et al., 2007; Tidhar et al., 2009; Feodorova and Motin, 2012; Dentovskaya et al., 2015; Derbise et al., 2015; Tiner et al., 2016; Verma and Tuteja, 2016).

Protection against plague can be achieved by reiterated administrations of live EV76-based vaccines, which elicit a strong adaptive protective immune response. As of today, the only well-established molecular basis for the attenuation of these vaccines is attributed to the absence of the pigmentation locus (*pgm*)-which results in iron acquisition deficiency, a process essential for the survival and expansion of the pathogen in the host (Fetherston et al., 1992; Perry and Fetherston, 1997). Whether live vaccines such as EV76 are merely attenuated mutants or whether they manifest protection-inducing activities that are silent in their virulent parental strains remains an unanswered issue.

In the current report, we evaluated the efficacy of the *Y. pestis* EV76 live vaccine strain in providing immediate protection against both bubonic and pneumonic plague, and we characterized the mechanism involved in this innate immune response.

MATERIALS AND METHODS

Bacterial Strains

The *Y. pestis* strains used in this study included Kimberley53 (Kim53), a fully virulent *Y. pestis* strain (biovar orientalis), the live vaccine strain EV76 (*pgm*$^-$ [Girard's strain]) and the avirulent Kim53Δ70Δ10 strain (Ben-Gurion and Shafferman, 1981; Flashner et al., 2004; Zauberman et al., 2013). Kim53Δ70Δ10 strain was spontaneously cured of pCD1 (carrying the genes coding for elements of the Type III secretion system, essential for manifestation of virulence, Perry and Fetherston, 1997) and pPCP1 (carrying the gene coding for the virulence factor plasminogen-activating protease, Sebbane et al., 2006; Lathem et al., 2007).

To construct a bioluminescent *Y. pestis*, the plasmid pGEN-luxCDABE (a generous gift from Professor H. Mobley, Lane et al., 2007) was introduced into the *Y. pestis* Kim53 strain by electroporation, generating the Kim53-lux strain. Maintenance of the virulence-associated plasmids pMT1, pCD1, and pPCP1 and the *pgm* locus in the Kim53-lux strain was verified by PCR analysis.

Ethics Statement

This study was performed in strict accordance with the recommendations in the Guide for the Care and Use of Laboratory Animals from the National Institutes of Health. All of the animal experiments were performed in accordance with Israeli law and were approved by the Ethics Committee for animal experiments at the Israel Institute for Biological Research. (Protocols M-03-14, M-28-14, M-47-15, M-20-16, and M-37-16).

Animal Studies

Female 8 to 12-week-old C57BL/6 mice (Harlan, Israel) were used in this study. For s.c. infections in the mice, *Y. pestis* bacteria were grown on brain heart infusion agar (BHIA, Difco) for 48 h at 28°C and were then suspended in saline solution (0.9% NaCl). Protection experiments were carried out by challenging vaccinated animals by two routes of infection-s.c. or i.n. (i) Mice were infected simultaneously with 1×10^7 CFU of EV76 in the upper back (s.c. vaccination) and with 100 CFU (100 LD_{50}), of Kim53 in the lower back (s.c. challenge). (ii) Mice were infected with 1×10^7 CFU of EV76 in the upper back (s.c. vaccination) simultaneously or 2 days prior to i.n. infection (challenge) with 1×10^4 CFU (10 LD_{50}) of Kim53. Mice infections were performed as described previously (Zauberman et al., 2009; Vagima et al., 2015). Bacteria were quantified by CFU counting on BHIA plates. For bacterial dissemination to internal organs and blood, groups of at least 4 mice were anesthetized; tail vein blood was collected; spleens, draining inguinal lymph nodes (I-LNs), draining axillary lymph nodes (Ax-LNs) and mediastinal lymph nodes were harvested; and then tissue homogenates were prepared in 1 ml of PBS/organ. Bacterial quantification in the tissue homogenates or in blood samples was performed by plating serial dilutions in PBS on BHIA and by calculating the CFU/organ or CFU/1 ml of blood. To differentiate between EV76 and Kim53 in the organs, the samples were plated on BHIA supplemented with 100 μg/ml streptomycin, conditions that allow for the growth of only the Kim53 streptomycin-resistant strain.

Whole-Animal Luminescent Imaging

Anesthetized mice previously infected s.c. with 100 CFU of Kim53-lux were analyzed by visualizing photon emission using an *in vivo* Imaging System-IVIS (Caliper Life Sciences, Hopkinton, MA, USA). Image acquisition was performed with the binning set to 2. The acquisition time ranged between 1 and 4 min. The luminescence signals for all of the images were normalized using Living image® 4 software (PerkinElmer, USA) and are reported as photons/second/cm^2/sr.

Ex vivo Y. pestis Growth Assay

For *ex vivo* growth assays, mouse serum were mixed with 1×10^3 *Y. pestis* bacteria (total volume of 100 μl) and incubated in microtiter plates at 28°C. Dilution of mouse serum was done in RPMI medium supplemented with 10% fetal calf serum. Test samples and control samples contained identical amounts of mouse serum. Kim53 or Kim53Δ70Δ10 bacterial growth was determined by serial dilution and viable cell counts. The inhibitory effect was similar in both strains. To assess bacterial growth in immunized mouse serum in the presence of iron, iron dextran (Sigma D8517) was added at concentrations between 1.3 μg/ml to 1 mg/ml in 3-fold serial dilutions.

Proteinase K Digestion

Proteolysis was performed by incubating the serum samples with proteinase K-conjugated beads (Sigma Aldrich P9290) for 2 h at 37°C according to the manufacturer's recommendations.

Proteinase K-treated serum samples were centrifuged to remove the beads, and the supernatants were collected for analysis.

SDS-Page, Western Blot Analysis and Anti-F1 Elisa

Serum proteins (10 μl) were separated by 4–12% gradient SDS-PAGE (Invitrogen) and were stained using a Silver Stain Plus kit (Bio-Rad). For Western blot analysis, electrophoresed samples were transferred to nitrocellulose membranes (Invitrogen). Membranes were developed with polyclonal antibodies against hemopexin (Abcam ab 90947), transferrin (Abcam ab 82411) and β-actin (Sigma A5060), followed by HRP-conjugated goat anti-rabbit IgG. Anti-F1 ELISA in the serum of immunized mice was performed as described previously (Levy et al., 2011, 2016). Briefly, microtiter plates were coated with 500 ng of purified rF1 [provided by the Biotechnology Department at IIBR, produced as described in Holtzman et al. (2006)]. Tested sera were serially diluted in 2-fold dilutions in a final volume of 50 μl and were incubated in the wells for 1 h at 37°C. Alkaline phosphatase-conjugated goat anti-rabbit IgG (1/2,000 dilution, Sigma) was used as the 2nd layer for rabbit anti-F1 IgG titer determination. Titers were defined as the reciprocal values of the endpoint serum dilutions that displayed OD_{405} values 2-fold higher than the normal serum controls.

Ion-Exchange Chromatography

A pooled serum sample from EV76-infected mice (48 h post-infection) was first diluted and filtered through a 100 k-Da size exclusion membrane (VIVASPIN, Sartorius). The *Y. pestis ex vivo* growth inhibitory activity was identified to be in the upper fraction. The upper fraction was diluted 1:5 in buffer A (25 mM HEPES, pH 8.0) and was loaded onto a HiTrapQ HP 5-ml column from GE Healthcare equilibrated in the same buffer, using an AKTA Explorer system (GE-Healthcare) at 4°C. After loading, the column was washed with 10 column volumes (cv) of 100% buffer A at 4 ml/min, and it was eluted using a composite gradient between buffer A and B (25 mM HEPES, pH 8.0, and 1 M NaCl) with 20 cv of 10–30% B, 2 cv of 30% B, and 3 cv of 30–100% B at 2 ml/min, collecting 2 ml fractions. Finally, the column was eluted with 3 cv of 100% B at 2 ml/min, collecting 4 ml fractions. The fractions were sampled and used for *ex vivo* bacterial growth assays.

The fraction containing the inhibitory growth activity was subjected to a second purification step using anion exchange chromatography. After loading the sample, the column was washed with 5 cv of 100% A at 2 ml/min, collecting 4 ml fractions, and was eluted using a composite gradient between buffer A and C (25 mM HEPES, pH 8.0, and 150 mM NaCl) with 20 cv of 0–15% C at 1 ml/min, collecting 2 ml fractions. Then, the elution was continued with 5 cv of 15% C, 4 cv of 20% C, 3 cv of 25% C, 3 cv of 25–100% C and 3 cv of 100% C at 2 ml/min, collecting 2 ml fractions. Finally, the column was eluted with 3 cv of 100% C at 2 ml/min, collecting 4 ml fractions. The fractions were sampled and used for *ex vivo* bacterial growth assays. Faction 26 from the second chromatographic purification step exhibited the highest growth inhibitory activity.

Mass Spectrometry

Fraction 26, which contained most of the growth inhibitory activity, was subjected to in-solution digestion and was partially dried in an Eppendorf SpeedVac, and the remaining sample was resuspended in 100 mM ammonium bicarbonate to a final volume of 50 μl. Prior to enzymatic digestion with trypsin, the sample was reduced with dithiothreitol (DTT) and alkylated with iodoacetamide. Briefly, reduction was conducted at a final concentration of 10 mM DTT at 56° for 1 h. Iodoacetamide was then added to a final concentration of 55 mM, and the reaction was incubated at room temperature for 30 min. Finally, the reaction was quenched with 10 mM DTT. Enzymatic digestion was conducted overnight at 37°C with trypsin at an enzyme to protein ratio of 1:50 (wt/wt). The sample was partially dried in a SpeedVac. The resulting peptide mixtures were diluted in 80% formic acid and were then diluted 1:10 with Milli-Q water immediately before inline reverse-phase nano-LC (liquid chromatography)-electro spray ionization (ESI) tandem mass spectrometric analysis (MS/MS).

Samples were analyzed using an LTQ Orbitrap (Thermo Fisher Scientific, Bremen, Germany) operated in the positive ion mode. Nano-LC-ESI-MS/MS peptide mixtures were separated by inline reversed-phase nanoscale capillary LC and were analyzed by ESI-MS/MS. For LC-MS/MS, the samples were injected onto a 15 cm reversed-phase spraying fused-silica capillary column [constructed in-house; inner diameter 75 μm and packed with 3 μm of ReproSil-Pur C18A18 media (Dr. Maisch GmbH, Ammerbuch-Entringen, Germany)] using an UltiMate 3000 Capillary/Nano LC System (Dionex). The LC setup was connected to an LTQ Orbitrap mass spectrometer (Thermo Fisher Scientific, Bremen, Germany) equipped with a nanoelectrospray ion source (Thermo Fisher Scientific, Bremen, Germany). The flow rate through the column was 300 nl/min. An acetonitrile gradient was employed with a mobile phase containing 0.2% formic acid in Milli-Q water. The injection volume was 5 μl. The peptides were separated by 4 h gradients that ranged from 5 to 65% acetonitrile. The voltage applied to the union to produce an electrospray was 1.2 kV. Helium was introduced as a collision gas at a pressure of 3 psi. The mass spectrometer was operated in the data-dependent mode. Survey MS scans were acquired in the Orbitrap with the resolution set to a value of 60,000. For the analysis of tryptic peptides, survey scans were recorded in the FT mode, followed by data-dependent collision-induced dissociation (CID) of the 7 most intense ions in the linear ion trap (LTQ). Raw data were searched with MASCOT (Matrix Science, London, UK) against a UniProt mouse database. The search parameters included variable modifications of 57.02146 Da (carboxyamidomethylation) for Cys, 15.99491 Da (oxidation) for Met and 0.984016 Da (deamidation) for Asn and Gln. The search parameters were as follows: a maximum of 2 missed cleavages; initial precursor ion mass tolerance of 10 ppm; and fragment ion mass tolerance 0.6 Da.

Statistical Analysis

Statistical significance was measured using Student's unpaired *t*-test. Survival curves were compared using the log-rank test. In all of the analyses, *p*-values equal to 0.05 served as the limit of

significance. Calculations were performed using GraphPad Prism software.

RESULTS

Y. pestis EV76 Provides Immediate Robust Protection against Plague

To discover novel innate immune responses that could result in the rapid onset of protective immunity against infection, we evaluated the ability of the live attenuate *Y. pestis* EV76 strain to induce protection against subcutaneous (s.c.) lethal challenge with the fully virulent *Y. pestis* Kimberley53 strain (Kim53), when both strains were administered concomitantly to mice. Accordingly, the mice were infected by s.c. injection of a single dose (1×10^7 CFU) of the attenuated strain and were immediately challenged subcutaneously with a lethal dose of 100 LD_{50} of the virulent strain. To avoid possible direct interaction between the two co-administered strains, the attenuated strain was injected in the upper right back close to the right axillary lymph node (RAx-LN), whereas the virulent strain was injected in the lower left back, close to the left inguinal lymph node (LI-LN). Control mice were injected with saline and were challenged with the virulent *Y. pestis* strain (see scheme in **Figure 1A**).

As shown in **Figure 1B**, all of the control mice died within 5 days of the challenge. In contrast, simultaneous co-administration of the attenuated and virulent strains provided a very high protection level of 91%. This result clearly indicated that the EV76 strain was able to elicit an unforeseen, rapid and potent protective response against plague, strongly suggesting that upon immunization, some unknown protective mechanisms manifested prior to the establishment of an adaptive protected state. Simultaneous co-administration of the virulent *Y. pestis* strain with 1×10^7 CFU of another attenuated *Y. pestis* strain (Kim53Δ70Δ10, which lacks the plasmids that carry major *Y. pestis* virulence determinants), could not protect the infected mice (**Figure 1B**). This observation indicated that the early protective response promoted by EV76 could not be attributed merely to the large amount of bacteria administered but to a particular feature of this strain, and/or to its relative ability to replicate and disseminate in the host.

To examine whether protection could also be achieved by post-challenge administration of the EV76 strain, the mice were injected with EV76 5 h post-challenge. Under this condition, a significantly increased survival rate of 34% was also observed (**Figure 1B**).

In light of these results, we addressed the question of whether EV76-administration might promote rapid protection against pneumonic plague, which is considered to be a more challenging and severe manifestation of the disease. Accordingly, the mice were challenged intra-nasally (i.n.) with a lethal dose of the virulent *Y. pestis* strain 2 days after s.c. administration of the EV76 strain. As seen in **Figure 1C**, all of the control mice died at 3 days post-challenge, whereas 60% of the immunized mice survived the challenge. When mice were concomitantly infected with both strains, the mean time to death was extended from 3 to 6.8 days (**Figure 1C**). These results indicated that exposure to the *Y. pestis* EV76 live vaccine strain induced a very potent protective mechanism within a time window of less than 4 days, which is much earlier than the time usually required for the manifestation of an adaptive protective response.

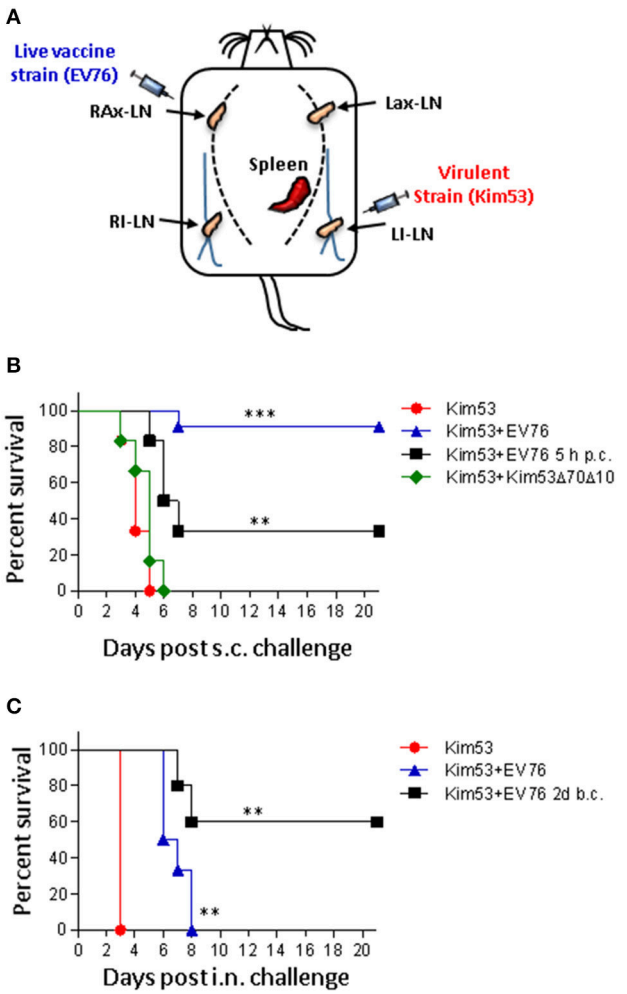

FIGURE 1 | The EV76 strain confers rapid protection against bubonic and pneumonic plague. **(A)** Schematic illustration of the injection sites of the EV76 vaccine strain and the virulent *Y. pestis* Kim53 strain. RAx-LN (right axillary lymph node), LAx-LN (left axillary lymph node), RI-LN (right inguinal lymph node), and LI-LN (left inguinal lymph node). **(B)** Kaplan-Meier survival profiles of mice challenged s.c. in the lower left side with 100 CFU of the virulent *Y. pestis* strain with concomitant immunization in the upper right side with 1×10^7 CFU of the EV76 strain (blue triangles), with 1×10^7 CFU of the Kim53Δ70Δ10 attenuated strain (green diamonds), or with saline (red circles). The black line represents the survival profiles of mice immunized with 1×10^7 CFU of the EV76 strain 5 h after s.c. challenge (p.c.) with the virulent Kim53 *Y. pestis* strain (100 CFU). **(C)** Mice were infected i.n. with 10^4 CFU of the virulent Kim53 *Y. pestis* strain and were then immediately infected s.c. with the EV76 strain (blue triangle) or with saline (red circle). The black line represents the survival of mice immunized s.c. with 1×10^7 CFU of EV76 2 days before i.n. challenge with 1×10^4 CFU of Kim53 (b.c.); $n = 6$ to $n = 11$ mice per group in at least 2 independent experiments. The *p*-values were calculated using Kaplan-Meier analysis with a log-rank (Mental-Cox) test compared to sham controls. $^{**}p < 0.01$ and $^{***}p < 0.001$.

Co-administration of the Protective EV76 Strain Restricts the Growth and Dissemination of the Virulent *Y. pestis* Strain

To further characterize the early protective activity induced by the EV76 strain, the effects of the administration of the attenuated strain on the expansion and dissemination of the virulent bacteria in the host were inspected using whole-animal luminescent imaging of individual animals with an *in vivo* imaging system (IVIS). Subcutaneous co-administration of the bacterial strains was performed as described above; however, the virulent strain used for the challenge expressed a bioluminescent tag (Kim53-lux). The animals were monitored daily for bioluminescence emission from 1 day post-infection until death. As depicted in **Figure 2A** (upper panel), in the non-immunized group, a luminescent signal marking the presence of at least 5×10^6 bacteria (the detection limit) was visible 48 h after the challenge and was limited to the site of injection or to the inguinal lymph node proximal to the injection site. Dissemination of the virulent bacteria into internal organs was first observed 72 h post-challenge. Five days post-challenge, 4 of 6 mice died, and the two remaining mice exhibited strong systemically dispersed luminescent signals. In contrast, mice injected with the protective EV76 strain simultaneously with the virulent strain did not exhibit any luminescent signals throughout the experiment, apart from a single mouse in which a minor and transient signal was observed at 72 h post-challenge at the draining lymph node (**Figure 2A**, lower panel). No mortality was observed in the immunized group. These results suggested that the protective strain rapidly induced a bacterial inhibitory effect following its administration that blocked the replication and dissemination of the virulent strain early in the course of infection.

To determine the effects of EV76 administration during the early stages of infection when the quantity of virulent bacteria in the host is less than the threshold enabling IVIS-mediated detection, the bacterial loads in organs were quantified by direct CFU counts. The mice were injected s.c. with EV76, with the virulent strain or with both, as above. At different time points post-infection, the tissues of infected mice were harvested, and the bacterial loads in the draining lymph nodes, spleen and blood were determined.

In the mice infected s.c. with 1×10^7 CFU of EV76, bacteria reached the draining RAx-LN proximal to the injection site within 1 h. Then, the bacteria persisted in the lymph node for at least 4 days and typically did not disseminate to other internal organs (**Figure 2B**). In the mice injected with the virulent Kim53 strain (100 CFU), a small amount of bacteria was found in the draining LI-LN, close to the injection site, within 1 h. The bacterial load at the LI-LN grew rapidly to 6×10^5 CFU (geometric mean) after 72 h and was paralleled by dissemination to the spleen and blood (**Figure 2C**).

When the virulent strain was co-administered with the protective EV76 strain, it disseminated to the draining LI-LN within 1 h (**Figure 2D**). However, in contrast to the pattern of distribution observed for the virulent strain in the absence of EV76, by 24 h, the number of bacteria detected in the LI-LN was notably lower, and by 72 h post-challenge, in 4 of 5 mice, the virulent bacteria were cleared from the draining LN and were not detected in the spleen or blood (**Figure 2D**). These results suggested that EV76 has rapid and systemic effects that inhibit the growth and dissemination of the virulent strain from the draining lymph node to internal organs and indicated that direct interaction between the two strains of the bacteria was not involved in this process. Furthermore, the persistence of EV76 bacteria in the lymph node for at least 4 days post-immunization (**Figure 2B**) could enable continuous induction of this putative protective mechanism.

Serum Derived from Mice Following Exposure to the Protective EV76 Strain Exerts Potent Protein-Based Antimicrobial Activity against *Y. pestis*

The results of the dissemination experiments strongly suggested that an antibacterial component was produced upon immunization with the protective EV76 strain, and it possibly migrated through the circulation, affecting propagation of the virulent strain.

To probe a putative non-cellular antibacterial effector, an *ex vivo* growth assay was designed (**Figure 3A**) in which *Y. pestis* bacteria were subjected to mouse serum from mice 24 h post-immunization (p.i.) with EV76 or to saline-immunized mouse serum (control serum) (**Figure 3B**). During the first 6 h of incubation, *Y. pestis* bacteria incubated with serum derived from control mice or with EV76-immunized mouse serum exhibited similar growth curves. However, *Y. pestis* growth continued with the control serum for an additional 72 h, reaching a concentration of 2.8×10^9 CFU/ml. In sharp contrast, at 24 h post-incubation, *Y. pestis* growth in the EV76-immunized mouse serum ceased, resulting in significantly lower bacterial concentrations of only 4×10^5 CFU/ml at 72 h. Therefore, the time course of the *Y. pestis* growth inhibition *ex vivo* was correlated with the protection observed *in vivo*. Furthermore, serum collected from mice exposed to the attenuated *Y. pestis* strain Kim53Δ70Δ10, which did not confer protection to mice (**Figure 1B**), failed to demonstrate inhibition of *Y. pestis* growth *ex vivo* (**Figure 3C**). Notably, inspection of sera by anti-F1 ELISA clearly demonstrated that the induction of humoral immunity against the immunogenic F1 capsular antigen of *Y. pestis*, which is known to provide anti-plague protection, was observed only on day 8 p.i. with EV76 (anti-F1 IgG titer of 1:1250). Thus, the data suggested that at 24 h p.i. with EV76, the murine serum contained an innate-derived antibacterial component that inhibited bacterial growth.

To define the kinetics of the antibacterial agent, the mice were immunized with EV76, and serum was collected at different time points post-immunization for *ex vivo Y. pestis* growth assays. Between 1 and 6 h p.i., the serum did not exhibit any anti-growth inhibitory effects (**Figure 4A**). Inhibition of bacterial growth was observed beginning with serum collected 24 h p.i., and it persisted until day 13. The maximal growth

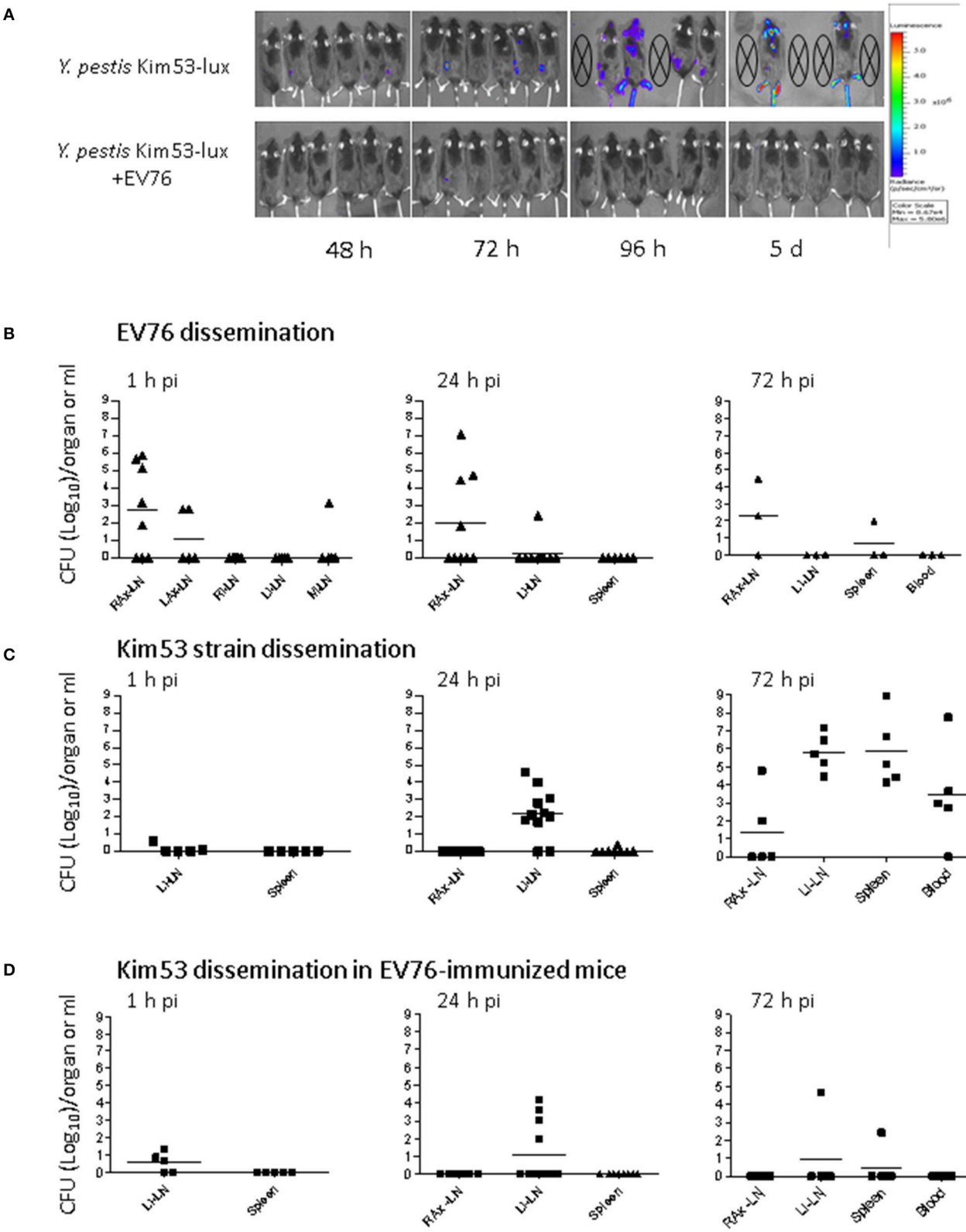

FIGURE 2 | Co-administration of the protective EV76 strain restricts the growth and dissemination of the virulent *Y. pestis* Kim53 strain. **(A)** Dissemination of bacteria in mice was analyzed using an IVIS lumina imaging system at different time points (h, hours; d, days) after s.c. injection of the virulent *Y. pestis* strain Kim53-lux

(Continued)

FIGURE 2 | Continued
(100 CFU) together with saline (upper panel) or after s.c. injection of *Y. pestis* Kim53-lux (100 CFU) together with 1×10^7 CFU of the EV76 strain (EV76-immunized, lower panel), as schematically described in **Figure 1A**. **(B)** Mice were infected s.c. with the protective EV76 strain, the virulent Kim53 strain **(C)** or both **(D)**, as described above. At different time points post-infection, the bacterial loads in the draining lymph nodes, spleen and blood were determined; $n = 3$ to $n = 11$ mice per group. Values represent the total bacterial loads in organs (CFU/organ) or the bacterial concentrations in blood (CFU/ml). The limit of detection was 3 CFU. RAx-LN (right axillary lymph node), LAx-LN (left axillary lymph node), RI-LN (right inguinal lymph node), LI-LN (left inguinal lymph node), M-LN (mediastinal lymph node), spleen, and blood. Each dot indicates the value quantified in one animal; bars represent geometric means.

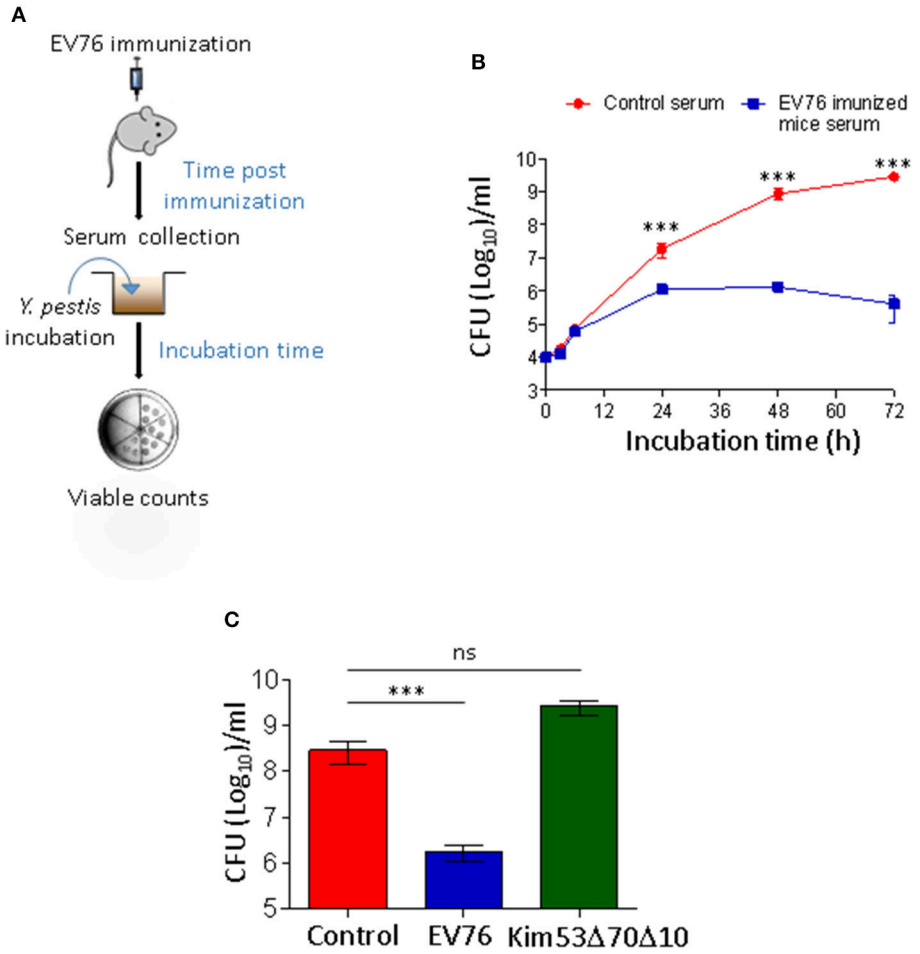

FIGURE 3 | Sera collected from mice immunized with the EV76 strain exhibit growth inhibitory effect against *Y. pestis*. **(A)** Schematic illustration of the *ex vivo* bacterial growth assay; mice were immunized with 1×10^7 CFU of the EV76 strain, and serum was collected at the indicated time points post-immunization (pi). *Y. pestis* bacteria (1×10^3 CFU) were incubated in the presence of murine sera for the indicated incubation times. Growth was monitored by viable counts. **(B)** *Y. pestis* bacteria were subjected to *ex vivo* growth assays as described above, with serum derived from saline-injected mice (red circle) or EV76-immunized mice 24 h p.i. (blue square). Growth was monitored by viable counts following incubation periods of 0–72 h. **(C)** *Y. pestis* bacteria were subjected to *ex vivo* growth assays in the presence of sera derived from control mice or from mice injected with the EV76 strain or the Kim53Δ70Δ10 attenuated strain, as indicated (24 h p.i.). Viable counts were determined after 48 h of incubation. In all of the experiments, the data depict the mean and the standard error of the mean (SEM) of at least 3 individual sera of at least two independent experiments. Statistical significance was measured using Student's unpaired *t*-test with log-transformed values (***$p < 0.001$, and ns, not significant).

inhibitory effect was observed in serum collected at 48 h and 72 h p.i and the antibacterial activity was found to be highly potent and active even at high dilution (**Figure 4B**). As depicted in **Figure 4C**, proteinase K digestion completely eliminated the growth inhibitory effect of the serum, indicating that the antibacterial activity might be attributed to a proteinaceous component.

Identification of the Host Proteins Hemopexin and Transferrin in the Serum Fraction That Inhibits Bacterial Growth

To identify the antibacterial component in the circulation of EV76-immunized mice, serum samples exhibiting *Y. pestis* inhibitory activity were subjected to HiTrapQ HP anion

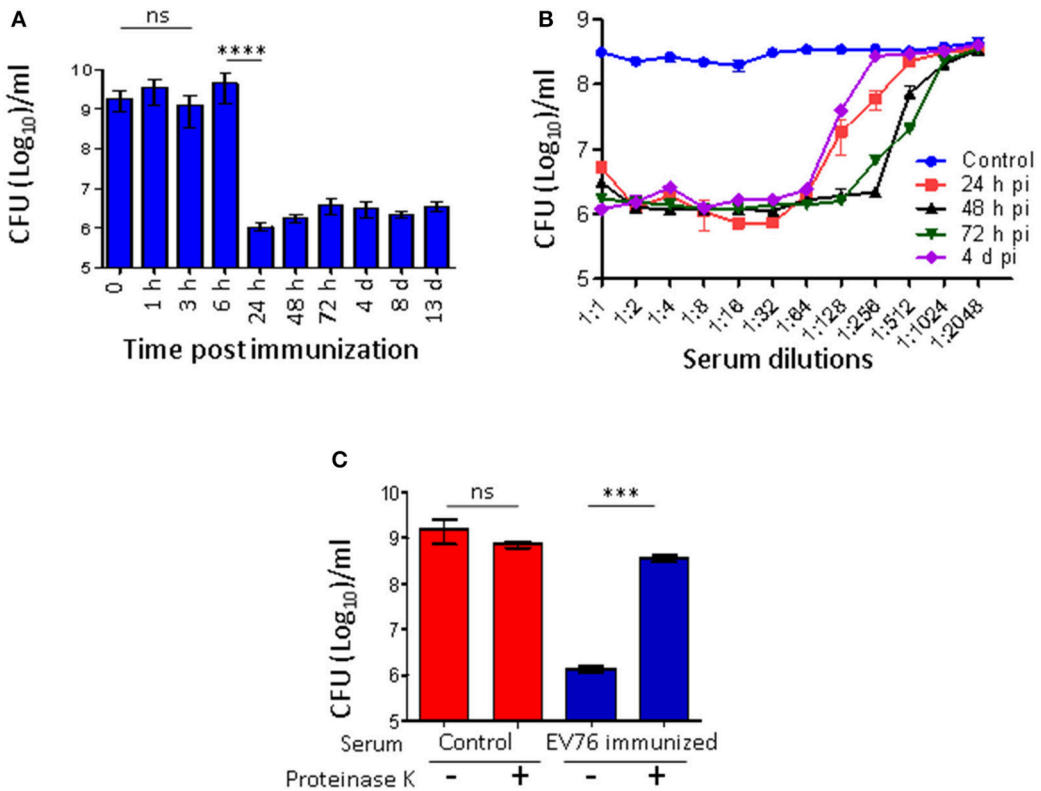

FIGURE 4 | A protenious antibacterial activity is present in the serum 24 h after immunization with the EV76 live vaccine strain. **(A)** Sera collected from EV76-immunized mice at the indicated time points post-infection (1 h–13 d) were analyzed by the *Y. pestis ex vivo* growth assays. **(B)** Serum samples were collected from saline-injected or EV76-immunized mice at the indicated time points p.i. (24 h–4 d), were serial diluted and analyzed for affecting *Y. pestis* growth by *ex vivo* assays. **(C)** Serum derived from control and EV76-immunized mice was subjected to proteinase K digestion and used for *Y. pestis ex vivo* growth assays. In all of the experiments, the data depict the mean and the standard error of the mean (SEM) of at least 3 individual sera, of at least two independent experiments. Statistical significance was measured using Student's unpaired *t*-test with log-transformed values (****$p < 0.0001$, ***$p < 0.001$, and ns, not significant).

exchange chromatography fractionations (**Figure 5A**). The eluted fractions were collected, and their antimicrobial properties were assessed by *ex vivo Y. pestis* growth assays (**Figure 5B**). Fraction 26 exhibited the maximal growth inhibitory effect. This fraction contained two protein bands visible by silver-stained SDS-PAGE analysis (**Figure 5C**, left panel). Mass spectrometric tryptic-protein fingerprinting analysis established that the two proteins were host-borne hemopexin (a heme-sequestering protein) and transferrin (an iron-sequestering protein). Using specific antibodies, the identities of these proteins were further confirmed by Western blot analysis (**Figure 5C**, right panels). Thus, the proteins that seemed to be associated with the inhibitory activity present in the serum of the immunized animals exhibited biological functions involved in iron limitation.

To directly investigate the possibility that the antibacterial activity of serum derived from EV76-immunized mice resulted from iron starvation, the *Y. pestis ex vivo* serum-mediated growth inhibition assay was performed in the presence of increasing amounts of iron dextran. Growth inhibition was clearly reversed by iron dextran in a dose-dependent manner (**Figure 6A**).

Serum Hemopexin and Transferrin Levels Following EV76 Immunization

To monitor the expression levels of hemopexin and transferrin following the immunization of mice with EV76, serum samples were collected from EV76-inoculated mice at different time points post-immunization and were subjected to SDS-PAGE and Western blot analysis using specific anti-transferrin and anti-hemopexin antibodies. As shown in **Figure 6B**, 24 h after EV76 inoculation, hemopexin was dramatically upregulated as compare to control mice. A further increase in hemopexin was detected 48 h following immunization, and this expression level was sustained for at least 4 days. The hemopexin expression pattern strongly correlated with the appearance of antibacterial activity in EV76-immunized mouse serum *ex vivo* (**Figures 4A,B**). A basal level of transferrin was detected in the serum of non-immunized mice, and its expression level increased slightly upon immunization (**Figure 6B**). These results suggested that both transferrin and hemopexin were responsible for the antimicrobial activity, however, hemopexin was the major component induced in EV76-immunized mouse serum. The correlation between hemopexin protein levels and the rapid protective response against plague was further substantiated

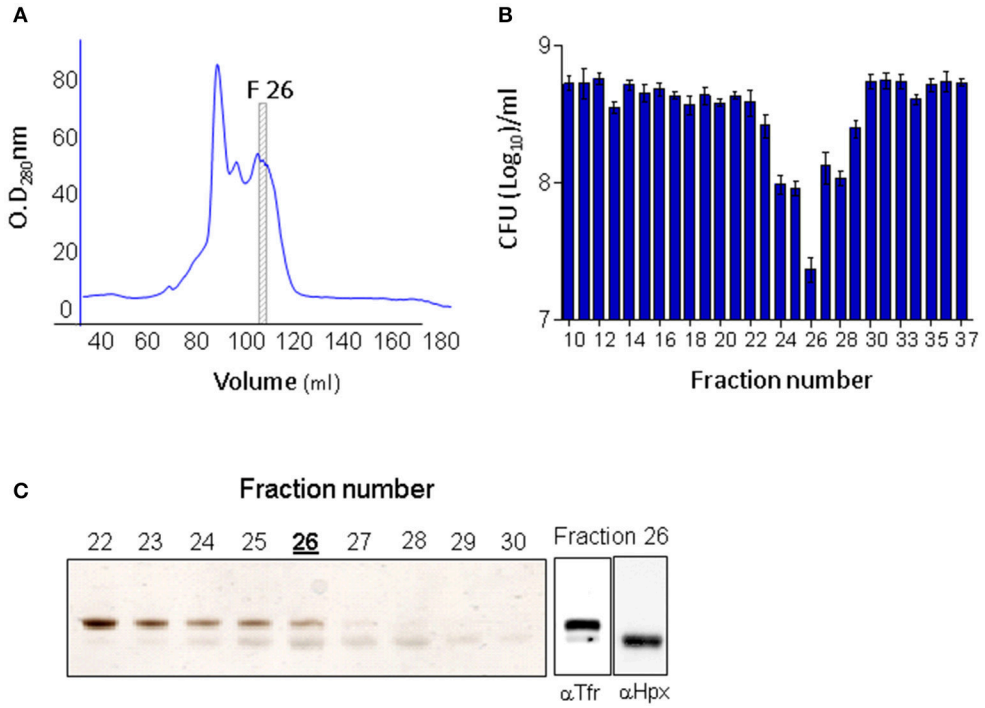

FIGURE 5 | Hemopexin and transferrin are present in the active fraction of EV76-immunized murine serum exhibiting *ex vivo* antibacterial activity. **(A)** Ion-exchange chromatography (second out of two constitutive rounds) of EV76-immunized mice sera. Fraction no. 26 is boxed and marked F26 (it exhibited the highest antibacterial activity, see **B**). **(B)** Antibacterial activity measured in the ion-exchange fractions of the EV76-immunized murine sera. **(C)** Ion-exchange fractions 22–30 inspected by SDS-PAGE visualized by silver staining (left panel). Fraction 26 was subjected to Western blot analysis using anti-transferrin (αTfr) or anti-hemopexin (αHpx antibodies (right).

by the observation that injection of the Kim53Δ70Δ10 strain (which did not protect mice from simultaneous challenge with the virulent strain; **Figure 1B**) did not induce the expression of hemopexin or transferrin in mouse serum (**Figure 6C**).

DISCUSSION

The live attenuated *Y. pestis* vaccine strain EV76 confers robust protection against plague due to its elicitation of strong acquired immune responses targeting *Y. pestis* key virulent factors and structural bacterial constituents, such as the F1 antigen (Walker et al., 1953; Tidhar et al., 2009). The establishment of an adaptive immune response is a relatively slow process, requiring several weeks to attain the amplitude needed for manifestation of its protective value. Since post-exposure prophylactic measures are highly relevant in the case of pathogens against which mass vaccination is not routinely conducted or in the case of bacterial pathogens potentially associated with intentional bioterror use, we inspected the effects of EV76 vaccination administered concomitantly with exposure of the experimental animals to a lethal dose of a fully virulent *Y. pestis* strain. Here, we provided evidence that upon s.c. immunization with a single dose of the EV76 live vaccine strain of *Y. pestis*, the mice acquired a protected state almost instantaneously that conferred high resistance to s.c. infection by a lethal *Y. pestis* strain. This effect was prevalent even when the live vaccine was administered several hours post-infection and was also effective when the mice were infected via pulmonary exposure only 2 days after immunization. Early induction of the protected state could not be attributed to an acquired response, which typically requires a much longer time to manifest (in the current study, a minimal 8-day period was measured for the detection of anti-F1 antibodies). To the best of our knowledge, this was the first time that such an immediate and effective stimulation of a protective response to plague by a live vaccine strain was shown. Furthermore, the effect appeared to be due to a particular ability of the EV76 strain because it could not be replicated by the administration of a commensurate dose of another attenuated *Y. pestis* strain. One may speculate that the specificity of the response could be related to the residual ability of EV76 to replicate and disseminate in the host.

Bacterial dissemination data obtained by IVIS-mediated visualization or by direct quantification of the bacterial load in the organs confirmed that the early innate protective response induced by the EV76 strain resulted in complete blockage of the spread of the virulent strain as well as profound limitation of its proliferation. *Ex vivo* assays showed that mouse sera collected 24 h after EV76 immunization (but not from control mice) exhibited a strong anti-*Y. pestis* growth inhibitory effect that was maximal at 48 h post-immunization and was maintained at least until the development of specific antibodies. To address the mechanistic basis for this early systemic antimicrobial activity induced by

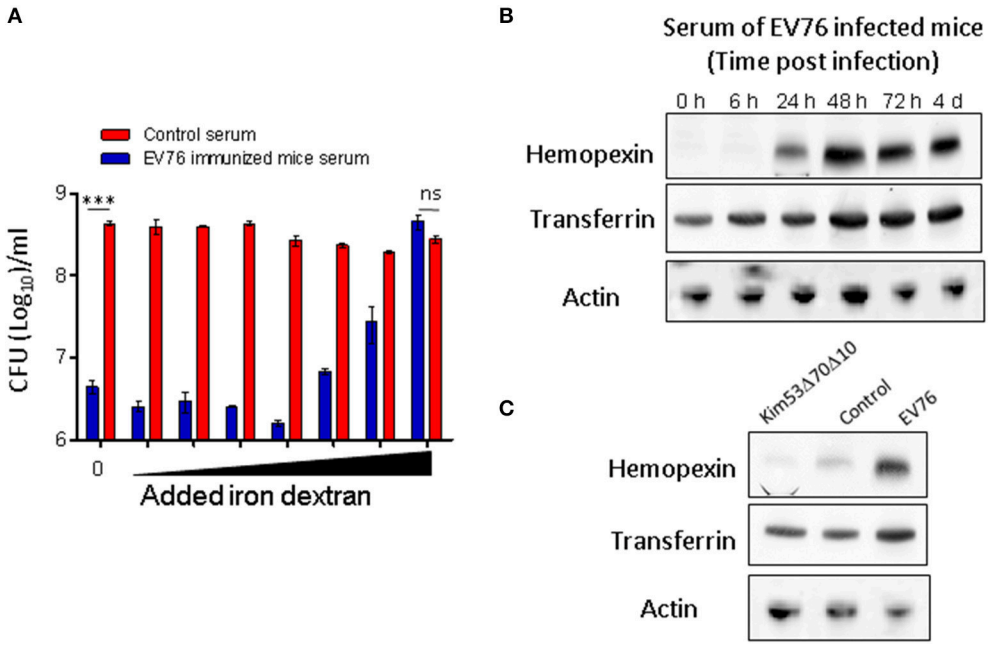

FIGURE 6 | *Y. pestis* growth inhibition by serum collected from EV76-immunized mice is associated with iron deprivation and is induced following EV76 immunization of mice *in vivo*. **(A)** *Y. pestis* incubated in serum (pooled serum samples, $n = 3$) derived from either control mice (red) or EV76–immunized mice (blue) in the presence of increasing amounts of iron (see Materials and Methods). Growth was determined by viable counts. The data depict the mean and SEM. Statistical significance was evaluated using Student's unpaired *t*-test with log-transformed values (***$p < 0.001$ and ns, not significant). **(B)** Pooled sera of mice infected with EV76 at time points from 0 to 4 days post-infection were inspected by Western blot analysis using anti-hemopexin, anti-transferrin or anti-β actin antibodies. **(C)** Pooled sera, collected from mice 24 h post-infection with EV76 or Kim53Δ70Δ10, were examined by Western blot analysis using the indicated antibodies.

the EV76 strain, a protein anion exchange chromatographic fractionation of the sera collected from the immunized mice was implemented, enabling mass spectrometric identification of the two host proteins, hemopexin and transferrin, that co-eluted in the antibacterial active fractions. While both proteins appeared to be associated with the antibacterial activity, transferrin was present in control mice sera, and its level was only moderately increased following immunization with EV76. Hemopexin, in contrast, was barely detected in control mice sera, and its expression level was upregulated dramatically soon after EV76 immunization in strong correlation with the antimicrobial activity observed in the *ex vivo* assays with post-immunization sera.

The data therefore strongly suggested that the protective state induced by immunization could be attributed to the biological activities of the host iron and heme-binding proteins. Maintenance of low levels of free iron is a major host innate defense strategy that limits the growth of infectious bacteria and thus establishes nutritional immunity (Weinberg, 1975; Cassat and Skaar, 2013; Parrow et al., 2013; Elphinstone et al., 2016). Accordingly, pathogens have evolved mechanisms to overcome this limitation to gain access to the host iron supply by expressing siderophores and hemophores, which are able to exploit iron that is trapped by host proteins, such as transferrin and hemopexin (Cornelis, 2010; Cassat and Skaar, 2013; Parrow et al., 2013). In the case of *Y. pestis*, extensive studies have documented that deletion of the pigmentation (*pgm*) locus, which is composed of genes encoding for the siderophore-mediated iron acquisition system and hemin storage, is associated with significant virulence attenuation (Perry and Fetherston, 1997; Carniel, 2001). Notably, the EV76 strain itself owes its significantly attenuated phenotype to the absence of the *pgm* pathogenicity locus.

Transferrin was previously shown to participate in host nutritional immunity, which can prevent the availability of free iron in the organism (Sridhar et al., 2000). Induction of hemopexin in response to systemic infection was thought to protect infected host from heme-induced cell damage (Larsen et al., 2010; Medzhitov et al., 2012). Recently, hemopexin was also shown to limit the availability of heme in the context of an IL-22-induced response to systemic infection by enteropathogens (Sakamoto et al., 2017). Our observation that *Y. pestis* growth inhibition appeared to depend on the presence of transferrin and hemopexin and that these effects could be reversed by elevating the amounts of available iron is in good agreement with these studies. Moreover, while in previous studies, iron limitation was associated with the host response to bacterial challenge; our data indicated that this phenomenon, which may not be effectively activated in the case of plague infection, was exploited for the early manifestation of protection by a live attenuated vaccine.

The sequestration of iron promoted by hemopexin and transferrin could explain the early antibacterial effect induced by immunization with EV76. In fact, exogenously elevating the level of the serum iron-binding protein transferrin was suggested to represent a therapeutic approach to preventing iron acquisition

by pathogens, such as *Staphylococcus aureus*, *Acinetobacter*, *Candida* and *B. anthracis,* consequently improving the survival of the infected host (Rooijakkers et al., 2010; Lin et al., 2014; Bruhn and Spellberg, 2015).

In this study, we showed for the first time that a *Y. pestis* live vaccine brings about a rapid and significant upregulation of the host hemopexin protein. Rapid elevation of hemopexin levels could, in turn, lead to effective heme withdrawal, which, together with preexisting transferrin, limits the availability of iron that is necessary for the growth and dissemination of the virulent strain. This rapid response was followed by the development of additional innate and adoptive immune responses in later stages of the infection. We speculate that the EV76-mediated rapid induction of hemopexin expression involves a bacterial factor that directly or indirectly interacts with host cells after immunization.

The data strongly suggest that the novel EV76-mediated mechanism described in this study may be relevant in the context of other bacterial infections. Yet, at this stage, it is early to speculate on the ability of other live attenuated vaccines to mount similar responses. Studies addressing these issues are currently being conducted in our laboratory.

This study provides the proof of principle for a new concept by which live attenuated vaccines have the potential to induce rapid, broad-range iron nutritional immunity, which could prove beneficial for post-exposure scenarios by enabling the extension of the time window necessary for the development of an acquired specific immune response or by providing additional countermeasures against antibiotic-resistant pathogens.

AUTHOR CONTRIBUTIONS

AZ and EM conceived and designed the study. AZ, YV, AT, MA, DG, YL, and EM conducted the experiments. AZ, EM, SR, and TC analyzed the data. AZ, EM, and TC wrote the paper.

FUNDING

Israel Institute for Biological Research funds, grant number SB-5112-81.

ACKNOWLEDGMENTS

We thank Professor H. Mobley for providing the plasmid used to generate the Kim53-lux derivative. We are deeply grateful to Dr. Mario Lebendiker from the Protein Purification Facility at the Hebrew University of Jerusalem for chromatographic fractionation of the active sera and to Dr. Tevie Mehlman from the Weizmann Institute of Science for the mass spectrometric analysis.

REFERENCES

Ben-Gurion, R., and Shafferman, A. (1981). Essential virulence determinants of different Yersinia species are carried on a common plasmid. *Plasmid* 5, 183–187. doi: 10.1016/0147-619X(81)90019-6

Bertherat, E. G. (2016). Plague around the world. *Wkly. Epidemiol. Rec.* 91, 89–104.

Bruhn, K. W., and Spellberg, B. (2015). Transferrin-mediated iron sequestration as a novel therapy for bacterial and fungal infections. *Curr. Opin. Microbiol.* 27, 57–61. doi: 10.1016/j.mib.2015.07.005

Carniel, E. (2001). The Yersinia high-pathogenicity island: an iron-uptake island. *Microbes Infect.* 3, 561–569. doi: 10.1016/S1286-4579(01)01412-5

Cassat, J. E., and Skaar, E. P. (2013). Iron in infection and immunity. *Cell Host Microbe* 13, 509–519. doi: 10.1016/j.chom.2013.04.010

Cornelis, P. (2010). Iron uptake and metabolism in pseudomonads. *Appl. Microbiol. Biotechnol.* 86, 1637–1645. doi: 10.1007/s00253-010-2550-2

Coward, C., Restif, O., Dybowski, R., Grant, A. J., Maskell, D. J., and Mastroeni, P. (2014). The effects of vaccination and immunity on bacterial infection dynamics *in vivo*. *PLoS Pathog.* 10:e1004359. doi: 10.1371/journal.ppat.1004359

Dentovskaya, S. V., Ivanov, S. A., Kopylov, P., Shaikhutdinova, R. Z., Platonov, M. E., Kombarova, T. I., et al. (2015). Selective protective potency of *Yersinia pestis* DeltanlpD Mutants. *Acta Nat.* 7, 102–108.

Derbise, A., Hanada, Y., Khalife, M., Carniel, E., and Demeure, C. E. (2015). Complete protection against pneumonic and bubonic plague after a single oral vaccination. *PLoS Negl. Trop. Dis.* 9:e0004162. doi: 10.1371/journal.pntd.0004162

Elphinstone, R., Conroy, A., Hawkes, M., Hermann, L., Namasopo, S., Warren, H., et al. (2016). Alterations in systemic extracellular heme and hemopexin are associated with adverse clinical outcomes in ugandan children with severe malaria. *J. Infect. Dis.* 214, 1268–1274. doi: 10.1093/infdis/jiw357

Feodorova, V. A., and Motin, V. L. (2012). Plague vaccines: current developments and future perspectives. *Emerg. Microbes Infect.* 1:e36. doi: 10.1038/emi.2012.34

Feodorova, V. A., Pan'kina, L. N., Savostina, E. P., Sayapina, L. V., Motin, V. L., Dentovskaya, S. V., et al. (2007). A *Yersinia pestis* lpxM-mutant live vaccine induces enhanced immunity against bubonic plague in mice and guinea pigs. *Vaccine* 25, 7620–7628. doi: 10.1016/j.vaccine.2007.08.055

Fetherston, J. D., Schuetze, P., and Perry, R. D. (1992). Loss of the pigmentation phenotype in *Yersinia pestis* is due to the spontaneous deletion of 102 kb of chromosomal DNA which is flanked by a repetitive element. *Mol. Microbiol.* 6, 2693–2704. doi: 10.1111/j.1365-2958.1992.tb01446.x

Flashner, Y., Mamroud, E., Tidhar, A., Ber, R., Aftalion, M., Gur, D., et al. (2004). Generation of *Yersinia pestis* attenuated strains by signature-tagged mutagenesis in search of novel vaccine candidates. *Infect. Immun.* 72, 908–915. doi: 10.1128/IAI.72.2.908-915.2004

Holtzman, Z., Levy, L., Marcus, D., Flashner, Y., Mamroud, E., Cohen, S., et al. (2006). Production and purification of high molecular weight oligomers of *Yersinia pestis* F1 capsular antigen released by high cell density culture of recombinant *Escherichia coli* cells carrying the caf1 operon. *Microb. Cell Factor.* 5(Suppl. 1):P98. doi: 10.1186/1475-2859-5-S1-P98

Inglesby, T. V., Dennis, D. T., Henderson, D. A., Bartlett, J. G., Ascher, M. S., Eitzen, E., et al. (2000). Plague as a biological weapon: medical and public health management. Working Group on Civilian Biodefense. *JAMA* 283, 2281–2290. doi: 10.1001/jama.283.17.2281

Lane, M. C., Alteri, C. J., Smith, S. N., and Mobley, H. L. (2007). Expression of flagella is coincident with uropathogenic *Escherichia coli* ascension to the upper urinary tract. *Proc. Natl. Acad. Sci. U.S.A.* 104, 16669–16674. doi: 10.1073/pnas.0607898104

Larsen, R., Gozzelino, R., Jeney, V., Tokaji, L., Bozza, F. A., Japiassu, A. M., et al. (2010). A central role for free heme in the pathogenesis of severe sepsis. *Sci. Transl. Med.* 2:51ra71. doi: 10.1126/scitranslmed.3001118

Lathem, W. W., Price, P. A., Miller, V. L., and Goldman, W. E. (2007). A plasminogen-activating protease specifically controls the development of primary pneumonic plague. *Science* 315, 509–513. doi: 10.1126/science.1137195

Levy, Y., Flashner, Y., Tidhar, A., Zauberman, A., Aftalion, M., Lazar, S., et al. (2011). T cells play an essential role in anti-F1 mediated rapid protection against bubonic plague. *Vaccine* 29, 6866–6873. doi: 10.1016/j.vaccine.2011.07.059

Levy, Y., Vagima, Y., Tidhar, A., Zauberman, A., Aftalion, M., Gur, D., et al. (2016). Adjunctive corticosteroid treatment against *yersinia pestis* improves bacterial clearance, immunopathology, and survival in the mouse model of bubonic plague. *J. Infect. Dis.* 214, 970–977. doi: 10.1093/infdis/jiw290

Lin, L., Pantapalangkoor, P., Tan, B., Bruhn, K. W., Ho, T., Nielsen, T., et al. (2014). Transferrin iron starvation therapy for lethal bacterial and fungal infections. *J. Infect. Dis.* 210, 254–264. doi: 10.1093/infdis/jiu049

Medzhitov, R., Schneider, D. S., and Soares, M. P. (2012). Disease tolerance as a defense strategy. *Science* 335, 936–941. doi: 10.1126/science.1214935

Minor, P. D. (2015). Live attenuated vaccines: historical successes and current challenges. *Virology* 479–480, 379–392. doi: 10.1016/j.virol.2015.03.032

Parrow, N. L., Fleming, R. E., and Minnick, M. F. (2013). Sequestration and scavenging of iron in infection. *Infect. Immun.* 81, 3503–3514. doi: 10.1128/IAI.00602-13

Perry, R. D., and Fetherston, J. D. (1997). *Yersinia pestis*–etiologic agent of plague. *Clin. Microbiol. Rev.* 10, 35–66.

Rooijakkers, S. H., Rasmussen, S. L., McGillivray, S. M., Bartnikas, T. B., Mason, A. B., Friedlander, A. M., et al. (2010). Human transferrin confers serum resistance against *Bacillus anthracis*. *J. Biol. Chem.* 285, 27609–27613. doi: 10.1074/jbc.M110.154930

Sakamoto, K., Kim, Y. G., Hara, H., Kamada, N., Caballero-Flores, G., Tolosano, E., et al. (2017). IL-22 controls iron-dependent nutritional immunity against systemic bacterial infections. *Sci. Immunol.* 2:eaai8371. doi: 10.1126/sciimmunol.aai8371

Sebbane, F., Jarrett, C. O., Gardner, D., Long, D., and Hinnebusch, B. J. (2006). Role of the *Yersinia pestis* plasminogen activator in the incidence of distinct septicemic and bubonic forms of flea-borne plague. *Proc. Natl. Acad. Sci. U.S.A.* 103, 5526–5530. doi: 10.1073/pnas.0509544103

Sridhar, S., Ahluwalia, M., Brummer, E., and Stevens, D. A. (2000). Characterization of an anticryptococcal protein isolated from human serum. *Infect. Immun.* 68, 3787–3791. doi: 10.1128/IAI.68.6.3787-3791.2000

Tidhar, A., Flashner, Y., Cohen, S., Levi, Y., Zauberman, A., Gur, D., et al. (2009). The NlpD lipoprotein is a novel *Yersinia pestis* virulence factor essential for the development of plague. *PLoS ONE* 4:e7023. doi: 10.1371/journal.pone.0007023

Tiner, B. L., Sha, J., Cong, Y., Kirtley, M. L., Andersson, J. A., and Chopra, A. K. (2016). Immunisation of two rodent species with new live-attenuated mutants of *Yersinia pestis* CO92 induces protective long-term humoral- and cell-mediated immunity against pneumonic plague. *npj Vaccines* 1:16020. doi: 10.1038/npjvaccines.2016.20

Titball, R. W., and Williamson, E. D. (2004). *Yersinia pestis* (plague) vaccines. *Expert Opin. Biol. Ther.* 4, 965–973. doi: 10.1517/14712598.4.6.965

Vagima, Y., Zauberman, A., Levy, Y., Gur, D., Tidhar, A., Aftalion, M., et al. (2015). Circumventing *Y. pestis* virulence by early recruitment of neutrophils to the lungs during pneumonic plague. *PLoS Pathog* 11:e1004893. doi: 10.1371/journal.ppat.1004893

Verma, S. K., and Tuteja, U. (2016). Plague vaccine development: current research and future trends. *Front. Immunol.* 7:602. doi: 10.3389/fimmu.2016.00602

Walker, D. L., Foster, L. E., Chen, T. H., Larson, A., and Meyer, K. F. (1953). Studies on immunization against plague. V. Multiplication and persistence of virulent and avirulent Pasteurella pestis in mice and guinea pigs. *J. Immunol.* 70, 245–252.

Weinberg, E. D. (1975). Nutritional immunity. Host's attempt to withold iron from microbial invaders. *JAMA* 231, 39–41. doi: 10.1001/jama.1975.03240130021018

Zauberman, A., Flashner, Y., Levy, Y., Vagima, Y., Tidhar, A., Cohen, O., et al. (2013). YopP-expressing variant of *Y. pestis* activates a potent innate immune response affording cross-protection against yersiniosis and tularemia [corrected]. *PLoS ONE* 8:e83560. doi: 10.1371/journal.pone.0083560

Zauberman, A., Tidhar, A., Levy, Y., Bar-Haim, E., Halperin, G., Flashner, Y., et al. (2009). *Yersinia pestis* endowed with increased cytotoxicity is avirulent in a bubonic plague model and induces rapid protection against pneumonic plague. *PLoS ONE* 4:e5938. doi: 10.1371/journal.pone.0005938

Conflict of Interest Statement: The authors declare that the research was conducted in the absence of any commercial or financial relationships that could be construed as a potential conflict of interest.

frontiers in Cellular and Infection Microbiology

ORIGINAL RESEARCH
published: 08 August 2017
doi: 10.3389/fcimb.2017.00361

Secreted Citrate Serves as Iron Carrier for the Marine Pathogen *Photobacterium damselae* subsp *damselae*

*Miguel Balado[1], Beatriz Puentes[1], Lucía Couceiro[1], Juan C. Fuentes-Monteverde[2], Jaime Rodríguez[2], Carlos R. Osorio[1], Carlos Jiménez[2] and Manuel L. Lemos[1]**

[1] Department of Microbiology and Parasitology, Institute of Aquaculture, University of Santiago de Compostela, Santiago de Compostela, Spain, [2] Department of Chemistry, Faculty of Sciences and Center for Advanced Scientific Research (CICA), University of A Coruña, A Coruña, Spain

Photobacterium damselae subsp *damselae* (*Pdd*) is a *Vibrionaceae* that has a wide pathogenic potential against many marine animals and also against humans. Some strains of this bacterium acquire iron through the siderophore vibrioferrin. However, there are virulent strains that do not produce vibrioferrin, but they still give a strong positive reaction in the CAS test for siderophore production. In an *in silico* search on the genome sequences of this type of strains we could not find any ORF which could be related to a siderophore system. To identify genes that could encode a siderophore-mediated iron acquisition system we used a mini-Tn*10* transposon random mutagenesis approach. From more than 1,400 mutants examined, we could isolate a mutant (BP53) that showed a strong CAS reaction independently of the iron levels of the medium. In this mutant the transposon was inserted into the *idh* gene, which encodes an isocitrate dehydrogenase that participates in the tricarboxylic acid cycle. The mutant did not show any growth impairment in rich or minimal media, but it accumulated a noticeable amount of citrate (around 7 mM) in the culture medium, irrespective of the iron levels. The parental strain accumulated citrate, but in an iron-regulated fashion, being citrate levels 5–6 times higher under iron restricted conditions. In addition, a null mutant deficient in citrate synthase showed an impairment for growth at high concentrations of iron chelators, and showed almost no reaction in the CAS test. Chemical analysis by liquid chromatography of the iron-restricted culture supernatants resulted in a CAS-positive fraction with biological activity as siderophore. HPLC purification of that fraction yielded a pure compound which was identified as citrate from its MS and NMR spectral data. Although the production of another citrate-based compound with siderophore activity cannot be ruled out, our results suggest that *Pdd* secretes endogenous citrate and use it for iron scavenging from the cell environment.

Keywords: *Photobacterium damselae*, citrate, iron uptake, siderophores, vibrioferrin

OPEN ACCESS

Edited by:
Pierre Cornelis,
Vrije Universiteit Brussel, Belgium

Reviewed by:
Iain Lamont,
University of Otago, New Zealand
Paul Edward Carlson,
United States Food and Drug Administration, United States

****Correspondence:***
Manuel L. Lemos
manuel.lemos@usc.es

Received: *31 May 2017*
Accepted: *26 July 2017*
Published: *08 August 2017*

Citation:
Balado M, Puentes B, Couceiro L, Fuentes-Monteverde JC, Rodríguez J, Osorio CR, Jiménez C and Lemos ML (2017) Secreted Citrate Serves as Iron Carrier for the Marine Pathogen Photobacterium damselae subsp damselae. Front. Cell. Infect. Microbiol. 7:361. doi: 10.3389/fcimb.2017.00361

INTRODUCTION

Iron restriction is an important host defense strategy, thus successful pathogens must possess mechanisms to acquire iron from host sources in order to cause disease. Although there are several strategies for iron acquisition, heme uptake and siderophore-based systems are certainly two of the most widespread among pathogenic bacteria and the most relevant to virulence (Hider and Kong, 2010; Cassat and Skaar, 2013; Saha et al., 2013; Ellermann and Arthur, 2017).

Photobacterium damselae is a member of *Vibrionaceae* that has been divided in two different subspecies: subsp. *damselae* (hereafter *Pdd*) and subsp. *piscicida* (*Pdp*). *Pdd* is an autochthonous marine bacterium resident in both natural and fish farms ecosystems that can behave as an opportunistic pathogen for fish and mammals (Labella et al., 2017). It is also a primary emerging pathogen causing haemorraghic septicemia in a variety of marine species including wild and cultured fish, sharks, crustaceans and marine mammals. In addition, *Pdd* can cause infections in humans due to exposure to marine fish, seawater or raw seafood (Rivas et al., 2013). In some of the reported human cases, the infection progressed into a severe necrotizing fasciitis leading to a fatal outcome (Yamane et al., 2004). In this bacterium it was demonstrated a positive correlation between iron availability in host fluids and degree of virulence (Fouz et al., 1997). Previous works proved that all *Pdd* strains are capable of utilizing hemoglobin and ferric ammonium citrate as the sole iron sources and that they also have the ability to produce siderophores (Fouz et al., 1994, 1997). It was postulated that the siderophore produced by *Pdd* could be a hydroxamate type different from aerobactin and desferal (Fouz et al., 1997), but the precise nature of the siderophores produced was not elucidated up to date.

In previous works, we described the presence of a functional heme uptake system in *Pdd* (Rio et al., 2005), but at present nothing is known about the siderophore-based systems used by *Pdd* to get iron from its hosts. In a recent work about *Pdd* proteome variations under diverse iron conditions (Puentes et al., 2017), we showed that some *Pdd* strains are likely able to produce the siderophore vibrioferrin, that was firstly described as the main siderophore of *Vibrio parahaemolyticus* and *V. alginolyticus* (Yamamoto et al., 1994). We showed that some *Pdd* strains express proteins with high similarity to the main proteins involved in the biosynthesis and transport of vibrioferrin in these vibrios (Puentes et al., 2017). However, many other pathogenic *Pdd* strains, including the reference strain CIP 102761 (ATCC 33539), do not express those proteins and lack the gene clusters involved in vibrioferrin production, but they still display a CAS reactivity, suggesting the existence of an alternative siderophore in these strains.

In this work we show that most pathogenic strains of *Pdd* secrete endogenous citrate and use it for iron scavenging from the cell environment.

MATERIALS AND METHODS

Strains, Media, and Reagents

Pdd strains were routinely grown at 25°C on Tryptone Soy Broth or Agar (Cultimed) supplemented with 1% NaCl (TSB-1 or TSA-1 respectively). Differential iron availability conditions were achieved by adding to CM9 minimal medium (Lemos et al., 1988) final concentrations of 10 μM $Fe_2(SO_4)_3$ (high iron conditions), or different concentrations of the non-assimilable and non-toxic iron chelator 2,2′-dipyridyl (TCI): 40 μM to get low iron conditions or 75 μM for very low iron conditions. The addition of 2,2′-dipyridyl to culture media mimics the low iron conditions found in the host environment. Strains and plasmids used are listed in **Table 1**.

Growth under Iron Limiting Conditions and Test of Siderophore Production

To test the ability of *Pdd* strains to grow under iron limiting conditions, overnight cultures in LB were adjusted to an OD_{600} of 0.5 and diluted 1:100 in CM9 minimal medium containing the iron chelator 2,2′-dipyridyl at 40 or 75 μM. 2,2′-dipyridyl (TCI) was dissolved in distilled water to prepare a stock solution at 20 mM that was added to the sterile media at appropriated concentrations. When required, ferric-ammonium citrate (Panreac) was added to CM9 medium at 10 μM final concentration. Cultures were incubated at 25°C with shaking at 150 rpm, and OD_{600} was measured after 12 h of incubation. Siderophore production was measured using the colorimetric liquid assay of the Chrome-Azurol-S (CAS) dye, as previously described (Schwyn and Neilands, 1987; Balado et al., 2015, 2017b). For CAS-reactivity assays, strains were grown at 40 μM 2,2′-dipyridyl to allow enough growth to make iron-chelating

TABLE 1 | Strains and plasmids used in this work.

Strain or plasmid	Description	References/ source
STRAIN		
Photobacterium damselae* subsp. *damselae		
RM71	Isolated from turbot (see **Table 3**)	Laboratory stock
RM71-rif	RM71 derivative, spontaneous rifampin-resistant mutant; Rif^r	Rivas et al., 2011
BP53	RM71 with mini-Tn*10* disrupting *idh* gene	This study
RM71Δ*gltA*	RM71 with in-frame deletion of *gltA* gene	This study
RG91	Isolated from turbot (see **Table 3**)	Laboratory stock
RG91Δ*pvsD*	RG91 with in-frame deletion of *pvsD* gene	Laboratory stock
E. coli		
DH5α	Cloning strain	Laboratory stock
S17-1 *λpir*	RP4 (Km::Tn7, Tc::Mu-1) *pro-82 λpir recA1 endA1 thiE1 hsdR17 creC510*	Herrero et al., 1990
Plasmids		
pLOFKm	Tn*10*-based delivery plasmid; Km^r	Herrero et al., 1990
pKNG101	Suicide vector; St^r	Kaniga et al., 1991
pUC118	High-copy-number cloning vector; Ap^r	Vieira and Messing, 1987

activity detectable. A non-inoculated CM9 sample with the same 2,2′-dipyridyl concentration was used as spectrophotometric blank and as negative control for CAS liquid assays. Growth curves and CAS assays were carried out in triplicate, and results shown are the means of three independent experiments.

Cross-Feeding Assays

Bioassays were designed to detect the production of vibrioferrin and to detect the production of other iron-chelating molecules. To detect vibrioferrin synthesis we used a mutant (AR13) of *Vibrio alginolyticus* deficient in *pvsA*, a gene involved in the synthesis of this siderophore (Osorio et al., 2015). For the detection of biological active supernatants we used strain RM71. The indicator strains were inoculated into CM9 plates containing the iron chelator 2,2′-dipyridyl at 100 μM, a concentration at which they are unable to growth. Strains to be tested were cultured on LB agar plates, cells were harvested with a sterile loop, placed on top of the indicator strain plates and incubated at 25°C for 48 h. The results were scored as positive when a growth halo of the indicator strains was visible around cells. A disc containing 10 μl of a solution of $Fe_2(SO_4)_3$ 10 mM was used as positive growth control.

DNA Purification and Analysis and PCR

Total genomic DNA from *Pdd* was purified with the Easy–DNA kit (Invitrogen). Plasmid DNA purification and extraction of DNA from agarose gels were carried out using kits from Fermentas (Thermo–Fisher). PCR reactions were routinely carried out in a T–Gradient Thermal Cycler (Biometra), with *Taq* polymerase KAPA Taq (Kapa Biosystems). Since all *Pdd* strains with genomic sequences available lack vibrioferrin genes, detection of *pvsD* gene by PCR was performed using degenerated oligonucleotides (**Table 2**) designed from conserved *pvsD* sequences from several *Vibrio* species aligned with the *ClustalW Multiple Alignment* tool of BioEdit program (http://www.mbio.ncsu.edu/BioEdit/bioedit.html). The choosen sequences were those of *pvsD* from *V. parahaemolyticus* (accession No: AB082123.1; GI: 23307114), *V. alginolyticus* (accession No: DQ201184.2; GI: 120564760), *V. splendidus* (accession No: NC_011744.2; GI: 294510242), *V. caribbenthicus* (accession No: EFP94847.1; GI: 309367283) and *V. harveyi* (accession No: EMR36193.1; GI: 471343428).

TABLE 2 | Oligonucleotides used in this work for mutant construction and detection of *pvsD* gene by PCR.

Oligonucleotide	Sequences (5′–>3′)
***gltA* mutant construction**	
gltA-ISA-1	CCCCTGCAGGTCGACGGATCGAGCTTCTGTTTGAGCCAGC
gltA-ISA-2	ACATGAGAACCAAGGAGAATAGATTCACATGAGGCAGTAG
gltA-ISA-3	AGTACCTAGCCAAGGTGTGCGATCAACGTGAGTTTAGTCC
gltA-ISA-4	ACTTATGGTACCCGGGGATCTGAGTATAGCCGTCTGCAAG
Degenerated primers for RG91 *pvsD* amplification	
pvsD_deg_F	CCCTTGYCAYCCTTGGGAAA
pvsD_deg_R	GAATCCADACRCARCABGGC
***Photobacterium damselae pvsD* PCR screening**	
pvsD-damsela_Fw	GCTTCACTGATGTTGTTGAT
pvsD-damsela_Rv	CGAGCAAAAAGAAGATCTGA

Mutagenesis by Mini-Tn*10* Transposon

A mini-Tn*10* insertion library was constructed in *Pdd* strain RM71 using the conjugative suicide plasmid pLOF/Km, carrying a mini-Tn*10* transposon with an isopropyl-beta-D-thiogalactopyranoside (IPTG)-inducible transposase located outside the mobile element, and a kanamycin-resistant gene flanked by transposable elements (Herrero et al., 1990; Rivas et al., 2015). Conjugation of pLOF/Km into *Pdd* RM71 was achieved my mixing equal amounts of the *E. coli* S17(pLOF/Km) (previously cultured in LB at 37°C for 5 h) and RM71-Rif (rifampicin-resistant) (cultured in TSB-1 at 25°C for 12 h). One mL of the mixture plus 10 μL IPTG was deposited in Marine Agar (Difco) plates and incubated at 25°C for 72 h. Appropriate dilutions of the growing cells were then plated on LB agar containing kanamycin (50 μg/mL) and rifampicin (50 μg/mL) and incubated at 25°C for 48 h to select for *Pdd* transformants. An Km^R Rif^R clone was considered a mini-Tn*10* insertion mutant. Growth and CAS-reactivity for each mutant was tested in 96-wells microtiter plates containing 100 μL of CM9 with 25 μM 2,2′-dipyridyl. Sequencing of DNA fragments flanking transposon sequences in the clones with expected phenotypes was achieved by partial digestion of genomic DNA with restriction enzyme *Bfu*CI (New England Biolabs) for 35 s. The restriction products were ligated into plasmid pUC118 previously treated with *BamH*I and alkaline phosphatase. The ligation products were transformed into *E. coli* DH5α, and clones were selected in LB with Km 50 μg/mL. pUC118-cloned inserts containing the kanamycin resistance gene of mini-Tn*10* plus flanking chromosomal DNA were purified using the GeneJET Plasmid Miniprep Kit (Thermo Fisher Scientific) and finally sequenced using a primer targeted to the extreme of the kanamycin cassette (TCCAGTTTACTT TGCAGGGC). DNA sequences were obtained using a capillary DNA Sequencer ABI 3730xl (Applied Biosystems), and then analyzed by BLAST (Altschul et al., 1990) to identify the insertion points.

Allelic Exchange Mutagenesis

In-frame deletion of *gltA* gene in *Pdd* RM71 was constructed by allelic exchange using the nucleotide sequence of locus A0J47_03095, protein with accession No. ODA26781.1, from *Pdd* RM71 genome sequence. PCR amplifications of two fragments of the gene and flanking regions, when ligated together result in an in–frame (nonpolar) deletion. Primers used are listed in **Table 2**. The construction was ligated into the suicide vector pKNG101 (Kaniga et al., 1991). The resulting plasmids were mated from *E. coli* S17-1-λ*pir* (Herrero et al., 1990) into *Pdd* RM71 wild type strain (Rif^R) and exconjugants with the plasmid ($Streptomycin^R$) integrated in the chromosome by homologous recombination were selected. A second recombination event was obtained by selecting for sucrose (15%) resistance and further checking for plasmid loss and for allelic exchange, generating the mutant RM71Δ*gltA*. Deletion of the parental gene was checked by DNA

sequencing of the region involved to ensure that mutation was in-frame.

Citrate Quantification

Bacterial cultures under high- and low-iron conditions in early exponential growth (OD_{600} = 0.6) were centrifuged (5 min at 8,000 × g) and filtered through 0.22 μm pore size to obtain a cell-free supernatant. The citrate concentration in these supernatants was measured using a colorimetric Citrate Assay Kit (Sigma-Aldrich) according to the manufacturer protocol. To remove oxaloacetate and pyruvate background a blank sample was included for each sample, omitting the Citrate Enzyme Mix provided by the kit, according to the manufacturer instructions. The citrate concentration standard curve was made with increasing concentrations (ranging from 0.1 to 12.5 mM) of sodium citrate (Merck) in CM9 medium. Concentrations of citrate lower than 0.1 mM gave reactions that were indistinguishable from CM9 alone. Three biological replicates were measured in duplicate.

Isolation and Identification of Citrate from Culture Supernatants

Pdd strain RM71 was cultured in CM9 minimal medium supplemented with 35 μM 2,2′-dipyridyl. Cultures were carried out in 2 L Erlenmeyer flasks containing 1 L of medium. These flasks were inoculated with 20 mL of a fresh culture in TSB-1. Flasks were incubated during 24 h at 25°C with continuous shaking at 190 rpm. After incubation, bacterial cells were pelleted by centrifugation at 10,000 rpm in a Beckman J-21 high speed centrifuge. The supernatant was filtered through a continuous filtration cartridge with a 0.45 μm pore size membrane (Millipore) to remove any cell and organic debris from the supernatant. Siderophore activity present was evaluated by the CAS method as above. Equal volumes of supernatants and CAS solution were mixed and the absorbance at 630 nm was measured in a spectrophotometer after 20 min. Siderophore activity of fractions and purified compounds were monitored by bioassays as described above.

A 6-L batch of centrifuged cell-free culture broth was divided into five portions which were loaded onto a XAD-4 resin (Radius Column: 2.8 cm, resin mass: 120 g). After washing with distilled water (1.3 L) with a flow rate of 0.8 mL/min, the resin was eluted with a methanol/water (1:1) mixture followed by methanol. The siderophore and CAS activities remained in the fraction eluted with water which was then lyophilized to give 86.2 g of a solid. This solid was washed with MeOH (4 times × 290 mL) to yield, after removal of the solvent, 54.53 g of a siderophore/CAS active non-methanol-soluble white solid. The material was dissolved in H_2O and chromatographed on a Sephadex LH-20 column which was eluted with a 9:1 mixture of H_2O in MeOH at a flow rate of 1.8 mL/min. The collected fractions were submitted to CAS assay and the fractions of interest were concentrated under vacuum to afford a CAS-positive fraction (37.6 g). Part of that fraction (21.0 g) was divided in three batches and chromatographed on a Sephadex® G-25 Fine column which was eluted with 760 mL of H_2O using a flow rate of 4.5 mL/min. The eluted fractions were submitted to CAS assay and a chloride test for the presence of salts. Fractions displaying an intense color change with the CAS reagent and with a relatively low amount of salts were pooled and lyophilized. The lyophilized material (400 mg) was dissolved in H_2O and chromatographed on a Sephadex® G-10 column using H_2O (87 mL) as eluent at a flow rate of 1.6 mL/min. Again, the eluted fractions were submitted to the same tests as before to afford 53.5 mg of a salt-free and CAS–positive fraction. Final purification of this fraction was achieved by HPLC using a Discovery® HS F5 (100 × 4.6 mm, 5 μm) column with a mobile phase consisting of an isocratic mixture of 0.3% of CH_3CN in H_2O (each containing 0.1% HCO_2H) for 1.4 min and then, a gradient from 0.3 to 6.0% of CH_3CN in H_2O (each containing 0.1% HCO_2H) over 15.8 min at a flow rate of 1.2 mL/min. The CAS-positive fractions, eluted with a retention time of 2.98 min, were pooled and concentrated *in vacuo* to provide 2.1 mg of compound **1** which was identified as citrate by its ^{1}H NMR and (–)-ESIMS data. *Compound* **1**: ^{1}H NMR (500 MHz in D_2O) δ (ppm): 3.00 (2H, d, J = 15.7, 2H, 2-H), 2.84 (2H, d, J =15.7, 2H, 4-H); (–)-ESIMS m/z 191 $[M - H]^-$.

RESULTS

In order to identify the siderophore system in *Pdd*, two strategies were used simultaneously: (1) identification of genes that could be related to siderophore biosynthesis and uptake by screening a transposon-generated mutant collection; and (2) isolation of compounds with siderophore activity by HPLC fractionation of iron-deprived cell-free supernatants and further chemical characterization of the fractions that retained the biological activity.

Only Some *Pdd* Strains Harbor Vibrioferrin Biosynthetic Genes

In previous works we have shown that some strains of *Pdd*, when cultured under iron limitation, express several proteins likely involved in the synthesis of the siderophore vibrioferrin (Puentes et al., 2017). In order to confirm the presence of vibrioferrin related genes, we checked by PCR the presence of *pvsD*, one of the main genes involved in the biosynthesis of this siderophore in other vibrios (Tanabe et al., 2003; Wang et al., 2007), in a collection of *Pdd* strains. The results are shown in **Table 3**. Some strains isolated from different hosts and different origins harbor the *pvsD* gene and give a strong reaction in the CAS test. Vibrioferrin production by these strains was assessed by a growth promotion bioassay using the *V. alginolyticus* AR13 mutant defective in vibrioferrin biosynthesis (Osorio et al., 2015). However, as seen in **Table 3**, there are many other virulent strains from different origins that clearly lack *pvsD* and do not produce vibrioferrin, but they still give a positive reaction in the CAS test for siderophore production, although with lower intensity.

Search of Candidate Genes Encoding a Siderophore System in Vibrioferrin-Negative Strains

Pdd RM71 strain was chosen to decipher the putative siderophore-based iron uptake system present in *Pdd* strains lacking vibrioferrin system. This strain has been widely used

TABLE 3 | Results of the PCR assays to detect the presence of *pvsD* and results of the CAS test and bioassays to detect vibrioferrin production in a collection of *Pdd* strains.

Strain	Origin	Host	Presence of *pvsD*	CAS test[a]	Vibrioferrin Production[b]
ATCC33539	USA	Damselfish (*Chromis punctipinnis*)	−	+	−
RG91	Spain	Turbot (*Psetta maxima*)	+	++	+
LD-07	Spain	Gilthead seabream (*Sparus aurata*)	−	+	−
RM71	Spain	Turbot (*Psetta maxima*)	−	+	−
RG214	Spain	Turbot (*Psetta maxima*)	+	++	+
CDC2227-81	USA	Human	−	+	−
ATCC35083	USA	Shark (*Carcharhinus plumbeus*)	−	+	−
ACR208.1	Spain	Turbot (*Psetta maxima*)	+	++	+
ACRp-72.1	Spain	Turbot (*Psetta maxima*)	−	+	−
TW294 L2	Spain	Seabass (*Dicentrarchus labrax*)	−	+	−
TW250/03	Spain	Gilthead seabream (*Sparus aurata*)	−	+	−
J3G-801	Taiwan	Shrimp (*Penaeus monodon*)	−	+	−
238	USA	Dolphin (*Tursiops truncatus*)	−	+	−
158	Belgium	Eel (*Anguilla anguilla*)	−	+	−
RG153	Spain	Turbot (*Psetta maxima*)	+	++	+
309	Spain	Mussel (*Mytilus edulis*)	−	+	−
PG-801	Taiwan	Shrimp (*Penaeus monodon*)	−	+	−
430	Spain	Seawater	−	+	−
H22060601R	Spain	Redbanded seabream (*Pagrus auriga*)	+	++	+
D20040408U	Spain	Gilthead seabream (*Sparus aurata*)	−	+	−
H011004020	Spain	Redbanded seabream (*Pagrus auriga*)	−	+	−
LB07070501R	Spain	Seabass (*Dicentrarchus labrax*)	−	+	−
S04070503C	Spain	Sargo (*Diplodus sargus*)	−	+	−
LCA24907	Spain	Barramundi perch (*Lates calcarifer*)	−	+	−
9FT1M-3	USA	Shark (*Carcharhinus* sp.)	−	+	−
RS80L1V1	USA	Red snapper (*Lutjanus campechanus*)	−	+	−
ST-1	USA	Trout	−	+	−
RS78SPL1	USA	Red snapper (*Lutjanus campechanus*)	−	+	−
9FT2B-2	USA	Shark (*Carcharhinus* sp.)	+	+	+

[a] *Reaction in CAS liquid test after growth in CM9 plus 40 μM 2,2′-dypiridyl; +, $A_{630} < -0.6$; ++, A_{630} ranging from −0.6 to −0.8.*
[b] *Detected by growth promotion of Vibrio alginolyticus AR13 (Osorio et al., 2015).*

in previous works of our research group to characterize diverse virulence factors (Rivas et al., 2011). To try to find candidate genes that could encode a siderophore-mediated iron acquisition system, we performed an *in silico* search on the genome sequence of strain RM71 (GenBank accession No. NZ_LYBT01000000) and on the reference genome from strain CIP 102761 (GenBank accession No. NZ_ADBS00000000). After this search, we were unable to find any ORF which could be potentially involved in siderophore synthesis or transport according to its homology to other siderophore-related genes.

Since *in silico* search gave negative results we performed a random mutagenesis approach in strain RM71, using the mini-Tn*10* transposon, to isolate mutants with siderophore production inactivated or altered. Essentially, we sought mutants that, compared to parental strain, showed a growth deficiency or a negative CAS reaction when they were grown under iron deficiency conditions. We also looked at potentially deregulated mutants that were positive in CAS assay under iron excess conditions. Any of these phenotypes could be indicative of inactivation of a component of a siderophore-mediated iron uptake system.

From a total of 1,400 mutants screened with the above phenotypic criteria we could found one mutant (BP53) that showed a strong CAS-positive reaction under both iron-deprivation and iron-excess conditions, which suggested an overproduction of iron-chelating compounds (**Figure 1**). Since the transposon library coverage was low (ca. 37%) we cannot discard the existence of other genes involved in iron uptake. Nucleotide sequence analysis revealed that mutant BP53 had the transposon inserted into *idh* gene (acc. No. ODA21722.1). This gene (named *icg* in *Vibrio cholerae*) encodes a NADP-dependent isocitrate dehydrogenase that participates in the tricarboxylic acid (TCA) cycle and convert D-isocitrate to 2-oxoglutarate with the production of one molecule of CO_2. Inactivation of *icg* in *V. cholerae* and other bacteria results in an accumulation of large amounts of citrate and a slight growth impairment compared to its parental strain, especially during

the late exponential phase of growth (Lakshmi and Helling, 1976; Minato et al., 2013). However, it is noticeable that BP53 did not show any growth defect in TSA-1 or CM9 media under high, low or very low iron (see methods) conditions (**Figure 2**). Furthermore, a significant citrate accumulation in the supernatant (ranging from 6 to 8 mM) could be detected (**Figure 3**). Based in these findings we could hypothesize that BP53 mutant secretes endogenous citrate to the extracellular medium and that the CAS-positive reaction observed could be caused by citrate accumulation.

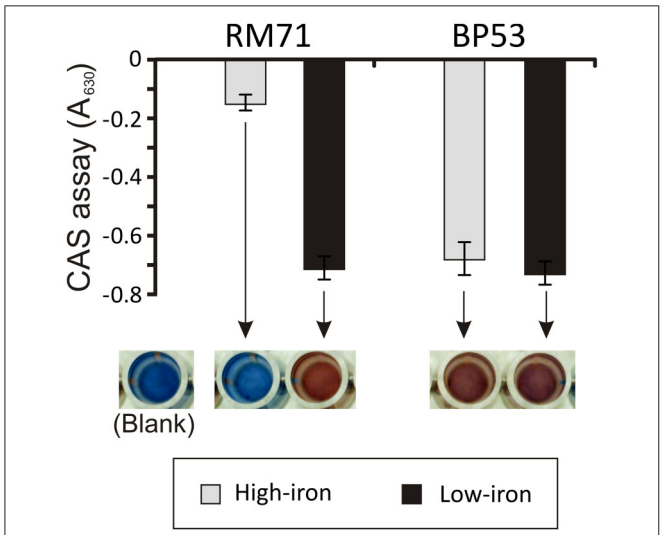

FIGURE 1 | CAS assay of cell-free supernatants obtained from RM71 and BP53 mutant cultures at OD_{600} = 0.6 under high- and low-iron conditions. Each bar represents mean values from three replicates. Error bars indicate standard deviations. Color pictures show wells from a microtiter plate with representative CAS test results.

Extracellular Citrate Accumulation by *Pdd* Strains

To confirm presence of citrate in culture media of *Pdd* strains we measured citrate levels under different culture conditions using a colorimetric citrate assay kit. We showed that RM71 produces noticeable levels of citrate, around 5.5 mM, when cultured in

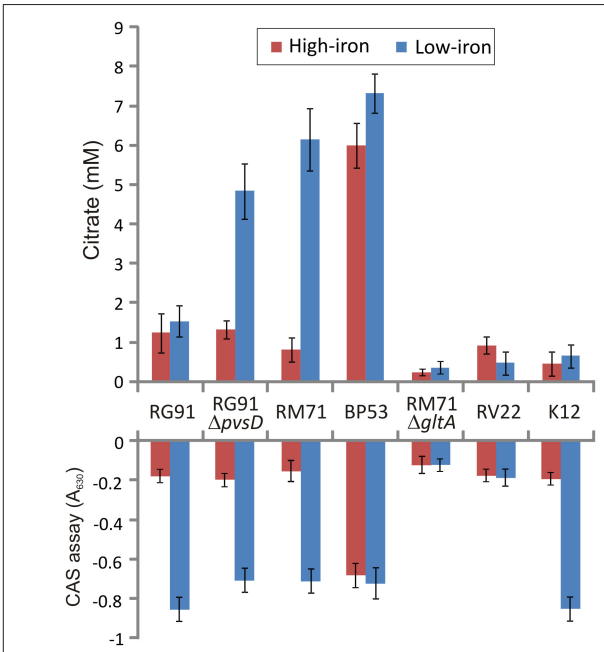

FIGURE 3 | Extracelular citrate accumulation and CAS reactivity in cell free supernatants after growing *Pdd* strains under iron-excess or iron-deficient conditions. *Vibrio anguillarum* RV22 and *E. coli* K12 were used as controls. CAS reactivity of *E. coli* K12 is due to enterobactin production. Each bar represents mean values from three replicates. Error bars indicate standard deviations.

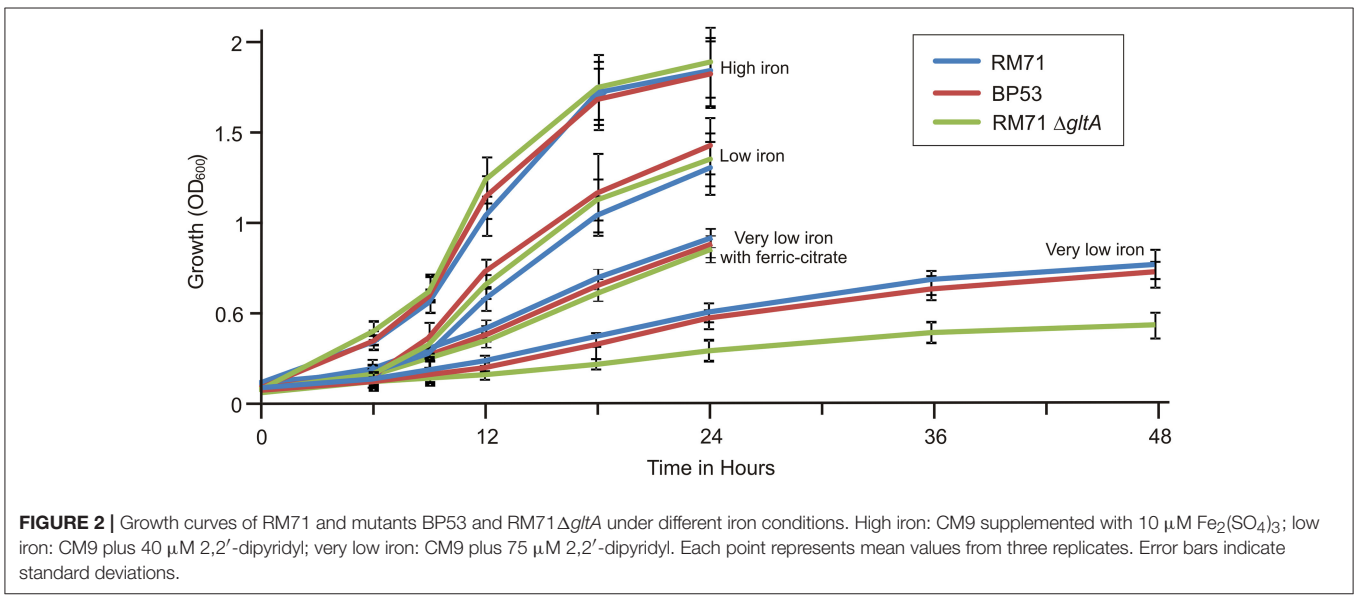

FIGURE 2 | Growth curves of RM71 and mutants BP53 and RM71Δ*gltA* under different iron conditions. High iron: CM9 supplemented with 10 μM $Fe_2(SO_4)_3$; low iron: CM9 plus 40 μM 2,2′-dipyridyl; very low iron: CM9 plus 75 μM 2,2′-dipyridyl. Each point represents mean values from three replicates. Error bars indicate standard deviations.

CM9 plus 40 μM 2,2′-dipyridyl, but under iron excess conditions the levels of extracellular citrate were under 1 mM (**Figure 3**). As CM9 does not include citrate in its formulation, the citrate present in the cell-free spent medium must come from bacterial cells synthesis. As comparative purposes we used *E. coli* K12 and *Vibrio anguillarum* RV22. The citrate amount present in these controls ranged from 0.8 to 1.3 mM and did not show any significant variation with iron availability. These data are in agreement with extracellular citrate amounts described for *E. coli* (Bennett et al., 2009). Thus, under iron-excess conditions the citrate amount found in RM71 supernatant (ca. 0.9 mM) is equivalent to the amount found in *E. coli* or *V. anguillarum*. Instead, citrate levels of RM71 increased 4- to 6-fold under low iron conditions. Hence, low levels of iron in the cell environment seem to trigger citrate synthesis and secretion in *Pdd* strains lacking the vibrioferrin system.

Interestingly, when citrate accumulation was measured in a vibrioferrrin-producing strain (strain RG91, see **Table 3**), the citrate levels were 5- to 6-fold lower (ca. 1.5 mM) and independent of the iron levels of the medium (**Figure 3**). This observation could be explained by the hypothesis that if cells get enough iron through the likely much more efficient vibrioferrin system, citrate levels are kept in the minimal amounts needed for TCA cycle functionality. Only when a high affinity siderophore is not present, citrate would be synthesized at high levels to act as iron carrier for the cell. To confirm this hypothesis extracellular citrate levels were measured in a vibrioferrin-deficient mutant of RG91 lacking *pvsD* (RG91Δ*pvsD*). The results showed that in this mutant citrate accumulation reached the levels of strain RM71 and were also iron-dependent. In this mutant, the CAS-reactivity levels were also equivalent to those of RM71. Further evaluation of citrate accumulation in the supernatants of other *Pdd* strains, including vibrioferrin-producing and non-producing strains (**Table 3**), showed that the described behavior for each type of strain is not restricted to RG91or RM71 strains, but it seems a common feature in *Pdd* strains (**Figure 4**): citrate accumulates extracellularly only when vibrioferrin is not produced. All this suggests that citrate is being secreted by *Pdd* strains to the medium in high amounts when no other siderophore-based iron acquisition system is available.

To further confirm that citrate is involved in iron uptake in *Pdd*, a mutant lacking citrate synthase (GltA) was constructed in strain RM71 (RM71Δ*gltA*) and its phenotype was compared with parental strain RM71 and mutant BP53 (deficient in isocitrate deshidrogenase). All three strains showed identical growth curves under high iron conditions (**Figure 2**). When CM9 contained 40 μM 2,2′-dipyridyl (low-iron conditions, 50% of 2,2′-dipyridyl minimal inhibitory concentration, MIC) RM71, BP53, and RM71Δ*gltA* also showed indistinguishable growth curves (**Figure 2**). However, under very low-iron conditions (75 μM 2,2′-dipyridyl, 80% of MIC) RM71Δ*gltA* mutant showed a growth which was 45% lower with respect to BP53 and RM71. Interestingly, when ferric-ammonium citrate was added to the medium, RM71Δ*gltA* showed a growth curve identical to RM71 and BP53 strains (**Figure 2**). Therefore, RM71Δ*gltA* showed a significant decrease in the growth ability under iron deprivation conditions when the concentration of 2,2′-dipyridyl is close to the MIC of this iron chelator for the parental strain RM71.

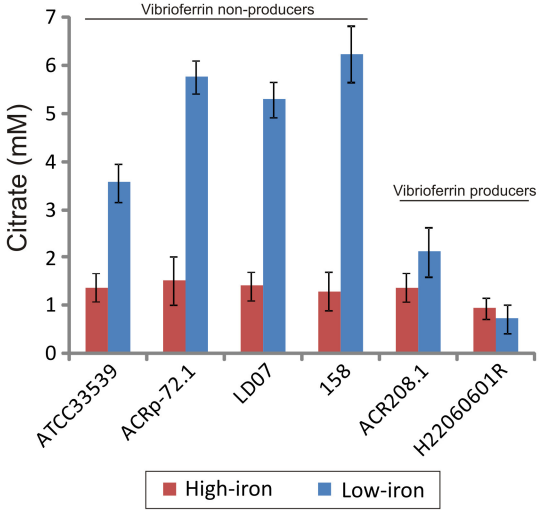

FIGURE 4 | Citrate accumulation of several representative strains of *Pdd* producing and non-producing vibrioferrin. Each bar represents mean values from three replicates. Error bars indicate standard deviations.

Citrate as Siderophore for *Pdd*

The RM71 supernatant produces a CAS-positive reaction under low-iron, being the absorbance between 5- and 7-fold lower than in iron-excess conditions, which denotes that, as expected, siderophore activity is stronger under iron-deprived conditions. The iron homeostasis is strictly controlled by Fur repression, therefore the genes involved in iron uptake, like siderophore synthesis, are expressed only under iron starvation (Fillat, 2014; Porcheron and Dozois, 2015). As previously mentioned, BP53 showed a strong CAS-positive reaction under both iron-restricted and iron-excess conditions which denotes that *idh* inactivation causes an overproduction of siderophore. Interestingly, the supernatants from the RM71Δ*gltA* mutant showed a CAS-negative reaction in both high- and low-iron conditions (**Figure 3**) indicating that no detectable amount of siderophores was produced. Therefore, inactivation of citrate synthesis in RM71 abolishes siderophore production.

To further confirm that citrate serves as iron source for *Pdd*, we used the stretonigrin sensitivity method. Streptonigrin is a metal-dependent quinone-containing antibiotic which at high values of intracellular iron (Fe^{2+} and Fe^{3+}) increases its bactericidal action by the formation of reactive oxygen radicals (Yeowell and White, 1982). So that, the presence in the cell of an active iron-uptake mechanism implies a growth defect when streptonigrin is added to the medium. In our case, while under iron limitation streptonigrin 10 μM was sufficient to inhibit the growth of RM71 and BP53 strains, the growth of RM71Δ*gltA* was inhibited only when streptonigrin was above 75 μM (**Figure 5**), indicating that no iron was entering into the cell. This result shows that blocking the endogenous citrate synthesis in *Pdd* RM71 prevents siderophore production, resulting in a decrease

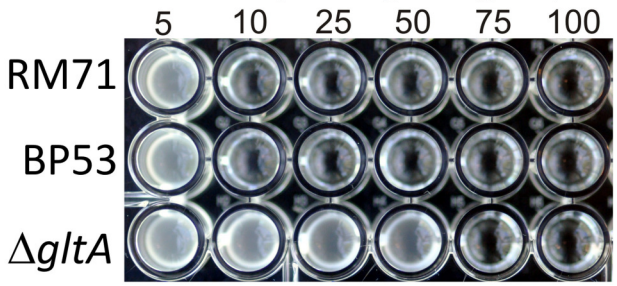

FIGURE 5 | Growth of RM71 and mutants BP53 and RM71 *ΔgltA* in presence of different concentrations (from 5 to 100 μM) of the iron-dependent antibiotic streptonigrin. Picture shows growth in a 96-well microtiter plate.

of growth under extreme iron deprivation. Altogether our results clearly suggest that citrate or a citrate-like compound serves as an iron scavenging system in RM71.

Identification of CAS-Reactive Compounds in Culture Supernatants

To identify compounds with siderophore activity secreted by strain RM71, the cells were grown under iron restricted conditions (CM9 with 35 μM 2,2′-dipyridyl) and the spent medium was subjected to chemical analysis using the CAS reactivity and biological activity as purification guides. The cell-free supernatants were fractionated by successive column chromatography (Amberlite XAD4 resin and size exclusion on Sephadex LH-20, G-25, and G-10) to give a CAS reactive and bioassay active fraction (**Figure 6**). From a final HPLC purification of this fraction we obtained a pure compound which spectral data (NMR, MS) were coincident to those of citrate (**Figure 7**). Hence, the CAS-reactive molecule produced by *Pdd* strain RM71 was unequivocally identified as citrate, and no other molecules with siderophore activity could be identified in the supernatants.

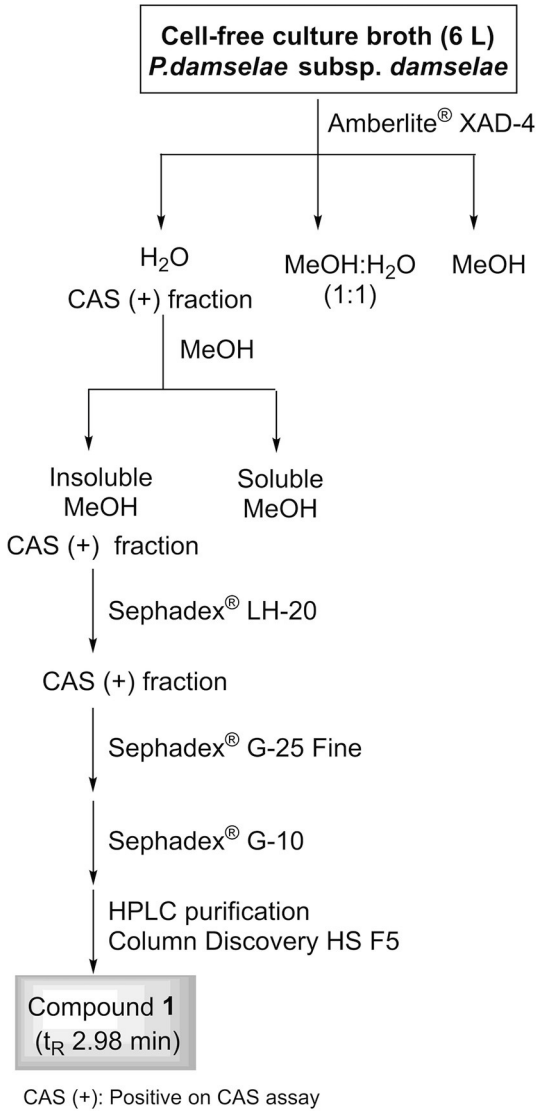

FIGURE 6 | Fractionation flowchart and isolation of citrate (compound **1**) from the iron-restricted culture supernatants of *Pdd* strain RM71.

DISCUSSION

Citrate is produced by most microorganisms via the TCA cycle (Breusch, 1943) and, although it is not a powerful chelator, it binds Fe(III) forming a ferric-dicitrate complex (Silva et al., 2009). In this form, citrate can be used by many bacteria, including *Pdd*, as a source of iron (Pressler et al., 1988; Mazoy and Lemos, 1991; Fouz et al., 1994; Mazoy et al., 1997). Besides, citrate is a common moiety of many polycarboxilic siderophores (Hider and Kong, 2010).

Although, at neutral pH, citrate has lower affinity for iron than conventional siderophores, it is considered a high-affinity iron carrier, and it produces a CAS-positive reaction at concentrations above 0.1 mM (Frawley et al., 2013). Endogenous citrate secretion was described previously in other pathogenic bacteria and it is associated to intracellular iron homeostasis. However, while most bacteria can use externally supplied ferric citrate to fulfill their nutritional requirement for iron, there are two examples of bacteria which secrete citrate in order to get iron: *Pseudomonas syringae* (Jones and Wildermuth, 2011) and *Bradyrhizobium japonicum* (Guerinot et al., 1990). This property depends on the existence of a secretion system that secretes citrate under appropriate conditions. In *Salmonella typhimurium* it was described a major facilitator superfamily pump (IceT) that regulates intracellular iron content by Fe-citrate secretion (Frawley et al., 2013). *in silico* searches on *Pdd* genomes did not detect IceT homologs. Whether citrate is host or endogenous derived, bacterial cells require an energy-dependent transporter to acquire it, with the likely participation of outer membrane transporters from the TonB family (Ogierman and Braun, 2003). In *E. coli* and *Pseudomonas aeruginosa* this role is played by outer membrane protein FecA (Pressler et al., 1988; Marshall

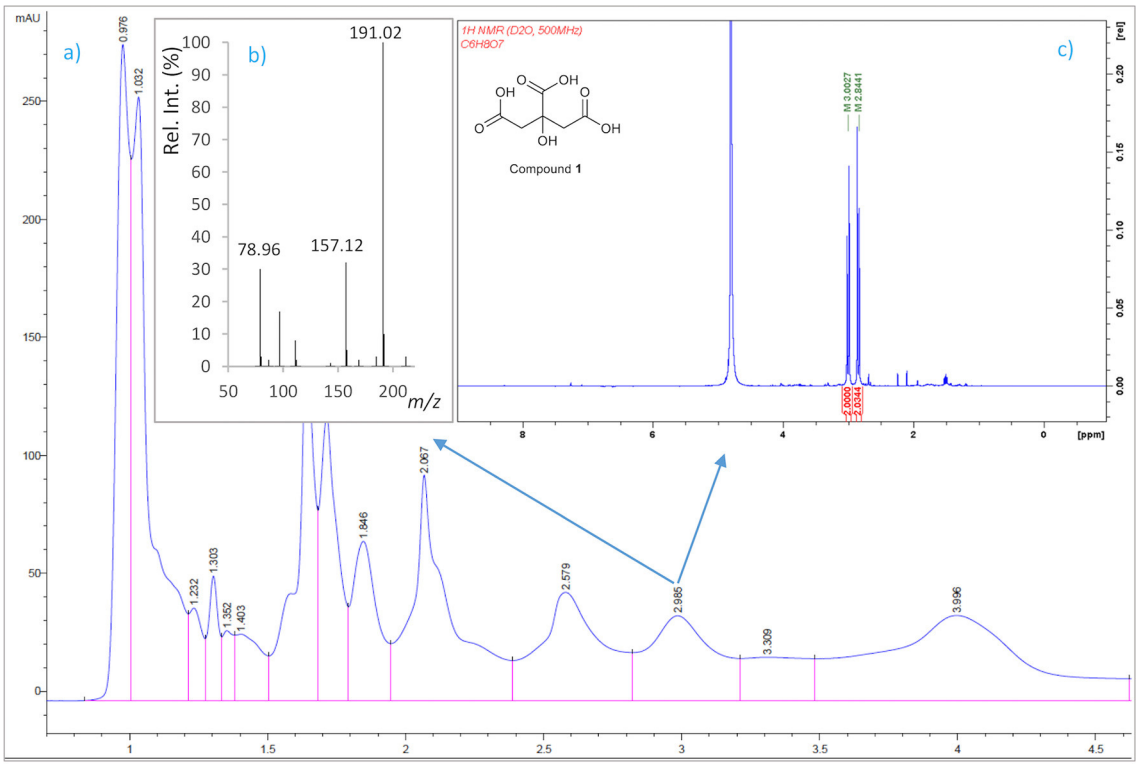

FIGURE 7 | Isolation by HPLC and chemical analysis of compound **1**: **(a)** HPLC chromatogram of the CAS active and salt-free fraction eluted from the Sephadex® G-10 column. **(b)** (–)ESI mass spectrum and **(c)** ^{1}H NMR spectrum in D_2O (500 MHz) of compound **1**.

et al., 2009). Although up to five TonB-dependent transporters are present in *Pdd* genomes, a FecA homolog seems to be absent. However, a FecB homolog, a periplasmic transporter which is part of the ferric-citrate transport system in *E. coli* (Banerjee et al., 2016), has been previously identified as a protein expressed under low iron conditions in *Pdd* (Puentes et al., 2017). More work is needed to clarify the ferric-citrate transport in this bacterium.

Besides acting as iron chelator, citrate seems to play different roles. In *S. typhimurium* it was reported the existence of a stress-induced citrate secretion that would reduce the intracellular iron amount and arrest growth, increasing tolerance to antibiotics and to reactive oxygen species produced by the host defenses (Frawley et al., 2013).

It is known that TCA cycle is suppressed in anaerobiosis or in media containing glucose and that it is activated in presence of oxygen and acetate (Park et al., 1994). Fur is a negative regulator of iron acquisition systems that also exert a regulatory role in energy metabolism (Thompson et al., 2002). In addition, Fur regulates some TCA cycle steps. While citrate synthase is repressed by the Fe^{2+}-Fur complex, the Aconitase A (that converts citrate into isocitrate) is induced by Fe^{2+}-Fur, suggesting that some bacteria, like *E. coli*, respond to iron restriction by producing citrate (Thompson et al., 2002; McHugh et al., 2003).

Our results indicate that inactivation of TCA cycle observed in *Pdd* BP53 mutant results in a dramatic increase of citrate in the extracellular medium but it did not affect growth in glucose-containing media. These findings clearly suggest the necessary existence of a citrate secretion system that prevents intracellular citrate accumulation. Overproduction of citrate is deleterious to most bacteria. It was proved that cytoplasmic citrate accumulation causes a growth defect and promotes a strong selection pressure for mutations inactivating citrate synthase. Such mutations restore the growth potential in mutant strains that accumulate citrate. This was demonstrated for many microorganisms such as *E. coli* (Gruer et al., 1997), *Corynebacterium glutamicum* (Baumgart et al., 2011), *Sinorhizobium meliloti* (Koziol et al., 2009), *Vibrio fischeri* (Septer et al., 2015), and *Bacillus subtilis* (Pechter et al., 2013). Nevertheless, the accumulation of citrate seems to have no negative effect on *Pdd* growth, suggesting that most citrate excess must be secreted to the extracellular medium to avoid intracellular accumulation. In contrast, inactivation of citrate synthase in *Pdd* produces a significant decrease in growth capacity under extreme iron-restriction. Therefore, citrate secretion by *Pdd* has a positive effect on cell fitness and could be used for extracellular high-affinity iron scavenging, which suggests that *Pdd* likely synthesizes a citrate excess to use it for iron uptake from the cell surroundings. This is reinforced by the observation that a vibrioferrin-producing *Pdd* strain does not accumulate citrate, but when the vibrioferrin system is inactivacted, the mutant behaves like a strain lacking the

vibrioferrin system, and accumulate extracellular citrate in an iron-dependent fashion (**Figure 3**). One plausible explanation of this result is that since citrate is a precursor for vibrioferrin (Tanabe et al., 2003), mutation of a vibrioferrin biosynthetic gene would result in the accumulation of precursors, and in this case citrate would be exported out of the cell to avoid toxicity. The cell would then use external citrate as an alternative iron carrier.

The advantages of using citrate or vibrioferrin for iron uptake are unclear. From the results described here we could deduce that vibrioferrin use would be a better strategy since all strains that produce this siderophore do not accumulate citrate. However, the vibrioferrin affinity constant for iron is not particularly high, with respect to citrate (Amin et al., 2009; Silva et al., 2009). Furthermore, and despite that the information available is scarce, seems that there are not clear differences in the virulence degree between the two types of strains (data not shown). In addition, it is likely that the use of citrate could be an ancestral mechanism to get iron since *Pdd* and *Pdp* subspecies share a common evolutionary origin (Balado et al., 2017a), and we have some evidence that *Pdp* seems to use also secreted citrate for iron uptake. Some strains of each subspecies could have later acquired by horizontal transfer additional siderophore-based mechanisms for iron uptake, like the plasmid-encoded piscibactin in *Pdp* (Osorio et al., 2015) or vibrioferrin in *Pdd*, resulting in the inactivation of the use of secreted citrate for iron uptake.

As conclusion, this work shows that although some strains of the marine pathogen *Pdd* produce vibrioferrin as siderophore, most pathogenic strains release endogenous citrate to the extracellular environment in response to iron deprivation, and that this trait have a positive effect in the cell fitness when it grows under extreme iron-restricted conditions. Although the production of another citrate-based or other compounds with siderophore activity cannot be completely discarded, our results suggest that endogenous citrate, besides being part of other siderophores, can be itself used for iron uptake by *Pdd*.

AUTHOR CONTRIBUTIONS

MB, CO, CJ, and ML conceived and designed the experiments. BP, LC, MB, and JF performed the laboratory experiments. CO and JR made substantial contributions to conception and design. MB, LC, CJ, and ML participated in experimental design and data analysis. MB, CJ, and ML drafted and wrote the manuscript. All authors read and approved the final manuscript.

ACKNOWLEDGMENTS

This work was supported by grants AGL2012-39274-C02-01/02 and AGL2015-63740-C2-1/2-R (AEI/FEDER, EU) from the State Agency for Research (AEI) of Spain, and co-funded by the FEDER Programme from the European Union. The support of Xunta de Galicia (Spain) with grant GRC-2014/007 is also acknowledged.

REFERENCES

Altschul, S. F., Gish, W., Miller, W., Myers, E. W., and Lipman, D. J. (1990). Basic local alignment search tool. *J. Mol. Biol.* 215, 403–410. doi: 10.1016/S0022-2836(05)80360-2

Amin, S. A., Green, D. H., Küpper, F. C., and Carrano, C. J. (2009). Vibrioferrin, an unusual marine siderophore: iron binding, photochemistry, and biological implications. *Inorg. Chem.* 48, 11451–11458. doi: 10.1021/ic901688 3

Balado, M., Benzekri, H., Labella, A. M., Claros, M. G., Manchado, M., Borrego, J. J., et al. (2017a). Genomic analysis of the marine fish pathogen *Photobacterium damselae* subsp. *piscicida*: insertion sequences proliferation is associated with chromosomal reorganisations and rampant gene decay. *Infect. Genet. Evol.* 54, 221–229. doi: 10.1016/j.meegid.2017.07.007

Balado, M., Segade, Y., Rey, D., Osorio, C. R., Rodriguez, J., Lemos, M. L., et al. (2017b). Identification of the ferric-acinetobactin outer membrane receptor in *Aeromonas salmonicida* subsp. *salmonicida* and structure-activity relationships of synthetic acinetobactin analogues. *ACS Chem. Biol.* 12, 479–493. doi: 10.1021/acschembio.6b00805

Balado, M., Souto, A., Vences, A., Careaga, V. P., Valderrama, K., Segade, Y., et al. (2015). Two Catechol siderophores, acinetobactin and amonabactin, are simultaneously produced by *Aeromonas salmonicida* subsp. *salmonicida* sharing part of the biosynthetic pathway. *ACS Chem. Biol.* 10, 2850–2860. doi: 10.1021/acschembio.5b00624

Banerjee, S., Paul, S., Nguyen, L. T., Chu, B. C., and Vogel, H. J. (2016). FecB, a periplasmic ferric-citrate transporter from *E. coli,* can bind different forms of ferric-citrate as well as a wide variety of metal-free and metal-loaded tricarboxylic acids. *Metallomics* 81, 125–133. doi: 10.1039/C5MT00218D

Baumgart, M., Mustafi, N., Krug, A., and Bott, M. (2011). Deletion of the aconitase gene in *Corynebacterium glutamicum* causes strong selection pressure for secondary mutations inactivating citrate synthase. *J. Bacteriol.* 193, 6864–6873. doi: 10.1128/JB.05465-11

Bennett, B. D., Kimball, E. H., Gao, M., Osterhout, R., Van Dien, S. J., and Rabinowitz, J. D. (2009). Absolute metabolite concentrations and implied enzyme active site occupancy in *Escherichia coli*. *Nat. Chem. Biol.* 58, 593–599. doi: 10.1038/nchembio.186

Breusch, F. L. (1943). Citric acid cycle; sugar and fatbreakdown in tissue metabolism. *Science* 97, 490–492. doi: 10.1126/science.97.2526.490

Cassat, J. E., and Skaar, E. P. (2013). Iron in infection and immunity. *Cell Host Microbe* 13, 509–519. doi: 10.1016/j.chom.2013.04.010

Ellermann, M., and Arthur, J. C. (2017). Siderophore-mediated iron acquisition and modulation of host-bacterial interactions. *Free Radic. Biol. Med.* 105, 68–78. doi: 10.1016/j.freeradbiomed.2016.10.489

Fillat, M. F. (2014). The FUR (ferric uptake regulator) superfamily: diversity and versatility of key transcriptional regulators. *Arch. Biochem. Biophys.* 546, 41–52. doi: 10.1016/j.abb.2014.01.029

Fouz, B., Biosca, E. G., and Amaro, C. (1997). High affinity iron-uptake systems in *Vibrio damsela*: role in the acquisition of iron from transferrin. *J. Appl. Microbiol.* 82, 157–167. doi: 10.1111/j.1365-2672.1997.tb02846.x

Fouz, B., Toranzo, A. E., Biosca, E. G., Mazoy, R., and Amaro, C. (1994). Role of iron in the pathogenicity of *Vibrio damsela* for fish and mammals. *FEMS Microbiol. Lett.* 121, 181–188. doi: 10.1111/j.1574-6968.1994.tb07097.x

Frawley, E. R., Crouch, M. L., Bingham-Ramos, L. K., Robbins, H. F., Wang, W., Wright, G. D., et al. (2013). Iron and citrate export by a major facilitator superfamily pump regulates metabolism and stress resistance in *Salmonella Typhimurium*. *Proc. Natl. Acad. Sci. U.S.A.* 110, 12054–12059. doi: 10.1073/pnas.1218274110

Gruer, M. J., Bradbury, A. J., and Guest, J. R. (1997). Construction and properties of aconitase mutants of *Escherichia coli*. *Microbiology* 143, 1837–1846. doi: 10.1099/00221287-143-6-1837

Guerinot, M. L., Meidl, E. J., and Plessner, O. (1990). Citrate as a siderophore in *Bradyrhizobium japonicum*. *J. Bacteriol.* 172, 3298–3303. doi: 10.1128/jb.172.6.3298-3303.1990

Herrero, M., de Lorenzo, V., and Timmis, K. N. (1990). Transposon vectors containing non-antibiotic resistance selection markers for cloning and stable chromosomal insertion of foreign genes in gram-negative bacteria. *J. Bacteriol.* 172, 6557–6567. doi: 10.1128/jb.172.11.6557-6567.1990

Hider, R. C., and Kong, X. (2010). Chemistry and biology of siderophores. *Nat. Prod. Rep.* 27, 637–657. doi: 10.1039/b906679a

Jones, A. M., and Wildermuth, M. C. (2011). The phytopathogen *Pseudomonas syringae* pv. tomato DC3000 has three high-affinity iron-scavenging systems functional under iron limitation conditions but dispensable for pathogenesis. *J. Bacteriol.* 193, 2767–2775. doi: 10.1128/JB.00069-10

Kaniga, K., Delor, I., and Cornelis, G. R. (1991). A wide-host-range suicide vector for improving reverse genetics in gram-negative bacteria: inactivation of the *blaA* gene of *Yersinia enterocolitica*. *Gene* 109, 137–141. doi: 10.1016/0378-1119(91)90599-7

Koziol, U., Hannibal, L., Rodriguez, M. C., Fabiano, E., Kahn, M. L., and Noya, F. (2009). Deletion of citrate synthase restores growth of *Sinorhizobium meliloti* 1021 aconitase mutants. *J. Bacteriol.* 191, 7581–7586. doi: 10.1128/JB.00777-09

Labella, A. M., Arahal, D. R., Castro, D., Lemos, M. L., and Borrego, J. J. (2017). Revisiting the genus *Photobacterium*: taxonomy, ecology and pathogenesis. *Int. Microbiol.* 20, 1–10. doi: 10.2436/20.1501.01.280

Lakshmi, T. M., and Helling, R. B. (1976). Selection for citrate synthase deficiency in icd mutants of *Escherichia coli*. *J. Bacteriol.* 127, 76–83.

Lemos, M. L., Salinas, P., Toranzo, A. E., Barja, J. L., and Crosa, J. H. (1988). Chromosome-mediated iron uptake system in pathogenic strains of *Vibrio anguillarum*. *J. Bacteriol.* 170, 1920–1925. doi: 10.1128/jb.170.4.1920-1925.1988

Marshall, B., Stintzi, A., Gilmour, C., Meyer, J. M., and Poole, K. (2009). Citrate-mediated iron uptake in *Pseudomonas aeruginosa*: involvement of the citrate-inducible FecA receptor and the FeoB ferrous iron transporter. *Microbiology* 155, 305–315. doi: 10.1099/mic.0.023531-0

Mazoy, R., Botana, L. M., and Lemos, M. L. (1997). Iron uptake from ferric citrate by *Vibrio anguillarum*. *FEMS Microbiol. Lett.* 154, 145–150. doi: 10.1111/j.1574-6968.1997.tb12636.x

Mazoy, R., and Lemos, M. L. (1991). Iron-binding proteins and heme compounds as iron sources for *Vibrio anguillarum*. *Curr. Microbiol.* 23, 221–226. doi: 10.1007/BF02092282

McHugh, J. P., Rodriguez-Quinones, F., Abdul-Tehrani, H., Svistunenko, D. A., Poole, R. K., Cooper, C. E., et al. (2003). Global iron-dependent gene regulation in *Escherichia coli*. a new mechanism for iron homeostasis. *J. Biol. Chem.* 278, 29478–29486. doi: 10.1074/jbc.M303381200

Minato, Y., Fassio, S. R., Wolfe, A. J., and Hase, C. C. (2013). Central metabolism controls transcription of a virulence gene regulator in *Vibrio cholerae*. *Microbiology* 159, 792–802. doi: 10.1099/mic.0.064865-0

Ogierman, M., and Braun, V. (2003). Interactions between the outer membrane ferric citrate transporter FecA and TonB: studies of the FecA TonB box. *J. Bacteriol.* 185, 1870–1885. doi: 10.1128/JB.185.6.1870-1885.2003

Osorio, C. R., Rivas, A. J., Balado, M., Fuentes-Monteverde, J. C., Rodriguez, J., Jimenez, C., et al. (2015). A transmissible plasmid-borne pathogenicity island confers piscibactin biosynthesis in the fish pathogen *Photobacterium damselae* subsp. *piscicida*. *Appl. Environ. Microbiol.* 81, 5867–5879. doi: 10.1128/AEM.01580-15

Park, S. J., McCabe, J., Turna, J., and Gunsalus, R. P. (1994). Regulation of the citrate synthase (gltA) gene of *Escherichia coli* in response to anaerobiosis and carbon supply: role of the arcA gene product. *J. Bacteriol.* 176, 5086–5092. doi: 10.1128/jb.176.16.5086-5092.1994

Pechter, K. B., Meyer, F. M., Serio, A. W., Stulke, J., and Sonenshein, A. L. (2013). Two roles for aconitase in the regulation of tricarboxylic acid branch gene expression in *Bacillus subtilis*. *J. Bacteriol.* 195, 1525–1537. doi: 10.1128/JB.01690-12

Porcheron, G., and Dozois, C. M. (2015). Interplay between iron homeostasis and virulence: fur and RyhB as major regulators of bacterial pathogenicity. *Vet. Microbiol.* 179, 2–14. doi: 10.1016/j.vetmic.2015.03.024

Pressler, U., Staudenmaier, H., Zimmermann, L., and Braun, V. (1988). Genetics of the iron dicitrate transport system of *Escherichia coli*. *J. Bacteriol.* 170, 2716–2724. doi: 10.1128/jb.170.6.2716-2724.1988

Puentes, B., Balado, M., Bermudez-Crespo, J., Osorio, C. R., and Lemos, M. L. (2017). A proteomic analysis of the iron response of *Photobacterium damselae* subsp. *damselae* reveals metabolic adaptations to iron levels changes and novel potential virulence factors. *Vet. Microbiol.* 201, 257–264. doi: 10.1016/j.vetmic.2017.01.040

Rio, S. J., Osorio, C. R., and Lemos, M. L. (2005). Heme uptake genes in human and fish isolates of *Photobacterium damselae*: existence of *hutA* pseudogenes. *Arch. Microbiol.* 183, 347–358. doi: 10.1007/s00203-005-0779-4

Rivas, A. J., Balado, M., Lemos, M. L., and Osorio, C. R. (2011). The *Photobacterium damselae* subsp. *damselae* hemolysins damselysin and HlyA are encoded within a new virulence plasmid. *Infect. Immun.* 79, 4617–4627. doi: 10.1128/IAI.05436-11

Rivas, A. J., Lemos, M. L., and Osorio, C. R. (2013). *Photobacterium damselae* subsp. *damselae,* a bacterium pathogenic for marine animals and humans. *Front. Microbiol.* 4:283. doi: 10.3389/fmicb.2013.00283

Rivas, A. J., Vences, A., Husmann, M., Lemos, M. L., and Osorio, C. R. (2015). *Photobacterium damselae* subsp. *damselae* major virulence factors Dly, plasmid-encoded HlyA, and chromosome-encoded HlyA are secreted via the type II secretion system. *Infect. Immun.* 83, 1246–1256. doi: 10.1128/IAI.02608-14

Saha, R., Saha, N., Donofrio, R. S., and Bestervelt, L. L. (2013). Microbial siderophores: a mini review. *J. Basic Microbiol.* 53, 303–317. doi: 10.1002/jobm.201100552

Schwyn, B., and Neilands, J. B. (1987). Universal chemical assay for the detection and determination of siderophores. *Anal. Biochem.* 160, 47–56. doi: 10.1016/0003-2697(87)90612-9

Septer, A. N., Bose, J. L., Lipzen, A., Martin, J., Whistler, C., and Stabb, E. V. (2015). Bright luminescence of *Vibrio fischeri* aconitase mutants reveals a connection between citrate and the Gac/Csr regulatory system. *Mol. Microbiol.* 95, 283–296. doi: 10.1111/mmi.12864

Silva, A. M., Kong, X., Parkin, M. C., Cammack, R., and Hider, R. C. (2009). Iron(III) citrate speciation in aqueous solution. *Dalton Trans.* 40, 8616–8625. doi: 10.1039/b910970f

Tanabe, T., Funahashi, T., Nakao, H., Miyoshi, S., Shinoda, S., and Yamamoto, S. (2003). Identification and characterization of genes required for biosynthesis and transport of the siderophore vibrioferrin in *Vibrio parahaemolyticus*. *J. Bacteriol.* 185, 6938–6949. doi: 10.1128/JB.185.23.6938-6949.2003

Thompson, D. K., Beliaev, A. S., Giometti, C. S., Tollaksen, S. L., Khare, T., Lies, D. P., et al. (2002). Transcriptional and proteomic analysis of a ferric uptake regulator (fur) mutant of *Shewanella oneidensis*: possible involvement of fur in energy metabolism, transcriptional regulation, and oxidative stress. *Appl. Environ. Microbiol.* 68, 881–892. doi: 10.1128/AEM.68.2.881-892.2002

Vieira, J., and Messing, J. (1987). Production of single-stranded plasmid DNA. *Methods Enzymol.* 153, 3–11. doi: 10.1016/0076-6879(87)53044-0

Wang, Q., Liu, Q., Ma, Y., Zhou, L., and Zhang, Y. (2007). Isolation, sequencing and characterization of cluster genes involved in the biosynthesis and utilization of the siderophore of marine fish pathogen *Vibrio alginolyticus*. *Arch. Microbiol.* 188, 433–439. doi: 10.1007/s00203-007-0261-6

Yamamoto, S., Okujo, N., Yoshida, T., Matsuura, S., and Shinoda, S. (1994). Structure and iron transport activity of vibrioferrin, a new siderophore of *Vibrio parahaemolyticus*. *J. Biochem.* 115, 868–874. doi: 10.1093/oxfordjournals.jbchem.a124432

Yamane, K., Asato, J., Kawade, N., Takahashi, H., Kimura, B., and Arakawa, Y. (2004). Two cases of fatal necrotizing fasciitis caused by *Photobacterium damsela* in Japan. *J. Clin. Microbiol.* 42, 1370–1372. doi: 10.1128/JCM.42.3.1370-1372.2004

Yeowell, H. N., and White, J. R. (1982). Iron requirement in the bactericidal mechanism of streptonigrin. *Antimicrob. Agents Chemother.* 22, 961–968. doi: 10.1128/AAC.22.6.961

Conflict of Interest Statement: The authors declare that the research was conducted in the absence of any commercial or financial relationships that could be construed as a potential conflict of interest.

frontiers in Cellular and Infection Microbiology

REVIEW
published: 25 July 2017
doi: 10.3389/fcimb.2017.00342

Iron Acquisition Strategies of *Vibrio anguillarum*

Yingjie Li[1,2] *and Qingjun Ma*[1,2]*

[1] *Key Laboratory of Experimental Marine Biology, Institute of Oceanology, Chinese Academy of Sciences, Qingdao, China,*
[2] *Laboratory for Marine Biology and Biotechnology, Qingdao National Laboratory for Marine Science and Technology, Qingdao, China*

The hemorrhagic septicemic disease vibriosis caused by *Vibrio anguillarum* shows noticeable similarities to invasive septicemia in humans, and in this case, the *V. anguillarum*–host system has the potential to serve as a model for understanding native eukaryotic host–pathogen interactions. Iron acquisition, as a fierce battle occurring between pathogenic *V. anguillarum* and the fish host, is a pivotal step for virulence. In this article, advances in defining the roles of iron uptake pathways in growth and virulence of *V. anguillarum* have been summarized, divided into five aspects, including siderophore biosynthesis and secretion, iron uptake, iron release, and regulation of iron uptake. Understanding the molecular mechanisms of iron acquisition will have important implications for the pathogenicity of this organism.

Keywords: *Vibrio anguillarum*, siderophore biosynthesis, siderophore secretion, iron uptake, iron release, iron acquisition mechanism

INTRODUCTION

The Gram-negative bacterium *Vibrio anguillarum* is a pathogen that causes vibriosis with lethal hemorrhagic septicemia in aquatic animals worldwide (Toranzo et al., 2005). Although up to 23 O serotypes of *V. anguillarum* are identified in the European serotyping system, with most serotypes encompassing free-living environmental strains (Pedersen et al., 1999), only serotypes O1, O2, and partial O3 are found to be implicated in vibriosis outbreaks (Toranzo et al., 2005). Many studies have been performed in an attempt to understand the virulence mechanism in *V. anguillarum*. Several main virulence factors have been recognized by using genetic approaches, including iron acquisition components (Naka and Crosa, 2011), hemolysins (Hirono et al., 1996; Rodkhum et al., 2005; Rock and Nelson, 2006; Li et al., 2008; Xu et al., 2011; Mou et al., 2013), metalloproteases (Milton et al., 1992; Yang et al., 2007; Varina et al., 2008; Mo et al., 2010), chemotaxis and motility (O'Toole et al., 1999; Ormonde et al., 2000), exopolysaccharides (Croxatto et al., 2007), and lipopolysaccharides (Welch and Crosa, 2005). Among them, iron uptake systems are a critical component for infection of the host fish leading to disease (Wolf and Crosa, 1986).

V. anguillarum, like most other organisms, has an absolute requirement for iron to synthesize a large number of crucial enzymes, which are involved in many fundamental cellular processes, such as cytochromes for cell respiration, ribonucleotide reductase for the biosynthesis of DNA precursors, and enzymes for the tricarboxylic acid (TCA) cycle (Crosa et al., 2004). However, due to the low solubility of iron ($\sim 10^{-18}$ M) at physiological pH in aerobic environments, ferric iron mainly forms insoluble hydroxides, whereas a cytoplasmic iron concentration of $\sim 10^{-6}$ M is required for bacterial growth (Hantke, 1981). Therefore, iron is suggested to be the growth-limiting factor in ocean environments (Martin et al., 1991). To respond to this selective pressure, bacteria have evolved numerous mechanisms for iron acquisition, including transport of iron from

OPEN ACCESS

Edited by:
Pierre Cornelis,
Vrije Universiteit Brussel, Belgium

Reviewed by:
Manuel L. Lemos,
Universidade de Santiago de Compostela, Spain
Isabelle Jeanne Schalk,
Centre National de la Recherche Scientifique (CNRS), France

***Correspondence:**
Qingjun Ma
qma@qdio.ac.cn

Received: *03 May 2017*
Accepted: *11 July 2017*
Published: *25 July 2017*

Citation:
Li Y and Ma Q (2017) Iron Acquisition Strategies of Vibrio anguillarum. Front. Cell. Infect. Microbiol. 7:342. doi: 10.3389/fcimb.2017.00342

the mammalian iron carriers, transferrin and heme, and synthesis of small ferric iron-binding molecules, known as siderophores. Some of these iron transport systems are conserved among all *Vibrio* species, reflecting their common ancestry, while other acquisition systems appear to have been developed by horizontal transfer, such as the anguibactin transport system that is mainly specific to *V. anguillarum*. It has been shown that *V. anguillarum* harbors a number of genes encoding for iron uptake and regulation, which are essential for its virulence beyond simple iron chelation (Lemos and Osorio, 2007; Naka et al., 2013b). In this article, we describe the developments in understanding the molecular mechanisms of iron acquisition systems in *V. anguillarum*, divided into the following aspects: siderophore biosynthesis and secretion, iron uptake, iron release, and regulation of iron uptake.

SIDEROPHORE BIOSYNTHESIS

Two different siderophore-dependent systems have been identified in *V. anguillarum* strains. One is mediated by a 65 kb pJM1 plasmid, which contains most of the genes encoding for biosynthesis and transport proteins of the siderophore anguibactin (Naka et al., 2013b). This anguibactin system is only found in pathogenic plasmid-bearing strains of serotype O1. The other system, existing in all serotype O2 strains tested thus far, and some plasmidless serotype O1 strains, synthesizes a catecholated-type siderophore, vanchrobactin (Alice et al., 2005; Balado et al., 2006).

Biosynthesis of Anguibactin

The structure of anguibactin is unique in containing both catechol and hydroxamate metal-chelating functional groups (Actis et al., 1986), derived from 2,3-dihydroxybenzoic acid (DHBA) and *N*-hydro-histamine, respectively. Utilizing the chorismate, plasmid-carrying *V. anguillarum* strain 775 generates a repertoire of molecules through a ribosome-independent process and finally synthesizes anguibactin. This biosynthesis is controlled by a number of genetic determinants. To date, more than 10 different genes have been described and yield anguibactin-related phenotypes in plasmid-carrying *V. anguillarum* strains when mutated by genetic approaches (Table S1). Most are located on the plasmid pJM1 or pJM1-like plasmids while some are on the chromosomes (**Figure 1**). First, chorismate is catalyzed stepwise by a series of proteins, AngC/VabC (isochrorismate synthase), AngB/VabB (isochrorismatase; Du et al., 2017), and VabA (2,3-dihydro-2,3-dehydroxybenzoate dehydrogenase), to synthesize DHBA (**Figure 2**; Alice et al., 2005; Balado et al., 2008). In later steps, phosphopantetheine transferase AngD is required to transfer a phosphopantetheinyl moiety to a serine residue of AngB and AngM (Balado et al., 2008). AngE/VabE (2,3-dehydroxybenzoate-AMP ligase) activates DHBA to form acyl adenylate and further transfers it to the free thiol of the phosphopantetheine AngB (Liu et al., 2004; Alice et al., 2005). AngC, AngB, and AngE are pJM1-encoded proteins while VabC, VabB, VabA, and VabE are chromosomally encoded with VabC, VabB, and VabE showing functional redundancy with AngC, AngB, and AngE, respectively. AngN catalyzes this DHBA thioester to combine with cysteine, which is activated by AngR and tethered by AngM, thereby producing a dihydroxyphenyl-thiazoline-thioester. AngH (histidine decarboxylase; Tolmasky et al., 1995; Barancin et al., 1998) and possibly AngU (Naka et al., 2013b) modify the histidine to form *N*-hydro-histamine, which is then transferred to dihydroxyphenyl-thiazoline-thioester to yield anguibactin. It is interesting to note that homologs of these plasmid-located genes are all present on the chromosome of *Vibrio harveyi*, which is also able to produce anguibactin, suggesting that the plasmid-mediated anguibactin system might originate from *V. harveyi* or vice versa (Naka et al., 2013a,b) .

Biosynthesis of Vanchrobactin

Plasmidless O1 strains and those belonging to a number of other *V. anguillarum* serotypes synthesize a chromosome-mediated siderophore, vanchrobactin (Lemos et al., 1988; Soengas et al., 2008). In a similar way to anguibactin synthesis, DHBA of these *V. anguillarum* strains is also produced from chorismate by the sequential activities of VabC, VabB, and VabA. However, how vanchrobactin is synthesized from the DHBA precursor remains obscure, even though some genes have been found to be indispensable for this process, including *vabB*, *vabD*, *vabE*, and *vabF* (Balado et al., 2006, 2008). According to well-studied pathways for synthesis of anguibactin and vibriobactin, a siderophore produced by *Vibrio cholerae*, late steps for vanchrobactin formation in *V. anguillarum* have been proposed during which DHBA is assembled (**Figure 3**; Balado et al., 2006). Specifically, VabD contributes to transfer of a phosphopantetheinyl moiety to the aryl carrier domain of VabB and the peptidyl carrier domain of VabF, respectively. Like anguibactin formation, VabE activates DHBA and arginine to yield acyl adenylates, and then delivers them to VabB and VabF, respectively. The DHBA-VabB is combined with arginine by the condensation domain of VabF to form (2,3-dihydroxybenzoyl)argininate. Finally, the condensation domain of VabF in (2,3-dihydroxybenzoyl)argininate-VabF may be loaded with VabE-activated serine, which adheres to the peptidyl carrier domain of VabF to produce vanchrobactin. Although similar roles of AngB and VabB are proposed in these processes, the aryl carrier protein (ArCP) domain of VabB is not able to complement the function of the AngB ArCP domain (Di Lorenzo et al., 2011), suggesting different but unknown roles may occur between AngB and VabB during anguibactin and vanchrobactin formation.

SIDEROPHORE EXPORT

Siderophore secretion is an essential step in iron uptake, yet the mechanisms of this process remain largely unknown. Two siderophore export systems have been found so far, including the ATP-dependent efflux pump and the major facilitator superfamily protein (MFS)-mediated efflux pump. PvdRT-OpmQ is the first ATP-dependent export system to be identified in *Pseudomonas aeruginosa* (reviewed by Schalk and Guillon, 2013). Schalk and colleagues found that this system exports not only the newly synthesized mature siderophore

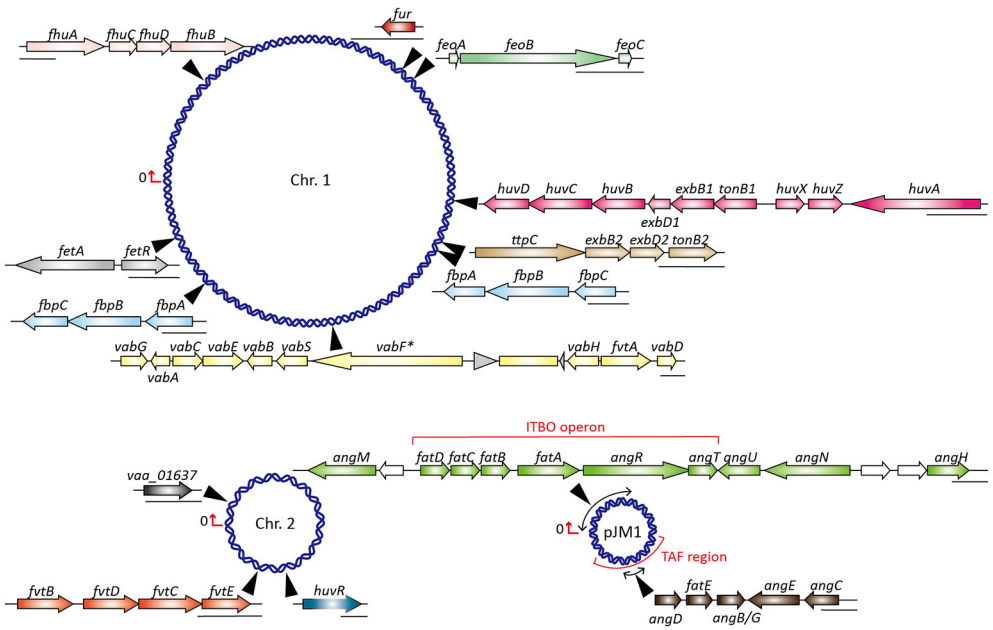

FIGURE 1 | Map of *V. anguillarum* 775 chromosomes and plasmid pJM1 showing locations and molecular organization of known and putative iron transport genes. Chr., chromosome; ITBO, iron transport biosynthesis operon; TAF, *trans*-acting factor; *vabF** indicates *vabF* is inactivated by the insertion sequence RS1.

pyoverdine but also pyoverdine that has already delivered iron into the bacterium (Hannauer et al., 2010; Yeterian et al., 2010). In addition, PvdRT-OpmQ can secrete unwanted metal-pyoverdine complexes into the periplasm of *P. aeruginosa* (Hannauer et al., 2012). By using the respective protein sequences from *P. aeruginosa* as a query in BLASTP analysis, only genes encoding for PvdR and PvdT are identified (Table S2) while the *ompQ* gene is absent in the genomes of the sequenced *V. anguillarum* strains, suggesting that the MFS system rather than PvdRT-OpmQ may participate in siderophore secretion in *V. anguillarum*.

The secretion of enterobactin in *Escherichia coli* is the best-studied paradigm of siderophore export via the MFS system (Horiyama and Nishino, 2014). Based on this, a proposed siderophore-export pathway is depicted in **Figure 4**, and putative genes involved in this process are listed in Table S2. First, siderophores are exported to the periplasm from the cytoplasm via the MSF VabS, a homolog of *E. coli* EntS that has been shown to transport enterobactin across the cytoplasmic membrane (Furrer et al., 2002). Subsequently, the resistance-nodulation-cell division (RND) family proteins, which have been found to play a role in multidrug resistance in many microbes including *V. cholerae* strains (Rahman et al., 2007; Bina et al., 2008), capture the periplasmic siderophores and secrete them to the environment via the outer membrane channel TolC. In agreement with this model, a RND efflux system recently described in *V. cholerae* plays an essential role in maintenance of cellular homeostasis by secreting the siderophore vibriobactin (Kunkle et al., 2017), which again indicates that a MFS-mediated efflux pump system might be used for siderophore export in *V. anguillarum*.

IRON UPTAKE

V. anguillarum strains contain several iron transport systems to sequester the different sources of iron, including anguibactin or vanchrobactin, heme, free Fe^{2+}, free Fe^{3+}, and ferrichrome, which are summarized in **Figure 5**.

Ferrisiderophore Import

Once siderophores are produced and exported to the environment, they capture iron to form a ferric-siderophore complex, which is recognized by a specific transporter on the surface of the outer membrane. In *V. anguillarum*, ferric-anguibactin is translocated across the outer membrane via its specific transporter FatA, which is essential for ferric-anguibactin uptake (Walter et al., 1983; Actis et al., 1988; Lopez and Crosa, 2007; Lopez et al., 2007). This process requires the TonB2 system for energy transmission, which originates from the proton-motive force of the inner membrane (Stork et al., 2004).

The TonB2 complex is located across the inner membrane and comprises TonB2, ExbB2, ExbD2, and TtpC (TonB2 complex-associated transport protein C), all of which are indispensable for ferric-anguibactin import to the periplasmic space. Deletion of either of these genes completely abolishes ferric-anguibactin uptake, and they are thereby considered essential virulence factors for *V. anguillarum* since ferrisiderophore transport during iron uptake is a critical step for virulence (Stork et al., 2004, 2007). Notably, TtpC which shows homology to the TolR protein of *E. coli*, has been identified to be part of the TonB2 system in several *Vibrio* species, including *V. anguillarum* (Stork et al., 2007), *V. cholerae* (Stork et al., 2007), *Vibrio alginolyticus* (Wang et al., 2008), *Vibrio parahaemolyticus* (Kuehl and Crosa,

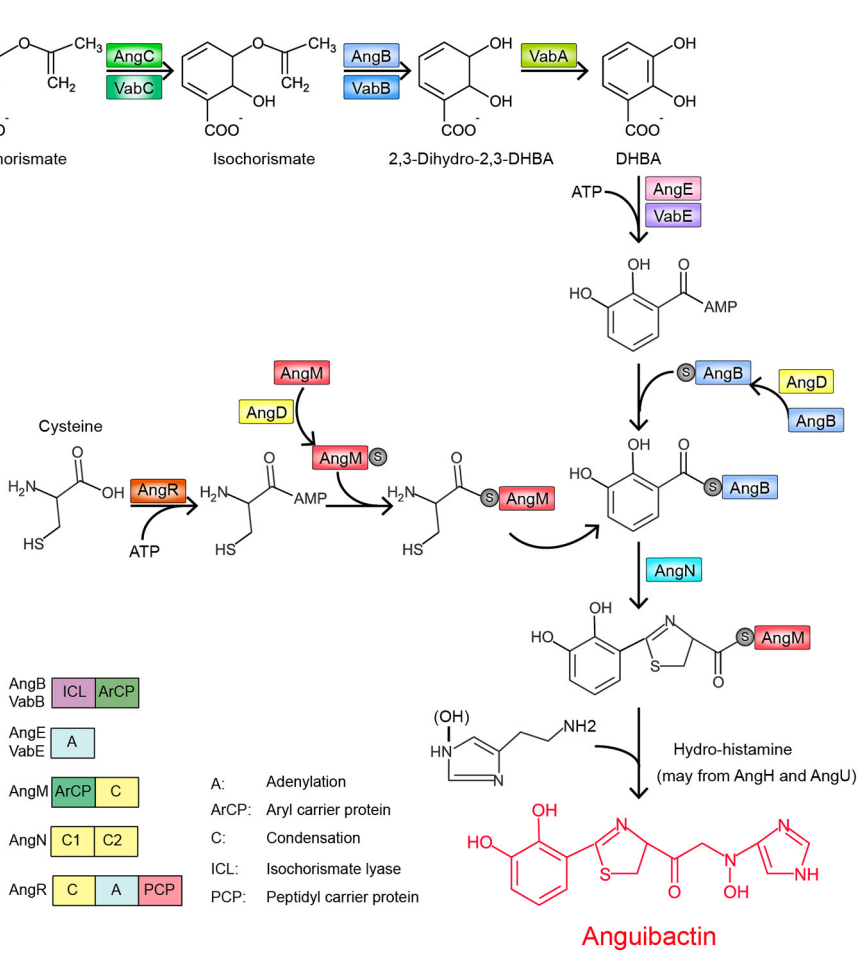

FIGURE 2 | Proposed pathway of anguibactin biosynthesis in *V. anguillarum* plasmid-carrying strains (modified from Naka et al., 2013b).

2010), and *Vibrio vulnificus* (Kuehl and Crosa, 2009). Despite a high similarity among all pathogenic vibrios studied thus far, the TtpC proteins likely play an important role in specific iron transport mediated by the TonB2 system, a conclusion drawn based on the observation that *V. anguillarum* Δ*ttpC* cannot be complemented by the TtpC protein from *V. cholerae* (Stork et al., 2007; Kuehl and Crosa, 2009).

In addition to anguibactin transport, the TonB2 system is also involved in the uptake of vanchrobactin and the xenosiderophore (siderophore produced by other organisms) enterobactin. The transport of vanchrobactin and enterobactin is mediated by another outer membrane transporter, FvtA, which displays vanchrobactin-dependent expression (Balado et al., 2008, 2009; Naka et al., 2008). In the serotype O2 *V. anguillarum* strain RV22, loss of *fvtA* leads to impaired growth under iron-limiting conditions due to incapability of vanchrobactin transport in cells (Balado et al., 2009). Besides FvtA, during transport of the xenosiderophore enterobactin, it seems another transporter, FetA, is present that shows specific binding to enterobactin, and the expression of FetA is regulated by FetR (Naka and Crosa, 2012). This *fetA-fetR* cluster in *V. anguillarum* is speculated to derive from *V. cholerae* based on similar molecular organization and high similarity (Naka and Crosa, 2012).

Subsequently, when combined with the periplasmic lipoprotein FatB, ferric-anguibactin passes through the cytoplasmic membrane by using an ATP-binding cassette (ABC) transporter, which includes inner membrane permeases consisting of a heterodimer of FatC and FatD, and an ATPase FatE (Köster et al., 1991; Actis et al., 1995; Naka et al., 2010, 2013c). FatBCD are required for ferric-anguibactin transport while a *fatE* mutant is still capable of ferric-anguibactin transport due to the presence of its homolog FvtE (Naka et al., 2013c). Double deletion of *fatE* and *fvtE* significantly impairs ferric-anguibactin uptake (Naka et al., 2013c). Similarly, the passage of vanchrobactin through the inner membrane is also achieved in a stepwise manner by a periplasmic protein, FvtB, and an ABC transporter, FvtCDE, which together are essential for ferric-vanchrobactin or ferric-enterobactin import; deletion of either protein causes a defect in ferric-vanchrobactin and ferric-enterobactin transport (Naka et al., 2013c). Different from the specific involvement of FatE in the uptake of anguibactin, FvtE can transport both

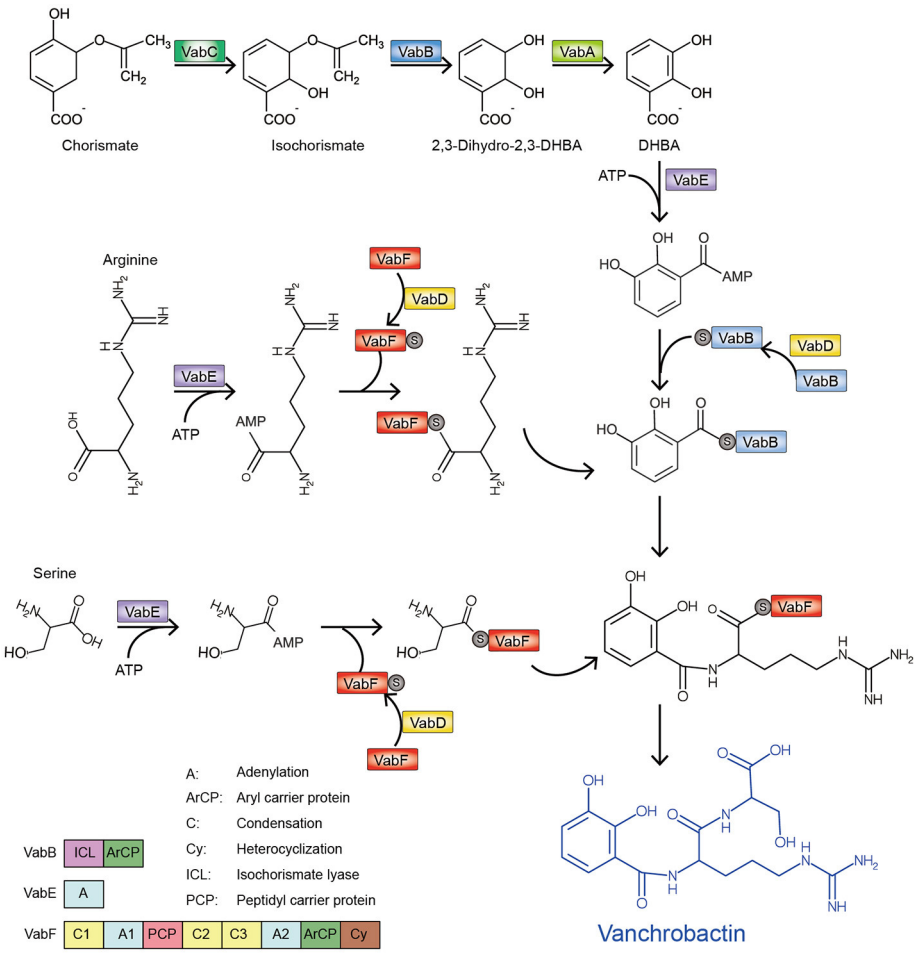

FIGURE 3 | Proposed pathway of vanchrobactin biosynthesis in *V. anguillarum* plasmidless strains (modified from Balado et al., 2006).

anguibactin and vanchrobactin/enterobactin (Naka et al., 2013c).

It is noteworthy that although *fatDCBA* encoding for ferric-anguibactin transport are located on the pJM1-type plasmid in serotype O1 strains, they are also present on the chromosomes of plasmidless vanchrobactin-synthesizing strains, albeit *fatA* is inactivated by an insertion sequence (Bay et al., 2007; Balado et al., 2009). In fact, gene clusters coding for vanchrobactin synthesis and uptake are ubiquitous in both anguibactin- and vanchrobactin-producing *V. anguillarum* strains (Balado et al., 2009), while plasmid-harboring strains do not produce vanchrobactin due to an inactivated chromosomal *vabF* gene (**Figure 1**; Naka et al., 2008). This is caused by the presence of the insertion sequence RS1, observed in all serotype O1 strains carrying a pJM1-type plasmid, and when RS1 is removed, pJM1-containing strains can simultaneously produce the siderophore vanchrobactin (Naka et al., 2008). However, because anguibactin appears to have a higher affinity for iron than does vanchrobactin, it is suggested to be the primary siderophore for iron import even though vanchrobactin is produced in the cell (Naka et al., 2008). Nevertheless, the minimal inhibitory concentration (MIC) values for iron chelators in plasmid-bearing strains seem to be lower than those of plasmidless *V. anguillarum* strains, which might be caused by higher stoichiometry of vanchrobactin in the plasmidless strains (Conchas et al., 1991).

Heme Uptake

Heme usually exists abundantly but not freely as a chemical compound in host cells. Therefore, bacteria secrete exotoxins such as cytolysins, proteases, or hemolysins to release it for further uptake. In *V. anguillarum*, several hemolysin genes have been identified and some of them are involved in *V. anguillarum* virulence (Hirono et al., 1996; Rodkhum et al., 2005; Rock and Nelson, 2006; Li et al., 2008, 2013; Xu et al., 2011) . After its release, free heme is captured by a putative outer membrane transporter, HuvA, which has been shown to be essential for heme uptake because the *huvA* mutant does not grow when heme is used as the sole iron source (Mazoy et al., 2003). However, compared with the wild type, the *huvA* mutant still maintains heme-binding activity under the conditions tested (Mazoy et al., 2003), indicating that HuvA is not the only protein capable of binding heme. In line with this, two heme-binding proteins

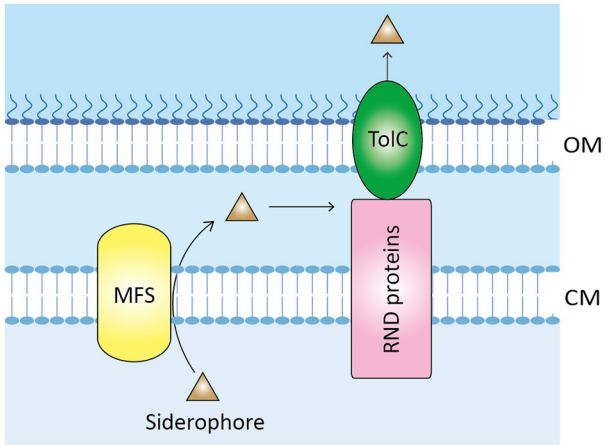

FIGURE 4 | Proposed model of siderophore export in *V. anguillarum*. When produced in the cytoplasm, siderophores such as anguibactin or vanchrobactin are exported to the periplasmic space by MFS protein. Subsequently, RND proteins capture and further secrete the siderophores to the environment through the outer membrane protein TolC. OM, outer membrane; CM, cytoplasmic membrane; MFS, major facilitator superfamily protein; RND, resistance-nodulation-cell division.

with molecular masses of 39 and 37 kDa were isolated from *V. anguillarum* serotype O1 and O2 strains, respectively, which are completely different from the 79 kDa HuvA protein (Mazoy and Lemos, 1996b; Mazoy et al., 1996). Therefore, Mazoy et al. speculate that, besides HuvA, additional proteins are probably present in *V. anguillarum* and function in heme binding, but not in its transport (Mazoy et al., 2003; Lemos and Osorio, 2007). Like siderophore import, this process is also energy-dependent, where HuvA is energized by TonB systems. The difference is that not only is the TonB2 complex involved in heme utilization, but a TonB1 system composed of TonB1-ExbB1-ExbD1 is also available for energy supply (Stork et al., 2004). Deletion of all genes for these two TonB systems leads to a complete defect in heme uptake and thus avirulence to the host, suggesting a key role of TonB systems in *V. anguillarum* virulence (Stork et al., 2004). The recent structural studies of the Ton complex from *E. coli* provide a mechanistic insight into this complex (Celia et al., 2016). It is proposed that the functional unit of the Ton complex contains an ExbB pentamer, an ExbD dimer, and at least one TonB. Electrophysiology experiments suggest that the ExbB-ExbD forms pH-sensitive channels, by which the Ton complex likely harnesses the proton-motive force for energy production and transduction.

Bioinformatic studies indicate that genes of the two TonB systems exist ubiquitously among all *Vibrio* species, and moreover, a third TonB system is even observed in some vibrios and other marine organisms (Kuehl and Crosa, 2010; Kustusch et al., 2011). However, it remains unclear why so many TonB systems are present in the *Vibrio* species. The *V. anguillarum* strains lack HuvA but contain an alternative heme transporter, HuvS, which is able to restore heme transport in a *huvA* mutant (Mouriño et al., 2005). The observation that *huvS* and *huvA* possess similar flanking DNA sequences implies that horizontal transmission and recombination might have occurred and thus be responsible for this genetic diversity (Mouriño et al., 2005).

Furthermore, the *huvA* gene is located in a gene cluster coding for nine heme uptake-related proteins, including HuvA, HuvZ, HuvX, TonB1, ExbB1, ExbD1, HuvB, HuvC, and HuvD (Mouriño et al., 2004). The periplasmic heme-binding protein HuvB delivers periplasmic heme to an inner membrane complex consisting of a permease, HuvC, and an ATPase, HuvD, which subsequently transport heme into the cytosol (Mouriño et al., 2004). Therefore, HuvBCD are required for heme transport, and deletion of either gene results in heme transport deficiencies (Mouriño et al., 2004). HuvZ also plays an import role in heme uptake, and loss of *huvZ* severely affects the growth of cells when heme serves as the sole iron source (Mouriño et al., 2004). Little is known about the function of HuvZ in heme utilization, and in *V. cholerae* it is suggested to have a role in heme storage (Wyckoff et al., 2004). HuvX, a predicted intracellular heme delivery protein in *V. cholerae* (Sekine et al., 2016), is not required for heme uptake in the *V. anguillarum* 775 plasmidless avirulent strain because deletion of *huvX* does not cause obvious differences in growth and heme utilization compared with the wild type (Mouriño et al., 2004). However, it is still under debate whether heme utilization is indeed involved in *V. anguillarum* virulence in nature.

Other Iron Acquisition Systems

Besides the anguibactin/vanchrobactin and heme uptake systems, four operons encoding putative iron transport systems, including transport of unchelated ferrous (*feoABC*) and ferric iron (*fbpABC1* and *fbpABC2*), and siderophore ferrichrome transport (*fhuABCD*), have been identified in the genomes of *V. anguillarum* strains (**Figures 1**, **5**). The presence of different iron transport systems in *V. anguillarum* probably results from differences in growth conditions because siderophores can only promote growth under limited iron conditions that must be insufficient for iron uptake under all environmental conditions. In line with this, all the vibrios examined have been shown to have additional iron acquisition systems (Table S3; Payne et al., 2016).

The ferrous iron transporter FeoABC is speculated to be the most ancient iron transport system and widely found among bacterial species including *Vibrio* species. In *V. cholerae*, all *feoABC* genes are required for ferrous iron uptake although their functions have not been fully characterized (Wyckoff et al., 2006; Weaver et al., 2013). However, it is still unknown how ferrous iron passes through the outer membrane for transport by the Feo system in the periplasm. FbpABC, a ferric iron transporter, is also found in vibrios and has been shown to promote better growth at alkaline pH in *V. cholerae* (Peng et al., 2016). FhuABCD, responsible for siderophore ferrichrome utilization, have been demonstrated to be required for ferrichrome utilization in *V. parahaemolyticus* and *V. cholerae* (Rogers et al., 2000; Funahashi et al., 2009).

Notably, although it has been demonstrated that *V. anguillarum* is capable of using ferric citrate as the only iron source by a siderophore-independent mechanism (Mazoy et al., 1997), we do not find any genes involved in ferric citrate

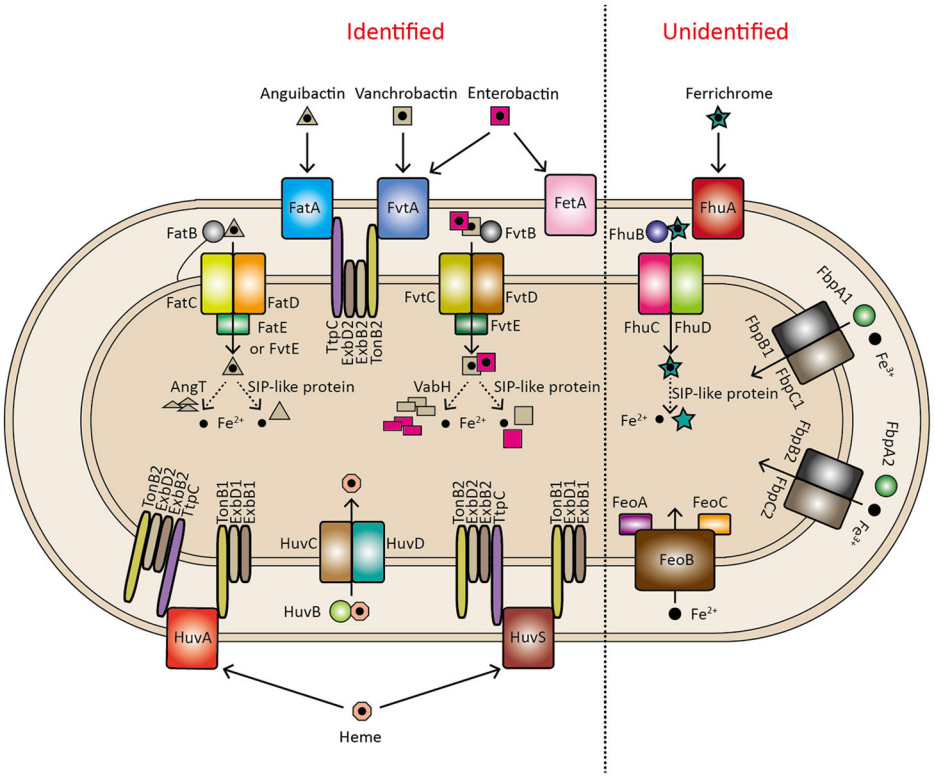

FIGURE 5 | Identified and unidentified iron transport systems in *V. anguillarum*. A ferrisiderophore release model is proposed, indicated by a dashed line, including two mechanisms: degradation of the siderophore (achieved by AngT for anguibactin hydrolysis and VabH for vanchrobactin hydrolysis) and reduction of the ferrisiderophore [achieved by a siderophore-interacting protein (SIP)-like protein].

transport in the genome of *V. anguillarum* or other vibrios. In *P. aeruginosa*, iron delivered by citrate is suggested to enter the cell as Fe^{2+}, and FeoB is further required for citrate-mediated Fe^{2+} uptake (Marshall et al., 2009). Therefore, it is plausible that FeoB of *V. anguillarum* may also play a role in Fe^{2+} uptake from ferric citrate to maintain iron homeostasis.

IRON RELEASE FROM FERRISIDEROPHORES

When iron–siderophore complexes are transported into the cell cytoplasm, bacteria can use different strategies to release iron:

- Via the reduction of ferric iron.
- Via the degradation or modification of siderophores.
- Via both iron reduction and siderophore degradation.

Genes predicted for iron reduction and siderophore degradation occur in the genome of *V. anguillarum*, and proposed pathways are shown in **Figure 5**. VabH, a putative cytoplasmic esterase, exhibits homology to *E. coli* Fes, which can hydrolyze enterobactin during iron release (Brickman and McIntosh, 1992). Therefore, VabH may serve as a vanchrobactin degradation enzyme during ferric-vanchrobactin compound dissociation. Similarly, a putative thioesterase gene, *angT*, may be involved in iron release from ferric-anguibactin. However, deletion of *vabH* or *angT* does not completely block siderophore uptake (Wertheimer et al., 1999; Balado et al., 2006), indicating that additional pathways for iron release may occur. In accordance with this, a nicotinamide adenine dinucleotide phosphate (NADPH)-dependent ferric reductase has been identified in the genomes of *V. anguillarum* strains. It shows high homology to the reported siderophore-interacting proteins (SIP) YqjH of *E. coli* and FscN of *Thermobifida fusca*, which are suggested to participate in iron reduction during ferrisiderophore dissociation (Miethke et al., 2011; Li et al., 2015). Furthermore, Mazoy and Lemos observed that ferric reductase activities of cell fractions are significantly increased in the presence of NADPH compared to its absence (Mazoy and Lemos, 1996a), indicating a functional NADPH-dependent ferric reductase may occur in *V. anguillarum*. In addition, they also found it is only in the cytoplasmic, but not in periplasmic or membrane faction, where ferric reductase activity is stimulated under iron-limiting conditions (Mazoy and Lemos, 1996a). This implies iron release from ferrisiderophore might happen in the cytoplasm. Further investigation of the role of SIP in the ferrisiderophore dissociation pathway will provide more detail to elucidate the strategies deployed by *V. anguillarum* to release iron for utilization.

REGULATION OF IRON TRANSPORT

As excess iron is lethal and may lead to oxidative damage to DNA when free Fe^{2+} reacts with hydrogen peroxide via the Fenton reaction (Imlay, 2002), tight regulation of iron transport is a prerequisite to meet, but not exceed, the requirement for iron. To date, several regulators have been identified in *V. anguillarum* to control the uptake of the iron, including the negative regulators Fur and an antisense RNA (RNAα), and the positive regulators AngR, TAFr, and anguibactin.

In Gram-negative bacteria, Fur is the major global regulator of iron metabolism, which serves as a sensor of intracellular iron concentration. It can bind to a Fe^{2+}-bound dimer at a specific site, termed the Fur box, in the promoter region and thereby negatively regulate the transcription of corresponding genes (Troxell and Hassan, 2013). Therefore, it is not surprising that the Fur protein of *V. anguillarum* blocks or depresses the expression of most genes involved in iron acquisition systems, such as those coding for anguibactin and vanchrobactin synthesis (Salinas and Crosa, 1995; Chen et al., 1996; Di Lorenzo et al., 2004; Alice et al., 2005; Balado et al., 2008), TonB systems (Mouriño et al., 2006), and iron transport systems (Waldbeser et al., 1993; Tolmasky et al., 1994; Chen and Crosa, 1996; Chai et al., 1998; Mouriño et al., 2006; Balado et al., 2008; Naka and Crosa, 2012). In addition to Fur, an antisense RNA, RNAα, is capable of negatively modulating the expression of the *fatA* and *fatB* genes involved in iron transport by specifically binding to *fatA* and *fatB* mRNAs and thus repressing their transcription under iron-rich conditions (Waldbeser et al., 1995; Chen and Crosa, 1996). Moreover, the Fur protein is also crucial for RNAα synthesis and regulates its transcription initiation, which is independent of the iron status of the cell (Chen and Crosa, 1996).

AngR is a bifunctional protein, involved not only in the formation of anguibactin but also in the positive regulation of transport and biosynthesis genes (Salinas et al., 1989; Singer et al., 1991). Although AngR consists of two helix-turn-helix (HTH) regulatory motifs, only the first HTH is essential for gene regulation, as demonstrated by the finding that modulation of an *angR* deletion mutant is restored by a construct containing a frame shift and leaving only the first HTH motif (Wertheimer et al., 1999). These data again suggest that AngR plays an important role in both anguibactin synthesis and regulation of gene expression. The transcription of genes including the iron transport biosynthesis operon (ITBO; **Figure 1**) and *angN* is tightly controlled by AngR, and they display the highest expression level when iron is limited (Actis et al., 1995; Chen and Crosa, 1996; Di Lorenzo et al., 2008). The TAF (*trans*-acting factor) region shown in **Figure 1** is essential for anguibactin biosynthesis and for maximal expression of the ITBO genes, which are achieved by two separate entities: one involved in anguibactin biosynthesis (TAFb) and the other in regulation (TAFr) (Tolmasky et al., 1988; Welch et al., 2000). Studies have demonstrated that TAFr and AngR work in a synergistic manner to modulate the level of anguibactin synthesis under iron-limiting conditions (Salinas et al., 1989; Salinas and Crosa, 1995). In addition, anguibactin by itself is also capable of increasing the transcriptional level of the ITBO, which reaches the highest level when AngR, TAFr, and anguibactin are all acting synergistically (Chen and Crosa, 1996).

Besides iron, many other environmental factors have been identified in vibrios, including *V. anguillarum*, that affect the expression of genes associated with iron transport, such as oxygen, temperature, carbon sources, and quorum sensing molecules (Mou et al., 2013; Payne et al., 2016). Therefore, an expanded search for sensors involved in other environmental signals may lead to a more complete picture of the strategies of iron regulation in *V. anguillarum*.

OUTLOOK

Despite the challenges of iron acquisition in various environments, such as competition with other organisms on host surfaces, or sequestration by the high-affinity iron-binding host proteins lactoferrin and transferrin, growth of *V. anguillarum* is proficient in both host and marine habitats, achieved by multiple iron transport systems. Moreover, there is increasing evidence for the position of iron uptake, especially siderophores, at the crux of the microbial infection process, thereby reducing the appeal of siderophores as antimicrobial targets. In this context, it is important to investigate the whole of the iron acquisition systems of *V. anguillarum*, which will not only provide new insights to explain the evolutionary origin of versatile iron transport systems but also supply more evidence to understand the pathogenicity of this organism.

However, despite the exciting developments in understanding siderophore synthesis and ferrisiderophore transport in some vibrios, such as *V. anguillarum* and *V. cholerae*, there are many unsolved aspects of the iron uptake systems. For example, the mechanisms that govern the synthesis of anguibactin or vanchrobactin are still not fully elucidated, and how proteins are regulated for anguibactin or vanchrobactin synthesis is not yet well understood. How is mature siderophore secreted to the environment, and how is the iron released to the periplasm or cytoplasm from the ferric-siderophore complex? To answer these questions, an effective way is required to monitor anguibactin or vanchrobactin in real time. Finally, the different iron uptake systems that are responsible for the utilization of diverse iron sources will need to be established at the genetic level in order to uncover the relationship between iron uptake and virulence.

AUTHOR CONTRIBUTIONS

All authors listed have made a substantial, direct and intellectual contribution to the work, and approved it for publication.

FUNDING

YL was supported by the China Postdoctoral Science Foundation (no. 2016M602200). QM was supported by grants from the "1000 Talents Program" of China, "100 Talents Program" of the Chinese Academy of Sciences, and "AoShan Talents Program" of Qingdao National Laboratory for Marine Science and Technology (no. 2015ASTP).

ACKNOWLEDGMENTS

Wenteng Xu, Yellow Sea Fisheries Research Institute, Chinese Academy of Fishery Sciences, is greatly acknowledged for language proofing.

SUPPLEMENTARY MATERIAL

The Supplementary Material for this article can be found online at: http://journal.frontiersin.org/article/10.3389/fcimb.2017.00342/full#supplementary-material

REFERENCES

Actis, L. A., Fish, W., Crosa, J. H., Kellerman, K., Ellenberger, S. R., Hauser, F. M., et al. (1986). Characterization of anguibactin, a novel siderophore from *Vibrio anguillarum* 775(pJM1). *J. Bacteriol.* 167, 57–65. doi: 10.1128/jb.167.1.57-65.1986

Actis, L. A., Tolmasky, M. E., Crosa, L. M., and Crosa, J. H. (1995). Characterization and regulation of the expression of FatB, an iron transport protein encoded by the pJM1 virulence plasmid. *Mol. Microbiol.* 17, 197–204. doi: 10.1111/j.1365-2958.1995.mmi_17010197.x

Actis, L. A., Tolmasky, M. E., Farrell, D. H., and Crosa, J. H. (1988). Genetic and molecular characterization of essential components of the *Vibrio anguillarum* plasmid mediated iron transport system. *J. Biol. Chem.* 263, 2853–2860.

Alice, A. F., Lopez, C. S., and Crosa, J. H. (2005). Plasmid- and chromosome-encoded redundant and specific functions are involved in biosynthesis of the siderophore anguibactin in *Vibrio anguillarum* 775: a case of chance and necessity? *J. Bacteriol.* 187, 2209–2214. doi: 10.1128/JB.187.6.2209-2214.2005

Balado, M., Osorio, C. R., and Lemos, M. L. (2006). A gene cluster involved in the biosynthesis of vanchrobactin, a chromosome-encoded siderophore produced by *Vibrio anguillarum*. *Microbiology* 152, 3517–3528. doi: 10.1099/mic.0.29298-0

Balado, M., Osorio, C. R., and Lemos, M. L. (2008). Biosynthetic and regulatory elements involved in the production of the siderophore vanchrobactin in *Vibrio anguillarum*. *Microbiology* 154, 1400–1413. doi: 10.1099/mic.0.2008/016618-0

Balado, M., Osorio, C. R., and Lemos, M. L. (2009). FvtA is the receptor for the siderophore vanchrobactin in *Vibrio anguillarum*: utility as a route of entry for vanchrobactin analogues. *Appl. Environ. Microbiol.* 75, 2775–2783. doi: 10.1128/AEM.02897-08

Barancin, C. E., Smoot, J. C., Findlay, R. H., and Actis, L. A. (1998). Plasmid-mediated histamine biosynthesis in the bacterial fish pathogen *Vibrio anguillarum*. *Plasmid* 39, 235–244. doi: 10.1006/plas.1998.1345

Bay, L., Larsen, J. L., and Leisner, J. J. (2007). Distribution of three genes involved in the pJM1 iron-sequestering system in various *Vibrio anguillarum* serogroups. *Syst. Appl. Microbiol.* 30, 85–92. doi: 10.1016/j.syapm.2006.03.006

Bina, X. R., Provenzano, D., Nguyen, N., and Bina, J. E. (2008). *Vibrio cholerae* RND family efflux systems are required for antimicrobial resistance, optimal virulence factor production, and colonization of the infant mouse small intestine. *Infect. Immun.* 76, 3595–3605. doi: 10.1128/IAI.01620-07

Brickman, T. J., and McIntosh, M. A. (1992). Overexpression and purification of ferric enterobactin esterase from *Escherichia coli*. demonstration of enzymatic hydrolysis of enterobactin and its iron complex. *J. Biol. Chem.* 267, 12350–12355.

Celia, H., Noinaj, N., Zakharov, S. D., Bordignon, E., Botos, I., Santamaria, M., et al. (2016). Structural insight into the role of the Ton complex in energy transduction. *Nature* 538, 60–65. doi: 10.1038/nature19757

Chai, S. H., Welch, T. J., and Crosa, J. H. (1998). Characterization of the interaction between Fur and the iron transport promoter of the virulence plasmid in *Vibrio anguillarum*. *J. Biol. Chem.* 273, 33841–33847. doi: 10.1074/jbc.273.50.33841

Chen, Q., and Crosa, J. H. (1996). Antisense RNA, Fur, iron, and the regulation of iron transport genes in *Vibrio anguillarum*. *J. Biol. Chem.* 271, 18885–18891. doi: 10.1074/jbc.271.31.18885

Chen, Q., Wertheimer, A. M., Tolmasky, M. E., and Crosa, J. H. (1996). The AngR protein and the siderophore anguibactin positively regulate the expression of iron-transport genes in *Vibrio anguillarum*. *Mol. Microbiol.* 22, 127–134. doi: 10.1111/j.1365-2958.1996.tb02662.x

Conchas, R. F., Lemos, M. L., Barja, J. L., and Toranzo, A. E. (1991). Distribution of plasmid- and chromosome-mediated iron uptake systems in *Vibrio anguillarum* strains of different origins. *Appl. Environ. Microbiol.* 57, 2956–2962.

Crosa, J. H., Payne, S. M., and Mey, A. R. (2004). *Iron Transport in Bacteria*. Washington, DC: ASM Press.

Croxatto, A., Lauritz, J., Chen, C., and Milton, D. L. (2007). *Vibrio anguillarum* colonization of rainbow trout integument requires a DNA locus involved in exopolysaccharide transport and biosynthesis. *Environ. Microbiol.* 9, 370–382. doi: 10.1111/j.1462-2920.2006.01147.x

Di Lorenzo, M., Poppelaars, S., Stork, M., Nagasawa, M., Tolmasky, M. E., and Crosa, J. H. (2004). A nonribosomal peptide synthetase with a novel domain organization is essential for siderophore biosynthesis in *Vibio anguillarum*. *J. Bacteriol.* 186, 7327–7336. doi: 10.1128/JB.186.21.7327-7336.2004

Di Lorenzo, M., Stork, M., and Crosa, J. H. (2011). Genetic and biochemical analyses of chromosome and plasmid gene homologues encoding ICL and ArCP domains in *Vibrio anguillarum* strain 775. *Biometals* 24, 629–643. doi: 10.1007/s10534-011-9416-7

Di Lorenzo, M., Stork, M., Naka, H., Tolmasky, M. E., and Crosa, J. H. (2008). Tandem heterocyclization domains in a nonribosomal peptide synthetase essential for siderophore biosynthesis in *Vibrio anguillarum*. *Biometals* 21, 635–648. doi: 10.1007/s10534-008-9149-4

Du, J. S., Deng, T., and Ma, Q. J. (2017). Crystal structures of the isochorismatase domains from *Vibrio anguillarum*. *Biochem. Biophys. Res. Commun.* 490, 827–833. doi: 10.1016/j.bbrc.2017.06.125

Funahashi, T., Tanabe, T., Shiuchi, K., Nakao, H., and Yamamoto, S. (2009). Identification and characterization of genes required for utilization of desferri-ferrichrome and aerobactin in *Vibrio parahaemolyticus*. *Biol. Pharm. Bull.* 32, 359–365. doi: 10.1248/bpb.32.359

Furrer, J. L., Sanders, D. N., Hook-Barnard, I. G., and McIntosh, M. A. (2002). Export of the siderophore enterobactin in *Escherichia coli*: involvement of a 43 kDa membrane exporter. *Mol. Microbiol.* 44, 1225–1234. doi: 10.1046/j.1365-2958.2002.02885.x

Hannauer, M., Braud, A., Hoegy, F., Ronot, P., Boos, A., and Schalk, I. J. (2012). The PvdRT-OpmQ efflux pump controls the metal selectivity of the iron uptake pathway mediated by the siderophore pyoverdine in *Pseudomonas aeruginosa*. *Environ. Microbiol.* 14, 1696–1708. doi: 10.1111/j.1462-2920.2011.02674.x

Hannauer, M., Yeterian, E., Martin, L. W., Lamont, I. L., and Schalk, I. J. (2010). An efflux pump is involved in secretion of newly synthesized siderophore by *Pseudomonas aeruginosa*. *FEBS Lett.* 584, 4751–4755. doi: 10.1016/j.febslet.2010.10.051

Hantke, K. (1981). Regulation of ferric iron transport in *Escherichia coli* K12 isolation of a constitutive mutant. *Mol. Gen. Genet.* 182, 288–292. doi: 10.1007/BF00269672

Hirono, I., Masuda, T., and Aoki, T. (1996). Cloning and detection of the hemolysin gene of *Vibrio anguillarum*. *Microb. Pathog.* 21, 173–182. doi: 10.1006/mpat.1996.0052

Horiyama, T., and Nishino, K. (2014). AcrB, AcrD, and MdtABC multidrug efflux systems are involved in enterobactin export in *Escherichia coli*. *PLoS ONE* 9:e108642. doi: 10.1371/journal.pone.0108642

Imlay, J. A. (2002). How oxygen damages microbes: oxygen tolerance and obligate anaerobiosis. *Adv. Microb. Physiol.* 46, 111–153. doi: 10.1016/S0065-2911(02)46003-1

Köster, W. L., Actis, L. A., Waldbeser, L. S., Tolmasky, M. E., and Crosa, J. H. (1991). Molecular characterization of the iron transport system mediated by the pJM1 plasmid in *Vibrio anguillarum* 775. *J. Biol. Chem.* 266, 23829–23833.

Kuehl, C. J., and Crosa, J. H. (2009). Molecular and genetic characterization of the TonB2-cluster TtpC protein in pathogenic vibrios. *Biometals* 22, 109–115. doi: 10.1007/s10534-008-9194-z

Kuehl, C. J., and Crosa, J. H. (2010). The TonB energy transduction systems in *Vibrio* species. *Future Microbiol.* 5, 1403–1412. doi: 10.2217/fmb.10.90

Kunkle, D. E., Bina, X. R., and Bina, J. E. (2017). The *Vibrio cholerae* VexGH RND efflux system maintains cellular homeostasis by efluxing vibriobactin. *mBio* 8:e00126-17. doi: 10.1128/mBio.00126-17

Kustusch, R. J., Kuehl, C. J., and Crosa, J. H. (2011). Power plays: iron transport and energy transduction in pathogenic vibrios. *Biometals* 24, 559–566. doi: 10.1007/s10534-011-9437-2

Lemos, M. L., and Osorio, C. R. (2007). Heme, an iron supply for vibrios pathogenic for fish. *Biometals* 20, 615–626. doi: 10.1007/s10534-006-9053-8

Lemos, M. L., Salinas, P., Toranzo, A. E., Barja, J. L., and Crosa, J. H. (1988). Chromosome-mediated iron uptake system in pathogenic strains of *Vibrio anguillarum*. *J. Bacteriol.* 170, 1920–1925. doi: 10.1128/jb.170.4.1920-1925.1988

Li, K. H., Chen, W. H., and Bruner, S. D. (2015). Structure and mechanism of the siderophore-interacting protein from the fuscachelin gene cluster of *Thermobifida fusca*. *Biochemistry* 54, 3989–4000. doi: 10.1021/acs.biochem.5b00354

Li, L., Mou, X. Y., and Nelson, D. R. (2013). Characterization of Plp, a phosphatidylcholine-specific phospholipase and hemolysin of *Vibrio anguillarum*. *BMC Microbiol.* 13:271. doi: 10.1186/1471-2180-13-271

Li, L., Rock, J. L., and Nelson, D. R. (2008). Identification and characterization of a repeat-in-toxin gene cluster in *Vibrio anguillarum*. *Infect. Immun.* 76, 2620–2632. doi: 10.1128/IAI.01308-07

Liu, Q., Ma, Y., Wu, H. Z., Shao, M. F., Liu, H. F., and Zhang, Y. X. (2004). Cloning, identification and expression of an *entE* homologue *angE* from *Vibrio anguillarum* serotype O1. *Arch. Microbiol.* 181, 287–293. doi: 10.1007/s00203-004-0652-x

Lopez, C. S., Alice, A. F., Chakraborty, R., and Crosa, J. H. (2007). Identification of amino acid residues required for ferric-anguibactin transport in the outer-membrane receptor FatA of *Vibrio anguillarum*. *Microbiology* 153, 570–584. doi: 10.1099/mic.0.2006/001735-0

Lopez, C. S., and Crosa, J. H. (2007). Characterization of ferric-anguibactin transport in *Vibrio anguillarum*. *Biometals* 20, 393–403. doi: 10.1007/s10534-007-9084-9

Marshall, B., Stintzi, A., Gilmour, C., Meyer, J. M., and Poole, K. (2009). Citrate-mediated iron uptake in *Pseudomonas aeruginosa*: involvement of the citrate-inducible FecA receptor and the FeoB ferrous iron transporter. *Microbiology* 155, 305–315. doi: 10.1099/mic.0.023531-0

Martin, J. H., Gordon, R. M., and Fitzwater, S. E. (1991). Iron limitation? The case for iron. *Limnol. Oceanogr.* 36, 1793–1802. doi: 10.4319/lo.1991.36.8.1793

Mazoy, R., Botana, L. M., and Lemos, M. L. (1997). Iron uptake from ferric citrate by *Vibrio anguillarum*. *FEMS Microbiol. Lett.* 154, 145–150. doi: 10.1111/j.1574-6968.1997.tb12636.x

Mazoy, R., and Lemos, M. L. (1996a). Ferric-reductase activities in whole cells and cell fractions of *Vibrio (Listonella) anguillarum*. *Microbiol-UK* 142, 3187–3193. doi: 10.1099/13500872-142-11-3187

Mazoy, R., and Lemos, M. L. (1996b). Identification of heme-binding proteins in the cell membranes of *Vibrio anguillarum*. *FEMS Microbiol. Lett.* 135, 265–270. doi: 10.1111/j.1574-6968.1996.tb07999.x

Mazoy, R., Osorio, C. R., Toranzo, A. E., and Lemos, M. L. (2003). Isolation of mutants of *Vibrio anguillarum* defective in haeme utilisation and cloning of *huvA*, a gene coding for an outer membrane protein involved in the use of haeme as iron source. *Arch. Microbiol.* 179, 329–338. doi: 10.1007/s00203-003-0529-4

Mazoy, R., Vazquez, F., and Lemos, M. L. (1996). Isolation of heme-binding proteins from *Vibrio anguillarum* using affinity chromatography. *FEMS Microbiol. Lett.* 141, 19–23. doi: 10.1111/j.1574-6968.1996.tb08357.x

Miethke, M., Hou, J., and Marahiel, M. A. (2011). The siderophore-interacting protein YqjH acts as a ferric reductase in different iron assimilation pathways of *Escherichia coli*. *Biochemistry* 50, 10951–10964. doi: 10.1021/bi201517h

Milton, D. L., Norqvist, A., and Wolfwatz, H. (1992). Cloning of a metalloprotease gene involved in the virulence mechanism of *Vibrio anguillarum*. *J. Bacteriol.* 174, 7235–7244. doi: 10.1128/jb.174.22.7235-7244.1992

Mo, Z. L., Guo, D. S., Mao, Y. X., Ye, X. H., Zou, Y. X., Xiao, P., et al. (2010). Identification and characterization of the *Vibrio anguillarum prtV* gene encoding a new metalloprotease. *Chin. J. Oceanol. Limnol.* 28, 55–61. doi: 10.1007/s00343-010-9246-4

Mou, X. Y., Spinard, E. J., Driscoll, M. V., Zhao, W. J., and Nelson, D. R. (2013). H-NS is a negative regulator of the two hemolysin/cytotoxin gene clusters in *Vibrio anguillarum*. *Infect. Immun.* 81, 3566–3576. doi: 10.1128/IAI.00506-13

Mouriño, S., Osorio, C. R., and Lemos, M. L. (2004). Characterization of heme uptake cluster genes in the fish pathogen *Vibrio anguillarum*. *J. Bacteriol.* 186, 6159–6167. doi: 10.1128/JB.186.18.6159-6167.2004

Mouriño, S., Osorio, C. R., Lemos, M. L., and Crosa, J. H. (2006). Transcriptional organization and regulation of the *Vibrio anguillarum* heme uptake gene cluster. *Gene* 374, 68–76. doi: 10.1016/j.gene.2006.01.014

Mouriño, S., Rodriguez-Ares, I., Osorio, C. R., and Lemos, M. L. (2005). Genetic variability of the heme uptake system among different strains of the fish pathogen *Vibrio anguillarum*: identification of a new heme receptor. *Appl. Environ. Microbiol.* 71, 8434–8441. doi: 10.1128/aem.71.12.8434-8441.2005

Naka, H., Actis, L. A., and Crosa, J. H. (2013a). The anguibactin biosynthesis and transport genes are encoded in the chromosome of *Vibrio harveyi*: a possible evolutionary origin for the pJM1 plasmid-encoded system of *Vibrio anguillarum*? *Microbiology* 2, 182–194. doi: 10.1002/mbo3.65

Naka, H., and Crosa, J. H. (2011). Genetic determinants of virulence in the marine fish pathogen *Vibrio anguillarum*. *Fish Pathol.* 46, 1–10. doi: 10.3147/jsfp.46.1

Naka, H., and Crosa, J. H. (2012). Identification and characterization of a novel outer membrane protein receptor FetA for ferric enterobactin transport in *Vibrio anguillarum* 775 (pJM1). *Biometals* 25, 125–133. doi: 10.1007/s10534-011-9488-4

Naka, H., Liu, M. Q., Actis, L. A., and Crosa, J. H. (2013b). Plasmid- and chromosome-encoded siderophore anguibactin systems found in marine vibrios: biosynthesis, transport and evolution. *Biometals* 26, 537–547. doi: 10.1007/s10534-013-9629-z

Naka, H., Liu, M. Q., and Crosa, J. H. (2013c). Two ABC transporter systems participate in siderophore transport in the marine pathogen *Vibrio anguillarum* 775 (pJM1). *FEMS Microbiol. Lett.* 341, 79–86. doi: 10.1111/1574-6968.12092

Naka, H., Lopez, C. S., and Crosa, J. H. (2008). Reactivation of the vanchrobactin siderophore system of *Vibrio anguillarum* by removal of a chromosomal insertion sequence originated in plasmid pJM1 encoding the anguibactin siderophore system. *Environ. Microbiol.* 10, 265–277. doi: 10.1111/j.1462-2920.2007.01450.x

Naka, H., Lopez, C. S., and Crosa, J. H. (2010). Role of the pJM1 plasmid-encoded transport proteins FatB, C and D in ferric anguibactin uptake in the fish pathogen *Vibrio anguillarum*. *Environ. Microbiol. Re.* 2, 104–111. doi: 10.1111/j.1758-2229.2009.00110.x

Ormonde, P., Horstedt, P., O'toole, R., and Milton, D. L. (2000). Role of motility in adherence to and invasion of a fish cell line by *Vibrio anguillarum*. *J. Bacteriol.* 182, 2326–2328. doi: 10.1128/JB.182.8.2326-2328.2000

O'Toole, R., Lundberg, S., Fredriksson, S. A., Jansson, A., Nilsson, B., and Wolf-Watz, H. (1999). The chemotactic response of *Vibrio anguillarum* to fish intestinal mucus is mediated by a combination of multiple mucus components. *J. Bacteriol.* 181, 4308–4317.

Payne, S. M., Mey, A. R., and Wyckoff, E. E. (2016). *Vibrio* iron transport: evolutionary adaptation to life in multiple environments. *Microbiol. Mol. Biol. Rev.* 80, 69–90. doi: 10.1128/MMBR.00046-15

Pedersen, K., Grisez, L., Van Houdt, R., Tiainen, T., Ollevier, F., and Larsen, J. L. (1999). Extended serotyping scheme for *Vibrio anguillarum* with the definition and characterization of seven provisional O-serogroups. *Curr. Microbiol.* 38, 183–189. doi: 10.1007/PL00006784

Peng, E. D., Wyckoff, E. E., Mey, A. R., Fisher, C. R., and Payne, S. M. (2016). Nonredundant roles of iron acquisition systems in *Vibrio cholerae*. *Infect. Immun.* 84, 511–523. doi: 10.1128/IAI.01301-15

Rahman, M. M., Matsuo, T., Ogawa, W., Koterasawa, M., Kuroda, T., and Tsuchiya, T. (2007). Molecular cloning and characterization of all RND-Type efflux transporters in *Vibrio cholerae* non-O1. *Microbiol. Immunol.* 51, 1061–1070. doi: 10.1111/j.1348-0421.2007.tb04001.x

Rock, J. L., and Nelson, D. R. (2006). Identification and characterization of a hemolysin gene cluster in *Vibrio anguillarum*. *Infect. Immun.* 74, 2777–2786. doi: 10.1128/IAI.74.5.2777-2786.2006

Rodkhum, C., Hirono, I., Crosa, J. H., and Aoki, T. (2005). Four novel hemolysin genes of *Vibrio anguillarum* and their virulence to rainbow trout. *Microb. Pathog.* 39, 109–119. doi: 10.1016/j.micpath.2005.06.004

Rogers, M. B., Sexton, J. A., Decastro, G. J., and Calderwood, S. B. (2000). Identification of an operon required for ferrichrome iron utilization in *Vibrio cholerae*. *J. Bacteriol.* 182, 2350–2353. doi: 10.1128/JB.182.8.2350-2353.2000

Salinas, P. C., and Crosa, J. H. (1995). Regulation of *angR*, a gene with regulatory and biosynthetic functions in the pJM1 plasmid-mediated iron uptake system of *Vibrio anguillarum*. *Gene* 160, 17–23. doi: 10.1016/0378-1119(95)00213-P

Salinas, P. C., Tolmasky, M. E., and Crosa, J. H. (1989). Regulation of the iron uptake system in *Vibrio anguillarum*: evidence for a cooperative effect between two transcriptional activators. *Proc. Natl. Acad. Sci. U.S.A.* 86, 3529–3533. doi: 10.1073/pnas.86.10.3529

Schalk, I. J., and Guillon, L. (2013). Pyoverdine biosynthesis and secretion in *Pseudomonas aeruginosa*: implications for metal homeostasis. *Environ. Microbiol.* 15, 1661–1673. doi: 10.1111/1462-2920.12013

Sekine, Y., Tanzawa, T., Tanaka, Y., Ishimori, K., and Uchida, T. (2016). Cytoplasmic heme-binding protein (HutX) from *Vibrio cholerae* is an intracellular heme transport protein for the heme-degrading enzyme, HutZ. *Biochemistry* 55, 884–893. doi: 10.1021/acs.biochem.5b01273

Singer, J. T., Schmidt, K. A., and Reno, P. W. (1991). Polypeptides p40, pOM2, and pAngR are required for iron uptake and for virulence of the marine fish pathogen *Vibrio anguillarum* 775. *J. Bacteriol.* 173, 1347–1352. doi: 10.1128/jb.173.3.1347-1352.1991

Soengas, R. G., Larrosa, M., Balado, M., Rodriguez, J., Lemos, M. L., and Jimenez, C. (2008). Synthesis and biological activity of analogues of vanchrobactin, a siderophore from *Vibrio anguillarum* serotype O2. *Org. Biomol. Chem.* 6, 1278–1287. doi: 10.1039/b719713f

Stork, M., Di Lorenzo, M., Mourino, S., Osorio, C. R., Lemos, M. L., and Crosa, J. H. (2004). Two tonB systems function in iron transport in *Vibrio anguillarum*, but only one is essential for virulence. *Infect. Immun.* 72, 7326–7329. doi: 10.1128/IAI.72.12.7326-7329.2004

Stork, M., Otto, B. R., and Crosa, J. H. (2007). A novel protein, TtpC, is a required component of the TonB2 complex for specific iron transport in the pathogens *Vibrio anguillarum* and *Vibrio cholerae*. *J. Bacteriol.* 189, 1803–1815. doi: 10.1128/JB.00451-06

Tolmasky, M. E., Actis, L. A., and Crosa, J. H. (1988). Genetic analysis of the iron uptake region of the *Vibrio anguillarum* plasmid pJM1: molecular cloning of genetic determinants encoding a novel trans activator of siderophore biosynthesis. *J. Bacteriol.* 170, 1913–1919. doi: 10.1128/jb.170.4.1913-1919.1988

Tolmasky, M. E., Actis, L. A., and Crosa, J. H. (1995). A histidine decarboxylase gene encoded by the *Vibrio anguillarum* plasmid pJM1 is essential for virulence: histamine is a precursor in the biosynthesis of anguibactin. *Mol. Microbiol.* 15, 87–95. doi: 10.1111/j.1365-2958.1995.tb02223.x

Tolmasky, M. E., Wertheimer, A. M., Actis, L. A., and Crosa, J. H. (1994). Characterization of the *Vibrio anguillarum fur* gene: role in regulation of expression of the FatA outer membrane protein and catechols. *J. Bacteriol.* 176, 213–220. doi: 10.1128/jb.176.1.213-220.1994

Toranzo, A. E., Magarinos, B., and Romalde, J. L. (2005). A review of the main bacterial fish diseases in mariculture systems. *Aquaculture* 246, 37–61. doi: 10.1016/j.aquaculture.2005.01.002

Troxell, B., and Hassan, H. M. (2013). Transcriptional regulation by ferric uptake regulator (Fur) in pathogenic bacteria. *Front. Cell. Infect. Microbiol.* 3:59. doi: 10.3389/fcimb.2013.00059

Varina, M., Denkin, S. M., Staroscik, A. M., and Nelson, D. R. (2008). Identification and characterization of *epp*, the secreted processing protease for the *Vibrio anguillarum* EmpA metalloprotease. *J. Bacteriol.* 190, 6589–6597. doi: 10.1128/JB.00535-08

Waldbeser, L. S., Chen, Q. A., and Crosa, J. H. (1995). Antisense RNA regulation of the *fatB* iron transport protein gene in *Vibrio anguillarum*. *Mol. Microbiol.* 17, 747–756. doi: 10.1111/j.1365-2958.1995.mmi_17040747.x

Waldbeser, L. S., Tolmasky, M. E., Actis, L. A., and Crosa, J. H. (1993). Mechanisms for negative regulation by iron of the *fatA* outer membrane protein gene expression in *Vibrio anguillarum* 775. *J. Biol. Chem.* 268, 10433–10439.

Walter, M. A., Potter, S. A., and Crosa, J. H. (1983). Iron uptake system mediated by *Vibrio anguillarum* plasmid pJM1. *J. Bacteriol.* 156, 880–887.

Wang, Q. Y., Liu, Q., Cao, X. D., Yang, M. J., and Zhang, Y. X. (2008). Characterization of two TonB systems in marine fish pathogen *Vibrio alginolyticus*: their roles in iron utilization and virulence. *Arch. Microbiol.* 190, 595–603. doi: 10.1007/s00203-008-0407-1

Weaver, E. A., Wyckoff, E. E., Mey, A. R., Morrison, R., and Payne, S. M. (2013). FeoA and FeoC are essential components of the *Vibrio cholerae* ferrous iron uptake system, and FeoC interacts with FeoB. *J. Bacteriol.* 195, 4826–4835. doi: 10.1128/JB.00738-13

Welch, T. J., Chai, S. H., and Crosa, J. H. (2000). The overlapping *angB* and *angG* genes are encoded within the *trans*-acting factor region of the virulence plasmid in *Vibrio anguillarum*: essential role in siderophore biosynthesis. *J. Bacteriol.* 182, 6762–6773. doi: 10.1128/JB.182.23.6762-6773.2000

Welch, T. J., and Crosa, J. H. (2005). Novel role of the lipopolysaccharide O1 side chain in ferric siderophore transport and virulence of *Vibrio anguillarum*. *Infect. Immun.* 73, 5864–5872. doi: 10.1128/IAI.73.9.5864-5872.2005

Wertheimer, A. M., Verweij, W., Chen, Q., Crosa, L. M., Nagasawa, M., Tolmasky, M. E., et al. (1999). Characterization of the *angR* gene of *Vibrio anguillarum*: essential role in virulence. *Infect. Immun.* 67, 6496–6509.

Wolf, M. K., and Crosa, J. H. (1986). Evidence for the role of a siderophore in promoting *Vibrio anguillarum* infections. *J. Gen. Microbiol.* 132, 2949–2952. doi: 10.1099/00221287-132-10-2949

Wyckoff, E. E., Mey, A. R., Leimbach, A., Fisher, C. F., and Payne, S. M. (2006). Characterization of ferric and ferrous iron transport systems in *Vibrio cholerae*. *J. Bacteriol.* 188, 6515–6523. doi: 10.1128/JB.00626-06

Wyckoff, E. E., Schmitt, M., Wilks, A., and Payne, S. M. (2004). HutZ is required for efficient heme utilization in *Vibrio cholerae*. *J. Bacteriol.* 186, 4142–4151. doi: 10.1128/JB.186.13.4142-4151.2004

Xu, Z., Wang, Y., Han, Y., Chen, J., and Zhang, X. H. (2011). Mutation of a novel virulence-related gene *mltD* in *Vibrio anguillarum* enhances lethality in zebra fish. *Res. Microbiol.* 162, 144–150. doi: 10.1016/j.resmic.2010.08.003

Yang, H., Chen, J. X., Yang, G. P., Zhang, X. H., Li, Y., and Wang, M. (2007). Characterization and pathogenicity of the zinc metalloprotease EmpA of *Vibrio anguillarum* expressed in *Escherichia coli*. *Curr. Microbiol.* 54, 244–248. doi: 10.1007/s00284-006-0495-6

Yeterian, E., Martin, L. W., Lamont, I. L., and Schalk, I. J. (2010). An efflux pump is required for siderophore recycling by *Pseudomonas aeruginosa*. *Environ. Microbiol. Rep.* 2, 412–418. doi: 10.1111/j.1758-2229.2009.00115.x

Conflict of Interest Statement: The authors declare that the research was conducted in the absence of any commercial or financial relationships that could be construed as a potential conflict of interest.

frontiers in Cellular and Infection Microbiology

REVIEW
published: 06 November 2017
doi: 10.3389/fcimb.2017.00460

Iron Acquisition Mechanisms and Their Role in the Virulence of *Burkholderia* Species

*Aaron T. Butt and Mark S. Thomas**

Department of Infection, Immunity and Cardiovascular Disease, Faculty of Medicine, Dentistry and Health, University of Sheffield, Sheffield, United Kingdom

Burkholderia is a genus within the *β-Proteobacteriaceae* that contains at least 90 validly named species which can be found in a diverse range of environments. A number of pathogenic species occur within the genus. These include *Burkholderia cenocepacia* and *Burkholderia multivorans,* opportunistic pathogens that can infect the lungs of patients with cystic fibrosis, and are members of the *Burkholderia cepacia* complex (Bcc). *Burkholderia pseudomallei* is also an opportunistic pathogen, but in contrast to Bcc species it causes the tropical human disease melioidosis, while its close relative *Burkholderia mallei* is the causative agent of glanders in horses. For these pathogens to survive within a host and cause disease they must be able to acquire iron. This chemical element is essential for nearly all living organisms due to its important role in many enzymes and metabolic processes. In the mammalian host, the amount of accessible free iron is negligible due to the low solubility of the metal ion in its higher oxidation state and the tight binding of this element by host proteins such as ferritin and lactoferrin. As with other pathogenic bacteria, *Burkholderia* species have evolved an array of iron acquisition mechanisms with which to capture iron from the host environment. These mechanisms include the production and utilization of siderophores and the possession of a haem uptake system. Here, we summarize the known mechanisms of iron acquisition in pathogenic *Burkholderia* species and discuss the evidence for their importance in the context of virulence and the establishment of infection in the host. We have also carried out an extensive bioinformatic analysis to identify which siderophores are produced by each *Burkholderia* species that is pathogenic to humans.

Keywords: *Burkholderia,* iron, siderophores, haem uptake, cystic fibrosis, melioidosis

OPEN ACCESS

Edited by:
Pierre Cornelis,
Vrije Universiteit Brussel, Belgium

Reviewed by:
Vittorio Venturi,
International Centre for Genetic Engineering and Biotechnology, India
Jonathan Mark Warawa,
University of Louisville, United States

****Correspondence:***
Mark S. Thomas
m.s.thomas@shef.ac.uk

Received: *18 August 2017*
Accepted: *18 October 2017*
Published: *06 November 2017*

Citation:
Butt AT and Thomas MS (2017) Iron Acquisition Mechanisms and Their Role in the Virulence of Burkholderia Species. Front. Cell. Infect. Microbiol. 7:460. doi: 10.3389/fcimb.2017.00460

THE ROLE OF IRON IN BACTERIA AND SOURCES OF IRON WITHIN THE HOST

Iron mainly occurs in either of two oxidation states in biological systems, Fe^{2+} and Fe^{3+} (also referred to as Fe(II) and Fe(III) or ferrous and ferric, respectively), the latter being the oxidized form that also prevails in the earth's crust, whereas the former is favored by low pH and low oxygen concentrations (Sanchez et al., 2017). It is the ability of iron to be interconverted between these two states that is the basis of many redox reactions that occur in cells (Andrews et al., 2003). For almost all species of bacteria, iron is essential as it is an important component of many proteins. It may occur as part of the haem cofactor, as in cytochromes and haem-type catalases, or as an iron-sulfur

center, as in ferredoxins, rubredoxins, nitrogenase, sulfite reductase, and other iron-sulfur proteins, or as mono- or dinuclear non-haem iron that occurs in Fe-dependent superoxide dismutase and in class Ia ribonucleotide reductases, respectively (Caza and Kronstad, 2013). However, despite the relatively high iron content within humans and animals, it is not freely available due to sequestration by proteins that include hemoglobin, transferrin, lactoferrin, and ferritin, and the fact that it is largely present in the intracellular compartment (Skaar, 2010). This presents a problem to pathogenic microbes that demands the possession of high affinity iron capturing systems if they are to cope with the otherwise bacteriostatic environment. The reader is referred to the following reviews for a more comprehensive discussion of this subject (Nairz et al., 2010; Skaar, 2010; Parrow et al., 2013; Runyen-Janecky, 2013).

THE GENUS *BURKHOLDERIA*

Burkholderia is a genus within the *β-Proteobacteriaceae* that contains at least 90 validly named species but will almost certainly include many more (Depoorter et al., 2016). Members of the genus are diverse and may be found as free-living species within soil or water, or in association with other hosts, including plants, fungi, animals and humans (Smith et al., 1995; Parke and Gurian-Sherman, 2001). They contain large genomes in the range of 7–9 Mb that are typically organized into two or three chromosomes. Based on 16S rRNA sequences, two major clades account for almost all of the currently described species (the endosymbionts *B. rhizoxinica* and *B. endofungorum* being the two exceptions; **Figure 1**). One clade consists of a large group of environmental and plant-associated species referred to as the *Burkholderia xenovorans* group, together with the deeper branching species *B. caryophylli*, *B. soli,* and *B. symbiotica*. The other clade consists of two large groups [the *B. glathei* group and the *B. cepacia* complex (or Bcc)] and two smaller groups (the *Burkholderia pseudomallei* group and a plant pathogenic group consisting of *Burkholderia gladioli*, *B. glumae,* and *B. plantarii*) (Depoorter et al., 2016). More recently, most of the non-pathogenic species (i.e., the *B. xenovorans* and *B. glathei* groups along with *B. caryophylli*, *B. soli,* and *B. symbiotica*) have been transferred to the new genus *Paraburkholderia* (Sawana et al., 2014; Oren and Garrity, 2015) and subsequently the *B. glathei* group has been transferred to the new genus *Caballeronia* (Dobritsa and Samadpour, 2016; **Figure 1**), although it is not clear whether the new classification schemes will be accepted by the scientific community (Depoorter et al., 2016). For the purposes of this review we will refer to all species as belonging to the genus *Burkholderia* (whichever classification scheme is adopted, the pathogenic species will remain within the genus *Burkholderia*). Of the pathogenic species, members of the Bcc and *B. pseudomallei* group can cause life-threatening infections in humans, and this feature will be discussed in this review in the context of their iron acquisition mechanisms. The phytopathogen *B. gladioli* also causes opportunistic infections in humans, but as little is known concerning its iron acquisition mechanisms it will not be discussed in detail.

BCC INFECTIONS AND CYSTIC FIBROSIS

The Bcc constitute a group of at least 20 closely related species within the genus (**Table 1**). Members of the Bcc are well-known for causing infections in the lungs of cystic fibrosis (CF) patients, although they are also associated with infections of patients with chronic granulomatous disease and in individuals who are compromised for other reasons (Song et al., 2011). Although almost all Bcc species have been recovered from CF patient sputum, the most prevalent species are *B. cenocepacia* and *B. multivorans*, and consequently they have been the subject of most studies on potential virulence mechanisms (Reik et al., 2005; Drevinek and Mahenthiralingam, 2010; Zlosnik et al., 2015). Infections with Bcc have variable outcomes and may include transient or chronic asymptomatic infections, or they may cause a rapid decline in lung function which in some cases is accompanied by bacteraemia leading to death of the patient ("Cepacia syndrome;" Isles et al., 1984; Mahenthiralingam et al., 2001; Courtney et al., 2004; Jones et al., 2004). Infections with Bcc species are extremely difficult to eradicate due to their high level of intrinsic resistance to many antibiotics and biocides (Rose et al., 2009; Rhodes and Schweizer, 2016) [Note: prior to 2005, bacteria described as *B. cepacia* (and as *Pseudomonas cepacia* prior to the proposal of the genus *Burkholderia* in 1992) largely included members of related species within the Bcc that were not recognized as such at the time (Yabuuchi et al., 1992; Lipuma, 2005). This needs to be borne in mind when considering the results from some of the earlier investigations described below, particularly those in which a large number of "*P. cepacia*" or "*B. cepacia*" isolates were analyzed].

Cystic fibrosis (CF) is the most common autosomal recessive disorder among Caucasians. It is caused by mutations to the gene encoding the CF transmembrane conductor regulator (CFTR), which primarily functions as a gated chloride ion transporter but also regulates other apical membrane ion transporters (Davies et al., 2007). This defect leads to a more viscous lung mucus that impairs the action of the mucociliary escalator (Matsui et al., 1998, 2005; Boucher, 2007). Moreover, the high viscosity of the mucosal secretions may hinder the access of secreted cationic antimicrobial peptides from submucosal glands to the epithelial surface and may also restrict migration of neutrophils (see Doring et al., 2011; Tang et al., 2014 for reviews). Additional effects of a defective CFTR are also likely to be at play in facilitating pathogen survival in the airway surface liquid (ASL) of the CF lung (reviewed in Doring and Gulbins, 2009; Tang et al., 2014; Elborn, 2016), including increased abundance of amino acids (Barth and Pitt, 1996; Thomas et al., 2000), lowered pH (Song et al., 2006; Yoon et al., 2006), increased neutrophil-mediated oxidative stress (Kolpen et al., 2010), inflammation (Perez et al., 2007), hypoxic regions (Worlitzsch et al., 2002), and an altered iron status (see below). These phenomena conspire to make CF patients particularly susceptible to infection from a variety of bacterial, viral and fungal pathogens (Harrison, 2007).

Despite extensive research, the key virulence determinants of Bcc members that lead to establishment of an infection, persistence and morbidity in CF patients still remain to be established. Potential virulence determinants associated with the

TABLE 1 | Siderophore biosynthesis in human pathogenic members of the genus *Burkholderia*[a].

Species	Ornibactin[b]	Malleobactin[c]	Cepaciachelin[d]	Pyochelin[e]	Cepabactin[f]
BCC[g]					
B. ambifaria	+	−	+[h]	−	?
B. metallica	+	−	+	−	?
B. multivorans	+	−	+[i]	−	?
B. pseudomultivorans	+	−	+[j]	−	?
B. pyrrocinia	+	−	+	−	?
B. stagnalis	+	−	+	−	?
B. ubonensis	+	−	+	−	?
Bcc ATCC 31433[k]	+	−	+	−	?
B. anthina	+	−	−	+	?
B. cenocepacia	+	−	−	+	−
B. cepacia	+	−	−[l]	+[m]	+
B. lata	+	−	−	+	?
B. paludis	−[n]	−	−	+	?
B. seminalis	+	−	−	+	?
B. stabilis[o]	+	−	−	+	?
B. arboris[p]	?	?	−	?	?
B. contaminans	+	−	−	−	?
B. diffusa	+	−	−	−	?
B. dolosa	+	−	−	−	?
B. latens	+	−	−	−	?
B. territorii	+	−	−	−[q]	?
B. vietnamiensis	+	−	−	−[r]	−
PSEUDOMALLEI GROUP					
B. pseudomallei	−	+	−	+	?
B. mallei	−	+	−	−	?
OTHERS					
B. gladioli	−	−	−	−	?

[a] *The potential of the listed species to produce each siderophore was deduced from a bioinformatic analysis of genome sequences using genes known to encode the biosynthesis of each siderophore as a search query (except for cepabactin where the biosynthetic genes remain to be identified). In some cases, the production (or not) of a siderophore by a specific strain has been demonstrated (see below and main text for details).*

[b] *Ornibactin production has been confirmed in B. ambifaria, B. cenocepacia, B. cepacia, and B. vietnamiensis (Stephan et al., 1993; Meyer et al., 1995; Barelmann et al., 1996; Darling et al., 1998; Agnoli et al., 2006).*

[c] *Presumed to be malleobactin E for B. pseudomallei and B. mallei based on the known structure of the B. thailandensis siderophore (Franke et al., 2015).*

[d] *Cepaciachelin production has only been confirmed in B. ambifaria (Meyer et al., 1989).*

[e] *B. cenocepacia, B. cepacia, B. paludis, and B. pseudomallei have been demonstrated to produce pyochelin whereas B. vietnamiensis isolates do not (Meyer et al., 1995; Darling et al., 1998; Alice et al., 2006; Kvitko et al., 2012; Ong et al., 2016).*

[f] *Cepabactin has been identified in culture supernatants from two B. cepacia environmental strains (ATCC 25416 and ATCC17759) but not in environmental or clinical isolates of B. vietnamiensis [including the type strain TVV75 (LMG 10929)] (Meyer et al., 1989, 1995). It was not detected in culture supernatants of B. cenocepacia clinical isolates K56-2 and 715j (Darling et al., 1998).*

[g] *Member species of the Bcc are as listed in Depoorter et al. (2016) with the addition of B. paludis (Ong et al., 2016) and a potential new member Bcc ATCC 31433 (Loveridge et al., 2017).*

[h] *B. ambifaria PHP7 (LMG 11351) and the type strain AMMD (LMG 19182) have been shown to produce cepaciachelin, whereas strains MC40-6, MEX-5 and IOP40-10 do not possess the required genes (this study; Barelmann et al., 1996; Esmaeel et al., 2016).*

[i] *Although, several B. multivorans strains encode the capacity to produce cepaciachelin, some (including ATCC 17616 and the type strain LMG 13010) do not (this study; Esmaeel et al., 2016).*

[j] *Cepaciachelin gene cluster is present in B. pseudomultivorans strain MSMB368 but not in other strains currently in the database.*

[k] *Bcc ATCC 31433 is closely related to B. ubonensis, but possibly constitutes a separate species (Loveridge et al., 2017).*

[l] *B. cepacia LK29 has the genetic capacity to produce cepaciachelin but other B. cepacia strains for which genome sequences are available do not (this study; Esmaeel et al., 2016).*

[m] *B. cepacia ATCC 25416 (the type strain) and ATCC 17759 produce pyochelin whereas strain GG4 does not encode the capacity to produce this siderophore (Meyer et al., 1995; Deng et al., 2016; Esmaeel et al., 2016).*

[n] *B. paludis encodes the ferric ornibactin transport system but not the biosynthetic apparatus. The fact that it retains OrbE may suggest recycling of the siderophore.*

[o] *At the time of writing, three B. stabilis complete genome sequences had been deposited in the database. The type strain (ATCC BAA-67) and FERMP-21014 contain the pyochelin biosynthesis and utilization genes on chromosome 2, whereas strain LA20W lacks these genes and carries the cepaciachelin gene cluster.*

[p] *Siderophore status is unknown due to unavailability of genome sequence information.*

[q] *B. territorii A63 contains the pyochelin gene cluster. Other strains, including the type strain, do not have it.*

[r] *Pyochelin was not detected in culture supernatants of clinical and environmental isolates of B. vietnamiensis (Meyer et al., 1995).*

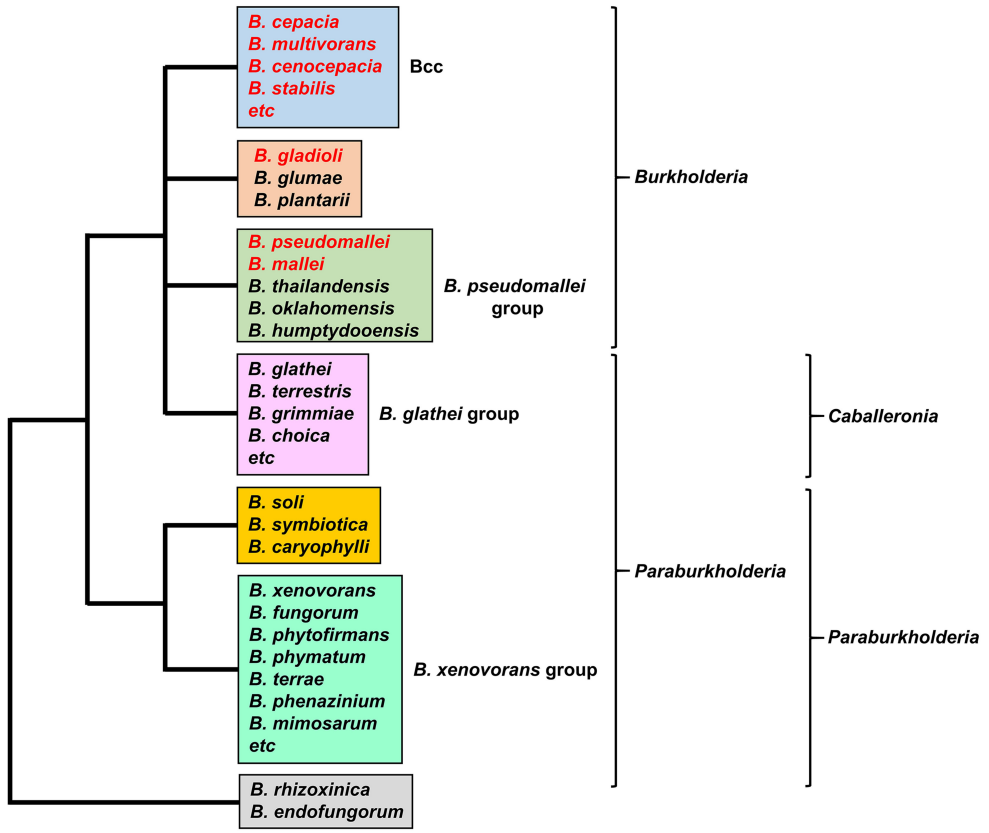

FIGURE 1 | The major groups of *Burkholderia* species. Groups are based on the 16S rRNA-based phylogenetic tree (see, for example, Depoorter et al., 2016). Species most commonly associated with infections in humans are shown in red font (for a full list of the Bcc species see **Table 1**). Alternative classification schemes involving the proposed new genera *Paraburkholderia* and *Caballeronia* are also indicated (see text for details). Recently, it has been proposed that *B. rhizoxinica* should be transferred to a new, as yet unnamed genus (Beukes et al., 2017).

Bcc, including their ability to survive intracellularly (including within macrophages) (Lamothe and Valvano, 2008; Vergunst et al., 2010; Valvano, 2015; Mesureur et al., 2017), have been the subject of several comprehensive reviews and are not discussed here (Drevinek and Mahenthiralingam, 2010; Loutet and Valvano, 2010; Sousa et al., 2011). One of the problems in identifying the pathogenic mechanisms is that there are few candidate virulence determinants that are associated with all member species of the Bcc, and indeed even among different strains within the same species some these determinants may not be conserved. However, one trait that does appear to be required for virulence in Bcc species is the ability to acquire iron from iron depleted environments such as within the human host. A large number of studies have been carried out on the virulence strategies of the most commonly isolated bacterial pathogen from CF patients, *P. aeruginosa*, particularly in relation to its ability to colonize the CF lung and the role that iron acquisition mechanisms may play in this process. This knowledge may inform our understanding of the conditions prevailing within the CF lung and the iron acquisition mechanisms that are important for establishment of an infection by Bcc species. Where relevant, pertinent data obtained from studies on *P. aeruginosa* will be discussed in this review.

THE ROLE OF IRON ACQUISITION MECHANISMS IN BCC INFECTIONS

Iron Availability in the CF Lung

In considering the potential role of iron acquisition systems in the CF lung it is worth reviewing what we know considering the iron content of CF sputum and its bioavailability. Based on the known iron limiting environment of the ASL of the healthy lung, where iron is sequestered by lactoferrin, transferrin, and ferritin, it was long assumed that the CF lung also generated an iron-deficient environment (Drevinek et al., 2008). Indeed, the results of some investigations into the regulation of iron acquisition genes in the major CF pathogen, *Pseudomonas aeruginosa*, appeared to lend support to this contention (see below). However, measurements of the iron content of the CF lung have led to a reappraisal of this environment. It is now clear that the lungs of CF patients have, on average, a higher iron content than that of a healthy individual. For example, it was shown that the abundance of the iron storage

protein, ferritin, was on average nearly 20-fold higher in the lungs of CF patients compared to healthy individuals, while there was ∼50% less transferrin (Stites et al., 1998). Other investigators have confirmed the high ferritin concentrations in CF sputum (Reid et al., 2002, 2004). In a more recent investigation, the total iron content and the fractions that were in the Fe(II) and Fe(III) forms were measured in CF patients experiencing differing degrees of disease severity (Hunter et al., 2013). This showed a strong positive correlation between the iron content of CF sputum and the progression of the disease. Thus, patients with severe disease (as judged by their low FEV) had a high mean iron concentration in their sputum of 72 μM compared to those with a milder condition where the mean was 18 μM. Moreover, a substantial fraction of iron was present in the soluble ferrous form which increased in line with disease severity, such that in the most severe disease stage, ferrous iron constituted ∼40% of the total iron load (Hunter et al., 2013). The increased abundance of Fe(II) in severe or late-stage CF disease is likely to be due to the reduction of Fe(III) by neutrophil-generated superoxides and stabilization of the resultant ferrous form by the increased prevalence of hypoxic zones in parts of the lung and acidification of the ASL.

Another source of iron that is more abundant in the CF lung is haem. This molecule becomes available through its release from hemoglobin which can occur following oxidation of the coordinated ferrous iron atom or following proteolysis of hemoglobin by host- or pathogen-derived proteases (Balla et al., 1993; Cosgrove et al., 2011). Lung tissue may release iron, including sources of haem, through injury due to the ravages of chronic inflammation (Reid et al., 2004). Moreover, CF patients experience a high frequency of micro-bleeds in their lung tissue that results in hemoglobin entering their ASL (Cosgrove et al., 2011). The frequency of airway bleeding in CF patients increases during pulmonary exacerbations where symptoms become more severe (Reid et al., 2009). The availability of ferrous iron and haem, particularly in the later stages of the disease, has potential implications for the iron acquisition systems that may be deployed by a colonizing pathogen. This change in our understanding of the iron status of the CF lung has led some workers to propose that the CF lung environment actually facilitates the growth of organisms such as *P. aeruginosa* (Reid et al., 2007).

Iron Acquisition Mechanisms of the Bcc

Many bacteria synthesize and secrete low molecular weight, high affinity iron chelating compounds known as siderophores which they employ to capture iron from their local environment, particularly when this element is scarce (Chu et al., 2010). Due to its propensity to form poorly soluble hydroxides in solution, such as $Fe(OH)_2^+$, an important role of the siderophore is to solubilize the ferric form of iron (Chipperfield and Ratledge, 2000; Ratledge and Dover, 2000). The affinities of some siderophores for iron are sufficiently high to allow them to obtain iron from host iron transport proteins such as lactoferrin and transferrin, but not from haem (Skaar, 2010). These compounds contain one, two, or three bidentate ligands that allow them to coordinate to a single Fe(III) ion, the predominant form of iron in aerobic environments at physiological pH. As iron forms hexavalent coordination complexes with its ligands, a single siderophore molecule containing three bidentate ligands (i.e., a hexadentate siderophore) will form a 1:1 complex with one ferric ion giving rise to an overall octahedral geometry (Neilands, 1995; Ratledge and Dover, 2000). Under iron replete conditions, synthesis of these molecules (and expression of other iron acquisition systems) is, in most cases, strongly downregulated in order to prevent cytoplasmic iron overload that may generate high levels of toxic reactive oxygen intermediates via the Fenton reaction (for reviews see Andrews et al., 2003; Cornelis et al., 2011).

Members of the Bcc have been shown to produce one or more of four different siderophores with which they can acquire iron: ornibactin, cepaciachelin, pyochelin, and cepabactin (Meyer et al., 1989, 1995; Stephan et al., 1993; Barelmann et al., 1996; Darling et al., 1998). These siderophores include all three types (bidentate, tetradentate, and hexadentate) and all of the most common iron binding ligands are represented among them (hydroxamate, hydroxycarboxylate, catechol, and 2-hydroxyphenylthiazoline; **Figure 2**). The biosynthesis of pyochelin and ornibactin and the genetic regulation of their synthesis have been reviewed elsewhere, while the biosynthetic genes for cepaciachelin have been recently identified (Thomas, 2007; Esmaeel et al., 2016). For this review, we have surveyed the distribution of ornibactin, cepaciachelin, and pyochelin among the Bcc by carrying out a bioinformatic analysis of the genomes of 21 Bcc members using the corresponding biosynthetic genes as search queries (**Table 1**). The results accord with more limited surveys carried out previously (Deng et al., 2016; Esmaeel et al., 2016). We have also augmented the bioinformatics analysis by referencing those cases where production of a particular siderophore by specific Bcc species has actually been demonstrated. Currently, this is the only way of ascertaining which species specify cepabactin, as the biosynthetic genes remain to be identified.

Based on bioinformatic analysis of genome sequences, all Bcc species (apart from the recently described *Burkholderia paludis*) are predicted to produce the siderophore ornibactin, which is likely to act as the primary secreted iron chelator in these organisms based on its hexadenticity (**Table 1** and **Figure 3**). Although ornibactin and malleobactin E (the siderophore produced by members of the *B. pseudomallei* group) are very similar (**Figure 2**), and therefore require similar biosynthetic enzymes for their assembly (**Figure 3**), a key feature that distinguishes the type of siderophore produced by each species is the presence of a distinct amino acid activation (adenylation) domain at the N-terminus of the larger of the two non-ribosomal peptide synthetases (NRPSs) that assemble these tetrapeptide siderophores (OrbI in the case of ornibactin). This domain activates the derivatized ornithine that will be located at the N-terminus of the tetrapeptide (for further details the reader is referred to Thomas, 2007 and the legend to **Figure 3**). In addition, as the δ-amino group of the N-terminal ornithine residue of ornibactin is acylated with a β-hydroxycarboxylic acid (rather than formic acid as in malleobactin E), the ornibactin gene cluster is distinguished by the presence of at least one of two genes (*orbK* and *orbL*) that are predicted to encode an acylase that

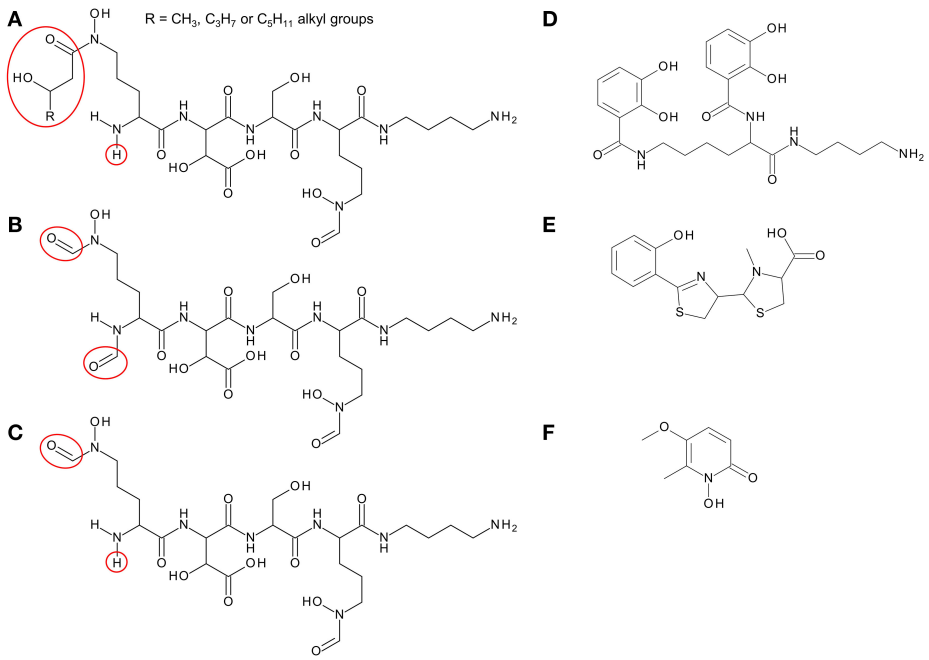

FIGURE 2 | Structure of siderophores produced by *Burkholderia* species. **(A)** Ornibactins contain an N-terminal ornithine that is acylated with a C4, C6, or C8 β-hydroxycarboxylic acid on the δ-amino nitrogen atom, giving rise to ornibactin-C4, -C6, or -C8. The δ-amino nitrogen atom is also hydroxylated. The other three amino acids in the tetrapeptide are D-hydroxyaspartate, L-serine, and the C-terminal ornithine that is formylated and hydroxylated on the δ-amino nitrogen atom and the carboxyl group is conjugated to putrescine. As with the malleobactins, they contain two bidentate hydroxamate ligands and a single bidentate α-hydroxycarboxylate ligand. **(B)** Malleobactin E, the siderophore-active malleobactin congener of *B. thailandensis*. **(C)** The siderophore-active malleobactin congener of *B. xenovorans*, tentatively referred to here as "malleobactin X." **(D)** Cepaciachelin contains two 2,3-DHBA groups that form amide linkages with the two amino groups of lysine, which in turn is conjugated to a molecule of putrescine (1,4-diaminobutane) on its α-carboxyl group. **(E)** Pyochelin contains two less commonly occurring bidentate iron-chelating groups (2-hydroxyphenyl thiazoline and N-methylthiazolidine-4-carboxylate). **(F)** Cepabactin, a cyclic hydroxamate bidentate siderophore. Chemical groups that distinguish the ornibactins and malleobactins are indicated in red circles or ellipses.

catalyses this condensation reaction (**Figure 3**). Whereas *orbL* is always present, *orbK* may contain an internal deletion (as in *B. ubonensis*) or be absent from the cluster altogether (as in *B. vietnamiensis*). Although, the single reported *B. paludis* strain is an environmental isolate, it should be noted that in a survey of "*B. cepacia*" CF isolates carried out prior to the taxonomic reorganization of *B. cepacia* into separate Bcc species, two clinical strains were found not to produce detectable levels of ornibactin (Darling et al., 1998). It is not clear to which Bcc member species they belong or whether they are indeed members of the Bcc. One possibility is that these strains were capable of producing ornibactin prior to infection but this ability was lost through mutation during prolonged carriage as has been observed with respect to production of the major siderophore pyoverdine by some *P. aeruginosa* strains isolated from chronically infected CF patients (De Vos et al., 2001; Smith et al., 2006; Andersen et al., 2015).

In addition, most Bcc species produce one or more secondary siderophores that are likely to have lower affinity for iron than ornibactin. The gene clusters specifying the biosynthesis and utilization of two of these siderophores, cepaciachelin and pyochelin, are shown in **Figures 4A,B**. Based on our bioinformatics survey, at least 7 species of Bcc, including *B. cenocepacia* and *B. lata*, produce pyochelin as the secondary siderophore, a feature associated with some *Pseudomonas* species (Cornelis and Matthijs, 2002), whereas in 8 other species, including some strains of *B. ambifaria* and *B. multivorans*, the secondary siderophore is cepaciachelin (**Table 1**). We have not identified a species possessing the genetic information required to produce both cepaciachelin and pyochelin. Both compounds are tetradentate siderophores, although the former belongs to the 2-hydroxyphenylthiazoline family whereas cepaciachelin is a bis-catecholate siderophore (Barelmann et al., 1996; Thomas, 2007; Inahashi et al., 2017). Some species do not appear to produce either of these two compounds as a secondary siderophore (**Table 1**). Another siderophore, the bidentate cyclic hydroxamate, cepabactin, has been detected in culture supernatants of some environmental *B. cepacia* strains in addition to ornibactin and pyochelin (see **Table 1**; Meyer et al., 1989, 1995). The ability of some clinical Bcc isolates of unknown taxonomic status to produce cepabactin has also been observed (Darling et al., 1998). Currently, it is not possible to infer from bioinformatics how widespread the synthesis or utilization of this siderophore is likely to be among the Bcc, although its production has not been observed in *B. cenocepacia* and *B. vietnamiensis* strains (**Table 1**).

The uptake of ferric-siderophore complexes by Gram-negative bacteria such as the *Burkholderia* requires an outer

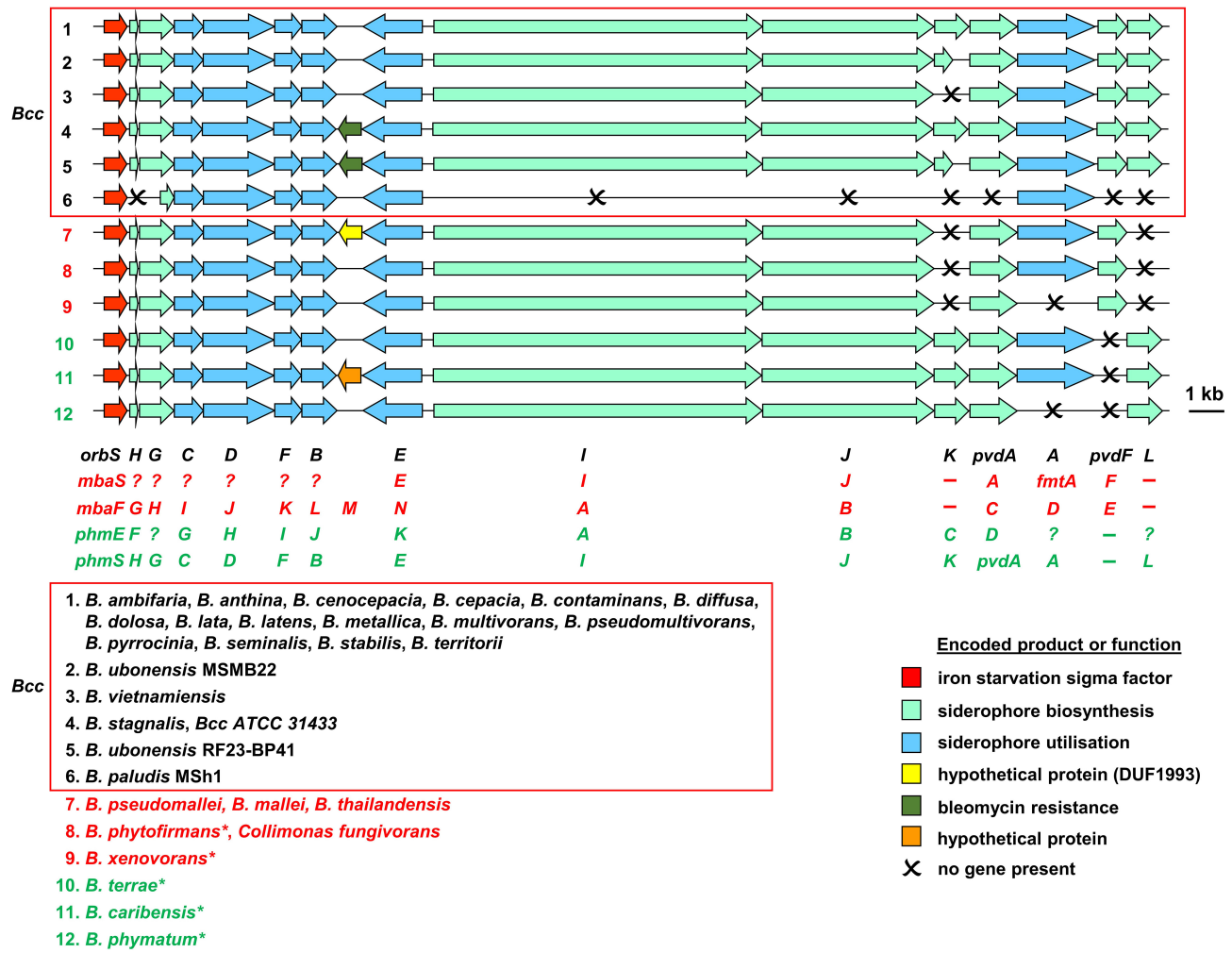

FIGURE 3 | Organization of ornibactin, malleobactin, and phymabactin biosynthesis and utilization genes in pathogenic *Burkholderia* and related species. Genes are represented by block arrows and are color coded as indicated in the figure [the precise role of the MbtH-like OrbH/MbaG/PhmF proteins is unknown but they are assumed to be required for biosynthesis of the siderophore based on the requirement for other MbtH-like proteins for NRPS-mediated biosynthesis of some peptides; (Wolpert et al., 2007; Baltz, 2011)]. The numbering of each gene cluster corresponds to the numbering system for the species listed at the bottom of the figure. The font color used for each species name corresponds to the siderophore produced as follows: black, ornibactin; red, malleobactins; green, phymabactin. NRPSpredictor2 (Rottig et al., 2011) was used to predict the siderophore product based on the substrates accepted by the four adenylation domains present in OrbI/OrbJ, MbaA/MbaB, and PhmA/PhmB for each species. For systems known to specify ornibactin, the first and last (N- and C-terminal) adenylation domains of the OrbI-OrbJ NRPS pair are both predicted to accept leucine with highest probability, reflecting the presence of N^5-3-hydroxyacyl-N^5-hydroxyornithine and N^5-formyl-N^5-hydroxyornithine, respectively, at these positions in the tetrapeptide product. For malleobactin, the predicted specificity of the N-terminal adenylation domain changes to β-hydroxytyrosine although the accepted substrate is N^5-formyl-N^5-hydroxyornithine. In some species, such as *B. thailandensis*, the N-terminal N^5-formyl-N^5-hydroxyornithine is formylated on the N^2-amino group upon formation of the tetrapeptide to generate malleobactin E (Franke et al., 2015), whereas in *B. xenovorans* the N-terminal N^5-formyl-N^5-hydroxyornithine does not appear to undergo such a tailoring reaction (Vargas-Straube et al., 2016) and so we tentatively refer to this siderophore as "malleobactin X." The N- and C-terminal adenylation domains of PhmA-PhmB are predicted to accept aspartate and cysteine, respectively, but the structure of the product, phymabactin, is unknown, although it is predicted to have siderophore activity based on its genomic context (Esmaeel et al., 2016). In all cases, the second and third adenylation domains are predicted to accept aspartate and serine, respectively, which correspond to β-hydroxy-D-aspartate and L-serine in the final product. The nomenclature proposed for each gene is shown below the gene clusters, and the gene designations are color coded as follows: ornibactin, black (Agnoli et al., 2006); the two systems for malleobactin, red (upper, Alice et al., 2006; lower, Franke et al., 2013); the two systems for phymabactin, green (upper, Esmaeel et al., 2016; lower, this study). Genes indicated by a single letter have the same prefix as the gene name at the extreme left. Dashes indicate the absence of a gene. Question mark indicates where a gene name has not been proposed. The initial annotation of the phymabactin gene cluster (Esmaeel et al., 2016) did not include the third and last genes in the cluster or the fact that a TBDR gene occurs in other species bearing this gene cluster (upper annotation in green font). Therefore, we have proposed an alternative nomenclature based on the ornibactin gene cluster (lower annotation in green font). Scale bar refers to gene lengths and not intergenic regions, which in some cases have been exaggerated to permit alignment of each gene cluster. Species marked with an asterisk belong to a subclade within the *B. xenovorans* group and have been reassigned to the new genus *Paraburkholderia* (Sawana et al., 2014). *Collimonas* is a genus within the *Oxalobacteraceae*, a family belonging to the order *Burkholderiales*. Member species of the Bcc are enclosed in a box (*B. arboris* is not listed as its genome sequence is not currently available). Gene loci are shown in Supplementary Table 1.

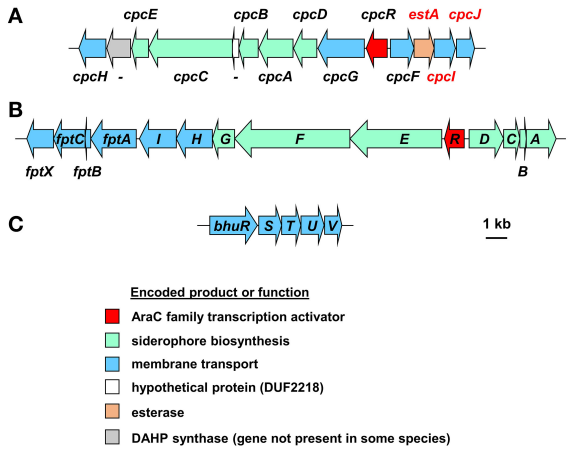

FIGURE 4 | Organization of the cepaciachelin and pyochelin biosynthesis and utilization genes and the genes for the haem uptake system in *Burkholderia* species. **(A)** The cepaciachelin gene cluster in *Burkholderia* species encodes enzymes for the synthesis of the precursor 2,3-dihydroxybenzoic acid (DHBA) from chorismate and its assembly into the siderophore. Genes encoding possible cepaciachelin transport proteins are also present, including the TonB-dependent receptor, CpcG, and an MFS transporter, CpcH. Most of the genes have been previously annotated (Esmaeel et al., 2016) but the annotation has been extended here (genes labeled in red font) and includes components of a cytoplasmic membrane ABC transporter which may be involved in uptake of ferric cepaciachelin (CpcF, -I, and -J). EstA is homologous to the cytoplasmic enterobactin and salmochelin esterases Fes and IroD that are required for removal of iron from ferric-enterobactins following their uptake. However, it contains a putative Sec-dependent signal peptide and so may be periplasmically located like the *C. jejuni* enterobactin esterase, Cee (Zeng et al., 2013). This may suggest that the putative cepaciachelin receptor (CpcG) and the cytoplasmic membrane transporter also recognizes ferric-enterobactin. With the exception of *B. ambifaria* and *B. pseudomultivorans* the cepaciachelin gene cluster includes a gene encoding a DAHP synthase which catalyses the first step in the shikimate pathway that leads to the biosynthesis of chorismate from erythrose-4-phosphate and PEP. Note that in Esmaeel et al. (2016) *cphA-cphC* should be annotated as *cpcA-cpcC*, as shown here (V. Leclere, personal communication). -, gene not assigned a four letter name. Gene loci are shown in Supplementary Table 2. **(B)** The pyochelin gene cluster. Genes annotated with a single letter are designated with the prefix *pch*. Products of the biosynthetic genes generate the precursor salicylic acid from chorismate (PchAB), activate it (PchD) and assemble it into pyochelin along with two molecules of cysteine (PchCEFG). The *pchHI* and *fptABCX* genes encode membrane proteins, of which two (FptA and FptX) are involved in the transport of exogenous ferric-pyochelin across the outer and inner membranes, respectively. *fptBC* and *pchHI* appear not to be essential for export of pyochelin nor for uptake of iron-bound pyochelin (see Youard et al., 2011 for a review). Gene loci are shown in Supplementary Table 3. **(C)** Organization of the *Burkholderia* haem uptake genes, *bhuRSTUV* (Shalom et al., 2007; Thomas, 2007), also referred to as *hmuRSTUV*, *huvA-hmuSTUV* or *omr-hmuSTUV* (Yuhara et al., 2008; Kvitko et al., 2012; Tyrrell et al., 2015). Note that in *B. stagnalis* a VOC family protein is encoded between *bhuU* and *bhuV*, and in *B. gladioli* the *bhu* genes are organized into two operons present on separate chromosomes. Gene loci of representative species are given in Supplementary Table 4.

membrane receptor, a 75–85 kDa polypeptide that folds into a β-barrel containing a central plug domain. Binding of a ferric-siderophore complex to the external face of the receptor triggers a conformational change in the gated receptor that allows access of the complex to the periplasmic space. The energy required for this process is derived from the proton motive force through the action of the TonB system, a complex of three different cytoplasmic membrane-anchored protein subunits: TonB, ExbB, and ExbD (Noinaj et al., 2010; Celia et al., 2016). For this reason, ferric-siderophore receptors are referred to as TonB-dependent receptors (TBDRs) or TonB-dependent transporters (TBDTs). As an example, OrbA is the TBDR for ferric-ornibactin (**Figure 5A**). Once the ferric-siderophore complex has entered the periplasmic space, the ferric ion is transported across the cytoplasmic membrane, either in complex with the siderophore or following release from the siderophore (depending on the system). The cytoplasmic membrane transporters are often ATP-binding cassette (ABC) transporters that consist of a periplasmic binding protein, an intrinsic membrane protein (the permease) and an ATPase located on the cytoplasmic face of the permease (Krewulak and Vogel, 2008). This type of system operates for the uptake of ferric ornibactin (Orb-B, -C, and -D) and possibly also for cepaciachelin (CpcF, -I, and -J) in the Bcc, as well as for the import of ferric malleobactin in *B. pseudomallei* and related bacteria (**Figures 5A,B**; Agnoli et al., 2006). In the case of ferric-pyochelin, a single subunit permease, FptX, appears to serve as the cytoplasmic membrane transporter (**Figure 5C**; Cuiv et al., 2004; Cunrath et al., 2015). For ferric-siderophore complexes that enter the cytoplasm, the iron is removed from the siderophore through its reduction to Fe(II), which is presumed to occur for ornibactin (Agnoli et al., 2006), or through modification or hydrolysis of the siderophore (Brickman and McIntosh, 1992; Hannauer et al., 2010).

Like many other bacterial species, *Burkholderia* spp. encode additional TBDRs that may allow them to utilize siderophores that are produced by other bacteria and fungi ("xenosiderophores"), although the potential importance of these compounds for pathogenicity is only likely to be realized in the context of a polymicrobial infection. Based on an analysis of its translated genome, *B. cenocepacia* is predicted to encode at least 20 TBDRs, many of which are likely to be involved in utilization of xenosiderophores (our unpublished results). At present, little is known concerning the nature of the xenosiderophores that can be utilized by the *Burkholderia*. However, the presence of the ornibactin transport genes in *B. paludis*, but not the biosynthetic genes, strongly suggests that ornibactin is likely to be utilized as a xenosiderophore by this species.

Members of the Bcc also specify iron acquisition systems that are not siderophore-dependent. For example, it has been shown that *B. cenocepacia* can utilize haem as an iron source (Whitby et al., 2006; Mathew et al., 2014; Tyrrell et al., 2015). *B. cenocepacia* and *B. multivorans* contain a cluster of genes (*bhuRSTUV*) that are predicted to be required for uptake of this molecule (**Figure 4C**; Thomas, 2007; Yuhara et al., 2008). [Note that there is currently a lack of consistency regarding the genetic nomenclature for this system in the *Burkholderia* (see below and legend to **Figure 4**).] Our bioinformatic survey shows that the *bhu* cluster is present on chromosome 2 in nearly all Bcc species for which whole genome sequence information is available (Supplementary Table 4). The exception is *B. vietnamiensis* which completely lacks the *bhuRSTUV* gene cluster. Although, there

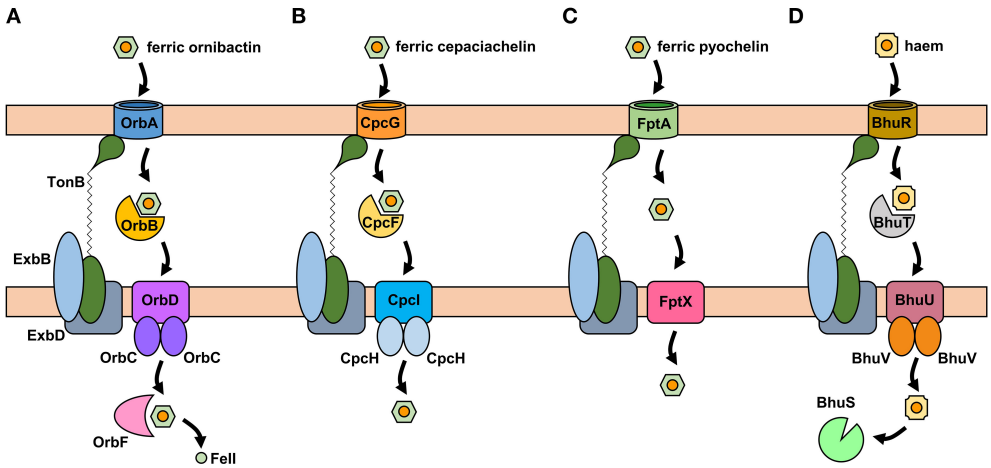

FIGURE 5 | Proposed iron uptake pathways in the *Burkholderia*. **(A)** The ornibactin/malleobactin uptake system. Ferric-ornibactin is recognized by the OrbA/MbaD TBDR and is translocated into the periplasmic space through a conformational change in the plug domain of the TBDR that requires energy transduction by the TonB complex (TonB-ExbB-ExbD). The iron-siderophore complex is then transported across the cytoplasmic membrane by a periplasmic binding protein-dependent ABC transporter (OrbBCD/MbaLIJ). Oncethe ferric-siderophore complex has been internalized, iron is released from ornibactin through its reduction to the ferrous form by OrbF/MbaK. **(B)** Ferric-cepaciachelin is proposed to require the CpcG TBDR. Genes neighboring *cpcG* encode a periplasmic binding protein-dependent ABC transporter (CpcFHI) that may be involved in transport of the bis-catecholate complex across the cytoplasmic membrane. **(C)** Ferric-pyochelin uptake requires the FptA TBDR and the single subunit cytoplasmic membrane transporter, FptX. **(D)** Uptake of haem via the Bhu system. Haem uptake is proposed to follow an analogous pathway to that of ornibactin/malleobactin and cepaciachelin. Cytoplasmic haem is bound by the BhuS protein which is proposed to play a role in haem trafficking and haemostasis. If required, iron can be released form haem by haem oxygenases (not shown). The FtrABCD system is not shown. OM, outer membrane; CM, cytoplasmic membrane.

have not been any major studies carried out to investigate the role of this system in haem acquisition in the Bcc, this function has been established for the *bhuRSTUV* system in *B. pseudomallei* (see below), and so one can confidently infer its role in haem uptake in the Bcc. Haem appears to be an important source of iron for *P. aeruginosa* during colonization of the CF lung, and therefore one might expect members of the Bcc to take advantage of this nutrient (Konings et al., 2013). *B. cenocepacia* can also obtain iron from ferritin in a protease-dependent process (Whitby et al., 2006; Mathew et al., 2014; Tyrrell et al., 2015). Interestingly, although iron is present in the ferric form when sequestered by ferritin, siderophores are not required for uptake of ferritin-derived iron in *B. pseudomallei* (Kvitko et al., 2012).

Ferrous iron is very soluble and can passage across the outer membrane of Gram-negative bacteria through porins in an energy-independent process. However, it requires specific transporters for translocation across the cytoplasmic membrane in all bacteria. The Feo system is one such ferrous iron-specific uptake system that is present in many Gram-positive and Gram-negative bacteria (Lau et al., 2016). This system consists of a cytoplasmic membrane transport protein (FeoB) and (in most cases) a cytoplasmic component of unknown function (FeoA). In some cases, a third component (FeoC) is also present. Ferrous iron is likely to be an important source of this essential nutrient for bacteria colonizing the CF lung based on its increased abundance in the ASL of more severely afflicted CF patients. Accordingly, it has been shown that the Feo system of *P. aeruginosa* is upregulated during colonization of the lungs of every individual in a cohort of 23 infected CF patients (Konings et al., 2013). For this reason, we conducted a survey of human pathogenic *Burkholderia* species for the presence of *feoA* and *feoB*. However, only a small a minority of *B. multivorans* and *B. pseudomultivorans* strains (not the type strains), as well as the single currently identified *B. paludis* strain (MSh1), were found to encode a FeoB-like protein, although these proteins lacked a region of ∼100 amino acids that is present in *P. aeruginosa* FeoB. There were no matches when FeoA was used as the query in a BLASTP search of the Bcc and *B. pseudomallei*. We conclude that the vast majority of pathogenic *Burkholderia* species lack this particular ferrous iron uptake system.

B. cenocepacia encodes a siderophore-independent mechanism for iron assimilation that is very similar to the FtrABCD systems reported in *Bordetella* and *Brucella* (Brickman and Armstrong, 2012; Elhassanny et al., 2013; Mathew et al., 2014). These systems share similarities with components of the *Escherichia coli* EfeUOB system that serves to import ferrous iron under aerobic conditions at low pH (Cao et al., 2007). Accordingly, in *Bordetella* spp. and *Brucella abortus*, ferrous iron is efficiently transported into these bacteria by the FtrABCD system over the pH range 6.0–7.5, in a process where the Fe(II) ion is oxidized to the ferric form using the FtrB cupredoxin component before translocation across the cytoplasmic membrane. In contrast, the *B. cenocepacia* FtrABCD system appears to utilize ferric iron as the substrate. Given the absence of a Feo system in *B. cenocepacia*, this begs the question as to the mechanism by which this species can uptake ferrous iron. *B. multivorans* also possesses an FtrABCD system, but in contrast to that of *B. cenocepacia* it does utilize ferrous

iron as the substrate (S.C. Andrews, unpublished results). Therefore, it is possible that this system may play a role in ferrous iron acquisition in the CF lung for at least some Bcc species, particularly given the abundance of ferrous iron in combination with the relatively low pH of CF ASL.

Although, the substantial proportion of iron that is in the ferrous form and the increased abundance of haem in the ASL may implicate the siderophore-independent iron acquisition mechanisms of the Bcc in establishing CF lung infections, as yet, the role of these systems in the context of CF have not been investigated in any detail (see below).

Experimental Evidence for the Role of Iron Acquisition Systems in the Virulence of the Bcc

In Vivo Studies

The earliest study on the role of iron acquisition mechanisms in the virulence of members of the Bcc was carried out prior to the discovery of the primary siderophore, ornibactin, in this group of bacteria (Sokol, 1986). Here, it was observed that from a collection of 43 "*P. cepacia*" CF isolates, ∼50% produced detectable levels of pyochelin during iron limited growth *in vitro* (Pch^+ phenotype). However, 86% of the Pch^+ strains were associated with infections which had led to the death of the patient or were responsible for severe infections, whereas only 41% of Pch^- strains were associated with such outcomes. Thus, while the ability to colonize a CF patient could not be linked to the ability to produce this siderophore, there was a link between pyochelin production and the morbidity/mortality of disease in CF patients. Similarly, while addition of exogenous pyochelin to two pyochelin-negative Bcc strains did not increase bacterial numbers or bacterial persistence in infected rat lungs, it did increase the severity of infection as assessed by lung pathology (Sokol and Woods, 1988). It was proposed that the observed enhancement of lung damage brought about by exogenous addition of pyochelin to these strains was most likely due to increased dissemination of the bacteria throughout the lungs. However, it is not clear from these studies whether it was the role of pyochelin in iron acquisition that was responsible for the more severe outcome or some other effect of the siderophore. In this regard, it is known that apart from binding iron and other metals (Cuppels et al., 1987; Visca et al., 1992; Baysse et al., 2000; Braud et al., 2009) pyochelin possesses an inherent chemical reactivity that may contribute to disease severity. For example, it can promote the degradation of organotin derivatives (Sun et al., 2006), and perhaps pertinently, it can catalyse the generation of ROS such as hydroxyl radicals that result in tissue damage (Coffman et al., 1990; Britigan et al., 1994, 1997; Adler et al., 2012). The latter property is proposed to contribute to the known antibiotic activity of this siderophore (Adler et al., 2012; Ong et al., 2016). It should be noted that one important Bcc pathogen of CF patients, *B. multivorans*, does not produce pyochelin (**Table 1**) and the clonally related *B. cenocepacia* CF epidemic strains K56-2 and J2315 produce very little of this siderophore (see below).

A direct genotypic-phenotypic link between iron acquisition and the virulence of *B. cenocepacia* was observed during an investigation of the virulence potential of ornibactin deficient mutants in rodent models of both chronic and acute respiratory infection (Sokol et al., 1999). In this study, mutants derived from the highly transmissible epidemic *B. cenocepacia* strain, K56-2, which contained an insertionally inactivated *pvdA* gene that is required for ornibactin synthesis (**Figure 3**), were generated by transposon mutagenesis (*pvdA*::Tn*5*-OT182) and allelic replacement (*pvdA*::tp). Both mutants were significantly attenuated in these models. Thus, in a rat lung chronic infection model, the number of *pvdA*::Tn*5*-OT182 bacterial cells recovered from the lung was 4 logs lower than that of the wild type K56-2 strain at 28 days post infection. Furthermore, the *pvdA*::tp strain could not be recovered from the lungs after the same length of time, suggesting the infection had been cleared. The degree of pathology, as determined by the amount of inflammatory cell infiltration and exudate in the lungs, was also significantly reduced in the K56*pvdA*::tp strain compared to that of K56-2. Aerosol administration of K56-2 and the *pvdA*::Tn*5*-OT182 mutant into neutropenic mice as an acute respiratory infection model revealed that whereas the wild type strain was able to persist in the lung 7 days post infection, the *pvdA* mutant was cleared from most of the mice after 3 days. These experiments suggested the importance of ornibactin-mediated iron acquisition by the bacteria for initial colonization, persistence and resulting pathological changes within the host. However, given the difference in the iron content of the lungs of a healthy individual compared to those of a CF patient, it is not clear to what extent the conclusions from this study, which did not involve CF mice or rats, can be extrapolated to the situation in the CF lung.

While the data indicated an important role for ornibactin in lung colonization in these models, the K56-2 strain (and other members of the highly transmissible ET12 epidemic lineage) produces very low amounts of the siderophore pyochelin compared to other *B. cenocepacia* strains due to a frameshift mutation in *pchF* (Darling et al., 1998; Holden et al., 2009) (Based on perusal of the genome sequence, we presume pyochelin biosynthesis in these strains occurs through independent initiation of translation from an internal in-frame GUG codon located upstream of the frameshift site that results in production of PchF as two separate components). Thus, the role of pyochelin in the lung infection model could not be established using ET12 strains. However, given that ET12 strains cause life-threatening infections in CF patients, this would again appear to rule out an important role for pyochelin in colonization of the CF lung by *B. cenocepacia*. Later work using a *B. cenocepacia* strain (Pc715j*orbA*::tp) that produced normal amounts of pyochelin but was unable to utilize ferric-ornibactin due to disruption of the gene encoding the ferric-ornibactin TBDR, OrbA, revealed that it was cleared from rat lungs much more quickly than the WT strain (Visser et al., 2004). A ferric-pyochelin receptor mutant (Pc715j*fptA*::tp) persisted with the same efficiency as that of the WT. These data suggested that while pyochelin may have a role in the severity of infection, it is unable to compensate for the loss of a functional ornibactin utilization system. Therefore, it is

ornibactin which appears to be important in order to establish an infection in this system. This may be explained by the presumed lower affinity of pyochelin than ornibactin for iron (Cox and Graham, 1979; Visca et al., 1993).

The importance of the ornibactin system for the virulence of *B. cenocepacia* has also been assessed in other infection models, including invertebrates and plants. Both a K56-2 *orbA* mutant and a K56-2 *pvdA* mutant were attenuated in the *Caenorhabditis elegans* and *Galleria mellonella* invertebrate models. The *pvdA* mutant was also slightly attenuated in the plant alfalfa model (Uehlinger et al., 2009). An *orbJ* mutant of the *B. cenocepacia* CF strain, H111, that is also deficient in the production of ornibactin, was also attenuated in the *G. mellonella* system (Mathew et al., 2014). Consistent with the virulence of the K56-2 strain in the rat lung chronic infection model, an H111 Δ*pchAB* pyochelin deficient mutant was still virulent in *G. mellonella*.

Using a modified signature-tagged mutagenesis (STM) procedure to identify genes required for survival in the rat chronic lung infection model, one of the attenuated *B. cenocepacia* K56-2 mutants which could not survive for 10 days in this model contained a transposon inserted just upstream of an ORF that encoded a haem TBDR-like protein (Hunt et al., 2004). The authors of this study indicated that the gene was the first in a cluster of genes associated with haem uptake that were located on chromosome 2, and the encoded protein was very similar to the 79 kDa RS03722 gene product of *Ralstonia solanacearum* strain GMI1000 (now reannotated as RSp0244). As RSp0244 is highly similar to BhuR we conclude that the plasposon insertion exerted polar effects on expression of the *bhuRSTUV* operon that impaired or abolished haem uptake. In contrast, genes involved in the biosynthesis and transport of ornibactin and pyochelin were not implicated in this study (Hunt et al., 2004). These observations would suggest that haem acquisition, and not siderophore-mediated iron acquisition, is an essential trait for persistence in the rat lung. Notwithstanding the different time courses of the chronic lung infection models, it is not clear why the ornibactin system should be implicated in some studies (Sokol et al., 1999; Visser et al., 2004) but not in the STM study, particularly as the ornibactin gene cluster presents a large target for plasposon-mediated disruption. One possible explanation is the selection procedure employed to construct the *B. cenocepacia* transposon mutant library. Here, mutants were selected on a mineral salts based medium in order to exclude auxotrophs. A K56-2 mutant in which the plasposon has disrupted a gene required for ornibactin synthesis or utilization would effectively be unable to obtain iron in a siderophore-dependent manner. We have observed that *B. cenocepacia* siderophore deficient mutants grow more slowly that the parental wild type strain on mineral salts medium (see for example Asghar et al., 2011), and it is possible that such mutants were omitted from the library of Hunt et al. This is not a complete explanation, however, as the haem uptake deficient mutants in the STM study can still produce ornibactin and so they might be expected to retain virulence based on other studies. This may suggest that a combination of both iron acquisition systems (haem- and ornibactin-mediated) is required for efficient colonization and persistence in the rat lung model.

Finally, the *B. cenocepacia* FtrABCD system was also investigated for a potential role in virulence in the *Galleria* wax moth model. Whereas deletion of the *ftr* system in isolation did not result in reduced virulence, when deleted in a strain that was unable to biosynthesise ornibactin and pyochelin, the mutant was more attenuated in comparison to an ornibactin-negative strain. This observation suggests that while ornibactin is the more important iron acquisition system for virulence in this model, the FtrABCD system can play a role in iron acquisition during infection in the absence of siderophores (Mathew et al., 2014).

In Vitro Studies

Changes in the environmental iron concentration or availability can also trigger adaptive changes in expression of virulence traits that are not directly connected to iron acquisition but rather serve other roles that contribute to survival of the bacterium under the prevailing conditions. Such examples include regulating biofilm formation in *P. aeruginosa* and capsule production in *Cryptococcus neoformans* (Singh et al., 2002; Banin et al., 2005; Jung et al., 2006). For *B. cenocepacia* it has been shown that modulating the concentration of iron causes a switch from planktonic to sessile growth. Thus, supplementing liquid cultures with ferric iron concentrations ranging from 1 to 100 μM resulted in increased levels of extracellular matrix production by strain PVI as the iron concentration was increased. Furthermore, biofilm formation induced by growth under high iron conditions resulted in more efficient invasion of A549 epithelial monolayers compared to cells grown in lower iron conditions that did not produce biofilm (Berlutti et al., 2005). In contrast, adherence of *B. cenocepacia* to A549 cells was more efficient under iron limiting conditions. The consequences of this for *B. cenocepacia* CF lung infections are not yet clear.

Gene Expression and Omics Studies

Transcriptomic and proteomic analyses can be used to identify sets of genes or proteins that may be required for survival under particular conditions by virtue of their differential expression. A few such studies have been carried out with *B. cenocepacia* that have suggested an important role for iron uptake mechanisms in bacterial persistence within CF patients. However, as we discuss below, the experimental set up may not necessarily be appropriate for addressing this particular question. The first notable study looked at global gene expression during growth of *B. cenocepacia* J2315 in a basal salts medium supplemented with CF sputum in comparison to growth in unsupplemented medium (Drevinek et al., 2008). The microarray revealed upregulation of 287 genes and downregulation of 437 other genes during growth in CF sputum medium. However, only two of the upregulated genes were associated with characterized iron acquisition systems in this bacterium. These two genes (*pchR* and *pchD*) encode the transcription activator of the pyochelin gene cluster and an enzyme required for biosynthesis of the pyochelin precursor, salicylic acid, respectively, but their expression increased only 2-fold. Transcription of the ornibactin genes was not upregulated, although the gene encoding the global iron repressor, Fur, that represses the ornibactin gene cluster, was found to be

downregulated 2- to 3-fold (Agnoli et al., 2006; Drevinek et al., 2008).

The authors of this work measured the iron content of their sputum medium and found it to be ∼35 μM, which is more than adequate to sustain growth of *B. cenocepacia* in standard laboratory medium without upregulating siderophore biosynthesis (Drevinek et al., 2008; Madeira et al., 2013; our unpublished results). Despite the presence of CF sputum in the medium, which has been argued by some investigators to sequester iron due to the presence of various iron binding components (Wang et al., 1996; Palmer et al., 2007), their results imply that sufficient iron is available to effect repression of the ornibactin system. Accordingly, the observed induction of the *pch* genes may not be related to iron depletion but is rather a response to the presence of another component in CF sputum. It is noteworthy that genes encoding other components of the pyochelin biosynthesis machinery (particularly those enzymes required to assemble pyochelin from salicylate and cysteine) and alternative iron uptake systems (FtrABCD and BhuRSTUV) were also not upregulated. The authors contend that the CF medium they employed restricted the available iron based on the observed gross upregulation of the BCAL0270 gene, which they considered to be involved in iron acquisition (described in the study as a "ferric reductase-like transmembrane component"). However, in a basal salts medium without iron supplementation, this gene was upregulated only 2-fold compared to medium containing the standard amount of ferrous sulfate (43 μM). Moreover, this gene is currently annotated in the NCBI database as encoding a "sulfoxide reductase heme-binding subunit YedZ" and it is transcriptionally linked to BCAL0269, a gene that encodes a YedY-homologous protein. Our own bioinformatics analysis supports this annotation (results not shown). The *E. coli* YedYZ complex is a membrane anchored haem-molybdoenzyme that serves to reduce an as yet unknown S- or N-oxide (Iobbi-Nivol and Leimkuhler, 2013). Therefore, there is little evidence to support the suggestion that BCAL0270 is involved in iron acquisition. The possibility that the CF sputum medium of Drevinek et al. (2008) is iron sufficient accords with the high iron concentration included in the basal salts medium used to generate the medium. Notwithstanding the fact that the sputum is present at only 10% (w/v) in the medium, the inability of the added CF sputum to induce iron acquisition systems may suggest that its ability to sequester iron is somewhat limited and/or it is iron replete.

The results of Drevinek et al. (2008) contrast with those of Palmer et al. (2005), who monitored gene expression in the CF pathogen *P. aeruginosa* growing in a mineral salts based medium containing only CF sputum as the source of carbon and energy ("MOPS-sputum medium"), and noted that a large number of genes specifying the biosynthesis of the major siderophore, pyoverdine, as well as the entire cluster of genes specifying the biosynthesis and transport of the secondary siderophore, pyochelin, were considerably upregulated relative to their transcription in cells growing in sputum-free MOPS-glucose medium. However, although MOPS-sputum medium contained a similar amount of CF sputum to that used by Drevinek et al. (2008), the iron content (3.5 μM) was approximately one tenth of that present in the medium used in the *B. cenocepacia* experiment (in both cases iron was added as ferrous sulfate). Thus, although it should be borne in mind that two different CF pathogens are being compared, each possessing a different primary siderophore system, the amount of iron added ranged from iron replete (in the *B. cenocepacia* experiment) to a concentration that will support bacterial growth but may require a degree of upregulation of the siderophore-mediated iron acquisition system (in the *P. aeruginosa* experiment), (pyoverdine synthesis is fully repressed at ∼4 μM iron and is upregulated to a progressively greater degree as concentrations of iron are decreased below 4 μM; Meyer and Abdallah, 1978). The reader may wish to consider which version of CF sputum medium more closely represents the true environment of the CF lung with respect to iron availability. The other variable at play that may influence the iron content is the source of the sputum. As discussed above, the iron content of sputum shows marked variation among CF patients, particularly in relation to the severity of the disease (Stites et al., 1998; Reid et al., 2002; Hunter et al., 2013). To illustrate the potential for a different outcome that may reflect variation in the iron content of CF sputum, in an IVET study conducted on *P. aeruginosa* growing in a mineral salts medium containing 10% CF mucus, and otherwise with no iron supplementation, only a single iron-regulated gene, *fptA* (encoding the ferric-pyochelin outer membrane receptor), was identified as being upregulated (Wang et al., 1996).

Global changes in *B. cenocepacia* gene expression have also been analyzed in a synthetic CF sputum medium (SCFM). SCFM is a defined (i.e., sputum-free) medium containing the average concentrations of ions, free amino acids, glucose and lactate as those found in the sputum of CF patients and has been shown to support similar growth rates and elicit similar changes in expression of some subsets of genes in *P. aeruginosa* to those observed during growth in MOPS-sputum medium (Palmer et al., 2007). It also contains 3.6 μM ferrous iron (i.e., similar to that of MOPS-sputum medium). Although the iron concentration of SCFM may be low enough to cause upregulation of *P. aeruginosa* siderophore gene expression relative to iron replete conditions, these genes were not (unsurprisingly) upregulated relative to cells growing in a MOPS-glucose based mineral salts medium containing an almost identical concentration of iron (Palmer et al., 2007). The contrasting high level of siderophore gene expression observed in *P. aeruginosa* growing in MOPS-sputum medium relative to cells growing in MOPS-glucose medium (Palmer et al., 2005) was rationalized on the basis that CF sputum also contains iron sequestering components which have been proposed to restrict the availability of iron (Palmer et al., 2007). Other analogous attempts to mimic CF sputum conditions using semi-synthetic media, such as ASMDM or Modified ASMDM, and comparing gene expression in *P. aeruginosa* to that in cells growing in standard laboratory media have likewise not suggested a requirement for the main siderophore-mediated iron acquisition systems in synthetic sputum-like media [apart from one case where a small (2-fold) increase in some pyochelin biosynthesis and transport genes was observed; Fung et al., 2010; Hare et al., 2012].

In apparent contrast to the observations with *P. aeruginosa*, the entire ornibactin gene cluster of *B. cenocepacia*, as well as genes encoding a number of TBDRs and a cluster of genes that encode a putative bacterioferritin-associated ferredoxin and a TonB system (BCAL2290-BCAL2293) were found to be strongly upregulated during growth of *B. cenocepacia* J2315 in SCFM in comparison to growth in soil extract medium, although the pyochelin biosynthesis genes were not upregulated in SCFM (Yoder-Himes et al., 2010). These results also contrast with those observed for *B. cenocepacia* growing in a basal salts medium supplemented with glucose, casamino acids and CF sputum (see above; Drevinek et al., 2008). The most likely reason for the latter difference is that there was a 10-fold higher concentration of iron in the CF sputum medium in comparison to SCFM. It might seem intriguing that SCFM stimulates ornibactin gene expression in *B. cenocepacia* but not expression of pyoverdine genes in *P. aeruginosa*. However, again one must proceed with caution in interpreting these data, as the fold induction of gene expression in *P. aeruginosa* cells growing in SCFM was expressed relative to medium containing the same iron concentration, whereas the comparator for the *B. cenocepacia* experiment were cells growing in soil extract medium, which has an indeterminate iron concentration. In fact, it is likely that relative to cells growing in an iron replete, nutrient rich laboratory medium, both the pyoverdine and ornibactin gene clusters may actually be upregulated in cells growing in SCFM.

To summarize the above, it is difficult to make informed judgements regarding the requirement or otherwise for various iron acquisition systems based on gene expression analysis in cells growing in defined or semi-defined media that seek to mimic CF conditions when the concentration of iron and its relative availability may not accurately reflect the situation in the patient. As an example, we note that in some more recent attempts to mimic CF conditions using synthetic media, a higher iron concentration has been used by including ferritin to better reflect the prevailing view that the iron content of the CF lung is relatively high (Hare et al., 2012). Moreover, experiments involving media which incorporate CF-derived sputa may be prone to a high degree of experimental variation according to the disease severity and consequential iron status of the sputa. Finally, obvious though this must appear, consideration of the comparator is fundamentally important in assessing whether or not iron acquisition genes are upregulated in such media.

The difficulty in reproducing CF conditions *in vitro* can be bypassed by measuring gene expression in bacterial pathogens that are present in sputum following collection of samples from CF patients. As an example, in one such study, a microarray experiment was performed using *P. aeruginosa* mRNA isolated from sputum obtained from a single patient (Son et al., 2007). In this investigation, genes specifying the biosynthesis of pyochelin were upregulated but not those encoding the biosynthesis and transport of the major siderophore pyoverdine. In a later study, an RT-qPCR analysis of gene expression in *P. aeruginosa* strains that were present in the lungs of a cohort of CF patients suggested that the siderophore pyoverdine was likely to contribute to iron acquisition in this context (Konings et al., 2013), and indeed the presence of the siderophore could be detected in CF sputa (Martin et al., 2011). In contrast, to our knowledge, studies involving direct sampling of RNA from Bcc bacteria colonizing the CF lung have not been carried out. However, sampling of *B. cenocepacia* mRNA directly from an animal model of a chronic lung infection has been carried out (O'Grady and Sokol, 2011). As discussed earlier, the ability to biosynthesise ornibactin plays an important role in chronic infections of the rat lung by *B. cenocepacia* (7 and 14 days post-infection; Visser et al., 2004). However, microarray data in which gene expression in *B. cenocepacia* K56-2 cells that were recovered from the rat lung model 3 days post-infection was compared to cells that were grown to stationary phase in a nutrient-rich broth (iron replete medium), showed no difference in ornibactin gene expression levels (O'Grady and Sokol, 2011). Therefore, the simplest interpretation of these data is that ornibactin is not required to establish an infection in this particular model system but it is required for persistence. Moreover, in contrast to the STM analysis of Hunt et al. (2004), the microarray analysis did not reveal a difference in expression of the *bhuR* and *bhuS* genes (referred to as *huvA* and *hmuS* by the authors) in the rat lung model compared to growth in iron replete medium (O'Grady and Sokol, 2011). As the STM study was conducted with animals that were infected for 10 days, one possible explanation is that haem utilization becomes important for longer term infections as has been observed in *P. aeruginosa* (see below).

Transcriptomics has been used to monitor *B. cenocepacia* adaptation to the host over time, although in this case RNA was isolated following *in vitro* culture of the bacteria. In one such study, gene expression was compared in two clonal variants that were isolated 3 years apart from a CF patient who died of cepacia syndrome. This study revealed that in the later clone, seven genes located within the ornibactin gene cluster were upregulated 1.9- to 5.9-fold compared to those in the earlier isolate when both strains were cultured on a nutrient-rich agar. Other genes potentially involved in iron uptake were also found to be more transcriptionally active in this isolate, including three genes that encode TBDRs that are not involved in ornibactin or pyochelin uptake, and two genes, *bhuR* and *bhuS* (referred to as *huvA* and *hmuS* by the authors), from the *bhuRSTUV* gene cluster that is proposed to be required for the uptake of haem (**Figure 4C**; Mira et al., 2011). A subsequent proteomic study employing the same pair of isolates, along with a third isolate collected just before the death of the patient, showed that the two later isolates exhibited an increased abundance of four proteins involved in siderophore-mediated iron uptake compared to the earliest clone (Madeira et al., 2013). These proteins included two TBDRs (one of which was FptA) that had increased in abundance by <2-fold, and one component of the ferric-ornibactin cytoplasmic membrane transporter (OrbC) which showed a relatively small increase in abundance (∼50%) in the third isolate compared to the first. However, in contrast to the transcriptomic study, a general increase in abundance of iron acquisition proteins was not observed. Moreover, based on a CAS assay, the latter two isolates were considered to be more tolerant to low iron concentrations (siderophore production was induced at 4 or 5 μM iron, whereas in the primary isolate siderophore production was upregulated at 6 μM iron).

In a later study carried out on the same sequential clonal isolates, the upregulation of ornibactin gene expression observed in response to the iron chelating activity of exogenously added pyoverdine was significantly less pronounced in the last isolate compared to the earlier isolates (Tyrrell et al., 2015). These observations are consistent with a scenario in which selection for genetic alterations has occurred upon long term colonization of the CF lung that lead to a decreased reliance on siderophore-dependent iron acquisition by the bacterium. This may indicate a switchover to another means of iron acquisition or it may reflect a general downregulation of iron acquisition mechanisms due to increased inflammatory damage that occurs in the CF lung as the disease progresses and the consequent increased availability of iron (Cohen and Prince, 2012).

The results are analogous to those obtained from studies carried out on *P. aeruginosa*, in which it was observed that during infection of the CF lung mutations accrue in the bacterial population that result in a reduction or abolition of production of the major siderophore, pyoverdine (Marvig et al., 2014; Nguyen et al., 2014 and refs within). Evidence was also provided for increased haem usage as an iron source concomitant with a reduction in pyoverdine synthesis during the later stages of infection (Marvig et al., 2014; Nguyen et al., 2014). Consistent with this, in a separate microarray study carried out on mRNA isolated directly from a *P. aeruginosa*-infected CF patient, two genes from the pyochelin gene cluster (*pchA* and *pchC*) were observed to be upregulated 2- to 3-fold, but no pyoverdine genes were identified as being upregulated (Son et al., 2007). Although these results were obtained from work on a different CF pathogen, they are consistent with the idea that siderophore-mediated iron acquisition in the CF lung may not be of major importance to some pathogenic bacteria, particularly later on in an infection.

While these types of analyses may provide useful pointers as to the iron acquisition mechanisms that may be employed by pathogenic bacteria colonizing the CF lung, particularly if the isolate has accrued mutations that have inactivated a particular uptake system, the fact that these systems are subject to genetic regulation means that a true understanding of the iron uptake mechanisms at play during an infection will also require analysis of bacterial gene expression *in vivo*, i.e., in the CF lung.

Studies on the effects of other environmental parameters on global gene expression in *B. cenocepacia* have also been conducted that have potential implications for iron acquisition in this organism. In one investigation, the effect of oxygen depletion on gene expression was assessed, as there is evidence to suggest that within the CF lung a steep oxygen gradient is generated due to increased activity of airway epithelial Na^+-K^+-ATPase pumps and excessive mucin secretion. This results in the deepest layers of mucus providing a hypoxic environment that can support high densities of micro-oxic and anaerobic microbes in the CF lung (Tunney et al., 2008). In this study it was shown that *B. cenocepacia* can grow in an atmosphere with oxygen concentrations as low as 0.1% (Pessi et al., 2013). The possibility that *B. cenocepacia* may therefore occupy a low oxygen niche when colonizing the lungs of CF patients prompted an RNA-seq and shotgun proteome analysis of *B. cenocepacia* H111 growing under micro-oxic conditions (0.5% oxygen) in comparison to aerobic growth (21% oxygen). RNA-seq showed strong down regulation of the pyochelin biosynthesis genes *pchD*, *pchE,* and *pchF* in addition to the gene encoding the ferric-pyochelin outer membrane receptor, FptA, in micro-oxic conditions. Overall production of siderophores was also reduced in micro-oxic conditions as assessed by the CAS agar assay (Pessi et al., 2013). This kind of environment promotes the increased stabilization of Fe(II) and may favor the use of ferrous iron transport systems, such as the FtrABCD system in *B. multivorans*, over siderophore based systems.

Another environmental parameter that appears to affect the expression of iron acquisition genes that may be pertinent in the context of CF lung infections is oxidative stress. Thus, it has been observed that exposure of *B. cenocepacia* biofilms to hydrogen peroxide causes increased expression of the first few genes of the ornibactin gene cluster (*orbS*, *orbH,* and *orbG*; Peeters et al., 2010). While the oxygen and oxidative stress status of the niche occupied by *B. cenocepacia* in the CF lung has not yet been established, these observations bring into focus the requirement to mimic, as close as possible, the conditions of the CF lung when assessing the potential role of iron acquisition mechanisms in the virulence of respiratory pathogens.

To summarize, there appears to be a role for ornibactin-mediated iron acquisition in the virulence of *B. cenocepacia* in both vertebrate and invertebrate models of infection, including infections of the respiratory tract. However, in the context of a CF infection the role of ornibactin is less certain and there is a possibility that haem acquisition may come into play. Moreover, the severity of the disease and the particular niche that is occupied by Bcc bacteria in the lung—for example, whether it is oxygen rich or hypoxic—are also likely to dictate which iron acquisition mechanism(s) are primarily deployed. Currently, there is little evidence to support a role for the secondary siderophores in colonization and persistence by Bcc bacteria, although this is partly due to the fact that no studies on the possible roles of cepaciachelin and cepabactin have been reported. Further studies are required to establish the relative importance of the various iron acquisition mechanisms available to Bcc bacteria for colonization of the CF lung.

BURKHOLDERIA PSEUDOMALLEI AND *BURKHOLDERIA MALLEI*

B. pseudomallei is both an environmental saprophyte and the causative agent of the tropical disease melioidosis (Wiersinga et al., 2006). This disease is endemic in South East Asia and Northern Australia with sporadic cases increasingly reported in other topical regions (Perumal Samy et al., 2017). Contraction of the disease is via cuts and abrasions, inhalation or ingestion (Wiersinga et al., 2012). Although apparently healthy individuals can become infected, conditions such as diabetes and liver disease are highly associated risk factors of melioidosis (Perumal Samy et al., 2017). The disease manifests in a range of forms from acute infections, chronic reoccurring infections, fatal sepsis or even persistent asymptomatic infections lasting for up to 60 years

(White, 2003; Ngauy et al., 2005). The lung is the most commonly infected organ with the liver, spleen, skeletal muscle and prostate other sites of infection (White, 2003).

B. mallei is a host restricted obligate pathogen with no known environmental reservoir (Whitlock et al., 2007). This bacterium causes the zoonotic disease glanders, which is spread directly or indirectly through secretions and excretions of infected animals. This disease is chronic in horses and an acute form of the disease occurs in donkeys and mules. Infection of humans is rare and is usually the result of occupational exposure (Verma et al., 2014). *B. mallei* is considered to be a clone of *B. pseudomallei* that has undergone a process of genome reduction during host adaptation (Godoy et al., 2003; Nierman et al., 2004).

Experimental Evidence for the Role of Iron Acquisition Systems in the Virulence of *B. pseudomallei*

The role of iron in *B. pseudomallei* and *B. mallei* virulence has been less well-studied than in *B. cenocepacia* mainly due to the increased hazard associated with handling these organisms which necessitates a more stringent level of containment and has also restricted the range of available selective genetic markers. Nevertheless, with the recent development of biosafety compliant tools for the genetic manipulation of these bacteria important progress has been made in our understanding of their iron acquisition systems and the role that these systems play in virulence. It is now well-established that access to iron is important for virulence by *B. pseudomallei*. For example, it has been demonstrated that the severity of *B. pseudomallei* infection of A549 macrophages and HeLa cells is increased if the cell lines are supplemented with iron. Thus, *B. pseudomallei* K96243 formed more plaques on iron-supplemented HeLa cells and invasion was significantly increased in iron-supplemented A549 cells. Furthermore, the intracellular survival of *B. pseudomallei* in A549 monolayers and the ability to induce MNGC formation, was greater when the A549 monolayers were supplemented with iron compared to non-iron supplemented controls (Amornrit et al., 2012). Interestingly, iron has also been shown to down regulate one of the type VI secretion systems (specifically T6SS-5) in *B. pseudomallei* and *B. mallei* (Burtnick and Brett, 2013). T6SS-5 is essential for virulence in hamsters and is required for multinucleated giant cell formation in infected tissue culture monolayers, a phenomenon that may facilitate cell-to-cell spread of the bacterium (Burtnick et al., 2011) [Note: T6SS-5, as designated by Shalom et al. (2007), is also referred to as T6SS-1 or the cluster 1 type VI secretion system by some authors (Schell et al., 2007; Burtnick et al., 2011)].

A limited number of studies have been carried out to determine the role of siderophores and other iron uptake systems on the virulence of *B. pseudomallei* and *B. mallei*. Both species produce the siderophore malleobactin (or more precisely, malleobactin E), that is structurally related to ornibactin (Yang et al., 1991; Alice et al., 2006; Franke et al., 2013, 2015; **Figure 2**). This siderophore was shown to be able to acquire iron from human transferrin and lactoferrin (Yang et al., 1993). *B. pseudomallei,* like several members of the Bcc, also produces pyochelin as a secondary siderophore (Alice et al., 2006; Kvitko et al., 2012), whereas in *B. mallei*, which has undergone extensive genome reduction, the gene cluster needed for pyochelin production is absent (Esmaeel et al., 2016). This is consistent with other evidence that pyochelin has a limited role in *Burkholderia* virulence, and loss of the ability to manufacture this siderophore in *B. mallei* may point to a more important role of pyochelin in environmental survival among other *Burkholderia* species. Moreover, *B. mallei* also produces reduced levels of malleobactin (as determined by the CAS assay) compared to *B. pseudomallei* and *B. thailandensis* which may also reflect the narrower range of niches in which it inhabits (Ong et al., 2004). *B. pseudomallei* may also secrete a third compound with iron chelating activity, although this compound has not yet been characterized (Kvitko et al., 2012).

The BPSS0240-BPSS0244 genes of *B. pseudomallei* K96243 were proposed to serve as a haem uptake system and were observed to be upregulated during growth under low iron conditions (Tuanyok et al., 2005). Based on an IVET screen, this system was shown to be induced during growth of *B. pseudomallei* NCTC 10274 within macrophages, suggesting that it may play an important role in iron acquisition during intracellular survival. In this study the authors referred to the uptake system as the Bhu (*Burkholderia* haem uptake) system based on the *Pseudomonas* Phu system (Shalom et al., 2007). By analogy with the Phu system and the related Shu system of *Shigella*, the Bhu system consists of the TBDR, BhuR (BPSS0244), a periplasmic binding protein-dependent type II ABC transporter (BhuT-BhuV) for translocation of haem across the cytoplasmic membrane, and a cytoplasmic haem binding protein (BhuS) that plays a role in haem trafficking and may also initiate haem degradation (**Figure 5D**; O'Neill and Wilks, 2013; Naoe et al., 2016; see Choby and Skaar, 2016) for a review. Based on a bioinformatic analysis, *B. pseudomallei* K96243 was predicted to specify two additional outer membrane receptors for haem (BPSL2724 and BPSS1742) with the former also associated with an ABC transporter system (Harland et al., 2007). However, neither of these systems shows a strong homology to characterized haem uptake systems. The BPSL2721-BPSL2724 and BPSS0240-BPSS0244 (Bhu) transport systems were later referred to as the Hem and Hmu systems, respectively, in a study conducted on strain 1710b (Kvitko et al., 2012). These authors observed that whereas deletion of the *bhu/hmu* locus compromised the ability of *B. pseudomallei* to utilize haem or hemoglobin as iron sources, deletion of the *hem* locus did not abrogate the ability to utilize haem, strongly indicating that the Bhu/Hmu system serves as the haem uptake system in this organism.

Kvitko and colleagues went on to explore the relative contributions of siderophore- and haem-mediated uptake systems to *B. pseudomallei* virulence in an acute murine melioidosis model following intranasal infection. They found that although utilization of lactoferrin-bound iron *in vitro* relied on malleobactin, inactivation of the malleobactin uptake

system in strain 1710b did not cause attenuation in the murine melioidosis model (Kvitko et al., 2012). Interestingly, a strain that was defective for malleobactin, pyochelin, and haem uptake was also fully virulent in the melioidosis model, although the titres of bacteria recovered from some organs was significantly lower. As this mutant could still grow with ferritin as an iron source, it was suggested that another iron uptake system is present that could compensate for the loss of the other uptake pathways. There are at least two possibilities that could account for this. First, the CAS agar assay indicated that *B. pseudomallei* mutants lacking the ability to biosynthesise malleobactin and pyochelin specify an additional secreted iron-chelating compound of unknown identity (Kvitko et al., 2012). Secondly, *B. pseudomallei* encodes the FtrABCD system which may play a role in iron acquisition during infection (Mathew et al., 2014). Perhaps surprisingly, although *B. pseudomallei* 708a (a strain containing a >130 kb genome deletion that removes the malleobactin synthesis genes) was virulent in the mouse model used by Kvitko and colleagues, it was attenuated in *G. mellonella* (Wand et al., 2011; Kvitko et al., 2012).

The outer membrane receptors required for uptake of ferric-siderophore complexes and haem require the action of the cytoplasmic membrane-anchored TonB-ExbB-ExbD complex to energize transport of these iron sources. A *B. mallei tonB* mutant, which is unable to internalize ferric-malleobactin or haem, was shown to be completely attenuated in mice at 10^5 CFU, in comparison to an LD_{50} of 7.4 x 10^4 CFU for the wild type, and it also exhibited lower titres in target organs (lungs and spleen). Supplementation of the medium with ferrous iron, which is assimilated by a TonB-independent mechanism, partially restored virulence and led to higher titres of *tonB* mutant bacteria in the spleen, indicating that the inability to acquire iron is the main reason for the loss of virulence in the mutant (Mott et al., 2015). However, as TonB systems in other species have been shown to be involved in transport of other large molecules, including some enzyme cofactors (thiamine, cobalamin) and saccharides (sialic acid, sucrose, maltodextrins) the possibility exists that there are other transport requirements served by the *B. mallei* TonB system that must be met for full virulence (Schauer et al., 2008; Roy et al., 2010).

Another study in which potential novel therapeutics were screened for their ability to counteract *B. pseudomallei* killing of *C. elegans* suggested an important role for iron acquisition in virulence. Exposure of *B. pseudomallei* to the plant alkaloid curcumin (diferuloylmethane), prior to their administration to *C. elegans*, significantly enhanced the survival of the worms (Eng and Nathan, 2015). Curcumin is structurally related to bis-catecholates, which include bacterial siderophores such as azotochelin, cepaciachelin, and serratiochelin, and is itself a known iron chelator that may serve to cause a decrease in iron availability (Jiao et al., 2006). Accordingly, microarray data showed that *B. pseudomallei* treated with curcumin upregulated genes for iron transport, including those for malleobactin, pyochelin and haem uptake, as well as genes encoding the TonB system. Moreover, genes encoding the biosynthesis of malleobactin and pyochelin were upregulated and increased secretion of siderophores by treated *B. pseudomallei* was observed. The authors suggest that the anti-infective effects observed by curcumin are due to the bacteria diverting their metabolism away from virulence and toward iron uptake to ensure growth and maintenance. These observations provide suggestive evidence for the importance of iron acquisition for virulence in this organism.

BURKHOLDERIA GLADIOLI

B. gladioli was originally identified as a pathogen of *Iridaceae*, specifically irises and gladioli, and then later was recognized as the cause of infections in certain groups of immunocompromised patients, particularly among those with CF and CGD (Boyanton et al., 2005; Kennedy et al., 2007). The iron acquisition systems of this organism have yet to be determined. However, the genome sequence offers a few clues. We note that it does not contain orthologs of the genes for the biosynthesis of ornibactin, malleobactin, pyochelin, or cepaciachelin (**Table 1**). However, it does contain orthologs of the *bhuRSTUV* genes. Unusually, these genes are organized into two separate operons that are present on chromosome 1 (*bhuRST*) and chromosome 2 (*bhuUV*) (results not shown), but nevertheless suggest that *B. gladioli* may be able to utilize haem as an iron source during infection of human hosts. The *B. gladioli* genome also encodes a FtrABCD system. It is not known whether one or both of these systems is important for establishing an infection in humans.

CLOSING REMARKS

To conclude, we are still far from ascertaining the relative importance of the different iron acquisition mechanisms available to the *Burkholderia* that are brought to bear during infection of a human host. A number of studies have been carried out with *B. cenocepacia* to address this question which have provided what might at first appear to be conflicting results. However, as the model systems are so varied, and the iron content and/or availability in these systems is also markedly different, we believe that most of these apparent contradictory results can be rationalized. Nonetheless, in terms of whether high affinity iron acquisition systems are essential for successful colonization of the CF lung and which ones are deployed, further studies are required. Due to the difficulty of working safely with *B. pseudomallei* and *B. mallei* fewer studies have been conducted, but it would appear that neither the known siderophores of *B. pseudomallei* nor its haem uptake system are important for systemic melioidosis. There is great scope for further work into the role of iron acquisition in the virulence of this important group of bacteria.

AUTHOR CONTRIBUTIONS

AB and MT contributed equally to writing the manuscript. MT prepared the figures, table and Supplementary Material.

ACKNOWLEDGMENTS

We would like to thank the BBSRC who are supporting the current work of AB and MT on the regulation of iron acquisition in *Burkholderia* (research grant BB/M003531/1).

SUPPLEMENTARY MATERIAL

The Supplementary Material for this article can be found online at: https://www.frontiersin.org/articles/10.3389/fcimb.2017.00460/full#supplementary-material

REFERENCES

Adler, C., Corbalan, N. S., Seyedsayamdost, M. R., Pomares, M. F., De Cristobal, R. E., Clardy, J., et al. (2012). Catecholate siderophores protect bacteria from pyochelin toxicity. *PLoS ONE* 7:e46754. doi: 10.1371/journal.pone.0046754

Agnoli, K., Lowe, C. A., Farmer, K. L., Husnain, S. I., and Thomas, M. S. (2006). The ornibactin biosynthesis and transport genes of *Burkholderia cenocepacia* are regulated by an extracytoplasmic function sigma factor which is a part of the Fur regulon. *J. Bacteriol.* 188, 3631–3644. doi: 10.1128/JB.188.10.3631-3644.2006

Alice, A. F., Lopez, C. S., Lowe, C. A., Ledesma, M. A., and Crosa, J. H. (2006). Genetic and transcriptional analysis of the siderophore malleobactin biosynthesis and transport genes in the human pathogen *Burkholderia pseudomallei* K96243. *J. Bacteriol.* 188, 1551–1566. doi: 10.1128/JB.188.4.1551-1566.2006

Amornrit, W. M. V., and Wangteeraprasert, T., and Korbsrisate, S. (2012). Elevated intracellular levels of iron in host cells promotes *Burkholderia pseudomallei* infection. *Asian Biomed.* 6, 465–471. doi: 10.5372/1905-7415.0603.078

Andersen, S. B., Marvig, R. L., Molin, S., Johansen, H. K., and Griffin, A. S. (2015). Long-term social dynamics drive loss of function in pathogenic bacteria. *Proc. Natl. Acad. Sci. U.S.A.* 112, 10756–10761. doi: 10.1073/pnas.1508324112

Andrews, S. C., Robinson, A. K., and Rodriguez-Quinones, F. (2003). Bacterial iron homeostasis. *FEMS Microbiol. Rev.* 27, 215–237. doi: 10.1016/S0168-6445(03)00055-X

Asghar, A. H., Shastri, S., Dave, E., Wowk, I., Agnoli, K., Cook, A. M., et al. (2011). The *pobA* gene of *Burkholderia cenocepacia* encodes a group I Sfp-type phosphopantetheinyltransferase required for biosynthesis of the siderophores ornibactin and pyochelin. *Microbiology* 157, 349–361. doi: 10.1099/mic.0.045559-0

Balla, J., Jacob, H. S., Balla, G., Nath, K., Eaton, J. W., and Vercellotti, G. M. (1993). Endothelial-cell heme uptake from heme proteins: induction of sensitization and desensitization to oxidant damage. *Proc. Natl. Acad. Sci. U.S.A.* 90, 9285–9289. doi: 10.1073/pnas.90.20.9285

Baltz, R. H. (2011). Function of MbtH homologs in nonribosomal peptide biosynthesis and applications in secondary metabolite discovery. *J. Ind. Microbiol. Biotechnol.* 38, 1747–1760. doi: 10.1007/s10295-011-1022-8

Banin, E., Vasil, M. L., and Greenberg, E. P. (2005). Iron and *Pseudomonas aeruginosa* biofilm formation. *Proc. Natl. Acad. Sci. U.S.A.* 102, 11076–11081. doi: 10.1073/pnas.0504266102

Barelmann, I., Meyer, J. M., Taraz, K., and Budzikiewicz, H. (1996). Cepaciachelin, a new catecholate siderophore from *Burholderia* (Pseudomonas) *cepacia*. *Z. Nat.* 51, 627–630.

Barth, A. L., and Pitt, T. L. (1996). The high amino-acid content of sputum from cystic fibrosis patients promotes growth of auxotrophic *Pseudomonas aeruginosa*. *J. Med. Microbiol.* 45, 110–119. doi: 10.1099/00222615-45-2-110

Baysse, C., De Vos, D., Naudet, Y., Vandermonde, A., Ochsner, U., Meyer, J. M., et al. (2000). Vanadium interferes with siderophore-mediated iron uptake in *Pseudomonas aeruginosa*. *Microbiology* 146 (Pt 10), 2425–2434. doi: 10.1099/00221287-146-10-2425

Berlutti, F., Morea, C., Battistoni, A., Sarli, S., Cipriani, P., Superti, F., et al. (2005). Iron availability influences aggregation, biofilm, adhesion and invasion of Pseudomonas aeruginosa and *Burkholderia cenocepacia*. *Int. J. Immunopathol. Pharmacol.* 18, 661–670. doi: 10.1177/039463200501800407

Beukes, C. W., Palmer, M., Manyaka, P., Chan, W. Y., Avontuur, J. R., Van Zyl, E., et al. (2017). Genome data provides high support for generic boundaries in *Burkholderia* sensu lato. *Front Microbiol* 8:1154. doi: 10.3389/fmicb.2017.01154

Boucher, R. C. (2007). Airway surface dehydration in cystic fibrosis: pathogenesis and therapy. *Annu. Rev. Med.* 58, 157–170. doi: 10.1146/annurev.med.58.071905.105316

Boyanton, B. L. Jr., Noroski, L. M., Reddy, H., Dishop, M. K., Hicks, M. J., Versalovic, J., et al. (2005). *Burkholderia gladioli* osteomyelitis in association with chronic granulomatous disease: case report and review. *Pediatr. Infect. Dis. J.* 24, 837–839. doi: 10.1097/01.inf.0000177285.44374.dc

Braud, A., Hoegy, F., Jezequel, K., Lebeau, T., and Schalk, I. J. (2009). New insights into the metal specificity of the *Pseudomonas aeruginosa* pyoverdine-iron uptake pathway. *Environ. Microbiol.* 11, 1079–1091. doi: 10.1111/j.1462-2920.2008.01838.x

Brickman, T. J., and Armstrong, S. K. (2012). Iron and pH-responsive FtrABCD ferrous iron utilization system of *Bordetella* species. *Mol. Microbiol.* 86, 580–593. doi: 10.1111/mmi.12003

Brickman, T. J., and McIntosh, M. A. (1992). Overexpression and purification of ferric enterobactin esterase from *Escherichia coli*. Demonstration of enzymatic hydrolysis of enterobactin and its iron complex. *J. Biol. Chem.* 267, 12350–12355.

Britigan, B. E., Rasmussen, G. T., and Cox, C. D. (1997). Augmentation of oxidant injury to human pulmonary epithelial cells by the *Pseudomonas aeruginosa* siderophore pyochelin. *Infect. Immun.* 65, 1071–1076.

Britigan, B. E., Serody, J. S., and Cohen, M. S. (1994). The role of lactoferrin as an anti-inflammatory molecule. *Adv. Exp. Med. Biol.* 357, 143–156. doi: 10.1007/978-1-4615-2548-6_14

Burtnick, M. N., and Brett, P. J. (2013). *Burkholderia mallei* and *Burkholderia pseudomallei* cluster 1 type VI secretion system gene expression is negatively regulated by iron and zinc. *PLoS ONE* 8:e76767. doi: 10.1371/journal.pone.0076767

Burtnick, M. N., Brett, P. J., Harding, S. V., Ngugi, S. A., Ribot, W. J., Chantratita, N., et al. (2011). The cluster 1 type VI secretion system is a major virulence determinant in *Burkholderia pseudomallei*. *Infect. Immun.* 79, 1512–1525. doi: 10.1128/IAI.01218-10

Cao, J., Woodhall, M. R., Alvarez, J., Cartron, M. L., and Andrews, S. C. (2007). EfeUOB (YcdNOB) is a tripartite, acid-induced and CpxAR-regulated, low-pH Fe^{2+} transporter that is cryptic in *Escherichia coli* K-12 but functional in *E. coli* O157:H7. *Mol. Microbiol.* 65, 857–875. doi: 10.1111/j.1365-2958.2007.05977.x

Caza, M., and Kronstad, J. W. (2013). Shared and distinct mechanisms of iron acquisition by bacterial and fungal pathogens of humans. *Front. Cell Infect. Microbiol.* 3:80. doi: 10.3389/fcimb.2013.00080

Celia, H., Noinaj, N., Zakharov, S. D., Bordignon, E., Botos, I., Santamaria, M., et al. (2016). Structural insight into the role of the Ton complex in energy transduction. *Nature* 538, 60–65. doi: 10.1038/nature19757

Chipperfield, J. R., and Ratledge, C. (2000). Salicylic acid is not a bacterial siderophore: a theoretical study. *Biometals* 13, 165–168. doi: 10.1023/A:1009227206890

Choby, J. E., and Skaar, E. P. (2016). Heme synthesis and acquisition in bacterial pathogens. *J. Mol. Biol.* 428, 3408–3428. doi: 10.1016/j.jmb.2016.03.018

Chu, B. C., Garcia-Herrero, A., Johanson, T. H., Krewulak, K. D., Lau, C. K., Peacock, R. S., et al. (2010). Siderophore uptake in bacteria and the battle for iron with the host; a bird's eye view. *Biometals* 23, 601–611. doi: 10.1007/s10534-010-9361-x

Coffman, T. J., Cox, C. D., Edeker, B. L., and Britigan, B. E. (1990). Possible role of bacterial siderophores in inflammation. Iron bound to the *Pseudomonas siderophore* pyochelin can function as a hydroxyl radical catalyst. *J. Clin. Invest.* 86, 1030–1037. doi: 10.1172/JCI114805

Cohen, T. S., and Prince, A. (2012). Cystic fibrosis: a mucosal immunodeficiency syndrome. *Nat. Med.* 18, 509–519. doi: 10.1038/nm.2715

Cornelis, P., and Matthijs, S. (2002). Diversity of siderophore-mediated iron uptake systems in fluorescent pseudomonads: not only pyoverdines. *Environ. Microbiol.* 4, 787–798. doi: 10.1046/j.1462-2920.2002.00369.x

Cornelis, P., Wei, Q., Andrews, S. C., and Vinckx, T. (2011). Iron homeostasis and management of oxidative stress response in bacteria. *Metallomics* 3, 540–549. doi: 10.1039/c1mt00022e

Cosgrove, S., Chotirmall, S. H., Greene, C. M., and McElvaney, N. G. (2011). Pulmonary proteases in the cystic fibrosis lung induce interleukin 8 expression from bronchial epithelial cells via a heme/meprin/epidermal growth factor receptor/Toll-like receptor pathway. *J. Biol. Chem.* 286, 7692–7704. doi: 10.1074/jbc.M110.183863

Courtney, J. M., Dunbar, K. E., McDowell, A., Moore, J. E., Warke, T. J., Stevenson, M., et al. (2004). Clinical outcome of *Burkholderia cepacia* complex infection in cystic fibrosis adults. *J. Cyst. Fibros.* 3, 93–98. doi: 10.1016/j.jcf.2004.01.005

Cox, C. D., and Graham, R. (1979). Isolation of an iron-binding compound from *Pseudomonas aeruginosa*. *J. Bacteriol.* 137, 357–364.

Cuiv, P. O., Clarke, P., Lynch, D., and O'connell, M. (2004). Identification of *rhtX* and *fptX*, novel genes encoding proteins that show homology and function in the utilization of the siderophores rhizobactin 1021 by *Sinorhizobium meliloti* and pyochelin by *Pseudomonas aeruginosa*, respectively. *J. Bacteriol.* 186, 2996–3005. doi: 10.1128/JB.186.10.2996-3005.2004

Cunrath, O., Gasser, V., Hoegy, F., Reimmann, C., Guillon, L., and Schalk, I. J. (2015). A cell biological view of the siderophore pyochelin iron uptake pathway in *Pseudomonas aeruginosa*. *Environ. Microbiol.* 17, 171–185. doi: 10.1111/1462-2920.12544

Cuppels, D., Stipanovic, R., Stoessl, A., and Stothers, J. (1987). The constitution and properties of a pyochelin–zinc complex. *Can. J. Chem.* 65, 2126–2130. doi: 10.1139/v87-354

Darling, P., Chan, M., Cox, A. D., and Sokol, P. A. (1998). Siderophore production by cystic fibrosis isolates of *Burkholderia cepacia*. *Infect. Immun.* 66, 874–877.

Davies, J. C., Alton, E. W. F. W., and Bush, A. (2007). Cystic fibrosis. *BMJ* 335, 1255–1259. doi: 10.1136/bmj.39391.713229.AD

De Vos, D., De Chial, M., Cochez, C., Jansen, S., Tummler, B., Meyer, J. M., et al. (2001). Study of pyoverdine type and production by *Pseudomonas aeruginosa* isolated from cystic fibrosis patients: prevalence of type II pyoverdine isolates and accumulation of pyoverdine-negative mutations. *Arch. Microbiol.* 175, 384–388. doi: 10.1007/s002030100278

Deng, P., Wang, X., Baird, S. M., Showmaker, K. C., Smith, L., Peterson, D. G., et al. (2016). Comparative genome-wide analysis reveals that *Burkholderia contaminans* MS14 possesses multiple antimicrobial biosynthesis genes but not major genetic loci required for pathogenesis. *Microbiologyopen* 5, 353–369. doi: 10.1002/mbo3.333

Depoorter, E., Bull, M. J., Peeters, C., Coenye, T., Vandamme, P., and Mahenthiralingam, E. (2016). Burkholderia: an update on taxonomy and biotechnological potential as antibiotic producers. *Appl. Microbiol. Biotechnol.* 100, 5215–5229. doi: 10.1007/s00253-016-7520-x

Dobritsa, A. P., and Samadpour, M. (2016). Transfer of eleven species of the genus *Burkholderia* to the genus *Paraburkholderia* and proposal of *Caballeronia* gen. nov. to accommodate twelve species of the genera *Burkholderia* and *Paraburkholderia*. *Int. J. Syst. Evol. Microbiol.* 66, 2836–2846. doi: 10.1099/ijsem.0.001065

Doring, G., and Gulbins, E. (2009). Cystic fibrosis and innate immunity: how chloride channel mutations provoke lung disease. *Cell Microbiol.* 11, 208–216. doi: 10.1111/j.1462-5822.2008.01271.x

Doring, G., Parameswaran, I. G., and Murphy, T. F. (2011). Differential adaptation of microbial pathogens to airways of patients with cystic fibrosis and chronic obstructive pulmonary disease. *FEMS Microbiol. Rev.* 35, 124–146. doi: 10.1111/j.1574-6976.2010.00237.x

Drevinek, P., and Mahenthiralingam, E. (2010). *Burkholderia cenocepacia* in cystic fibrosis: epidemiology and molecular mechanisms of virulence. *Clin. Microbiol. Infect.* 16, 821–830. doi: 10.1111/j.1469-0691.2010.03237.x

Drevinek, P., Holden, M. T., Ge, Z., Jones, A. M., Ketchell, I., Gill, R. T., et al. (2008). Gene expression changes linked to antimicrobial resistance, oxidative stress, iron depletion and retained motility are observed when *Burkholderia cenocepacia* grows in cystic fibrosis sputum. *BMC Infect. Dis.* 8:121. doi: 10.1186/1471-2334-8-121

Elborn, J. S. (2016). Cystic fibrosis. *Lancet* 388, 2519–2531. doi: 10.1016/S0140-6736(16)00576-6

Elhassanny, A. E., Anderson, E. S., Menscher, E. A., and Roop, R. M. II. (2013). The ferrous iron transporter FtrABCD is required for the virulence of *Brucella abortus* 2308 in mice. *Mol. Microbiol.* 88, 1070–1082. doi: 10.1111/mmi.12242

Eng, S. A., and Nathan, S. (2015). Curcumin rescues *Caenorhabditis elegans* from a *Burkholderia pseudomallei* infection. *Front. Microbiol.* 6:290. doi: 10.3389/fmicb.2015.00290

Esmaeel, Q., Pupin, M., Kieu, N. P., Chataigné, G., Béchet, M., Deravel, J., et al. (2016). *Burkholderia* genome mining for nonribosomal peptide synthetases reveals a great potential for novel siderophores and lipopeptides synthesis. *Microbiologyopen* 5, 512–526. doi: 10.1002/mbo3.347

Franke, J., Ishida, K., and Hertweck, C. (2015). Plasticity of the malleobactin pathway and its impact on siderophore action in human pathogenic bacteria. *Chemistry* 21, 8010–8014. doi: 10.1002/chem.201500757

Franke, J., Ishida, K., Ishida-Ito, M., and Hertweck, C. (2013). Nitro versus hydroxamate in siderophores of pathogenic bacteria: effect of missing hydroxylamine protection in malleobactin biosynthesis. *Angew. Chem. Int. Ed. Engl.* 52, 8271–8275. doi: 10.1002/anie.201303196

Fung, C., Naughton, S., Turnbull, L., Tingpej, P., Rose, B., Arthur, J., et al. (2010). Gene expression of *Pseudomonas aeruginosa* in a mucin-containing synthetic growth medium mimicking cystic fibrosis lung sputum. *J. Med. Microbiol.* 59, 1089–1100. doi: 10.1099/jmm.0.019984-0

Godoy, D., Randle, G., Simpson, A. J., Aanensen, D. M., Pitt, T. L., Kinoshita, R., et al. (2003). Multilocus sequence typing and evolutionary relationships among the causative agents of melioidosis and glanders, *Burkholderia pseudomallei* and *Burkholderia mallei*. *J. Clin. Microbiol.* 41, 2068–2079. doi: 10.1128/JCM.41.5.2068-2079.2003

Hannauer, M., Barda, Y., Mislin, G. L., Shanzer, A., and Schalk, I. J. (2010). The ferrichrome uptake pathway in *Pseudomonas aeruginosa* involves an iron release mechanism with acylation of the siderophore and recycling of the modified desferrichrome. *J. Bacteriol.* 192, 1212–1220. doi: 10.1128/JB.01539-09

Hare, N. J., Solis, N., Harmer, C., Marzook, N. B., Rose, B., Harbour, C., et al. (2012). Proteomic profiling of *Pseudomonas aeruginosa* AES-1R, PAO1 and PA14 reveals potential virulence determinants associated with a transmissible cystic fibrosis-associated strain. *BMC Microbiol.* 12:16. doi: 10.1186/1471-2180-12-16

Harland, D. N., Dassa, E., Titball, R. W., Brown, K. A., and Atkins, H. S. (2007). ATP-binding cassette systems in *Burkholderia pseudomallei* and *Burkholderia mallei*. *BMC Genomics* 8:83. doi: 10.1186/1471-2164-8-83

Harrison, F. (2007). Microbial ecology of the cystic fibrosis lung. *Microbiology* 153, 917–923. doi: 10.1099/mic.0.2006/004077-0

Holden, M. T., Seth-Smith, H. M., Crossman, L. C., Sebaihia, M., Bentley, S. D., Cerdeno-Tarraga, A. M., et al. (2009). The genome of *Burkholderia cenocepacia* J2315, an epidemic pathogen of cystic fibrosis patients. *J. Bacteriol.* 191, 261–277. doi: 10.1128/JB.01230-08

Hunt, T. A., Kooi, C., Sokol, P. A., and Valvano, M. A. (2004). Identification of *Burkholderia cenocepacia* genes required for bacterial survival *in vivo*. *Infect. Immun.* 72, 4010–4022. doi: 10.1128/IAI.72.7.4010-4022.2004

Hunter, R. C., Asfour, F., Dingemans, J., Osuna, B. L., Samad, T., Malfroot, A., et al. (2013). Ferrous iron is a significant component of bioavailable iron in cystic fibrosis airways. *Mbio* 4:e00557–13. doi: 10.1128/mBio.00557-13

Inahashi, Y., Zhou, S., Bibb, M. J., Song, L., Al-Bassam, M. M., Bibb, M. J., et al. (2017). Watasemycin biosynthesis in *Streptomyces venezuelae*: thiazoline C-methylation by a type B radical-SAM methylase homologue. *Chem. Sci.* 8, 2823–2831. doi: 10.1039/C6SC03533G

Iobbi-Nivol, C., and Leimkuhler, S. (2013). Molybdenum enzymes, their maturation and molybdenum cofactor biosynthesis in *Escherichia coli*. *Biochim. Biophys. Acta* 1827, 1086–1101. doi: 10.1016/j.bbabio.2012.11.007

Isles, A., Maclusky, I., Corey, M., Gold, R., Prober, C., Fleming, P., et al. (1984). *Pseudomonas cepacia* infection in cystic fibrosis: an emerging problem. *J. Pediatr.* 104, 206–210. doi: 10.1016/S0022-3476(84)80993-2

Jiao, Y., Wilkinson, J. T., Christine Pietsch, E., Buss, J. L., Wang, W., Planalp, R., et al. (2006). Iron chelation in the biological activity of curcumin. *Free Radic. Biol. Med.* 40, 1152–1160. doi: 10.1016/j.freeradbiomed.2005.11.003

Jones, A. M., Dodd, M. E., Govan, J. R., Barcus, V., Doherty, C. J., Morris, J., et al. (2004). *Burkholderia cenocepacia* and *Burkholderia multivorans*: influence on survival in cystic fibrosis. *Thorax* 59, 948–951. doi: 10.1136/thx.2003.017210

Jung, W. H., Sham, A., White, R., and Kronstad, J. W. (2006). Iron regulation of the major virulence factors in the AIDS-associated pathogen

Cryptococcus neoformans. *PLoS Biol.* 4:e410. doi: 10.1371/journal.pbio.0040410

Kennedy, M. P., Coakley, R. D., Donaldson, S. H., Aris, R. M., Hohneker, K., Wedd, J. P., et al. (2007). *Burkholderia gladioli:* five year experience in a cystic fibrosis and lung transplantation center. *J. Cyst. Fibros.* 6, 267–273. doi: 10.1016/j.jcf.2006.10.007

Kolpen, M., Hansen, C. R., Bjarnsholt, T., Moser, C., Christensen, L. D., Van Gennip, M., et al. (2010). Polymorphonuclear leucocytes consume oxygen in sputum from chronic *Pseudomonas aeruginosa* pneumonia in cystic fibrosis. *Thorax* 65, 57–62. doi: 10.1136/thx.2009.114512

Konings, A. F., Martin, L. W., Sharples, K. J., Roddam, L. F., Latham, R., Reid, D. W., et al. (2013). *Pseudomonas aeruginosa* uses multiple pathways to acquire iron during chronic infection in cystic fibrosis lungs. *Infect. Immun.* 81, 2697–2704. doi: 10.1128/IAI.00418-13

Krewulak, K. D., and Vogel, H. J. (2008). Structural biology of bacterial iron uptake. *Biochim. Biophys. Acta* 1778, 1781–1804. doi: 10.1016/j.bbamem.2007.07.026

Kvitko, B. H., Goodyear, A., Propst, K. L., Dow, S. W., and Schweizer, H. P. (2012). *Burkholderia pseudomallei* known siderophores and hemin uptake are dispensable for lethal murine melioidosis. *PLoS Negl. Trop. Dis.* 6:e1715. doi: 10.1371/journal.pntd.0001715

Lamothe, J., and Valvano, M. A. (2008). *Burkholderia cenocepacia*-induced delay of acidification and phagolysosomal fusion in cystic fibrosis transmembrane conductance regulator (CFTR)-defective macrophages. *Microbiology* 154, 3825–3834. doi: 10.1099/mic.0.2008/023200-0

Lau, C. K., Krewulak, K. D., and Vogel, H. J. (2016). Bacterial ferrous iron transport: the Feo system. *FEMS Microbiol. Rev.* 40, 273–298. doi: 10.1093/femsre/fuv049

Lipuma, J. J. (2005). Update on the *Burkholderia cepacia* complex. *Curr. Opin. Pulm. Med.* 11, 528–533. doi: 10.1097/01.mcp.0000181475.85187.ed

Loutet, S. A., and Valvano, M. A. (2010). A decade of *Burkholderia cenocepacia* virulence determinant research. *Infect. Immun.* 78, 4088–4100. doi: 10.1128/IAI.00212-10

Loveridge, E. J., Jones, C., Bull, M. J., Moody, S. C., Kahl, M. W., Khan, Z., et al. (2017). Reclassification of the specialized metabolite producer *Pseudomonas mesoacidophila* ATCC 31433 as a member of the *Burkholderia cepacia* complex. *J. Bacteriol.* 199:e00125-17. doi: 10.1128/JB.00125-17

Madeira, A., Dos Santos, S. C., Santos, P. M., Coutinho, C. P., Tyrrell, J., McClean, S., et al. (2013). Proteomic profiling of *Burkholderia cenocepacia* clonal isolates with different virulence potential retrieved from a cystic fibrosis patient during chronic lung infection. *PLoS ONE* 8:e83065. doi: 10.1371/journal.pone.0083065

Mahenthiralingam, E., Vandamme, P., Campbell, M. E., Henry, D. A., Gravelle, A. M., Wong, L. T., et al. (2001). Infection with *Burkholderia cepacia* complex genomovars in patients with cystic fibrosis: virulent transmissible strains of genomovar III can replace *Burkholderia multivorans*. *Clin. Infect. Dis.* 33, 1469–1475. doi: 10.1086/322684

Martin, L. W., Reid, D. W., Sharples, K. J., and Lamont, I. L. (2011). *Pseudomonas* siderophores in the sputum of patients with cystic fibrosis. *Biometals* 24, 1059–1067. doi: 10.1007/s10534-011-9464-z

Marvig, R. L., Damkiaer, S., Khademi, S. M. H., Markussen, T. M., Molin, S., and Jelsbak, L. (2014). Within-host evolution of *Pseudomonas aeruginosa* reveals adaptation toward iron acquisition from hemoglobin. *Mbio* 5:e00966-14. doi: 10.1128/mBio.00966-14

Mathew, A., Eberl, L., and Carlier, A. L. (2014). A novel siderophore-independent strategy of iron uptake in the genus *Burkholderia*. *Mol. Microbiol.* 91, 805–820. doi: 10.1111/mmi.12499

Matsui, H., Grubb, B. R., Tarran, R., Randell, S. H., Gatzy, J. T., Davis, C. W., et al. (1998). Evidence for periciliary liquid layer depletion, not abnormal ion composition, in the pathogenesis of cystic fibrosis airways disease. *Cell* 95, 1005–1015. doi: 10.1016/S0092-8674(00)81724-9

Matsui, H., Verghese, M. W., Kesimer, M., Schwab, U. E., Randell, S. H., Sheehan, J. K., et al. (2005). Reduced three-dimensional motility in dehydrated airway mucus prevents neutrophil capture and killing bacteria on airway epithelial surfaces. *J. Immunol.* 175, 1090–1099. doi: 10.4049/jimmunol.175.2.1090

Mesureur, J., Feliciano, J. R., Wagner, N., Gomes, M. C., Zhang, L., Blanco-Gonzalez, M., et al. (2017). Macrophages, but not neutrophils, are critical for proliferation of *Burkholderia cenocepacia* and ensuing host-damaging inflammation. *PLoS Pathog.* 13:e1006437. doi: 10.1371/journal.ppat.1006437

Meyer, J. M., and Abdallah, M. A. (1978). The fluorescent pigment of pseudomonas fluorescens: biosynthesis, purification and physicochemical properties. *Microbiology* 107, 319–328. doi: 10.1099/00221287-107-2-319

Meyer, J. M., Hohnadel, D., and Halle, F. (1989). Cepabactin from *Pseudomonas cepacia*, a new type of siderophore. *J. Gen. Microbiol.* 135, 1479–1487. doi: 10.1099/00221287-135-6-1479

Meyer, J.-M., Van Van, T., Stintzi, A., Berge, O., and Winkelmann, G. (1995). Ornibactin production and transport properties in strains of *Burkholderia vietnamiensis* and *Burkholderia cepacia* (formerly *Pseudomonas cepacia*). *Biometals* 8, 309–317. doi: 10.1007/BF00141604

Mira, N. P., Madeira, A., Moreira, A. S., Coutinho, C. P., and Sa-Correia, I. (2011). Genomic expression analysis reveals strategies of *Burkholderia cenocepacia* to adapt to cystic fibrosis patients' airways and antimicrobial therapy. *PLoS ONE* 6:e28831. doi: 10.1371/journal.pone.0028831

Mott, T. M., Vijayakumar, S., Sbrana, E., Endsley, J. J., and Torres, A. G. (2015). Characterization of the *Burkholderia mallei tonB* mutant and its potential as a backbone strain for vaccine development. *PLoS Negl. Trop. Dis.* 9:e0003863. doi: 10.1371/journal.pntd.0003863

Nairz, M., Schroll, A., Sonnweber, T., and Weiss, G. (2010). The struggle for iron - a metal at the host-pathogen interface. *Cell Microbiol.* 12, 1691–1702. doi: 10.1111/j.1462-5822.2010.01529.x

Naoe, Y., Nakamura, N., Doi, A., Sawabe, M., Nakamura, H., Shiro, Y., et al. (2016). Crystal structure of bacterial haem importer complex in the inward-facing conformation. *Nat. Commun.* 7:13411. doi: 10.1038/ncomms13411

Neilands, J. B. (1995). Siderophores: structure and function of microbial iron transport compounds. *J. Biol. Chem.* 270, 26723–26726. doi: 10.1074/jbc.270.45.26723

Ngauy, V., Lemeshev, Y., Sadkowski, L., and Crawford, G. (2005). Cutaneous melioidosis in a man who was taken as a prisoner of war by the Japanese during World War II. *J. Clin. Microbiol.* 43, 970–972. doi: 10.1128/JCM.43.2.970-972.2005

Nguyen, A. T., O'Neill, M. J., Watts, A. M., Robson, C. L., Lamont, I. L., Wilks, A., et al. (2014). Adaptation of iron homeostasis pathways by a *Pseudomonas aeruginosa* pyoverdine mutant in the cystic fibrosis lung. *J. Bacteriol.* 196, 2265–2276. doi: 10.1128/JB.01491-14

Nierman, W. C., Deshazer, D., Kim, H. S., Tettelin, H., Nelson, K. E., Feldblyum, T., et al. (2004). Structural flexibility in the *Burkholderia mallei* genome. *Proc. Natl. Acad. Sci. U.S.A.* 101, 14246–14251. doi: 10.1073/pnas.0403306101

Noinaj, N., Guillier, M., Barnard, T. J., and Buchanan, S. K. (2010). TonB-dependent transporters: regulation, structure, and function. *Annu. Rev. Microbiol.* 64, 43–60. doi: 10.1146/annurev.micro.112408.134247

O'Grady, E. P., and Sokol, P. A. (2011). *Burkholderia cenocepacia* differential gene expression during host-pathogen interactions and adaptation to the host environment. *Front. Cell. Infect. Microbiol.* 1:15. doi: 10.3389/fcimb.2011.00015

O'Neill, M. J., and Wilks, A. (2013). The *P. aeruginosa* heme binding protein PhuS is a heme oxygenase titratable regulator of heme uptake. *ACS Chem. Biol.* 8, 1794–1802. doi: 10.1021/cb400165b

Ong, C., Ooi, C. H., Wang, D., Chong, H., Ng, K. C., Rodrigues, F., et al. (2004). Patterns of large-scale genomic variation in virulent and avirulent *Burkholderia* species. *Genome Res.* 14, 2295–2307. doi: 10.1101/gr.1608904

Ong, K. S., Aw, Y. K., Lee, L. H., Yule, C. M., Cheow, Y. L., and Lee, S. M. (2016). *Burkholderia paludis* sp. nov., an antibiotic-siderophore producing novel *Burkholderia cepacia* complex species, isolated from Malaysian tropical peat swamp soil. *Front. Microbiol.* 7:2046. doi: 10.3389/fmicb.2016.02046

Oren, A., and Garrity, A. G. (2015). Proposal to modify rule 27 of the international code of nomenclature of prokaryotes. *Int. J. Syst. Evol. Microbiol.* 65:2342. doi: 10.1099/ijs.0.000288

Palmer, K. L., Aye, L. M., and Whiteley, M. (2007). Nutritional cues control *Pseudomonas aeruginosa* multicellular behavior in cystic fibrosis sputum. *J. Bacteriol.* 189, 8079–8087. doi: 10.1128/JB.01138-07

Palmer, K. L., Mashburn, L. M., Singh, P. K., and Whiteley, M. (2005). Cystic fibrosis sputum supports growth and cues key aspects of *Pseudomonas aeruginosa* physiology. *J. Bacteriol.* 187, 5267–5277. doi: 10.1128/JB.187.15.5267-5277.2005

Parke, J. L., and Gurian-Sherman, D. (2001). Diversity of the *Burkholderia cepacia* complex and implications for risk assessment of biological control strains. *Annu. Rev. Phytopathol.* 39, 225–258. doi: 10.1146/annurev.phyto.39.1.225

Parrow, N. L., Fleming, R. E., and Minnick, M. F. (2013). Sequestration and scavenging of iron in infection. *Infect. Immun.* 81, 3503–3514. doi: 10.1128/IAI.00602-13

Peeters, E., Sass, A., Mahenthiralingam, E., Nelis, H., and Coenye, T. (2010). Transcriptional response of *Burkholderia cenocepacia* J2315 sessile cells to treatments with high doses of hydrogen peroxide and sodium hypochlorite. *BMC Genomics* 11:90. doi: 10.1186/1471-2164-11-90

Perez, A., Issler, A. C., Cotton, C. U., Kelley, T. J., Verkman, A. S., and Davis, P. B. (2007). CFTR inhibition mimics the cystic fibrosis inflammatory profile. *Am. J. Physiol. Lung Cell Mol. Physiol.* 292, L383–L395. doi: 10.1152/ajplung.00403.2005

Perumal Samy, R., Stiles, B. G., Sethi, G., and Lim, L. H. K. (2017). Melioidosis: clinical impact and public health threat in the tropics. *PLoS Negl. Trop. Dis.* 11:e0004738. doi: 10.1371/journal.pntd.0004738

Pessi, G., Braunwalder, R., Grunau, A., Omasits, U., Ahrens, C. H., and Eberl, L. (2013). Response of *Burkholderia cenocepacia* H111 to micro-oxia. *PLoS ONE* 8:e72939. doi: 10.1371/journal.pone.0072939

Ratledge, C., and Dover, L. G. (2000). Iron metabolism in pathogenic bacteria. *Annu. Rev. Microbiol.* 54, 881–941. doi: 10.1146/annurev.micro.54.1.881

Reid, D. W., Anderson, G. J., and Lamont, I. L. (2009). Role of lung iron in determining the bacterial and host struggle in cystic fibrosis. *Am. J. Physiol. Lung Cell. Mol. Physiol.* 297, L795–L802. doi: 10.1152/ajplung.00132.2009

Reid, D. W., Carroll, V., O'may, C., Champion, A., and Kirov, S. M. (2007). Increased airway iron as a potential factor in the persistence of *Pseudomonas aeruginosa* infection in cystic fibrosis. *Eur. Respir. J.* 30, 286–292. doi: 10.1183/09031936.00154006

Reid, D. W., Lam, Q. T., Schneider, H., and Walters, E. H. (2004). Airway iron and iron-regulatory cytokines in cystic fibrosis. *Eur. Respir. J.* 24, 286–291. doi: 10.1183/09031936.04.00104803

Reid, D. W., Withers, N. J., Francis, L., Wilson, J. W., and Kotsimbos, T. C. (2002). Iron deficiency in cystic fibrosis: relationship to lung disease severity and chronic *Pseudomonas aeruginosa* infection. *Chest* 121, 48–54. doi: 10.1378/chest.121.1.48

Reik, R., Spilker, T., and Lipuma, J. J. (2005). Distribution of *Burkholderia cepacia complex* species among isolates recovered from persons with or without cystic fibrosis. *J. Clin. Microbiol.* 43, 2926–2928. doi: 10.1128/JCM.43.6.2926-2928.2005

Rhodes, K. A., and Schweizer, H. P. (2016). Antibiotic resistance in *Burkholderia* species. *Drug Resist. Update* 28, 82–90. doi: 10.1016/j.drup.2016.07.003

Rose, H., Baldwin, A., Dowson, C. G., and Mahenthiralingam, E. (2009). Biocide susceptibility of the *Burkholderia cepacia* complex. *J. Antimicrob. Chemother.* 63, 502–510. doi: 10.1093/jac/dkn540

Rottig, M., Medema, M. H., Blin, K., Weber, T., Rausch, C., and Kohlbacher, O. (2011). NRPSpredictor2–a web server for predicting NRPS adenylation domain specificity. *Nucleic Acids Res.* 39, W362–W367. doi: 10.1093/nar/gkr323

Roy, S., Douglas, C. W., and Stafford, G. P. (2010). A novel sialic acid utilization and uptake system in the periodontal pathogen *Tannerella forsythia*. *J. Bacteriol.* 192, 2285–2293. doi: 10.1128/JB.00079-10

Runyen-Janecky, L. J. (2013). Role and regulation of heme iron acquisition in gram-negative pathogens. *Front. Cell. Infect. Microbiol.* 3:55. doi: 10.3389/fcimb.2013.00055

Sanchez, M., Sabio, L., Galvez, N., Capdevila, M., and Dominguez-Vera, J. M. (2017). Iron chemistry at the service of life. *IUBMB Life* 69, 382–388. doi: 10.1002/iub.1602

Sawana, A., Adeolu, M., and Gupta, R. S. (2014). Molecular signatures and phylogenomic analysis of the genus *Burkholderia*: proposal for division of this genus into the emended genus *Burkholderia* containing pathogenic organisms and a new genus *Paraburkholderia* gen. nov. harboring environmental species. *Front. Genet.* 5:429. doi: 10.3389/fgene.2014.00429

Schauer, K., Rodionov, D. A., and De Reuse, H. (2008). New substrates for TonB-dependent transport: do we only see the "tip of the iceberg"? *Trends Biochem. Sci.* 33, 330–338. doi: 10.1016/j.tibs.2008.04.012

Schell, M. A., Ulrich, R. L., Ribot, W. J., Brueggemann, E. E., Hines, H. B., Chen, D., et al. (2007). Type VI secretion is a major virulence determinant in *Burkholderia mallei*. *Mol. Microbiol.* 64, 1466–1485. doi: 10.1111/j.1365-2958.2007.05734.x

Shalom, G., Shaw, J. G., and Thomas, M. S. (2007). *In vivo* expression technology identifies a type VI secretion system locus in *Burkholderia pseudomallei* that is induced upon invasion of macrophages. *Microbiology* 153, 2689–2699. doi: 10.1099/mic.0.2007/006585-0

Singh, P. K., Parsek, M. R., Greenberg, E. P., and Welsh, M. J. (2002). A component of innate immunity prevents bacterial biofilm development. *Nature* 417, 552–555. doi: 10.1038/417552a

Skaar, E. P. (2010). The battle for iron between bacterial pathogens and their vertebrate hosts. *PLoS Pathog.* 6:e1000949. doi: 10.1371/journal.ppat.1000949

Smith, E. E., Buckley, D. G., Wu, Z., Saenphimmachak, C., Hoffman, L. R., D'argenio, D. A., et al. (2006). Genetic adaptation by *Pseudomonas aeruginosa* to the airways of cystic fibrosis patients. *Proc. Natl. Acad. Sci. U.S.A.* 103, 8487–8492. doi: 10.1073/pnas.0602138103

Smith, M. D., Wuthiekanun, V., Walsh, A. L., and White, N. J. (1995). Quantitative recovery of *Burkholderia pseudomallei* from soil in Thailand. *Trans. R. Soc. Trop. Med. Hyg.* 89, 488–490. doi: 10.1016/0035-9203(95)90078-0

Sokol, P. A. (1986). Production and utilization of pyochelin by clinical isolates of *Pseudomonas cepacia*. *J. Clin. Microbiol.* 23, 560–562.

Sokol, P. A., and Woods, D. E. (1988). Effect of pyochelin on *Pseudomonas cepacia* respiratory infections. *Microb. Pathog.* 5, 197–205. doi: 10.1016/0882-4010(88)90022-8

Sokol, P. A., Darling, P., Woods, D. E., Mahenthiralingam, E., and Kooi, C. (1999). Role of ornibactin biosynthesis in the virulence of *Burkholderia cepacia*: characterization of pvdA, the gene encoding L-ornithine N(5)-oxygenase. *Infect. Immun.* 67, 4443–4455.

Son, M. S., Matthews, W. J. Jr., Kang, Y., Nguyen, D. T., and Hoang, T. T. (2007). *In vivo* evidence of *Pseudomonas aeruginosa* nutrient acquisition and pathogenesis in the lungs of cystic fibrosis patients. *Infect. Immun.* 75, 5313–5324. doi: 10.1128/IAI.01807-06

Song, E., Jaishankar, G. B., Saleh, H., Jithpratuck, W., Sahni, R., and Krishnaswamy, G. (2011). Chronic granulomatous disease: a review of the infectious and inflammatory complications. *Clin. Mol. Allergy* 9:10. doi: 10.1186/1476-7961-9-10

Song, Y., Salinas, D., Nielson, D. W., and Verkman, A. S. (2006). Hyperacidity of secreted fluid from submucosal glands in early cystic fibrosis. *Am. J. Physiol. Cell Physiol.* 290, C741–C749. doi: 10.1152/ajpcell.00379.2005

Sousa, S. A., Ramos, C. G., and Leitao, J. H. (2011). *Burkholderia cepacia* complex: emerging multihost pathogens equipped with a wide range of virulence factors and determinants. *Int. J. Microbiol.* 2011:607575. doi: 10.1155/2011/607575

Stephan, H., Freund, S., Beck, W., Jung, G., Meyer, J. M., and Winkelmann, G. (1993). Ornibactins–a new family of siderophores from *Pseudomonas*. *Biometals* 6, 93–100. doi: 10.1007/BF00140109

Stites, S. W., Walters, B., O'brien-Ladner, A. R., Bailey, K., and Wesselius, L. J. (1998). Increased iron and ferritin content of sputum from patients with cystic fibrosis or chronic bronchitis. *Chest* 114, 814–819. doi: 10.1378/chest.114.3.814

Sun, G. X., Zhou, W. Q., and Zhong, J. J. (2006). Organotin decomposition by pyochelin, secreted by *Pseudomonas aeruginosa* even in an iron-sufficient environment. *Appl. Environ. Microbiol.* 72, 6411–6413. doi: 10.1128/AEM.00957-06

Tang, A. C., Turvey, S. E., Alves, M. P., Regamey, N., Tummler, B., and Hartl, D. (2014). Current concepts: host-pathogen interactions in cystic fibrosis airways disease. *Eur. Respir. Rev.* 23, 320–332. doi: 10.1183/09059180.00006113

Thomas, M. S. (2007). Iron acquisition mechanisms of the *Burkholderia cepacia* complex. *Biometals* 20, 431–452. doi: 10.1007/s10534-006-9065-4

Thomas, S. R., Ray, A., Hodson, M. E., and Pitt, T. L. (2000). Increased sputum amino acid concentrations and auxotrophy of *Pseudomonas aeruginosa* in severe cystic fibrosis lung disease. *Thorax* 55, 795–797. doi: 10.1136/thorax.55.9.795

Tuanyok, A., Kim, H. S., Nierman, W. C., Yu, Y., Dunbar, J., Moore, R. A., et al. (2005). Genome-wide expression analysis of iron regulation in *Burkholderia pseudomallei* and *Burkholderia mallei* using DNA microarrays. *FEMS Microbiol. Lett.* 252, 327–335. doi: 10.1016/j.femsle.2005.09.043

Tunney, M. M., Field, T. R., Moriarty, T. F., Patrick, S., Doering, G., Muhlebach, M. S., et al. (2008). Detection of anaerobic bacteria in high numbers in sputum from patients with cystic fibrosis. *Am. J. Respir. Crit. Care Med.* 177, 995–1001. doi: 10.1164/rccm.200708-1151OC

Tyrrell, J., Whelan, N., Wright, C., Sa-Correia, I., McClean, S., Thomas, M., et al. (2015). Investigation of the multifaceted iron acquisition strategies of *Burkholderia cenocepacia*. *Biometals* 28, 367–380. doi: 10.1007/s10534-015-9840-1

Uehlinger, S., Schwager, S., Bernier, S. P., Riedel, K., Nguyen, D. T., Sokol, P. A., et al. (2009). Identification of specific and universal virulence factors in *Burkholderia cenocepacia* strains by using multiple infection hosts. *Infect. Immun.* 77, 4102–4110. doi: 10.1128/IAI.00398-09

Valvano, M. A. (2015). Intracellular survival of *Burkholderia cepacia* complex in phagocytic cells. *Can. J. Microbiol.* 61, 607–615. doi: 10.1139/cjm-2015-0316

Vargas-Straube, M. J., Camara, B., Tello, M., Montero-Silva, F., Cardenas, F., and Seeger, M. (2016). Genetic and functional analysis of the biosynthesis of a non-ribosomal peptide siderophore in *Burkholderia xenovorans* LB400. *PLoS ONE* 11:e0151273. doi: 10.1371/journal.pone.0151273

Vergunst, A. C., Meijer, A. H., Renshaw, S. A., and O'callaghan, D. (2010). *Burkholderia cenocepacia* creates an intramacrophage replication niche in zebrafish embryos, followed by bacterial dissemination and establishment of systemic infection. *Infect. Immun.* 78, 1495–1508. doi: 10.1128/IAI.00743-09

Verma, A. K., Saminathan, M., Neha, Tiwari, R., Dhama, K., and Vir Singh, S. (2014). Glanders-A re-emerging zoonotic disease: a review. *J. Biol. Sci.* 14, 38–51. doi: 10.3923/jbs.2014.38.51

Visca, P., Ciervo, A., Sanfilippo, V., and Orsi, N. (1993). Iron-regulated salicylate synthesis by *Pseudomonas* spp. *J. Gen. Microbiol.* 139, 1995–2001. doi: 10.1099/00221287-139-9-1995

Visca, P., Colotti, G., Serino, L., Verzili, D., Orsi, N., and Chiancone, E. (1992). Metal regulation of siderophore synthesis in *Pseudomonas aeruginosa* and functional effects of siderophore-metal complexes. *Appl. Environ. Microbiol.* 58, 2886–2893.

Visser, M. B., Majumdar, S., Hani, E., and Sokol, P. A. (2004). Importance of the ornibactin and pyochelin siderophore transport systems in *Burkholderia cenocepacia* lung infections. *Infect. Immun.* 72, 2850–2857. doi: 10.1128/IAI.72.5.2850-2857.2004

Wand, M. E., Muller, C. M., Titball, R. W., and Michell, S. L. (2011). Macrophage and *Galleria mellonella* infection models reflect the virulence of naturally occurring isolates of *B. pseudomallei, B. thailandensis* and *B. oklahomensis*. *BMC Microbiol.* 11:11. doi: 10.1186/1471-2180-11-11

Wang, J., Lory, S., Ramphal, R., and Jin, S. (1996). Isolation and characterization of *Pseudomonas aeruginosa* genes inducible by respiratory mucus derived from cystic fibrosis patients. *Mol. Microbiol.* 22, 1005–1012. doi: 10.1046/j.1365-2958.1996.01533.x

Whitby, P. W., Vanwagoner, T. M., Springer, J. M., Morton, D. J., Seale, T. W., and Stull, T. L. (2006). *Burkholderia cenocepacia* utilizes ferritin as an iron source. *J. Med. Microbiol.* 55, 661–668. doi: 10.1099/jmm.0.46199-0

White, N. J. (2003). Melioidosis. *Lancet* 361, 1715–1722. doi: 10.1016/S0140-6736(03)13374-0

Whitlock, G. C., Estes, D. M., and Torres, A. G. (2007). Glanders: off to the races with *Burkholderia mallei*. *FEMS Microbiol. Lett.* 277, 115–122. doi: 10.1111/j.1574-6968.2007.00949.x

Wiersinga, W. J., Currie, B. J., and Peacock, S. J. (2012). Melioidosis. *N. Engl. J. Med.* 367, 1035–1044. doi: 10.1056/NEJMra1204699

Wiersinga, W. J., Van Der Poll, T., White, N. J., Day, N. P., and Peacock, S. J. (2006). Melioidosis: insights into the pathogenicity of *Burkholderia pseudomallei*. *Nat. Rev. Microbiol.* 4, 272–282. doi: 10.1038/nrmicro1385

Wolpert, M., Gust, B., Kammerer, B., and Heide, L. (2007). Effects of deletions of mbtH-like genes on clorobiocin biosynthesis in *Streptomyces coelicolor*. *Microbiology* 153, 1413–1423. doi: 10.1099/mic.0.2006/002998-0

Worlitzsch, D., Tarran, R., Ulrich, M., Schwab, U., Cekici, A., Meyer, K. C., et al. (2002). Effects of reduced mucus oxygen concentration in airway *Pseudomonas* infections of cystic fibrosis patients. *J. Clin. Invest.* 109, 317–325. doi: 10.1172/JCI0213870

Yabuuchi, E., Kosako, Y., Oyaizu, H., Yano, I., Hotta, H., Hashimoto, Y., et al. (1992). Proposal of *Burkholderia* gen. nov. and transfer of seven species of the genus *Pseudomonas* homology group II to the new genus, with the type species *Burkholderia cepacia* (Palleroni and Holmes 1981) comb. nov. *Microbiol. Immunol.* 36, 1251–1275. doi: 10.1111/j.1348-0421.1992.tb02129.x

Yang, H. M., Chaowagul, W., and Sokol, P. A. (1991). Siderophore production by *Pseudomonas pseudomallei*. *Infect. Immun.* 59, 776–780.

Yang, H., Kooi, C. D., and Sokol, P. A. (1993). Ability of *Pseudomonas pseudomallei* malleobactin to acquire transferrin-bound, lactoferrin-bound, and cell-derived iron. *Infect. Immun.* 61, 656–662.

Yoder-Himes, D. R., Konstantinidis, K. T., and Tiedje, J. M. (2010). Identification of potential therapeutic targets for *Burkholderia cenocepacia* by comparative transcriptomics. *PLoS ONE* 5:e8724. doi: 10.1371/journal.pone.0008724

Yoon, S. S., Coakley, R., Lau, G. W., Lymar, S. V., Gaston, B., Karabulut, A. C., et al. (2006). Anaerobic killing of mucoid *Pseudomonas aeruginosa* by acidified nitrite derivatives under cystic fibrosis airway conditions. *J. Clin. Invest.* 116, 436–446. doi: 10.1172/JCI24684

Youard, Z. A., Wenner, N., and Reimmann, C. (2011). Iron acquisition with the natural siderophore enantiomers pyochelin and enantio-pyochelin in *Pseudomonas* species. *Biometals* 24, 513–522. doi: 10.1007/s10534-010-9399-9

Yuhara, S., Komatsu, H., Goto, H., Ohtsubo, Y., Nagata, Y., and Tsuda, M. (2008). Pleiotropic roles of iron-responsive transcriptional regulator Fur in *Burkholderia multivorans*. *Microbiology* 154, 1763–1774. doi: 10.1099/mic.0.2007/015537-0

Zeng, X., Mo, Y., Xu, F., and Lin, J. (2013). Identification and characterization of a periplasmic trilactone esterase, Cee, revealed unique features of ferric enterobactin acquisition in *Campylobacter*. *Mol. Microbiol.* 87, 594–608. doi: 10.1111/mmi.12118

Zlosnik, J. E., Zhou, G., Brant, R., Henry, D. A., Hird, T. J., Mahenthiralingam, E., et al. (2015). *Burkholderia* species infections in patients with cystic fibrosis in British Columbia, Canada. 30 years' experience. *Ann. Am. Thorac. Soc.* 12, 70–78. doi: 10.1513/AnnalsATS.201408-395OC

Conflict of Interest Statement: The authors declare that the research was conducted in the absence of any commercial or financial relationships that could be construed as a potential conflict of interest.

frontiers in Cellular and Infection Microbiology

MINI REVIEW
published: 04 April 2017
doi: 10.3389/fcimb.2017.00107

Iron and Virulence in *Francisella tularensis*

Girija Ramakrishnan *

Department of Medicine/Division of Infectious Diseases, University of Virginia, Charlottesville, VA, USA

Francisella tularensis, the causative agent of tularemia, is a Gram-negative bacterium that infects a variety of cell types including macrophages, and propagates with great efficiency in the cytoplasm. Iron, essential for key enzymatic and redox reactions, is among the nutrients required to support this pathogenic lifestyle and the bacterium relies on specialized mechanisms to acquire iron within the host environment. Two distinct pathways for iron acquisition are encoded by the *F. tularensis* genome- a siderophore-dependent ferric iron uptake system and a ferrous iron transport system. Genes of the Fur-regulated *fslABCDEF* operon direct the production and transport of the siderophore rhizoferrin. Siderophore biosynthesis involves enzymes FslA and FslC, while export across the inner membrane is mediated by FslB. Uptake of the rhizoferrin- ferric iron complex is effected by the siderophore receptor FslE in the outer membrane in a TonB-independent process, and FslD is responsible for uptake across the inner membrane. Ferrous iron uptake relies largely on high affinity transport by FupA in the outer membrane, while the Fur-regulated FeoB protein mediates transport across the inner membrane. FslE and FupA are paralogous proteins, sharing sequence similarity and possibly sharing structural features as well. This review summarizes current knowledge of iron acquisition in this organism and the critical role of these uptake systems in bacterial pathogenicity.

Keywords: Siderophore, FeoB, intracellular pathogen, FslE, FupA, TonB-independent, *Francisella tularensis*

OPEN ACCESS

Edited by:
Pierre Cornelis,
Vrije Universiteit Brussel, Belgium

Reviewed by:
Charles Martin Dozois,
Institut National de la Recherche Scientifique, Canada
Erin R. Murphy,
Ohio University, USA
Paul Edward Carlson,
US Food and Drug Administration, USA

***Correspondence:**
Girija Ramakrishnan
girija@virginia.edu

Received: *30 January 2017*
Accepted: *16 March 2017*
Published: *04 April 2017*

Citation:
Ramakrishnan G (2017) Iron and Virulence in Francisella tularensis. Front. Cell. Infect. Microbiol. 7:107. doi: 10.3389/fcimb.2017.00107

INTRODUCTION

Francisella tularensis, the etiological agent of the zoonosis tularemia, is a Gram-negative gamma-proteobacterium with a small genome of 1.89 Mb (Sjöstedt, 2007). The species is further differentiated into three subspecies, of which *tularensis* causes a more severe disease than *holarctica*, while *mediasiatica* is less well-studied. The closely related species *F. novicida*, considered to be of a more ancestral lineage (Svensson et al., 2005) and with a genome sequence identity of ~98% (Larsson et al., 2009) is an opportunistic human pathogen, but can cause a virulent tularemia-like disease in mice.

In the laboratory, studies have largely focused on virulent strain Schu S4 of the *tularensis* subspecies, the attenuated live vaccine strain (LVS) derived from a *holarctica* isolate and the strain U112 of *F. novicida*. These three isolates share many biological attributes although their genetic and functional differences significantly impact virulence (Jones et al., 2012; Celli and Zahrt, 2013; Kingry et al., 2014). For this reason, all three strains are referred to in this review as *F. tularensis* unless specifically identified in order to highlight particular differences.

F. tularensis is a facultative intracellular pathogen infecting a wide variety of cells, including mammalian and arthropod cells (Ozanic et al., 2015). Following uptake into the macrophage, the bacteria at first reside within a phagosome, but then rapidly escape into the cytoplasm. Phagosomal

escape is dependent on the *igl* operon and associated genes in the *Francisella* Pathogenicity Island (FPI) that encode components of a putative Type VI secretion system (Barker et al., 2009; de Bruin et al., 2011). The bacteria replicate to high numbers in the cytoplasm resulting finally in apoptotic death of the host cell. Adaptation to the specialized intracellular lifestyle is associated with evolutionary loss of genes for many metabolic pathways (Rohmer et al., 2007; Larsson et al., 2009), but *F. tularensis* has retained or evolved mechanisms to efficiently acquire essential nutrients within the intracellular niche of the different cell types that it infects (Meibom and Charbit, 2010).

Mice have been extensively used to model animal infection (Lyons and Wu, 2007). Phagocytic cells are thought to be the first infected (Hall et al., 2008); subsequently infection is disseminated to other tissues in the body. *F. tularensis* exercises several strategies to evade immune responses and is able to replicate to high levels in the liver, spleen and lungs before the immune system is provoked to respond with a destructive cytokine storm (Sharma et al., 2011; Jones et al., 2012).

Iron and Francisella

Francisella requires iron for essential cellular functions. Early studies reported that infection with *F. tularensis* induces an iron-withholding response typical of the innate nutritional immunity defense mechanism (Pekarek et al., 1969). However, the intracellular pathogen manipulates host cell iron metabolism to support growth; LVS induces infected macrophages to increase iron flow through the cell by enhanced expression of the transferrin receptor TfR1 for uptake of iron and in parallel, increased expression of Dmt1 that moves endosomal iron into the cytoplasm and a slight increase in ferroportin that promotes outflow of iron from the cell (Pan et al., 2010). A functional Nramp1protein that also transports endosomal iron into the cytoplasm restricts growth of endosome-resident bacteria but enhances *Francisella* growth (Kovářová et al., 2000, 2002), highlighting the importance of cytoplasmic iron availability for pathogenesis. However, the nature of the host iron sources accessed by the organism remains to be characterized. Iron-limitation restricts growth of bacteria in culture (Deng et al., 2006; Sullivan et al., 2006) as well as within the macrophage (Fortier et al., 1995).

As might be predicted, growth of *F. tularensis* is inhibited by gallium, which competes with ferric iron for uptake and also interferes with iron-dependent biological processes (Olakanmi et al., 2010; Lindgren and Sjöstedt, 2016). Inhibition of the iron-associated enzymes catalase and superoxide dismutase leads to increased susceptibility to oxidative stress (Bakshi et al., 2006; Lindgren et al., 2007; Olakanmi et al., 2010; Binesse et al., 2015).

Iron metabolism appears to differ among *F. tularensis* isolates. LVS expresses higher levels of bacterioferritin as compared to Schu S4 (Hubálek et al., 2003, 2004). Consistent with these findings, isolates of the *holarctica* subspecies have greater iron stores than *tularensis* isolates, and since iron is closely associated with generation of reactive oxygen species, *holarctica* strains are more susceptible to oxidative stress (Lindgren et al., 2011).

Fur and Iron Regulation of Genes

A *fur* ortholog is encoded in the *F. tularensis* genome and the predicted Fur protein contains elements known to be important for Fur function (Pérard et al., 2016). The *fur* gene is adjacent to the *fsl* operon encoding components of a siderophore- mediated iron uptake pathway, and a canonical Furbox is located upstream of the first gene of the operon, *fslA* (**Figure 1A**). Expression of the *fsl* operon is induced in iron-limiting media (Deng et al., 2006; Sullivan et al., 2006; Buchan et al., 2008). Loss of the *fur* gene results in deregulated transcription of the *fsl* operon and increased siderophore production (Buchan et al., 2008; Ramakrishnan et al., 2008). Expression of the inner membrane ferrous iron transporter *feoB* is also upregulated in a *fur* mutant (Pérez and Ramakrishnan, 2014).

Exposure to iron limitation was also shown to increase virulence of an *F. tularensis* isolate, suggesting that pathogenicity is influenced by iron levels (Bhatnagar et al., 1995). Microarray analysis of RNA indicated that besides the *fsl* operon, transcription of the *igl* operon was increased under iron limitation (Deng et al., 2006). Proteomic analysis also confirmed that iron limitation results in increased levels of the IglC protein (Lenco et al., 2007). However, although an *fslB-lacZ* reporter could be repressed by overexpression of Fur, an *iglB-lacZ* reporter was not similarly repressible (Buchan et al., 2008), suggesting that a mechanism besides Fur regulates the *igl* genes in response to iron levels in *F. tularensis*.

Siderophore-Mediated Iron Acquisition

A "growth inducing substance (GIS)" that promoted growth of *F. tularensis* bacteria from small inocula was reported in the 1960s (Halmann and Mager, 1967; Halmann et al., 1967); in all likelihood this substance was the siderophore now identified as the polycarboxylate rhizoferrin (Drechsel et al., 1991; Thieken and Winkelmann, 1992; Sullivan et al., 2006). Rhizoferrin is structurally simple, comprising 2 citrate moieties linked through amide bonds to a putrescine backbone (**Figure 1B**). Originally identified as a fungal siderophore (Drechsel et al., 1991; Thieken and Winkelmann, 1992), rhizoferrin was subsequently also isolated from a strain of the bacterium *Ralstonia pickettii* (Münzinger et al., 1999). The identification of the siderophore made by *F. tularensis* as rhizoferrin (Sullivan et al., 2006), and the subsequent identification of the *Legionella pneumophila* siderophore legiobactin as also rhizoferrin (Burnside et al., 2015) suggests that this siderophore may be more widely prevalent in bacteria than suspected. Structurally related siderophores made by bacteria include staphyloferrin A (Konetschny-Rapp et al., 1990) and corynebactin (Zajdowicz et al., 2012), where D-ornithine and lysine, respectively, constitute the siderophore backbone in place of the putrescine present in rhizoferrin. The *R. pickettii* rhizoferrin was shown by CD spectroscopy to be an S-S enantiomer in contrast to the R-R fungal molecule (Münzinger et al., 1999). Whether all bacterial rhizoferrins adopt the S-S conformation is not clear, but bacteria making rhizoferrin are capable of utilizing the fungal form for iron uptake (Münzinger et al., 1999; Kiss et al., 2008).

Genes for synthesis and transport of *Francisella* rhizoferrin are located on the siderophore operon *fslABCDEF* (also designated

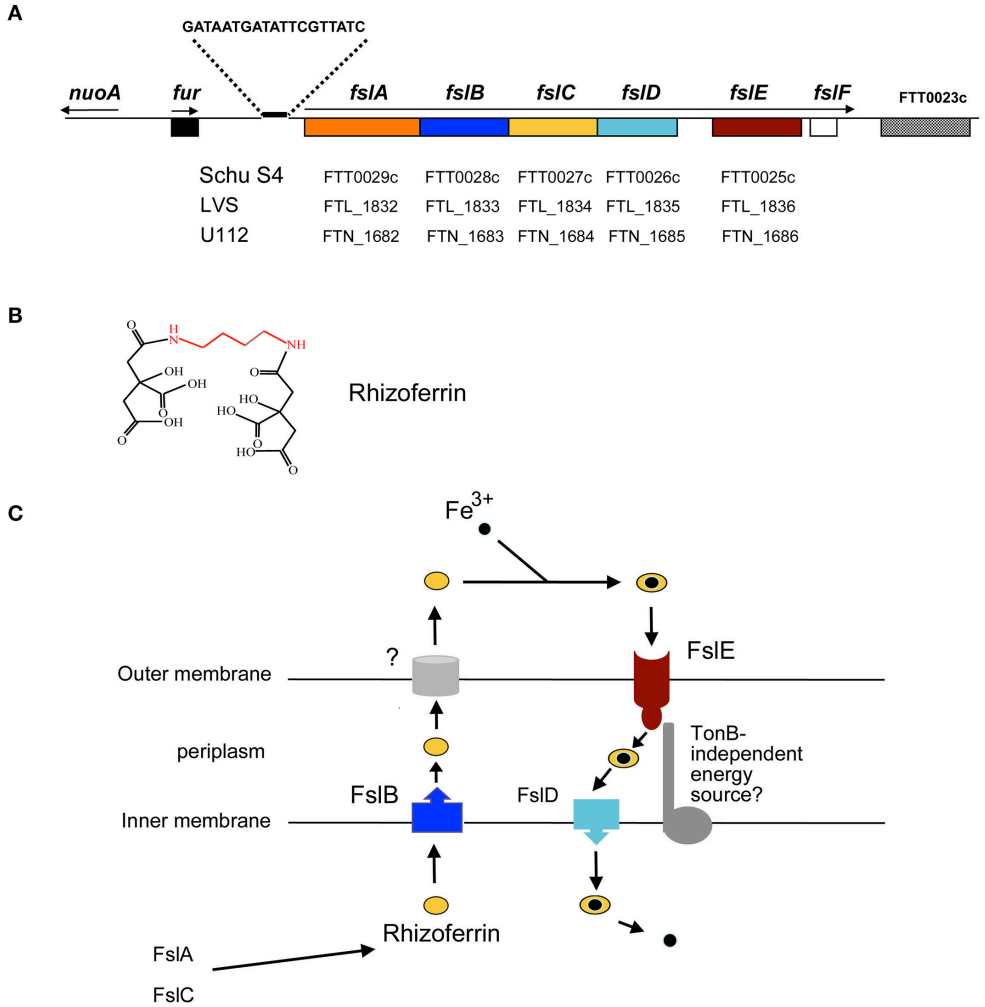

FIGURE 1 | Siderophore-mediated iron acquisition in *F. tularensis*. (A) The *fur-fsl* locus of the *F. tularensis* subsp. *tularensis* chromosome is depicted and the corresponding gene designations in the Schu S4, LVS, and U112 genomes are indicated. The Furbox upstream of the *fslABCDEF* operon is shown. Arrows indicate the direction and extent of transcribed regions. **(B)** A schematic of the *F. tularensis* siderophore, rhizoferrin comprising two citrate molecules linked by amide bonds to a putrescine backbone (in red). **(C)** Current model for siderophore-mediated iron acquisition in *F. tularensis* and the roles of the *fsl* operon products. FslA and FslC encode enzymes for biosynthesis of the siderophore. The siderophore is released into the extracellular medium by the action of FslB and an as yet unknown outer membrane component. The outer membrane siderophore receptor FslE, and FslD in the inner membrane mediate uptake of the ferric-siderophore complex. It is not known if a TonB analog facilitates FslE function.

figABCDEF; (Deng et al., 2006; Sullivan et al., 2006; Milne et al., 2007; Buchan et al., 2008; Ramakrishnan et al., 2008); **Figures 1A,C**). Analysis of individual mutants as well as complementation of a strain carrying a complete deletion of the *fslA-F* genes helped to determine the roles played by the different genes in siderophore-mediated iron acquisition, as detailed below.

fslA and *fslC* and share homology with genes found in siderophore biosynthetic loci of other bacteria. FslA is similar to the aerobactin synthetases IucA/IucC and a member of the non-ribosomal peptide synthetase-independent siderophore (NIS) synthetases, enzymes that assemble non-peptide siderophores using dicarboxylic acids and diamines or amino-alcohols (Challis, 2005). FslC is predicted to be a member of the pyridoxal phosphate-dependent decarboxylases. Mutant analysis demonstrated that both *fslA* and *fslC* are required for *Francisella* rhizoferrin production (Deng et al., 2006; Sullivan et al., 2006; Lindgren et al., 2009; Thomas-Charles et al., 2013). Rhizoferrin biosynthesis in *F. tularensis*, involving just two dedicated enzymes, may be the simplest siderophore biosynthetic pathway identified thus far.

fslB encodes a transporter of the Major Facilitator superfamily (MFS) and deletion of this gene in *F. novicida* results in reduced levels of siderophore activity in the culture medium (Kiss et al., 2008). Additionally, detection of siderophore activity in culture supernatants of an LVS Δ*fslA-F* mutant

required complementation with the *fslB* gene in addition to the biosynthetic genes *fslA* and *fslC* (Pérez et al., 2016). These observations support a role for FslB in export of the siderophore across the cytoplasmic membrane. How the siderophore is channeled through the outer membrane into the extracellular space is currently not known.

fslD encodes an inner membrane MFS protein and deletion of this gene was found to have little effect on siderophore production (Kiss et al., 2008). The role of this protein in siderophore-mediated iron uptake across the cytoplasmic membrane was deduced on the basis of complementation studies: a Schu S4 Δ*fslA-F* mutant is able to transport $^{55}Fe^{3+}$ complexed to siderophore only when complemented with the *fslD* gene in addition to the *fslE* receptor gene (see below; Pérez et al., 2016).

fslE, the fifth gene in the operon, encodes an outer membrane protein unique to the *Francisella* genus Larsson et al., 2005; Huntley et al., 2007). Δ*fslE* mutants are impaired for growth in iron-limiting media and are unable to utilize exogenous siderophore for growth (Kiss et al., 2008; Ramakrishnan et al., 2008). In transport assays, *fslE* mutants proved incapable of siderophore-mediated $^{55}Fe^{3+}$ uptake, establishing a role for FslE as receptor for the siderophore (Ramakrishnan et al., 2012). FslE can also transport the iron mimic gallium in complex with rhizoferrin as shown by the resistance of *fslA* and *fslE* mutants to gallium (Pérez et al., 2016).

The last gene of the *fsl* operon, *fslF*, varies structurally among the *tularensis* and the *novicida* species, being truncated in the *tularensis* isolates. Studies with a Δ*fslF* mutant in Schu S4 indicate that the gene does not influence iron transport in *F. tularensis* (Pérez et al., 2016).

Siderophore-mediated iron transport by outer membrane receptors in Gram-negative bacteria is typically dependent on the proton motive force transduced by the TonB-ExbB-ExbD complex (Noinaj et al., 2010). The *Francisella* genome, however, does not encode orthologs of *tonB*, *exbB,* and *exbD*, implying that alternative mechanisms must facilitate siderophore -iron uptake.

Ferrous Iron Uptake

The *F. tularensis* genome encodes an inner membrane ferrous iron transport system comprising unlinked genes *feoA* and *feoB*. Δ*feoB* mutants of LVS and Schu S4 are deficient for growth on iron-limiting media (Thomas-Charles et al., 2013; Pérez and Ramakrishnan, 2014; Pérez et al., 2016). ^{55}Fe uptake assays demonstrated that the *F. tularensis* Δ*feoB* mutants are completely deficient in ferrous iron uptake (Pérez and Ramakrishnan, 2014; Pérez et al., 2016), implying that the Feo system is the sole ferrous iron transporter across the inner membrane (**Figure 2**). It is likely that FeoA supports FeoB function as seen in *Salmonella* Typhimurium (Kim et al., 2012) and *Vibrio cholerae* (Weaver et al., 2013; Stevenson et al., 2016).

Given the soluble nature of ferrous iron, the general assumption has been that it diffuses into the periplasmic space through non-specific porin proteins in the outer membrane. However, growth and ^{55}Fe transport assays indicate that *F. tularensis* is capable of high-affinity uptake of ferrous iron mediated by the specific outer membrane protein FupA (Ramakrishnan et al., 2012). FupA was initially characterized as a virulence factor in Schu S4 (Twine et al, 2005) and found to influence bacterial intracellular replication (Twine et al, 2005; Asare et al., 2010). An involvement in iron acquisition was established by the finding that Schu S4 Δ*fupA* mutant grew poorly under iron limitation, had lowered internal iron levels and was deregulated for siderophore production (Lindgren et al., 2009). A link to ferrous iron uptake was indicated by the finding that ferrous and ferric iron supplements supported growth of a *fupA* mutant to different extents on agar plates (Ramakrishnan et al., 2012). ^{55}Fe transport assays clearly demonstrated that the *fupA* mutant was unable to transport ferrous iron at limiting concentrations (~0.1 μM) although low affinity ferrous iron transport at high concentrations (~3 μM) could still be observed, and siderophore-iron uptake was not perturbed (Ramakrishnan et al., 2012). These findings suggest that FupA serves as a *F. tularensis* adaptation to efficiently acquire ferrous iron even in low abundance settings when general diffusion-based transport across the outer membrane might prove inadequate (**Figure 2**).

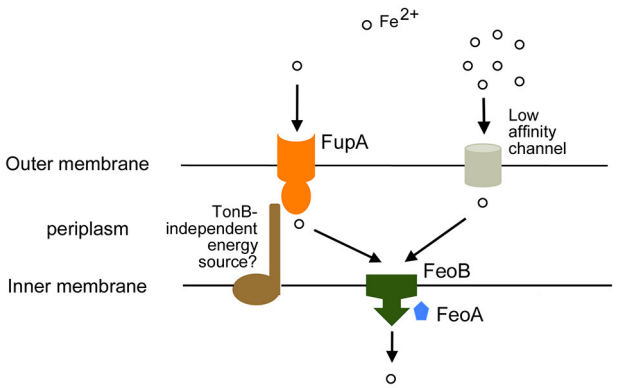

FIGURE 2 | Ferrous iron acquisition in *F. tularensis*. Transport of ferrous iron relies on the high affinity transporter FupA and uncharacterized low affinity channels in the outer membrane. Inner membrane transport is dependent on the FeoB transporter with likely involvement of FeoA. We raise the possibility that an accessory protein may facilitate FupA function.

FslE and FupA: Related High-Affinity Iron Transport Proteins

FupA and FslE are paralogs belonging to a family of proteins unique to *Francisella* (Larsson et al., 2005). Both proteins have been localized to the outer membrane of *F. tularensis* (Huntley et al., 2007; Ramakrishnan and Sen, 2014) and share a global 54% identity and 69% similarity in amino acid sequence. FupA with 557 amino acid residues is larger than FslE (509 residues). The Hidden Markov Model-based PRED-TMBB program (Bagos et al., 2004a,b) predicts that both FupA and FslE fold as β-barrels in the outer membrane with amino-terminal periplasmic domains. FupA is predicted to form a 16-stranded barrel with a periplasmic domain of 201 residues while FslE could form a 14-stranded barrel with a 152 residue periplasmic domain. This structure is reminiscent of typical TonB-dependent transporters (Noinaj et al., 2010). The greatest similarity between FslE and FupA is in the predicted β-barrel domains.

The *fupA* gene is located adjacent to a paralog *fupB* on the chromosome. Infrequent recombinational deletion events have been observed leading to formation of *fupA/B* hybrid genes (Twine et al, 2005; Rohmer et al., 2006); such recombination accounts for a significant reduction in virulence as seen in LVS, which can be reversed by restoration of the full length *fupA* gene (Salomonsson et al., 2009). The FupA/B hybrid protein encoded by LVS is less efficient at high-affinity ferrous iron uptake than FupA, but gains siderophore-iron uptake capability (Sen et al., 2010; Ramakrishnan and Sen, 2014). The structural and functional overlap in protein function raises the intriguing possibility that a common mechanism may underlie transport by FslE and FupA.

fupA expression is independent of iron and *fur* regulation, suggesting that FupA may have functions in addition to iron transport. *fupA* mutants have increased resistance to copper, and transport assays indicated that copper competes with ferrous iron for transport (Pérez et al., 2016). A role for FupA in maintenance of outer membrane integrity has also been proposed (Nallaparaju et al., 2011). Alhough, the *fsl* operon is regulated in response to iron levels, it was reported recently that calcium and magnesium limitation also result in increased *fslE* transcription (Wu et al., 2016). These observations are consistent with the idea that the high affinity iron transport proteins in the outer membrane of *F. tularensis* may assume roles in transport of additional substrates under stress.

Interestingly, FslE appears structurally different from rhizoferrin receptors of other bacteria. The LbtU siderophore receptor of *L. pneumophila* is not predicted to have a distinct periplasmic domain (Chatfield et al., 2011). RumA, the rhizoferrin receptor in *Morganella morganii* is a TonB-dependent transporter (Kühn et al., 1996). Mechanisms for rhizoferrin transport thus appear to have evolved independently in different bacteria.

Iron Uptake and Pathogenesis

Analysis of the transcriptome of Schu S4-infected macrophages demonstrated that the *fsl* genes are among the most highly induced genes in the intracellular niche (Wehrly et al., 2009). Similar results were obtained using LVS infected hepatocytes (Thomas-Charles et al., 2013), suggesting that the siderophore uptake system contributes to survival within different tissue types. *fsl* mutants were identified in a negative selection screen of a U112 transposon mutant library in mice (Weiss et al., 2007) and a signature-tagged mutant screen identified *fslA* and *feoB* to be important for pulmonary infection by LVS (Su et al., 2007). Nevertheless, individual mutants in the *fsl*, *fupA,* and *feoB* genes are capable of intracellular growth although the reduced growth of the *feoB* mutants in hepatocytes suggests that ferrous iron is likely the major iron source within these cells (Lindgren et al., 2009; Ramakrishnan et al., 2012; Thomas-Charles et al., 2013; Pérez and Ramakrishnan, 2014; Pérez et al., 2016). Both iron uptake pathways appear to contribute to utilization of iron from heme for growth (Lindgren et al., 2015), suggesting that iron needs to be released from the heme for use by the bacteria. Screens with U112 mutants have implicated additional genes in iron acquisition, but they have not been definitively characterized (Crosa et al., 2009).

A Schu Δ*fslE* Δ*fupA* mutant deficient for both siderophore and high affinity ferrous iron uptake grows slowly, is attenuated for growth in macrophages and completely avirulent in mice (Ramakrishnan et al., 2012). Δ*fslA* Δ*feoB* mutants of LVS and Schu S4 deficient for siderophore biosynthesis and for all ferrous iron uptake have an even more severe defect, with dependence on extraneous siderophore for growth, loss of all capacity for intracellular growth and complete loss of virulence (Pérez and Ramakrishnan, 2014; Pérez et al., 2016). These findings indicate that both subspecies of *F. tularensis* have a similar repertoire of iron uptake mechanisms, limited to just the *fsl* and *feo*-mediated mechanisms. Interestingly, although the Δ*fslE* Δ*fupA* and the Δ*fslA* Δ*feoB* mutants are avirulent in mice, exposure to these strains protects from subsequent challenge with the virulent strain (Ramakrishnan et al., 2012; Pérez et al., 2016), making them good candidates for further exploration as live vaccines.

CONCLUSIONS

With a reduced genome, *F. tularensis* has evolved to efficiently support its lifestyle as an intracellular pathogen with a minimal set of two iron acquisition pathways. Host iron sources utilized and mechanisms regulating the transport proteins FslE and FupA are interesting questions for future investigations.

AUTHOR CONTRIBUTIONS

The author confirms being the sole contributor of this work and approved it for publication.

FUNDING

Work in the author's lab has been supported by grants AI056227, AI067823, and AI119471 from the National Institute of Allergy and Infectious Diseases (NIH) and by intramural support from the School of Medicine, University of Virginia.

REFERENCES

Asare, R., Akimana, C., Jones, S., and Abu Kwaik, Y. (2010). Molecular bases of proliferation of *Francisella tularensis* in arthropod vectors. *Environ. Microbiol.* 12, 2587–2612. doi: 10.1111/j.1462-2920.2010.02230.x

Bagos, P. G., Liakopoulos, T. D., Spyropoulos, I. C., and Hamodrakas, S. J. (2004a). A hidden markov model method, capable of predicting and discriminating β barrel outer membrane proteins. *BMC Bioinformatics* 5:29. doi: 10.1186/1471-2105-5-29

Bagos, P. G., Liakopoulos, T. D., Spyropoulos, I. C., and Hamodrakas, S. J. (2004b). PRED-TMBB: a web server for predicting the topology of β barrel outer membrane proteins. *Nucleic Acids Res.* 32, W400–W404. doi: 10.1093/nar/gkh417

Bakshi, C. S., Malik, M., Regan, K., Melendez, J. A., Metzger, D. W., Pavlov, V. M., et al. (2006). Superoxide dismutase B gene (sodB)-deficient mutants

of *Francisella tularensis* demonstrate hypersensitivity to oxidative stress and attenuated virulence. *J. Bacteriol.* 188, 6443–6448. doi: 10.1128/JB.00266-06

Barker, J. R., Chong, A., Wehrly, T. D., Yu, J. J., Rodriguez, S. A., Liu, J., et al. (2009). The *Francisella tularensis* pathogenicity island encodes a secretion system that is required for phagosome escape and virulence. *Mol. Microbiol.* 74, 1459–1470. doi: 10.1111/j.1365-2958.2009.06947.x

Bhatnagar, N. B., Elkins, K. L., and Fortier, A. H. (1995). Heat stress alters the virulence of a rifampin-resistant mutant of *Francisella tularensis* LVS. *Infect. Immun.* 63, 154–159.

Binesse, J., Lindgren, H., Lindgren, L., Conlan, W., and Sjöstedt, A. (2015). Roles of reactive oxygen species-degrading enzymes of *Francisella tularensis* SCHU S4. *Infect. Immun.* 83, 2255–2263. doi: 10.1128/IAI.02488-14

Buchan, B. W., McLendon, M. K., and Jones, B. D. (2008). Identification of differentially regulated *Francisella tularensis* genes by use of a newly developed Tn5-based transposon delivery system. *Appl. Environ. Microbiol.* 74, 2637–2645. doi: 10.1128/AEM.02882-07

Burnside, D. M., Wu, Y., Shafaie, S., and Cianciotto, N. P. (2015). The *Legionella pneumophila* siderophore legiobactin is a polycarboxylate that is identical in structure to rhizoferrin. *Infect. Immun.* 83, 3937–3945. doi: 10.1128/IAI.00808-15

Celli, J., and Zahrt, T. C. (2013). Mechanisms of *Francisella tularensis* intracellular pathogenesis. *Cold Spring Harb. Perspect. Med.* 3:a010314. doi: 10.1101/cshperspect.a010314

Challis, G. L. (2005). A widely distributed bacterial pathway for siderophore biosynthesis independent of nonribosomal peptide synthetases. *ChemBioChem* 6, 601–611. doi: 10.1002/cbic.200400283

Chatfield, C. H., Mulhern, B. J., Burnside, D. M., and Cianciotto, N. P. (2011). *Legionella pneumophila* LbtU acts as a novel, tonb-independent receptor for the legiobactin siderophore. *J. Bacteriol.* 193, 1563–1575. doi: 10.1128/JB.01111-10

Crosa, L. M., Crosa, J. H., and Heffron, F. (2009). Iron Transport in *Francisella* in the absence of a recognizable TonB protein still requires energy generated by the proton motive force. *Biometals* 22, 337–344. doi: 10.1007/s10534-008-9170-7

de Bruin, O. M., Duplantis, B. N., Ludu, J. S., Hare, R. F., Nix, E. B., Schmerk, C. L., et al. (2011). The biochemical properties of the Francisella Pathogenicity Island (FPI)-encoded proteins IglA, IglB, IglC, PdpB and DotU Suggest roles in Type VI secretion. *Microbiology* 157, 3483–3491. doi: 10.1099/mic.0.052308-0

Deng, K., Blick, R. J., Liu, W., and Hansen, E. J. (2006). Identification of *Francisella tularensis* genes affected by iron limitation. *Infect. Immun.* 74, 4224–4236. doi: 10.1128/IAI.01975-05

Drechsel, H., Metzger, J., Freund, S., Jung, G., Boelaert, J. R., and Winkelmann, G. (1991). Rhizoferrin- a novel siderophore from the fungus *Rhizopus microsporus* Var. *Rhizopodiformis*. *Biometals* 4, 238–243.

Fortier, A. H., Leiby, D. A., Narayanan, R. B., Asafoadjei, E., Crawford, R. M., Nacy, C. A., et al. (1995). Growth of *Francisella tularensis* LVS in Macrophages: the acidic intracellular compartment provides essential iron required for growth. *Infect. Immun.* 63, 1478–1483.

Hall, J. D., Woolard, M. D., Gunn, B. M., Craven, R. R., Taft-Benz, S., Frelinger, J. A., et al. (2008). Infected-host-cell repertoire and cellular response in the lung following inhalation of *Francisella tularensis* Schu S4, LVS, or U112. *Infect. Immun.* 76, 5843–5852. doi: 10.1128/IAI.01176-08

Halmann, M., and Mager, J. (1967). An endogenously produced substance essential for growth initiation of *Pasteurella tularensis*. *J. Gen. Microbiol.* 49, 461–468. doi: 10.1099/00221287-49-3-461

Halmann, M., Magda, B., and Mager, J. (1967). Nutritional requirements of *Pasteurella tularensis* for growth from small inocula. *J. Gen. Microbiol.* 49, 451–460. doi: 10.1099/00221287-49-3-451

Hubálek, M., Hernychová, L., Brychta, M., Lenčo, J., Zechovská, J., and Stulík, J. (2004). Comparative proteome analysis of cellular proteins extracted from highly virulent *Francisella tularensis* ssp. tularensis and less virulent, *F. tularensis* ssp. holarctica and *F. tularensis* ssp. mediaasiatica. *Proteomics* 4, 3048–3060. doi: 10.1002/pmic.200400939

Hubálek, M., Hernychová, L., Havlasová, J., Kasalová, I., Neubauerová, V., Stulík, J., et al. (2003). Towards proteome database of *Francisella tularensis*. *J. Chromatogr. B Analyt. Technol. Biomed. Life Sci.* 787, 149–177. doi: 10.1016/S1570-0232(02)00730-4

Huntley, J. F., Conley, P. G., Hagman, K. E., and Norgard, M. V. (2007). Characterization of *Francisella tularensis* outer membrane proteins. *J. Bacteriol.* 189, 561–574. doi: 10.1128/JB.01505-06

Jones, C. L., Napier, B. A., Sampson, T. R., Llewellyn, A. C., Schroeder, M. R., and Weiss, D. S. (2012). Subversion of host recognition and defense systems by *Francisella* spp. *Microbiol. Mol. Biol. Rev.* 76, 383–404. doi: 10.1128/MMBR.05027-11

Kim, H., Lee, H., and Shin, D. (2012). The FeoA protein is necessary for the FeoB transporter to import ferrous iron. *Biochem. Biophys. Res. Commun.* 423, 733–738. doi: 10.1016/j.bbrc.2012.06.027

Kingry, L. C., and, Petersen, J. M., (2014). Comparative review of *Francisella tularensis* and *Francisella novicida*. *Front. Cell. Infect. Microbiol.* 4:35. doi: 10.3389/fcimb.2014.00035

Kiss, K., Liu, W., Huntley, J. F., Norgard, M. V., and Hansen, E. J. (2008). Characterization of fig operon mutants of *Francisella novicida* U112. *FEMS Microbiol. Lett.* 285, 270–277. doi: 10.1111/j.1574-6968.2008.01237.x

Konetschny-Rapp, S., Jung, G., Meiwes, J., and Zähner, H. (1990). Staphyloferrin a: a structurally new siderophore from staphylococci. *Eur. J. Biochem.* 191, 65–74. doi: 10.1111/j.1432-1033.1990.tb19094.x

Kovářová, H., Halada, P., Man, P., Golovliov, I., Kovářová, Z., Špaček, J., et al. (2002). Proteome Study of *Francisella tularensis* Live vaccine strain-containing phagosome in *Bcg/Nramp1* congenic macrophages: resistant allele contributes to permissive environment and susceptibility to infection. *Proteomics* 2, 85–93. doi: 10.1002/1615-9861(200201)2:1<85::AID-PROT85>3.0.CO;2-S

Kovářová, H., Hernychova, L., Hajduch, M., Sirova, M., and Macela, A. (2000). Influence of the *Bcg* locus on natural resistance to primary infection with the facultative intracellular bacterium *Francisella tularensis* in mice. *Infect. Immun.* 68, 1480–1484. doi: 10.1128/IAI.68.3.1480-1484.2000

Kühn, S., Braun, V., and Köster, W. (1996). Ferric rhizoferrin uptake into *Morganella morganii*: characterization of genes involved in the uptake of a polyhydroxycarboxylate siderophore. *J. Bacteriol.* 178, 496–504. doi: 10.1128/jb.178.2.496-504.1996

Larsson, P., Elfsmark, D., Svensson, K., Wikström, P., Forsman, M., Brettin, T., et al. (2009). Molecular evolutionary consequences of niche restriction in *Francisella tularensis*, a facultative intracellular pathogen. *PLoS Pathog.* 5:e1000472. doi: 10.1371/journal.ppat.1000472

Larsson, P., Oyston, P. C., Chain, P., Chu, M. C., Duffield, M., Fuxelius, H. H., et al. (2005). The complete genome sequence of *Francisella tularensis*, the causative agent of tularemia. *Nat. Genet.* 37, 153–159. doi: 10.1038/ng1499

Lenco, J., Hubalek, M., Larsson, P., Fucikova, A., Brychta, M., Macela, A., et al. (2007). Proteomics analysis of the *Francisella tularensis* LVS response to iron restriction: induction of the *F.* tularensis pathogenicity island proteins IglABC. *FEMS Microbiol. Lett.* 269, 11–21. doi: 10.1111/j.1574-6968.2006.00595.x

Lindgren, H., and Sjöstedt, A. (2016). Gallium potentiates the antibacterial effect of gentamicin against *Francisella tularensis*. *Antimicrob. Agents Chemother.* 60, 288–295. doi: 10.1128/AAC.01240-15

Lindgren, H., Honn, M., Golovlev, I., Kadzhaev, K., Conlan, W., and Sjostedt, A. (2009). The 58-kilodalton major virulence factor of *Francisella tularensis* Is required for efficient utilization of iron. *Infect. Immun.* 77, 4429–4436. doi: 10.1128/IAI.00702-09

Lindgren, H., Honn, M., Salomonsson, E., Kuoppa, K., Forsberg, Å., and Sjöstedt, A. (2011). Iron content differs between *Francisella tularensis Subspecies tularensis* and *Subspecies holarctica* strains and correlates to their susceptibility to H(2)O(2)-induced killing. *Infect. Immun.* 79, 1218–1224. doi: 10.1128/IAI.01116-10

Lindgren, H., Lindgren, L., Golovliov, I., and Sjöstedt, A. (2015). Mechanisms of heme utilization by *Francisella tularensis*. *PLoS ONE* 10:e0119143. doi: 10.1371/journal.pone.0119143

Lindgren, H., Shen, H., Zingmark, C., Golovliov, I., Conlan, W., and Sjöstedt, A. (2007). Resistance of *Francisella tularensis* strains against reactive nitrogen and oxygen species with special reference to the role of KatG. *Infect. Immun.* 75, 1303–1309. doi: 10.1128/IAI.01717-06

Lyons, R. C., and Wu, T. H. (2007). Animal models of *Francisella tularensis* infection. *Ann. N. Y. Acad. Sci.* 1105, 238–265. doi: 10.1196/annals.1409.003

Meibom, K. L., and Charbit, A. (2010). *Francisella tularensis* metabolism and its relation to virulence. *Front. Microbiol.* 1:140. doi: 10.3389/fmicb.2010.00140

Milne, T. S., Michell, S. L., Diaper, H., Wikström, P., Svensson, K., Oyston, P. C., et al. (2007). A 55 kDa hypothetical membrane protein is an iron-regulated

virulence factor of *Francisella tularensis* subsp. Novicida U112. *J. Med. Microbiol.* 56(Pt 10), 1268–1276. doi: 10.1099/jmm.0.47190-0

Münzinger, M., Taraz, K., Budzikiewicz, H., Drechsel, H., Heymann, P., Winkelmann, G., et al. (1999). S,S-Rhizoferrin (Enantio-Rhizoferrin) - a siderophore of *Ralstonia* (*Pseudomonas*) *pickettii* DSM 6297 - the optical antipode of R,R-rhizoferrin isolated from fungi. *Biometals* 12, 189–193. doi: 10.1023/A:1009259118034

Nallaparaju, K. C., Yu, J. J., Rodriguez, S. A., Zogaj, X., Manam, S., Guentzel, M. N., Seshu, J., et al. (2011). Evasion of IFN- γ signaling by *Francisella novicida* is dependent upon *Francisella* outer membrane protein, C. *PLoS ONE* 6:e18201. doi: 10.1371/journal.pone.0018201

Noinaj, N., Guillier, M., Barnard, T. J., and Buchanan, S. K. (2010). TonB-dependent transporters: regulation, structure, and function. *Annu. Rev. Microbiol.* 64, 43–60. doi: 10.1146/annurev.micro.112408.134247

Olakanmi, O., Gunn, J. S., Su, S., Soni, S., Hassett, D. J., and Britigan, B. E. (2010). Gallium disrupts iron uptake by intracellular and extracellular *Francisella* strains and exhibits therapeutic efficacy in a murine pulmonary infection model. *Antimicrob. Agents Chemother.* 54, 244–253. doi: 10.1128/AAC.00655-09

Ozanic, M., Marecic, V., Abu Kwaik, Y., and Santic, M. (2015). The divergent intracellular lifestyle of *Francisella tularensis* in evolutionarily distinct host cells. *PLoS Pathog.* 11:e1005208. doi: 10.1371/journal.ppat.1005208

Pan, X., Tamilselvam, B., Hansen, E. J., and Daefler, S. (2010). Modulation of iron homeostasis in macrophages by bacterial intracellular pathogens. *BMC Microbiol.* 10:64. doi: 10.1186/1471-2180-10-64

Pekarek, R. S., Bostian, K. A., Bartelloni, P. J., Calia, F. M., and Beisel, W. R. (1969). The effects of *Francisella tularensis* infection on iron metabolism in man. *Am. J. Med. Sci.* 258, 14–25. doi: 10.1097/00000441-196907000-00003

Pérard, J., Covés, J., Castellan, M., Solard, C., Savard, M., Miras, R., Galop, S., et al. (2016). Quaternary structure of fur proteins, a new subfamily of tetrameric proteins. *Biochemistry* 55, 1503–1515. doi: 10.1021/acs.biochem.5b01061

Pérez, N. M., and Ramakrishnan, G. (2014). The reduced genome of the *Francisella tularensis* live vaccine strain (LVS) encodes two iron acquisition systems essential for optimal growth and virulence. *PLoS ONE* 9:e93558. doi: 10.1371/journal.pone.0093558

Pérez, N., Johnson, R., Sen, B., and Ramakrishnan, G. (2016). Two parallel pathways for ferric and ferrous iron acquisition support growth and virulence of the intracellular pathogen *Francisella tularensis* Schu S4. *Microbiologyopen* 5, 453–468. doi: 10.1002/mbo3.342

Ramakrishnan, G., and Sen, B. (2014). The FupA/B protein uniquely facilitates transport of ferrous iron and siderophore-associated ferric iron across the outer membrane of *Francisella tularensis* live vaccine strain. *Microbiology* 160(Pt 2), 446–457. doi: 10.1099/mic.0.072835-0

Ramakrishnan, G., Meeker, A., and Dragulev, B. (2008). Fsle is necessary for siderophore-mediated iron acquisition in *Francisella tularensis* Schu S4. *J. Bacteriol.* 190, 5353–5361. doi: 10.1128/JB.00181-08

Ramakrishnan, G., Sen, B., and Johnson, R. (2012). Paralogous outer membrane proteins mediate uptake of different forms of iron and synergistically govern virulence in *Francisella tularensis tularensis*. *J. Biol. Chem.* 287, 25191–25202. doi: 10.1074/jbc.M112.371856

Rohmer, L., Brittnacher, M., Svensson, K., Buckley, D., Haugen, E., Zhou, Y., et al. (2006). Potential source of *Francisella tularensis* live vaccine strain attenuation determined by genome comparison. *Infect. Immun.* 74, 6895–6906. doi: 10.1128/IAI.01006-06

Rohmer, L., Fong, C., Abmayr, S., Wasnick, M., Larson Freeman, T. J., Radey, M., et al. (2007). Comparison of *Francisella tularensis* genomes reveals evolutionary events associated with the emergence of human pathogenic strains. *Genome Biol.* 8:R102. doi: 10.1186/gb-2007-8-6-r102

Salomonsson, E., Kuoppa, K., Forslund, A. L., Zingmark, C., Golovliov, I., Sjöstedt, A., et al. (2009). Reintroduction of two deleted virulence loci restores full virulence to the live vaccine strain of *Francisella tularensis*. *Infect. Immun.* 77, 3424–3431. doi: 10.1128/IAI.00196-09

Sen, B., Meeker, A., and Ramakrishnan, G. (2010). The *fslE* Homolog, *FTL-0439* (*fupA/B*), Mediates siderophore-dependent iron uptake in *Francisella tularensis* LVS. *Infect. Immun.* 78:10. doi: 10.1128/IAI.00503-10

Sharma, J., Mares, C. A., Li, Q., Morris, E. G., and Teale, J. M. (2011). Features of sepsis caused by pulmonary infection with *Francisella tularensis* Type A strain. *Microb. Pathog.* 51, 39–47. doi: 10.1016/j.micpath.2011.03.007

Sjostedt, A. (2007). Tularemia: history, epidemiology, pathogen physiology, and clinical manifestations. *Ann. N. Y. Acad. Sci.* 1105, 1–29. doi: 10.1196/annals.1409.009

Stevenson, B., Wyckoff, E. E., and Payne, S. M. (2016). *Vibrio cholerae* FeoA, FeoB, and FeoC interact to form a complex. *J. Bacteriol.* 198, 1160–1170. doi: 10.1128/JB.00930-15

Su, J., Yang, J., Zhao, D., Kawula, T. H., Banas, J. A., and Zhang, J. R. (2007). Genome-wide identification of *Francisella tularensis* virulence determinants. *Infect. Immun.* 75, 3089–3101. doi: 10.1128/IAI.01865-06

Sullivan, J. T., Jeffery, E. F., Shannon, J. D., and Ramakrishnan, G. (2006). Characterization of the siderophore of *Francisella tularensis* and role of *fslA* in siderophore production. *J. Bacteriol.* 188, 3785–3795. doi: 10.1128/JB.00027-06

Svensson, K., Larsson, P., Johansson, D., Byström, M., Forsman, M., and Johansson, A. (2005). Evolution of Subspecies of *Francisella tularensis*. *J. Bacteriol.* 187, 3903–3908. doi: 10.1128/JB.187.11.3903-3908.2005

Thieken, A., and Winkelmann, G. (1992). Rhizoferrin: a complexone type siderophore of the *Mucorales* and *Entomophthorales* (Zygomycetes). *FEMS Microbiol. Lett.* 94, 37–41. doi: 10.1111/j.1574-6968.1992.tb05285.x

Thomas-Charles, C. A., Zheng, H., Palmer, L. E., Mena, P., Thanassi, D. G., and Furie, M. B. (2013). FeoB-mediated uptake of iron by *Francisella tularensis*. *Infect. Immun.* 81, 2828–2837. doi: 10.1128/IAI.00170-13

Twine, S., Byström, M., Chen, W., Forsman, M., Golovliov, I., Johansson, A., et al. (2005). A mutant of *Francisella tularensis* strain SCHU S4 lacking the ability to express a 58-kilodalton protein is attenuated for virulence and is an effective live vaccine. *Infect. Immun.* 73, 8345–8352. doi: 10.1128/IAI.73.12.8345-8352.2005

Weaver, E. A., Wyckoff, E. E., Mey, A. R., Morrison, R., and Payne, S. M. (2013). FeoA and FeoC are essential components of the *Vibrio cholerae* ferrous iron uptake system, and FeoC interacts with FeoB. *J. Bacteriol.* 195, 4826–4835. doi: 10.1128/JB.00738-13

Wehrly, T. D., Chong, A., Virtaneva, K., Sturdevant, D. E., Child, R., Edwards, J. A., et al. (2009). Intracellular biology and virulence determinants of *Francisella tularensis* revealed by transcriptional profiling inside macrophages. *Cell. Microbiol.* 11, 1128–1150. doi: 10.1111/j.1462-5822.2009.01316.x

Weiss, D. S., Brotcke, A., Henry, T., Margolis, J. J., Chan, K., and Monack, D. M. (2007). *In vivo* negative selection screen identifies genes required for *Francisella* virulence. *Proc. Natl. Acad. Sci. U.S.A.* 104, 6037–6042. doi: 10.1073/pnas.0609675104

Wu, X., Ren, G., Gunning, W. T. III, Weaver, D. A., Kalinoski, A. L., Khuder, S. A., et al. (2016). FmvB: a *Francisella tularensis* magnesium-responsive outer membrane protein that plays a role in virulence. *PLoS ONE* 11:e160977. doi: 10.1371/journal.pone.0160977

Zajdowicz, S., Haller, J. C., Krafft, A. E., Hunsucker, S. W., Mant, C. T., Duncan, M. W., et al. (2012). Purification and structural characterization of siderophore (Corynebactin) from *Corynebacterium diphtheriae*. *PLoS ONE* 7:e34591. doi: 10.1371/journal.pone.0034591

Conflict of Interest Statement: The author declares that the research was conducted in the absence of any commercial or financial relationships that could be construed as a potential conflict of interest.

frontiers in Cellular and Infection Microbiology

ORIGINAL RESEARCH
published: 26 January 2017
doi: 10.3389/fcimb.2017.00012

Gallium-Protoporphyrin IX Inhibits *Pseudomonas aeruginosa* Growth by Targeting Cytochromes

Sarah Hijazi, Paolo Visca and Emanuela Frangipani *

Department of Science, Roma Tre University, Rome, Italy

Pseudomonas aeruginosa is a challenging pathogen due to both innate and acquired resistance to antibiotics. It is capable of causing a variety of infections, including chronic lung infection in cystic fibrosis (CF) patients. Given the importance of iron in bacterial physiology and pathogenicity, iron-uptake and metabolism have become attractive targets for the development of new antibacterial compounds. *P. aeruginosa* can acquire iron from a variety of sources to fulfill its nutritional requirements both in the environment and in the infected host. The adaptation of *P. aeruginosa* to heme iron acquisition in the CF lung makes heme utilization pathways a promising target for the development of new anti-*Pseudomonas* drugs. Gallium [Ga(III)] is an iron mimetic metal which inhibits *P. aeruginosa* growth by interfering with iron-dependent metabolism. The Ga(III) complex of the heme precursor protoporphyrin IX (GaPPIX) showed enhanced antibacterial activity against several bacterial species, although no inhibitory effect has been reported on *P. aeruginosa.* Here, we demonstrate that GaPPIX is indeed capable of inhibiting the growth of clinical *P. aeruginosa* strains under iron-deplete conditions, as those encountered by bacteria during infection, and that GaPPIX inhibition is reversed by iron. Using *P. aeruginosa* PAO1 as model organism, we show that GaPPIX enters cells through both the heme-uptake systems *has* and *phu*, primarily *via* the PhuR receptor which plays a crucial role in *P. aeruginosa* adaptation to the CF lung. We also demonstrate that intracellular GaPPIX inhibits the aerobic growth of *P. aeruginosa* by targeting cytochromes, thus interfering with cellular respiration.

Keywords: aerobic respiration, antibacterial, cystic fibrosis, gallium, heme, infection, iron-uptake, terminal oxidases

OPEN ACCESS

Edited by:
Pierre Cornelis,
Vrije Universiteit Brussel, Belgium

Reviewed by:
Isabelle Schalk,
Ecole Superieure de Biotechnologie de Starsbourg, France
Christine Baysse,
University of Rennes 1, France

***Correspondence:**
Emanuela Frangipani
emanuela.frangipani@uniroma3.it

Received: *15 November 2016*
Accepted: *10 January 2017*
Published: *26 January 2017*

Citation:
Hijazi S, Visca P and Frangipani E (2017) Gallium-Protoporphyrin IX Inhibits Pseudomonas aeruginosa Growth by Targeting Cytochromes. Front. Cell. Infect. Microbiol. 7:12. doi: 10.3389/fcimb.2017.00012

INTRODUCTION

Pseudomonas aeruginosa is a challenging bacterial pathogen due to both innate and acquired resistance to several antibiotics (Moore and Flaws, 2011). This bacterium is capable of causing a variety of infections, including chronic lung infection, which represents the main cause of morbidity and mortality in patients suffering from cystic fibrosis (CF) (Murphy, 2006; Davies et al., 2007). The success of *P. aeruginosa* as an opportunistic pathogen relies, at least in part, on its metabolic versatility, including the ability to obtain energy from different sources under a variety of environmental conditions (Williams et al., 2007; Arai, 2011). *P. aeruginosa* possesses a branched respiratory chain terminated by oxygen or nitrogen oxides, to allow growth by aerobic respiration or by denitrification under anaerobic conditions, respectively (reviewed in Arai, 2011). Moreover,

P. aeruginosa is able to ferment arginine and pyruvate anaerobically (Vander et al., 1984; Eschbach et al., 2004). Aerobic respiration in *P. aeruginosa* relies on five terminal oxidases (Matsushita et al., 1982, 1983; Fujiwara et al., 1992; Cunningham and Williams, 1995; Cunningham et al., 1997; Stover et al., 2000; Comolli and Donohue, 2002, 2004). Three of these enzymes, the aa_3 terminal oxidase (Cox), the cbb_3-1 (Cco-1), and the cbb_3-2 (Cco-2) are cytochrome *c*-type oxidases, while the other two, i.e., the cyanide-insensitive oxidase (Cio) and the bo_3 oxidase (Cyo), are quinol oxidases (**Figure 1**). All these terminal oxidases contain heme, and are differentially expressed depending on the growth conditions, likely as a consequence to their different affinity for oxygen (Alvarez-Ortega and Harwood, 2007; Kawakami et al., 2010). Denitrification is ensured by a set of enzymes which sequentially convert nitrate (NO_3^-) to molecular nitrogen (N_2). Among the denitrification enzymes, only nitrite reductase (Nir) and nitric oxide reductase (Nor) contain heme as a cofactor (**Figure 1**).

Like almost all pathogenic bacteria, *P. aeruginosa* has an absolute need for iron to cause infections and to persist within the host (Ratledge and Dover, 2000). Iron is required as a cofactor of many key enzymes involved in respiration, DNA synthesis and defense against reactive oxygen species (Andrews et al., 2003). However, in the human host, iron is poorly available to bacteria due to its incorporation into heme-containing molecules (e.g., hemoglobin and myoglobin) and iron carrier proteins (e.g., transferrin and lactoferrin) (Weinberg, 2009). This iron-withholding capacity represents the first line of the host defense against invading pathogens, a phenomenon known as "nutritional immunity" (Skaar, 2010). To circumvent iron-limitation, *P. aeruginosa* possesses several systems that actively acquire this essential metal, such as (i) the production of the siderophores pyoverdine (Pvd, Meyer and Abdallah, 1978; Cox and Adams, 1985) and pyochelin (Pch, Cox et al., 1981; Heinrichs et al., 1991); (ii) the ability to utilize a wide range of siderophores synthesized by other organisms (Cornelis and Matthijs, 2002; Cornelis et al., 2009); (iii) the ability to acquire Fe(II) through the Feo system (Cartron et al., 2006). In addition, *P. aeruginosa* can utilize heme-iron, by expressing two distinct heme-uptake systems, namely *phu* and *has* (Ochsner et al., 2000). The *phu* system allows the direct acquisition of heme from hemoproteins, which bind to the outer membrane receptor PhuR (Ochsner et al., 2000). In the *has* system a secreted hemophore HasA withdraws heme from hemoproteins and delivers it to the outer membrane receptor HasR (Létoffé et al., 1998). Given the similarity with the well-known *has* system of *Serratia marcescens* (Rossi et al., 2003; Létoffé et al., 2004), it is likely that the *has* system of *P. aeruginosa* positively regulates its own expression, *via* the sigma factor HasI and anti-sigma HasS, upon interaction of heme-loaded HasA with the HasR receptor (Llamas et al., 2014). The expression of both *has* and *phu* heme-uptake systems is shut down in the presence of sufficient intracellular iron, due to the negative regulation exerted by the ferric-uptake regulator (Fur) protein (Ochsner et al., 2000).

It has been shown that *P. aeruginosa* aerobic respiration and iron-uptake capabilities play pivotal roles during chronic lung

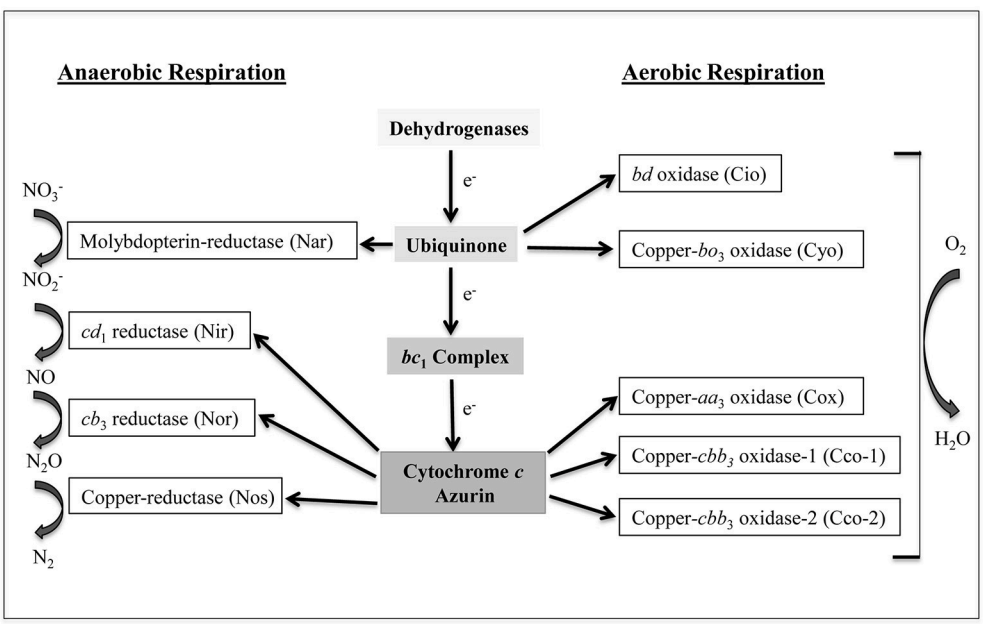

FIGURE 1 | Branched respiratory chain of *P. aeruginosa*. Cio, Cyo, Cox, Cco-1, and Cco-2 represent the five terminal oxidases that reduce oxygen to water under aerobic conditions. Cio and Cyo are quinol oxidases while Cox, Cco-1, and Cco-2 are cytochrome *c* oxidases. Nar, Nir, Nor, and Nos are nitrate reductase, nitrite reductase, nitric oxide reductase, and nitrous oxide reductase, respectively. These enzymes transfer electron to nitrogen oxides under anaerobic conditions. Nar receives electrons directly from the quinone pool while the other three receive electrons *via* the cytochrome *c* or from the small blue-copper protein azurin. *a*, *b*, *c,* and *d* represent different types of low-spin heme while a_3, b_3, d_1, and o_3 indicate the high-spin ones (modified from Arai, 2011).

infection in CF patients. In particular, three terminal oxidases (Cco-1, Cco-2, and Cio) sustain bacterial growth in the CF lung, a particular environment where *P. aeruginosa* iron-uptake abilities are sought to evolve toward heme utilization (Alvarez-Ortega and Harwood, 2007; Marvig et al., 2014; Nguyen et al., 2014).

The paucity of effective antibiotics to treat *P. aeruginosa* infections have made bacterial respiration and/or iron metabolism promising targets for the development of new anti-*Pseudomonas* drugs (Ballouche et al., 2009; Foley and Simeonov, 2012; Imperi et al., 2013). The possibility of using iron mimetics as novel therapeutics to interfere with iron metabolism has been exploited (Kaneko et al., 2007; Banin et al., 2008; Minandri et al., 2014). $Ga(NO_3)_3$, the active component of the FDA-approved formulation Ganite®, has successfully been repurposed as an antimicrobial drug (Bonchi et al., 2014; Rangel-Vega et al., 2015). Interestingly, $Ga(NO_3)_3$ has been shown to be very active against *P. aeruginosa*, by interfering with iron-dependent metabolic pathways (Kaneko et al., 2007; Bonchi et al., 2015). The antibacterial proprieties of Ga(III) reside in the fact that, different from Fe(III), Ga(III) cannot be reduced under physiological conditions. However, redox cycling is critical for many of iron-dependent biological functions, including respiration (Breidenstein et al., 2011). Moreover, the heme-mimetic GaPPIX [i.e., Ga(III) coupled with the heme precursor protoporphyrin IX] has been shown to possess a good antibacterial activity against several bacterial species, including *Staphylococcus aureus* and *Acinetobacter baumannii* (Stojiljkovic et al., 1999; Arivett et al., 2015; Chang et al., 2016). GaPPIX is likely to exploit heme-uptake routes to enter bacterial cells, where it could substitute for heme in heme-containing enzymes, including cytochromes, catalases, and peroxidases, resulting in the perturbation of vital cellular functions (Stojiljkovic et al., 1999). Due to the similarity between GaPPIX and heme, GaPPIX is predicted to interfere with heme-dependent *b*-type cytochromes, thus impairing their function and ultimately inhibiting bacterial respiration.

In this work, the *in vitro* effect of GaPPIX on *P. aeruginosa* was tested under iron-depleted conditions, as those encountered during infection. The entrance routes of GaPPIX into *P. aeruginosa* cells and possible targets of GaPPIX were investigated. We demonstrate that the sensitivity of *P. aeruginosa* to GaPPIX depends on both intracellular iron levels and the expression of heme-uptake systems. Furthermore, we show that GaPPIX enters *P. aeruginosa* cells mainly through the heme-uptake receptor PhuR. Evidence is also provided that intracellular GaPPIX inhibits the aerobic growth of *P. aeruginosa* by targeting heme-dependent *b*-type cytochromes.

MATERIALS AND METHODS

Bacterial Strains and Growth Conditions

Strains and plasmids used in this work are listed in **Table 1**. *P. aeruginosa* clinical isolates are listed in Table S1. *P. aeruginosa* strains from frozen cultures were maintained on Luria Bertani (LB) agar before being transferred to liquid culture media. Bacteria were cultured in iron-free Casamino Acids medium (DCAA, Visca et al., 1993) supplemented or not with 100 μM of $FeCl_3$ at 37°C, with vigorous shaking. When required, antibiotics were added to the media at the following concentrations for *Escherichia coli*, with the concentrations used for *P. aeruginosa* shown in parentheses: Ampicillin 100 μg/ml; carbenicillin (300 μg/ml in LB and 200 μg/ml in DCAA); and tetracycline 12.5 μg/ml (100 μg/ml). DCAA agar plates were prepared by the addition of 15 g/l bacteriological agar (Acumedia, Neogen corporation). When GaPPIX was required, a 50 mM of stock solution of GaPPIX (Frontier Scientific) was prepared in dimethyl sulfoxide (DMSO) and stored at 4°C in the dark. When $Ga(NO_3)_3$ was required, a 100 mM of stock solution of $Ga(NO_3)_3$ (Sigma-Aldrich), was prepared in double-distilled water and stored at −20°C.

Susceptibility Testing

The activity of GaPPIX, $Ga(NO_3)_3$ and Hemin (Hm) (Sigma-Aldrich) on *P. aeruginosa* was tested in 96-well microtiter plates (Falcon). Briefly, bacterial cells were grown over-night in DCAA supplemented with 100 μM $FeCl_3$ in order to obtain high cell densities, then washed in saline and diluted to an OD_{600} of 0.01 in 200 μl of DCAA containing increasing concentrations (0–100 μM) of GaPPIX, $Ga(NO_3)_3$ or Hm. Microtiter plates were incubated for 24 h at 37°C with gentle shaking (120 rpm). Growth (OD_{600}) was measured in a Wallac 1420 Victor3 V multilabel plate reader (PerkinElmer). The minimum inhibitory concentration (MIC) of gallium compounds was visually determined as the lowest concentration that completely inhibited *P. aeruginosa* growth. As a control experiment the same procedure was performed, except that 100 μM $FeCl_3$ was added in the medium containing the highest concentration of gallium compounds tested (100 μM).

The antibacterial activity of gallium compounds was also assessed by disk diffusion assays. Briefly, cells from an over-night culture in DCAA supplemented with 100 μM $FeCl_3$ were washed and diluted in saline to $OD_{600} = 0.1$, then seeded on the surface of DCAA agar plates supplemented or not with $FeCl_3$. Sterile 6-mm blank disks (ThermoFisher-Oxoid) soaked with 10 μl of a 15 mM solution of either GaPPIX or $Ga(NO_3)_3$ were deposited on the agar surface and the Zone Of growth Inhibition (ZOI) was measured (in mm) after 16 h of incubation at 37°C.

To observe the rescue effect of Hm and Hemoglobin (Hb), disks were soaked with 10 μl of a 7.5 mg/ml solution of bovine hemin chloride (Sigma-Aldrich) in 10 mM NaOH or bovine hemoglobin (Sigma-Aldrich) in phosphate buffered saline (PBS) and deposited on the plate surface nearby the disk soaked with GaPPIX. The appearance of a half-moon-shaped growth area around the disk soaked with Hm or Hb was detected after 16 h of incubation at 37°C.

Construction of Plasmids for the Expression of Heme Receptors

Plasmid preparations and DNA cloning were performed according to standards methods (Sambrook et al., 1989). Restriction and DNA modifying enzymes were used following the instructions of the manufacturers. Oligonucleotide primers are listed in **Table 1**. To express *hasR* in the Δ*hasR*Δ*phuR*

TABLE 1 | Bacterial strains and plasmids used in this study.

Strain or plasmid	Genotype and/or relevant characteristics	Reference or source
STRAINS		
P. aeruginosa		
PAO1	ATCC15692 (wild type, prototroph)	American type culture collection
Δ*hasR*	PAO1Δ*hasR*	This work
Δ*phuR*	PAO1Δ*phuR*	This work
Δ*hasR*Δ*phuR*	PAO1Δ*hasR*Δ*phuR*	Minandri et al., 2016
Δ*pvdA*	PAO1Δ*pvdA*	Imperi et al., 2008
Δ*pchD*	PAO1Δ*pchD*	Frangipani et al., 2014
Δ*pvdA*Δ*pchD*	PAO1Δ*pvdA*Δ*pchD*	Visca et al., 2013
Δ*cio*	PAO1 containing a 2400-bp deletion in the *cioAB* locus	This work
Δ*cox*	PAO1 containing a 4109-bp deletion in the *coxBA*-PA0107-*coIII* locus	This work
Δ*cyo*	PAO1 containing a 4830-bp deletion in the *cyoABCDE* operon	This work
Δ*cco*	PAO1 containing a 6445-bp deletion in the two adjacent *ccoNOQP1* and *ccoNOQP2* operons	This work
Δ*cyo*Δ*cio*	PAO1 mutated in both *cyo* and *cio*	This work
Δ*cyo*Δ*cco*	PAO1 mutated in both *cyo* and *cco*-1,2	This work
Δ*cyo*Δ*cio*Δ*cox*	PAO1 mutated in *cyo*, *cio* and *cox*	This work
Δ*cyo*Δ*cco*Δ*cox*	PAO1 mutated in *cyo*, *cco* and *cox*	This work
E. coli		
DH5αF′	*recA1 endA1 hsdR17 supE44 thi-1 gyrA96 relA1* Δ(*lacZYA-argF*) U169 [Φ*80dlacZ*Δ*M15*] Nal^R	Sambrook et al., 1989
S17-1 λpir	*recA*, *thi*, *pro*, *hsdR*-M+RP4: 2-Tc:Mu: Km Tn7 λpir, Tp^R Sm^R	Simon et al., 1983
PLASMIDS		
pDM4	Suicide vector; *sacBR*, *oriR6K*, Cm^R	Milton et al., 1996
pME7541	Suicide construct used for deletion of the *cioAB* operon; Tc^R	Frangipani et al., 2008
pME9302	Suicide construct used for deletion of the *coxB-coIII* cluster; Tc^R	Frangipani et al., 2008
pME9303	Suicide construct used for deletion of the *cyoABCDE* operon; Tc^R	Frangipani et al., 2008
pME9308	Suicide construct used for deletion of the two adjacent *ccoNOQP* operons; Tc^R	Frangipani et al., 2008
pUCP18	*E. coli-Pseudomonas* shuttle vector derived from pUC18; ColE1, pRO1600, Ap^R, Cb^R	Schweizer, 1991
pUCP*hasR*	pUCP18 derivative carrying the coding sequence of *hasR* with its own promoter	This study
pUCP*phuR*	pUCP18 derivative carrying the coding sequence of *phuR* with its own promoter	This study
pUCP*phuRhasR*	pUCP18 derivative carrying the coding sequence of *phuR* and *hasR* with their own promoters	Minandri et al., 2016
pDM4Δ*hasR*	pDM4 derivative carrying the flanking regions of the *hasR* coding sequence	Minandri et al., 2016
pDM4Δ*phuR*	pDM4 derivative carrying the flanking regions of the *phuR* coding sequence	Minandri et al., 2016

Oligonucleotides	Sequence 5′-3′	Restriction site
hasR compl FW	CGGGGTACCGGCGGGAGTGACGCTGC	KpnI
hasR compl RV	GAAGATCTCCTTCACTGGGCAAAACGG	BglII
phuR compl FW	CCGGAATTCGAAAGGCTGGGAGTGCTG	EcoRI
phuR compl RV	CGGGGTACCACCTGTGGCATGGAAAGC	KpnI

Tc^R, tetracycline resistant; Ap^R, ampicillin resistant; Cm^R, chloramphenicol resistant; Cb^R, carbenicillin resistant; restriction sites in the oligonucleotides are underlined.

mutant, a 2932 bp fragment containing the *hasR* gene with its own promoter region was amplified by PCR from the PAO1 genome using primers *hasR* compl FW and *hasR* compl RV (**Table 1**). The product was then digested with KpnI and BglII and directionally cloned into the corresponding sites of the shuttle vector pUCP18, giving plasmid pUCP*hasR*. To express *phuR* in Δ*hasR*Δ*phuR* mutant, a 2575 bp fragment containing the *phuR* gene with its own promoter region was amplified by PCR from the PAO1 genome using primers *phuR* compl FW and *phuR* compl RV (**Table 1**). The product was then digested with EcoRI and KpnI and directionally cloned into the corresponding sites of the shuttle vector pUCP18, giving plasmid pUCP*phuR*. To express *hasR* and *phuR* in the Δ*hasR*Δ*phuR* mutant strain, the pUCP*hasRphuR* plasmid previously described (Minandri et al., 2016) was used.

Generation of *P. aeruginosa* Mutants

For mutant construction, *E. coli* and *P. aeruginosa* strains were grown in LB, with or without antibiotics, at 37 and 42°C, respectively, with vigorous aeration. Previously described suicide plasmids (**Table 1**) were used according to procedures detailed elsewhere (Milton et al., 1996; Frangipani et al., 2008).

Measurement of Cytochrome *c* Oxidase Activity in *P. aeruginosa* Intact Cells

Cytochrome *c* oxidase activity was assayed by using the artificial electron donor *N*,*N*,*N*',*N*'tetramethyl-*p*-phenylene diamine (TMPD) (Fluka). Briefly, bacteria were grown over-night in DCAA supplemented with 100 μM $FeCl_3$, then washed in saline and inoculated in DCAA to a final $OD_{600} = 0.05$. When the mid-exponential growth phase was reached (≈6 h post inoculum), cells were washed once in saline and adjusted to an $OD_{600} = 1$ (corresponding to $\approx 10^9$ CFU/ml).

Then, 10^8 bacterial cells (100 μl) were suspended in 1.4 ml of 33 mM potassium phosphate buffer (KPi, pH 7.0). The reaction was started by the addition of 5 μl of a 0.54 M TMPD solution to the sample cuvette. The rate of TMPD oxidation was recorded spectrophotometrically at 520 nm for 8 min at 25°C. Results were expressed as μmol TMPD oxidized/min^{-1}/10^8cells using 6.1 as the millimolar extinction coefficient of TMPD (Matsushita et al., 1982).

Isolation of Outer Membrane Proteins (OMPs) and SDS-PAGE Analysis

OMPs were isolated following the sarcosyl solubilization method (Filip et al., 1973), with some modifications. Briefly, bacteria from over-night cultures in DCAA supplemented with 100 μM $FeCl_3$ and 200 μg/ml Cb were washed in saline, then diluted to $OD_{600} = 0.05$ in 60 ml DCAA supplemented with 200 μg/ml Cb, and incubated over-night at 37°C. Cells were collected by centrifugation (2500 × *g*, 20 min), washed with 5 ml of 30 mM Tris HCl (pH 8, Sigma-Aldrich) and suspended in 1 ml of the same buffer. Bacteria were lysed by sonication in an ice bath (8 × 20 s cycles in a Sonics Vibra-Cell™ VCX 130 sonicator), punctuated by 20 s intervals (50% power). Phenyl methyl sulfonyl fluoride (PMSF, Sigma-Aldrich) was added to cell lysate at 1 mM final concentration. Unbroken cells were removed by centrifugation at 2400 × *g* for 20 min, and supernatants were transferred to fresh tubes. Sarcosyl (N-laurylsarcosinate sodium salt, Sigma) was added to the supernatant to a final concentration of 2%. After 1 h incubation at room temperature with gentle shaking, the mixture was centrifuged for 2 h at 55,000 × *g* at 4°C. OMP pellets were suspended in 40 μl 2 x SDS-PAGE loading dye (Sambrook et al., 1989), boiled for 10 min, then separated by 8% SDS-PAGE and visualized by Coomassie brilliant blue staining.

Statistical Analysis

Statistical analysis was performed with the software GraphPad Instat (GraphPad Software, Inc., La Jolla, CA), using One-Way Analysis of Variance (ANOVA), followed by Tukey-Kramer Multiple Comparisons Test.

RESULTS

P. aeruginosa is Inhibited by GaPPIX under Iron-Deplete Conditions

It has been previously reported that GaPPIX has no effect on *P. aeruginosa* (Stojiljkovic et al., 1999). This results is quite surprising given that *P. aeruginosa* is able to utilize heme as an iron source, by expressing two heme-uptake systems, i.e., *has* and *phu* (Ochsner et al., 2000). However, since the effect of GaPPIX has previously been investigated in iron-rich media (Stojiljkovic et al., 1999), we sought that under these conditions iron availability would have impaired Ga(III) activity. To verify this hypothesis, we preliminary tested the effect of GaPPIX on *P. aeruginosa* PAO1 growth using the iron-poor medium DCAA (Visca et al., 1993), supplemented with increasing concentrations of GaPPIX, the iron-binding porphyrin Hemin, or $Ga(NO_3)_3$, the latter resulting very active on *P. aeruginosa* in this medium (Bonchi et al., 2015). $Ga(NO_3)_3$ completely inhibited *P. aeruginosa* growth at 12.5 μM, and its activity was abrogated by the addition of $FeCl_3$ (**Figure 2A**) consistent with previous findings (Kaneko et al., 2007; Frangipani et al., 2014). Although the minimal inhibitory concentration (MIC) could not be determined for up to 100 μM GaPPIX (**Figure 2A**), exposure of PAO1 to GaPPIX reduced bacterial growth by 50% (IC_{50}) at 12.5 μM (**Figure 2A**). Also in the case of GaPPIX, growth inhibition was completely reversed by the addition of $FeCl_3$ (**Figure 2A**). As expected, exposure *P. aeruginosa* PAO1 to Hemin promoted bacterial growth at concentrations ranging between 1.55 and 25 μM, in line with the ability of *P. aeruginosa* to use Hemin as an iron source (Ochsner et al., 2000).

The GaPPIX susceptibility of *P. aeruginosa* PAO1 was also tested using the disk diffusion assays in DCAA agar plates supplemented or not with an excess of $FeCl_3$ (600 μM) (**Figure 2B**). In $FeCl_3$-supplemented DCAA, both GaPPIX and $Ga(NO_3)_3$ caused no inhibition of PAO1 growth. Conversely, in DCAA a clear ZOI was observed around the GaPPIX and $Ga(NO_3)_3$ disks (**Figure 2B**). Different from the ZOI formed by $Ga(NO_3)_3$, the ZOI formed by GaPPIX was less transparent (**Figure 2B**), consistent with the evidence that no MIC (full inhibition) could be determined for GaPPIX in liquid DCAA (**Figure 2A**). Although more transparent, the ZOI caused by $Ga(NO_3)_3$ was smaller than that of GaPPIX (**Figure 2B**). These preliminary data indicate that iron-deplete conditions render *P. aeruginosa* PAO1 susceptible to GaPPIX-mediated growth inhibition.

The Response of *P. aeruginosa* Cells to GaPPIX Depends on Intracellular Iron Carryover

The above results prompted us to investigate the effect of the intracellular iron content on GaPPIX-dependent growth inhibition. To this aim, the effect of GaPPIX was compared between *P. aeruginosa* PAO1 cells that had been pre-cultured in either DCAA containing 100 μM $FeCl_3$ (to increase the intracellular iron content) or DCAA without $FeCl_3$ (to lower the intracellular iron content). Iron-starved bacterial cells were significantly more susceptible to GaPPIX ($P < 0.001$) compared with those pre-cultured with $FeCl_3$ (**Figure 3A**). In particular, upon the addition of 0.38 μM GaPPIX, the growth of iron-starved PAO1 cells was reduced by 40% compared with cells pre-cultured in the presence of 100 μM $FeCl_3$ (**Figure 3A**).

To further investigate the correlation between the intracellular iron content and GaPPIX-dependent growth inhibition, GaPPIX

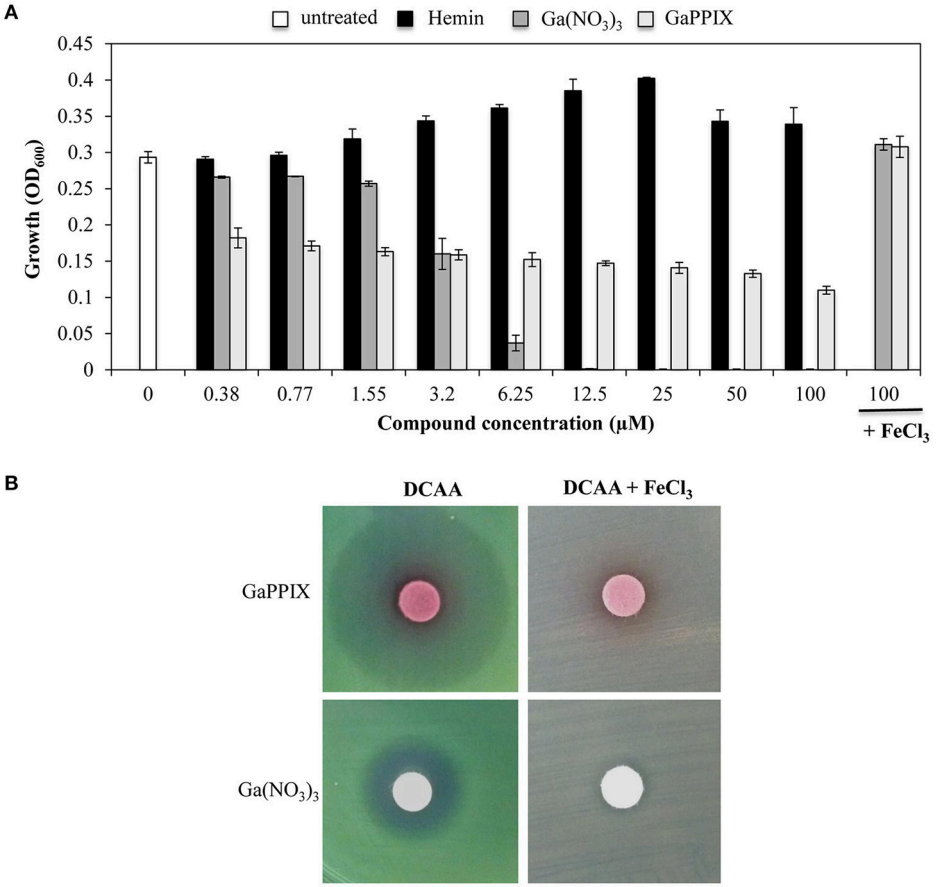

FIGURE 2 | GaPPIX inhibits *P. aeruginosa* PAO1 growth under iron-deplete conditions. (A) *P. aeruginosa* PAO1 was grown for 24 h at 37°C in DCAA in the presence of different concentrations of Hemin (black bars), $Ga(NO_3)_3$ (dark gray bars), GaPPIX (light gray bars), or nothing (white bar). Control cultures were supplemented with 100 μM $FeCl_3$ and 100 μM of either $Ga(NO_3)_3$ or GaPPIX. Values are the mean of 3 independent experiments, each one performed in duplicate ± the standard deviation. **(B)** Approximately 5×10^6 *P. aeruginosa* PAO1 cells were seeded on the surface of DCAA agar plates, supplemented or not with 600 μM $FeCl_3$, as indicated on top. Then, disks soaked with 10 μl of a 15 mM solution of either GaPPIX or $Ga(NO_3)_3$ were deposited on the agar surface, as indicated on the left. Plates were incubated for 16 h at 37°C. Images are representative of three independent experiments yielding similar results.

susceptibility was evaluated on *P. aeruginosa* mutants impaired in Fe(III)-siderophore uptake systems, i.e., mutants unable to synthesize pyoverdine (Δ*pvdA*), pyochelin (Δ*pchD*), or both siderophores (Δ*pvdA*Δ*pchD*) (**Figure 3B**). While GaPPIX-dependent growth inhibition was similar in the wild type and the Δ*pchD* mutant, both Δ*pvdA* and Δ*pvdA*Δ*pchD* mutants were extremely sensitive to GaPPIX (**Figure 3B**). In particular, 0.38 μM GaPPIX inhibited the growth of the Δ*pvdA* and Δ*pvdA*Δ*pchD* mutant strains by 75 and 78%, respectively, compared with the untreated cultures, while it reduced the growth of the wild-type strain and of the Δ*pchD* mutant by only 40 and 30%, respectively (**Figure 3B**). Altogether, these data indicate that the response of *P. aeruginosa* PAO1 to GaPPIX also depends on the carryover of intracellular iron.

GaPPIX is Preferentially Uptaken *via* the *P. aeruginosa* PhuR Receptor

To investigate the hypothesis that GaPPIX may enter *P. aeruginosa* cells by exploiting the same routes as heme, *P. aeruginosa* mutants carrying a deletion of either of the known heme receptors (Δ*hasR* and Δ*phuR* mutants; **Table 1**) were generated. The effect of GaPPIX on these mutants, as well as on a Δ*hasR*Δ*phuR* double mutant lacking both heme receptors (Minandri et al., 2016), was investigated in DCAA in the presence of 12.5 μM GaPPIX (IC_{50}; **Figure 4A**). While all strains showed the same growth profiles in the untreated medium, both Δ*phuR* and Δ*hasR*Δ*phuR* mutants grew better than the wild type or the Δ*hasR* mutant in the presence of 12.5 μM GaPPIX, displaying ≈50% higher growth levels relative to the wild type or the Δ*hasR* mutant (**Figure 4A**). These data suggest that, among the *P. aeruginosa* heme-uptake systems, *phu* has a more prominent role than *has* in the uptake of GaPPIX. Then, the effect of GaPPIX on heme-receptor mutants was evaluated in DCAA agar plates, by performing the disk diffusion assays (**Figure 4B**). Results showed a similar ZOI (27.6 ± 2.0 mm) for both the wild-type strain and the Δ*hasR* mutant, while a smaller ZOI (24.5 ± 0.7 mm) was observed for the Δ*phuR* mutant, indicating a less susceptible phenotype (**Figure 4B,** Table S2).

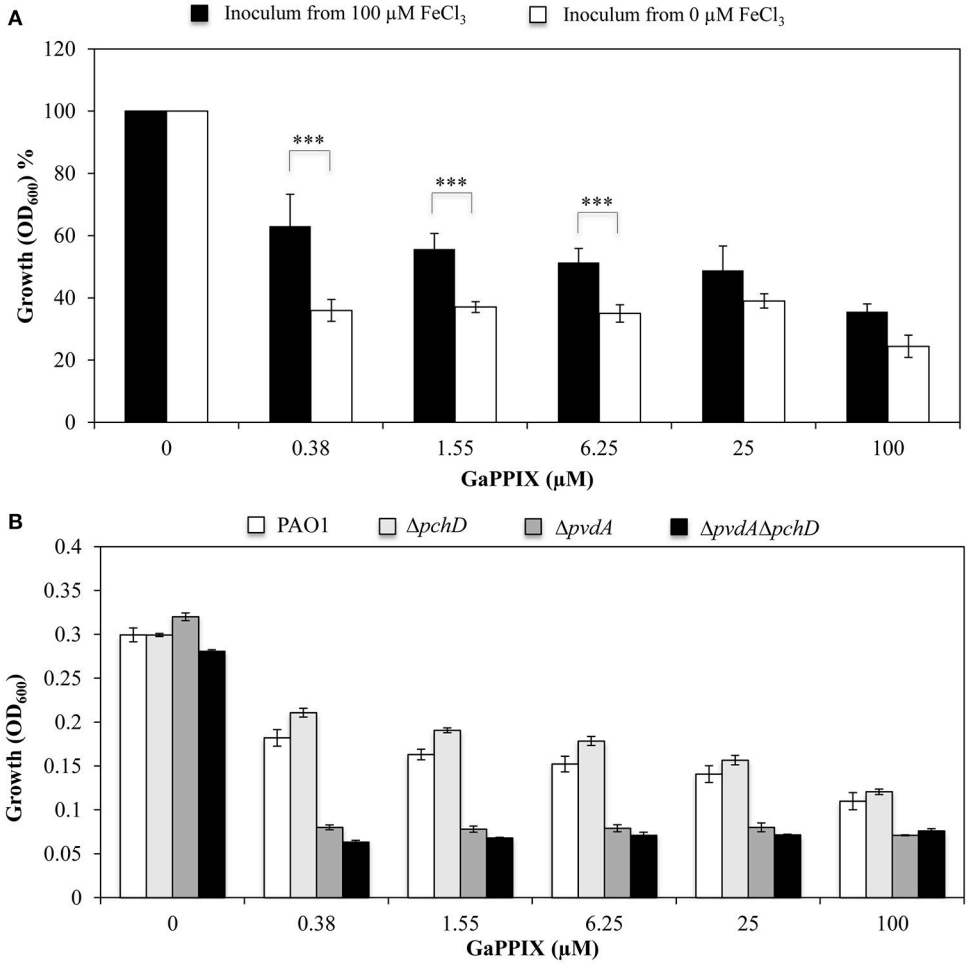

FIGURE 3 | The response of *P. aeruginosa* to GaPPIX depends on intracellular iron carryover. (A) *P. aeruginosa* PAO1 cells from an inoculum with 100 μM $FeCl_3$ (black bars) and without $FeCl_3$ (white bars) were grown in DCAA supplemented with increasing concentrations of GaPPIX for 24 h at 37°C. The values are expressed as the percentage relative to the untreated cultures, and represent the mean of four independent experiments, each one performed at least in duplicate ± the standard deviation. Asterisks indicate statistically significant differences relative to a culture derived from cells grown in the presence of 100 μM $FeCl_3$ (***$P <$ 0.001). **(B)** *P. aeruginosa* PAO1 (white bars), Δ*pchD* (light gray bars), Δ*pvdA* (dark gray bars), and Δ*pvdA*Δ*pchD* (black bars) were grown in DCAA supplemented with increasing concentrations of GaPPIX for 24 h at 37°C. Values are the mean of two independent experiments, each one performed in duplicate ± the standard deviation.

In addition, no ZOI was observed for the Δ*hasR*Δ*phuR* double mutant, indicating a fully resistant phenotype (**Figure 4B**). These observations indicate that both *has* and *phu* systems are implicated in GaPPIX transport, although the *phu* system appears to be the preferential route for the entrance of GaPPIX in *P. aeruginosa* cells (**Figure 4B**).

The Sensitivity of *P. aeruginosa* to GaPPIX Depends on the Expression of the Heme-Uptake Receptors

To further investigate the contribution of the HasR and PhuR receptors to GaPPIX-uptake, we individually expressed multicopy *hasR*, *phuR*, or both *hasR* and *phuR* in the Δ*hasR*Δ*phuR* mutant strain (using plasmids pUCP*hasR*, pUCP*phuR*, or pUCP*hasRphuR*, respectively) (**Figure 5A**). The effect of GaPPIX on these strains was initially tested by the disk diffusion assays (**Figure 5A**). While, the empty pUCP18 vector did not alter the susceptibility of Δ*hasR*Δ*phuR* to GaPPIX (**cfr Figures 5A**, **4B**), the expression of *hasR* from the multicopy plasmid pUCP*hasR* made the Δ*hasR*Δ*phuR* mutant more susceptible to GaPPIX (ZOI = 27.6 ± 2.0 mm) (**Figure 5A,** Table S2). The effect of GaPPIX was even more pronounced in the Δ*has*Δ*phuR* mutant overexpressing either *phuR* (Δ*has*Δ*phuR* carrying the multicopy plasmid pUCP*phuR*; ZOI = 34.0 ± 1.0 mm) or both *hasR* and *phuR* (Δ*has*Δ*phuR* carrying the multicopy plasmid pUCP*hasRphuR*; ZOI = 33.3 ± 0.5 mm) (**Figure 5A,** Table S2). GaPPIX sensitivity of the Δ*has*Δ*phuR* strain expressing *hasR, phuR,* or both genes, was also evaluated in DCAA liquid medium, in the presence of different concentrations of GaPPIX (**Figure 5B**). All strains grew equally in the untreated medium, and GaPPIX did not

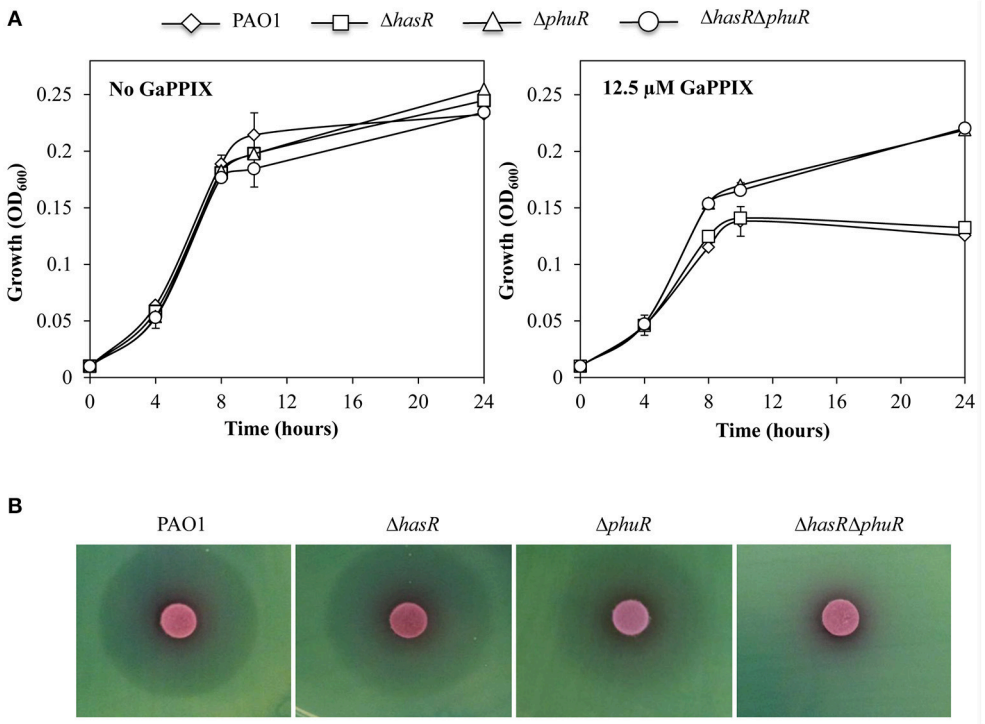

FIGURE 4 | GaPPIX enters *P. aeruginosa* cells through the heme-uptake systems. (A) Growth of *P. aeruginosa* wild type (diamond) and Δ*hasR* (square), Δ*phuR* (triangle), and Δ*hasR*Δ*phuR* (circle) mutant strains in DCAA supplemented or not with 12.5 μM GaPPIX at 37°C. Values are the mean of two independent experiments, each one performed in duplicate ± the standard deviation. **(B)** Approximately 5 × 10^6 bacterial cells were seeded on DCAA agar plates, then disks soaked with 10 μl of a 15 mM solution of GaPPIX were deposited on the agar surface. Plates were incubated for 16 h at 37°C. Images are representative of three independent experiments yielding similar results.

affect the growth of Δ*hasR*Δ*phuR*/pUCP18 up to 25 μM (**Figure 5B**). Conversely, strains Δ*hasR*Δ*phuR*/pUCP*hasR*, Δ*hasR*Δ*phuR*/pUCP*phuR,* and Δ*hasR*Δ*phuR*/pUCP*hasRphuR* were very sensitive to GaPPIX. In particular, 0.38 μM GaPPIX reduced the growth of the Δ*hasR*Δ*phuR*/pUCP*hasR* strain by 56%, and by >80% in both Δ*hasR*Δ*phuR*/pUCP*phuR* and Δ*hasR*Δ*phuR*/pUCP*hasRphuR* strains (**Figure 5B**). This effect was much more pronounced than that observed for the parental strain PAO1 (**Figure 2A**). Of note, no further growth reduction was observed for both the Δ*hasR*Δ*phuR*/pUCP*phuR* and Δ*hasR*Δ*phuR*/pUCP*hasRphuR* mutant strains at > 0.38 μM GaPPIX. The increased sensitivity of the Δ*hasR*Δ*phuR* strain expressing either *hasR* or *phuR*, relative to the wild type, can be explained by the overexpression of heme receptors from the multicopy plasmid pUCP18 (**Figure 5A**). To confirm this hypothesis, HasR and PhuR protein levels were visualized by SDS-PAGE analysis of OMPs purified from the different *P. aeruginosa* strains cultured in DCAA (**Figure 5C**). By comparing *P. aeruginosa* outer-membrane-proteins profiles of the wild type, the Δ*phuR* or the Δ*hasR*Δ*phuR* mutant strains, the lack of a *ca.* 75 kDa protein in the Δ*phuR* or the Δ*hasR*Δ*phuR* mutants, was observed. This was in good agreement with a predicted molecular mass of 82 kDa for the mature PhuR receptor. Moreover, a protein band at that position was evident in SDS-PAGE electropherograms of the Δ*hasR*Δ*phuR*/pUCP*phuR* and the Δ*hasR*Δ*phuR*/pUCP*hasRphuR* complemented mutants (**Figure 5C**). Similarly, a protein band corresponding to *ca.* 94 kDa, consistent with the HasR receptor mass, was absent in the Δ*hasR* and Δ*hasR*Δ*phuR* mutants, while it was clearly detectable in the Δ*hasR*Δ*phuR*/pUCP*hasR* and Δ*hasR*Δ*phuR*/pUCP*hasRphuR* complemented mutants (**Figure 5C**). In line with previous results (Ochsner et al., 2000), protein levels greatly differed between PhuR and HasR, the latter being poorly expressed in wild-type PAO1. These results confirm that both HasR and PhuR direct GaPPIX entrance in *P. aeruginosa* cells, and argue for a prominent role of PhuR as a consequence of its higher expression levels, compared with HasR.

To confirm the specificity of GaPPIX for both heme-uptake systems, we investigated whether the growth inhibitory effect of GaPPIX could be rescued by the presence of Hemin (Hm) or Hemoglobin (Hb), which are known to deliver iron *via* heme-uptake receptors (Ochsner et al., 2000). To this aim, the heme-uptake mutant Δ*hasR*Δ*phuR* overexpressing either PhuR or HasR was tested in the GaPPIX disk diffusion assays in the presence of Hm and Hb (**Figure 5D**). Both Hm and Hb partly rescued the growth of the Δ*hasR*Δ*phuR* mutant overexpressing either PhuR (from pUCP*phuR*) or HasR (from pUCP*hasR*) thus

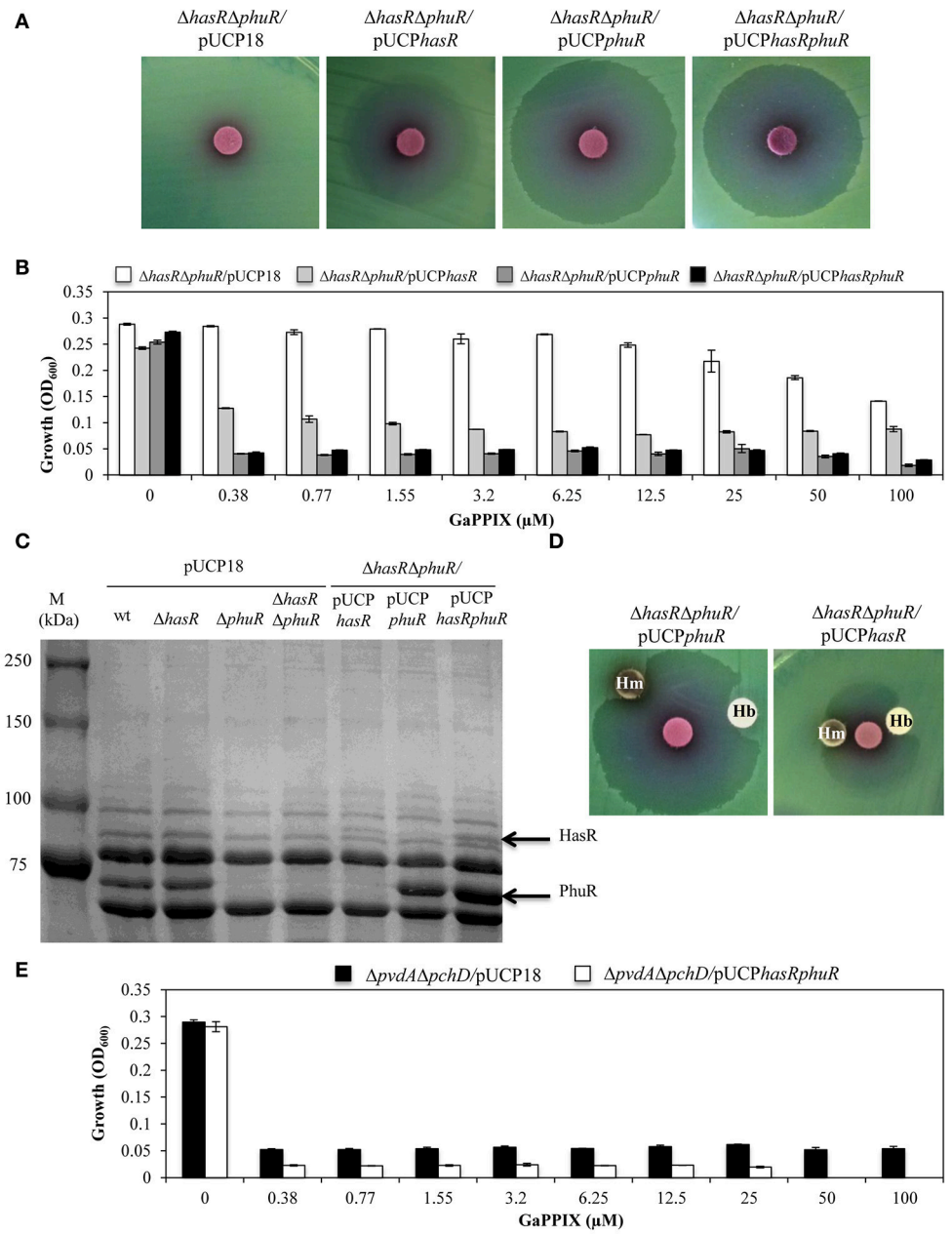

FIGURE 5 | The sensitivity of *P. aeruginosa* to GaPPIX depends on the expression of heme-uptake systems. (A) Approximately 5×10^6 bacterial cells were seeded on DCAA agar plates containing 200 μg/ml Cb, then disks soaked with 10 μl of a 15 mM solution of GaPPIX were deposited on the agar surface. Plates were incubated for 16 h at 37°C. **(B)** Growth of the *P. aeruginosa* Δ*hasR*Δ*phuR* mutant strain carrying the empty vector pUCP18 (white bars), or overexpressing *hasR* from plasmid pUCP*hasR* (light gray bars) or *phuR* from plasmid pUCP*phuR* (dark gray bars), or both *hasR* and *phuR* from plasmid pUCP*hasRphuR* (black bars), in DCAA supplemented with increasing concentrations of GaPPIX for 24 h at 37°C. **(C)** SDS-PAGE analysis of the outer membrane proteins of different *P. aeruginosa* PAO1 strains. Strains and plasmids are indicated on the top of each lane. M is the molecular mass marker (kDa), with band sizes on the left. The position of the putative 82 kDa PhuR and 94 kDa HasR outer membrane receptors is indicated by arrows on the right. **(D)** Rescue effect of hemin (Hm) or hemoglobin (Hb) from GaPPIX growth inhibition in the Δ*hasR*Δ*phuR* mutant strain overexpressing either *phu* from plasmid pUCP*phuR* or *hasR* from plasmid pUCP*hasR*. Approximately 5×10^6 bacterial cells were seeded on DCAA agar plates containing 200 μM Cb. Blank discs were soaked with 10 μl of a 15 mM solution of GaPPIX or with 75 μg of either Hm or Hb. Plates were incubated at 37°C for 16 h. **(E)** Growth of the *P. aeruginosa* Δ*pvdA*Δ*pchD* mutant strain carrying the empty vector pUCP18 (black bars), or overexpressing both *hasR* and *phuR* from plasmid pUCP*hasRphuR* (white bars), in DCAA supplemented with increasing concentrations of GaPPIX for 24 h at 37°C. Values are the mean of two independent experiments, each one performed in triplicate ± the standard deviation. Images in **B** and **D** are representative of two independent experiments yielding similar results.

confirming that (i) Hm, Hb and GaPPIX compete with heme receptors and (ii) GaPPIX enters *P. aeruginosa* cells through PhuR and HasR (**Figure 5D**).

It has been observed that *P. aeruginosa* isolates evolving during chronic lung infection in CF patients tend to accumulate mutations in siderophore loci, concomitant with preferential utilization of heme iron (Cornelis and Dingemans, 2013; Marvig et al., 2014; Andersen et al., 2015). To simulate this situation, we tested GaPPIX susceptibility of a siderphore-defective *P. aeruginosa* mutant overexpressing both PhuR and HasR receptors (Δ*pvdA*Δ*pchD*/pUCP*hasRphuR*). Whereas, exposure of the Δ*pvdA*Δ*pchD* mutant to GaPPIX reduced bacterial growth by 82% at 0.38 μM, expression of both *hasR* and *phuR* from multicopy plasmid pUCP*hasRphuR* made the Δ*pvdA*Δ*pchD* mutant extremely susceptible to GaPPIX, displaying 90% growth reduction (IC_{90}) at 0.38 μM (**Figure 5E**). Notably, full inhibition of the Δ*pvdA*Δ*pchD*/pUCP*hasRphuR* strain was observed upon challenge with 50 μM GaPPIX.

GaPPIX Targets the Aerobic Respiration of *P. aeruginosa*

GaPPIX has been proven effective against a wide range of pathogenic bacteria by targeting metabolic pathways that require heme as an enzymatic cofactor, such as cellular respiration (Stojiljkovic et al., 1999). Thus, we investigated whether GaPPIX could interfere with the activity of terminal oxidases implicated in *P. aeruginosa* aerobic respiration. In particular, we focused on Cco-1, Cco-2, and Cio, which have been shown to sustain *P. aeruginosa* growth under low oxygen conditions, as those encountered in the lung of CF patients (Alvarez-Ortega and Harwood, 2007; Kawakami et al., 2010). To this aim, we initially tested the sensitivity of cytochrome *c* oxidases (i.e., Cox, Cco-1, and Cco-2) to GaPPIX. Strains deleted of the whole operon encoding the terminal oxidase Cox (Δ*cox*) or both the Cco-1 and Cco-2 terminal oxidases (Δ*cco*) were generated in the same parental strain used to generate the heme-receptor mutants (**Table 1**). The effect of GaPPIX was then assayed on these cytochrome-defective mutants using the TMPD redox indicator, which is an artificial electron donor to the cytochrome *c* (Matsushita et al., 1982). Oxidation of TMPD to a blue indophenol compound indicates electron flow to the cytochrome *c* terminal oxidases. Thus, cytochrome *c* oxidase activity was measured on *P. aeruginosa* PAO1 and in the Δ*cox* and Δ*cco* mutants grown in DCAA supplemented or not with a sub-inhibitory concentration of GaPPIX (4 μM). In whole cells cultured in the untreated medium, no cytochrome *c* oxidase activity could be measured in the Δ*cco* strain (**Figure 6A**), confirming that in our conditions the TMPD test mainly measures the activity of Cco. Indeed, the Δ*cox* mutation does not affect the TMPD oxidase activity (**Figure 6A**), as previously reported (Frangipani and Haas, 2009). This is because Cox is known to be poorly expressed during *P. aeruginosa* exponential growth (Kawakami et al., 2010). Interestingly, 4 μM GaPPIX reduced the respiratory activity by more than 50% in the wild-type strain PAO1 and the Δ*cox* mutant, compared with the untreated condition (**Figure 6A**). These observations suggest that Cco-1 and Cco-2 terminal oxidases are sensitive to GaPPIX. To confirm these preliminary results, the effect of GaPPIX was tested on a mutant expressing only Cco-1 and Cco-2. To this aim, a Δ*cyo*Δ*cio*Δ*cox* triple mutant strain was generated. Disk diffusion assays showed that the Δ*cyo*Δ*cio*Δ*cox* mutant was more sensitive to GaPPIX than the wild type (ZOI = 34.6 ± 1.24 vs 27.6 ± 2.0 mm, respectively) (**Figure 6B,** Table S2). Similar results were obtained in DCAA liquid cultures. PAO1 wild type and the Δ*cyo*Δ*cio*Δ*cox* mutant showed a similar growth profile in the untreated medium (**Figure 6C**), whereas exposure to 0.38 μM GaPPIX reduced bacterial growth by 40% and 68%, respectively, relative to the untreated cultures (**Figure 6C**). Interestingly, it was possible to determine an IC_{90} at 82 μM for the Δ*cyo*Δ*cio*Δ*cox* mutant strain (**Figure 6C**). These results confirm that Cco-1 and Cco-2 are targeted by GaPPIX.

Then, the effect of GaPPIX on the Cio terminal oxidase was assessed. To this purpose, sodium azide (NaN_3) was used as a specific inhibitor of copper-dependent oxidases, i.e., all terminal oxidases except Cio (Cunningham and Williams, 1995). Preliminarily, we determined the minimal NaN_3 concentration inhibiting all terminal oxidases except Cio in DCAA, by comparing the growth of wild-type PAO1 and the Δ*cio* mutant in the presence of increasing NaN_3 concentrations (250–1000 μM). We observed that 350 μM of NaN_3 completely inhibited the Δ*cio* mutant without affecting PAO1 growth (data not shown). Then, the sensitivity of Cio to GaPPIX was tested by performing a GaPPIX disk diffusion assays with wild-type PAO1 in DCAA supplemented or not with 350 μM NaN_3. It was observed that PAO1 remains sensitive to GaPPIX in the presence of 350 μM NaN_3, displaying a ZOI even greater than that obtained for PAO1 without NaN_3 (36.6 ± 3.0 vs 27.6 ± 2.0 mm, respectively) (**Figure 7A,** Table S2). This result provides evidence that Cio is a target for GaPPIX. To strengthen this evidence, a *P. aeruginosa* Δ*cyo*Δ*cco*Δ*cox* triple mutant, which expresses only Cio (**Table 1**) was constructed and assayed for GaPPIX susceptibility. Disk diffusion assay results showed that the Δ*cyo*Δ*cco*Δcox mutant was more sensitive to GaPPIX than the wild-type PAO1 (ZOI = 30.0 ± 0.7 vs 27.6 ± 2.0 mm, respectively) (**Figure 7A,** Table S2). Similar results were also obtained in DCAA liquid medium, showing that GaPPIX significantly reduced ($P < 0.001$) the growth of the Δ*cyo*Δ*cco*Δcox mutant relative to the wild type, at concentrations ranging between 0.38 and 6.25 μM (**Figure 7B**). Altogether, the above results indicate that *P. aeruginosa* Cco-1, Cco-2, and Cio terminal oxidases are targets for GaPPIX.

P. aeruginosa Clinical Isolates Are Sensitive to GaPPIX

The expression of *P. aeruginosa* genes encoding heme-uptake systems has recently been detected in sputum samples collected from CF patients (Konings et al., 2013), and an evolution toward preferential heme utilization has been documented in *P. aeruginosa* during the course of chronic lung infection in CF patients (Marvig et al., 2014; Nguyen et al., 2014). Given the importance of heme in sustaining *P. aeruginosa* growth during infection, we have comparatively assessed the response to $Ga(NO_3)_3$ and GaPPIX in a collection of *P. aeruginosa* clinical

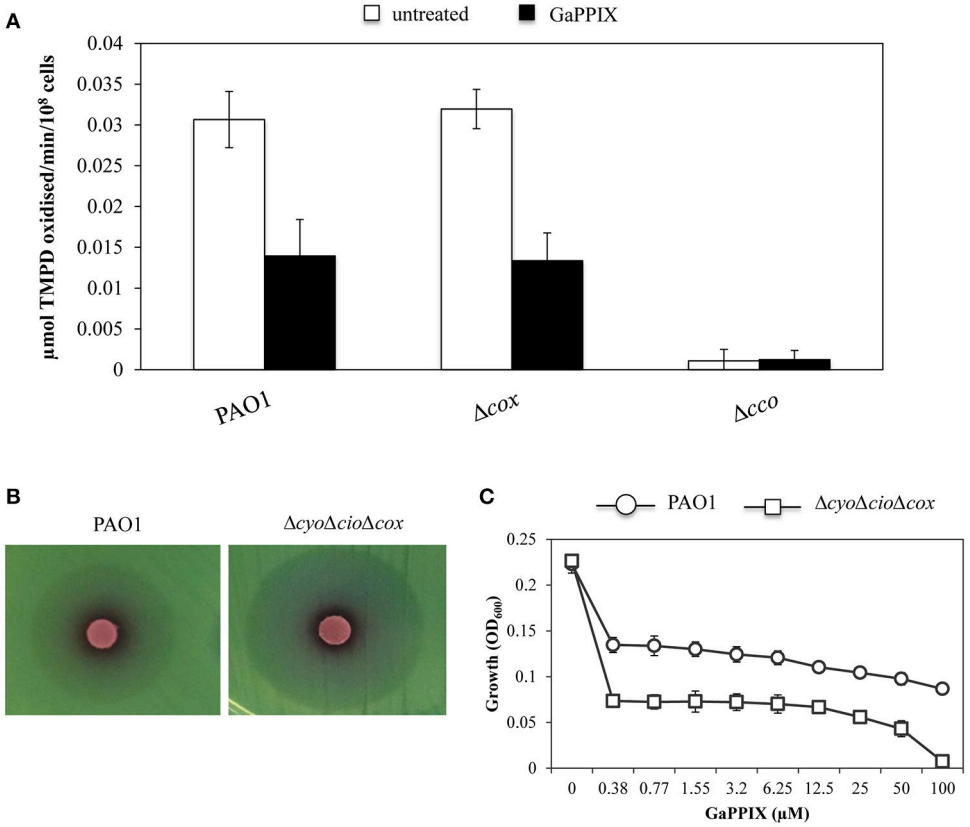

FIGURE 6 | GaPPIX inhibits *P. aeruginosa* PAO1 growth by targeting Cco. (A) TMPD oxidase activity on whole cells of wild-type PAO1, Δ*cox* and Δ*cco* mutants grown for 6 h in DCAA supplemented (black bars) or not (white bars) with 4 μM GaPPIX. Activity is expressed as μmol TMPD oxidized/min^{-1}/10^8 cells at pH 7.0 and 25°C. Each value is the average of three independent experiments, each one performed in triplicate ± the standard deviation. **(B)** Approximately 5 × 10^6 bacterial cells of wild-type PAO1 and the Δ*cyo*Δ*cio*Δ*cox* triple mutant were seeded on DCAA agar plates, then disks soaked with 10 μl of a 15 mM solution of GaPPIX were deposited on the agar surface. Plates were incubated for 16 h at 37°C. Images are representative of two independent experiments giving similar results. **(C)** Growth of wild type PAO1 (open circle) and the Δ*cyo*Δ*cio*Δ*cox* triple mutant (open square) in DCAA supplemented with increasing GaPPIX concentrations, for 24 h at 37°C. Values are representative of two independent experiments, each one performed in triplicate ± the standard deviation.

isolates from CF and non-CF patients (**Figure 8**, Table S1). Although GaPPIX (up to 100 μM) never abolished *P. aeruginosa* growth, the majority of clinical isolates (>70%) was sensitive to GaPPIX, displaying an IC_{50} values in the range 0.1–15.2 μM (Table S1). Moreover, all but one *P. aeruginosa* clinical isolates were significantly more susceptible than the reference PAO1 strain (**Figure 8**). In line with previous reports (Bonchi et al., 2015), all clinical isolates except one (FM1, Table S1) were very sensitive to $Ga(NO_3)_3$, showing IC_{50} values ranging from 0.2 to 9 μM (Table S1).

DISCUSSION

The ability of pathogenic bacteria to colonize the host and cause infections is dependent on their capability to acquire iron and generate energy to sustain *in vivo* growth (Ratledge and Dover, 2000; Alvarez-Ortega and Harwood, 2007; Hammer et al., 2013). The success of *P. aeruginosa* as a pathogen relies on the presence of several iron-uptake systems (reviewed in Llamas et al., 2014), as well as on a multiplicity of terminal oxidases which allow bacterial respiration *in vivo*. Both iron-uptake systems and respiratory cytochromes have been shown to contribute to *P. aeruginosa* fitness during chronic lung infection in CF patients (Alvarez-Ortega and Harwood, 2007; Konings et al., 2013). Recent observations have documented an adaptation of *P. aeruginosa* toward heme iron acquisition in the CF lung, where bacterial energy metabolism mainly relies on the three terminal oxidases Cco-1, Cco-2, and Cio, all of which have high affinity for oxygen (Alvarez-Ortega and Harwood, 2007). These data suggest that heme utilization pathways and respiratory cytochromes could represent candidate targets for the development of new anti-*Pseudomonas* drugs (Alvarez-Ortega and Harwood, 2007; Marvig et al., 2014; Nguyen et al., 2014). Indeed, targeting bacterial membrane functions such as cellular respiration, are considered promising therapeutic opportunities, especially in the case of persistent or chronic infections (Hurdle et al., 2011). Given that all terminal oxidases require heme as a cofactor, and that heme-uptake systems are expressed during chronic lung infection, in this work we have investigated the effect of the heme-mimetic GaPPIX against *P. aeruginosa*. We focused on

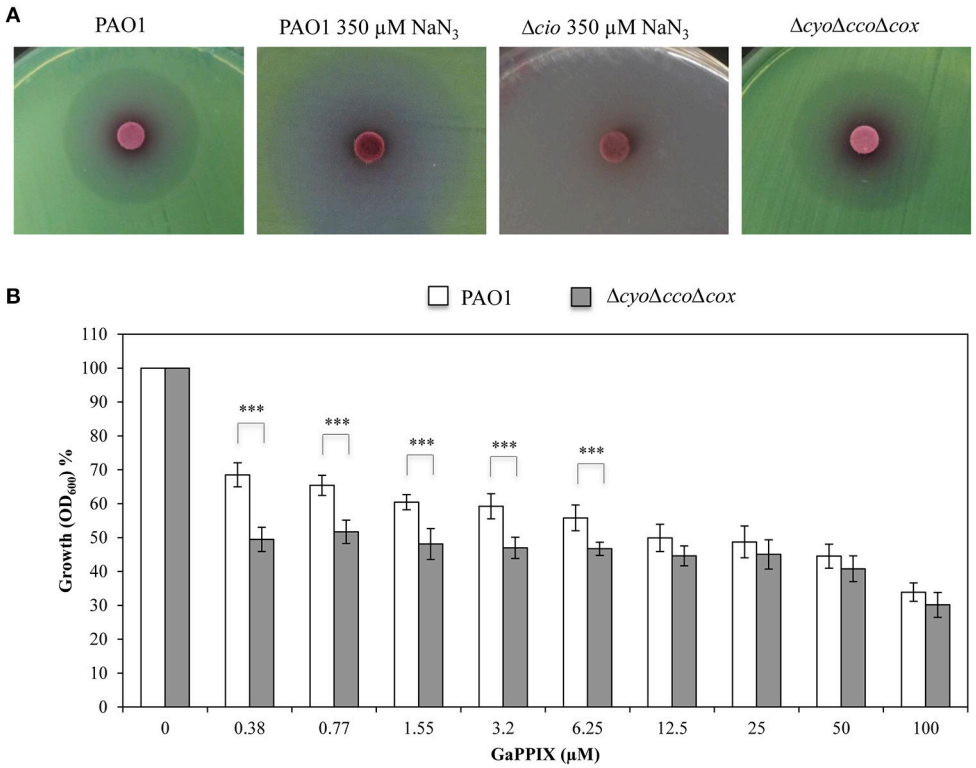

FIGURE 7 | GaPPIX inhibits *P. aeruginosa* PAO1 growth by targeting Cio. (A) Approximately 5×10^6 bacterial cells were seeded on DCAA agar plates, then disks soaked with 10 μl of a 15 mM solution of GaPPIX were deposited on the surface of DCAA agar plates supplemented or not with 350 μM NaN_3. Plates were incubated for 16 h at 37°C. Strains and conditions are indicated on top of each panel. Images are representative of two independent experiments giving similar results. **(B)** Growth inhibition (%) of wild type PAO1 (white bars) and the Δ*cyo*Δ*cco*Δ*cox* triple mutant (gray bars) in DCAA supplemented with increasing concentrations of GaPPIX relative to the untreated controls (no GaPPIX). Growth was measured after 24 h incubation at 37°C. Values are representative of four independent experiments, each one performed at least in duplicate ± the standard deviation. Asterisks indicate statistically significant differences between the wild type PAO1 and the Δ*cyo*Δ*cco*Δ*cox* triple mutant ($P < 0.001$).

Cco-1, Cco-2, and Cio since *P. aeruginosa* uses any of these three terminal oxidases to support the microaerobic growth necessary to thrive in the lung of CF patients. Cox and Cyo are not expressed or strongly repressed under these conditions (Alvarez-Ortega and Harwood, 2007).

We have initially demonstrated that GaPPIX is able to reduce the growth of *P. aeruginosa* only under iron-limiting growth conditions. However, different from $Ga(NO_3)_3$, bacterial growth was never completely inhibited at GaPPIX concentrations up to 100 μM (**Figure 2A**), in line with the fact that the ZOI for GaPPIX was less transparent compared with that generated by $Ga(NO_3)_3$ in the disk diffusion assays (**Figure 2B**). This diverse response of *P. aeruginosa* upon exposure to GaPPIX or $Ga(NO_3)_3$ (**Figures 2A,B**) could be explained by the fact that GaPPIX and $Ga(NO_3)_3$ enter bacterial cells through different pathways. $Ga(NO_3)_3$ may enter *P. aeruginosa* cells (i) by diffusion; (ii) through the HitAB iron transport proteins (García-Contreras et al., 2013); or (iii) *via* the siderophore Pch (Frangipani et al., 2014). On the other hand, we have demonstrated that GaPPIX can cross the *P. aeruginosa* outer membrane only through the heme-receptors HasR and PhuR, since a Δ*hasR*Δ*phuR* mutant is fully resistant to GaPPIX (**Figure 4**). Indeed, overexpression of heme receptors in the Δ*hasR*Δ*phuR* mutant makes this strain susceptible to GaPPIX, at even lower GaPPIX concentrations compared with wild-type PAO1 (**Figures 5A,B**). However, it should also be taken into consideration that GaPPIX and $Ga(NO_3)_3$ likely have different targets. In fact, while $Ga(NO_3)_3$ is known to target a variety of essential iron-containing enzymes (Bernstein, 1998; Soo et al., 2016), less is known about GaPPIX targets. Several studies have demonstrated that the antibacterial activity of GaPPIX relies on the molecule as a whole, since GaPPIX cannot be cleaved by bacterial enzymes (Stojiljkovic et al., 1999; Hammer et al., 2013). In fact, we demonstrated that the homolog of GaPPIX (Hemin) did not affect *P. aeruginosa* PAO1 growth. Indeed, Hemin promoted bacterial growth at concentrations ranging between 1.55 and 25 μM (**Figure 2A**), likely as a consequence of iron delivery to the cell, combined with positive regulation of the *has* system (Llamas et al., 2014). Hence, GaPPIX might be erroneously incorporated in heme-containing proteins such as cytochromes. However, due to the multiplicity of pathways involving cytochromes, exposure to GaPPIX never results in a complete growth inhibition. This

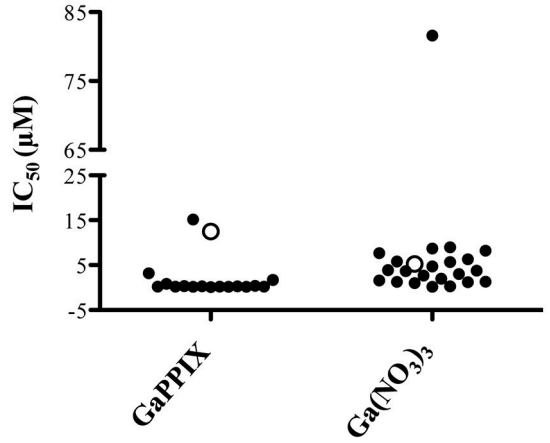

FIGURE 8 | Susceptibility of *P. aeruginosa* clinical isolates to GaPPIX. IC_{50} values of GaPPIX or $Ga(NO_3)_3$ in a collection of *P. aeruginosa* clinical isolates (black) and in the reference strains PAO1 (white). Bacteria were grown for 24 h at 37°C in DCAA with increasing concentrations of GaPPIX or $Ga(NO_3)_3$ to determine the IC_{50}. The IC_{50} of PAO1 was 12.5 μM for GaPPIX and 5.2 μM for $Ga(NO_3)_3$.

hypothesis is supported by the observation that GaPPIX is more active against *P. aeruginosa* mutants deleted in some of the cytochrome-dependent terminal oxidases (**Figures 6**, **7**). In fact, a *P. aeruginosa* mutant that only expresses the terminal oxidases Cco-1 and Cco-2 (Δ*cyo*Δ*cio*Δ*cox*) is much more sensitive to GaPPIX than the wild-type strain. In addition, the Δ*cyo*Δ*cio*Δ*cox* mutant showed a 68% growth reduction in liquid DCAA at 0.38 μM GaPPIX, compared to the untreated cultures, and an IC_{90} of 82 μM (**Figures 6B,C**). Along the same lines, a *P. aeruginosa* strain that only relies on the terminal oxidase Cio to respire oxygen, is more sensitive to GaPPIX than the wild-type strain (**Figure 7**). Taken together, our results demonstrate that GaPPIX targets *P. aeruginosa* respiratory cytochromes Cco-1, Cco-2, and Cio, which are exclusively found in bacteria (Cunningham and Williams, 1995; Pitcher and Watmough, 2004), although we cannot discriminate which of the Cco cytochromes is preferentially targeted by GaPPIX (the Δ*cco*-1,2 strain is mutated in both). Moreover, it is tempting to speculate that GaPPIX may also inhibit the other terminal oxidases Cyo and Cox (**Figure 1**), as well as some of the enzymes involved in denitrification, such as the heme-containing protein complexes Nir and Nor (**Figure 1**). Moreover, GaPPIX could also be incorporated into heme-containing enzymes involved in the protection from oxidative stress, increasing the susceptibility of *P. aeruginosa* to reactive oxygen species.

Although it was not possible to determine the MIC of GaPPIX for wild-type PAO1, it is worth to point out that GaPPIX was extremely active against a *P. aeruginosa* mutant impaired in siderophore production (Δ*pvdA*Δ*pchD*) and overexpressing both HasR and PhuR heme receptors from plasmid pUCP*hasRphuR* (**Figure 5**). Ninety percent growth reduction and full inhibition were observed upon exposure of this mutant to 0.38 and 50.0 μM GaPPIX, respectively. It is tempting to speculate that such strong inhibition could also occur in the CF lung, where siderophore-defective *P. aeruginosa* variants emerge during chronic infection, and heme represents the principal iron source (Marvig et al., 2014; Nguyen et al., 2014). Inhibition could further be enhanced under the microaerobic conditions encountered by *P. aeruginosa* in the CF airways (Hogardt and Heesemann, 2010), where the three high affinity terminal oxidases targeted by GaPPIX (Cco-1, Cco-2, and Cio) are essential for bacterial growth (Alvarez-Ortega and Harwood, 2007). Irrespective of the Ga(III) delivery system and of the energy metabolism adopted by *P. aeruginosa*, the balance between Fe(III) and Ga(III) availability *in vivo* will be the main determinant of Ga(III) efficacy. The inhibitory activity of GaPPIX was not limited to the prototypic strain PAO1, as it was also exerted on a representative collection of *P. aeruginosa* clinical isolates (Table S1). The great majority of clinical isolates (>70%) was sensitive to GaPPIX, irrespective of their origin, and all but one were significantly more susceptible than PAO1 ($IC_{50} \leq 3.2$ μM, Table S1).

Interestingly, studies on several human cell lines report that GaPPIX does not show cytotoxicity at concentrations ≤ 128 μM (Stojiljkovic et al., 1999; Chang et al., 2016), far above the concentrations that we found active on *P. aeruginosa* clinical isolates. Moreover, GaPPIX did not show to affect the health and behavior of mice, when administered by intraperitoneal injections (25–30 mg/kg) followed by four daily doses of (10–12 mg/kg) (Stojiljkovic et al., 1999), though it reduced the survival of *Galleria mellonella* larvae by 50% (LC_{50}) when injected at 25 mM (Arivett et al., 2015).

Although further studies are needed to assess the effect of GaPPIX against *P. aeruginosa* infection *in vivo*, our work should encourage future research directed to the development of heme-mimetic drugs targeting cellular respiration for the treatment of *P. aeruginosa* chronic lung infection.

AUTHOR CONTRIBUTIONS

PV and EF designed research; SH performed research; SH, EF, and PV analyzed data; SH, EF, and PV wrote the paper.

ACKNOWLEDGMENTS

This work was supported by grants from the Italian Ministry of University and Research PRIN-2012 (prot. 2012WJSX8K) and from the Italian Cystic Fibrosis Foundation (grant FFC#21/2015) to PV.

SUPPLEMENTARY MATERIAL

The Supplementary Material for this article can be found online at: http://journal.frontiersin.org/article/10.3389/fcimb.2017.00012/full#supplementary-material

REFERENCES

Alvarez-Ortega, C., and Harwood, C. S. (2007). Responses of *Pseudomonas aeruginosa* to low oxygen indicate that growth in the cystic fibrosis lung is by aerobic respiration. *Mol. Microbiol.* 65, 153–165. doi: 10.1111/j.1365-2958.2007.05772.x

Andersen, S. B., Marvig, R. L., Molin, S., Krogh Johansen, H., and Griffin, A. S. (2015). Long-term social dynamics drive loss of function in pathogenic bacteria. *Proc. Natl. Acad. Sci. U.S.A.* 112, 10756–10761. doi: 10.1073/pnas.1508324112

Andrews, S. C., Robinson, A. K., and Rodríguez-Quiñones, F. (2003). Bacterial iron homeostasis. *FEMS Microbiol. Rev.* 27, 215–237. doi: 10.1016/S0168-6445(03)00055-X

Arai, H. (2011). Regulation and function of versatile aerobic and anaerobic respiratory metabolism in *Pseudomonas aeruginosa*. *Front. Microbiol.* 2:103. doi: 10.3389/fmicb.2011.00103

Arivett, B. A., Fiester, S. E., Ohneck, E. J., Penwell, W. F., Kaufman, C. M., Relich, R. F., et al. (2015). Antimicrobial activity of gallium protoporphyrin IX against *Acinetobacter baumannii* strains displaying different antibiotic resistance phenotypes. *Antimicrob. Agents Chemother.* 59, 7657–7665. doi: 10.1128/AAC.01472-15

Ballouche, M., Cornelis, P., and Baysse, C. (2009). Iron metabolism: a promising target for antibacterial strategies. *Recent Pat. Antiinfect. Drug. Discov.* 4, 190–205. doi: 10.2174/157489109789318514

Banin, E., Lozinski, A., Brady, K. M., Berenshtein, E., Butterfield, P. W., Moshe, M., et al. (2008). The potential of desferrioxamine-gallium as an anti-*Pseudomonas* therapeutic agent. *Proc. Natl. Acad. Sci. U.S.A.* 105, 16761–16766. doi: 10.1073/pnas.0808608105

Bernstein, L. R. (1998). Mechanisms of therapeutic activity for gallium. *Pharmacol. Rev.* 50, 665–682.

Bonchi, C., Frangipani, E., Imperi, F., and Visca, P. (2015). Pyoverdine and proteases affect the response of *Pseudomonas aeruginosa* to gallium in human serum. *Antimicrob. Agents Chemother.* 59, 5641–5646. doi: 10.1128/AAC.01097-15

Bonchi, C., Imperi, F., Minandri, F., Visca, P., and Frangipani, E. (2014). Repurposing of gallium-based drugs for antibacterial therapy. *Biofactors* 40, 303–312. doi: 10.1002/biof.1159

Breidenstein, E. B., de la Fuente-Núñez, C., and Hancock, R. E. (2011). *Pseudomonas aeruginosa*: all roads lead to resistance. *Trends Microbiol.* 19, 419–426. doi: 10.1016/j.tim.2011.04.005

Cartron, M. L., Maddocks, S., Gillingham, P., Craven, C. J., and Andrews, S. C. (2006). Feo-transport of ferrous iron into bacteria. *Biometals* 19, 143–157. doi: 10.1007/s10534-006-0003-2

Chang, D., Garcia, R. A., Akers, K. S., Mende, K., Murray, C. K., Wenke, J. C., et al. (2016). Activity of gallium meso-and protoporphyrin IX against biofilms of multidrug-resistant *Acinetobacter baumannii* isolates. *Pharmaceuticals* 9:16. doi: 10.3390/ph9010016

Comolli, J. C., and Donohue, T. J. (2002). *Pseudomonas aeruginosa* RoxR, a response regulator related to *Rhodobacter sphaeroides* PrrA, activates expression of the cyanide-insensitive terminal oxidase. *Mol. Microbiol.* 45, 755–768. doi: 10.1046/j.1365-2958.2002.03046.x

Comolli, J. C., and Donohue, T. J. (2004). Differences in two *Pseudomonas aeruginosa* cbb_3 cytochrome oxidases. *Mol. Microbiol.* 51, 1193–1203. doi: 10.1046/j.1365-2958.2003.03904.x

Cornelis, P., and Dingemans, J. (2013). *Pseudomonas aeruginosa* adapts its iron uptake strategies in function of the type of infections. *Front. Cell. Infect. Microbiol.* 3:75. doi: 10.3389/fcimb.2013.00075

Cornelis, P., and Matthijs, S. (2002). Diversity of siderophore-mediated iron uptake systems in fluorescent pseudomonads: not only pyoverdines. *Environ. Microbiol.* 4, 787–7898. doi: 10.1046/j.1462-2920.2002.00369.x

Cornelis, P., Matthijs, S., and Van Oeffelen, L. (2009). Iron uptake regulation in *Pseudomonas aeruginosa*. *Biometals* 22, 15–22. doi: 10.1007/s10534-008-9193-0

Cox, C. D., and Adams, P. (1985). Siderophore activity of pyoverdin for *Pseudomonas aeruginosa*. *Infect. Immun.* 48, 130–138.

Cox, C. D., Rinehart, K. L. Jr., Moore, M. L., and Cook, J. C. Jr. (1981). Pyochelin: novel structure of an iron-chelating growth promoter for *Pseudomonas aeruginosa*. *Proc. Natl. Acad. Sci. U.S.A.* 78, 4256–4260.

Cunningham, L., Pitt, M., and Williams, H. D. (1997). The *cioAB* genes from *Pseudomonas aeruginosa* code for a novel cyanide-insensitive terminal oxidase related to the cytochrome *bd* quinol oxidases. *Mol. Microbiol.* 24, 579–591. doi: 10.1046/j.1365-2958.1997.3561728.x

Cunningham, L., and Williams, H. D. (1995). Isolation and characterization of mutants defective in the cyanide-insensitive respiratory pathway of *Pseudomonas aeruginosa*. *J. Microbiol.* 177, 432–438. doi: 10.1128/jb.177.2.432-438.1995

Davies, J. C., Alton, E. W., and Bush, A. (2007). Cystic fibrosis. *BMJ* 335, 1255–1259. doi: 10.1136/bmj.39391.713229.AD

Eschbach, M., Schreiber, K., Trunk, K., Buer, J., Jahn, D., Schobert, M., et al. (2004). Long-term anaerobic survival of the opportunistic pathogen *Pseudomonas aeruginosa* via pyruvate fermentation. *J. Bacteriol.* 186, 4596–4604. doi: 10.1128/JB.186.14.4596-4604.2004

Filip, C., Fletcher, G., Wulff, J. L., and Earhart, C. F. (1973). Solubilization of the cytoplasmic membrane of *Escherichia coli* by the ionic detergent sodium-lauryl sarcosinate. *J. Bacteriol.* 115, 717–722.

Foley, T. L., and Simeonov, A. (2012). Targeting iron assimilation to develop new antibacterials. *Expert Opin. Drug. Discov.* 7, 831–847. doi: 10.1517/17460441.2012.708335

Frangipani, E., Bonchi, C., Minandri, F., Imperi, F., and Visca, P. (2014). Pyochelin potentiates the inhibitory activity of gallium on *Pseudomonas aeruginosa*. *Antimicrob. Agents Chemother.* 58, 5572–5575. doi: 10.1128/AAC.03154-14

Frangipani, E., and Haas, D. (2009). Copper acquisition by the SenC protein regulates aerobic respiration in *Pseudomonas aeruginosa* PAO1. *FEMS Microbiol.* 298, 234–240. doi: 10.1111/j.1574-6968.2009.01726.x

Frangipani, E., Slaveykova, V. I., Reimmann, C., and Haas, D. (2008). Adaptation of aerobically growing *Pseudomonas aeruginosa* to copper starvation. *J. Bacteriol.* 190, 6706–6717. doi: 10.1128/JB.00450-08

Fujiwara, T., Fukumori, Y., and Yamanaka, T. (1992). A novel terminal oxidase, cytochrome baa_3 purified from aerobically grown *Pseudomonas aeruginosa*: it shows a clear difference between resting state and pulsed state. *J. Biochem.* 112, 290–298.

García-Contreras, R., Lira-Silva, E., Jasso-Chávez, R., Hernández-González, I. L., Maeda, T., Hashimoto, T., et al. (2013). Isolation and characterization of gallium resistant *Pseudomonas aeruginosa* mutants. *Int. J. Med. Microbiol.* 303, 574–582. doi: 10.1016/j.ijmm.2013.07.009

Hammer, N. D., Reniere, M. L., Cassat, J. E., Zhang, Y., Hirsch, A. O., Hood, M. I., et al. (2013). Two heme-dependent terminal oxidases power *Staphylococcus aureus* organ-specific colonization of the vertebrate host. *MBio* 4, e00241–e00213. doi: 10.1128/mBio.00241-13

Heinrichs, D. E., Young, L., and Poole, K. (1991). Pyochelin-mediated iron transport in *Pseudomonas aeruginosa*: involvement of a high-molecular-mass outer membrane protein. *Infect. Immun.* 59, 3680–3684.

Hogardt, M., and Heesemann, J. (2010). Adaptation of *Pseudomonas aeruginosa* during persistence in the cystic fibrosis lung. *Int. J. Med. Microbiol.* 300, 557–562. doi: 10.1016/j.ijmm.2010.08.008

Hurdle, J. G., O'Neill, A. J., Chopra, I., and Lee, R. E. (2011). Targeting bacterial membrane function: an underexploited mechanism for treating persistent infections. *Nat. Rev. Microbiol.* 9, 62–75. doi: 10.1038/nrmicro2474

Imperi, F., Massai, F., Facchini, M., Frangipani, E., Visaggio, D., Leoni, L., et al. (2013). Repurposing the antimycotic drug flucytosine for suppression of *Pseudomonas aeruginosa* pathogenicity. *Proc. Nat1. Acad. Sci. U.S.A.* 110, 7458–7463. doi: 10.1073/pnas.1222706110

Imperi, F., Putignani, L., Tiburzi, F., Ambrosi, C., Cipollone, R., Ascenzi, P., et al. (2008). Membrane-association determinants of the ω-amino acid monooxygenase PvdA, a pyoverdine biosynthetic enzyme from *Pseudomonas aeruginosa*. *Microbiology* 154, 2804–2813. doi: 10.1099/mic.0.2008/018804-0

Kaneko, Y., Thoendel, M., Olakanmi, O., Britigan, B. E., and Singh, P. K. (2007). The transition metal gallium disrupts *P. aeruginosa* iron metabolism and has antimicrobial and antibiofilm activity. *J. Clin. Invest.* 117, 877–888. doi: 10.1172/JCI30783

Kawakami, T., Kuroki, M., Ishii, M., Igarashi, Y., and Arai, H. (2010). Differential expression of multiple terminal oxidases for aerobic respiration in *Pseudomonas aeruginosa*. *Environ. Microbiol.* 12, 1399–1412. doi: 10.1111/j.1462-2920.2009.02109.x

Konings, A. F., Martin, L. W., Sharples, K. J., Roddam, L. F., Latham, R., Reid, D. W., et al. (2013). *Pseudomonas aeruginosa* uses multiple pathways to acquire iron during chronic infection in cystic fibrosis lungs. *Infect. Immun.* 81, 2697–2704. doi: 10.1128/IAI.00418-13

Létoffé, S., Delepelaire, P., and Wandersman, C. (2004). Free and hemophore-bound heme acquisitions through the outer membrane receptor HasR have different requirements for the TonB-ExbB-ExbD complex. *J. Bacteriol.* 186, 4067–4074. doi: 10.1128/JB.186.13.4067-4074.2004

Létoffé, S., Redeker, V., and Wandersman, C. (1998). Isolation and characterization of an extracellular haem-binding protein from *Pseudomonas aeruginosa* that shares function and sequence similarities with the *Serratia marcescens* HasA haemophore. *Mol. Microbiol.* 28, 1223–1234. doi: 10.1046/j.1365-2958.1998.00885.x

Llamas, M. A., Imperi, F., Visca, P., and Lamont, I. L. (2014). Cell-surface signaling in *Pseudomonas*: stress responses, iron transport, and pathogenicity. *FEMS Microbiol. Rev.* 38, 569–597. doi: 10.1111/1574-6976.12078

Marvig, R. L., Damkiær, S., Khademi, S. H., Markussen, T. M., Molin, S., Jelsbak, L., et al. (2014). Within-host evolution of *Pseudomonas aeruginosa* reveals adaptation toward iron acquisition from hemoglobin. *MBio* 5, e00966–e00914. doi: 10.1128/mBio.00966-14

Matsushita, K., Shinagawa, E., Adachi, O., and Ameyama, M. (1982). *o*-Type cytochrome oxidase in the membrane of aerobically grown *Pseudomonas aeruginosa*. *FEBS Lett.* 139, 255–258. doi: 10.1016/0014-5793(82)80864-8

Matsushita, K., Yamada, M., Shinagawa, E., Adachi, O., and Ameyama, M. (1983). Membrane-bound respiratory chain of *Pseudomonas aeruginosa* grown aerobically. A KCN-insensitive alternate oxidase chain and its energetics. *J. Microbiol.* 93, 1137–1144.

Meyer, J. M., and Abdallah, M. A. (1978). The fluorescent pigment of *Pseudomonas fluorescens*: biosynthesis, purification and physicochemical properties. *J. Gen. Microbiol.* 107, 319–328. doi: 10.1099/00221287-107-2-319

Milton, D. L., O'Toole, R., Horstedt, P., and Wolf-Watz, H. (1996). Flagellin A is essential for the virulence of *Vibrio anguillarum*. *J. Bacteriol.* 178, 1310–1319. doi: 10.1128/jb.178.5.1310-1319.1996

Minandri, F., Bonchi, C., Frangipani, E., Imperi, F., and Visca, P. (2014). Promises and failures of gallium as an antibacterial agent. *Future Microbiol.* 9, 379–397. doi: 10.2217/fmb.14.3

Minandri, F., Imperi, F., Frangipani, E., Bonchi, C., Visaggio, D., Facchini, M., et al. (2016). Dissecting the role of iron uptake systems in *Pseudomonas aeruginosa* virulence and airways infection. *Infect. Immun.* 84, 2324–2335. doi: 10.1128/IAI.00098-16

Moore, N. M., and Flaws, M. L. (2011). Antimicrobial resistance mechanisms in *Pseudomonas aeruginosa*. *Clin. Lab. Sci.* 24, 47–51.

Murphy, T. F. (2006). The role of bacteria in airway inflammation in exacerbations of chronic obstructive pulmonary disease. *Curr. Opin. Infect. Dis.* 19, 225–230. doi: 10.1097/01.qco.0000224815.89363.15

Nguyen, A. T., O'Neill, M. J., Watts, A. M., Robson, C. L., Lamont, I. L., Wilks, A., et al. (2014). Adaptation of iron homeostasis pathways by a *Pseudomonas aeruginosa* pyoverdine mutant in the cystic fibrosis lung. *J. Bacteriol.* 196, 2265–2276. doi: 10.1128/JB.01491-14

Ochsner, U. A., Johnson, Z., and Vasil, M. L. (2000). Genetics and regulation of two distinct haem-uptake systems, *phu* and *has*, in *Pseudomonas aeruginosa*. *Microbiology* 146, 185–198. doi: 10.1099/00221287-146-1-185

Pitcher, R. S., and Watmough, N. J. (2004). The bacterial cytochrome cbb_3 oxidases. *Biochim. Biophys. Acta* 1655, 388–399. doi: 10.1016/j.bbabio.2003.09.017

Rangel-Vega, A., Bernstein, L. R., Mandujano Tinoco, E. A., García-Contreras, S. J., and García-Contreras, R. (2015). Drug repurposing as an alternative for the treatment of recalcitrant bacterial infections. *Front. Microbiol.* 6:282. doi: 10.3389/fmicb.2015.00282

Ratledge, C., and Dover, L. G. (2000). Iron metabolism in pathogenic bacteria. *Annu. Rev. Microbiol.* 54, 881–941. doi: 10.1146/annurev.micro.54.1.881

Rossi, M. S., Paquelin, A., Ghigo, J. M., and Wandersman, C. (2003). Haemophore-mediated signal transduction across the bacterial cell envelope in *Serratia marcescens*: the inducer and the transported substrate are different molecules. *Mol. Microbiol.* 48, 1467–1480. doi: 10.1046/j.1365-2958.2003.03516.x

Sambrook, J., Fitsch, E. F., and Maniatis, T. (1989). *Molecular Cloning*: *A Laboratori Manual*, *2nd Edn.* Cold Spring Harbor, NY: Cold Spring Harbor Laboratory.

Schweizer, H. P. (1991). *Escherichia-Pseudomonas* shuttle vectors derived from pUC18/19. *Gene* 97, 109–112. doi: 10.1016/0378-1119(91)90016-5

Simon, R., Priefer, U., and Puhler, A. (1983). A broad host range mobilization system for *in vivo* genetic engineering: transposon mutagenesis in Gram-negative bacteria. *Nat. Biotech.* 1, 784–791. doi: 10.1038/nbt1183-784

Skaar, E. P. (2010). The battle for iron between bacterial pathogens and their vertebrate hosts. *PLoS Pathog.* 6:e1000949. doi: 10.1371/journal.ppat.1000949

Soo, V. W., Kwan, B. W., Quezada, H., Castillo-Juárez, I., Pérez-Eretza, B., García-Contreras, S. J., et al. (2016). Repurposing of anticancer drugs for the treatment of bacterial infections. *Curr. Top. Med. Chem.* doi: 10.2174/1568026616666160930131737. [Epub ahead of print].

Stojiljkovic, I., Kumar, V., and Srinivasan, N. (1999). Non-iron metalloporphyrins: potent antibacterial compounds that exploit haem/Hb uptake systems of pathogenic bacteria. *Mol. Microbiol.* 31, 429–442. doi: 10.1046/j.1365-2958.1999.01175.x

Stover, C. K., Pham, X. Q., Erwin, A. L., Mizoguchi, S. D., Warrener, P., Hickey, M. J., et al. (2000). Complete genome sequence of *Pseudomonas aeruginosa* PAO1, an opportunistic pathogen. *Nature* 406, 959–964. doi: 10.1038/35023079

Vander, W. C., Piérard, A., Kley-Raymann, M., and Haas, D. (1984). *Pseudomonas aeruginosa* mutants affected in anaerobic growth on arginine: evidence for a four-gene cluster encoding the arginine deiminase pathway. *J. Bacteriol.* 160, 928–934.

Visca, P., Bonchi, C., Minandri, F., Frangipani, E., and Imperi, F. (2013). The dual personality of iron chelators: growth inhibitors or promoters? *Antimicrob. Agents Chemother.* 57, 2432–2433. doi: 10.1128/AAC.02529-12

Visca, P., Ciervo, A., Sanfilippo, V., and Orsi, N. (1993). Iron-regulated salicylate synthesis by *Pseudomonas* spp. *J. Gen. Microbiol.* 139, 1995–2001. doi: 10.1099/00221287-139-9-1995

Weinberg, E. D. (2009). Iron availability and infection. *Biochem. Biophys. Acta* 1790, 600–605. doi: 10.1016/j.bbagen.2008.07.002

Williams, H. D., Zlosnik, J. E., and Ryall, B. (2007). Oxygen, cyanide and energy generation in the cystic fibrosis pathogen *Pseudomonas aeruginosa*. *Adv. Microb. Physiol.* 52, 1–71. doi: 10.1016/S0065-2911(06)52001-6

Conflict of Interest Statement: The authors declare that the research was conducted in the absence of any commercial or financial relationships that could be construed as a potential conflict of interest.

frontiers in Cellular and Infection Microbiology

ORIGINAL RESEARCH
published: 19 January 2018
doi: 10.3389/fcimb.2017.00535

Iron Starvation Conditions Upregulate *Ehrlichia ruminantium* Type IV Secretion System, *tr1* Transcription Factor and *map1* Genes Family through the Master Regulatory Protein ErxR

Amal Moumène[1,2,3], *Silvina Gonzalez-Rizzo*[4,5], *Thierry Lefrançois*[1,2], *Nathalie Vachiéry*[1,2] *and Damien F. Meyer*[1,2]*

[1] Centre de Coopération Internationale en Recherche Agronomique Pour le Développement, UMR ASTRE, Petit-Bourg, France, [2] ASTRE, Univ Montpellier, Centre de Coopération Internationale en Recherche Agronomique Pour le Développement, Institut National de la Recherche Agronomique, Montpellier, France, [3] UFR Sciences Exactes et Naturelles, Université des Antilles, Pointe-à-Pitre, France, [4] Institut de Biologie Paris Seine (EPS - IBPS), Sorbonne Universités, UPMC Univ Paris 06, Univ Antilles, Univ Nice Sophia Antipolis, Centre National de la Recherche Scientifique Evolution Paris Seine, Paris, France, [5] Equipe Biologie de la Mangrove, UFR Sciences Exactes et Naturelles, Université des Antilles, Pointe-à-Pitre, France

OPEN ACCESS

Edited by:
Susu M. Zughaier, Emory University, United States

Reviewed by:
Jere W. McBride, University of Texas Medical Branch, United States
David O'Callaghan, Université de Montpellier, France

***Correspondence:**
Damien F. Meyer
damien.meyer@cirad.fr

Received: *19 June 2017*
Accepted: *22 December 2017*
Published: *19 January 2018*

Citation:
Moumène A, Gonzalez-Rizzo S, Lefrançois T, Vachiéry N and Meyer DF (2018) Iron Starvation Conditions Upregulate Ehrlichia ruminantium Type IV Secretion System, tr1 Transcription Factor and map1 Genes Family through the Master Regulatory Protein ErxR. Front. Cell. Infect. Microbiol. 7:535. doi: 10.3389/fcimb.2017.00535

Ehrlichia ruminantium is an obligatory intracellular bacterium that causes heartwater, a fatal disease in ruminants. Due to its intracellular nature, *E. ruminantium* requires a set of specific virulence factors, such as the type IV secretion system (T4SS), and outer membrane proteins (Map proteins) in order to avoid and subvert the host's immune response. Several studies have been conducted to understand the regulation of the T4SS or outer membrane proteins, in *Ehrlichia*, but no integrated approach has been used to understand the regulation of *Ehrlichia* pathogenicity determinants in response to environmental cues. Iron is known to be a key nutrient for bacterial growth both in the environment and within hosts. In this study, we experimentally demonstrated the regulation of *virB*, *map1*, and *tr1* genes by the newly identified master regulator ErxR (for *Ehrlichia ruminantium* expression *r*egulator). We also analyzed the effect of iron depletion on the expression of *erxR* gene, *tr1* transcription factor, T4SS and *map1* genes clusters in *E. ruminantium*. We show that exposure of *E. ruminantium* to iron starvation induces *erxR* and subsequently *tr1*, *virB,* and *map1* genes. Our results reveal tight co-regulation of T4SS and *map1* genes via the ErxR regulatory protein at the transcriptional level, and, for the first time link *map* genes to the virulence function *sensu stricto*, thereby advancing our understanding of *Ehrlichia's* infection process. These results suggest that *Ehrlichia* is able to sense changes in iron concentrations in the environment and to regulate the expression of virulence factors accordingly.

Keywords: *Ehrlichia ruminantium*, master regulator, iron regulation, T4SS, *map* genes, *tr1* transcription factor, environmental cues

INTRODUCTION

Ehrlichia ruminantium, the causal agent of heartwater, a fatal disease of ruminants in sub-Saharan African and other tropical regions, belongs to the *Anaplasmataceae* family and is transmitted by ticks of the genus *Amblyomma* (Dumler et al., 2001; Allsopp, 2010). In the mammalian host, *E. ruminantium* mainly infects brain capillary endothelial cells and replicates inside membrane-bound vacuoles (Zweygarth and Josemans, 2001). *E. ruminantium* has a biphasic developmental cycle in which elementary bodies (EB), the infectious form of the bacterium, first adhere and enter host cells. After internalization, EB differentiate into reticulate bodies (RB), the vegetative and non-infectious form, which divide by binary fission. Within 4–5 days, RB reorganize into EB, which are released from the vacuole by the lysis of the host cell to initiate a new infectious cycle (Moumène and Meyer, 2015).

Intracellular pathogenic bacteria belonging to the *Anaplasmataceae* family such as *Ehrlichia*, use a dedicated system, the type IV secretion system (T4SS), to inject some bacterial proteins, named effectors, to evade the host's immune responses and to hijack host cell processes in order to survive and proliferate in a safe replicative niche (Moumène and Meyer, 2015). T4SS is well conserved in the *Anaplasmataceae* family and several T4SS effectors (T4Es) have been shown to be crucial for the pathogenicity of *Anaplasma phagocytophilum, Anaplasma marginale,* and *Ehrlichia chaffeensis* (as reviewed by Rikihisa, 2010). Little is known about T4SS in *E. ruminantium* and no T4Es have yet been characterized (Collins et al., 2005; Frutos et al., 2007).

In several bacteria, it has been shown that the expression of T4SS is tightly regulated by transcription factors (Li and Carlow, 2012; Martín-Martín et al., 2012). Cheng et al. (2008) showed that the five *virB/D4* genetic loci of *E. chaffeensis* T4SS are co-regulated by the transcription factor EcxR to allow specific expression, depending on the developmental stage of the bacteria (Cheng et al., 2008). Previous studies have also demonstrated developmental regulation of the expression of T4SS components during the intracellular life cycle of *A. phagocytophilum* in human peripheral blood neutrophils (Niu et al., 2006). A *ecxR* ortholog, *apxR*, has been found in several *A. phagocytophilum* strains (Wang et al., 2007a,b). ApxR regulates the expression of the transcription factor *tr1* (Wang et al., 2007b) and of the downstream *p44E* locus (Wang et al., 2007a). Interestingly, the *virB/D4* loci of *A. phagocytophilum*, *E. chaffensis,* and *E. canis* are flanked by genes encoding outer membrane proteins (OMP) belonging to the *p44/msp2* family, which are paralogs of *Ehrlichia ruminantium map1* genes (Dunning Hotopp et al., 2006; Rikihisa, 2011). The exact environmental cues, which stimulate the expression of *apxR* and *ecxR*, are not known.

Considering all these observations, we analyzed the genome of *E. ruminantium* and found an ortholog of *ecxR* and *apxR* in *E. ruminantium*, hereafter termed *erxR,* for the *Ehrlichia ruminantium* expression regulator. Moreover, as we observed in *A. phagocytophilum*, *tr1* is present in *E. ruminantium* upstream of the cluster of *map1* OMPs (Wang et al., 2007b). In *E. ruminantium*, the 16 paralogs of the *map1* multigene family are expressed in bovine endothelial cells and some are preferentially transcribed in the tick or in the mammalian host (van Heerden et al., 2004). However, whether or not ErxR is a regulatory protein, which drives the expression of *tr1* gene, the *map1* genes family, and the *virB/D4* loci in *E. ruminantium* and the triggering stimuli are currently unknown.

Microorganisms have evolved sensory mechanisms to regulate their cellular activities in response to environmental changes. This is particularly true for bacterial pathogens whose expression of virulence factors is tightly regulated in response to host and non-host environments (Hyytiäinen et al., 2003). Thus, the regulation of T4SS in response to host cues enables the efficient use of bacterial resources and facilitates colonization, leading to full infection (Abromaitis et al., 2013). One such environmental signal is iron, which is an essential cofactor in various enzymatic reactions like respiration, DNA replication, oxygen transport, response to oxidative stress, but can be toxic at excessive intracellular concentrations (Andrews et al., 2003). Therefore, iron scavenging from the limited sources of free iron available in the host is a crucial determinant of bacterial pathogenicity (Ratledge and Dover, 2000). Pathogens have evolved several ways to scavenge iron from the host, including the expression of iron acquisition genes in response to low iron concentrations (Brickman et al., 2011; Portier et al., 2014). In Gram negative bacteria, TonB-dependent outer membrane receptors (TBDR) are required to transfer iron chelates and heme into the periplasm under poor iron conditions, with subsequent transport to the cytoplasm (Shultis et al., 2006). Whether Map1 proteins play a similar role in *E. ruminantium's* iron uptake or sensing is currently not known.

In this study, we consequently investigated the effect of the newly identified ErxR protein and iron conditions on the regulation of the *virB/D4*, *tr1* and *map* genes expression in *E. ruminantium*. For the first time in *Ehrlichia,* we identified (i) a master regulatory protein responsible for the coordinated regulation of the expression of *virB/D4, tr1*, and *map* genes, and (ii) one triggering environmental signal i.e., iron depletion, which activates this regulation cascade. Our work also demonstrates that *map* genes share at least one regulatory pathway with genes encoding the T4SS and may therefore be important pathogenicity determinants for iron acquisition or host cell infection.

MATERIALS AND METHODS

Culture Conditions

E. ruminantium Gardel strain (passages 30 to 52) was routinely propagated in bovine aortic endothelial (BAE) cells as previously described (Marcelino et al., 2005). To evaluate the growth characteristics of *E. ruminantium* under iron depletion conditions, the strain was grown in TC25 cm^2 flasks in BHK-21 cell medium supplemented with 2 mM glutamine, 10% heat inactivated fotal bovine serum (FBS), penicillin (100 IU/ml), streptomycin (100 mg/ml). For iron response experiments, the medium was supplemented with iron (100 μM $FeSO_4$) or an iron chelator (100 μM 2,2′-bipyridyl; BPD) as described in Breuer et al. (1995) and Romeo et al. (2001). The cells were kept in a humidified atmosphere supplemented with 5% CO_2 at 37°C.

$FeSO_4$ or 2,2′-bipyridyl was added when 80% cell lysis was observed, at 120 h post-inoculation (hpi). The *E. ruminantium* infected cell monolayer (1 TC25 cm^2 flask) was harvested by trypsinisation 24 h after chemical inoculation. From the 6 ml of infected cell supernatant, a 600 µl sample was collected by centrifugation at 20,000 × g for 10 min. The pellet was stored at −80°C until DNA extraction. The remaining 5,400 µl of infected cells were centrifuged at 20,000 × g for 10 min. The pellet was resuspended in TRIzol reagent (Invitrogen) and stored at −80°C until RNA extraction (Pruneau et al., 2012).

Quantitative Detection of *E. ruminantium*

Genomic DNA was extracted from the 600 µl samples described above using the QIAamp DNA Mini Kit (Qiagen, France). The number of bacteria per sample was quantified by q-PCR, targeting the single copy of *map1* gene encoding a major antigenic protein. The primer sequences are shown in **Supplementary Table 1** (Pruneau et al., 2012). A standard curve was established using gDNA of Gardel serially diluted from 7×10^6 to 7×10^1 copies $\mu L^{-}1$, to determine the number of bacteria per microliter (Pruneau et al., 2012). Four microliters were added to Taqman master mix (Applied Biosystems, France), following the manufacturer's instructions. PCR conditions were as follows: 2 min at 50°C, 10 min at 95°C, and 40 cycles with 15 s at 95°C and 1 min at 60°C.

Relative Gene Expression: RNA Preparation and qRT-PCR

Total RNA was extracted using TRIzol reagent. RNA pellets were dissolved in 100 µl of DEPC water and treated with turboDNAse (Ambion, France). The purity and concentration of the isolated RNA were assessed using a NanoDrop 2000c (Thermo Scientific, France). RNA samples were diluted in RNase-free water to obtain a final concentration of 0.5 µg/µL. RNA samples were reverse-transcribed with the SuperScript VILO cDNA Synthesis Kit (Invitrogen, France), according to the manufacturer's instructions. Quantitative PCR was performed in a 7500 Real-Time PCR System (Applied Biosystems, France) using a Power SYBR Green PCR Master Mix (Applied Biosystems, France) and the primers listed in **Supplementary Table 2**. Reactions were performed in 25 µl volume with 5 ng template cDNA and 5 µM of each primer. The amplification conditions were as follows: 2 min at 50°C, 10 min at 95°C and 40 PCR cycles (30 s at 95°C and 1 min at 60°C). An additional dissociation step of 15 s at 95°C, 20 s at 60°C and 15 s at 95°C was added to assess non-specific amplification. A negative control without cDNA template was included for each primer combination. Amplifications were performed in technical replicates consisting of independent cDNA syntheses derived from the same RNA sample and in three independent biological replicates. The relative expression of *erxR* was calculated by dividing the number of transcripts by the total number of bacteria at each time point. Fold change was then calculated by comparing the relative expression at each time point and the relative expression at 96 hpi, the stationary phase. Ratios were calculated from the number of transcripts and normalized to *recA* as described in Gonzalez-Rizzo et al. (2006).

Identification of Orthologs of EcxR in the *E. ruminantium* Genome

To identify orthologs of *E. chaffeensis ecxR* in the genome of *E. ruminantium*, we used the same strategy as that described in Li and Carlow (2012). The protein sequence of ECH_0795 (YP_507593) was used as a query to search the genome of *E. ruminantium*. Multiple sequence alignment was performed using ClustalW (http://www.ebi.ac.uk/Tools/msa/clustalw2/) (Larkin et al., 2007). Sequence identity values between the two sequences were generated using BlastP. A Helix-Turn-Helix motif was determined using Pfam (https://www.ebi.ac.uk/Tools/hmmer/search/hmmscan) to find domains and motifs present in the protein sequence.

Cloning and Expression of *erxR*

Full-length *erxR* was PCR amplified using the primers listed in **Supplementary Table 2**, and ligated into the *Nde*I and *Xho*I sites of the pET29a(+) vector (Novagen). The resulting plasmid, defined herein as pErxR, was cloned into *E. coli* DH5α (Invitrogen) for amplification, purified using the QIAGEN Plasmid Maxi Kit (Qiagen, France), and cloned into *E. coli* BL21 (DE3) (Invitrogen) for protein expression. Protein expression was induced with 4 mM isopro-pyl-β-D-thiogalactopyranoside (IPTG) in 250 ml terrific broth. The protein then was purified using the Ni-NTA Fast Start Kit (Qiagen, France). ErxR expression was determined by Western blot analysis using anti-His tag antibody (Qiagen, France).

Construction of pUA66-Derived Promoter Plasmids

The pUA66 plasmid was used to analyse promoter activity based on the expression of a green fluorescent protein (GFP). The promoter regions were PCR amplified from the genomic DNA of *Ehrlichia ruminantium* Gardel strain, using the primers listed in **Supplementary Table 2**. Forward and reverse primers contained *Hind*III and *BamH*I restriction sites for cloning into the pET29a(+) plasmid. After cloning in pET29a(+), the promoters were digested with *Xho*I and *BamH*I for directed cloning into the pUA66 plasmid (Castaño-Cerezo et al., 2011). BL21 (DE3) cells were co-transformed with pErxR and each of the GFP reporter constructs, individually. The pET29a(+) vector alone was used as a negative control. Cotransformants were grown in LB medium supplemented with 50 µg/ml kanamycin at 37°C for 2 h, followed by induction with 1 mM IPTG for 4 h. Induced bacteria were visualized as described below.

Microscopy

A 6-µl drop of *E. coli* BL21 (DE3) co-transformed with the pUA66 promoter containing one of the different promoters and the pET29a-erxR plasmid (**Supplementary Table 3**), resuspended in LB growth medium, was spotted onto a Superfrost Plus slide (Fisher Scientific Ltd, UK) and visualized using a Nikon Eclipse 80i epifluorescence microscope (Nikon, France). Fluorescent images were acquired with a Nikon DXM1200F digital camera (Nikon, France), using Nikon ACT-1 software (Nikon, France). Fluorescence intensity was calculated by measuring the area, integrated intensity and mean gray

value of the fluorescent bacteria and the background with ImageJ (National Institute of Health, USA). Corrected total cell fluorescence (CTCF) was calculated using the following formula: integrated density—(area of the cell × mean background readings). The average and statistical differences between the bacteria containing the plasmids with the different promoters and controls were calculated using the CTCF values of all the bacteria in four different fields of view. Images were processed to size, and brightness and contrast were adjusted after the measurements, using Adobe Photoshop cs5 (Adobe Systems Inc., California, USA).

Statistical Analyses

Statistical analyses used Student's *t*-test and a $P < 0.05$ was considered significant.

RESULTS

Identification of One *ecxR* Ortholog in the *E. ruminantium* Genome

We used the *ecxR* sequence (YP_507593.1) from *E. chaffeensis* to search NCBI databases using the BLAST tool. With this approach, we identified ERGA_CDS_03000 (YP_196226.1) in the genome of *E. ruminantium* as the closest ortholog to *ecxR*. The results of the BLAST search revealed a putative conserved domain belonging to the HXT_XRE superfamily of DNA binding proteins (cl17200). We identified a helix-turn-helix structure by comparing it with the structure found in *Wolbachia* (Li and Carlow, 2012) and further confirmed by Pfam (https://www.ebi.ac.uk/Tools/hmmer/search/hmmscan). This protein comprising 124 amino acids has a predicted molecular mass of 14.25 kDa. Alignment of the deduced amino acid sequences of the various orthologs is shown in **Figure 1A**. By homology with ApxR and EcxR, we named this protein *E. ruminantium* expression regulator, ErxR. Comparison of the sequence identities of these proteins revealed a high degree of conservation (82% identity) between EcxR and ErxR. ApxR and ErxR showed 40% identity at the amino acid level. Structural analyses indicated that all orthologs shared a conserved helix-turn-helix domain that may function as a sequence specific DNA binding domain, such as in transcription regulators (Aravind et al., 2005).

Architecture of T4SS and *map1* Genes Clusters of *E. ruminantium*

We compared the genetic arrangement of *E. ruminantium* to that of *E. chaffeensis*. The five *virBD* loci are represented in **Figures 1B,C**. In *E. ruminantium*, the genome sequence revealed the presence of two major operons. *virD4*, *virB11*, *virB10*, *virB9a*, and *virB8a* were located in operon 1. Operon 2 was seen to be located in the negative strand and contained four copies of *virB6*, along with one copy of *virB4a* and *virB3,* all located downstream of *sodB*. Four duplicated versions of *virB2* were also located upstream of *virB4b*, while copies of *virB8* and *virB9* (namely *virBb8* and *virB9b*) were scattered along the genome. We also present the arrangement of the *map1* gene family previously reported by Postigo et al. (2007) (**Figure 1C**).

Analysis of *erxR* Expression during the Life Cycle of *E. ruminantium*

To determine the relative expression of *erxR* throughout the developmental cycle of *E. ruminantium*, *erxR* mRNA expression was analyzed by qRT-PCR. Compared to 96 hpi, the expression of *erxR* decreased at 24, 48, and 72 hpi, and peaked at 120 hpi, having increased 4 fold (**Figure 2A**), which corresponds to the time of lysis (early time point in the following round of infection). Data from previous independent microarray experiments (Pruneau et al., 2012) also demonstrated that the maximal expression of *erxR* in the post-exponential growth phase is significant and reproducible (data not shown). These results suggest that the up-regulation expression of *erxR* correlates with early stages in the development cycle *in vitro* before the bacteria enter the host cell.

rErxR Activates *gfp* Reporter Fusions

The promoter regions (hatched boxes in **Figure 1**) for *virBD* genes, *map1, tr1,* and *erxR* were cloned into a *gfp* reporter plasmid and transformed into *E. coli* BL21 (DE3) carrying pErxR or an empty pET29a(+) vector to investigate if ErxR regulatory protein drove their expression. The *virB3-gfp* reporter constructs presented a significant increase in fluorescence intensity after IPTG induction (270,000 units of fluorescence intensity) compared to samples lacking IPTG (10,000 units of fluorescence) or compared to the control (50,000 units of fluorescence) (**Figure 2B**). Similarly, the reporter construct showed an induction of *virB2a* by the recombinant ErxR protein. Activation was also observed for *tr1* (200,000 units), *erxR* promoter (250,000), and *map1* promoter (∼45,000) (**Figure 2B**). Western blot experiments confirmed that the expression of ErxR (14 kDa band) was only detected following induction with IPTG (**Figure 3**).

The Expression of T4SS, *erxR*, *tr1,* and *map* Genes Is Induced by Iron Depletion in *E. ruminantium*

As iron uptake mechanisms are closely associated with bacterial pathogenesis and may be connected to the expression of certain virulence determinants in *E. ruminantium,* we investigated the expression of T4SS, *tr1* and *map* genes clusters in response to iron starvation. We incubated the bacteria in media containing iron or an iron chelator (BPD) for 24 h after lysis. The five T4SS transcription units of *E. ruminantium* were significantly up-regulated under iron depletion (25 to 190 fold increase as shown for *virB3*, *virB4a*, *virB4b*, *virB8a*, *virB8b*, and *virB9b*) (**Figure 4A**). *virB2a* was the only gene that did not present a significant change in expression (**Figure 4A**). Moreover, the *erxR* gene was up-regulated 25 fold during iron starvation (**Figure 4B**). We tested the expression of the *map1* gene cluster under iron starvation in the two genes at the border of the cluster (*tr1* and *map1+1*) as well as in the archetypal *map1* and *map1-6, which* are located in a central position in the cluster. Culture under iron limitation strongly increased the expression of all genes (**Figure 4C**), however *map1+1* showed the highest change in expression with 400-fold up-regulation (**Figure 4C**),

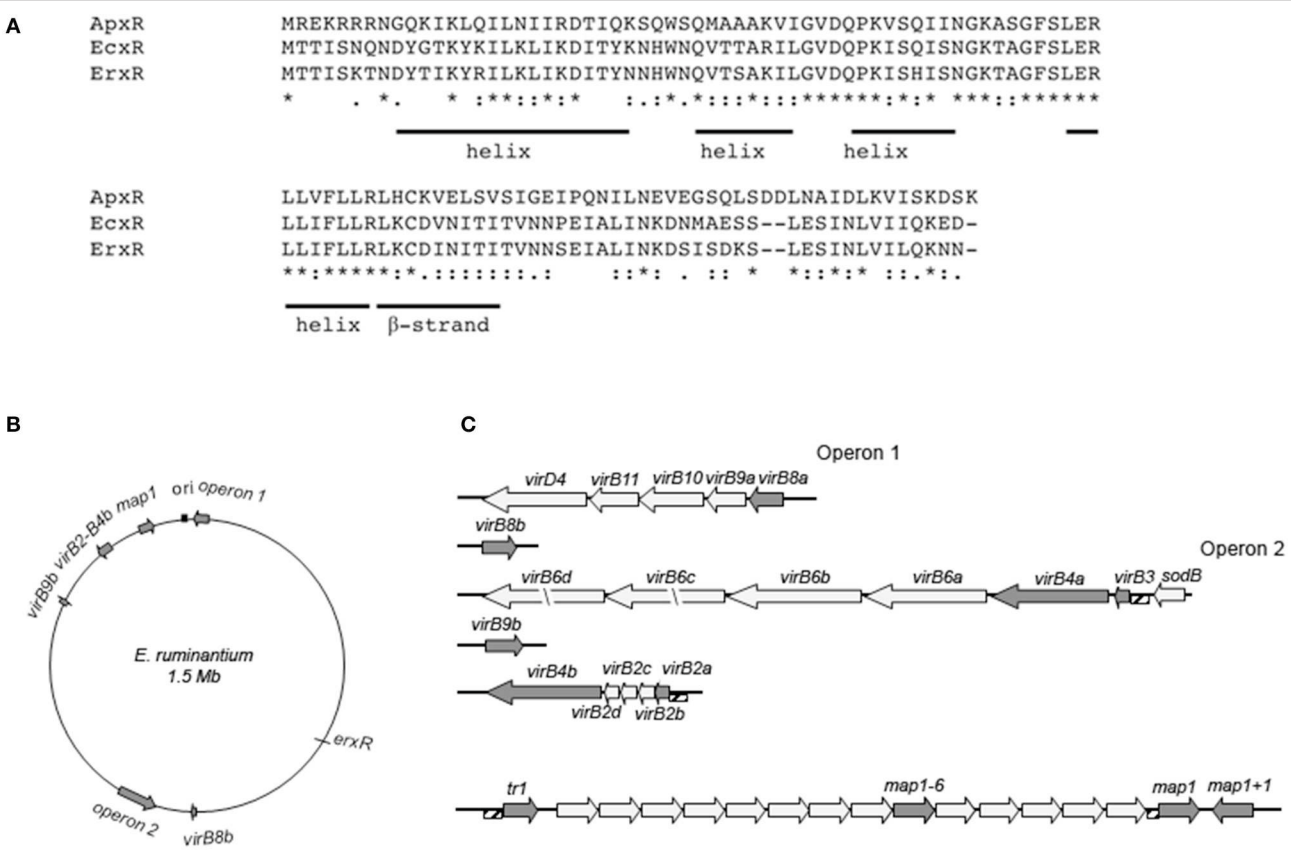

FIGURE 1 | Potential ortholog of the *Ehrlichia* type IV secretion system regulator EcxR in *E. ruminantium* and organization of *virBD* loci and *map1* cluster. **(A)** Amino acid alignment of EcxR and its orthologs from *E. ruminantium* (ERGA_CDS_03000) and *A. phagocytophilum* (ApxR). Identical and conserved residues are indicated by stars and dots, respectively. The positions of amino acids predicted to form a helix structure and beta-strand are shown. **(B)** The genomic map of *E. ruminantium* is represented by a circle. The origin of replication (ori) is indicated by a black box. Gray arrows show the *virBD* gene loci and cluster *map1*. T4SS operon 1 consists in *virB8a, virB9a, virB10, virB11,* and *virD4* and operon 2 consists in *sodB*, *virB3*, *virB4a*, *virB6a*, *virB6b*, *virB6c,* and *virB6d*. Four copies of *virB2* were identified upstream of *virB4b*. *map1* genes belong to a multigenic family organized in one cluster of 16 paralogs located downstream of the transcriptional factor *tr1*. The length of the arrows is proportional to the length of the gene. **(C)** Cluster structure of *virBD* gene loci and *map1* genes. *virBD* and *map1* genes whose expression under iron starvation condition was tested and are represented by gray arrows. The names and length of the genes are indicated above and below the arrows. The upstream regions amplified by PCR for regulation assays (hatched boxes) are indicated.

suggesting that this gene may play a key role during iron starvation.

DISCUSSION

The preferential expression of virulence factors with diverse functions in response to host and environmental cues has already been characterized in several bacteria (Oogai et al., 2011; Weber et al., 2014). Thus, several *Ehrlichia* and other members of the *Anaplasmataceae* family have been shown to differentially express certain genes in response to the host cells (Singu et al., 2006; Nelson et al., 2008).

These genes include genes encoding components of the T4SS, which have been shown to play an essential role in pathogenicity (Rikihisa, 2010; Moumène and Meyer, 2015). Many intracellular bacterial pathogens use T4SS to deliver effector molecules, which subvert the eukaryotic host cell defenses and other cellular processes to their own advantage (Trokter et al., 2014). The genetic arrangement of the 18 genes encoding the T4SS apparatus in *E. ruminantium* T4SS genes resembles that of *E. chaffeensis* (**Figure 1**).

Likewise, OMPs are often regulated by environmental signals and play an important role in bacterial pathogenesis by enhancing the ability of the bacteria to adapt to different environments (Blanvillain et al., 2007). Interestingly, T4SS affects outer membrane properties, which might be important for the adaptation of *Brucella* to growth both *in vitro* and *in vivo* (Wang et al., 2010). Herein, we have described the effects of one environmental cue, iron concentration, on the expression of the transcriptional regulator *erxR*, the components of the T4SS apparatus and members of the Map1 family during *E. ruminantium* infection cycle of BAE cells.

Regulatory proteins are known to play an important role in the survival and persistence of intracellular pathogens in their host (Cheng et al., 2008). EcxR (ECH_0795) is the only transcriptional regulator to be associated with the expression

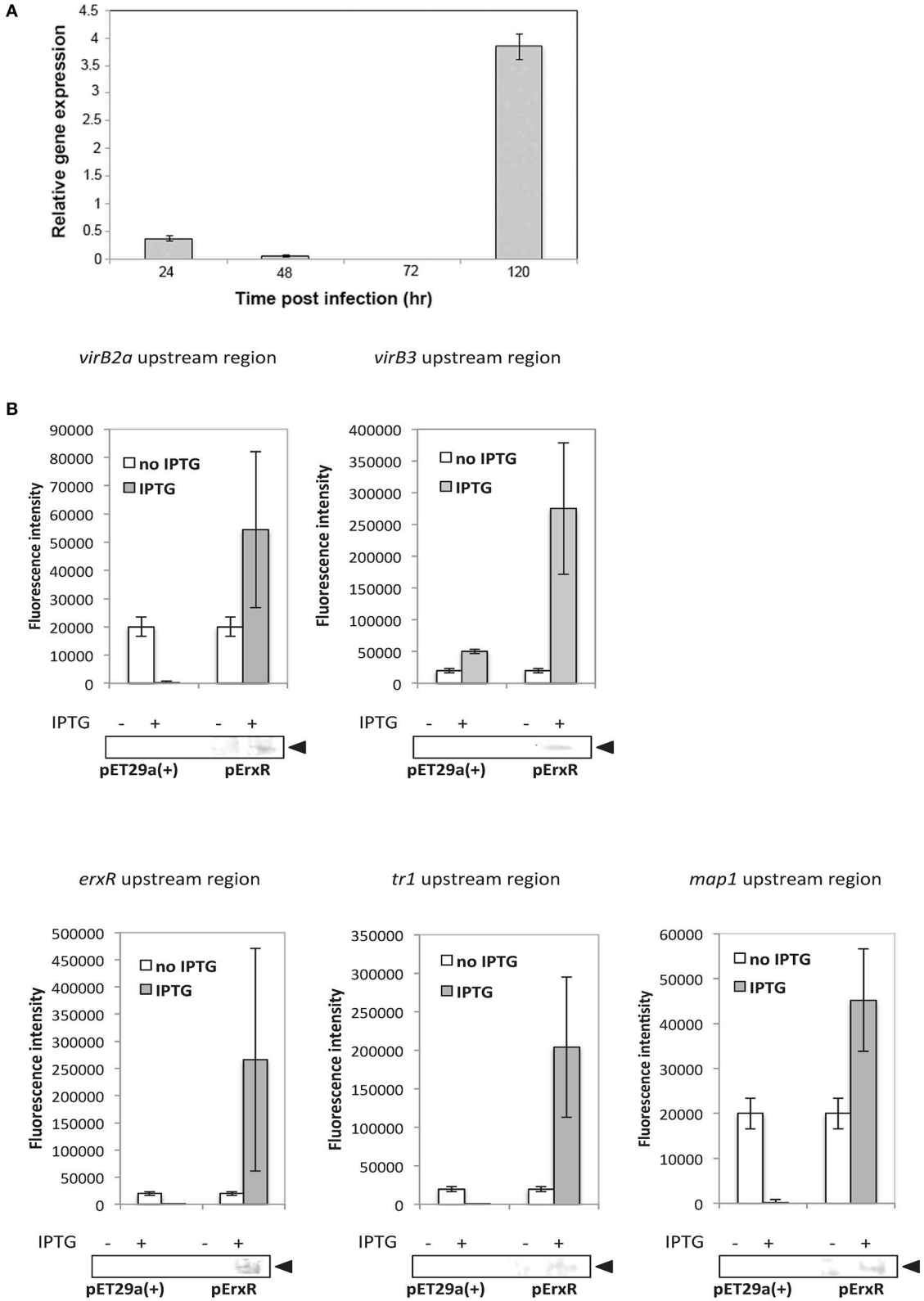

FIGURE 2 | (A) *erxR* expression peaks at 120 hpi in *E. ruminantium*. Quantitative RT-PCR was used to determine the temporal expression of *erxR*. Relative expression at different developmental stages was normalized by dividing the transcripts number by the number of bacteria. Fold differences were evaluated by comparing each

(Continued)

FIGURE 2 | time point to 96 hpi (the stationary phase). Data were obtained from triplicate samples and are expressed as means + standard deviation. **(B)** ErxR activates the transcription of *virBD*, *tr1* and *map* genes. Fluorescence intensity was used to measure the transcriptional activities of *gfp* reporter constructs. The values are means + standard deviations for three specimens, and measurements were taken from four different view fields. An asterisk indicates that values differ significantly ($P < 0.001$) from the controls. Western blot analyses were performed of samples from the fluorescence assays using an anti-His antibody to verify the expression of rErxR. Arrowheads indicate the position of rErxR.

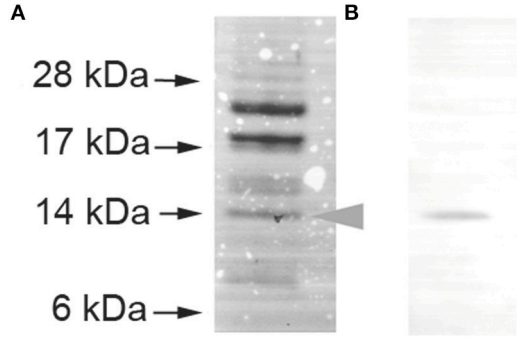

FIGURE 3 | Production of rErxR in *E. coli*. *E. ruminantium erxR* was cloned into the pET29a(+) vector, expressed, and purified using nickel chelate chromatography. The purified protein was subjected to SDS- PAGE analysis, followed by Coomassie blue staining **(A)** and Western blot analysis using an anti-His tag antibody **(B)**. We used pre-stained protein size standards. Each lane contained 8 μg of recombinant protein.

of T4SS components in *E. chaffeensis* (Cheng et al., 2008). In *E. ruminantium,* we identified *erxR,* an orthologous gene of *ecxR* (**Figure 1A**), by sequence homology. ErxR (*Ehrlichia ruminantium expression regulator*) binds and regulates its own promoter and the promoters of some *virBD* genes. These results show that ErxR is the regulatory protein of the T4SS of *E. ruminantium*. Using qRT-PCR at different time points, we also show that *erxR* is strongly expressed at an elementary body stage (120 hpi), like that demonstrated in *E. chaffeensis* (Cheng et al., 2008).

ErxR orthologs in other *Anaplasmataceae* also appear to be associated with the expression of important antigenic OMPs. Thus, ApxR regulates the transcription of *p44* transcription by binding to the *tr1* promoter during *A. phagocytophilum* infection of mammalian host cells (Wang et al., 2007a,b). *p44E* encodes the immunodominant pleomorphic 44-kDa major surface protein, which shows homology with the Map1 family in *E. ruminantium* as well as the P30 family in *E. canis* and the P28 family in *E. chaffeensis* (Dunning Hotopp et al., 2006). The major antigenic protein Map1 is part of a multigene family containing 16 paralogs tandemly organized in a head to tail arrangement that are located downstream of a hypothetical transcriptional regulator gene (*tr1*) (Postigo et al., 2007; **Figure 1C**), a similar arrangement to that reported for *p44, p30,* and *p28* in the other *Anaplasmataceae* (Dunning Hotopp et al., 2006). *tr1* is one of the three promoters identified in the *p44* expression locus and shown to be the strongest promoter driving the expression of a polycistronic mRNA containing OMP1, *p44ESup,* and *p44* (Barbet et al., 2005). *tr1* harbors a winged helix-turn-helix and a DNA binding motif and its part of the xenobiotic response element family of transcriptional regulators. However, the function of *tr1* remains unclear (Nelson et al., 2008), and whether or not *tr1* drives the expression of a polycistronic tandem mRNA containing several *map* homologs is still not known. According to our results, ErxR binds to *tr1* and to *map1* promoters (**Figure 3**). It is thus possible that it regulates the expression of the *map1* members in a similar way to *tr1* in *A. phagocytophilum* for *p44* expression.

Taken together, our results show that ErxR binds to *tr1*, *map1,* and *virBD* promoters, suggesting for the first time coordinated regulation of T4SS and OMP in *Anaplasmataceae*. Interestingly, in the endosymbiotic bacterium *Wolbachia* (wBm) wBmxR1 and wBmxR2, which are orthologs of ErxR, have been shown to co-regulate genes of the T4SS and riboflavin biosynthesis pathway (Li and Carlow, 2012). Riboflavin is an important co-factor for the survival of the endosymbiont's host, the filarial parasite *Brugia malayi* (Li and Carlow, 2012).

Next, we investigated whether the regulation of genes encoding the T4SS and members of the Map1 family by ErxR could be triggered by environmental and nutritional cues in the host cell. Our transcriptional analysis showed that *erxR, virBD, tr1,* and *map1* genes were upregulated in response to iron starvation (**Figure 4**). Interestingly, the fact that *virB2a* is not expressed under iron depletion could be due to a functional redundancy depending on the environment (*e.g.* mammalian host, vector cell, etc.) as previously shown for PopF1 and PopF2 proteins of the T3SS of *Ralstonia solanacearum* (Meyer et al., 2006). Similarly, *A. phagocytophilum* appears to express specific *virB2* paralogs in a host cell dependent manner as well as differential expression of *virB2* gene in tick cells or in human cells (Nelson et al., 2008). Many bacterial pathogens sense iron depletion as a signal indicating that they are within a vertebrate host (Skaar, 2010).

Although the sensing mechanisms of changes in iron concentration are not known in *E. ruminantium,* three pathways are possible. One possibility is that the regulator ErxR is activated by an unidentified sensor kinase which responds to this environmental signal and up-regulates expression of the T4SS genes and certain *map1* genes in response to iron starvation (**Figure 5**). Sensor kinases are part of two component systems (TCS), which regulate the differential expression of genes in bacteria in response to environmental cues. Three TCS composed of three response regulators and three sensor kinases have been identified in *A. phagocytophilum* and *E. chaffeensis* (Cheng et al., 2006). All three sets of TCS have orthologs in *E. ruminantium* and one of these TCS could thus be involved in the regulation of pathogenic factors in response to changes in iron abundance.

Another possibility is the presence of an unknown Fur repressor in the *Anaplasmataceae* family. This sensing involves transcriptional control mediated by the transcriptional repressor,

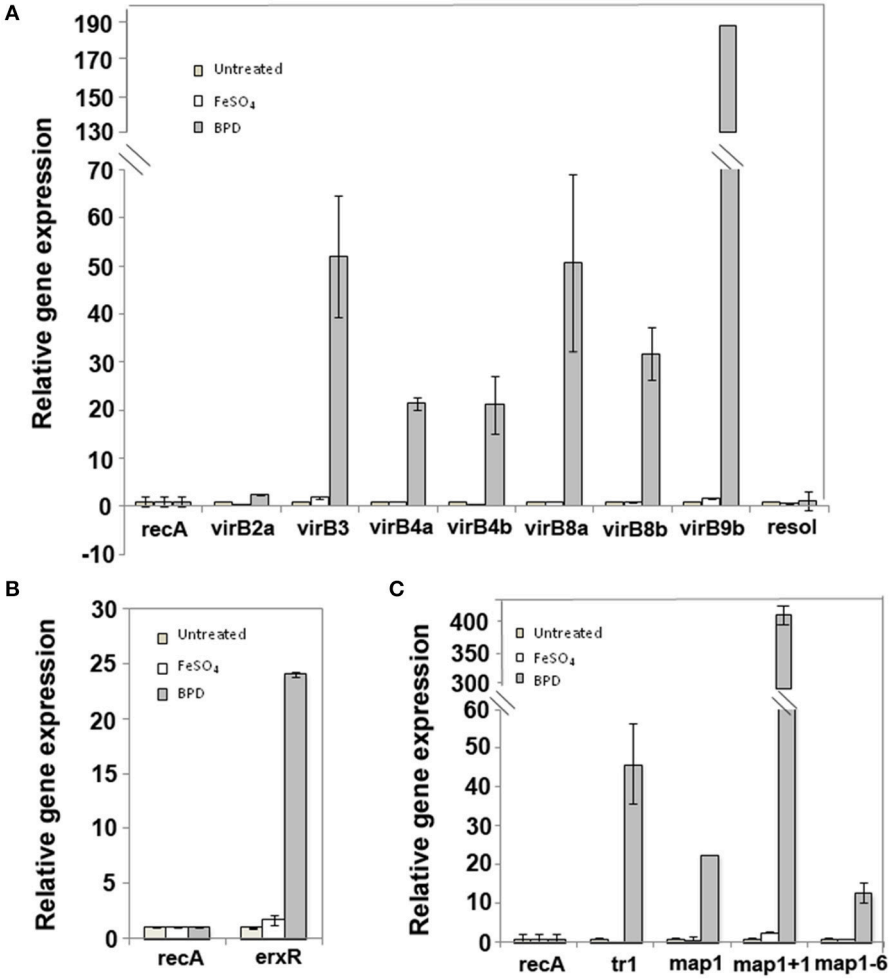

FIGURE 4 | *virBD*, *tr1* and *map* genes as well as *erxR* are up-regulated under iron-depletion. The expression of the *virB* **(A)**, *erxR* **(B)**, *tr1* and *map1* **(C)** genes were measured during the lysis phase of infection under iron repletion or iron depletion using quantitative real-time PCR. The data represent the mean + SD of 2 or 3 biological replicates, each of which comprised 3 technical replicates. Ratios were calculated from the transcript numbers and normalized to *recA*. The *resol* gene was used as negative control.

Fur (Escolar et al., 1998). But many organisms, including *E. coli*, *Campylobacter jejuni*, and *Vibrio cholera*, have been shown to use Fur to negatively regulate gene expression with increasing concentrations of iron (O'Sullivan et al., 1994; Palyada et al., 2004; Mey et al., 2005). For example, Fur activates *sodB*, an iron superoxide dismutase, under iron repletion. SODs are metalloproteins, which play an important role in protection against oxidative stress by catalyzing dismutation of the superoxide radical (O_2^-). Interestingly, in *E. ruminantium*, *sodB* is located upstream of operon 2 of the T4SS and is co-transcribed along these genes in *Ehrlichia* and *Anaplasma*, suggesting an effect of iron in the expression of *virBD* genes. Moreover, it has been demonstrated that the regulator ApxR binds to the promoter regions upstream of *sodB* (Wang et al., 2007b). We searched for putative Fur boxes in the genome of *E. ruminantium* and found one located upstream of *erxR* (**Supplementary Figure 1**). The 19 bp sequence consisted in two repeated hexamers (nATWAT) flanking a 7 nt sequence, which is commonly found upstream of iron regulated enzymes such as succinate dehydrogenase iron-sulfur subunits, major ferric iron binding protein precursors, and adenosine tRNA methylthiotransferase (Escolar et al., 1998; Grifantini et al., 2003). Thus, it is possible that *E. ruminantium* is capable of sensing low iron concentrations in the environment and of regulating the expression of *ErxR* through this putative Fur box.

Finally, it is possible that some Map1 proteins play a role like that of TBDRs in the perception of environmental cues and in iron uptake (Blanvillain et al., 2007). As mentioned above, Map1 proteins are orthologs of members of the *p28* family in *E. chaffeensis*, which have been shown to function as porins and possibly act in nutrient uptake during intracellular infection (Kumagai et al., 2008). It has been shown that porins, such as OmpA and OmpC, bind to transferrin and act in iron uptake in

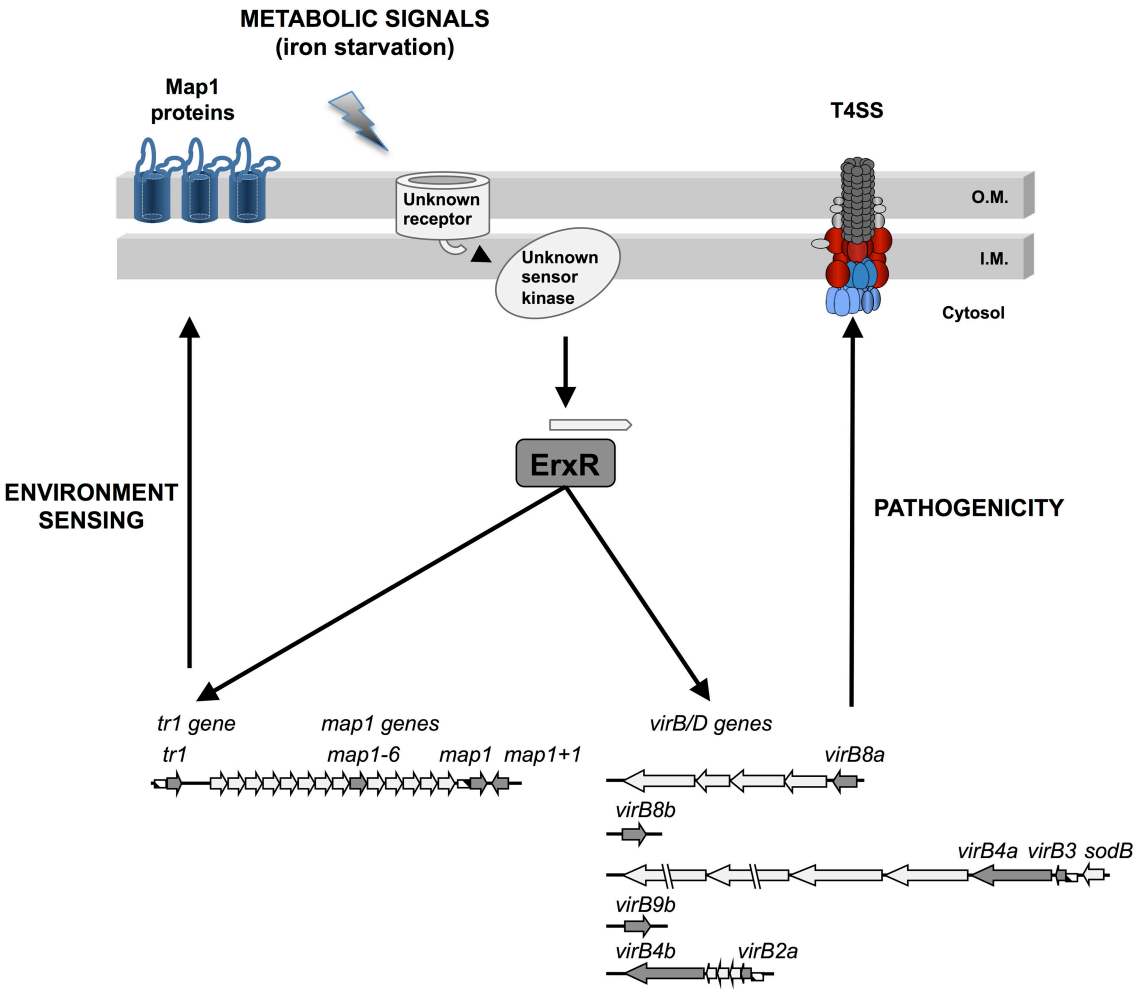

FIGURE 5 | Putative regulation model for ErxR, *virBD*, *tr1* and *map* genes in *E. ruminantium* under iron starvation conditions.

the enteropathogenic strains of *E. coli, Salmonella typhimurium,* and several *Shigella* species (Sandrini et al., 2013). Similarly, *Mycobacterium smegmatis* is able to acquire ferric ions through members of the Msp family of porins (Jones and Niederweis, 2010). The up-regulation of *map1*, *map1+1,* and *map1-6* showed under iron starvation suggests that these three porins play a role in iron acquisition and raises the possibility that Map1 proteins may also act as sensors, although more evidence is needed before concluding. These results suggest that the Map1 proteins may fulfil several functions during *E. ruminantium* infection. Characterizing these functions could advance our understanding of the adaptation of *E. ruminantium* to its host, as done by Blanvillain et al. (2007).

In conclusion, we have demonstrated that exposure of *E. ruminantium* to iron limitation induces ErxR-dependent expression of the T4SS apparatus and *map1* genes. These findings reveal an important degree of coordination between T4SS and *map1* genes at the transcriptional level and raise the possibility of the involvement of Map proteins in environmental sensing and in the infection process. The data presented herein enables us to propose a model for the regulation of *E. ruminantium* T4SS and *map1* genes in which ErxR acts as a global regulator integrating iron as an important triggering environmental signal (**Figure 5**). Understanding *Ehrlichia* gene regulation in response to environmental signals provides valuable cues for the development of alternative treatments.

AUTHOR CONTRIBUTIONS

DM, Conceived and designed the experiments. AM, SG-R, and DM, Performed the experiments. AM, SG-R, TL, NV, and DM, Analyzed the data. AM and DM, Wrote the paper.

ACKNOWLEDGMENTS

We are grateful to. S. Castaño-Cerezo at the *Universidad de Murcia* for providing pUA66 plasmid. We thank E. Albina for critical reading of the manuscript and A.O. Chavez for technical assistance in the regulation experiments. AM acknowledges

financial support from FEDER grant FED 1/1.4-30305, 2007–2013, "*Risque en santé animale et végétale*" (PhD grant to AM), and from EPIGENESIS RegPot European project (n°315988).

SUPPLEMENTARY MATERIAL

The Supplementary Material for this article can be found online at: https://www.frontiersin.org/articles/10.3389/fcimb.2017.00535/full#supplementary-material

Supplementary Figure 1 (A) | Nucleotide sequence of the predicted *erxR* promoter. The initiation codon of *erxR* is shown in capital letters at the end of the sequence. The sequence in red represents the nATWAT motif. The−35 and−10 boxes of the *erxR* promoter are capitalized. **(B)** The potential *erxR* Fur box is compared with the consensus *E. coli* Fur box. Conserved residues are shown in red.

Supplementary Table 1 | Oligonucleotide primers used for qPCR and qRT-PCR.

Supplementary Table 2 | Oligonucleotide primers used to construct plasmids.

Supplementary Table 3 | Strains and plasmids used in this work.

REFERENCES

Abromaitis, S., Nelson, C. S., Previte, D., Yoon, K. S., Clark, J. M., DeRisi, J. L., et al. (2013). *Bartonella quintana* deploys host and vector temperature-specific transcriptomes. *PLoS ONE* 8:e58773. doi: 10.1371/journal.pone.0058773

Allsopp, B. A. (2010). Natural history of *Ehrlichia ruminantium*. *Vet. Parasitol.* 167, 123–135. doi: 10.1016/j.vetpar.2009.09.014

Andrews, S. C., Robinson, A. K., and Rodríguez-Qui-ones, F. (2003). Bacterial iron homeostasis. *FEMS Microbiol. Rev.* 27, 215–237. doi: 10.1016/S0168-6445(03)00055-X

Aravind, L., Anantharaman, V., Balaji, S., Babu, M. M., and Iyer, L. M. (2005). The many faces of the helix-turn-helix domain: transcription regulation and beyond. *FEMS Microbiol. Rev.* 29, 231–262. doi: 10.1016/j.fmrre.2004.12.008

Barbet, A. F., Agnes, J. T., Moreland, A. L., Lundgren, A. M., Alleman, A. R., Noh, S. M., et al. (2005). Identification of functional promoters in the msp2 expression loci of *Anaplasma marginale* and *Anaplasma phagocytophilum*. *Gene* 353, 89–97. doi: 10.1016/j.gene.2005.03.036

Blanvillain, S., Meyer, D., Boulanger, A., Lautier, M., Guynet, C., Denancé, N., et al. (2007). Plant carbohydrate scavenging through tonB-dependent receptors: a feature shared by phytopathogenic and aquatic bacteria. *PLoS ONE* 2:e224. doi: 10.1371/journal.pone.0000224

Breuer, W., Epsztejn, S., and Cabantchik, Z. I. (1995). Iron acquired from transferrin by K562 cells is delivered into a cytoplasmic pool of chelatable iron(II). *J. Biol. Chem.* 270, 24209–24215. doi: 10.1074/jbc.270.41.24209

Brickman, T. J., Cummings, C. A., Liew, S.-Y., Relman, D. A., and Armstrong, S. K. (2011). Transcriptional profiling of the iron starvation response in *Bordetella pertussis* provides new insights into siderophore utilization and virulence gene expression. *J. Bacteriol.* 193, 4798–4812. doi: 10.1128/JB.05136-11

Castaño-Cerezo, S., Bernal, V., Blanco-Catalá, J., Iborra, J. L., and Cánovas, M. (2011). cAMP-CRP co-ordinates the expression of the protein acetylation pathway with central metabolism in *Escherichia coli*. *Mol. Microbiol.* 82, 1110–1128. doi: 10.1111/j.1365-2958.2011.07873.x

Cheng, Z., Kumagai, Y., Lin, M., Zhang, C., and Rikihisa, Y. (2006). Intra-leukocyte expression of two-component systems in *Ehrlichia chaffeensis* and *Anaplasma phagocytophilum* and effects of the histidine kinase inhibitor closantel. *Cell. Microbiol.* 8, 1241–1252. doi: 10.1111/j.1462-5822.2006.00704.x

Cheng, Z., Wang, X., and Rikihisa, Y. (2008). Regulation of type IV secretion apparatus genes during *Ehrlichia chaffeensis* intracellular development by a previously unidentified protein. *J. Bacteriol.* 190, 2096–2105. doi: 10.1128/JB.01813-07

Collins, N. E., Liebenberg, J., de Villiers, E. P., Brayton, K. A., Louw, E., Pretorius, A., et al. (2005). The genome of the heartwater agent *Ehrlichia ruminantium* contains multiple tandem repeats of actively variable copy number. *Proc. Natl. Acad. Sci. U.S.A.* 102, 838–843. doi: 10.1073/pnas.0406633102

Dumler, J. S., Barbet, A. F., Bekker, C. P., Dasch, G. A., Palmer, G. H., Ray, S. C., et al. (2001). Reorganization of genera in the families Rickettsiaceae and Anaplasmataceae in the order Rickettsiales: unification of some species of Ehrlichia with Anaplasma, Cowdria with Ehrlichia and Ehrlichia with Neorickettsia, descriptions of six new species combinations and designation of Ehrlichia equi and "HGE agent" as subjective synonyms of *Ehrlichia phagocytophila*. *Int. J. Syst. Evol. Microbiol.* 51, 2145–2165. doi: 10.1099/00207713-51-6-2145

Dunning Hotopp, J. C., Lin, M., Madupu, R., Crabtree, J., Angiuoli, S. V., Eisen, J. A., et al. (2006). Comparative genomics of emerging human ehrlichiosis agents. *PLoS Genet.* 2:e21. doi: 10.1371/journal.pgen.0020021

Escolar, L., Pérez-Martín, J., and de Lorenzo, V. (1998). Binding of the fur (ferric uptake regulator) repressor of *Escherichia coli* to arrays of the GATAAT sequence. *J. Mol. Biol.* 283, 537–547.

Frutos, R., Viari, A., Vachiery, N., Boyer, F., and Martinez, D. (2007). *Ehrlichia ruminantium*: genomic and evolutionary features. *Trends Parasitol.* 23, 414–419. doi: 10.1016/j.pt.2007.07.007

Gonzalez-Rizzo, S., Crespi, M., and Frugier, F. (2006). The *Medicago truncatula* CRE1 cytokinin receptor regulates lateral root development and early symbiotic interaction with *Sinorhizobium meliloti*. *Plant Cell* 18, 2680–2693. doi: 10.1105/tpc.106.043778

Grifantini, R., Sebastian, S., Frigimelica, E., Draghi, M., Bartolini, E., Muzzi, A., et al. (2003). Identification of iron-activated and -repressed Fur-dependent genes by transcriptome analysis of *Neisseria meningitidis* group B. *Proc. Natl. Acad. Sci. U.S.A.* 100, 9542–9547. doi: 10.1073/pnas.1033001100

Hyytiäinen, H., Sjöblom, S., Palomäki, T., Tuikkala, A., and Tapio Palva, E. (2003). The PmrA-PmrB two-component system responding to acidic pH and iron controls virulence in the plant pathogen *Erwinia carotovora* ssp. *carotovora*. *Mol. Microbiol.* 50, 795–807. doi: 10.1046/j.1365-2958.2003.03729.x

Jones, C. M., and Niederweis, M. (2010). Role of porins in iron uptake by *Mycobacterium smegmatis*. *J. Bacteriol.* 192, 6411–6417. doi: 10.1128/JB.00986-10

Kumagai, Y., Huang, H., and Rikihisa, Y. (2008). Expression and porin activity of P28 and OMP-1F during intracellular *Ehrlichia chaffeensis* development. *J. Bacteriol.* 190, 3597–3605. doi: 10.1128/JB.02017-07

Larkin, M. A., Blackshields, G., Brown, N. P., Chenna, R., McGettigan, P. A., McWilliam, H., et al. (2007). Clustal, W., and Clustal X version 2.0. *Bioinformatics* 23, 2947–2948. doi: 10.1093/bioinformatics/btm404

Li, Z., and Carlow, C. K. S. (2012). Characterization of transcription factors that regulate the type IV secretion system and riboflavin biosynthesis in Wolbachia of *Brugia malayi*. *PLoS ONE* 7:e51597. doi: 10.1371/journal.pone.0051597

Marcelino, I., Veríssimo, C., Sousa, M. F. Q., Carrondo, M. J. T., and Alves, P. M. (2005). Characterization of *Ehrlichia ruminantium* replication and release kinetics in endothelial cell cultures. *Vet. Microbiol.* 110, 87–96. doi: 10.1016/j.vetmic.2005.07.012

Martín-Martín, A. I., Sancho, P., de Miguel, M. J., Fernández-Lago, L., and Vizcaíno, N. (2012). Quorum-sensing and BvrR/BvrS regulation, the type IV secretion system, cyclic glucans, and BacA in the virulence of *Brucella ovis*: similarities to and differences from smooth brucellae. *Infect. Immun.* 80, 1783–1793. doi: 10.1128/IAI.06257-11

Mey, A. R., Wyckoff, E. E., Kanukurthy, V., Fisher, C. R., and Payne, S. M. (2005). Iron and fur regulation in *Vibrio cholerae* and the role of fur in virulence. *Infect. Immun.* 73, 8167–8178. doi: 10.1128/IAI.73.12.8167-8178.2005

Meyer, D. F., Cunnac, S., Guéneron, M., Declercq, C., Van Gijsegem, F., Lauber, E., et al. (2006). PopF1 and PopF2, two proteins secreted by the type III protein secretion system of *Ralstonia solanacearum*, are translocators belonging to the HrpF/NopX family. *J. Bacteriol.* 88, 4903–4917 doi: 10.1128/JB.00180-06

Moumène, A., and Meyer, D. F. (2015). Ehrlichia's molecular tricks to manipulate their host cells. *Microbes Infect.* 18, 172–179. doi: 10.1016/j.micinf.2015.11.001

Nelson, C. M., Herron, M. J., Felsheim, R. F., Schloeder, B. R., Grindle, S. M., Chavez, A. O., et al. (2008). Whole genome transcription profiling of *Anaplasma phagocytophilum* in human and tick host cells by tiling array analysis. *BMC Genomics* 9:364. doi: 10.1186/1471-2164-9-364

Niu, H., Rikihisa, Y., Yamaguchi, M., and Ohashi, N. (2006). Differential expression of VirB9 and VirB6 during the life cycle of *Anaplasma phagocytophilum* in human leucocytes is associated with differential binding and avoidance of lysosome pathway. *Cell. Microbiol.* 8, 523–534. doi: 10.1111/j.1462-5822.2005.00643.x

Oogai, Y., Matsuo, M., Hashimoto, M., Kato, F., Sugai, M., and Komatsuzawa, H. (2011). Expression of virulence factors by *Staphylococcus aureus* grown in serum. *Appl. Environ. Microbiol.* 77, 8097–8105. doi: 10.1128/AEM.05316-11

O'Sullivan, D. J., Dowling, D. N., deLorenzo, V., and O'Gara, F. (1994). *Escherichia coli* ferric uptake regulator (Fur) can mediate regulation of a pseudomonad iron-regulated promoter. *FEMS Microbiol. Lett.* 117, 327–332. doi: 10.1111/j.1574-6968.1994.tb06787.x

Palyada, K., Threadgill, D., and Stintzi, A. (2004). Iron acquisition and regulation in *Campylobacter jejuni*. *J. Bacteriol.* 186, 4714–4729. doi: 10.1128/JB.186.14.4714-4729.2004

Portier, E., Zheng, H., Sahr, T., Burnside, D. M., Mallama, C., Buchrieser, C., et al. (2014). IroT/mavN, a new iron-regulated gene involved in Legionella pneumophila virulence against amoebae and macrophages. *Environ. Microbiol.* 17, 1338–13350. doi: 10.1111/1462-2920.12604

Postigo, M., Taoufik, A., Bell-Sakyi, L., de Vries, E., Morrison, W. I., and Jongejan, F. (2007). Differential transcription of the major antigenic protein 1 multigene family of *Ehrlichia ruminantium* in *Amblyomma variegatum* ticks. *Vet. Microbiol.* 122, 298–305. doi: 10.1016/j.vetmic.2007.01.019

Pruneau, L., Emboulé, L., Gely, P., Marcelino, I., Mari, B., Pinarello, V., et al. (2012). Global gene expression profiling of *Ehrlichia ruminantium* at different stages of development. *FEMS Immunol. Med. Microbiol.* 64, 66–73. doi: 10.1111/j.1574-695X.2011.00901.x

Ratledge, C., and Dover, L. G. (2000). Iron metabolism in pathogenic bacteria. *Annu. Rev. Microbiol.* 54, 881–941. doi: 10.1146/annurev.micro.54.1.881

Rikihisa, Y. (2010). *Anaplasma phagocytophilum* and *Ehrlichia chaffeensis*: subversive manipulators of host cells. *Nat. Rev. Microbiol.* 8, 328–339. doi: 10.1038/nrmicro2318

Rikihisa, Y. (2011). Mechanisms of obligatory intracellular infection with *Anaplasma phagocytophilum*. *Clin. Microbiol. Rev.* 24, 469–489. doi: 10.1128/CMR.00064-10

Romeo, A. M., Christen, L., Niles, E. G., and Kosman, D. J. (2001). Intracellular chelation of iron by bipyridyl inhibits DNA virus replication: ribonucleotide reductase maturation as a probe of intracellular iron pools. *J. Biol. Chem.* 276, 24301–24308. doi: 10.1074/jbc.M010806200

Sandrini, S., Masania, R., Zia, F., Haigh, R., and Freestone, P. (2013). Role of porin proteins in acquisition of transferrin iron by enteropathogens. *Microbiology* 159, 2639–2650. doi: 10.1099/mic.0.071928-0

Shultis, D. D., Purdy, M. D., Banchs, C. N., and Wiener, M. C. (2006). Outer membrane active transport: structure of the BtuB:TonB complex. *Science* 312, 1396–1399. doi: 10.1126/science.1127694

Singu, V., Peddireddi, L., Sirigireddy, K. R., Cheng, C., Munderloh, U., and Ganta, R. R. (2006). Unique macrophage and tick cell-specific protein expression from the p28/p30-outer membrane protein multigene locus in *Ehrlichia chaffeensis* and *Ehrlichia canis*. *Cell. Microbiol.* 8, 1475–1487. doi: 10.1111/j.1462-5822.2006.00727.x

Skaar, E. P. (2010). The battle for iron between bacterial pathogens and their vertebrate hosts. *PLoS Pathog.* 6:e1000949. doi: 10.1371/journal.ppat.1000949

Trokter, M., Felisberto-Rodrigues, C., Christie, P. J., and Waksman, G. (2014). Recent advances in the structural and molecular biology of type IV secretion systems. *Curr. Opin. Struct. Biol.* 27, 16–23. doi: 10.1016/j.sbi.2014.02.006

van Heerden, H., Collins, N. E., Brayton, K. A., Rademeyer, C., and Allsopp, B. A. (2004). Characterization of a major outer membrane protein multigene family in *Ehrlichia ruminantium*. *Gene* 330, 159–168. doi: 10.1016/j.gene.2004.01.020

Wang, X., Cheng, Z., Zhang, C., Kikuchi, T., and Rikihisa, Y. (2007a). *Anaplasma phagocytophilum* p44 mRNA expression is differentially regulated in mammalian and tick host cells: involvement of the DNA binding protein ApxR. *J. Bacteriol.* 189, 8651–8659. doi: 10.1128/JB.00881-07

Wang, X., Kikuchi, T., and Rikihisa, Y. (2007b). Proteomic identification of a novel *Anaplasma phagocytophilum* DNA binding protein that regulates a putative transcription factor. *J. Bacteriol.* 189, 4880–4886. doi: 10.1128/JB.00318-07

Wang, Y., Chen, Z., Qiao, F., Zhong, Z., Xu, J., Wang, Z., et al. (2010). The type IV secretion system affects the expression of Omp25/Omp31 and the outer membrane properties of *Brucella melitensis*. *FEMS Microbiol. Lett.* 303, 92–100. doi: 10.1111/j.1574-6968.2009.01866.x

Weber, G. G., Kortmann, J., Narberhaus, F., and Klose, K. E. (2014). RNA thermometer controls temperature-dependent virulence factor expression in *Vibrio cholerae*. *Proc. Natl. Acad. Sci. U.S.A.* 111, 14241–14246. doi: 10.1073/pnas.1411570111

Zweygarth, E., and Josemans, A. I. (2001). Continuous *in vitro* propagation of *Cowdria ruminantium* (Welgevonden stock) in a canine macrophage-monocyte cell line. *Onderstepoort J. Vet. Res.* 68, 155–157. Available online at: http://hdl.handle.net/2263/18399

Conflict of Interest Statement: The authors declare that the research was conducted in the absence of any commercial or financial relationships that could be construed as a potential conflict of interest.

frontiers in Cellular and Infection Microbiology

ORIGINAL RESEARCH
published: 25 August 2017
doi: 10.3389/fcimb.2017.00382

The Role of the Regulator Fur in Gene Regulation and Virulence of *Riemerella anatipestifer* Assessed Using an Unmarked Gene Deletion System

Yunqing Guo[1,2], *Di Hu*[1,2], *Jie Guo*[1,2], *Xiaowen Li*[1,2], *Jinyue Guo*[1,2], *Xiliang Wang*[1,2], *Yuncai Xiao*[1,2], *Hui Jin*[1,3], *Mei Liu*[1,2], *Zili Li*[1,2], *Dingren Bi*[1,2,3]* and *Zutao Zhou*[1,2]*

[1] College of Veterinary Medicine, Huazhong Agricultural University, Wuhan, China, [2] Key Lab of Preventive Veterinary Medicine of Hubei Province, Huazhong Agricultural University, Wuhan, China, [3] State Key Laboratory of Agricultural Microbiology, Huazhong Agricultural University, Wuhan, China

OPEN ACCESS

Edited by:
Susu M. Zughaier,
Emory University, United States

Reviewed by:
Teresa Olczak,
University of Wrocław, Poland
Michael Marceau,
Université Lille 2 Droit et Santé, France

***Correspondence:**
Dingren Bi
bidingren@mail.hzau.edu.cn
Zutao Zhou
ztzhou@mail.hzau.edu.cn

Received: 15 May 2017
Accepted: 09 August 2017
Published: 25 August 2017

Citation:
Guo Y, Hu D, Guo J, Li X, Guo J, Wang X, Xiao Y, Jin H, Liu M, Li Z, Bi D and Zhou Z (2017) The Role of the Regulator Fur in Gene Regulation and Virulence of Riemerella anatipestifer Assessed Using an Unmarked Gene Deletion System. Front. Cell. Infect. Microbiol. 7:382. doi: 10.3389/fcimb.2017.00382

Riemerella anatipestifer, an avian pathogen, has resulted in enormous economic losses to the duck industry globally. Notwithstanding, little is known regarding the physiological, pathogenic and virulence mechanisms of *Riemerella anatipestifer* (RA) infection. However, the role of Ferric uptake regulator (Fur) in the virulence of *R. anatipestifer* has not, to date, been demonstrated. Using a genetic approach, unmarked gene deletion system, we evaluated the function of *fur* gene in the virulence of *R. anatipestifer*. For this purpose, we constructed a suicide vector containing *pheS* as a counter selectable marker for unmarked deletion of *fur* gene to investigate its role in the virulence. After successful transformation of the newly constructed vector, a mutant strain was characterized for genes regulated by iron and Fur using RNA-sequencing and a comparison was made between wild type and mutant strains in both iron restricted and enriched conditions. RNA-seq analysis of the mutant strain in a restricted iron environment showed the downregulation and upregulation of genes which were involved in either important metabolic pathways, transport processes, growth or cell membrane synthesis. Electrophoretic mobility shift assay was performed to identify the putative sequences recognized by Fur. The putative Fur-box sequence was 5′-GATAATGATAATCATTATC-3′. Lastly, the median lethal dose and histopathological investigations of animal tissues also illustrated mild pathological lesions produced by the mutant strain as compared to the wild type RA strain, hence showing declined virulence. Conclusively, an unmarked gene deletion system was successfully developed for RA and the role of the *fur* gene in virulence was explored comprehensively.

Keywords: ***Riemerella anatipestifer, fur, pheS,*** **unmarked gene deletion system, virulence, Fur-box, RNA-seq**

INTRODUCTION

Riemerella anatipestifer (*R. anatipestifer*, RA) is non-spore forming, non-motile, Gram-negative, rod-shaped bacterium belonging to the family *Flavobacteriaceae.* Other than ducks, RA can also affect the majority of poultry including turkeys, geese, which has resulted in significant economic losses to the poultry industry worldwide. Infection leads to polyserositis and septicaemia often with neurological symptoms. At least 21 serotypes have been identified in different countries, with serotypes 1, 2, and 10 most prevalent in China (Loh et al., 1992; Cheng et al., 2003). Due to extensive genomic divergences, even within a given serotype, there is often limited cross protection and variation of virulence (Higgins et al., 2000). Presently, little is known regarding RA pathogenesis, although a number of attempts have been made to explore the molecular mechanisms underlying virulence. In previous studies, the role of outer membrane protein A (OmpA), TonB dependent receptor 1 (TbdR1), TonB family protein (TbfA), siderophore interacting protein (Sip) and CAMP cohemolysin have all been proposed as virulence associated factors (Crasta et al., 2002; Hu et al., 2011; Lu et al., 2013; Tu et al., 2014; Liu et al., 2016). All of these studies were based on gene knockout, which result in modified expression of downstream genes, known as the polar effect. As a genetic analysis tool, unmarked gene deletion system is advantageous over gene knockout strategy, as well as able to provide a more accurate estimation of gene expression and has a limited polar effect. Indeed, in many species of bacteria, such as *Enterococcus faecalis*, *Burkholderia* family, *Streptococcus mutans*, *Bacillus amyloliquefaciens,* unmarked gene deletion system has been established to elucidate molecular mechanisms of pathogenesis and virulence (Kristich et al., 2007; Barrett et al., 2008; Xie et al., 2011; Zhou et al., 2016). To the best of our knowledge, no data is available on unmarked gene deletion system in RA. The development and application of such strategies will accelerate our understanding of the mechanism of pathogenesis, virulence and antibiotic resistance in RA.

Earlier studies have established the role of Ferric uptake regulator (Fur) proteins in virulence in a variety of bacterial species (Ernst et al., 2005a; Haraszthy et al., 2006; Yuhara et al., 2008; Porcheron and Dozois, 2015; Pi et al., 2016). Fur is a regulator of transcription in bacteria, involved in iron homeostasis, acid resistance, oxidative stress and virulence (Bijlsma et al., 2002; Ernst et al., 2005b; Mathieu et al., 2016). Iron is an essential element in various metabolic pathways of bacteria and eukaryotic host (Holmes et al., 2005). To date, the function of *fur* gene in virulence of RA has not been demonstrated in any previous study. In this novel study, the role of *fur* gene in virulence of RA has been examined by adopting unmarked gene deletion system. Having observed the limitations of other counter-selectable markers, *pheS* is an appropriate non-antibiotic resistance counter-selectable marker. Previously, the applications of the mutant *E. coli pheS* gene (A294G), the mutant *E. faecalis pheS* gene (A312G), the mutant *Burkholderia pheS* gene (A294G), and the mutant *S. mutans pheS* gene (A314G) were successful for allelic replacement in those organisms (Kast and Hennecke, 1991; Ibba et al., 1994; Kristich et al., 2007; Barrett et al., 2008; Xie et al., 2011). Therefore, we postulated the role of *pheS* gene for this purpose.

In summary, in this study, we engineered a suicide vector pRE-lacZ-mpheS-spc, using mutated *pheS* as a counter-selectable marker and *lacZ* to select a *fur* gene deletion mutant RA-YM Δ*fur*. This is the first successful attempt to construct mutant RA using an unmarked gene deletion system. The RA-YM Δ*fur* complemented strain was constructed to confirm virulence of the wild type strain, compared with the mutant. Lastly, using whole genome transcriptional sequencing, genes regulated by the *fur* gene were screened out in mutant and wild types. Moreover, the predictive sequence of Fur-box of RA was analyzed.

MATERIALS AND METHODS

Bacterial Strains, Plasmids, Media, and Growth Conditions

The bacterial strains and plasmids used in this study, and their relevant characteristics are described in **Table 1**. *R. anatipestifer* strains were grown at 37°C in tryptic soy broth (TSB) (Difco, Detroit, USA) in an atmosphere of 5% CO_2, *E. coli* strains were cultured at 37°C in Luria Bertani broth (Sigma-Aldrich, St. Louis, USA). Both *R. anatipestifer* strains and *E. coli* strains included in this study were obtained from laboratory stocks of the Department of Veterinary Microbiology and Immunology of Huazhong Agricultural University, China. Where necessary, the following antibiotics were added in to the selection media: ampicillin (Amp), 100 mg/mL; spectinomycin (Spc), 100 mg/mL; kanamycin (Kan), 100 mg/mL; and medium was supplemented with 2, 6-diaminopimelic acid (DAP), 100 mg/mL; 5-bromo-4-chloro-3-indolyl β-D-galactopyranoside (X-gal), 20 mg/mL; Isopropyl β-D-1-thiogalactopyranoside (IPTG), 20 mg/mL; 4-chloro-DL-phenylalanine (cPhe), 0.2% (w/v).

Construction of Suicide Vector pRE-lacZ-mpheS-spc and Complemented Shuttle Vector pRES-JXrep-spc

For the construction of suicide vector pRE-lacZ-mpheS-spc, a 3.9 kb fragment of pRE was amplified from suicide vector pRE112 using primer S1L (**Table 1**) (introducing *BamH*I, *Sal*I, and *Nde*I site) and S2R (**Table 1**) (introducing *Xho*I and *BamH*I site); then digested with *BamH*I enzyme and ligated to generate circular pRE which contained the essential components of the conjugational transfer. As RA cannot catabolize sucrose, the selected marker *SacB* was removed. The mutated *pheS* gene (*mpheS*) and the sequence of the multiple cloning sites were engineered into pUC57 to generate pUC57-mpheS and pUC57-MCS by the GenScript Corporation (Nanjing, China). This pUC57-mpheS vector contained the mutated *R. anatipestifer pheS* gene with altered DNA sequences (Supplemental Figure 1), which was driven by an upstream PS12 promoter of the *R. anatipestifer rpsL* gene. The 1.1 kb *spc* cassette was amplified from plasmid pIC333 using primers spcL and spcR (**Table 1**), *mpheS* was amplified from plasmid pUC57-mpheS using primers pheS1and pheS2 (**Table 1**). The *spc* cassette was then fused with the *mpheS* fragment using overlap PCR (introducing

TABLE 1 | Strains, plasmids and primers.

Strains or plasmids	Description	PCR product	Reference
STRAINS			
RA-YM	*Riemerella anatipestifer* wild-type strain, serotype 1		This study
RA-JX	*Riemerella anatipestifer* strain, serotype 1		
RAYM Δ*fur*	*fur* gene deletion mutant of RA-YM strain		This study
RAYM Δ*fur* (pRES-JXrep-spc-fur)	Complemented RA-YM Δ*fur* strain		This study
PLASMIDS			
pRE112	*SacB*,Cm^R		This study
pRE-lacZ-mpheS-spc	Cm^R,Spc		This study
pRES-JXrep-spc	Cm^R,Spc		This study
PRIMERS FOR CONSTRUCTION OF VECTOR pRE-lacZ-mpheS-spc			
S1L	5′-AGGATCCTGTCGACCATATGTCCTAACCTTTTGGTAATG-3′		This study
S1R	5′- AGGAAATTACAGATCTGAGGGGACAGGCGAGAGACGAT-3′		This study
S2L	5′- CTCAGATCTGTAATTTCCTGCATTTGCCTGT-3′		This study
S2R	5′-AGGATCCACTCGAGTCTATCTGTTTCTTTTCATTCTCTG-3′		This study
PrpsLF	5′- GGGGTACCACTTTATCCATTTATAAAACTACATCA-3′	rpsL Promoter	This study
PrpsLR	5′-ATCAATATACTCTAACATTTAATTGCTTTTATTTATTTTTAGTTTC-3′		This study
phesF	5′-GAAACTAAAAATAAATAAAAGCAATTAAATGTTAGAGTATATTGAT-3′	*mpheS* gene	This study
phesR	5′-TCTATAGTCAAAAGGATACCCATTAAAAATAAAAAAGGAAACT-3′		This study
spcL	5′-ATTTTTAATGGGTATCCTTTTGACTATAGAGGATCGATCT-3′	*spc* gene	This study
spcR	5′-GCTCTAGACAGTAGTTTTAAAAGTAAGCACCTG-3′		This study
rpsL-lacZ	5′-TCTCGAGAACTTTATCCATTTATAAAACTACATCA-3′	rpsL Promoter	This study
rpsR-LacZ	5′-ATCCGTAATCATGGTCATTTAATTGCTTTTATTTATTTTTAGTTTC-3′		This study
lacZL	5′-CTAAAAATAAATAAAAGCAATTAAATGACCATGATTACGGATTCA-3′	*lacZ* gene	This study
lacZR	5′-CGGGATCCATCCAAAAGTTTGTGTTTTTTAAATAGT-3′		This study
PRIMERS FOR CONSTRUCTION OF THE COMPLEMENTED SHUTTLE PLASMID pRES-JXrep-spc			
rep1	5′-CCCTCGAGAATGCTTTGTGTTCCTCCCTTGTCA-3′	Replicon and replicase gene	This study
rep2	5′-GTTTTCGTTCCACTGAACTTTAGGATTGTCTGCTTGCGCT-3′		This study
spcL1	5′-GACAATCCTAAAGTTCAGTGGAACGAAAACTCACGTT-3′	*spc* gene	This study
spcR1	5′-CGGGATCCCAGTAGTTTTAAAAGTAAGCACCTG-3′		This study
PRIMERS FOR CONSTRUCTION OF THE MUTANT Δ*fur* AND THE COMPLEMENTED STRAIN			
Fur-L1	5′-CATGCATGCTTGGATTACGGTAGTTCTTGCTG-3′	Upstream of *fur*	This study
Fur-L2	5′-GTATAATTAGCCTCATAGGTACTATTATTTTCTAGATTTA-3′		This study
Fur-R1	5′-AAAATAATAGTACCTATGAGGCTAATTATACTCGTACTAAT-3′	Downstream of *fur* gene	This study
Fur-R2	5′-GGGGTACCATGGTTTCTCCCGTGAGGACTTT-3′		This study
Promoter-fur1	5′- GGGGTACC ATAAAGTAATATTGCTATATTTA-3′	promoter of*fur* gene	This study
Promoter-fur2	5′- GAGAACTACAAGGTA ATATTAAAAACTTAATTTTTA-3′		This study
Fur-inL	5′- TTAAGTTTTTAATATTACCTTGTAGTTCTCTTTCTATA-3′	Coding sequence of *fur* gene	This study
Fur-inR	5′- CATGCATGCAATAGCAAAAAATACTGGCAT-3′		This study
PRIMERS FOR RT-PCR			
03924L	5′-GAAATACACGCTGATAGATGGTT-3′	*RAYM_03924*	This study
03924R	5′-TACCGTGGGCGTTATCATCTTCA-3′		This study
09824L	5′-TCCAAGTAGGCAACCAACGAGTC-3′	*RAYM_09824*	This study
09824R	5′-TGATGACAAGGCAGGACCGAGGG-3′		This study
09774L	5′-ATGTCCACCTCCAACTTATCTTC-3′	*RAYM_09774*	This study
09774R	5′-GGTTATCATCTTTCCGTCCACTT-3′		This study
00365L	5′-TTTTGACCATATTAGCGAACCTAC-3′	*RAYM_00365*	This study
00365R	5′-TTGATGCTACAATCCGTATGCTC-3′		This study
04506L	5′-TATCATCGTTCCCAAGGAGGTTT-3′	*RAYM_04506*	This study
04506R	5′-TCAAACGAAGGGAGCGAGGTCAT-3′		This study
00965L	5′-CGTCTGTAGTGATGAGGGTTTGA-3′	*RAYM_00965*	This study

(Continued)

TABLE 1 | Continued

Strains or plasmids	Description	PCR product	Reference
00965R	5′-CTATGTATTTGGCTTTATCCCTTC-3′		This study
01847L	5′-CGTTACTTATCATCGGAACTGGA-3′	*RAYM_01847*	This study
01847R	5′-AGCCAGCATTTCGTTAGAGTTAT-3′		This study
06180L	5′-GAGTGCCTACCACCGAATA-3′	*RAYM_06180*	This study
06180R	5′-TGGCAGGTGTAAGGTACGATTA-3′		This study
PRIMERS FOR EMSA			
Biotin-06180F	5′-CTATTTTGTTAGGCTGTTCCTCCAC-3′	Promoter of *RAYM_06180*	This study
Biotin-06180R	5′-GAACTTTGCCCCAATAGAGGTAATC-3′		This study
Biotin-01847F	5′-AAAGATGGTAAAGTAGCTAGCCCTG-3′	Promoter of *RAYM_01847*	This study
Biotin-01847R	5′-CGCCGAAGCTAATAGTATAAGAGGT-3′		This study
Biotin-03924L	5′-AGATTACTATAACGCCGTTCTTC-3′	Promoter of *RAYM_03924*	This study
Biotin-03924R	5′-ATAATAAGTGTTAGGCGTTGGGT-3′		This study
Biotin-09824L	5′-CCCTGCGACACGACCTTCTAACA-3′	Promoter of *RAYM_09824*	This study
Biotin-09824R	5′-ACCACAACGGAACAACTACAGGA-3′		This study

*Kpn*I and *Xba*I site). The fragment of mpheS-spc was inserted into pMD18T to generate pMD18T-mpheS-spc. The pMD18T-mpheS-spc was digested with *Kpn*I and *Xba*I enzymes, and 2.2 kb PS12-mpheS-spc fragment was ligated into pUC57-MCS and digested with *Kpn*I and *Xba*I to obtain pUC57-MCS-mpheS-spc. The pRE and pUC57-MCS-mpheS-spc were digested with *Xho*I and *Xba*I and ligated to generate pRE-mpheS-spc. The next step was to amplify a 3.3 kb fragment of *lacZ* from *E. coli* BL21 genome using primer lacZR and lacZL (**Table 1**) (introducing a *BamH*I site). A 135 bp fragment of PS12 promoter was amplified from RA-YM using primer rpsL-LacZ (introducing a *Xho*I site) and rpsR-LacZ (**Table 1**) and fused to *lacZ* fragment by overlap PCR using rpsL-LacZ and lacZR primers. pRE-mpheS-spc and *lacZ* fragments were digested with *BamH*I and *Xho*I and ligated to obtain 9 kb pRE-lacZ-mpheS-spc.

The shuttle plasmid pRES-JXrep-spc was constructed in several steps including the amplification of 2.5 kb fragment of replicon region and replicase gene (Genebank: KY806579) with primers rep1 and rep2 (**Table 1**) (introducing *a Xho*I site). The wild type plasmid of *R. anatipestifer* strain RA-JX was used as a template. A 1.1 kb *spc* cassette was amplified from plasmid pIC333 using primers spcL1 and spcR1 (**Table 1**), thereby introducing a *BamH*I site. The replicon region of RA-JX was joined with the *spc* cassette using overlap PCR. The JXrep-spc fragment was inserted into pMD18T to obtain pMD18T-JXrep-spc. In the next step, plasmid pRE and pMD18T-JXrep-spc were digested with *Xho*I and *BamH*I and ligated to generate the shuttle plasmid pRES-JXrep-spc.

Construction of Unmarked Deletion *R. anatipestifer* Δ*fur* and Complemented Mutant Strains

To obtain the suicide vector pRE-lacZ-mpheS-spc-fur for the deletion of whole *fur* gene from *R. anatipestifer* RA-YM strain, upstream (738 bp) and downstream (802 bp) DNA fragments were amplified using primers Fur-L1 and Fur-L2 (**Table 1**) (introducing *Sph*I site), Fur-R1 and Fur-R2 (**Table 1**) (introducing *Kpn*I site), respectively. The two fragments were joined together by overlap PCR. The LR fragment and pRE-lacZ-mpheS-spc were digested with *Sph*I and *Kpn*I; 1.5 kb LR fragment was inserted into pRE-lacZ-mpheS-spc to generate the suicide vector pRE-lacZ-mpheS-spc-fur. *E. coli* strain x7213 was used as a donor in conjugation step to introduce the suicide vector pRE-lacZ-mpheS-spc-fur into RA-YM strain as described previously (Hu et al., 2011). For phenotypic detection of mutant strains, conjugation filters were plated on tryptic soya agar (TSA) containing 100 μg/mL Spc. Colonies were then grown on TSA containing cPhe (0.2%) and X-gal (40 μg/mL). Appearance of white colonies confirmed successful construction of deletion mutant strains. For identification of recombinants carrying the chromosomal *fur* gene deletion, colonies were analyzed using PCR primers FurL1 and FurR2 to determine presence of wild-type or mutant allele at the target locus. The wild-type and deleted alleles could be differentiated on the basis of size of amplicon by agarose gel electrophoresis.

Similarly, for generation of complemented mutant strain, shuttle vector pRES-JXrep-spc-fur was constructed by amplification of the promoter sequence (171 bp) and the coding sequence (486 bp) of *fur* gene. The promoter sequence and the coding sequence were amplified using primers Promoter-fur1 and Promoter-fur2 (introducing *Kpn*I site, **Table 1**), primers Fur-inL and Fur-inR (introducing *Sph*I site, **Table 1**). The two fragments were joined together by overlap PCR. The plasmid pRES-JXrep-spc and *fur* gene fragment were digested with *Sph*I and *Kpn*I, then the fragment of 657 bp was inserted into plasmid pRES-JXrep-spc to obtain shuttle vector pRES-JXrep-spc-fur. The *E. coli* strain x7213 was used as donor in conjugation transfer of shuttle vector into the RA-YM Δ*fur* strain (Hu et al., 2011). The phenotypic identification of complemented mutant strain was conducted on TSA plates containing Spc 100 μg/mL. Furthermore, PCR reaction was performed using primers Fur inL and Fur inR to ensure that recombinant strains were harboring shuttle vectors.

RNA-Sequencing of Wild-Type and RA-YM Δ*fur* Deletion Mutant in Iron-Restricted and Enriched Conditions

The colonies of the wild-type and the RA-YM Δ*fur* mutant were suspended into tryptic soya broth (TSB) and incubated overnight with shaking at 37°C to an OD_{600} of 0.2. $FeCl_3$ (Sigma-Aldrich) or 2, 2-Dipyridyl (2, 2-DP, Sigma-Aldrich) was added to the bacterial suspension to produce a final concentration of 200 and 30 μM, as iron restricted and iron rich conditions, respectively and incubated at 37°C until the OD_{600} reached 0.8. Total RNA was extracted from bacteria solution using Bacterial RNA Kit (OMEGA, Norcross, USA) following the guidelines. Extracted RNA was purified with RNase-free DNase (Promega, Wisconsin, USA) at 37°C for 30 min to remove impurities of DNA, the DNA-free purified RNA was examined by 1% agarose gel electrophoresis. Purified RNA (23S rRNA and 16S rRNA) was sent to Huada Gene Center (Shenzhen, China) for RNA sequencing. All RNA samples were performed in two independent biological replicates (BioProject: SRP106941).

Quantitative Reverse Transcription PCR (RT-qPCR)

RT-qPCR was performed to quantify the expression of genes regulated by Fur. Primers were designed with Primer 5.0 software. RNA was extracted from wild-type and RA-YM Δ*fur* strains grown in iron-restricted and iron-rich medium. RNA was reverse transcribed to cDNA using PrimerScript RT regent Kit with gDNA Eraser (Takara, Dalian, China). Real-time PCR reaction was performed using SYBR Premix (Takara, Dalian, China). Each reaction was performed in triplicate. Relative quantification of gene expression was calculated according to $2^{-\Delta\Delta Ct}$ method, RA-YM 16S rRNA was used as reference gene for normalized expression for each RNA sample.

The Expression of Fur Protein and Electrophoretic Mobility-Shift Assay (EMSA) of the Putative Fur-Box Sequence

The fragment of *fur* gene was amplified using the primers Fur1 and Fur2 (introducing the *BamH*I and *Xho*I sites); the fragment and vector pET-28a were digested with *BamH*I and *Xho*I and restricted fragment was ligated into the expression vector pET-28a to generate the expression vector pET-28a-fur. The expression plasmid was then transformed into competent cells of *E. coli* BL21 (DE3). Then the Fur protein was purified with an ÄKTA Purifier (GE His Trap FF, USA).

EMSA was performed with the Lightshift Chemiluminescent EMSA Kit (Thermo fisher scientific, Waltham, USA). The reaction was incubated at 30°C for 1 h, then loaded into 6% non-denaturing polyacrylamide gel electrophoretic and exposured. The reaction mixture (20 μL) contained 1 μg biotin labeled DNA fragment, 2 μL binding buffer, 1 μL KCl, 1 μL $MgCl_2$, 1 μL glycerol, 1 μL NP-40 and 1 μL Poly(dI-dC) and desired concentration of Fur protein, the final concentration of Fur protein were 0, 0.1, 1, and 10 μg in four lanes. 16S rDNA was used as a negative control. DNA fragments to be identified were amplified by biotin labeled primer (Sangon, Shanghai, China). The length of DNA fragments ranged from 350 to 420 bp.

Assessment of Virulence *In vivo*

One-day-old Cherry Valley ducklings obtained from the Wuhan Duck Farm (Wuhan, China) housed in cages under 12-h light/dark cycle, at controlled temperature (28–30°C) and free access to food and water during the whole course of this study. Care and maintenance of all animals were in line with the standards of Institutional Animal Care. This experiment was approved by the Institutional Animal Experimental Committee of the Veterinary Faculty of Huazhong Agricultural University.

To determine the role of *fur* in virulence, the median lethal dose (LD_{50}) of the deletion mutant RA-YM Δ*fur* strain, the complemented mutant RA-YM Δ*fur* strain and the wild-type RA-YM was measured using the Reed–Muench method (Reed and Muench, 1938). For each wild type, mutant and complemented strains, 12-day-old ducklings were evenly divided into five groups (10 ducklings/group). All five groups were injected intramuscularly with 1.0×10^4, 1.0×10^5, 1.0×10^6, 1.0×10^7, and 1.0×10^8 colony forming units (CFU) of wild type strain, respectively. Similarly, mutant and complemented strains were injected to respective groups of ducklings for the evaluation of LD_{50}. Moribund ducklings were killed humanely and counted as dead. Dead ducklings were identified for the presence of RA. Mortality of the ducklings was recorded daily for a period of 10 days.

A comparative analysis of bacterial load in the blood of ducklings infected with mutants and wild type was made. Blood and target organs (brain, liver, heart and spleen) were collected at 24 and 48 h post-inoculation (five ducklings per group at each time-point). The target organs were homogenized with PBS to obtain supernatant. Blood and supernatant were plated on TSB agar plates for bacterial count with a 10-fold dilution method. In addition, the degree of lesions developing on the liver, spleen, heart and brain by the wild-type and the Δ*fur* mutant strains were also recorded. For pathological investigations, all tissues were immersed in 10% formalin solution, embedded in paraffin section and stained with hematoxylin and eosin (H E). The pathological findings of the wild-type and the RA-YM Δ*fur* mutant were compared.

RESULTS

Characterization of *R. anatipestifer* Δ*fur* Mutant and RA-YM Δ*fur* Complemented Mutant Strain

As homologous recombination follows a two-step procedure, the selection of the *R. anatipestifer* Δ*fur* mutant was carried out in two steps (Stibitz, 1994). The selection of mutant with Spc resistance was initially carried out, followed by the expression of *mpheS* gene. The function of *lacZ* gene could directly confirm whether the plasmid had been excised. The *pheS* gene was engineered by substituting alternative bases at

numerous positions. The sequence similarity rate between wild-type *pheS* and *mpheS* was 71%. However, no difference was observed in amino acid sequence with the exception of the A301G mutation. In this study, the *mpheS* gene was driven by the promoter of RA *rpsL* gene. The first process was obtained by growing RA-YM strains on TSA medium containing Spc resistance. The first process obtained the merodiploid strains, which harbored the suicide vector. Then, the merodiploid strains were screened on TSA medium containing 0.2% cPhe and X-gal to obtain the deletion mutant. The merodiploid strains grew on the plate containing Spc but had no growth on the agar plate with 0.2% cPhe. The wild strains could be grown on the plate contains cPhe (**Figures 1A2,A3**). In addition, the merodiploid strains appeared as blue colonies while the wild type strain was of a white color on the plate containing X-gal (**Figures 1A4,A5**). This finding demonstrated the effectiveness of the counter-selectable markers *pheS* in RA. A suicide vector pRE-lacZ-mpheS-spc-fur, containing mutated *pheS* as a counter-selectable marker (**Figure 1A1**) was constructed and successfully transformed into RA-YM strain to generate RA-YM Δ*fur* strain.

To determine whether the plasmid replicated and deleted *fur* gene after homologous recombination, no PCR amplification of *fur* gene and smaller LR fragment size (1,540 bp) from RA-YM Δ*fur* strain as compared to larger LR fragment size (2,008 bp) from RA-YM strain (**Figure 1C**) confirmed the plasmid activity and recombination. Similarly, development of a recombinant RA-YM Δ*fur* complemented mutant strain was confirmed by PCR amplification of *fur* and *spc* genes as shown in **Figure 1D**.

Transcriptional Response in Iron Enriched and Restricted Environment

A comparison of gene expression regulated by iron and/or Fur in wild type (WT) and mutant (Δ*fur*) strains grown in iron rich (+Fe) and iron restricted condition(−Fe) was exclusively established and comparison of RA-YM Δ*fur* deletion mutant strain with wild type RA-YM was also performed. In our

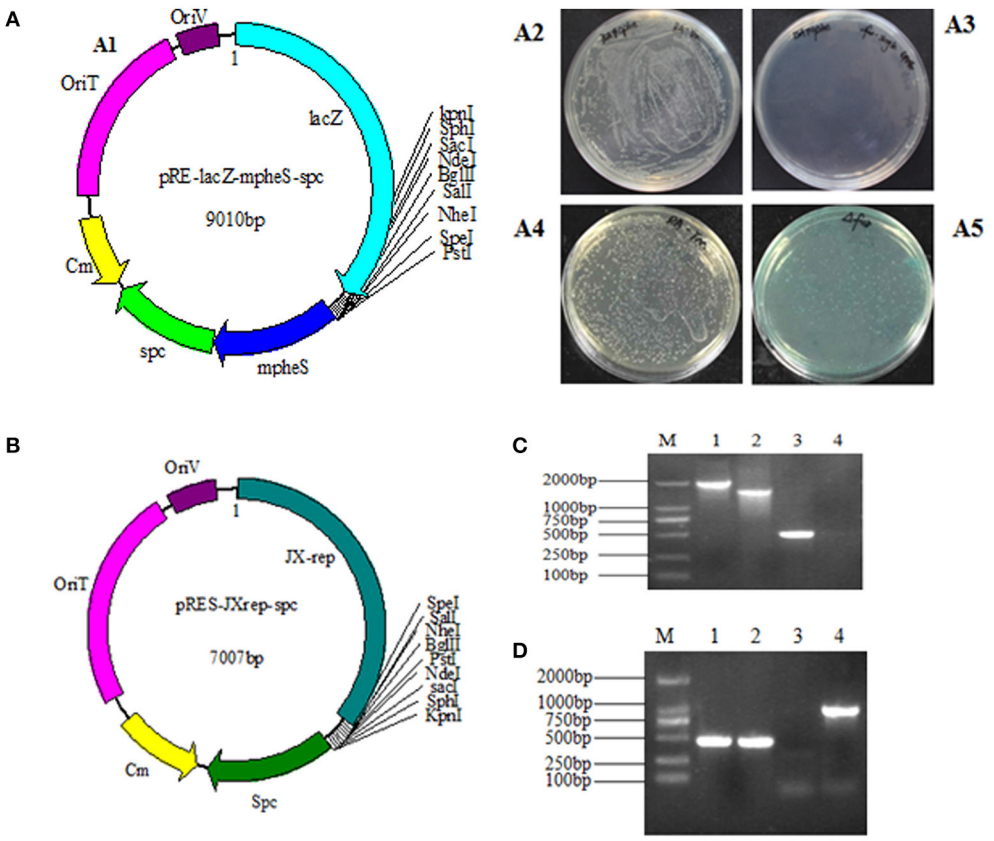

FIGURE 1 | (A1) The map of plasmid pRE-lacZ-mpheS-spc containing resistance gene *spc,* counter-selectable marker *mpheS* and *lacZ*; **(A2,A3)** show the growth of the wild type strain and the merodiploid strains on the TSA plate with 0.2% cPhe respectively. **(A4)** The color of the RA-YM on X-gal plate was white. **(A5)** The color of the merodiploid strains on X-gal plate was blue. **(B)** The map of the complemented shuttle plasmid pRES-JXrep-spc. **(C)** The PCR amplification of the RA-YM Δ*fur* deletion mutant strain and wild type RA-YM strain. Lane M: DL2000 DNA Marker; Lane 1: LR fragment amplification from RA-YM; Lane 2: LR fragment amplification from RA-YM Δ*fur* deletion mutant strain; Lan 3: Amplification of *fur* gene from RA-YM; Lane 4: Amplification of *fur* gene from RA-YM Δ*fur* deletion mutant strain; **(D)** The PCR amplification of RA-YM Δ*fur* mutant complemented strain. Lane M: DL2000 DNA Marker; Lan 1: Amplification of *fur* gene wild type RA-YM; Lane 2: Amplification of *fur* gene RA-YM Δ*fur* complemented mutant strain; Lane 3: Amplification of *spc* gene from wild type RA-YM; Lane 4: *spc* gene amplification from the RA-YM Δ*fur* complementary mutant strain.

experiments, the significance of differentially expressed genes was estimated by the false discovery rate (FDR) and was considered significant if FDR < 0.001 and the $|\log_2 \text{Ratio}| > 1$(Ernst et al., 2005a; Ledala et al., 2010). In total, 25 genes were downregulated and 45 genes were upregulated by iron when grown in iron-restricted conditions, in both parent and mutant. Seventeen genes were directly regulated by Fur. The expression of eight genes randomly selected regulated by iron and Fur was confirmed by real-time PCR in RA-YM and the Δ*fur* mutant (**Figure 7**). The real-time PCR result was in accordance to the transcriptional data.

Downregulation of Genes by Iron

Exclusively, 25 genes were downregulated when grown without iron in medium in both wild type RA-YM and RA-YM Δ*fur* deletion mutant strains. Furthermore, ratio (WT-Fe/WT+Fe ratio and Δ*fur*-Fe/Δ*fur*+Fe ratio) of gene expression were calculated in both iron-restricted (−Fe) and iron-rich (+Fe) conditions, which were ≥2. Of the 25 downregulated genes, five genes encoded proteins which acted as transporters; six genes encoded enzymes which participated in tricarboxylic acid cycle; six were involved in oxidation-reduction; six genes encoded hypothetical proteins and two genes actively participated in amino acid biosynthesis (**Table 2**).

Upregulation of Genes by Iron

Similarly, 45 genes were upregulated by iron both in the parent and the Δ*fur* mutant strain when iron was restricted. Gene ratio (WT-Fe/WT+Fe ratio and Δ*fur*-Fe/Δ*fur*+Fe ratio) was calculated ≥2. Among the 45 upregulated genes, nine genes participated in amino acids and cofactor biosynthesis; six were involved in cell envelope and surface structure formation; eight genes were involved in protein synthesis; transport and binding protein were encoded by six genes; three genes encoded regulators; cellular processes were regulated by three genes, and ten encoded hypothetical proteins (**Table 3**).

TABLE 2 | Genes downregulated by iron in response to iron restricted condition.

Gene name	Predicted function	Ratio			
		WT-Fe/WT+Fe	Δ*fur*-Fe/Δ*fur*+Fe	Δ*fur*-Fe/WT-Fe	Δ*fur*+Fe/WT+Fe
ENERGY METABOLISM					
RAYM_00925	Fumarate hydratase	−1.26	−2.78	−1.54	
RAYM_01977	Succinate dehydrogenase cytochrome b subunit, b558 family	−1.01	−2.47		
RAYM_08220	Aconitase	−1.56	−1.42		
RAYM_01982	Succinate dehydrogenase flavoprotein subunit	−1.04	−2.75		
RAYM_01987	Succinate dehydrogenase iron-sulfur subunit	−1.46	−2.79		
RAYM_02307	NADH-ubiquinone oxidoreductase chain G	−1.66	−1.72	−1.09	
TRANSPORTER					
RAYM_02992	Efflux transporter, RND family, MFP subunit	−2.33	−2.70		
RAYM_04896	TonB-dependent outer membrane receptor	−1.94	−2.57		−2.17
RAYM_04891	Amino acid/peptide transporter	−1.25	−1.64		
RAYM_00465	Co/Zn/Cd efflux system membrane fusion protein	−1.38	−1.56		
RAYM_02982	Integral membrane protein	−1.39	−1.82		
OXIDATION-REDUCTION					
RAYM_00020	Cytochrome c oxidoreductase quinone-binding subunit 1	−1.01	−3.47	−2.23	
RAYM_03017	Cytochrome c551/c552	−1.32	−1.57		
RAYM_01530	Cytochrome c oxidase subunit CcoP	−1.12	−1.07		
RAYM_01540	Cytochrome c oxidase subunit CcoN	−1.10	−1.09		
RAYM_07584	Cytochrome c nitrate reductase, small subunit	−2.06	−1.36		
RAYM_07589	Nitrite reductase (cytochrome; ammonia-forming)	−1.01	−1.01		
BIOSYNTHESIS OF CYSTEINE					
RAYM_04786	Cysteine synthase A	−3.23	−1.27		−2.50
RAYM_04791	Serine O-acetyltransferase	−2.10	−1.40	−1.45	−1.95
HYPOTHETICAL PROTEIN					
RAYM_05775	Hypothetical protein	−1.24	−1.09	1.37	
RAYM_05780	Hypothetical protein	−2.36	−1.67	1.49	
RAYM_00895	Hypothetical protein	−2.03	−1.01		
RAYM_03012	Hypothetical protein	−1.69	−1.34		
RAYM_03172	Hypothetical protein	−2.26	−1.13	2.15	
RAYM_01690	Hypothetical protein	−1.63	−2.39		

TABLE 3 | Genes upregulated by iron in response to iron restricted condition.

Gene name	Predicted function (gene)	Ratio			
		WT-Fe/WT+Fe	Δ*fur*-Fe/Δ*fur*+Fe	Δ*fur*-Fe/WT+Fe	Δ*fur*+Fe/WT+Fe
BIOSYNTHESIS OF AMINO ACIDS, COFACTORS, AND PROSTHETIC GROUPS					
RAYM_04219	Phosphoserine aminotransferase	1.35	1.25		
RAYM_04224	D-3-phosphoglycerate dehydrogenase	1.35	1.19		
RAYM_04506	Thiamine biosynthesis protein ApbE	1.84	3.37		
RAYM_06215	Aminodeoxychorismate lyase	1.08	1.12		
RAYM_06377	Para-aminobenzoate synthase component I	1.53	1.01		
CELL ENVELOPE AND SURFACE STRUCTURES					
RAYM_01390	GtrA family protein	2.00	1.80	−1.26	
RAYM_02732	Lipid A biosynthesis lauroyl acyltransferase	1.15	1.18		
RAYM_04004	Monofunctional biosynthetic peptidoglycan transglycosylase	1.70	1.31		−1.31
RAYM_08765	ATPase YjeE, predicted to have essential role in cell wall biosynthesis	1.13	1.21		
RAYM_06482	Outer membrane lipoprotein nlpE	1.28	2.45	1.14	
CELLULAR PROCESSES					
RAYM_00990	Non-specific DNA-binding protein Dps	2.00	3.24		
RAYM_01160	Ferritin	2.02	2.74		
RAYM_04501	Nitric oxide synthase	2.80	3.73		
DNA METABOLISM, RESTRICTION AND MODIFICATION					
RAYM_00455	Predicted DNA alkylation repair enzyme	1.99	1.14		
FATTY ACID AND PHOSPHOLIPID METABOLISM AND BIOSYNTHESIS					
RAYM_04164	Isopentenyl diphosphate isomerase	1.38	1.26		
HYPOTHETICAL PROTEINS/UNKNOWN FUNCTION					
RAYM_00065	Hypothetical protein	1.19	1.09		
RAYM_00865	Hypothetical protein	1.57	1.61		
RAYM_04229	Hypothetical protein	1.35	1.10		
RAYM_04491	Hypothetical protein	5.24	5.32		
RAYM_04496	Hypothetical protein	3.42	4.35		
RAYM_05980	Hypothetical protein	1.41	1.65		
RAYM_06462	Four helix bundle protein	1.41	2.09		
RAYM_06477	Hypothetical protein	1.43	2.49	1.32	
RAYM_06862	Rare lipoprotein A	3.23	1.83		
RAYM_09774	Leucine-rich repeat-containing protein	3.05	2.83		
PROTEIN SYNTHESIS					
RAYM_00750	RNA polymerase Rpb6	2.24	1.43	−1.08	
RAYM_01100	Nitrogen-fixing NifU domain protein	1.87	1.15		
RAYM_01495	FeS assembly SUF system protein	1.27	1.71		
RAYM_06457	Probable iron binding protein from the HesB_IscA_SufA family	1.53	2.58	1.04	
RAYM_06467	Cysteine desulfurase activator complex subunit SufB	1.87	1.85		
RAYM_06507	FeS assembly protein SufD	1.56	1.78		
RAYM_03082	Protein-(glutamine-N5) methyltransferase, release factor-specific	1.27	1.99		
RAYM_03087	tRNA methyltransferase	1.42	1.63		
PURINES, PYRIMIDINES, NUCLEOSIDES, AND NUCLEOTIDES					
RAYM_03724	Orotate phosphoribosyltransferase	2.10	3.30		
RAYM_06492	5-hydroxyisourate hydrolase	1.22	1.84	1.00	
REGULATORY FUNCTIONS					
RAYM_00365	RNA polymerase sigma-70 factor, ECF subfamily protein	1.93	1.51	−1.05	
RAYM_07184	Transcriptional regulator	1.61	1.25		
RAYM_08270	Transcriptional regulator, XRE family	1.02	1.05		
TRANSPORT AND BINDING PROTEINS					
RAYM_00510	Ferrous iron transport protein A	1.52	1.03	−2.75	−2.25
RAYM_00515	Ferrous iron transport protein B	1.33		−3.03	−2.22
RAYM_04481	TonB-dependent receptor	6.36	5.49		
RAYM_06602	Outer membrane efflux protein	1.07	1.05		
RAYM_06607	ABC transporter related protein	1.86	1.51		
RAYM_06472	Accessory colonization factor AcfC	1.14	2.15		

Gene Regulation by Fur under Iron Restricted Conditions

In almost all bacteria, Fur acted as a negative regulator. Genes directly regulated by Fur were observed to be upregulated when iron was restricted and when *fur* was mutated. The ratio (WT-Fe/WT+Fe ratio, Δ*fur*-Fe/Δ*fur*+Fe ratio and Δ*fur*+Fe/WT+Fe ratio) of 17 genes regulated by Fur was ≥2 (**Table 4**). Of the 17 genes directly regulated by Fur, five genes contributed in iron acquisition; two were involved in oxidation-reduction; one gene participated in activation of type IX secretion system (T9SS); the functions of six genes remained unknown, and three encoded hypothetical proteins (**Table 4**).

Identification of Putative Binding Sequences of Fur-Box Binding to Fur Protein

The putative Fur binding sequence and the distance from the start condon of the genes regulated by Fur is shown in **Table 5**. Promoter sequences were analyzed using software RegPredict and ClustalW for identification of putative binding sequence of Fur protein which was 19 bp long and sequence was predicted as 5′-ATTTAGAATTATTCTAAAT-3′ (**Figure 8A**). Therefore, the Fur binding sequence might be located within 100 bp of the translation initiation codon of the regulated genes (**Table 5**). To verify the putative role of the Fur-box sequence, the promoters of *hmuR*, *sprT*, *RAYM_01847*, *RAYM_09824* were selected for electrophoretic mobility shift assay (EMSA). Our findings illustrated that purified Fur protein could bind to the DNA fragment containing the putative Fur-box (**Figure 8B**).

In vivo Evaluation of Virulence of *R. anatipestifer* Δ*fur* Deletion Mutants

The LD_{50} values of RA-YM, RA-YM Δ*fur* deletion mutant and RA-YM Δ*fur* complemented strain were recorded as 2.0×10^6 CFU, 1.6×10^8 CFU, 1.2×10^7CFU, respectively. LD_{50} counted for wild type as compared to RA-YM Δ*fur* deletion mutant was approximately 80 times higher, whereas no significant difference was observed as in the case of wild type in comparison to RA-YM Δ*fur* complemented mutant that was six times higher. Due to slight difference between wild type and RA-YM Δ*fur* complemented mutant, a further comparison was established only between wild type and RA-YM Δ*fur* deletion mutant strains. As the *fur* gene was disrupted in RA-YM Δ*fur* deletion mutant strains resulted in attenuation of virulence of RA. However, virulence to ducklings was partially restored when the mutant was complemented with the plasmid pRES-JXrep-spc.

Microbiological analysis of heart, brain, liver and spleen showed that bacterial load was higher in wild type RA-YM strain compared to RA-YM Δ*fur* deletion mutant strain at 24 and 48 h post-infection collection, a detailed comparison is shown in **Figures 2A,B**. Correspondingly, the pathological investigations illustrated that lesions were more significant in wild type as compared to mutant strains. The epicardial tissue of ducklings infected with wild type bacteria consisted of a higher degree of fibrinous exudate and inflammatory cell infiltration as compared to infection with mutant pathogens after 24 and 48 h (**Figure 3**). The lesions in brain tissue after both 24 and 48 h, the subarachnoid space was examined where mild inflammatory cell infiltration was noted in case of RA-YM Δ*fur* deletion mutant strain as compared to wild type RA-YM strains (**Figure 4**). Similarly, a large number of hepatocytes expressed fatty degeneration and slight fibrotic

TABLE 4 | Putative genes regulated by Fur under iron restricted condition.

Gene name	Predicted function	Ratio			
		WT-Fe/WT+Fe	Δ*fur*-Fe/Δ*fur*+Fe	Δ*fur*-Fe/WT-Fe	Δ*fur*+Fe/WT+Fe
RAYM_00450	Oxidoreductase	3.31	3.67	1.67	1.73
RAYM_01847	TonB-dependent outer membrane protein receptor for Fe^{3+}-dicitrate	2.22	1.94	1.96	1.63
RAYM_03589	Rhodanese-like domain protein	1.63	2.18	1.77	1.21
RAYM_03864	3-hydroxyacyl-CoA dehydrogenase/Enoyl-CoA hydratase	1.44	2.01	1.76	1.20
RAYM_03869	Regulatory protein, MarR	2.48	4.05	1.71	1.37
RAYM_03924	SprT protein	1.01	1.17		1.08
RAYM_05635	L-asparaginase	1.76	1.26		1.30
RAYM_06175	Hypothetical protein (HmuY)	6.71	7.69	2.53	2.56
RAYM_06180	Outer membrane receptor for ferrienterochelin and colicins	7.89	8.44	1.93	2.64
RAYM_06185	Hypothetical protein	7.25	8.37	2.18	2.25
RAYM_07324	Mammalian cell entry protein	1.46	1.32	1.01	1.06
RAYM_07989	Hypothetical protein	1.14	1.59		2.36
RAYM_09779	TonB-dependent receptor	2.11	2.70		1.90
RAYM_09784	Vitamin K-dependent gamma-carboxylase	2.64	2.77		1.39
RAYM_09789	Putative lipoprotein Imelysin	3.07	2.92		1.93
RAYM_09794	Hypothetical protein	2.41	3.07	1.14	1.36
RAYM_09824	Putative outer membrane protein, mostly Fe transport	2.41	3.06	2.14	1.36

TABLE 5 | Identification of putative Fur binding sequences (Fur boxes).

Locus ID	Nucleotide position		Fur box sequence	Predicted function (Gene name)	ATG-distance
	Start	End			
RAYM_00450	91412	91430	ATTTAGAATAATTAAAAAA	Oxidoreductase	9
RAYM_01847	9623	9641	ATTTAGAATTATCCTAAAT	Outer membrane receptor for Fe^{3+}-dicitrate	67
RAYM_03589	76340	6358	ATTTAGAATTAGAATAAAT	Rhodanese-like domain protein	30
RAYM_03869	79344	79362	ATTTATAATATTGATTATT	Regulatory protein, MarR	87
RAYM_03924	86294	86312	AATGATAAACACTTTAACT	SprT protein	85
RAYM_05635	94340	94358	GTTTAAAATTTATCTAATT	L-asparaginase	27
RAYM_06180	205354	205372	ATTTAAAATTATTCTAAAT	HmuR	78
RAYM_06185	205354	205272	ATTTAGAATAATTTTAAAT	Hypothetical protein	25
RAYM_07324	79551	79569	ATTTATATTTATTTTTGAT	Mammalian cell entry protein	86
RAYM_07989	205419	205437	ATTTATTTTCAGTTTTAAT	Hypothetical protein	91
RAYM_09824	15328	15346	ATTTATACTTATTCTAATT	Putative outer membrane protein, mostly Fe transport	33

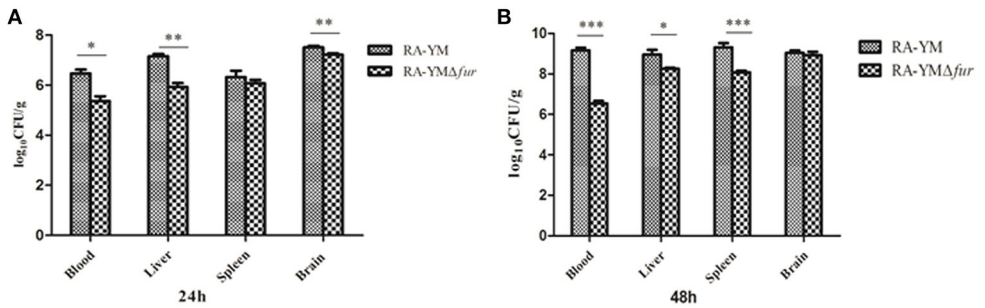

FIGURE 2 | Graphical presentation of bacterial load in blood, liver, spleen, and brain of ducklings infected with wild type RA-YM and RA-YM Δ*fur* deletion mutant strain. The error bars represent mean ± standard deviation from five ducks. **(A)** The tissue burden of the group infected with wild type and RA-YM Δ*fur* deletion mutant after 24 h. **(B)** The tissue burden of the group infected with wild type and RA-YM Δ*fur* deletion mutant after 48 h.

effusion when infected with wild type RA-YM bacteria, whereas, such lesions were hardly observed in ducklings infected with RA-YM Δ*fur* mutant bacteria after 24 h inoculation. A higher degree of fibrotic effusions in liver tissue was observed after 48 h of infection with wild type pathogens, in comparison to mutant pathogens. Collectively, severe hepatic congestion was noticed in ducklings infected with wild type RA-YM strains (**Figure 5**). Likely, both splenomegaly and congestion of spleen was observed in ducklings after 24 and 48 h in case of infection with wild type pathogens, whereas only splenomegaly was noticed in case of infection with mutant pathogens (**Figure 6**). Conclusively, all groups of ducklings, inoculated with wild type RA-YM strains, were severely infected in comparison to those inoculated with RA-YM Δ*fur* deletion mutant strains. The control group of ducklings showed no significant pathological lesions.

DISCUSSION

In the present study, we employed the suicide vector pRE-lacZ-mpheS-spc-fur to construct an unmarked mutant RA-YM Δ*fur* successfully. Using this technique, the traditional method of mutant development by inducing antibiotic resistance can be circumvented, and influence on the expression of downstream genes can be minimized in some cases. However, the expression of the *fur* downstream gene *RAYM_04841* remained unchanged. The counter-selectable marker *pheS* in combination with *lacZ* have been successfully developed for unmarked gene deletion in RA. Previously, *pheS* had been also successfully used in *Burkholderia* (Barrett et al., 2008) and *E. faecalis* (Kristich et al., 2007), and *S. mutans* (Xie et al., 2011). The technique was developed to determine the role of *fur* in the pathogenicity of RA. Indeed, the virulence of RA-YM Δ*fur* mutant strain was attenuated in comparison to wild type and virulence was partially restored when RA-YM Δ*fur* mutant strain was complemented with the plasmid pRES-JXrep-spc. Moreover, bacterial load in different tissues was significantly decreased in RA-YM Δ*fur* mutant infection as compared to wild type strain. Similarly significantly mild lesions were observed in case of RA-YM Δ*fur* mutant infection in comparison to wild type infection. Conclusively, it was observed that Fur regulated virulence factors of RA infection. Indeed, the role of Fur with respect to virulence has been previously examined in *Vibrio cholerae* (Mey et al., 2005) and *Staphylococcus aureus* (Johnson et al., 2011). Consequently, findings of this study depicted the role of *fur* in virulence of RA.

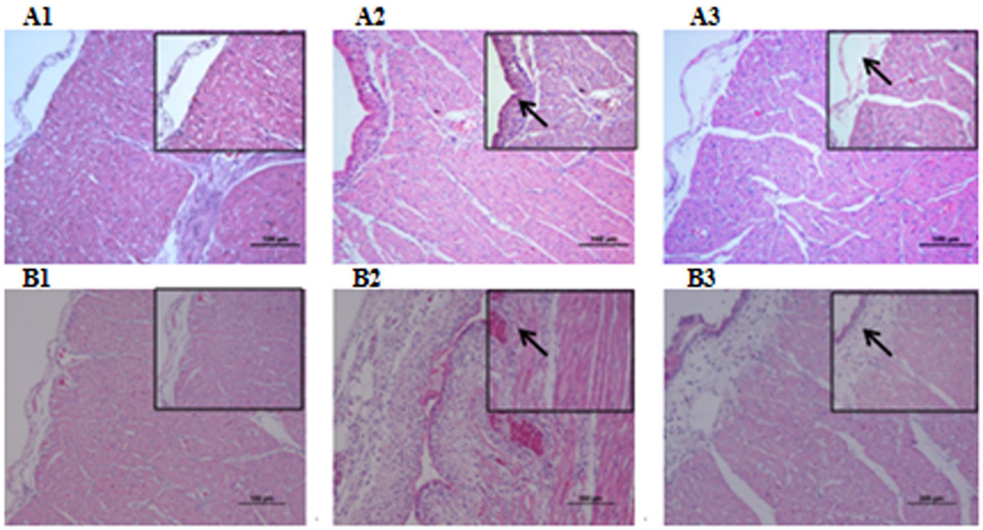

FIGURE 3 | Histopathological diagram of heart. **(A1)** The blank control group after 24 h, **(A2)** The group with wild type RA-YM strain after 24 h, **(A3)** The group with RA-YM Δ*fur* deletion mutant strain after 24 h. **(B1)** The blank control group after 48 h, **(B2)** The group with wild type RA-YM strain after 48 h, **(B3)** The group with RA-YM Δ*fur* deletion mutant strain after 48 h.

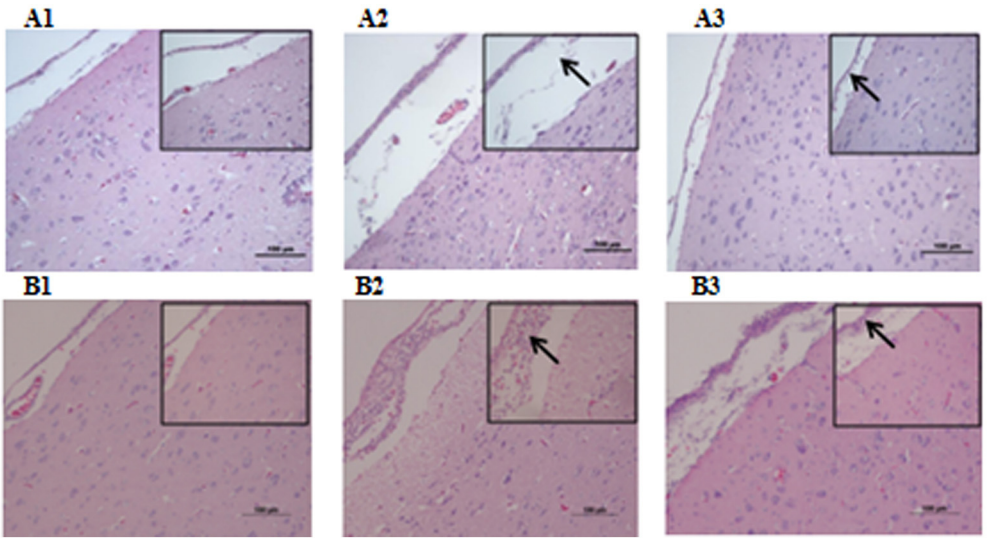

FIGURE 4 | Histopathological diagram of brain **(A1)** The blank control group after 24 h, **(A2)** The group with wild type RA-YM strain after 24 h, **(A3)** The group with RA-YM Δ*fur* deletion mutant strain after 24 h. **(B1)** The blank control group after 48 h, **(B2)** The group with wild type RA-YM strain after 48 h, **(B3)** The group with RA-YM Δ*fur* deletion mutant strain after 48 h.

In the current study, we also recorded the expression of the genes downregulated by iron under iron-restricted conditions. Among those genes, six downregulated genes were involved in regulation of tricarboxylic acid (TCA) cycle, which play an important role in metabolism, energy generation and synthesis of precursors (Vuoristo et al., 2016). Under iron-restricted conditions, certain key enzymes of the TCA cycle of RA-YM Δ*fur* strain were downregulated, which included succinate dehydrogenase (SDH) subunit (*RAYM_01977*, *RAYM_01982*, *RAYM_01987*), fumarate hydratase (*RAYM_00925*) and aconitase. SDH is involved in the respiratory chain and Krebs cycle of bacteria (Yankovskaya et al., 2003). Similarly, glyoxylate bypass pathways are also repressed in *Yersinia pestis* iron-restricted conditions (Pieper et al., 2010). In previous reports, downregulation of SDH, fumurase and aconitase were reported in *E. coli* (Massé et al., 2005) and *Bacillus subtilis* (Gaballa et al., 2008) in iron-sparing conditions. This phenomenon may be accounted for as the bacteria utilize an alternative iron-independent pathway of the TCA cycle and repressed numerous of iron-containing proteins under

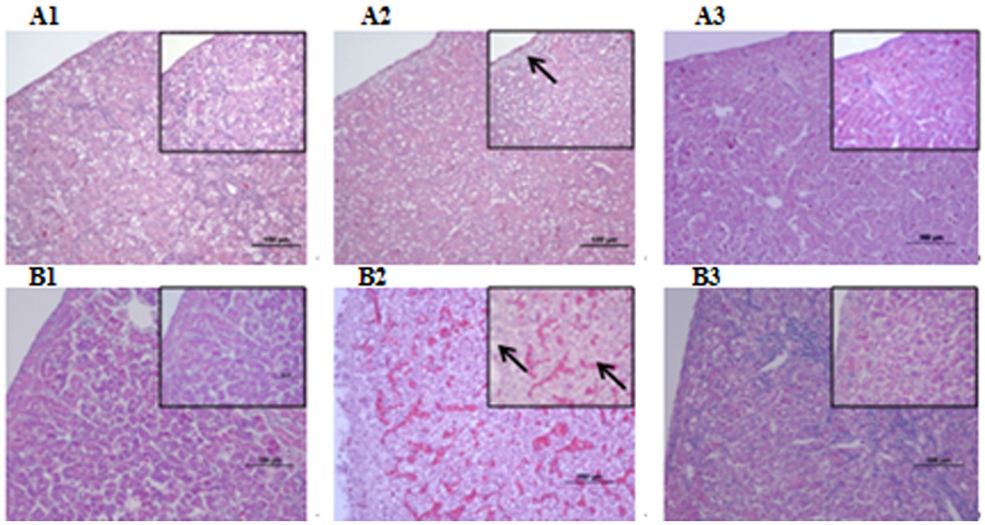

FIGURE 5 | Histopathological diagram of liver **(A1)** The blank control group after 24 h, **(A2)** The group with wild type RA-YM strain after 24 h, **(A3)** The group with RA-YM Δ*fur* deletion mutant strain after 24 h. **(B1)** The blank control group after 48 h, **(B2)** The group with wild type RA-YM strain after 48 h, **(B3)** The group with RA-YM Δ*fur* deletion mutant strain after 48 h.

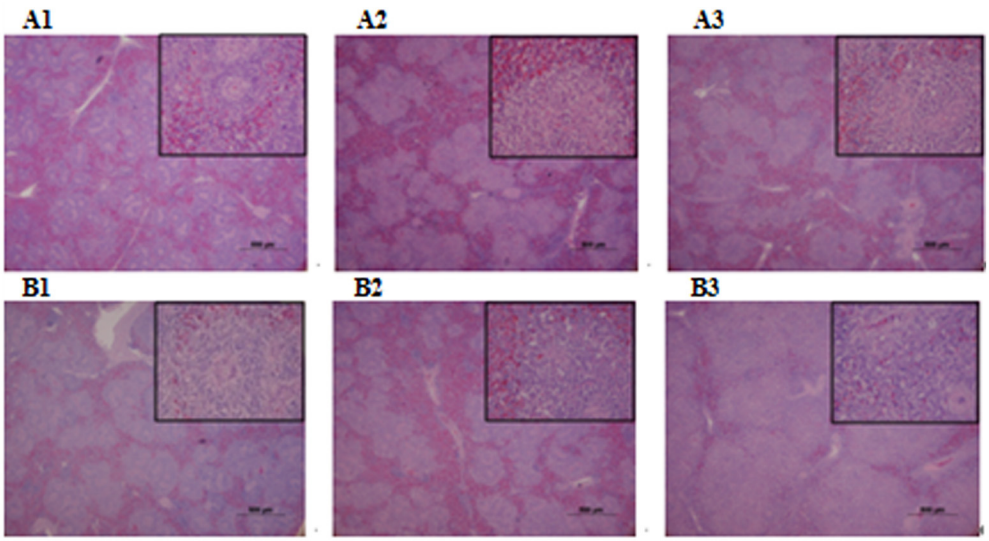

FIGURE 6 | Histopathological diagram of spleen. **(A1)** The blank control group after 24 h, **(A2)** The group with wild type RA-YM strain after 24 h, **(A3)** The group with RA-YM Δ*fur* deletion mutant strain after 24 h. **(B1)** The blank control group after 48 h, **(B2)** The group with wild type RA-YM strain after 48 h, **(B3)** The group with RA-YM Δ*fur* deletion mutant strain after 48 h.

iron–restricted conditions. Moreover, cysteine synthase A (*cysK*, a significant enzyme of cysteine biosynthesis) and serine O-acetyltransferase (*cysE*, catalyzes the acetylation of L-serine to O-acetyl-L-serine) involved in amino biosynthesis were also downregulated due to iron deficiency. This inhibition regulates the conversion of available serine to siderophore, enterobactin, which thereby increases iron acquisition (Salvail et al., 2010). The cytochrome c oxidase (Cco) family related to oxidation-reduction was also inhibited in response to iron limitation, which is comprised of four subunits, CcoN, CcoO, CcoP, and CcoQ, which act as the terminal enzyme of respiratory chain (Ahn et al., 2015; Steininger et al., 2016). The Cco family, a member of heme-copper oxidase superfamily, may play a role in iron- restricted conditions. In *Pseudomonas stutzeri*, the Cco family has also been reported as an essential element for nitrogen-fixing (Nyquist et al., 2001; Xie et al., 2014). Our data showed that nitrogen-fixing associated genes (*RAYM_07584*, *RAYM_07589*) were repressed in iron-restricted conditions. In conclusion, iron-sparing responses, which means the repression of iron-dependent genes when iron is deficient, was the vital

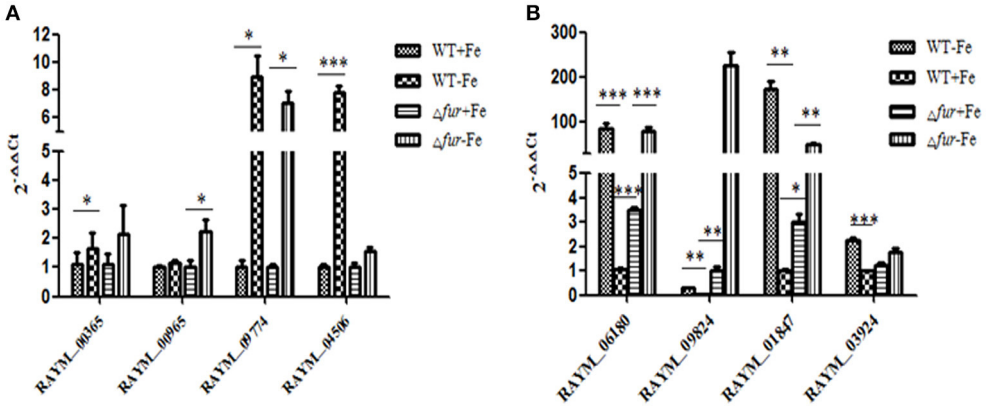

FIGURE 7 | Real-Time PCR analysis of the Fur-and Iron- regulated genes. **(A)** The genes (*RAYM_00365*, *RAYM_00965*, *RAYM_09774, RAYM_04506*) regulated by iron. **(B)** The genes (*RAYM_06180*, *RAYM_09824*, *RAYM_01847*, *RAYM_03924*) regulated by Fur.

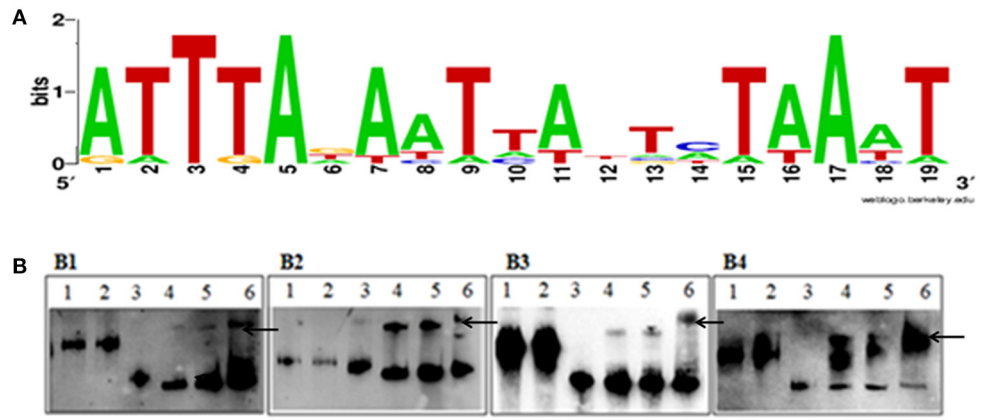

FIGURE 8 | (A) Sequence logo of the Fur box of RA-YM. The binding sequence was listed by using WEBLOGO program. **(B)** EMSA of the Fur protein and its putative target promoters. **(B1)** Lane 1, DNA fragment of 16S rRNA; Lane 2, DNA fragment of 16S rRNA and Fur protein; Lane 3, DNA fragment of *RAYM_01847*; Lane 4, DNA fragment of *RAYM_01847* and Fur protein (0.1 μg); Lane 5, DNA fragment of *RAYM_01847* and Fur protein (1 μg); Lane 6, DNA fragment of *RAYM_01847* and Fur protein (10 μg); **(B2)** Lane 1, DNA fragment of 16S rRNA; Lane 2, 1 DNA fragment of 16s rRNA and Fur protein; Lane 3, DNA fragment of *RAYM_03924*; Lane 4, DNA fragment of *RAYM_03924* and Fur protein (0.1 μg); Lane 5, DNA fragment of *RAYM_03924* and Fur protein (1 μg); Lane 6, DNA fragment of *RAYM_03924* and Fur protein (10 μg); **(B3)** Lane 1, DNA fragment of 16S rRNA; Lane 2, DNA fragment of 16S rRNA and Fur protein; Lane 3, DNA fragment of *RAYM_06180*; Lane 4, DNA fragment of *RAYM_06180* and Fur protein (0.1 μg); Lane 5, DNA fragment of *RAYM_06180* and Fur protein (1 μg); Lane 6, DNA fragment of *RAYM_06180* and Fur protein (10 μg); **(B4)** Lane 1, DNA fragment of 16S rRNA; Lane 2, DNA fragment of 16S rRNA and Fur protein; Lane 3, DNA fragment of *RAYM_09824*; Lane 4, DNA fragment of *RAYM_09824* and Fur protein (0.1 μg); Lane 5, DNA fragment of *RAYM_09824* and Fur protein (1 μg); Lane 6, DNA fragment of *RAYM_09824* and Fur protein (10 μg); each lane the concentration of DNA fragment was 1 μg. The band which marked by arrows shows the Fur protein and DNA fragment complex.

reason of the genes downregulated by iron in iron restricted conditions.

Among genes induced by iron, the genes (*RAYM_00510*, *RAYM_00515*) associated with iron acquisition were upregulated, which included Ferrous iron transport protein A (FeoA) and Ferrous iron transport protein B (FeoB). The *feoB* gene encodes an inner membrane Fe (II) transporter in multiple bacteria, such as *E. coli* and *V. cholerae* whereas *feoA* gene was demonstrated crucial for FeoB uptake of Fe(II) (Marlovits et al., 2002; Kim et al., 2012). Other genes involved in the iron-acquisition system were also upregulated, including Ferritin (*RAYM_01160*), ABC transporter related protein (*RAYM_06607*), TonB-dependent receptor (*RAYM_04481*). This is an apparent response to iron starvation in bacteria, which has also been demonstrated in *Klebsiella pneumonia* and *Listeria monocytogenes* (Ledala et al., 2010; Lin et al., 2011). Similarly, a group of genes contributed to the biosynthetic process of iron-sulfur (Fe-S) were also regulated by iron. In bacteria, Fe-S machinery is comprised of a nitrogen-fixing NifU domain protein (*RAYM_01100*), SUF system protein (*RAYM_01495, RAYM_06457, RAYM_06467, RAYM_06507*). Similar changes of NIF and SUF systems have been confirmed in *E. coli* in previous studies (Outten et al., 2004). Moreover, the genes Phosphoserine aminotransferase (*RAYM_04219*), D-3-phosphoglycerate-dehydrogenase (*RAYM_04224*) controlling the shikimate pathway were upregulated. D-3-phosphoglycerate-dehydrogenase (pabB)

converts chorismate to 4-amino-4-deoxychorismate (ADC) and phosphoserine aminotransferase (pabC) converts ADC to p-aminobenzoate (PABA) and pyruvate (Green et al., 1992). Shikimate pathway catalyzes serine to form siderophore, enterobactin (Prévost et al., 2007). The upregulation of the pabB and pabC in iron-limited conditions results in high levels of both aromatic amino acids and phenolate siderophore (Lemaître et al., 2014). Moreover, in our data, sigma factor protein (*RAYM _00365*) was upregulated by iron. Iron-starvation sigmas, a extracytoplamic function (ECFs) subfamily, have been demonstrated previously to play a role in iron acquisition in *P. aeruginosa* (Visca et al., 2002). In conclusion, the genes induced by iron are involved in iron-acquisition, some metabolic pathways and several transcriptional regulation factors. The series of regulatory responses under low-iron conditions resulted in increasing iron acquisition.

Among the genes regulated by Fur under iron-restricted conditions, Hmu system, comprised of *hmuY* (*RAYM_06175*) and *hmuR* (*RAYM_06180*), was observed to be regulated by Fur. The homologous Fur-box sequence has been identified upstream of the *hmuY* start codon in *Porphyromonas gingivalis* (Simpson et al., 2000). HmuR, the TonB-dependent receptor for ferric, has previously been illustrated to be regulated by Fur in *Y. pestis* (Branger et al., 2010). Furthermore, genes (*RAYM_01847*, *RAYM_09824,* and *RAYM_09779*) encoding TonB-dependent outer membrane proteins are also regulated by Fur under iron-restricted conditions. The accessory proteins of TonB system can transduce energy in Gram-negative bacteria (Postle and Kadner, 2003; Lim et al., 2012). Our data confirmed that TonB-ExbB-ExbD system was a significant component for ferric enterobactin acquisition, which was previously reported in *Campylobacter* (Zeng et al., 2013). In addition, *RAYM_00450* (oxidoreductase), *RAYM_03864* (3-hydroxyacyl-CoA dehydrogenase) were also regulated by Fur which was demonstrated in previous study as Fur regulated the response to oxidative stress in *C. jejuni* (Holmes et al., 2005). Interestingly, *sprT* gene (*RAYM_03924*), a component of the type IX secretion system (T9SS) was also regulated by Fur. Parallel findings were recorded in *Flavobacterium johnsoniae* (Kharade and McBride, 2015). T9SS was also characterized as a novel protein secretion system mediated outer membrane translocation to the cell surface in *P. gingivalis* (de Diego et al., 2016). In conclusion, Fur regulated processes included iron acquisition, oxidation and reduction, and regulation of some components of T9SS.

Fur has been reported to act as a negative regulator. It was demonstrated that Fur protein, together with iron, can bind to a consensus sequence, resulting in transcriptional inhibition (Baichoo and Helmann, 2002) which had been described in *E. coli*, *P. aeruginosa, Helicobacter pylori,* and *H. hepaticus* (Escolar et al., 1998; Vasil and Ochsner, 1999; Belzer et al., 2007; Pich et al., 2012). The Fur-box consensus sequence 5′-GATAATGATAATCATTATC-3, was slightly different among bacteria. It was identified as an adjacent hexamer unit of the sequence 5′-GATTAT-3′ or three repeat of the NATWAT (Lavrrar and McIntosh, 2003). Typically, the Fur binding sequence was located within 150 bp of the translation initiation codon of the regulated genes (Grifantini et al., 2003). The putative Fur-box sequence of RA-YM in our study was predicted as 5′-ATTTAGAATTATTCTAAAT- 3′, and the sequences might be located within 100 bp of the translation initiation codon of regulated genes which could be reasoned due to the unique promoter of the strain. RA-YM belongs to the *Flavobacterium*, where promoter have −7 and −33 consensus elements, whereas the promotor of *E. coli* has −10 and −35 consensus elements (Chen et al., 2007).

In summary, our work showed that *pheS* acted as effective counter-selectable marker for conjugal transfer. We successfully constructed an unmarked deletion mutant of RA with the suicide vector pRE-lacZ-mpheS-spc. In addition, we elucidated the role of the *fur* gene in virulence of RA. Furthermore, we screened out the genes regulated by iron and Fur. The putative Fur-box sequence of RA was also predicted. Conclusively, this was a comprehensive study on the metabolism of *R. anatipestifer* which may help facilitate the control of this pathogen.

AUTHOR CONTRIBUTIONS

YG designed, performed the experimentation, data analysis and wrote the manuscript. DH, JG, XL, and JYG performed experimentations. XW, YX, HJ, ML, and ZL designed and contributed to experimental work. ZZ and DB designed, analyzed the data and revised the manuscript. All authors read and approved the final manuscript.

ACKNOWLEDGMENTS

This work was supported by the National Natural Science Foundation of China (31201933) and the Fundamental Research Founds for the Central Universities (52902-0900206127).

SUPPLEMENTARY MATERIAL

The Supplementary Material for this article can be found online at: http://journal.frontiersin.org/article/10.3389/fcimb.2017.00382/full#supplementary-material

REFERENCES

Ahn, Y. O., Lee, H. J., Kaluka, D., Yeh, S. R., Rousseau, D. L., Ädelroth, P., et al. (2015). The two transmembrane helices of CcoP are sufficient for assembly of the cbb3-type heme-copper oxygen reductase from *Vibrio cholerae*. *Biochim. Biophys. Acta* 1847, 1231–1239. doi: 10.1016/j.bbabio.2015.06.013

Baichoo, N., and Helmann, J. D. (2002). Recognition of DNA by Fur: a reinterpretation of the Fur box consensus sequence. *J. Bacteriol.* 184, 5826–5832. doi: 10.1128/JB.184.21.5826-5832.2002

Barrett, A. R., Kang, Y., Inamasu, K. S., Son, M. S., Vukovich, J. M., and Hoang, T. T. (2008). Genetic tools for allelic replacement in *Burkholderia* species. *Appl. Environ. Microbiol.* 74, 4498–4508. doi: 10.1128/AEM.00531-08

Belzer, C., van schendel, B. A. M., Kuipers, E. J., Kusters, J. G., and van Vliet, A. H. M. (2007). Iron-responsive repression of urease expression in *Helicobacter hepaticus* is mediated by the transcriptional regulator Fur. *Infect. Immun.* 75, 745–752. doi: 10.1128/IAI.01163-06

Bijlsma, J. J. E., Waidner, B., Vliet, A. H., Hughes, N. J., Häg, S., Bereswill, S., et al. (2002). The *Helicobacter pylori* homologue of the ferric uptake regulator is involved in acid resistance. *Infect. Immun.* 70, 606–611.doi: 10.1128/IAI.70.2.606-611.2002

Branger, C. G., Sun, W., Torres-Escobar, A., Perry, R., Roland, K. L., Fetherston, J., et al. (2010). Evaluation of Psn, HmuR and a modified LcrV protein delivered to mice by live attenuated *Salmonella* as a vaccine against bubonic and pneumonic *Yersinia pestis* challenge. *Vaccine* 29, 274–282. doi: 10.1016/j.vaccine.2010.10.033

Chen, S., Bagdasarian, M. M., Kaufman, M. G., Bates, A. K., and Walker, E. D. (2007). Mutational Analysis of the ompA Promoter from *Flavobacterium johnsoniae*. *J. Bacteriol.*189, 5108–5118. doi: 10.1128/JB.00401-07

Cheng, A., Wang, M., Chen, X., Zhu, D., Huang, C., Fei, L., et al. (2003). Epidemiology and new serotypes of *Riemerella anatipestifer* isolated from ducks in China and studies on their pathogenic characteristics. *Chinese J. Vet. Sci.* 78, 1469–1473.

Crasta, K. C., Chua, K. L., Subramaniam, S., Frey, J., Loh, H., and Tan, H. M. (2002). Identification and characterization of CAMP cohemolysin as a potential virulence factor of *Riemerella anatipestifer*. *J. Bacteriol.* 184, 1932–1939. doi: 10.1128/JB.184.7.1932-1939.2002

de Diego, I., Ksiazek, M., Mizgalska, D., Koneru, L., Golik, P., Szmigielski, B., et al. (2016). The outer-membrane export signal of *Porphyromonas gingivalis* type IX secretion system (T9SS) is a conserved C-terminal β-sandwich domain. *Sci Rep.* 6:23123. doi: 10.1038/srep23123

Ernst, F. D., Bereswill, S., Waidner, B., Stoof, J., Mäder, U., Kusters, J. G., et al. (2005a). Transcriptional profiling of *Helicobacter pylori* Fur- and iron-regulated gene expression. *Microbiology* 151, 533–546. doi: 10.1099/mic.0.27404-0

Ernst, F. D., Homuth, G., Stoof, J., Mäder, U., Waidner, B., Kuipers, E. J., et al. (2005b). Iron-responsive regulation of the *Helicobacter pylori* iron-cofactored superoxide dismutase sodb is mediated by fur. *J. Bacteriol.* 187, 3687–3692. doi: 10.1128/JB.187.11.3687-3692.2005

Escolar, L., Pérez-Martín, J., and de Lorenzo, V. (1998). Binding of the fur (ferric uptake regulator) repressor of *Escherichia coli* to arrays of the GATAAT sequence. *J. Mol. Biol.* 283, 537–547. doi: 10.1006/jmbi.1998.2119

Gaballa, A., Antelmann, H., Aguilar, C., Khakh, S. K., Song, K. B., Smaldone, G. T., et al. (2008). The *Bacillus subtilis* Iron-Sparing Response Is Mediated by a Fur-Regulated Small RNA and Three Small, Basic Proteins. *Proc. Natl. Acad. Sci. U.S.A.* 105, 11927–11932. doi: 10.1073/pnas.07117 52105

Green, J. M., Merkel, W. K., and Nichols, B. P. (1992). Characterization and sequence of *Escherichia coli* pabC, the gene encoding aminodeoxychorismate lyase, a pyridoxal phosphate-containing enzyme. *J. Bacteriol.* 174, 5317–5323. doi: 10.1128/jb.174.16.5317-5323.1992

Grifantini, R., Sebastian, S., Frigimelica, E., Draghi, M., Bartolini, E., Muzzi, A., et al. (2003). Identification of iron-activated and-repressed Fur-dependent genes by transcriptome analysis of *Neisseria meningitidis* group B. *Proc. Natl. Acad. Sci. U.S.A.* 100, 9542–9547. doi: 10.1073/pnas.1033001100

Haraszthy, V. I., Jordan, S. F., and Zambon, J. J. (2006). Identification of Fur-regulated genes in *Actinobacillus actinomycetemcomitans*. *Microbiology* 152, 787–796. doi: 10.1099/mic.0.28366-0

Higgins, D. A., Henry, R. R., and Kounev, Z. V. (2000). Duck immune responses to *Riemerella anatipestifer* vaccines. *Dev. Comp. Immunol.* 24, 153–167. doi: 10.1016/S0145-305X(99)00070-1

Holmes, K., Mulholland, F., Pearson, B. M., Pin, C., McNicholl-Kennedy, J., Ketley, J. M., et al. (2005). *Campylobacter jejuni* gene expression in response to iron limitation and the role of Fur. *Microbiology* 151, 243–257. doi: 10.1099/mic.0.27412-0

Hu, Q., Han, X., Zhou, X., Ding, C., Zhu, Y., and Yu, S. (2011). OmpA is a virulence factor of *Riemerella anatipestifer*. *Vet. Microbiol.*150, 278–283. doi: 10.1016/j.vetmic.2011.01.022

Ibba, M., Kast, P., and Hennecke, H. (1994). Substrate specificity is determined by amino acid binding pocket size in *Escherichia coli* phenylalanyl-tRNA synthetase. *Biochem.* 33, 7107–7112.

Johnson, M., Sengupta, M., Purves, J., Tarrant, E., Williams, P. H., Cockayne, A., et al. (2011). Fur is required for the activation of virulence gene expression through the induction of the sae regulatory system in *Staphylococcus aureus*. *Int. J. Med. Microbiol.* 301, 44–52. doi: 10.1016/j.ijmm.2010.05.003

Kast, P., and Hennecke, H. (1991). Amino acid substrate specificity of *Escherichia coli* phenylalanyl-tRNA synthetase altered by distinct mutations. *J. Mol. Biol.* 222, 99–124. doi: 10.1016/0022-2836(91)90740-w

Kharade, S. S., and McBride, M. J. (2015). *Flavobacterium johnsoniae* PorV is required for secretion of a subset of proteins targeted to the type IX secretion system. *J. Bacteriol.* 197, 147–158. doi: 10.1128/JB.02085-14

Kim, H., Lee, H., and Shin, D. (2012). The FeoA protein is necessary for the FeoB transporter to import ferrous iron. *Biochem. Biophys. Res. Commun.* 423, 733–738. doi: 10.1016/j.bbrc.2012.06.027

Kristich, C. J., Chandler, J. G., and Dunny, G. M. (2007). Development of a host-genotype-independent counterselectable marker and a high-frequency conjugative delivery system and their use in genetic analysis of *Enterococcus faecalis*. *Plasmid* 57, 131–144. doi: 10.1016/j.plasmid.2006.08.003

Lavrrar, J. L., and McIntosh, M. A. (2003). Architecture of a Fur binding site: a comparative analysis. *J. Bacteriol.* 185, 2194–2202. doi: 10.1128/JB.185.7.2194-2202.2003

Ledala, N., Sengupta, M., Muthaiyan, A., Wilkinson, B. J., and Jayaswal, R. K. (2010). Transcriptomic response of *Listeria monocytogenes* to iron limitation and fur mutation. *Appl. Environ. Microbiol.* 76, 406–416.

Lemaître, C., Bidet, P., Benoist, J. F., Schlemmer, D., Sobral, E., d'Humières, C., et al. (2014). The *ssbL* gene harbored by the ColV plasmid of an *Escherichia coli* neonatal meningitis strain is an auxiliary virulence factor boosting the production of siderophores through the shikimate pathway. *J. Bacteriol.* 196, 1343–1349. doi: 10.1128/JB.01153-13

Lim, C. K., Hassan, K. A., Tetu, S. G., Loper, J. E., and Paulsen, I. T. (2012). The effect of iron limitation on the transcriptome and proteome of *Pseudomonas fluorescens* Pf-5. *PLoS ONE* 7:e39139. doi: 10.1371/journal.pone.0039139

Lin, C., Wu, C., Chen, Y., Lai, Y., Chi, C., Lin, J., et al. (2011). Fur regulation of the capsular polysaccharide biosynthesis and iron-acquisition systems in *Klebsiella pneumoniae* CG43. *Microbiology* 157, 419–429. doi: 10.1099/mic.0.044065-0

Liu, M., Wang, M., Zhu, D., Wang, M., Jia, R., Chen, S., et al. (2016). Investigation of TbfA in *Riemerella anatipestifer* using plasmid-based methods for gene over-expression and knockdown. *Sci Rep.* 6:37159. doi: 10.1038/srep37159

Loh, H., Teo, T. P., and Tan, H. C. (1992). Serotypes of *'Pasteurella' anatipestifer* isolates from ducks in Singapore: a proposal of new serotypes. *Avian Pathol.* 21, 453–459. doi: 10.1080/03079459208418863

Lu, F., Miao, S., Tu, J., Ni, X., Xing, L., Yu, H., et al. (2013). The role of TonB-dependent receptor TbdR1 in *Riemerella anatipestifer* in iron acquisition and virulence. *Vet. Microbiol.* 167, 713–718. doi: 10.1016/j.vetmic.2013.08.020

Marlovits, T. C., Haase, W., Herrmann, C., Aller, S. G., and Unger, V. M. (2002). The membrane protein FeoB contains an intramolecular G protein essential for Fe(II) uptake in bacteria. *Proc. Natl. Acad. Sci. U.S.A.* 99, 16243–16248. doi: 10.1073/pnas.242338299

Massé, E., Vanderpool, C. K., and Gottesman, S. (2005). Effect of RyhB small RNA on global iron use in *Escherichia coli*. *J. Bacteriol.* 187, 6962–6971. doi: 10.1128/JB.187.20.6962-6971.2005

Mathieu, S., Cissé, C., Vitale, S., Ahmadova, A., Degardin, M., Pérard, J., et al. (2016). From peptide aptamers to inhibitors of FUR, bacterial transcriptional regulator of iron homeostasis and virulence. *ACS Chem. Biol.* 11, 2519–2528. doi: 10.1021/acschembio.6b00360

Mey, A. R., Wyckoff, E. E., Kanukurthy, V., Fisher, C. R., and Payne, S. M. (2005). Iron and fur regulation in *Vibrio cholerae* and the role of fur in virulence. *Infect. Immun.* 73, 8167–8178. doi: 10.1128/IAI.73.12.8167-8178.2005

Nyquist, R. M., Heitbrink, D., Bolwien, C., Wells, T. A., Gennis, R. B., and Heberle, J. (2001). Perfusion-induced redox differences in cytochrome c oxidase: ATR/FT-IR spectroscopy. *FEBS Lett.* 505, 63–67. doi: 10.1016/S0014-5793(01)02769-7

Outten, F. W., Djaman, O., and Storz, G. (2004). A suf operon requirement for Fe–S cluster assembly during iron starvation in *Escherichia coli*. *Mol. Microbiol.* 52, 861–872. doi: 10.1111/j.1365-2958.2004.04025.x

Pi, H., Patel, S. J., Argüello, J. M., and Helmann, J. D. (2016). The *Listeria monocytogenes* Fur-regulated virulence protein FrvA is an Fe(II) efflux P1B4 -type ATPase. *Mol. Microbiol.* 100, 1066–1079. doi: 10.1111/mmi.13368

Pich, O. Q., Carpenter, B. M., Gilbreath, J. J., and Merrell, D. S. (2012). Detailed analysis of *Helicobacter pylori* Fur-regulated promoters reveals a Fur box core sequence and novel Fur-regulated genes. *Mol. Microbiol.* 84, 921–941. doi: 10.1111/j.1365-2958.2012.08066.x

Pieper, R., Huang, S. T., Parmar, P. P., Clark, D. J., Alami, H., Fleischmann, R. D., et al. (2010). Proteomic analysis of iron acquisition, metabolic and regulatory responses of *Yersinia pestis* to iron starvation. *BMC Microbiol.* 10:30. doi: 10.1186/1471-2180-10-30

Porcheron, G., and Dozois, C. M. (2015). Interplay between iron homeostasis and virulence: Fur and RyhB as major regulators of bacterial pathogenicity. *Vet. Microbiol.* 179, 2–14. doi: 10.1016/j.vetmic.2015.03.024

Postle, K., and Kadner, R. J. (2003). Touch and go: tying TonB to transport. *Mol. Microbiol.* 49, 869–882. doi: 10.1046/j.1365-2958.2003.03629.x

Prévost, K., Salvail, H., Desnoyers, G., Jacques, J. F., Phaneuf, E., and Massé, E. (2007). The small RNA RyhB activates the translation of shiA mRNA encoding a permease of shikimate, a compound involved in siderophore synthesis. *Mol. Microbiol.* 64, 1260–1273. doi: 10.1111/j.1365-2958.2007.05733.x

Reed, L. J., and Muench, H. (1938). A simple method of estimating fifty per cent endpoints. *Am. J. Epidemiol.* 27, 493–497. doi: 10.1093/oxfordjournals.aje.a118408

Salvail, H., Lanthier-Bourbonnais, P., Sobota, J. M., Caza, M., Benjamin, J. A., Mendieta, M. E., et al. (2010). A small RNA promotes siderophore production through transcriptional and metabolic remodeling. *Proc. Natl. Acad. Sci. U.S.A.* 107, 15223–15228. doi: 10.1073/pnas.1007805107

Simpson, W., Olczak, T., and Genco, C. A. (2000). Characterization and expression of HmuR, a TonB-dependent hemoglobin receptor of *Porphyromonas gingivalis*. *J. Bacteriol.* 182, 5737–5748. doi: 10.1128/JB.182.20.5737-5748.2000

Steininger, C., Reiner-Rozman, C., Schwaighofer, A., Knoll, W., and Naumann, R. L. C. (2016). Kinetics of cytochrome c oxidase from *R. sphaeroides* initiated by direct electron transfer followed by tr-SEIRAS. *Bioelectrochemistry.* 112, 1–8. doi: 10.1016/j.bioelechem.2016.06.005

Stibitz, S. (1994). Use of conditionally counterselectable suicide vectors for allelic exchange. *Meth. Enzymol.* 235, 458–465. doi: 10.1016/0076-6879(94)35161-9

Tu, J., Lu, F., Miao, S., Ni, X., Jiang, P., Yu, H., et al. (2014). The siderophore-interacting protein is involved in iron acquisition and virulence of *Riemerella anatipestifer* strain CH3. *Vet. Microbiol.* 168, 395–402. doi: 10.1016/j.vetmic.2013.11.027

Vasil, M. L., and Ochsner, U. A. (1999). The response of *Pseudomonas aeruginosa* to iron: genetics, biochemistry and virulence. *Mol. Microbiol.* 34, 399–413. doi: 10.1046/j.1365-2958.1999.01586.x

Visca, P., Leoni, L., Wilson, M. J., and Lamont, I. L. (2002). Iron transport and regulation, cell signalling and genomics: lessons from *Escherichia coli* and *Pseudomonas*. *Mol. Microbiol.* 45, 1177–1190. doi: 10.1046/j.1365-2958.2002.03088.x

Vuoristo, K. S., Mars, A. E., Sanders, J. P. M., Eggink, G., and Weusthuis, R. A. (2016). Metabolic engineering of TCA cycle for production of chemicals. *Trends Biotechnol.* 34, 191–197. doi: 10.1016/j.tibtech.2015.11.002

Xie, H., Buschmann, S., Langer, J. D., Ludwig, B., and Michel, H. (2014). Biochemical and biophysical characterization of the two isoforms of cbb3-type cytochrome c oxidase from *Pseudomonas stutzeri*. *J. Bacteriol.* 196, 472–482. doi: 10.1128/JB.01072-13

Xie, Z., Okinaga, T., Qi, F., Zhang, Z., and Merritt, J. (2011). Cloning-independent and counterselectable markerless mutagenesis system in *Streptococcus mutans*. *Appl. Environ. Microbiol.* 77, 8025–8033. doi: 10.1128/AEM.06362-11

Yankovskaya, V., Horsefield, R., Törnroth, S., Luna-Chavez, C., Miyoshi, H., Léger, C., et al. (2003). Architecture of succinate dehydrogenase and reactive oxygen species generation. *Science* 299, 700–704. doi: 10.1126/science.1079605

Yuhara, S., Komatsu, H., Goto, H., Ohtsubo, Y., Nagata, Y., and Tsuda, M. (2008). Pleiotropic roles of iron-responsive transcriptional regulator Fur in B*urkholderia multivorans*. *Microbiology* 154, 1763–1774. doi: 10.1099/mic.0.2007/015537-0

Zeng, X., Xu, F., and Lin, J. (2013). Specific TonB-ExbB-ExbD energy transduction systems required for ferric enterobactin acquisition in *Campylobacter*. *FEMS Microbiol. Lett.* 347, 83–91. doi: 10.1111/1574-6968.12221

Zhou, C., Shi, L., Ye, B., Feng, H., Zhang, J., Zhang, R., et al. (2016). *pheS* *, an effective host-genotype-independent counter-selectable marker for marker-free chromosome deletion in *Bacillus amyloliquefaciens*. *Appl. Microbiol. Biotechnol.* 101, 217–227. doi: 10.1007/s00253-016-7906-9

Conflict of Interest Statement: The authors declare that the research was conducted in the absence of any commercial or financial relationships that could be construed as a potential conflict of interest.

frontiers in Cellular and Infection Microbiology

ORIGINAL RESEARCH
published: 11 April 2017
doi: 10.3389/fcimb.2017.00110

Genetic and Dietary Iron Overload Differentially Affect the Course of *Salmonella* Typhimurium Infection

Manfred Nairz[1], Andrea Schroll[1], David Haschka[1], Stefanie Dichtl[1], Piotr Tymoszuk[1], Egon Demetz[1], Patrizia Moser[2], Hubertus Haas[3], Ferric C. Fang[4,5], Igor Theurl[1] and Günter Weiss[1]*

[1] Department of Internal Medicine II, Infectious Diseases, Immunology, Rheumatology, Pneumology, Medical University of Innsbruck, Innsbruck, Austria, [2] Department of Pathology, Medical University of Innsbruck, Innsbruck, Austria, [3] Division of Molecular Microbiology, Biocenter, Medical University of Innsbruck, Innsbruck, Austria, [4] Department of Laboratory Medicine, University of Washington, Seattle, WA, USA, [5] Department of Microbiology, University of Washington, Seattle, WA, USA

Genetic and dietary forms of iron overload have distinctive clinical and pathophysiological features. HFE-associated hereditary hemochromatosis is characterized by overwhelming intestinal iron absorption, parenchymal iron deposition, and macrophage iron depletion. In contrast, excessive dietary iron intake results in iron deposition in macrophages. However, the functional consequences of genetic and dietary iron overload for the control of microbes are incompletely understood. Using $Hfe^{+/+}$ and $Hfe^{-/-}$ mice in combination with oral iron overload in a model of *Salmonella enterica* serovar Typhimurium infection, we found animals of either genotype to induce hepcidin antimicrobial peptide expression and hypoferremia following systemic infection in an Hfe-independent manner. As predicted, $Hfe^{-/-}$ mice, a model of hereditary hemochromatosis, displayed reduced spleen iron content, which translated into improved control of *Salmonella* replication. *Salmonella* adapted to the iron-poor microenvironment in the spleens of $Hfe^{-/-}$ mice by inducing the expression of its siderophore iron-uptake machinery. Dietary iron loading resulted in higher bacterial numbers in both WT and $Hfe^{-/-}$ mice, although Hfe deficiency still resulted in better pathogen control and improved survival. This suggests that Hfe deficiency may exert protective effects in addition to the control of iron availability for intracellular bacteria. Our data show that a dynamic adaptation of iron metabolism in both immune cells and microbes shapes the host-pathogen interaction in the setting of systemic *Salmonella* infection. Moreover, Hfe-associated iron overload and dietary iron excess result in different outcomes in infection, indicating that tissue and cellular iron distribution determines the susceptibility to infection with specific pathogens.

Keywords: iron, macrophage, hepcidin, lipocalin, *Salmonella*, infection, siderophore

OPEN ACCESS

Edited by:
Susu M. Zughaier, Emory University, USA

Reviewed by:
Manuela Raffatellu, University of California, Irvine, USA
Susan M. Bueno, Pontifical Catholic University of Chile, Chile

****Correspondence:***
Manfred Nairz
manfred.nairz@i-med.ac.at

Received: *27 January 2017*
Accepted: *20 March 2017*
Published: *11 April 2017*

Citation:
Nairz M, Schroll A, Haschka D, Dichtl S, Tymoszuk P, Demetz E, Moser P, Haas H, Fang FC, Theurl I and Weiss G (2017) Genetic and Dietary Iron Overload Differentially Affect the Course of Salmonella Typhimurium Infection. Front. Cell. Infect. Microbiol. 7:110. doi: 10.3389/fcimb.2017.00110

INTRODUCTION

HFE encodes an atypical MHC class I molecule which plays a major role in the regulation of iron homeostasis under basal conditions (Feder et al., 1996; Ludwiczek et al., 2004). *HFE* mutations, especially the homozygous *C282Y* substitution, result in type I (AKA classical) hereditary hemochromatosis (HH) (Camaschella et al., 2002; Pietrangelo, 2004; Weiss, 2010), the

most frequent form of HH mainly found in people of Northern or Western European ancestry. HH is characterized by reduced serum levels of the antimicrobial peptide Hamp (hepcidin) and increased duodenal absorption of iron via divalent metal transporter 1 (Dmt1) and ferroportin 1 (Fpn1) despite progressive iron overload in parenchymal organs including the liver, pancreas, and heart (Zoller et al., 1999, 2001; Bridle et al., 2003; Pietrangelo, 2004; Bardou-Jacquet et al., 2013). The precise role of the HFE protein, however, remains incompletely understood. HFE binds to transferrin receptor 1 (TfR1) thus lowering its affinity for iron-laden transferrin (Feder et al., 1998; Lebrón et al., 1998; Bennett et al., 2000). This interaction controls cellular iron acquisition while also modifying the expression of the key iron-regulatory hormone Hamp (Ahmad et al., 2002; Nicolas et al., 2003; Ludwiczek et al., 2005; Vujic Spasic et al., 2008). The latter mechanism involves the sensing of circulating iron levels by TfR1 and TfR2, which reciprocally complex with HFE expressed on hepatocytes (Schmidt et al., 2008; Wallace et al., 2009). Mutations in *HFE* (or *TFR2*) impair this iron-sensing mechanism, resulting in the insufficient generation of Hamp and increased iron absorption (Goswami and Andrews, 2006; D'Alessio et al., 2012). Of note, macrophages lacking HFE display an iron-poor phenotype which has been attributed to enhanced iron export (Cairo et al., 1997; Drakesmith et al., 2002; Wang et al., 2003).

Systemic iron availability, erythropoietic iron demand, hypoxia, hormones, and inflammatory signals are key factors that modulate the production of the iron homeostatic regulator Hamp (Nemeth et al., 2004a; Bozzini et al., 2008; Theurl et al., 2010; Armitage et al., 2011; Kautz et al., 2014; Nairz et al., 2014; Canali et al., 2017). Hamp controls iron homeostasis upon binding Fpn1, which triggers Fpn1 internalization, degradation (Nemeth et al., 2004b) and blockade of iron efflux from duodenal enterocytes and macrophages, which recycle iron from senescent erythrocytes. Inflammation-driven Hamp induction thus causes iron sequestration within the mononuclear phagocyte system (MPS), which limits iron availability for extracellular pathogens (Bridle et al., 2003; Ludwiczek et al., 2003; Ganz, 2005; Theurl et al., 2008a).

In infections with the intracellular bacterium *Salmonella enterica* serovar Typhimurium, macrophages constitute an important habitat for pathogen replication and persistence (Malik-Kale et al., 2011). Because many bacteria are highly dependent on a sufficient supply of iron for their growth and pathogenicity, macrophage iron homeostasis is an important determinant of disease outcome (Nairz et al., 2014). On one hand, macrophage iron overload is associated with the inhibition of IFN-γ-driven antimicrobial immune effector pathways such as nitric oxide synthase 2 (Nos2) expression, resulting in impaired control of intracellular microbes (Weiss et al., 1994; Mencacci et al., 1997; Oexle et al., 2003). On the other hand, severe iron depletion of the host may result in reduced generation of ROS, which also impairs host defenses. In parallel, iron withholding from pathogens constitutes an efficient host defense strategy (Soares and Weiss, 2015). However, macrophages also contribute to host defense by the production of T-cell stimulatory cytokines and antimicrobial peptides (Graziadei et al., 1997). One of the latter, lipocalin 2 (Lcn2; also known as neutrophil gelatinase-associated lipocalin, siderocalin or 24p3), is secreted by neutrophils and macrophages in response to LPS, IL-1ß, IL-17, and IL-22 (Flo et al., 2004; Shen et al., 2006). In its best characterized function, Lcn2 captures iron-laden bacterial siderophores, small molecules that are enzymatically synthesized and actively secreted by many microbes to bind ferric iron with extraordinarily high affinity (Bachman et al., 2009). Lcn2-sensitive siderophores include enterobactin, carboxy-mycobactins, and bacillibactin. Upon neutralization of these siderophores, Lcn2 contributes to innate resistance against a range of pathogenic bacteria including enterobacteriaceae, mycobacteria and *Bacillus anthracis* by limiting their access to iron (Flo et al., 2004; Berger et al., 2006).

Salmonella Typhimurium, a facultative intracellular microbe, needs to gain sufficient access to host iron resources as a prerequisite for replication and virulence (Leung and Finlay, 1991; Vazquez-Torres et al., 1999). To acquire the metal from the host and within infected macrophages, *Salmonella* has evolved both siderophore-dependent and -independent strategies. *Salmonella* synthesizes catecholate-type siderophores such as enterochelin and salmochelins to capture and internalize ferric iron via siderophore receptors (Bäumler et al., 1998; Rabsch et al., 2003; Fischbach et al., 2005). Alternatively, *Salmonella* can incorporate non-siderophore-bound ionic iron using the Feo transport system. In addition, the SitABCD system, whose primary function is bacterial manganese import, may contribute through low-affinity uptake of iron (Zaharik et al., 2004). All three pathways of bacterial iron uptake are linked to *Salmonella* virulence (Tsolis et al., 1996; Janakiraman and Slauch, 2000; Boyer et al., 2002; Crouch et al., 2008; Kim et al., 2013).

Given the central importance of iron for the growth and proliferation of intracellular pathogens such as *Salmonella* and the important role of Hfe in the regulation of systemic iron balance, we performed experiments to assess the influence of Hfe and/or dietary iron overload on host iron homeostasis and immunity in response to *S.* Typhimurium infection. This is of specific interest because Hfe results in macrophage iron depletion whereas dietary iron overload leads to iron accumulation within the MPS.

MATERIALS AND METHODS

Salmonella Infection *In vivo*

All animal experiments described were performed in accordance with Austrian legal requirements. Design of the animal experiments was approved by the Austrian Federal Ministry of Science and Research (approvals BMWF-66.011/0074-C/GT/2007 and /0154-II/3b/2010). Mice were maintained at the central animal facilities of the Medical University of Innsbruck and given free access to water and food. $Hfe^{-/-}$ mice were generated as described (Bahram et al., 1999; Flo et al., 2004), crossed back on a C57BL/6 background for at least 10 generations and transferred to the SPF unit of the local Animal Facility by means of embryonic transfer. $Hfe^{+/-}$ mice were intercrossed and offspring were genotyped using the following primers (obtained from Microsynth): *Hfe* fw: 5′-GAATTAACA

GGCCGTTTCTAAAG-3′, *Hfe* rev: 5′-CTTGGAGTAGTGGCT CACACT-3′, *Hfe* neo: 5′-GAGATCAGCAGCCTCTGTTCC-3′.

For *in vivo* infection experiments (Supplementary Figure 1), male mice were used at 20–26 week of age and fed either an iron-enriched diet (C1038 from Altromin) supplemented with 25 g/kg carbonyl iron (Sigma) or a standard diet (180 mg Fe/kg, C1000 from Altromin) 3 week before and during infection. Mice were infected i.p. with 500 CFU *S.* Typhimurium strain ATCC14028 suspended in 200 μl PBS. Animals were monitored 3 times daily for 10 days for signs of illness, and moribund mice were euthanized. Forty-eight and ninety-six hours post-infection, mice were randomly selected for the determination of colony counts. Bacterial load in livers and spleens was determined by plating serial dilutions of organ homogenates on LB agar under sterile conditions. Mice selected for the determination of colony counts were not considered for the recording of survival times.

Blood Counts

Blood samples were drawn under anesthesia by retroorbital puncture and collected in heparinized tubes. An aliquot of heparinized blood was used for complete blood count analysis on a Vet-ABC Animal blood counter (Scil animal care company GmbH).

Measurement of Iron Parameters

Serum iron was measured using the QuantiChrom Iron Assay kit (BioAssay Systems) according to the manufacturer's instructions. Serum FT was measured by a specific ELISA kit (LifeSpan BioSciences) according to the manufacturer's protocol (Theurl et al., 2016). Total tissue iron content was measured as described (Sonnweber et al., 2012).

Histology

Histological examinations of tissues were performed on formalin-fixed tissue sections stained with hematoxylin and eosin (HE) according to a standard protocol (Nairz et al., 2011). Images with HE staining were acquired using a Nikon-Eclipse 80i microscope equipped with a 4x objective with a 0.10 numerical aperture. Image acquisition was performed using NIS-Elements BR3 software.

Cell Culture, *Salmonella* Infection *In vitro* and Determination of Bacterial Iron Acquisition

Thioglycolate-elicited primary peritoneal macrophages were harvested as described (Schleicher et al., 2005) from C57BL/6 mice of indicated genotypes (detailed below), matched for sex and age, and cultured in RPMI (purchased from Biochrom AG) containing 5% heat-inactivated fetal calf serum (FCS; from PAA), 100 U/mL penicillin, 0.1 mg/mL streptomycin and 10 mM HEPES (all from Sigma). After a 24 h incubation period, macrophages were extensively washed with phosphate-buffered saline (PBS purchased from Invitrogen) and incubated in complete RPMI without antibiotics. Only cell preparations of at least 90–95% purity, as determined by F4/80 surface expression in FACS analysis, were used for subsequent experiments. Macrophages were infected with *S.* Typhimurium ATCC14028 at a multiplicity of infection (MOI) of 10.

Measurement of bacterial iron acquisition was performed as described elsewhere (Nairz et al., 2008). Briefly, *Salmonella*-infected macrophages were washed three times and resuspended in serum-free HEPES-buffered RPMI. After the addition of 5 μM ^{59}Fe as citrate (NTBI) or loaded onto human apo-transferrin (TBI; Sigma), cells were incubated for an additional 8 h. Intracellular bacilli were harvested according to a modified protocol as described (Olakanmi et al., 2002; Nairz et al., 2008). An aliquot of the bacterial suspension was plated in serial dilutions onto agar plates to quantify released bacteria, while the remaining volume was filtered through centrifugal filter devices with a PDVF membrane of 0.22 μm pore size (Millipore). Filters containing the trapped bacteria were used to measure *Salmonella*-associated ^{59}Fe with a γ-counter. No association of ^{59}Fe to *S.* Typhimurium that had been heat-inactivated at 70°C for 20 min could be detected.

RNA Extraction and Quantitative Real-Time PCR

Preparation of total RNA and quantification of mRNA expression by Taqman® or SYBR Green® RT-PCR following reverse transcription was performed exactly as described (Crawford et al., 2016). Murine primers and probes (Microsynth), the latter carrying 5′-FAM and 3′-BHQ1 labels, were used as described elsewhere (Ludwiczek et al., 2005; Theurl et al., 2008b). Bacterial primers and probes have been described (Bearson et al., 2008; Crawford et al., 2016).

Statistical Analysis

Statistical analysis was carried out using a SPSS statistical package. Calculations for statistical differences between various groups were carried out by ANOVA and Tukey's correction for multiple tests. Otherwise, a two-tailed unpaired Student's *t*-test was used. For comparison of survival between subgroups, the Wilcoxon (Gehan) statistic was used. Non-parametric variables (CFU and serum FT) were log-transformed prior to testing. $P < 0.05$ was used to determine statistical significance, $0.05 \leq P < 1.0$ was considered a statistical trend and depicted.

RESULTS

Influence of Hfe, Dietary Iron Challenge and *Salmonella* Infection on Iron Parameters

To better understand the influence of Hfe and dietary iron loading on iron homeostasis and the outcome of infection, we used a well-established model of systemic *Salmonella* infection. Wildtype (WT) C57BL/6 ($Hfe^{+/+}$) and congenic $Hfe^{-/-}$ mice were fed either a standard rodent diet with adequate iron content (IA) or an iron-enriched (IE) diet for 3 weeks prior to and during infection. Congenic WT and $Hfe^{-/-}$ mice were then systemically infected with 500 colony-forming units (CFU) of *Salmonella enterica* serovar Typhimurium ATCC14028 (*S.* Typhimurium; *S.* Tm.) via intraperitoneal (i.p.) injection (as delineated in

Supplementary Figure 1). Mock-infected controls received a single i.p. injection of PBS as a control (Ctrl.). Animals were monitored for up to 10 days. On days 2 and 4 post-infection, randomly selected animals were sacrificed and bacterial loads (days 2 and 4), erythroid (Supplementary Figures 2B,C) and iron indices as well as the expression of iron metabolic genes (day 2) were evaluated.

As predicted, under control conditions $Hfe^{-/-}$ mice fed an iron-adequate (IA) diet showed elevated serum iron and serum ferritin (FT) levels as compared to $Hfe^{+/+}$ controls. Both $Hfe^{+/+}$ and $Hfe^{-/-}$ responded to systemic infection with a reduction of serum iron concentrations (hypoferremia) (**Figure 1A**). Of interest, serum iron levels increased upon dietary iron challenge independent of the *Hfe* genotype, as $Hfe^{-/-}$ and congenic $Hfe^{+/+}$ mice displayed comparable serum iron levels on an IE diet. Intriguingly, $Hfe^{+/+}$ and $Hfe^{-/-}$ mice maintained on an IE diet prior to and during *Salmonella* infection had even higher serum iron levels as compared to uninfected animals on an IE diet and did not mount a hypoferremic response. Serum FT levels were dramatically increased during dietary iron overload, whereas the stimulatory effect of *Salmonella* infection on serum FT levels was minimal (**Figure 1B**).

While $Hfe^{-/-}$ mice tended to have lower hepatic Hamp mRNA expression as compared to congenic WT mice, the

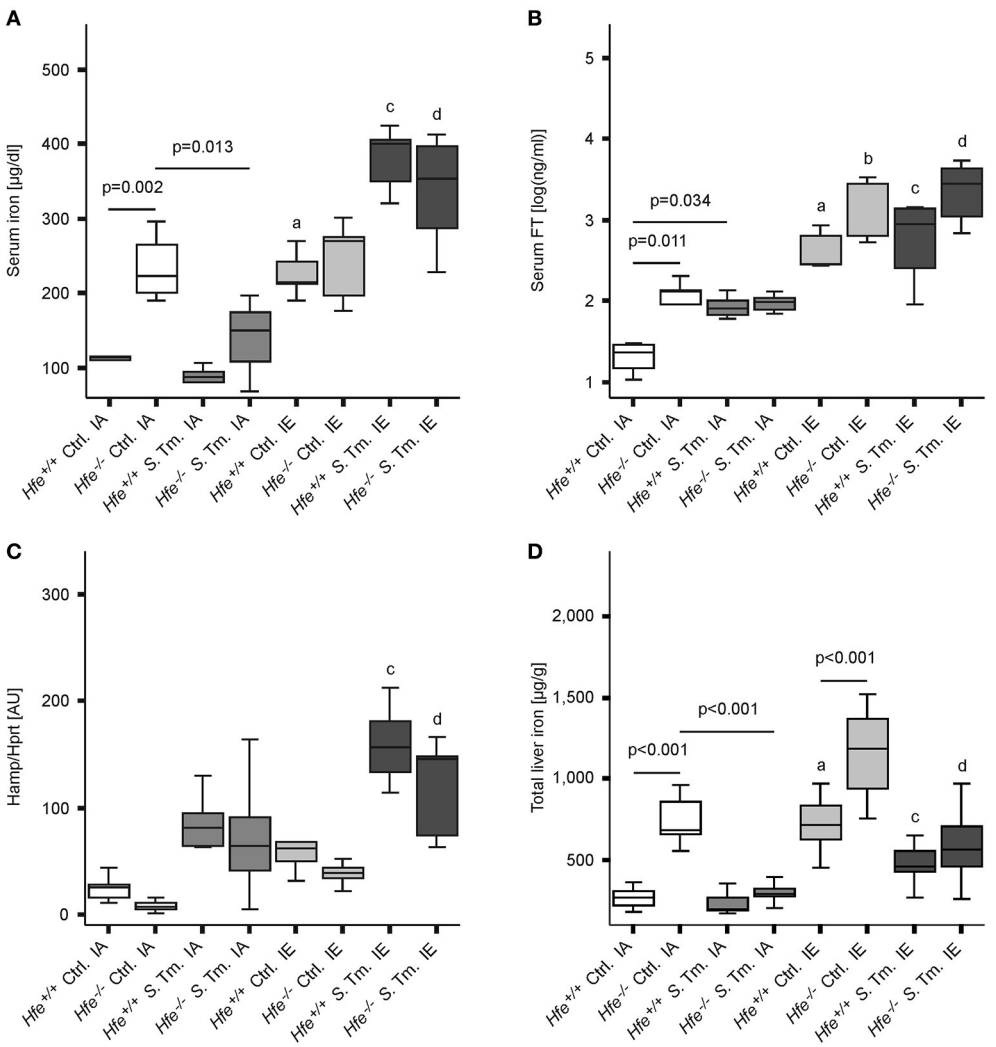

FIGURE 1 | Influence of Hfe, dietary iron challenge and *Salmonella* infection on systemic iron parameters. $Hfe^{-/-}$ and congenic C57BL/6 WT animals ($Hfe^{+/+}$) were fed either a standard iron-adequate diet (IA) or an iron-enriched diet (IE) and infected i.p. with 500 CFU of *S.* Typhimurium (*S.* Tm.). Mock-infected controls (Ctrl.) received diluent. Serum iron **(A)** and ferritin (FT) levels **(B)** were measured after 48 h. In parallel, the expression of Hamp mRNA **(C)** in the liver was determined relative to the house-keeping gene Hprt by quantitative RT-PCR. Total liver iron content 48 post-infection was measured colorimetrically and normalized for wet tissue weight **(D)**. Data were compared by means of ANOVA with Tukey's *post hoc* test. Values are depicted as lower quartile, median and upper quartile (boxes), and minimum/maximum ranges. Statistical significant differences within each diet group are indicated. Additional letters represent statistically significant differences ($P < 0.05$) as follows: (a) $Hfe^{+/+}$ Ctrl. IA vs. $Hfe^{+/+}$ Ctrl. IE; (b) $Hfe^{-/-}$ Ctrl. IA vs. $Hfe^{-/-}$ Ctrl. IE; (c) $Hfe^{+/+}$ *S.* Tm. IA vs. $Hfe^{+/+}$ *S.* Tm. IE; $Hfe^{-/-}$ *S.* Tm. IA vs. $Hfe^{-/-}$ *S.* Tm. IE. $n = 7$–10 per group.

induced Hamp expression in response to infection or dietary iron overload remained intact in $Hfe^{-/-}$ mice compared to WT littermates (**Figure 1C**). As expected, $Hfe^{-/-}$ mice had an elevated total iron content in the liver, and the IE diet resulted in hepatic iron accumulation (**Figure 1D**). Serum IL-6 concentrations were unaffected by the Hfe genotype (Supplementary Figure 2A).

As previously shown (Cairo et al., 1997; Nairz et al., 2009), $Hfe^{-/-}$ mice had reduced total iron content in the spleen is comparison to $Hfe^{+/+}$ mice (**Figure 2A**). Whereas, dietary iron challenge resulted in an increase in spleen iron levels, *Salmonella* infection caused a small yet significant reduction. Splenic Hamp mRNA expression was not significantly affected by either dietary iron content or infection (**Figure 2B**). In contrast, Fpn1 mRNA expression increased in response to *Salmonella* infection but was not affected by dietary iron overload or Hfe genotype (**Figure 2C**). Dmt1 and TfR1 mRNA levels were negatively affected by oral iron challenge (**Figures 2D,E**). Concurrent *Salmonella* infection reverted Dmt1 expression to basal levels, while TfR1 expression remained suppressed. However, there was no substantial influence of *Hfe* genotype on expression of these iron acquisition molecules. Splenic Lcn2 receptor (LcnR) expression was significantly reduced following *Salmonella* infection (**Figure 2F**), and Lcn2 mRNA expression in the spleen was higher in $Hfe^{-/-}$ as compared to congenic WT mice (**Figure 2G**).

Influence of Dietary Iron Content on the Course of *Salmonella* Typhimurium Infection in WT and $Hfe^{-/-}$ Mice

We next studied the influence of dietary iron overload on disease progression in systemic *Salmonella* infection in $Hfe^{-/-}$ and congenic C57BL/6 WT animals. All WT mice died by day 8 of infection independent of their dietary iron content, but animals on an iron-enriched (IE) diet succumbed 1–2 days earlier (**Figure 3A**). Of note, 33% of $Hfe^{-/-}$ mice on an iron-adequate (IA) or iron-enriched (IE) diet (3 of 9 mice in each group) survived the infection beyond day 10 of the observation period. Hepatic and splenic microbial loads of randomly selected animals were quantified on days 2 and 4 of infection. Dietary iron overload significantly increased the bacterial load in both organs in WT mice as well as in $Hfe^{-/-}$ animals 2 days post-infection (**Figures 3B,C**). By day 4 of infection, $Hfe^{-/-}$ mice fed an IE diet controlled microbial replication as efficiently as their WT littermates maintained on an IA diet (Supplementary Figures 3A,B). Moreover, tissue sections obtained on day 4 post-infection revealed that WT mice on an IA diet had microabscesses in the liver, which were partly confluent. WT mice on an IE diet also exhibited hepatic macroabscesses. In contrast, hardly any microabscesses were observed in the livers of $Hfe^{-/-}$ mice on an IA diet, and only solitary lesions were visible in $Hfe^{-/-}$ mice on an IE diet (**Figure 4A**). Similar observations were made in the spleens of *Salmonella*-infected mice on day 4 post-infection. Only $Hfe^{-/-}$ mice on an IA diet had a relatively normal spleen size (**Figure 4B**). These histopathologic findings were accompanied by corresponding alterations in spleen weight (Supplementary Figures 4A,B).

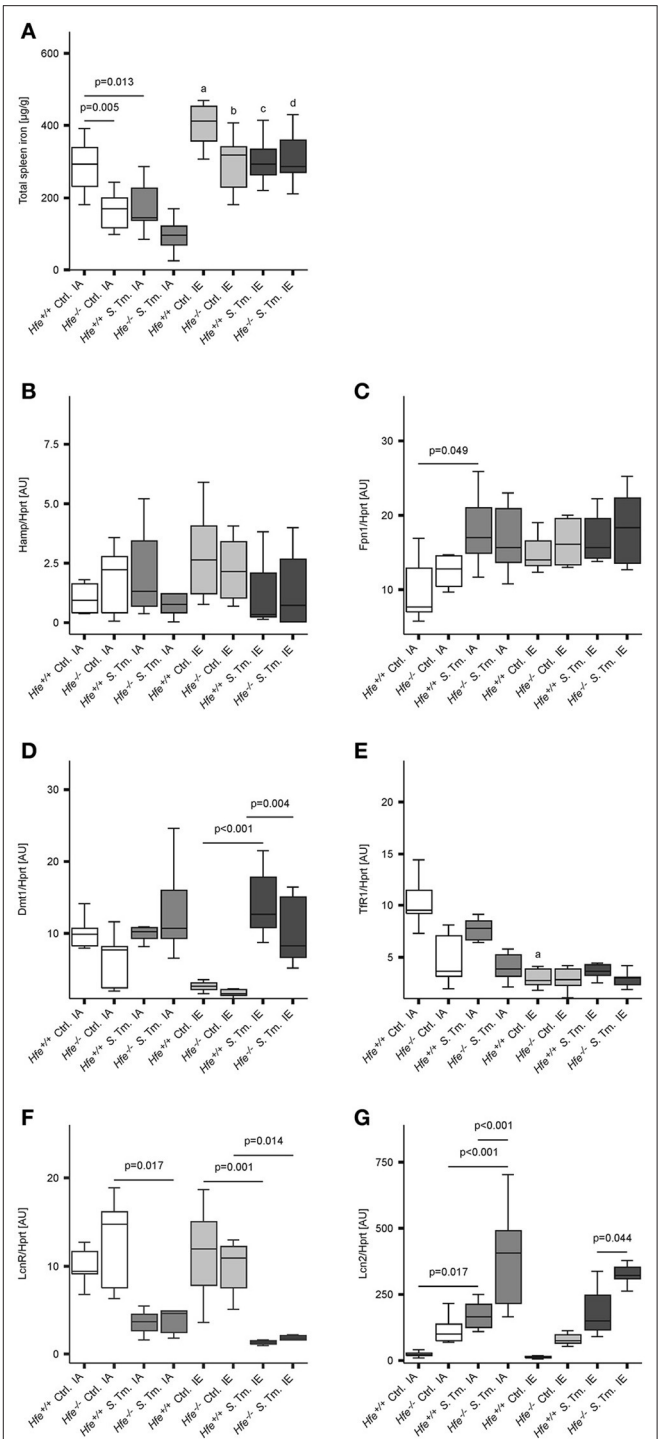

FIGURE 2 | Influence of Hfe, dietary iron challenge and *Salmonella* infection on splenic iron parameters. Total spleen iron content **(A)** and mRNA levels of iron metabolic genes **(B–G)** in the spleen as determined by quantitative RT-PCR were measured after 48 h. Hamp **(B)**, Fpn1 **(C)**, Dmt1 **(D)**, TfR1 **(E)**, LcnR **(F)**, and Lcn2 **(G)** mRNA levels were determined relative to the house-keeping gene Hprt at baseline and 48 h post-infection. Data were compared by means of ANOVA with Tukey's *post hoc* test. Values are depicted as lower quartile, median and upper quartile (boxes), and minimum/maximum ranges and only statistically significant differences are indicated exactly as described for **Figure 1**. Additional letters represent

(Continued)

FIGURE 2 | Continued
statistically significant differences ($P < 0.05$) as follows: (a) $Hfe^{+/+}$ Ctrl. IA vs. $Hfe^{+/+}$ Ctrl. IE; (b) $Hfe^{-/-}$ Ctrl. IA vs. $Hfe^{-/-}$ Ctrl. IE; (c) $Hfe^{+/+}$ *S.* Tm. IA vs. $Hfe^{+/+}$ *S.* Tm. IE; $Hfe^{-/-}$ *S.* Tm. IA vs. $Hfe^{-/-}$ *S.* Tm. IE. $n = 7$–10 per group.

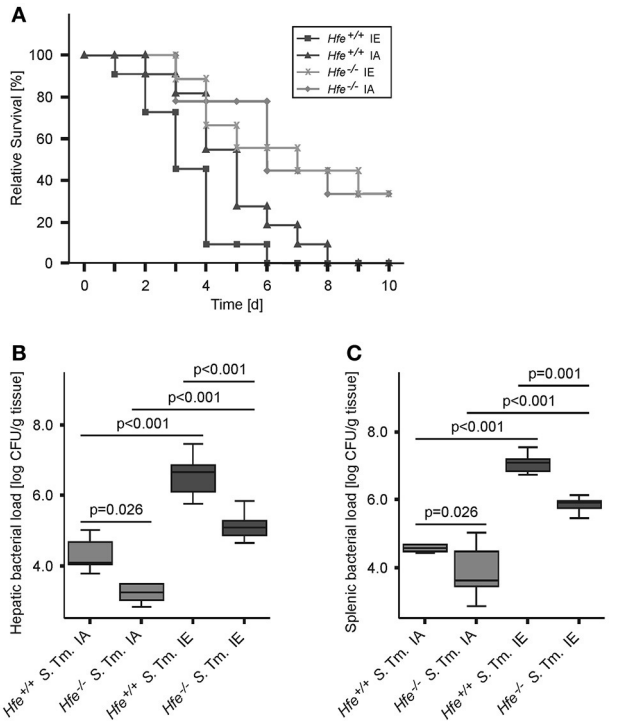

FIGURE 3 | Influence of dietary iron content on the course of *Salmonella* Typhimurium infection in *Hfe* WT and $Hfe^{-/-}$ mice. Survival during systemic infection with *Salmonella* Typhimurium was monitored over an observation period of 10 days **(A)**. Data are depicted as Kaplan-Meier curves and were compared by log rank test. $n = 9$–11 per group. Statistically signficant differences are as follows: $P = 0.031$ for $Hfe^{+/+}$ IA vs. $Hfe^{-/-}$ IA. $P = 0.028$ for $Hfe^{+/+}$ IA vs. $Hfe^{+/+}$ IE. $P = 0.954$ for $Hfe^{-/-}$ IA vs. $Hfe^{-/-}$ IE. $P = 0.002$ for $Hfe^{+/+}$ IE vs. $Hfe^{-/-}$ IE. $P = 0.041$ for $Hfe^{+/+}$ IA vs. $Hfe^{-/-}$ IE. $P = 0.003$ for $Hfe^{+/+}$ IE vs. $Hfe^{-/-}$ IA. Bacterial loads of at least 6 animals per group were determined in livers **(B)** and spleens **(C)** of randomly selected animals on d 2 post-infection. CFU data were log-transformed and compared by means of ANOVA with Tukey's *post hoc* test. All statistically significant differences are indicated as lines. Values are depicted as lower quartile, median, and upper quartile (boxes), and minimum/maximum ranges and statistical significances are indicated.

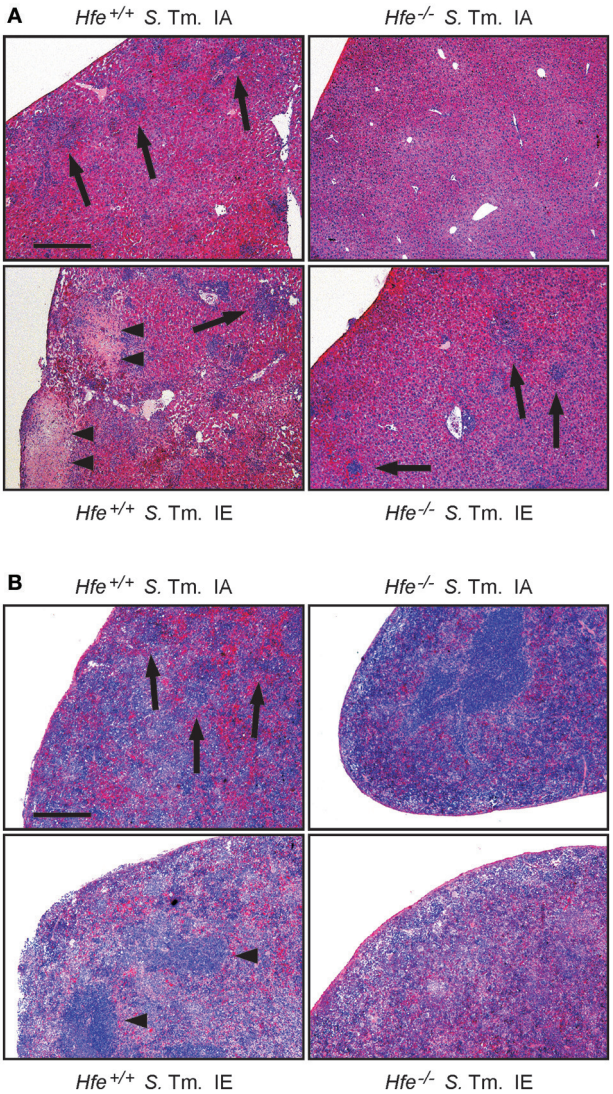

FIGURE 4 | Influence of dietary iron content on tissue damage during *Salmonella* Typhimurium infection in *Hfe* WT and $Hfe^{-/-}$ mice. HE-stained sections of livers **(A)** and spleens **(B)** of WT and $Hfe^{-/-}$ mice on day 4 of infection show macro-abscesses (arrow heads) in both organs of WT mice on an iron-excessive diet (IE) and scarce inflammatory foci (arrows) in $Hfe^{-/-}$ mice fed an iron-adequate diet (IA) with intermediate pathology in the other two treatment/genotype groups. Scale bars: 400 μm.

Classical Innate Immune Functions Are Hfe-Independent

To better define the role of Hfe and dietary iron overload in innate immune function, cytokine and antimicrobial effector system expression was measured on day 2 post-infection. Splenic mRNA levels of TNF, IL-1ß, IL-6, Nos2, and the p47 subunit of the NADPH oxidase (phox) were not affected by the Hfe-genotype (**Figures 5A–E**). Increased expression of NOS2 and IL-1ß in mice receiving an IE diet relative to those receiving an IA diet paralleled the increased number of bacteria isolated from the spleens of these groups.

Salmonella Adapts to the Iron-Restricted Myeloid Compartment of $Hfe^{-/-}$ Mice

The expression of bacterial iron uptake genes was measured in the spleens of *Salmonella*-infected mice on day 2 post-infection. We found that multiple genes involved in iron uptake were expressed at higher levels in the spleens of $Hfe^{-/-}$ mice on an IA diet as compared to the spleens of WT mice receiving the same diet. These genes encoded outer membrane siderophore receptors IroN, FepA, and CirA, as well as the siderophore exporter IroC (**Figures 6A–D**). In contrast, expression of FeoB (**Figure 6E**) and SitB (**Figure 6F**) were not substantially affected

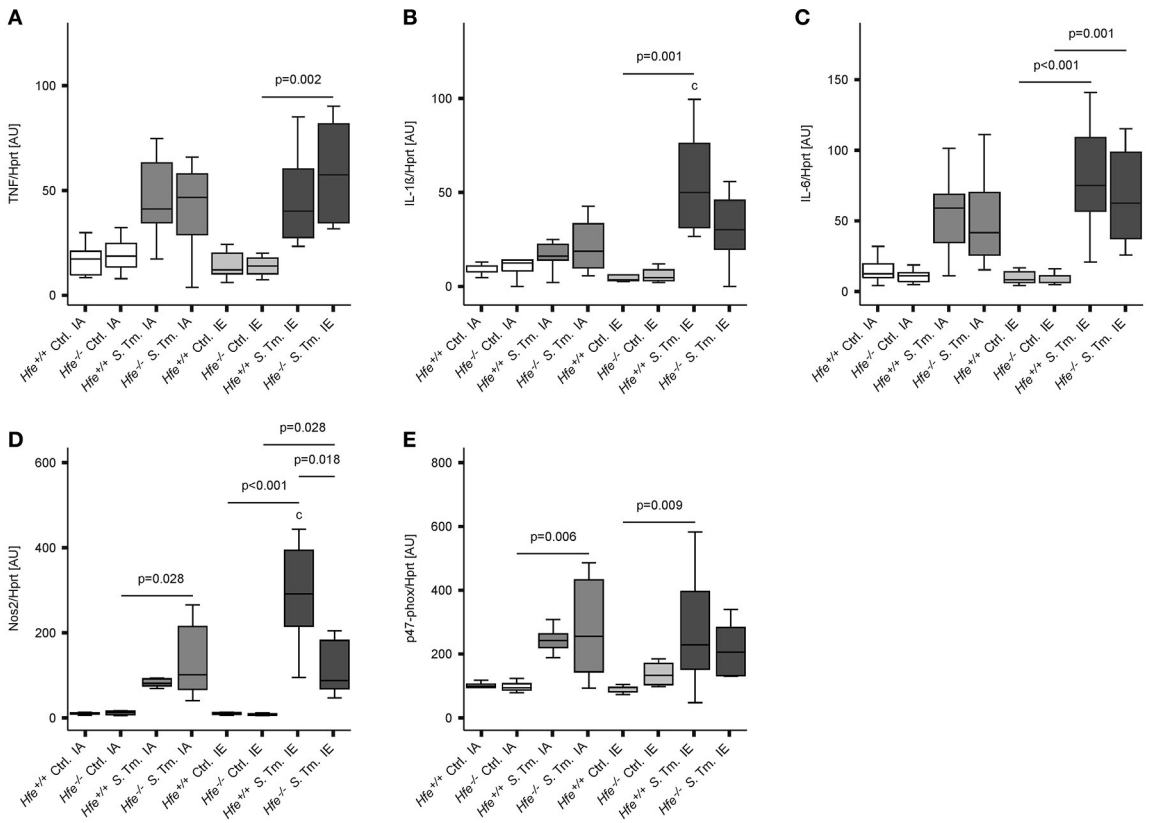

FIGURE 5 | Classical innate immune functions are Hfe-independent. The expression of TNF-α **(A)**, IL-1ß **(B)**, IL-6 **(C)**, Nos2 **(D)**, and the p47 phox subunit **(E)** in the spleen was determined relative to the housekeeping gene Hprt by quantitative RT-PCR. Data were analyzed and presented exactly as described in the legend to **Figure 1**. All statistically significant differences are indicated. Additional letters represent statistically significant differences ($P < 0.05$) as follows: (c) $Hfe^{+/+}$ *S*. Tm. IA vs. $Hfe^{+/+}$ *S*. Tm. IE. $n = 7$–10 per group.

by the Hfe status of the host. Notably, no differential induction of bacterial iron genes was observed when WT and $Hfe^{-/-}$ mice were on an IE diet, which resulted in splenic iron overload.

In keeping with the induction of siderophore-mediated iron uptake pathways in *Salmonella* residing in the spleens of IA diet-fed $Hfe^{-/-}$ mice *in vivo*, we observed that the uptake of host derived ^{59}Fe by intracellular *Salmonella*, provided as NTBI or TBI, was reduced in $Hfe^{-/-}$ peritoneal macrophages infected *in vitro* relative to congenic WT macrophages (**Figures 7A,B**).

DISCUSSION

Salmonella Typhimurium causes a systemic disease in mice characterized by a tropism for and replication within professional phagocytes (Richter-Dahlfors et al., 1997; Coburn et al., 2007). *S.* Typhimurium invades its preferred host cell type both by phagocytic uptake and active invasion (Pfeifer et al., 1999). Virulence factors such as those encoded by *Salmonella* Pathogenicity Island-2 are essential for both intracelullar survival and virulence (Hensel et al., 1995, 1998), suggesting that the ability to infect and replicate within macrophages provides a major benefit for the pathogen (Leung and Finlay, 1991). Nutrient availability within this host cell niche is therefore an important factor in *Salmonella* pathogenesis (Carver, 2014).

Iron is one of the essential nutrients that hold a central position in the interplay of host and pathogen (Weinberg, 1974; Schaible and Kaufmann, 2005; Skaar, 2009; Nairz et al., 2010; Drakesmith and Prentice, 2012; Ganz and Nemeth, 2015; Soares and Weiss, 2015). Sufficient access to this trace element is therefore a major determinant of the outcome of *Salmonella* infection. In general, the host response to any bacterial infection involves the restriction of serum iron levels (hypoferremia) through a combined limitation of intestinal iron absorption and macrophage iron recycling. Hamp and its receptor Fpn1 are primary mediators of the hypoferremia, and thereby influence *Salmonella*-host interactions (Nairz et al., 2013; Kim et al., 2014; Armitage et al., 2016). However, a range of additional genetic and environmental factors also influence bacterial iron availability during *Salmonella* infections.

The data presented herein suggest that both the local and systemic availability of iron within the mammalian host affect

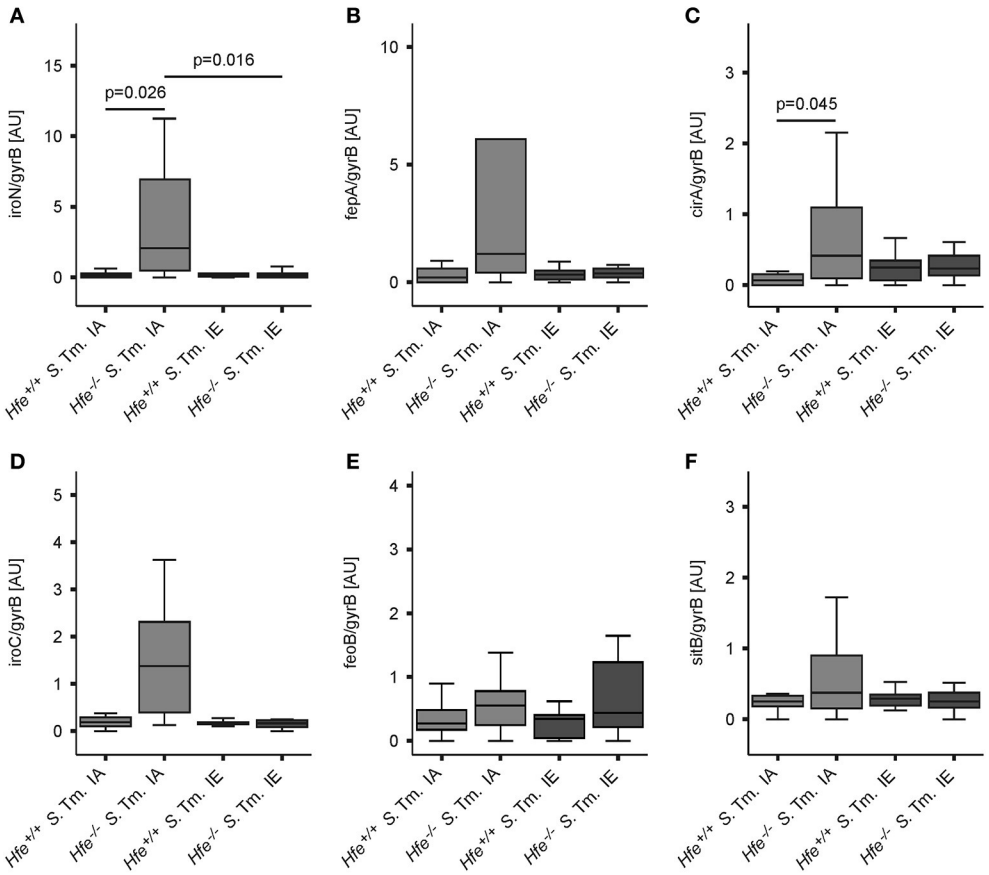

FIGURE 6 | *Salmonella* adapts to the iron-restricted myeloid compartment of *Hfe*$^{-/-}$ mice. The expression of bacterial iron metabolic genes in the spleen was measured by qPCR. Expression of *iroN* **(A)**, *fepA* **(B)**, *cirA* **(C)**, *iroC* **(D)**, *feoB* **(E)**, and *sitB* **(F)** was determined relative to the housekeeping gene *gyrB*. Data were compared by means of ANOVA with Tukey's *post hoc* test. Values are depicted as lower quartile, median and upper quartile (boxes), and minimum/maximum ranges and statistical significances are indicated. $n = 14–17$ per group.

infection outcome (Nairz et al., 2015a). Hfe deficiency results in reduced Hamp production and increased serum iron levels (Pietrangelo, 2004). Enhanced bacterial replication might be anticipated in an Hfe-deficient host as a result of increased iron availability, and this has been experimentally demonstrated for pathogens such as *Vibrio vulnificus*, *Yersinia enterocolitica,* and *Yersinia pestis* in the setting of HH (Quenee et al., 2012; Arezes et al., 2015; Miller et al., 2016). However, the opposite is true in the context of infection with an intracellular bacterium such as *S.* Typhimurium because Hfe-deficient macrophages are iron-poor and thus provide an inferior niche for bacterial replication (Nairz et al., 2009). We find that Hfe-deficient macrophages restrict the availability of both non-transferrin-bound (NTBI) and transferrin-bound (TBI) iron to intracellular *Salmonella* more efficiently than WT macrophages. This suggests that the underlying mechanism is independent of Dmt1 and TfR1 and may be attributable to differential iron turnover or efflux. While Fpn1 constitutes the primary pathway for the cellular release of ferrous iron, iron may also be exported via alternative pathways (Devireddy et al., 2005; Keel et al., 2008; Du and Galán, 2009; Nairz et al., 2015b; Lok et al., 2016).

Slc11a1 (also known as Nramp1) has long been known to influence the course of infection with *S.* Typhimurium and certain species of *Mycobacterium* and *Leishmania* (Vidal et al., 1993; Atkinson et al., 1997; Blackwell et al., 2003). Although these pathogens are taxonomically unrelated, they share the features of infecting macrophages, persisting in phagolysosomes and depending on iron. Slc11a1 is incorporated into the phagolysosomal membrane and shifts iron and other divalent ions out of this compartment, thus withdrawing it from phagocytosed microbes (Vidal et al., 1995; Jabado et al., 2000; Wyllie et al., 2002; Fritsche et al., 2007; Valdez et al., 2008). We used C57BL/6 mice for our studies, which carry two dysfunctional Slc11a1 alleles. Therefore, the phenotypes observed in our studies cannot be attributed to this transporter. Moreover, our findings are unlikely to be specific for infections with *S.* Typhimurium but are also relevant to other iron-dependent intracellular pathogens such as *Chlamydia*, *Legionella* and *Listeria* (Paradkar et al., 2008; Bellmann-Weiler et al., 2010, 2013; Haschka et al., 2015), as well as *Mycobacterium* and *Leishmania*. Accordingly, we note that Hfe deficiency impairs the growth of

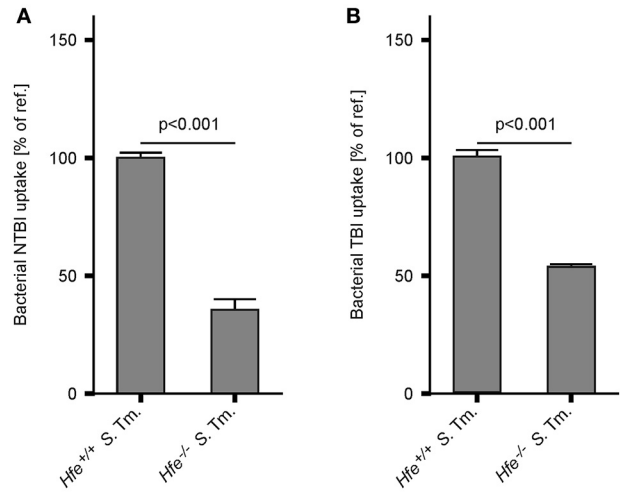

FIGURE 7 | *Hfe*$^{-/-}$ macrophages more efficiently restrict iron from bacteria. WT and *Hfe*$^{-/-}$ macrophages were infected with *S.* Typhimurium and exposed to ^{59}Fe for 24 h. Intracellular bacterial uptake of NTBI **(A)** and TBI **(B)**, respectively, was determined in ^{59}Fe-transport studies. The data were compared by a two-tailed unpaired Student's *t*-test and are shown as mean ± S.E.M of at least 3 independent experiments.

Mycobacterium tuberculosis in human macrophages (Olakanmi et al., 2007).

The iron content of macrophages is influenced by several mechanisms including iron levels in the extracellular microenvironment, expression of iron importers, and exporters, and the rates of erythrophagocytosis and heme-iron recycling (Canonne-Hergaux et al., 1999; Mitterstiller et al., 2016; Theurl et al., 2016). Our models of genetic (i.e., Hfe-associated) and dietary iron overload had different effects on macrophage iron content. Long-term oral iron overload results in increased iron content in virtually all cell types expressing Dmt1 and/or TfR1. In contrast, Hfe deficiency spares the myeloid compartment from iron. We found that oral iron overload results in an increased bacterial load in the spleens and livers of *Salmonella*-infected mice and that Hfe deficiency reduces the bacterial load. Of note, oral iron overload in the setting of Hfe deficiency resulted in intermediate pathogen numbers in spleen and liver on days 2 and 4 of infection. In contrast, the survival of *Hfe*$^{-/-}$ mice over a 10 day period was not affected by dietary iron. *Hfe*$^{-/-}$ mice with dietary iron overload remain more resistant to *Salmonella* infection than WT mice receiving the same diet, with reduced organ loads and increased survival (**Figure 3**) despite the alleviation of bacterial iron-deprivation by dietary iron supplementation as measured by siderophore gene expression (**Figure 6**). Albeit somewhat unexpected, these findings suggest that in the later stages of *Salmonella* infection, Hfe plays an immunoregulatory function that is independent of its effect on bacterial iron-restriction. However, the expression of innate immune genes known to mediate host defense against *S.* Typhimurium was not different between *Hfe*$^{-/-}$ and *Hfe*$^{+/+}$ mice (Vazquez-Torres et al., 2000; Vázquez-Torres et al., 2001), nor were differences in T cell-mediated pathways associated with immunity against *S.* Typhimurium such as IL-12, IFN-γ, IL-17, or IL-22, observed (data not shown) (Berger et al., 2006; Raffatellu et al., 2008; Saiga et al., 2008; Schulz et al., 2008; Chan et al., 2009; Godinez et al., 2009; Srinivasan et al., 2012). Given that Lcn2 was expressed at higher levels in *Hfe*$^{-/-}$ mice, it is possible that one of the siderophore-independent effects of Lcn2 may play a role. Lcn2 is a chemoattractant for neutrophils, but this is unlikely to account for a survival difference beyond day 3 of infection (Schroll et al., 2012). Furthermore, Lcn2 promotes macrophage antibacterial effector mechanisms including TNF, IL-6, and Nos2, but these were not observed to be differentially expressed on day 2 or 4 of infection of *Hfe*$^{-/-}$ and *Hfe*$^{+/+}$ mice (Nairz et al., 2015b). It is conceivable that the survival of mice in the late stages of systemic *Salmonella* infection is directly or indirectly influenced by the intestinal microbiome, which is modulated by Lcn2 (Raffatellu et al., 2009; Deriu et al., 2013; Moschen et al., 2016). Alternatively, the comparable survival of *Hfe*$^{-/-}$ mice on an IE on IA diet may involve an Lcn2-independent mechanism beyond innate immunity. For instance, Hfe deficiency may have beneficial effects on apoptosis, ferroptosis, autophagy, or the oxidative stress response within or outside of the myeloid compartment that is independent of dietary iron. If a vital organ system were to be involved, an effect on host survival would be a plausible. An unbiased approach such as RNA-sequencing may be required to identify such a mechanism.

A central and novel finding of our study is that both the host and the microbe adapt their iron metabolism during infection. *S.* Typhimurium expressed genes required for siderophore-mediated iron uptake *in vivo* in the iron-poor spleens of *Hfe*$^{-/-}$ mice. This induction was specifically abrogated by dietary iron overload. This observation raises the question whether virulence factors other than siderophore genes may have been repressed in the setting of dietary iron overload to enhance the survival of *Hfe*$^{-/-}$ mice. This possibility is supported by the known cross-regulation of bacterial iron homeostasis and virulence gene expression (Zaharik et al., 2002). Our data on the upregulation of bacterial iron uptake genes are further in line with the specific induction of iron import mechanisms reported for *Neisseria gonorrhoeae* residing within human monocytes (Zughaier et al., 2014). Both studies thus support the concept that both host myeloid cells and facultatively intracellular bacteria actively compete for iron as essential nutrient.

In summary, the present study highlights the central role of macrophage iron homeostasis in the outcome of infections with iron-dependent intracellular microbes and the differential effects of genetic and dietary iron overload. We also demonstrate that Hfe is not required for the induction of hypoferremia in infected animals on an iron-replete diet. Nevertheless, the *Hfe* mutation alters the iron content of macrophages, which renders the host more resistant to infections with the intracellular pathogen *S.* Typhimurium. The selective pressure imposed by intracellular pathogens may have contributed to the evolutionary conservation of the *HFE C282Y* mutation, accounting for its high allelic frequency in Caucasians (Datz et al., 1998; Moalem et al., 2004).

AUTHOR CONTRIBUTIONS

MN planned and performed experiments, analyzed the data and wrote the manuscript. AS, DH, SD, PT, ED, and PM performed experiments. HH, FF, and IT interpreted results and edited the manuscript. GW conceived the study, analyzed the data and wrote the manuscript.

ACKNOWLEDGMENTS

We are grateful to Sylvia Berger, Ines Brosch, Sabine Engl, and Markus Seifert for excellent technical support. This work was supported by the "Verein zur Förderung von Forschung und Weiterbildung in molekularer Immunologie und Infektiologie" and by grants from the Austrian Research Fund FWF (W1253-Doctoral college-HOROS to GW, HH, and SD as well as TRP-188 to GW). FF receives support from the National Institues of Health (AI118962).

SUPPLEMENTARY MATERIAL

The Supplementary Material for this article can be found online at: http://journal.frontiersin.org/article/10.3389/fcimb.2017.00110/full#supplementary-material

REFERENCES

Ahmad, K. A., Ahmann, J. R., Migas, M. C., Waheed, A., Britton, R. S., Bacon, B. R., et al. (2002). Decreased liver hepcidin expression in the Hfe knockout mouse. *Blood Cells Mol. Dis.* 29, 361–366. doi: 10.1006/bcmd.2002.0575

Arezes, J., Jung, G., Gabayan, V., Valore, E., Ruchala, P., Gulig, P. A., et al. (2015). Hepcidin-induced hypoferremia is a critical host defense mechanism against the siderophilic bacterium *Vibrio vulnificus*. *Cell Host Microbe* 17, 47–57. doi: 10.1016/j.chom.2014.12.001

Armitage, A. E., Eddowes, L. A., Gileadi, U., Cole, S., Spottiswoode, N., Selvakumar, T. A., et al. (2011). Hepcidin regulation by innate immune and infectious stimuli. *Blood* 118, 4129–4139. doi: 10.1182/blood-2011-04-351957

Armitage, A. E., Lim, P. J., Frost, J. N., Pasricha, S. R., Soilleux, E. J., Evans, E., et al. (2016). Induced disruption of the iron-regulatory hormone hepcidin inhibits acute inflammatory hypoferraemia. *J. Innate Immun.* 8, 517–528. doi: 10.1159/000447713

Atkinson, P. G., Blackwell, J. M., and Barton, C. H. (1997). Nramp1 locus encodes a 65 kDa interferon-gamma-inducible protein in murine macrophages. *Biochem. J.* 325(Pt 3), 779–786.

Bachman, M. A., Miller, V. L., and Weiser, J. N. (2009). Mucosal lipocalin 2 has pro-inflammatory and iron-sequestering effects in response to bacterial enterobactin. *PLoS Pathog.* 5:e1000622. doi: 10.1371/journal.ppat.1000622

Bahram, S., Gilfillan, S., Kuhn, L. C., Moret, R., Schulze, J. B., Lebeau, A., et al. (1999). Experimental hemochromatosis due to MHC class I HFE deficiency: immune status and iron metabolism. *Proc. Natl. Acad. Sci. U.S.A.* 96, 13312–13317. doi: 10.1073/pnas.96.23.13312

Bardou-Jacquet, E., Philip, J., Lorho, R., Ropert, M., Latournerie, M., Houssel-Debry, P., et al. (2013). Liver transplantation normalizes serum hepcidin level and cures iron metabolism alterations in HFE hemochromatosis. *Hepatology* 59, 839–847. doi: 10.1002/hep.26570

Bäumler, A. J., Norris, T. L., Lasco, T., Voight, W., Reissbrodt, R., Rabsch, W., et al. (1998). IroN, a novel outer membrane siderophore receptor characteristic of *Salmonella enterica*. *J. Bacteriol.* 180, 1446–1453.

Bearson, B. L., Bearson, S. M., Uthe, J. J., Dowd, S. E., Houghton, J. O., Lee, I., et al. (2008). Iron regulated genes of Salmonella enterica serovar Typhimurium in response to norepinephrine and the requirement of fepDGC for norepinephrine-enhanced growth. *Microbes Infect.* 10, 807–816. doi: 10.1016/j.micinf.2008.04.011

Bellmann-Weiler, R., Martinz, V., Kurz, K., Engl, S., Feistritzer, C., Fuchs, D., et al. (2010). Divergent modulation of *Chlamydia pneumoniae* infection cycle in human monocytic and endothelial cells by iron, tryptophan availability and interferon gamma. *Immunobiology* 215, 842–848. doi: 10.1016/j.imbio.2010.05.021

Bellmann-Weiler, R., Schroll, A., Engl, S., Nairz, M., Talasz, H., Seifert, M., et al. (2013). Neutrophil gelatinase-associated lipocalin and interleukin-10 regulate intramacrophage *Chlamydia pneumoniae* replication by modulating intracellular iron homeostasis. *Immunobiology* 218, 969–978. doi: 10.1016/j.imbio.2012.11.004

Bennett, M. J., Lebrón, J. A., and Bjorkman, P. J. (2000). Crystal structure of the hereditary haemochromatosis protein HFE complexed with transferrin receptor. *Nature* 403, 46–53. doi: 10.1038/47417

Berger, T., Togawa, A., Duncan, G. S., Elia, A. J., You-Ten, A., Wakeham, A., et al. (2006). Lipocalin 2-deficient mice exhibit increased sensitivity to *Escherichia coli* infection but not to ischemia-reperfusion injury. *Proc. Natl. Acad. Sci. U.S.A.* 103, 1834–1839. doi: 10.1073/pnas.0510847103

Blackwell, J. M., Searle, S., Mohamed, H., and White, J. K. (2003). Divalent cation transport and susceptibility to infectious and autoimmune disease: continuation of the Ity/Lsh/Bcg/Nramp1/Slc11a1 gene story. *Immunol. Lett.* 85, 197–203. doi: 10.1016/S0165-2478(02)00231-6

Boyer, E., Bergevin, I., Malo, D., Gros, P., and Cellier, M. F. (2002). Acquisition of Mn(II) in addition to Fe(II) is required for full virulence of *Salmonella* enterica serovar Typhimurium. *Infect. Immun.* 70, 6032–6042. doi: 10.1128/IAI.70.11.6032-6042.2002

Bozzini, C., Campostrini, N., Trombini, P., Nemeth, E., Castagna, A., Tenuti, I., et al. (2008). Measurement of urinary hepcidin levels by SELDI-TOF-MS in HFE-hemochromatosis. *Blood Cells Mol. Dis.* 40, 347–352. doi: 10.1016/j.bcmd.2007.10.001

Bridle, K. R., Frazer, D. M., Wilkins, S. J., Dixon, J. L., Purdie, D. M., Crawford, D. H., et al. (2003). Disrupted hepcidin regulation in HFE-associated haemochromatosis and the liver as a regulator of body iron homoeostasis. *Lancet* 361, 669–673. doi: 10.1016/S0140-6736(03)12602-5

Cairo, G., Recalcati, S., Montosi, G., Castrusini, E., Conte, D., and Pietrangelo, A. (1997). Inappropriately high iron regulatory protein activity in monocytes of patients with genetic hemochromatosis. *Blood* 89, 2546–2553.

Camaschella, C., Roetto, A., and De Gobbi, M. (2002). Genetic haemochromatosis: genes and mutations associated with iron loading. *Best Pract. Res. Clin. Haematol.* 15, 261–276. doi: 10.1016/S1521-6926(02)90207-0

Canali, S., Zumbrennen-Bullough, K. B., Core, A. B., Wang, C. Y., Nairz, M., Bouley, R., et al. (2017). Endothelial cells produce bone morphogenetic protein 6 required for iron homeostasis in mice. *Blood* 129, 405–411. doi: 10.1182/blood-2016-06-721571

Canonne-Hergaux, F., Gruenheid, S., Govoni, G., and Gros, P. (1999). The Nramp1 protein and its role in resistance to infection and macrophage function. *Proc. Assoc. Am. Physicians* 111, 283–289. doi: 10.1046/j.1525-1381.1999.99236.x

Carver, P. L. (2014). Metal ions and infectious diseases. An overview from the clinic. *Met. Ions Life Sci.* 13, 1–28. doi: 10.1007/978-94-007-7500-8_1

Chan, Y. R., Liu, J. S., Pociask, D. A., Zheng, M., Mietzner, T. A., Berger, T., et al. (2009). Lipocalin 2 is required for pulmonary host defense against Klebsiella infection. *J. Immunol.* 182, 4947–4956. doi: 10.4049/jimmunol.0803282

Coburn, B., Grassl, G. A., and Finlay, B. B. (2007). *Salmonella*, the host and disease: a brief review. *Immunol. Cell Biol.* 85, 112–118. doi: 10.1038/sj.icb.7100007

Crawford, M. A., Henard, C. A., Tapscott, T., Porwollik, S., McClelland, M., and Vázquez-Torres, A. (2016). DksA-dependent transcriptional regulation in salmonella experiencing nitrosative stress. *Front. Microbiol.* 7:444. doi: 10.3389/fmicb.2016.00444

Crouch, M. L., Castor, M., Karlinsey, J. E., Kalhorn, T., and Fang, F. C. (2008). Biosynthesis and IroC-dependent export of the siderophore salmochelin are

essential for virulence of *Salmonella* enterica serovar Typhimurium. *Mol. Microbiol.* 67, 971–983. doi: 10.1111/j.1365-2958.2007.06089.x

D'Alessio, F., Hentze, M. W., and Muckenthaler, M. U. (2012). The hemochromatosis proteins HFE, TfR2, and HJV form a membrane-associated protein complex for hepcidin regulation. *J. Hepatol.* 57, 1052–1060. doi: 10.1016/j.jhep.2012.06.015

Datz, C., Haas, T., Rinner, H., Sandhofer, F., Patsch, W., and Paulweber, B. (1998). Heterozygosity for the C282Y mutation in the hemochromatosis gene is associated with increased serum iron, transferrin saturation, and hemoglobin in young women: a protective role against iron deficiency? *Clin. Chem.* 44, 2429–2432.

Deriu, E., Liu, J. Z., Pezeshki, M., Edwards, R. A., Ochoa, R. J., Contreras, H., et al. (2013). Probiotic bacteria reduce salmonella typhimurium intestinal colonization by competing for iron. *Cell Host Microbe* 14, 26–37. doi: 10.1016/j.chom.2013.06.007

Devireddy, L. R., Gazin, C., Zhu, X., and Green, M. R. (2005). A cell-surface receptor for lipocalin 24p3 selectively mediates apoptosis and iron uptake. *Cell* 123, 1293–1305. doi: 10.1016/j.cell.2005.10.027

Drakesmith, H., and Prentice, A. M. (2012). Hepcidin and the iron-infection axis. *Science* 338, 768–772. doi: 10.1126/science.1224577

Drakesmith, H., Sweetland, E., Schimanski, L., Edwards, J., Cowley, D., Ashraf, M., et al. (2002). The hemochromatosis protein HFE inhibits iron export from macrophages. *Proc. Natl. Acad. Sci. U.S.A.* 99, 15602–15607. doi: 10.1073/pnas.242614699

Du, F., and Galán, J. E. (2009). Selective inhibition of type III secretion activated signaling by the *Salmonella* effector AvrA. *PLoS Pathog.* 5:e1000595. doi: 10.1371/journal.ppat.1000595

Feder, J. N., Gnirke, A., Thomas, W., Tsuchihashi, Z., Ruddy, D. A., Basava, A., et al. (1996). A novel MHC class I-like gene is mutated in patients with hereditary haemochromatosis. *Nat. Genet.* 13, 399–408. doi: 10.1038/ng0896-399

Feder, J. N., Penny, D. M., Irrinki, A., Lee, V. K., Lebrón, J. A., Watson, N., et al. (1998). The hemochromatosis gene product complexes with the transferrin receptor and lowers its affinity for ligand binding. *Proc. Natl. Acad. Sci. U.S.A.* 95, 1472–1477. doi: 10.1073/pnas.95.4.1472

Fischbach, M. A., Lin, H., Liu, D. R., and Walsh, C. T. (2005). *In vitro* characterization of IroB, a pathogen-associated C-glycosyltransferase. *Proc. Natl. Acad. Sci. U.S.A.* 102, 571–576. doi: 10.1073/pnas.0408463102

Flo, T. H., Smith, K. D., Sato, S., Rodriguez, D. J., Holmes, M. A., Strong, R. K., et al. (2004). Lipocalin 2 mediates an innate immune response to bacterial infection by sequestrating iron. *Nature* 432, 917–921. doi: 10.1038/nature03104

Fritsche, G., Nairz, M., Theurl, I., Mair, S., Bellmann-Weiler, R., Barton, H. C., et al. (2007). Modulation of macrophage iron transport by Nramp1 (Slc11a1). *Immunobiology* 212, 751–757. doi: 10.1016/j.imbio.2007.09.014

Ganz, T. (2005). Hepcidin–a regulator of intestinal iron absorption and iron recycling by macrophages. *Best Pract. Res. Clin. Haematol.* 18, 171–182. doi: 10.1016/j.beha.2004.08.020

Ganz, T., and Nemeth, E. (2015). Iron homeostasis in host defence and inflammation. *Nat. Rev. Immunol.* 15, 500–510. doi: 10.1038/nri3863

Godinez, I., Raffatellu, M., Chu, H., Paixão, T. A., Haneda, T., Santos, R. L., et al. (2009). Interleukin-23 orchestrates mucosal responses to *Salmonella* enterica serotype Typhimurium in the intestine. *Infect. Immun.* 77, 387–398. doi: 10.1128/IAI.00933-08

Goswami, T., and Andrews, N. C. (2006). Hereditary hemochromatosis protein, HFE, interaction with transferrin receptor 2 suggests a molecular mechanism for mammalian iron sensing. *J. Biol. Chem.* 281, 28494–28498. doi: 10.1074/jbc.C600197200

Graziadei, I., Weiss, G., Bohm, A., Werner-Felmayer, G., and Vogel, W. (1997). Unidirectional upregulation of the synthesis of the major iron proteins, transferrin-receptor and ferritin, in HepG2 cells by the acute-phase protein alpha1-antitrypsin. *J. Hepatol.* 27, 716–725. doi: 10.1016/S0168-8278(97)80089-X

Haschka, D., Nairz, M., Demetz, E., Wienerroither, S., Decker, T., and Weiss, G. (2015). Contrasting regulation of macrophage iron homeostasis in response to infection with Listeria monocytogenes depending on localization of bacteria. *Metallomics* 7, 1036–1045. doi: 10.1039/C4MT00328D

Hensel, M., Shea, J. E., Gleeson, C., Jones, M. D., Dalton, E., and Holden, D. W. (1995). Simultaneous identification of bacterial virulence genes by negative selection. *Science* 269, 400–403. doi: 10.1126/science.7618105

Hensel, M., Shea, J. E., Waterman, S. R., Mundy, R., Nikolaus, T., Banks, G. et al. (1998). Genes encoding putative effector proteins of the type III secretion system of Salmonella pathogenicity island 2 are required for bacterial virulence and proliferation in macrophages. *Mol. Microbiol.* 30, 163–174. doi: 10.1046/j.1365-2958.1998.01047.x

Jabado, N., Jankowski, A., Dougaparsad, S., Picard, V., Grinstein, S., and Gros, P. (2000). Natural resistance to intracellular infections: natural resistance-associated macrophage protein 1 (Nramp1) functions as a pH-dependent manganese transporter at the phagosomal membrane. *J. Exp. Med.* 192, 1237–1248. doi: 10.1084/jem.192.9.1237

Janakiraman, A., and Slauch, J. M. (2000). The putative iron transport system SitABCD encoded on SPI1 is required for full virulence of *Salmonella typhimurium*. *Mol. Microbiol.* 35, 1146–1155. doi: 10.1046/j.1365-2958.2000.01783.x

Kautz, L., Jung, G., Valore, E. V., Rivella, S., Nemeth, E., and Ganz, T. (2014). Identification of erythroferrone as an erythroid regulator of iron metabolism. *Nat. Genet.* 46, 678–684. doi: 10.1038/ng.2996

Keel, S. B., Doty, R. T., Yang, Z., Quigley, J. G., Chen, J., Knoblaugh, S., et al. (2008). A heme export protein is required for red blood cell differentiation and iron homeostasis. *Science* 319, 825–828. doi: 10.1126/science.1151133

Kim, D. K., Jeong, J. H., Lee, J. M., Kim, K. S., Park, S. H., Kim, Y. D., et al. (2014). Inverse agonist of estrogen-related receptor gamma controls *Salmonella typhimurium* infection by modulating host iron homeostasis. *Nat. Med.* 20, 419–424. doi: 10.1038/nm.3483

Kim, H., Lee, H., and Shin, D. (2013). The FeoC protein leads to high cellular levels of the Fe(II) transporter FeoB by preventing FtsH protease regulation of FeoB in *Salmonella enterica*. *J. Bacteriol.* 195, 3364–3370. doi: 10.1128/JB.00343-13

Lebrón, J. A., Bennett, M. J., Vaughn, D. E., Chirino, A. J., Snow, P. M., Mintier, G. A., et al. (1998). Crystal structure of the hemochromatosis protein HFE and characterization of its interaction with transferrin receptor. *Cell* 93, 111–123. doi: 10.1016/S0092-8674(00)81151-4

Leung, K. Y., and Finlay, B. B. (1991). Intracellular replication is essential for the virulence of *Salmonella typhimurium*. *Proc. Natl. Acad. Sci. U.S.A.* 88, 11470–11474. doi: 10.1073/pnas.88.24.11470

Lok, H. C., Sahni, S., Jansson, P. J., Kovacevic, Z., Hawkins, C. L., and Richardson, D. R. (2016). A nitric oxide storage and transport system that protects activated macrophages from endogenous nitric oxide cytotoxicity. *J. Biol. Chem.* 291, 27042–27061. doi: 10.1074/jbc.M116.763714

Ludwiczek, S., Aigner, E., Theurl, I., and Weiss, G. (2003). Cytokine-mediated regulation of iron transport in human monocytic cells. *Blood* 101, 4148–4154. doi: 10.1182/blood-2002-08-2459

Ludwiczek, S., Theurl, I., Artner-Dworzak, E., Chorney, M., and Weiss, G. (2004). Duodenal HFE expression and hepcidin levels determine body iron homeostasis: modulation by genetic diversity and dietary iron availability. *J. Mol. Med.* 82, 373–382. doi: 10.1007/s00109-004-0542-3

Ludwiczek, S., Theurl, I., Bahram, S., Schümann, K., and Weiss, G. (2005). Regulatory networks for the control of body iron homeostasis and their dysregulation in HFE mediated hemochromatosis. *J. Cell. Physiol.* 204, 489–499. doi: 10.1002/jcp.20315

Malik-Kale, P., Jolly, C. E., Lathrop, S., Winfree, S., Luterbach, C., and Steele-Mortimer, O. (2011). *Salmonella*–at home in the host cell. *Front. Microbiol.* 2:125. doi: 10.3389/fmicb.2011.00125

Mencacci, A., Cenci, E., Boelaert, J. R., Bucci, P., Mosci, P., Fè d'Ostiani, C., et al. (1997). Iron overload alters innate and T helper cell responses to *Candida albicans* in mice. *J. Infect. Dis.* 175, 1467–1476. doi: 10.1086/516481

Miller, H. K., Schwiesow, L., Au-Yeung, W., and Auerbuch, V. (2016). Hereditary hemochromatosis predisposes mice to *Yersinia pseudotuberculosis* infection even in the absence of the type III secretion system. *Front. Cell. Infect. Microbiol.* 6:69. doi: 10.3389/fcimb.2016.00069

Mitterstiller, A. M., Haschka, D., Dichtl, S., Nairz, M., Demetz, E., Talasz, H., et al. (2016). Heme oxygenase 1 controls early innate immune response of macrophages to *Salmonella* Typhimurium infection. *Cell. Microbiol.* 18, 1374–1389. doi: 10.1111/cmi.12578

Moalem, S., Weinberg, E. D., and Percy, M. E. (2004). Hemochromatosis and the enigma of misplaced iron: implications for infectious disease and survival. *Biometals* 17, 135–139. doi: 10.1023/B:BIOM.0000018375.20026.b3

Moschen, A. R., Gerner, R. R., Wang, J., Klepsch, V., Adolph, T. E., Reider, S. J., et al. (2016). Lipocalin 2 protects from inflammation and tumorigenesis associated with gut microbiota alterations. *Cell Host Microbe* 19, 455–469. doi: 10.1016/j.chom.2016.03.007

Nairz, M., Ferring-Appel, D., Casarrubea, D., Sonnweber, T., Viatte, L., Schroll, A., et al. (2015a). Iron regulatory proteins mediate host resistance to salmonella infection. *Cell Host Microbe* 18, 254–261. doi: 10.1016/j.chom.2015.06.017

Nairz, M., Fritsche, G., Brunner, P., Talasz, H., Hantke, K., and Weiss, G. (2008). Interferon-gamma limits the availability of iron for intramacrophage *Salmonella typhimurium*. *Eur. J. Immunol.* 38, 1923–1936. doi: 10.1002/eji.200738056

Nairz, M., Haschka, D., Demetz, E., and Weiss, G. (2014). Iron at the interface of immunity and infection. *Front. Pharmacol.* 5:152. doi: 10.3389/fphar.2014.00152

Nairz, M., Schleicher, U., Schroll, A., Sonnweber, T., Theurl, I., Ludwiczek, S., et al. (2013). Nitric oxide-mediated regulation of ferroportin-1 controls macrophage iron homeostasis and immune function in *Salmonella* infection. *J. Exp. Med.* 210, 855–873. doi: 10.1084/jem.20121946

Nairz, M., Schroll, A., Haschka, D., Dichtl, S., Sonnweber, T., Theurl, I., et al. (2015b). Lipocalin-2 ensures host defense against *Salmonella* Typhimurium by controlling macrophage iron homeostasis and immune response. *Eur. J. Immunol.* 45, 3073–3086. doi: 10.1002/eji.201545569

Nairz, M., Schroll, A., Moschen, A. R., Sonnweber, T., Theurl, M., Theurl, I., et al. (2011). Erythropoietin contrastingly affects bacterial infection and experimental colitis by inhibiting nuclear factor-kappaB-inducible immune pathways. *Immunity* 34, 61–74. doi: 10.1016/j.immuni.2011.01.002

Nairz, M., Schroll, A., Sonnweber, T., and Weiss, G. (2010). The struggle for iron–a metal at the host-pathogen interface. *Cell. Microbiol.* 12, 1691–1702. doi: 10.1111/j.1462-5822.2010.01529.x

Nairz, M., Theurl, I., Schroll, A., Theurl, M., Fritsche, G., Lindner, E., et al. (2009). Absence of functional Hfe protects mice from invasive *Salmonella* enterica serovar Typhimurium infection via induction of lipocalin-2. *Blood* 114, 3642–3651. doi: 10.1182/blood-2009-05-223354

Nemeth, E., Rivera, S., Gabayan, V., Keller, C., Taudorf, S., Pedersen, B. K., et al. (2004a). IL-6 mediates hypoferremia of inflammation by inducing the synthesis of the iron regulatory hormone hepcidin. *J. Clin. Invest.* 113, 1271–1276. doi: 10.1172/JCI20945

Nemeth, E., Tuttle, M. S., Powelson, J., Vaughn, M. B., Donovan, A., Ward, D. M., et al. (2004b). Hepcidin regulates cellular iron efflux by binding to ferroportin and inducing its internalization. *Science* 306, 2090–2093. doi: 10.1126/science.1104742

Nicolas, G., Viatte, L., Lou, D. Q., Bennoun, M., Beaumont, C., Kahn, A., et al. (2003). Constitutive hepcidin expression prevents iron overload in a mouse model of hemochromatosis. *Nat. Genet.* 34, 97–101. doi: 10.1038/ng1150

Oexle, H., Kaser, A., Möst, J., Bellmann-Weiler, R., Werner, E. R., Werner-Felmayer, G., et al. (2003). Pathways for the regulation of interferon-gamma-inducible genes by iron in human monocytic cells. *J. Leukoc. Biol.* 74, 287–294. doi: 10.1189/jlb.0802420

Olakanmi, O., Schlesinger, L. S., Ahmed, A., and Britigan, B. E. (2002). Intraphagosomal Mycobacterium tuberculosis acquires iron from both extracellular transferrin and intracellular iron pools. Impact of interferon-gamma and hemochromatosis. *J. Biol. Chem.* 277, 49727–49734. doi: 10.1074/jbc.M209768200

Olakanmi, O., Schlesinger, L. S., and Britigan, B. E. (2007). Hereditary hemochromatosis results in decreased iron acquisition and growth by *Mycobacterium tuberculosis* within human macrophages. *J. Leukoc. Biol.* 81, 195–204. doi: 10.1189/jlb.0606405

Paradkar, P. N., De Domenico, I., Durchfort, N., Zohn, I., Kaplan, J., and Ward, D. M. (2008). Iron depletion limits intracellular bacterial growth in macrophages. *Blood* 112, 866–874. doi: 10.1182/blood-2007-12-126854

Pfeifer, C. G., Marcus, S. L., Steele-Mortimer, O., Knodler, L. A., and Finlay, B. B. (1999). *Salmonella typhimurium* virulence genes are induced upon bacterial invasion into phagocytic and nonphagocytic cells. *Infect. Immun.* 67, 5690–5698.

Pietrangelo, A. (2004). Hereditary hemochromatosis–a new look at an old disease. *N. Engl. J. Med.* 350, 2383–2397. doi: 10.1056/NEJMra031573

Quenee, L. E., Hermanas, T. M., Ciletti, N., Louvel, H., Miller, N. C., Elli, D., et al. (2012). Hereditary hemochromatosis restores the virulence of plague vaccine strains. *J. Infect. Dis.* 206, 1050–1058. doi: 10.1093/infdis/jis433

Rabsch, W., Methner, U., Voigt, W., Tschäpe, H., Reissbrodt, R., and Williams, P. H. (2003). Role of receptor proteins for enterobactin and 2,3-dihydroxybenzoylserine in virulence of *Salmonella enterica*. *Infect. Immun.* 71, 6953–6961. doi: 10.1128/IAI.71.12.6953-6961.2003

Raffatellu, M., George, M. D., Akiyama, Y., Hornsby, M. J., Nuccio, S. P., Paixao, T. A., et al. (2009). Lipocalin-2 resistance confers an advantage to *Salmonella* enterica serotype Typhimurium for growth and survival in the inflamed intestine. *Cell Host Microbe* 5, 476–486. doi: 10.1016/j.chom.2009.03.011

Raffatellu, M., Santos, R. L., Verhoeven, D. E., George, M. D., Wilson, R. P., Winter, S. E., et al. (2008). Simian immunodeficiency virus-induced mucosal interleukin-17 deficiency promotes *Salmonella* dissemination from the gut. *Nat. Med.* 14, 421–428. doi: 10.1038/nm1743

Richter-Dahlfors, A., Buchan, A. M., and Finlay, B. B. (1997). Murine salmonellosis studied by confocal microscopy: *Salmonella typhimurium* resides intracellularly inside macrophages and exerts a cytotoxic effect on phagocytes *in vivo*. *J. Exp. Med.* 186, 569–580. doi: 10.1084/jem.186.4.569

Saiga, H., Nishimura, J., Kuwata, H., Okuyama, M., Matsumoto, S., Sato, S., et al. (2008). Lipocalin 2-dependent inhibition of mycobacterial growth in alveolar epithelium. *J. Immunol.* 181, 8521–8527. doi: 10.4049/jimmunol.181.12.8521

Schaible, U. E., and Kaufmann, S. H. (2005). A nutritive view on the host-pathogen interplay. *Trends Microbiol.* 13, 373–380. doi: 10.1016/j.tim.2005.06.009

Schleicher, U., Hesse, A., and Bogdan, C. (2005). Minute numbers of contaminant CD8+ T cells or CD11b+CD11c+ NK cells are the source of IFN-gamma in IL-12/IL-18-stimulated mouse macrophage populations. *Blood* 105, 1319–1328. doi: 10.1182/blood-2004-05-1749

Schmidt, P. J., Toran, P. T., Giannetti, A. M., Bjorkman, P. J., and Andrews, N. C. (2008). The transferrin receptor modulates Hfe-dependent regulation of hepcidin expression. *Cell Metab.* 7, 205–214. doi: 10.1016/j.cmet.2007.11.016

Schroll, A., Eller, K., Feistritzer, C., Nairz, M., Sonnweber, T., Moser, P. A., et al. (2012). Lipocalin-2 ameliorates granulocyte functionality. *Eur. J. Immunol.* 42, 3346–3357. doi: 10.1002/eji.201142351

Schulz, S. M., Kohler, G., Schutze, N., Knauer, J., Straubinger, R. K., Chackerian, A. A., et al. (2008). Protective immunity to systemic infection with attenuated *Salmonella* enterica serovar enteritidis in the absence of IL-12 is associated with IL-23-dependent IL-22, but not IL-17. *J. Immunol.* 181, 7891–7901. doi: 10.4049/jimmunol.181.11.7891

Shen, F., Hu, Z., Goswami, J., and Gaffen, S. L. (2006). Identification of common transcriptional regulatory elements in interleukin-17 target genes. *J. Biol. Chem.* 281, 24138–24148. doi: 10.1074/jbc.M604597200

Skaar, E. P. (2009). A precious metal heist. *Cell Host Microbe* 5, 422–424. doi: 10.1016/j.chom.2009.05.005

Soares, M. P., and Weiss, G. (2015). The Iron age of host-microbe interactions. *EMBO Rep.* 16, 1482–1500. doi: 10.15252/embr.20154055

Sonnweber, T., Ress, C., Nairz, M., Theurl, I., Schroll, A., Murphy, A. T., et al. (2012). High-fat diet causes iron deficiency via hepcidin-independent reduction of duodenal iron absorption. *J. Nutr. Biochem.* 23, 1600–1608. doi: 10.1016/j.jnutbio.2011.10.013

Srinivasan, G., Aitken, J. D., Zhang, B., Carvalho, F. A., Chassaing, B., Shashidharamurthy, R., et al. (2012). Lipocalin 2 deficiency dysregulates iron homeostasis and exacerbates endotoxin-induced sepsis. *J. Immunol.* 189, 1911–1919. doi: 10.4049/jimmunol.1200892

Theurl, I., Finkenstedt, A., Schroll, A., Nairz, M., Sonnweber, T., Bellmann-Weiler, R., et al. (2010). Growth differentiation factor 15 in anaemia of chronic disease, iron deficiency anaemia and mixed type anaemia. *Br. J. Haematol.* 148, 449–455. doi: 10.1111/j.1365-2141.2009.07961.x

Theurl, I., Hilgendorf, I., Nairz, M., Tymoszuk, P., Haschka, D., Asshoff, M., et al. (2016). On-demand erythrocyte disposal and iron recycling requires transient macrophages in the liver. *Nat. Med.* 22, 945–951. doi: 10.1038/nm.4146

Theurl, I., Theurl, M., Seifert, M., Mair, S., Nairz, M., Rumpold, H., et al. (2008a). Autocrine formation of hepcidin induces iron retention in human monocytes. *Blood* 111, 2392–2399. doi: 10.1182/blood-2007-05-090019

Theurl, M., Theurl, I., Hochegger, K., Obrist, P., Subramaniam, N., van Rooijen, N., et al. (2008b). Kupffer cells modulate iron homeostasis in mice via regulation of hepcidin expression. *J. Mol. Med.* 86, 825–835. doi: 10.1007/s00109-008-0346-y

Tsolis, R. M., Bäumler, A. J., Heffron, F., and Stojiljkovic, I. (1996). Contribution of TonB- and Feo-mediated iron uptake to growth of *Salmonella typhimurium* in the mouse. *Infect. Immun.* 64, 4549–4556.

Valdez, Y., Grassl, G. A., Guttman, J. A., Coburn, B., Gros, P., Vallance, B. A., et al. (2008). Nramp1 drives an accelerated inflammatory response during *Salmonella*-induced colitis in mice. *Cell Microbiol.* 11, 351–362. doi: 10.1111/j.1462-5822.2008.01258.x

Vázquez-Torres, A., Fantuzzi, G., Edwards, C. K. III., Dinarello, C. A., and Fang, F. C. (2001). Defective localization of the NADPH phagocyte oxidase to *Salmonella*-containing phagosomes in tumor necrosis factor p55 receptor-deficient macrophages. *Proc. Natl. Acad. Sci. U.S.A.* 98, 2561–2565. doi: 10.1073/pnas.041618998

Vazquez-Torres, A., Jones-Carson, J., Bäumler, A. J., Falkow, S., Valdivia, R., Brown, W., et al. (1999). Extraintestinal dissemination of *Salmonella* by CD18-expressing phagocytes. *Nature* 401, 804–808.

Vazquez-Torres, A., Jones-Carson, J., Mastroeni, P., Ischiropoulos, H., and Fang, F. C. (2000). Antimicrobial actions of the NADPH phagocyte oxidase and inducible nitric oxide synthase in experimental salmonellosis. I. Effects on microbial killing by activated peritoneal macrophages *in vitro*. *J. Exp. Med.* 192, 227–236. doi: 10.1084/jem.192.2.227

Vidal, S. M., Malo, D., Vogan, K., Skamene, E., and Gros, P. (1993). Natural resistance to infection with intracellular parasites: isolation of a candidate for Bcg. *Cell* 73, 469–485. doi: 10.1016/0092-8674(93)90135-D

Vidal, S., Tremblay, M. L., Govoni, G., Gauthier, S., Sebastiani, G., Malo, D., et al. (1995). The Ity/Lsh/Bcg locus: natural resistance to infection with intracellular parasites is abrogated by disruption of the Nramp1 gene. *J. Exp. Med.* 182, 655–666. doi: 10.1084/jem.182.3.655

Vujic Spasic, M., Kiss, J., Herrmann, T., Galy, B., Martinache, S., Stolte, J., et al. (2008). Hfe acts in hepatocytes to prevent hemochromatosis. *Cell Metab.* 7, 173–178. doi: 10.1016/j.cmet.2007.11.014

Wallace, D. F., Summerville, L., Crampton, E. M., Frazer, D. M., Anderson, G. J., and Subramaniam, V. N. (2009). Combined deletion of Hfe and transferrin receptor 2 in mice leads to marked dysregulation of hepcidin and iron overload. *Hepatology* 50, 1992–2000. doi: 10.1002/hep.23198

Wang, J., Chen, G., and Pantopoulos, K. (2003). The haemochromatosis protein HFE induces an apparent iron-deficient phenotype in H1299 cells that is not corrected by co-expression of beta 2-microglobulin. *Biochem. J.* 370(Pt 3), 891–899. doi: 10.1042/BJ20021607

Weinberg, E. D. (1974). Iron and susceptibility to infectious disease. *Science* 184, 952–956.

Weiss, G. (2010). Genetic mechanisms and modifying factors in hereditary hemochromatosis. *Nat. Rev. Gastroenterol. Hepatol.* 7, 50–58. doi: 10.1038/nrgastro.2009.201

Weiss, G., Werner-Felmayer, G., Werner, E. R., Grünewald, K., Wachter, H., and Hentze, M. W. (1994). Iron regulates nitric oxide synthase activity by controlling nuclear transcription. *J. Exp. Med.* 180, 969–976. doi: 10.1084/jem.180.3.969

Wyllie, S., Seu, P., and Goss, J. A. (2002). The natural resistance-associated macrophage protein 1 Slc11a1 (formerly Nramp1) and iron metabolism in macrophages. *Microbes Infect.* 4, 351–359. doi: 10.1016/S1286-4579(02)01548-4

Zaharik, M. L., Cullen, V. L., Fung, A. M., Libby, S. J., Kujat Choy, S. L., Coburn, B., et al. (2004). The *Salmonella* enterica serovar typhimurium divalent cation transport systems MntH and SitABCD are essential for virulence in an Nramp1G169 murine typhoid model. *Infect. Immun.* 72, 5522–5525. doi: 10.1128/IAI.72.9.5522-5525.2004

Zaharik, M. L., Vallance, B. A., Puente, J. L., Gros, P., and Finlay, B. B. (2002). Host-pathogen interactions: host resistance factor Nramp1 up-regulates the expression of *Salmonella* pathogenicity island-2 virulence genes. *Proc. Natl. Acad. Sci. U.S.A.* 99, 15705–15710. doi: 10.1073/pnas.252415599

Zoller, H., Koch, R. O., Theurl, I., Obrist, P., Pietrangelo, A., Montosi, G., et al. (2001). Expression of the duodenal iron transporters divalent-metal transporter 1 and ferroportin 1 in iron deficiency and iron overload. *Gastroenterology* 120, 1412–1419. doi: 10.1053/gast.2001.24033

Zoller, H., Pietrangelo, A., Vogel, W., and Weiss, G. (1999). Duodenal metal-transporter (DMT-1, NRAMP-2) expression in patients with hereditary haemochromatosis. *Lancet* 353, 2120–2123.

Zughaier, S. M., Kandler, J. L., and Shafer, W. M. (2014). Neisseria gonorrhoeae modulates iron-limiting innate immune defenses in macrophages. *PLoS ONE* 9:e87688. doi: 10.1371/journal.pone.0087688

Conflict of Interest Statement: The authors declare that the research was conducted in the absence of any commercial or financial relationships that could be construed as a potential conflict of interest.

frontiers in Cellular and Infection Microbiology

ORIGINAL RESEARCH
published: 08 June 2017
doi: 10.3389/fcimb.2017.00245

Mycobacterium tuberculosis Glyceraldehyde-3-Phosphate Dehydrogenase (GAPDH) Functions as a Receptor for Human Lactoferrin

*Himanshu Malhotra[1‡], Anil Patidar[1‡], Vishant M. Boradia[2†‡], Rajender Kumar[3†], Rakesh D. Nimbalkar[3], Ajay Kumar[2], Zahid Gani[2], Rajbeer Kaur[2], Prabha Garg[3], Manoj Raje[1] and Chaaya I. Raje[2]**

[1] Cell Biology and Immunology, Council of Scientific and Industrial Research-Institute of Microbial Technology, Chandigarh, India, [2] Department of Biotechnology, National Institute of Pharmaceutical Education and Research, Punjab, India, [3] Department of Pharmacoinformatics, National Institute of Pharmaceutical Education and Research, Punjab, India

OPEN ACCESS

Edited by:
Susu M. Zughaier,
Emory University, United States

Reviewed by:
Ashu Sharma,
University at Buffalo, United States
Teresa Olczak,
University of Wrocław, Poland

***Correspondence:**
Chaaya I. Raje
chaaya@niper.ac.in

†Present Address:
Vishant M. Boradia,
Department of Microbiology and Immunology, University of Maryland School of Medicine, Baltimore, MD, United States
Rajender Kumar,
Architecture et Fonction des Macromolécules Biologiques UMR 7257 Case 932, Marseille, France

‡These authors have contributed equally to this work.

Received: 21 March 2017
Accepted: 26 May 2017
Published: 08 June 2017

Citation:
Malhotra H, Patidar A, Boradia VM, Kumar R, Nimbalkar RD, Kumar A, Gani Z, Kaur R, Garg P, Raje M and Raje CI (2017) Mycobacterium tuberculosis Glyceraldehyde-3-Phosphate Dehydrogenase (GAPDH) Functions as a Receptor for Human Lactoferrin. Front. Cell. Infect. Microbiol. 7:245. doi: 10.3389/fcimb.2017.00245

Iron is crucial for the survival of living cells, particularly the human pathogen *Mycobacterium tuberculosis (M.tb)* which uses multiple strategies to acquire and store iron. *M.tb* synthesizes high affinity iron chelators (siderophores), these extract iron from host iron carrier proteins such as transferrin (Tf) and lactoferrin (Lf). Recent studies have revealed that *M.tb* may also relocate several housekeeping proteins to the cell surface for capture and internalization of host iron carrier protein transferrin. One of the identified receptors is the glycolytic enzyme Glyceraldehyde-3-phosphate dehydrogenase (GAPDH). This conserved multifunctional protein has been identified as a virulence factor in several other bacterial species. Considering the close structural and functional homology between the two major human iron carrier proteins (Tf and Lf) and the fact that Lf is abundantly present in lung fluid (unlike Tf which is present in plasma), we evaluated whether GAPDH also functions as a dual receptor for Lf. The current study demonstrates that human Lf is sequestered at the bacterial surface by GAPDH. The affinity of Lf-GAPDH (31.7 ± 1.68 nM) is higher as compared to Tf-GAPDH (160 ± 24 nM). Two GAPDH mutants were analyzed for their enzymatic activity and interaction with Lf. Lastly, the present computational studies offer the first significant insights for the 3D structure of monomers and assembled tetramer with the associated co-factor NAD^+. Sequence analysis and structural modeling identified the surface exposed, evolutionarily conserved and functional residues and predicted the effect of mutagenesis on GAPDH.

Keywords: ***Mycobacterium tuberculosis***, **iron, transferrin, lactoferrin, glyceraldehyde-3-phosphate dehydrogenase (GAPDH)**

INTRODUCTION

Iron acquisition is vital for the survival of *Mycobacterium tuberculosis,* the causative agent of tuberculosis. In order to survive and replicate within the iron restricted intracellular environment of the host cell, these pathogens utilize multiple strategies to pilfer iron from host resources. In the mammalian host iron remains tightly sequestered to either storage proteins or to transport proteins such as Tf and Lf. One strategy used by *M.tb* to acquire iron is to synthesize high affinity chelators known as siderophores (De Voss et al., 1999; Ratledge, 2004; Banerjee et al., 2011).

Recently an alternate siderophore–independent pathway has been identified wherein human holo-Tf is directly captured at the bacterial surface and subsequently internalized. The *M.tb* Tf receptors identified included several conserved proteins namely Glyceraldehyde-3-phosphate dehydrogenase (GAPDH, Rv1436); Lactate dehydrogenase (Rv1872c); Iron regulated Elongation factor tu (Rv0685); Acyl desaturase (Rv0824c); 50S ribosomal protein L2rplB (Rv0704); 50S ribosomal protein L1rplA (Rv0641) (Boradia et al., 2014). The essential house-keeping glycolytic enzyme GAPDH operates as a multifunctional protein in both eukaryotes (Sirover, 1999) and prokaryotes including *M.tb* (Bermudez et al., 1996; Carroll et al., 2010). Earlier GAPDH has been identified as a dual receptor for both Tf and Lf in mammalian cells (Raje et al., 2007; Rawat et al., 2012). GAPDH therefore plays analogous roles in Tf acquisition of iron by *M.tb* as well as its human host (Boradia et al., 2014).

Tf is predominantly present in the blood and is involved in iron transport to cells, while Lf is abundantly present in human milk, mucosal secretions, and neutrophil secretory granules. The two iron carrier proteins Lf and Tf share significant sequence identity (60%) and have a conserved bi-lobed structure that each bind single atom of Fe^{3+}. Lf plays a vital role in iron sequestration, transport, and as an immunomodulator. Several studies have revealed that it plays a protective role by enhancing phagocytosis, inhibiting biofilm formation, and preventing of microbe-host interactions (Testa, 2002; Siqueiros-Cendón et al., 2014).

While Tf iron acquisition in *M.tb* has been extensively assessed, limited information is available regarding acquisition of Lf iron in this pathogen. A few previous reports have indicated that *M.tb* bacilli in culture and intracellular bacilli can acquire Lf associated iron. Infact these studies have shown that iron is acquired several fold more efficiently from Lf than Tf (Olakanmi et al., 2004), however the exact mechanisms involved remain unknown.

In the current study using *in vitro* and cell based models, we demonstrate for the first time that *M.tb* acquires iron by utilizing GAPDH as receptor for Lf. Ligand binding analysis demonstrated that GAPDH had a greater affinity for Lf than Tf. Lf uptake by *M.tb* was evident in virulent, attenuated, and even siderophore negative *M.tb* strains with Lf being trafficked to the intraphagosomal bacilli. Taken together, these findings suggest that iron acquisition from Lf is independent of the siderophore pathway. Mutagenesis and *in silico* studies provided an insight into the structure and function of GAPDH. This study also provides the first 3D model for *M.tb* GAPDH and confirms that enzyme activity and Lf binding are unrelated.

MATERIALS AND METHODS

Plasmids and Strains

The *M.tb* H37Rv ΔmbtB::hyg, siderophore knockout strain was received as a kind gift from Dr. CE Barry, Tuberculosis Research Section, Laboratory of Host Defenses, National Institute of Allergy and Infectious Disease, Rockville, Maryland (De Voss et al., 2000). *M.tb* H37Ra and H37Rv strains were transformed with pSC301 plasmid (Cowley and Av-Gay, 2001) to generate the *M.tb* H37Ra-GFP and *M.tb* H37Rv-GFP strains. *M.tb* H37Ra strains expressing mCherry or GAPDH-mCherry were prepared previously in our laboratory (Boradia et al., 2014).

The full length *M.tb* GAPDH gene was cloned and expressed in *M.tb* H37Ra to obtain recombinant wild type GAPDH (wt rGAPDH) as described previously (Boradia et al., 2016). During plasmid screening two point mutations were detected (i) an Arginine to Serine mutation at position 142 (N142S) and (ii) a Proline to Leucine mutation at position 295 (P295L). Each plasmid was individually transformed into *M.tb* H37Ra using standard methods (Wards and Collins, 1996), recombinant proteins were purified as described previously (Boradia et al., 2016), the mutant proteins are referred to as rGAPDH(N142S) and rGAPDH(P295L) respectively.

Conjugation of Proteins

Human Lf (Sigma Chemical Co.) was biotinylated using Sulfo-NHS-LC-Biotin as per the manufacturer's instructions (Pierce). Hilyte Fluor (HF)-488 was conjugated to Lf using AnaTag™ HiLyte Fluor™ 488 Protein Labeling Kit according to the manufacturer's instructions.

Surface Binding of Holo-Lf-HiLyte Fluor488 (Lf-HF-488) by FACS Analysis

M.tb H37Ra cells were cultured to log phase, 2×10^8 cells were used per assay. Cells were washed with PBS and blocked for 1 h at 4°C with PBS containing 2% BSA. Cells were then incubated with 10 μg Lf-HF488 alone or in the presence of 100-fold excess unlabeled human holo-Lf at 4°C for 2 h. Finally, cells were washed extensively with PBS and the fluorescence data of 10^4 cells per assay was acquired using a Guava 8HT flow cytometer. Experiments were repeated thrice, statistical significance was determined by Student's *t*-test.

Cell Surface Binding of Lf-Gold by Transmission Electron Microscopy (TEM)

To assess Lf binding, *M.tb* H37Ra bacilli were cultured to log phase, 2×10^8 cells were used per assay. Cells were washed with PBS and blocked in PBS containing 2% casein at 4°C for 1 h. Cells were then incubated with 10 μg of Lf- gold (20 nm) in PBS containing 0.2% casein at 4°C for 2 h. Cells were washed and fixed in Karnovsky's fixative for 30 min, followed by two washes with 5 mM NaCl. Finally, cells were resuspended in PBS, placed on carbon coated grids and viewed in a JEOL 2100 Transmission Electron Microscope (TEM). As a negative control, samples were similarly incubated with streptavidin gold conjugate (20 nm, Sigma) instead of Lf. Gold particles were prepared as described previously (Boradia et al., 2014).

Lf Surface Binding and Uptake into *M.tb* H37Ra Bacilli Overexpressing GAPDH mCherry and mCherry

M.tb H37Ra mCherry and *M.tb* H37Ra GAPDH mCherry expressing cells were cultured to log phase, 1×10^8 cells were used per assay. Cells were washed with iron free Sauton's media and blocked for 1 h at 4°C with 2% BSA in PBS. Cells were then

incubated with Lf conjugated to Alexa fluor 647 (Lf-A647, 10 μg per 100 μl of iron free Sauton's media) at 4°C for 2 h. Finally, cells were washed extensively with iron free Sauton's media and fluorescence data of 10^4 cells per assay was acquired using a BD FACS Verse instrument. Experiments were repeated twice in duplicates, statistical significance was analyzed by Student's *t*-test. Data is represented as an overlay histogram and as a bar graph of MFI values.

For uptake experiments, cells were processed as before, blocking was done with SFM containing 2% BSA for 30 min at 4°C. Subsequently, bacteria were incubated with 10 μg Lf-A647 at 37°C for 2 h. Cells were then washed twice and treated with 0.1% pronase at 4°C for 5 min on ice to remove any residual surface bound proteins. Finally, cells were washed extensively with iron free Sauton's media and fluorescence data of 10^4 cells per assay was acquired using a BD FACS Verse instrument. Experiments were repeated twice in duplicates, statistical significance was analyzed by Student's *t*-test. Data is represented as an overlay histogram and as a bar graph of MFI values.

Evaluation of Lf-Iron Uptake

Log phase *M.tb* H37Ra mCh and *M.tb* H37Ra GAPDH-mCh cells, (2×10^8 cells / assay) were washed twice with Sauton's media without iron followed by incubation with the same media for 2 h at 37°C. Cells were then washed and incubated for a further 1 h at 37°C with media containing 50 μg of Lf-^{55}Fe in 100 μl Sauton's media without iron. Cells were washed thrice with iron-free media, centrifuged, and resuspended in 3.0 ml of scintillation fluid. The radioactivity associated with the cells was measured using a beta counter (Perkin Elmer), counts were normalized to cell number. Statistical significance was estimated by Student's *t*-test ($n = 6$) (Boradia et al., 2014).

FRET Analysis of Lf-GAPDH Interaction

Log phase *M.tb* H37Ra mCh and *M.tb* H37Ra GAPDH-mCh cells, (2×10^8 cells/assay) were washed and blocked with 2% BSA followed by incubation with 20 μg Lf-FITC in 100 μl PBS, for 2 h at 4°C. Samples were fixed in 4% buffered paraformaldehyde for 20 min and FRET analysis was carried out by the acceptor photobleaching method on a Nikon A1R confocal microscope as described previously (Raje et al., 2007). The intensities of a total of 70 regions of interest from multiple, randomly selected fields were measured before and after photobleaching, and FRET efficiency was calculated (Boradia et al., 2014). Statistical analysis was done by Student's *t*-test.

Lf Binding on *M.tb* H37Rv and *M.tb* H37RvΔmbtB::hyg Bacilli

M.tb H37Rv and *M.tb* H37Rv ΔmbtB::hyg strains were cultured to log phase, and 1×10^8 cells were used per assay. Cells were washed with phosphate-buffered saline (PBS) and blocked for 1 h at 4°C with 2% BSA in SFM (serum free media). Cells were then incubated with Lf-A647 (10 μg per 100 μl of SFM) alone or in the presence of 200-fold excess unlabeled human Lf at 4°C for 2 h. Finally, cells were washed extensively with SFM and fluorescence data of 10^4 cells per assay was acquired using a BD FACS Accuri instrument. Experiments were repeated thrice in duplicates. Statistical significance was analyzed by Student's *t*-test.

Lf Uptake in *M.tb* H37Rv and *M.tb* H37RvΔmbtB::hyg Bacilli

Cells (1×10^8 bacilli/assay) were blocked with SFM containing 2% BSA for 30 min at 4°C. Subsequently, bacteria were incubated with 10 μg Lf-A647. After incubation at 37°C for 2 h, cells were treated with 0.1% pronase at 4°C for 5 min to remove any residual surface bound proteins. Cells were washed extensively with SFM and fluorescence data of 10^4 cells per assay was acquired using a BD FACS Verse instrument, experiments were repeated thrice in triplicates. Statistical significance was analyzed by Student's *t*-test.

Trafficking of Lf to Intracellular Bacilli

The human macrophage cell line, THP-1, was utilized as an infection model. To study trafficking of Lf to bacteria resident within macrophages, THP-1 cells were plated into Matek glass bottom petri dishes (3×10^5 cells per dish). Cells were activated with 25 ng/ml PMA (Sigma) for 24 h and rested for an additional 24 h. Cells were then shifted to antibiotic-free RPMI media containing 10% fetal calf serum and infected with bacilli at a ratio of 1:20 (THP-1: bacteria) using log phase cultures of *M.tb* H37Rv-GFP, *M.tb* H37Ra mCherry, or *M.tb* H37Ra GAPDH-mCherry. After 6 h, cells were washed with serum-free media (SFM) to remove non-phagocytosed bacteria. A second wash with SFM was carried out after 24 h of infection and cells were shifted to SFM for 30 min at 37°C. Cells were then washed and incubated with 10 μg of Lf-A647 in 100 μl SFM media at 4°C for 30 min. Subsequently, for internalization of bound Lf cells were shifted to 37°C, 5% CO_2 for 1 h. After extensive rinsing with SFM, cells were fixed with 2% paraformaldehyde for 15 min and imaged on a Nikon A1R confocal microscope using a 60X oil immersion objective and an aperture of 1 airy unit.

Live Cell Imaging of *M.tb* H37Ra-GFP Infected THP-1 Cells

THP-1 cells were plated and processed for infection with log phase cultures of *M.tb* H37Ra-GFP and incubation with Lf-A647 as described above. Subsequently cells were imaged live on a Nikon A1R confocal microscope equipped with an Okolab bold line water-jacket cryo topstage CO_2 incubator system (Okolab Italy).

Immuno-Gold Labeling TEM to Detect Internalized Lf in *M.tb* H37Rv

Cells (2×10^9 bacilli per sample) were blocked with SFM containing 2% BSA for 30 min at 4°C. Subsequently, bacteria were incubated with 1 mg of Lf-conjugated with 20 nm gold particles for 2 h at 37°C. Subsequently cells were treated with 0.1% pronase at 4°C for 10 min to remove any residual surface bound proteins. Cells were then fixed, embedded in epoxy resin and ultrathin sections cut for visualization in TEM essentially as described previously (Boradia et al., 2014).

Expression and Purification of Mutants and GAPDH Enzymatic Activity

Both mutant forms of the protein were expressed and purified as described previously for wt rGAPDH (Boradia et al., 2016). Purification was confirmed by western blotting, detection was done after incubation with Mouse anti-His (Sigma) (1:3,000) for 1 h followed by incubation with anti-Mouse IgG HRP (Sigma) (1:8,000) for 1 h. The enzyme activity of wt rGAPDH, rGAPDH(N142S), and rGAPDH(P295L) purified from cytosol fraction was studied by measuring the increase in the absorbance at 340 nm due to oxidative reduction of NAD^+ to NADH. The reaction mixture containing 200 µl of enzyme assay buffer (50 mM HEPES, 10 mM sodium arsenate, and 5 mM EDTA, pH 8.5), 1 mM NAD^+ and 2 mM glyceraldehyde-3-phosphate (G-3-P) was added to wells containing 100 ng of each purified enzyme at 25°C. Enzyme activity was measured at 340 nm for 5 min on a Tecan Infinity M200 multimode microplate reader. Negative controls were set up without the specific substrate G-3-P and their values were subtracted from the final absorbance. The experiment was repeated thrice in triplicates. The enzymatic activity of wt rGAPDH was taken as 100% and data was plotted as % residual activity ± *SD*. Statistical analysis was done using Student's *t*-test.

Interaction of GAPDH Mutants with Human Lf

Lf (3 µg), BSA (5 µg), wt rGAPDH (1 µg), rGAPDH (N142S) (1 µg), or rGAPDH (P295L) (1 µg) were resolved on 10% SDS-PAGE and then transferred to nitrocellulose membrane. The membrane was then blocked with 5% BSA and probed with 10 µg/ml of either wt rGAPDH, rGAPDH(N142S) or rGAPDH(P295L) for 2 h, followed by incubation with mouse anti-His (Sigma) (1:3,000) for 1 h and anti-mouse IgG HRP (Sigma) (1:8,000) for 1 h. Finally, blots were washed and developed with TMB/H_2O_2; the experiment was repeated three times.

Analysis of Lf-GAPDH Interaction by Far Western Blotting

Recombinant *M.tb* H37Rv GAPDH, wild type (wt rGAPDH) was prepared as described previously (Boradia et al., 2016). Lf, BSA (3 µg each) and wt rGAPDH (400 ng) were run on a 10% SDS-PAGE and transferred to nitrocellulose membrane. The membrane was probed with 10 µg/ml of wt rGAPDH for 2 h, followed by incubation with rabbit anti-GAPDH (1:1,000) for 1 h and anti-rabbit IgG HRP (1:16,000) for 1 h; blots were developed with TMB/H_2O_2, experiments were repeated thrice.

Determination of Affinity of Interaction by Solid Phase Binding Assay

The affinity of the GAPDH and Lf interaction was estimated using a plate based solid phase binding assay. Polystyrene wells were coated overnight at 4°C using 2 µg/well of either wt rGAPDH, rGAPDH(N142S) or rGAPDH(P295L) mutant proteins in PBS (pH 7.4) and blocked using 5% cold fish skin gelatin prepared in PBS for 4 h at room temperature. GAPDH coated wells were then incubated at 25°C for 2 h with increasing concentrations (7.5−1,000 nM) of biotinylated Lf in PBS containing 1% fish skin gelatin. Control wells were incubated with buffer alone. Extensive washing with PBST was done out to remove any unbound Lf. Bound Lf was detected using primary antibody Mouse anti-Biotin (1:5,000), secondary antibody anti-Mouse IgG HRP (1:20,000) followed by the addition of TMB-H_2O_2 for development of color. Data was plotted as absorbance at 650 nm vs. concentration of biotinylated Lf after subtracting OD values of control wells. Experiments were performed thrice (with triplicates) and data was plotted for non-linear fit, one-site specific binding using Graph Pad Prism®.

Sequence Conservation Analysis of GAPDH

Initial evolutionary conservation sequence analysis to identify functionally and structurally important residues in *M.tb* GAPDH were performed by the ConSurf Program (Ashkenazy et al., 2010, 2016). The primary sequence of wild type, N142S and P295L mutants as well as *M.tb* GAPDH modeled structure were considered. For query sequences and structure the CSI-BLAST (Context-Specific Iterated-Basic Local Alignment Search Tool) homolog search algorithm were used with 0.00001 as E-value cutoff, set at a maximal 95% identity and minimal identity of 35% between sequences for homology searches. The protein database UNIREF-90 (http://www.uniprot.org/help/uniref) was utilized; all other parameters were kept at default values for calculation of conservation scores. The primary goal was to reveal the highly conserved regions and functionally and structurally important residues in *M.tb* GAPDH.

Comparative Modeling of GAPDH

GAPDH is a homo-tetramer composed of four identical 36 kDa subunits. The structure of GAPDH alongwith its associated cofactor NAD^+ has been reported for other homologous organisms. The sequence of *M.tb* H37Rv GAPDH was retrieved from NCBI (GenBank: CAB09248.1), the protein sequence is composed of 339 amino acids. The sequence was analyzed by NCBI protein BLAST search against Protein Data Bank (PDB) in order to get a template with a suitable identity. Tetrameric GAPDH from *Bacillus stearothermophilus* (PDB ID: 1GD1) was identified as the best template and was utilized for homology modeling of GAPDH using Modeller9v program (Webb and Sali, 2014).

Assembly of Monomer Units and Analysis of Mutants

GAPDH homo-tetramer assembled from four identical 36 kDa subunits was done using superimposition tool of Chimera program (Pettersen et al., 2004; Meng et al., 2006). The template (PDB ID: 1GD1) was assembled into its homo-tetrameric structure, each unit of modeled *M.tb* GAPDH was then superimposed upon this template. The assembled model was energy minimized to correct the unfavorable bond lengths, bond angles, torsion angles, and contacts. Subsequently, the final model was verified and validated using RAMPAGE Ramachandran plot analysis server (http://mordred.bioc.cam.ac.uk/~rapper/rampage.php) and native protein folding energy assessment by PRoSA program (https://prosa.services.came.sbg.

ac.at/prosa.php). The position of the two mutations was analyzed in context of the GAPDH tetramer and its proximity to the NAD^+ binding site.

Analysis of Mutants by Computational Methods

Two selected mutations (N142S and P295L) were experimentally tested for the two functions attributed to GAPDH i.e., (i) enzyme activity and (ii) ability to bind Lf. Of these Asparagine 142 is a conserved residue and mutation to serine resulted in a loss of enzyme activity. However, both mutants retained their ability to bind Lf in far-western blots. Both mutants were explored to predict the effect of these alterations on protein stability and proximity to substrate binding site. The effect of mutations on protein stability were analyzed using DUET (Pires et al., 2014), mCSM and Site Directed Mutator (SDM) (Worth et al., 2011).

RESULTS

Cell Surface Binding of Lf on *M.tb* H37Ra Cells

Flow cytometry clearly demonstrated the binding of Lf to *M.tb* H37Ra cells which was significantly inhibited ($p < 0.0001$) in the presence of 100-fold excess of unlabeled Lf, indicative of a specific interaction (**Figures 1A,B**). The binding of Lf-gold particles conjugated particles to *M.tb* H37Ra was confirmed by TEM analysis (**Figures 1C–E**).

GAPDH Mediated Lf-Iron Delivery

M.tb H37Ra strains overexpressing GAPDH-mCherry (GAPDH-mCh) or mCherry (mCh) alone were utilized to confirm whether Lf iron is GAPDH dependent. The overexpression of GAPDH in *M.tb* H37Ra resulted in enhanced binding (**Figures 2A,B**) and uptake of Lf when compared to control cells that over express mCherry alone ($p < 0.0005$) (**Figures 2C,D**). A correlated increase in iron uptake was also evident in the *M.tb* GAPDH-mCh strain as compared to the mCh strain (**Figure 2E**).

Confirmation of GAPDH-Lf Interaction on the *M.tb* Cell Surface

To confirm that GAPDH and Lf interact on the bacterial cell surface we carried out acceptor photobleaching Förster resonance energy transfer (FRET) analysis using *M.tb* H37Ra cells expressing GAPDH-mCh or mCh alone. This assay is based on the principle of two interacting partners which are fluorescently tagged. The fluorophores are selected such that the emission spectra of the donor overlaps with the absorption

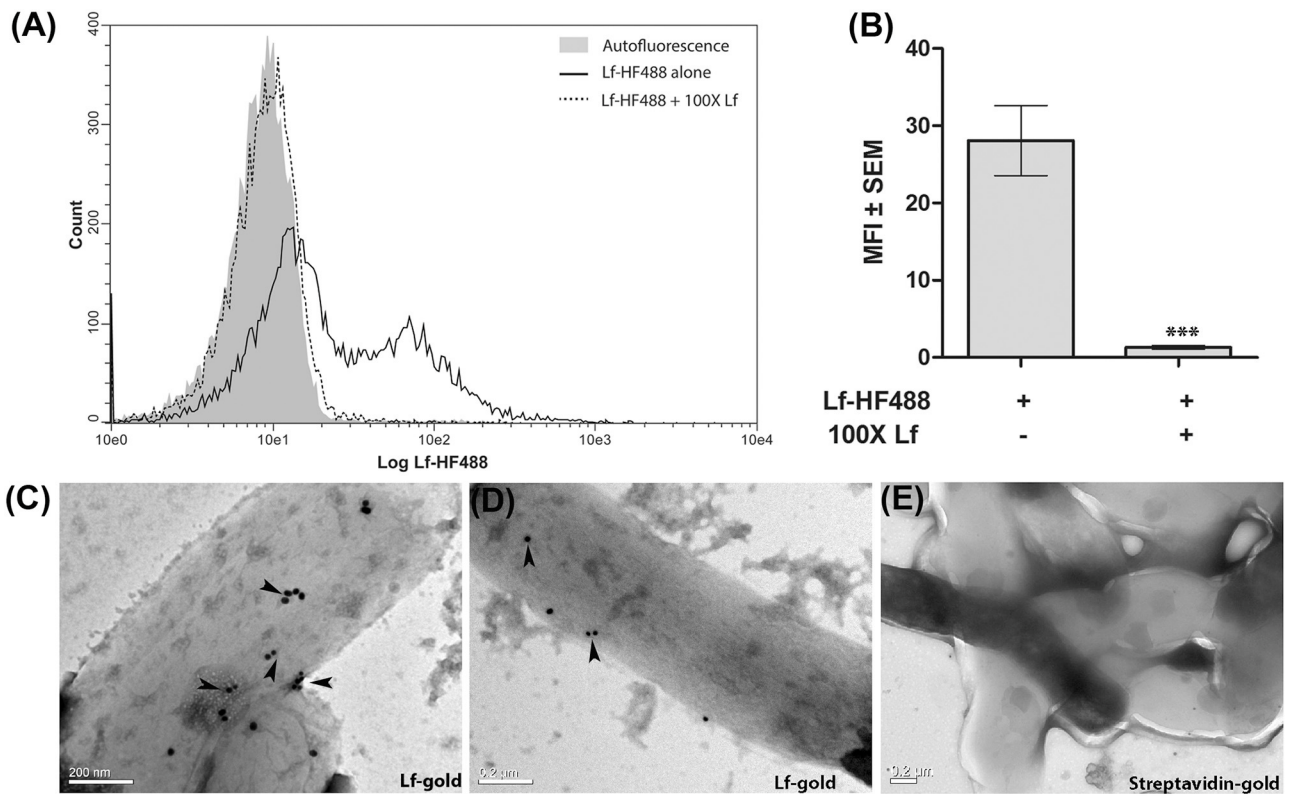

FIGURE 1 | Surface binding of Lf. **(A,B)** FACS analysis indicates specific binding of Lf-HF488 on the surface of *M.tb* H37Ra cells **(A)** Overlay histogram plot of one representative experiment indicating log fluorescence of Lf-HF488. **(B)** Bar graph depicting MFI ± SEM. **(C–D)** TEM images reveal the binding of Lf conjugated gold particles (indicated by arrow heads) and **(E)** Control cells treated with control Streptavidin gold particles, demonstrate no surface binding of gold particles. Scale bar 0.2 μM. Multiple fields were analyzed with each sample, representative images are shown.

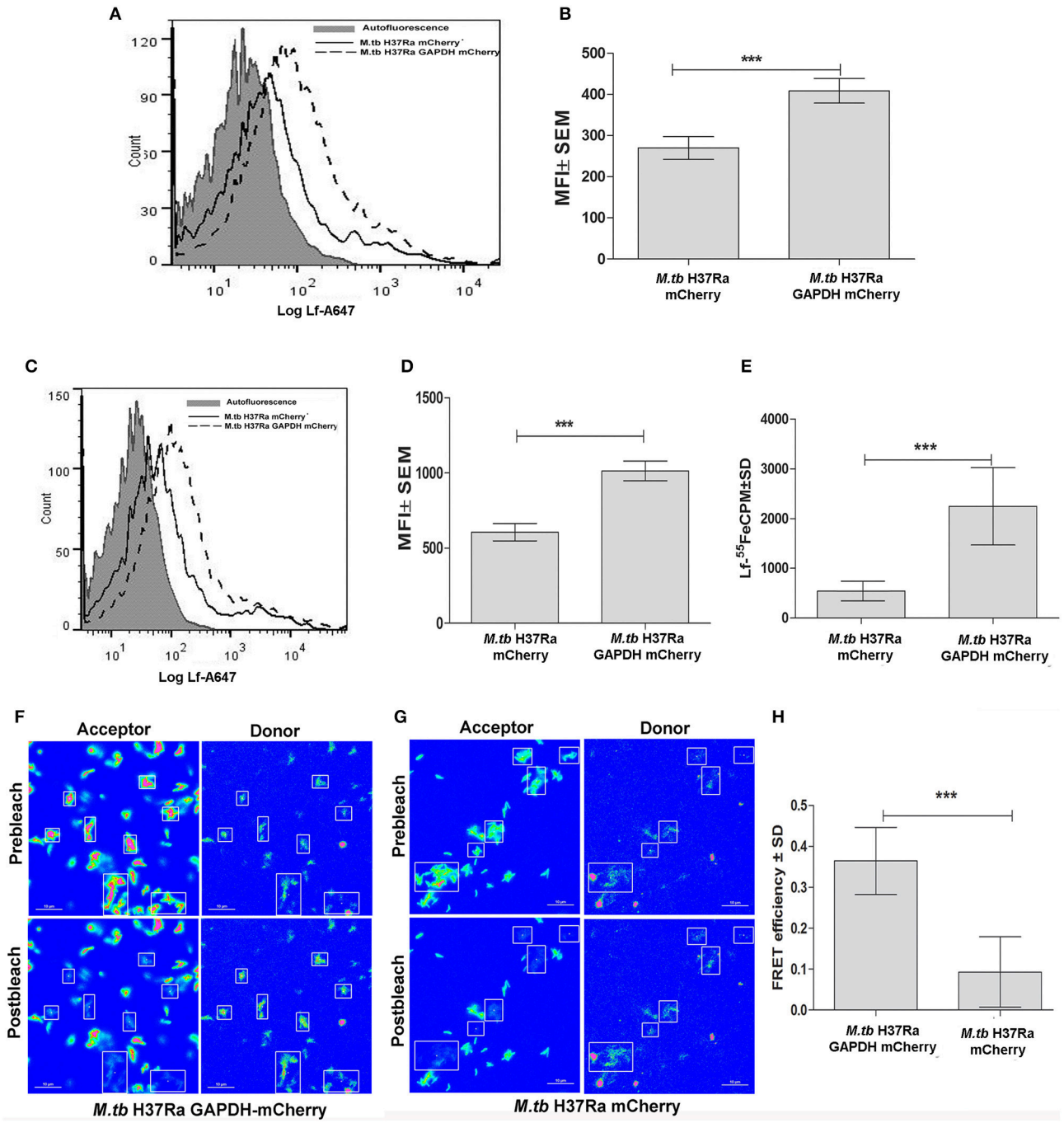

FIGURE 2 | Enhanced GAPDH promotes binding, uptake and iron acquisition via Lf: FACS analysis indicates **(A–B)** binding of Lf-A647 **(C–D)** uptake of labeled Lf **(E)** Iron uptake in *M.tb* H37Ra GAPDH mCherry and mCherry strains. ($p < 0.0005$; $n = 6$) **(F)** Acceptor photobleaching FRET analysis of the GAPDH-Lf interaction on the surface of *M.tb* H37Ra cells. Upper panels indicate the pre-bleach images of acceptor and donor respectively, while lower panels indicate post-bleach images of acceptor and donor. An increase in donor (Lf-FITC) signal is observed on photobleaching of acceptor (GAPDH-mCh) **(G)** A control experiment using *M.tb* H37Ra cells expressing mCh alone. **(H)** Quantitative analysis of FRET signal of 70 regions of interest from multiple, randomly selected fields were analyzed from both test and control samples. The FRET efficiency change ± s.d. of the donor and acceptor signals after photobleaching GAPDH-mCh and mCh was determined using NIS-Elements (Nikon) software. The % intensity change of the Lf-FITC signal was significantly higher in cells expressing GAPDH-mCh as compared to mCh alone (***$p < 0.0001$, Student's *t*-test, $n = 70$).

spectra of the acceptor. In the current study if Lf-FITC and GAPDH-mCherry interact, when excitation is done with the wavelength specific for Lf-FITC a strong fluorescence of mCherry is evident. When mCherry is destroyed (by photobleaching) an increase in donor signal is visible because the acceptor is no longer available to parasitize the light emitted from Lf-FITC

(Kenworthy, 2001). In the present study a significant increase in donor (Lf-FITC) fluorescence intensity was observed upon photobleaching of acceptor (mCh) in the *M.tb* H37Ra GAPDH-mCh strain (**Figures 2F,H**) as compared to the strain expressing mCh alone (**Figures 2G,H**). The occurrence of FRET between the GAPDH and Lf indicates that they are at proximity of 1–10 nm (Kenworthy, 2001).

Cell Surface Binding and Uptake of Lf by *M.tb* H37Rv and *M.tb* H37Rv ΔmbtB::hygr Strain

Both strains demonstrated cell surface binding of human Lf at 4°C that was competitively inhibited by the presence of 200X unlabeled Lf (**Figures 3A,B**). Lf binding was comparable in wild type and siderophore knockout strains (**Figure 3C**). Internalization of labeled Lf was also evident in both strains after incubation at 37°C (**Figure 3D**) indicating that GAPDH mediated Lf uptake is siderophore independent.

Internalization of Lf into *M.tb* H37Rv

Bacilli were analyzed by TEM to assess the internalization of Lf-gold conjugated particles, which were observed within the cell cytosol (**Figures 3E–G**).

Trafficking of Lf to Intraphagosomal *M.tb*

THP-1 cells were infected with either (i) *M.tb* H37Ra mCh (ii) *M.tb* H37Ra GAPDH-mCh or (iii) *M.tb* H37Rv-GFP strains (**Figures 4A–C** respectively). The trafficking of Lf-A647 to the intraphagosomal bacilli was assessed by confocal microscopy. In all cases the co-localization of Lf-A647 and bacilli was observed, live cell imaging of infected cells confirmed the endocytosis and subsequent co-localization of Lf with intraphagosomal *M.tb* H37Ra-GFP (**Movie 1**).

Expression and Purification of rGAPDH (N142S) and rGAPDH (P295L)

Both proteins were expressed using *M.tb* H37Ra as a host strain. The proteins were purified using Ni-NTA affinity chromatography and purity confirmed by western blotting with mouse anti-His antibody (**Figures 5A,B**).

Enzyme Activity of Mutants and Interaction with Lf

The N142S mutant showed a significant loss of activity ($p < 0.0001$), only 45% enzyme activity was retained as compared to the wild type enzyme. In contrast the P295L mutant protein demonstrated enzyme activity comparable to wt rGAPDH (**Figure 5C**). The GAPDH-Lf interaction was confirmed *in vitro* by far western blotting using recombinant *M.tb* rGAPDH (rGAPDH) (**Figure 5D**). Resolved Lf was able to capture rGAPDH as evident by far western blotting, rGAPDH, and BSA were utilized as positive and negative controls respectively. The N142S, P295L mutant proteins also retained their ability to bind Lf in far western blots (**Figures 5E,F**). ELISA was carried out using 125 nM Lf to obtain quantitative data, no significant difference was observed between the three proteins (**Figure 5G**)

M.tb GAPDH and Lf Binding Affinity

Lf binding to rGAPDH and mutants was observed to steadily increase with increasing concentration of Lf with saturation at 500 nM (**Figure 5H**). The K_D value of GAPDH-Lf interaction was estimated to be 31.7 ± 1.68 nM, a 5-fold higher affinity as compared to *M.tb* GAPDH and Tf (160 ± 24 nM). No significant difference in the affinity values were evident between wt and mutant proteins values. The N142S and P295L mutants were 38.22 ± 3.08 and 37.74 ± 2.63 nM respectively (**Figure 5H**).

Sequence Conservation of GAPDH

The *M.tb* GAPDH sequence was analyzed for its evolutionary conservation, it was observed that key active site residues as well as other surface exposed residues are highly conserved. Since it is known that GAPDH from multiple species binds to Tf (Modun and Williams, 1999), there is a high probability that the conserved regions (including active sites, co-factor binding site, and surface regions) may contribute to the interaction between Lf and Tf. Consurf server based evolutionary conservation analysis was carried out for the wt GAPDH sequence and the two point mutations N142S and P295L (http://consurf.tau.ac.il/2016/). Analysis of Asparagine 142 (N142) revealed that it is a highly conserved and exposed functional residue while Proline at 295 position is an exposed but variable residue (**Figure 6A**).

Comparative Homology Modeling of GAPDH and Mutant Analysis

The comparative modeling of *M.tb* GAPDH was performed, using highly identical template of GAPDH from *B. stearothermophilus* (PDB ID: 1GD1). The two sequences demonstrate a sequence identity of 60%. The modeled 3D structure of GAPDH was validated by the RAMPAGE Ramachandran plot analysis server (http://mordred.bioc.cam.ac.uk/ rapper/rampage.php). The quality of protein folds of GAPDH homology model was evaluated using ProSA protein structure analysis web server (https://prosa.services.came.sbg.ac.at/prosa.php). Modeled 3D structure aligned with the template (PDB ID: 1GD1) and assembled structural model was developed using UCSF Chimera software (https://www.cgl.ucsf.edu/chimera/), the RMSD score was 0.238 (**Figures 6B,C**).

Although, *in silico* analysis of the mutant N142S suggests that this mutation may result in a non-significant structural change, since Serine at position 142 also shows a similar characteristic to the wild type residues N142, experimentally the mutation resulted in a loss of enzyme activity. Several computational methods have been developed for predicting the stability of mutant proteins based on sequence, structure, and Gibbs free energy estimation, this combined feature based approach provides better prediction of changes due to mutations (Kulshreshtha et al., 2016). In the current study, two different methods were used to predict the stability change of mutated proteins, predictions also assessed the sequence conservation. A combined sequence conservation and protein modeling study indicates Asparagine (N142) is a highly conserved and exposed residue that is located in a flexible loop region of GAPDH. Predicted stability change energies in the mutant (ΔΔG)

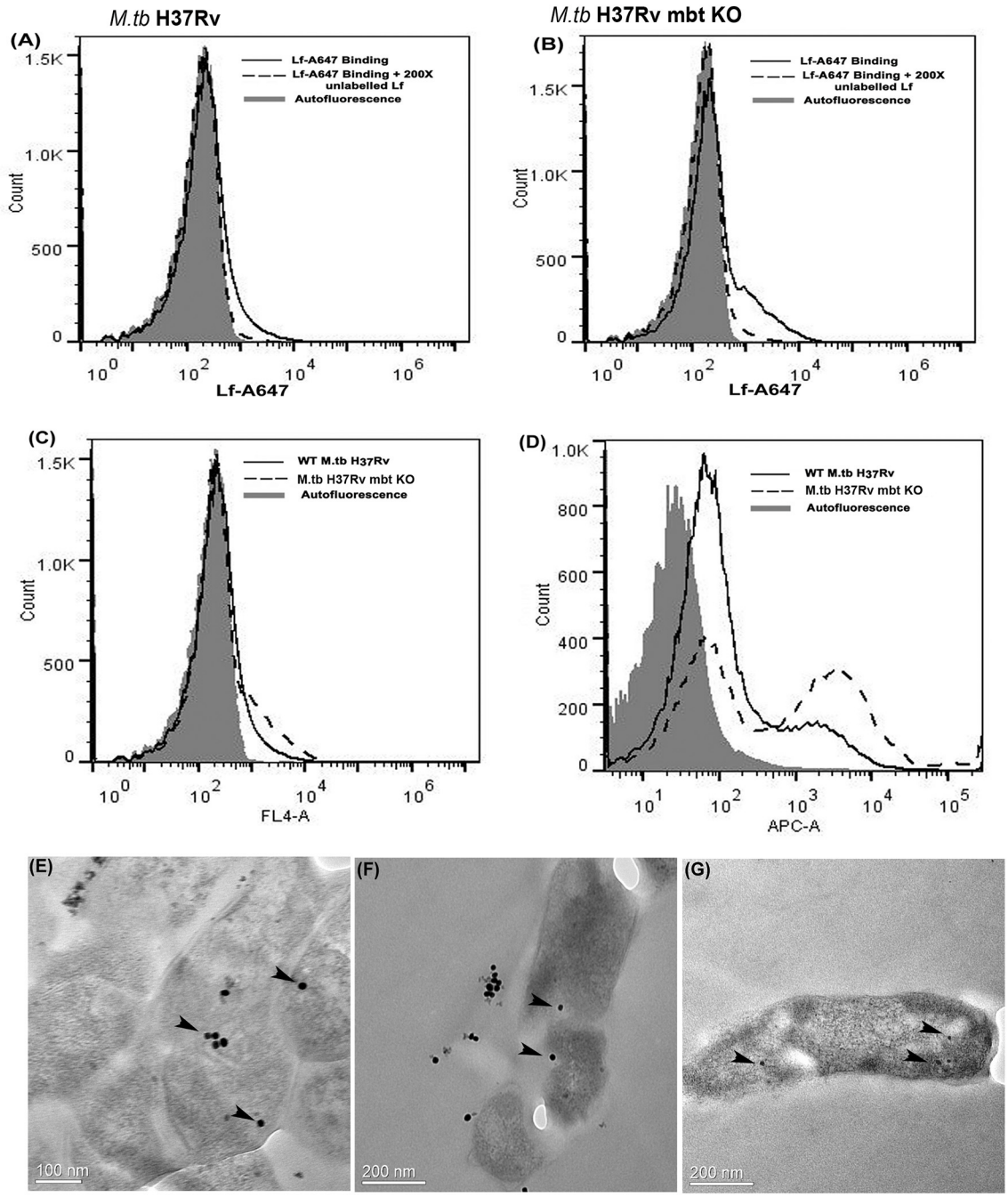

FIGURE 3 | Lf surface binding and internalization in *M.tb* H37Rv strains: FACS analysis indicates specific binding of Lf-A647 on the surface of **(A)** *M.tb* H37Rv cells and **(B)** *M.tb* H37Rv mbt KO strain. **(C)** Comparative binding of Lf-A47 on the surface of both strains **(D)** Internalization of Lf-A647 in *M.tb* H37Rv and H37Rv mbt KO strain. **(E–G)** TEM images reveal the internalization of Lf-gold particles into the bacilli of *M.tb* H37Rv cells. Scale bar 0.1, 0.2 μM.

indicate destabilization (**Table 1**). Structural analysis indicates that in *M.tb* GAPDH, the Glycine-Valine-Asparagine tripeptide sequence (at positions 140, 141, and 142 respectively) is also highly conserved in several GAPDH homologs. Additionally, it was observed that Asparagine 142 also has hydrogen bonding interactions with another highly conserved tripeptide region comprised of residues 136 to 138 (**Figures 6**, **7C**). This tripeptide is composed of the sequence Threonine136-X-Valine138 where X indicates a variable residue. In *M.tb* GAPDH the intervening residue is Isoleucine at position 137 (**Figure 6**). Replacement of Asparagine with serine results in a loss of hydrogen bonding with Threonine 136 (**Figure 7D**). Computational modeling of the

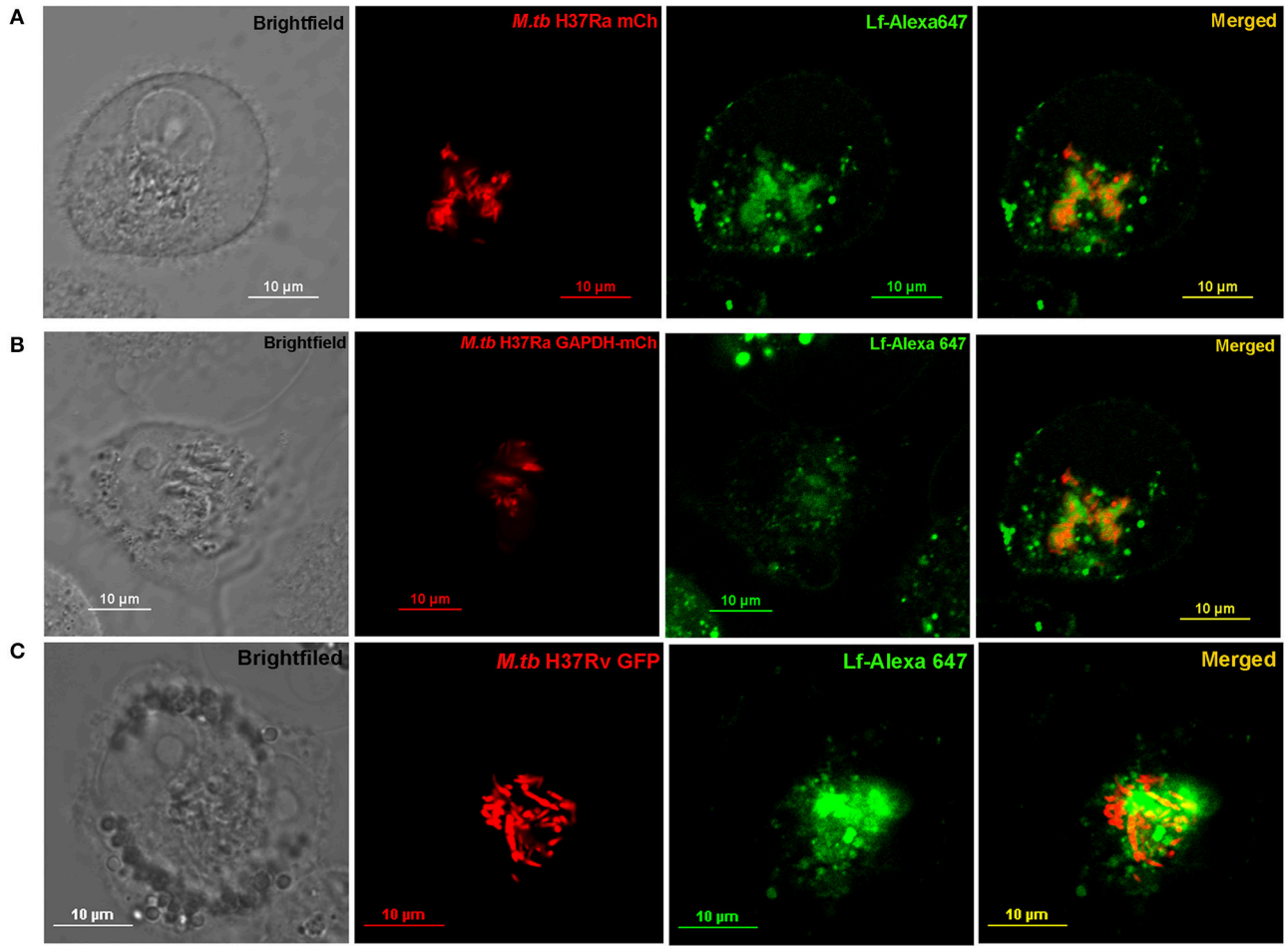

FIGURE 4 | Trafficking of Lf to Intraphagosomal bacilli: THP-1 cells were infected with **(A)** *M.tb* H37Ra mCh **(B)** *M.tb* H37Ra GAPDH-mCh or **(C)** *M.tb* H37Rv GFP strains. The trafficking of Lf-A647 to the phagosome and co-localization with the intracellular bacteria are evident.

N142S mutant revealed conformational changes in this region during loop refinement, suggesting that this mutation may alter the stability of the molecule or its interaction with a helix that lies in close proximity (**Figures 7A,B**). While biochemical assays confirm a loss of enzyme activity, detailed analysis by co-crystallization, molecular modeling, extensive dynamic simulation, and mutagenesis would be essential to ascertain the relevance of these residues (if any) in the GAPDH-Lf/Tf interaction. In contrast the Proline 295 residue occurs in a variable loop region adjoining a highly conserved helix, mutation to Leucine does not result in a structurally significant change as confirmed by experimental data (**Figures 7E,F**).

DISCUSSION

Due to its intracellular location, *M. tuberculosis* faces a unique challenge in acquiring iron from within the host cell. It adopts multiple strategies to acquire this essential micronutrient from host iron carrier/storage proteins such as Tf, Lf, ferritin, and hemoglobin. Among these, two well-established processes involve the synthesis of siderophores and hemophores (De Voss et al., 2000; Tullius et al., 2011). Tf and Lf are conserved iron carrier proteins that share a high degree of sequence identity (60%), they are also structurally conserved. Iron acquisition from human Tf and Lf by the siderophores mycobactin and carboxymycobactin is well-characterized. Iron is chelated by the siderophore and transported via specific iron regulated transporters (Ryndak et al., 2010; Banerjee et al., 2011). However, the recombinant strains *M.tb* H37Rv Δmbt:: hyg and BCG(mbt)30 that do not express siderophores retain the ability to acquire Tf iron *in vivo*, indicating the presence of a siderophore independent pathway (De Voss et al., 2000; Tullius et al., 2008). Similar studies with Lf have not been evaluated. Although *M.tb* thrive in the lung, an environment rich in Lf rather than Tf, relatively less is known about Lf mediated iron uptake by *M.tb*. While previous studies have demonstrated that *M.tb* acquires iron from Lf in broth cultures and also within host macrophage cells the exact process is yet to be defined.

In pathogens such as *S.aureus, S.epidermidis, Neisseria gonorrhea, N.meningitidis, H. influenzae* iron acquisition from Tf and Lf can occur by the direct capture of these proteins by

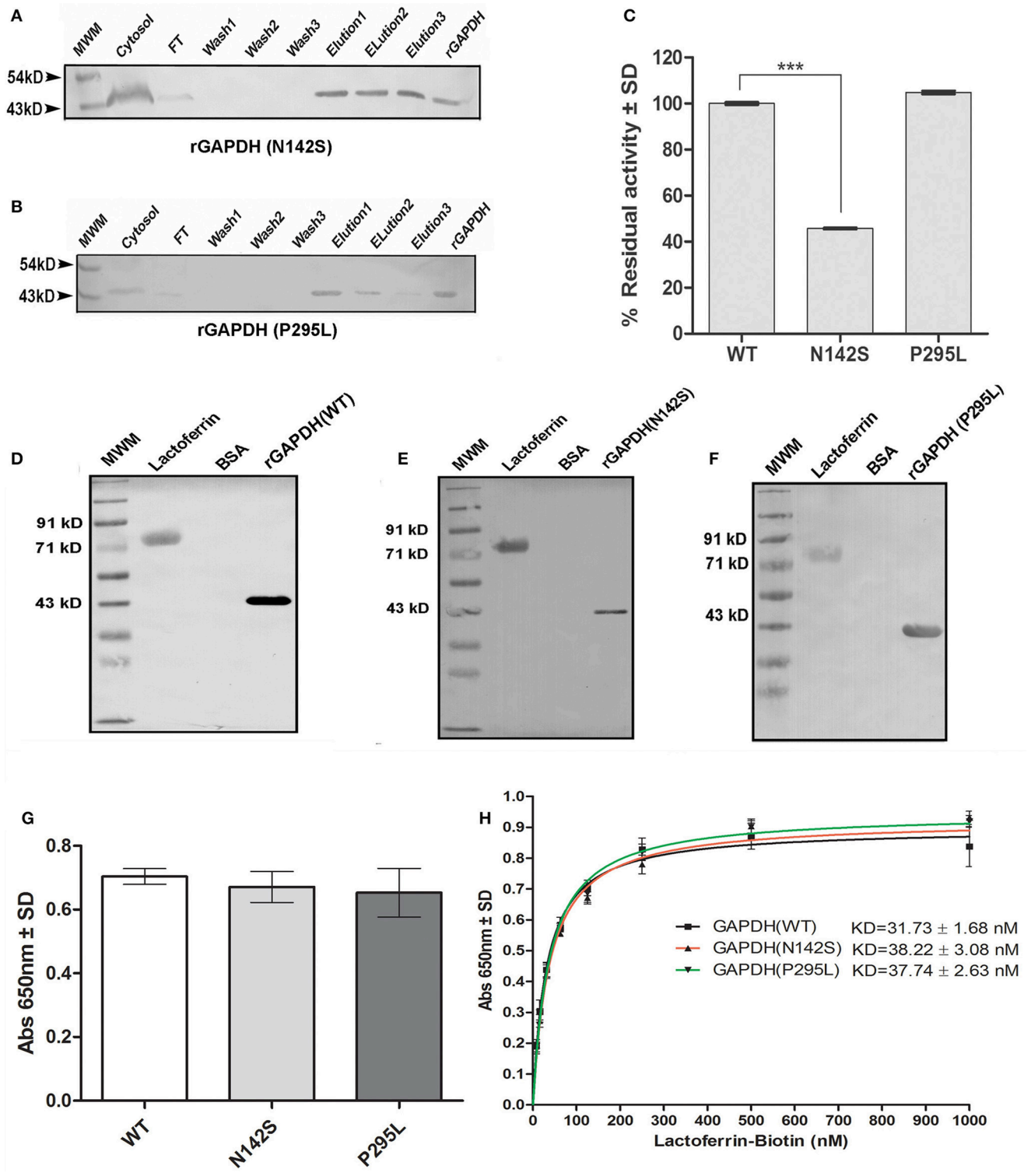

FIGURE 5 | Analysis of *M.tb* GAPDH point mutations: Purification of recombinant GAPDH mutant proteins as confirmed by western blot **(A)** rGAPDH (N142S) **(B)** rGAPDH (P295L) **(C)** Enzyme activity of mutants and wild type protein. ($p < 0.0001$, $n = 3$) **(D–F)** Far western blotting assessed the interaction of Lf with rGAPDH (wt), rGAPDH (N142S), rGAPDH (P295L) respectively. **(G)** ELISA to estimate the binding of 125 nM Lf to wt rGAPDH, rGAPDH (N142S), rGAPDH (P295L) **(H)** Determination of affinity of interaction (K_D) between rGAPDH, rGAPDH (N142S),or rGAPDH (P295L) with Lf.

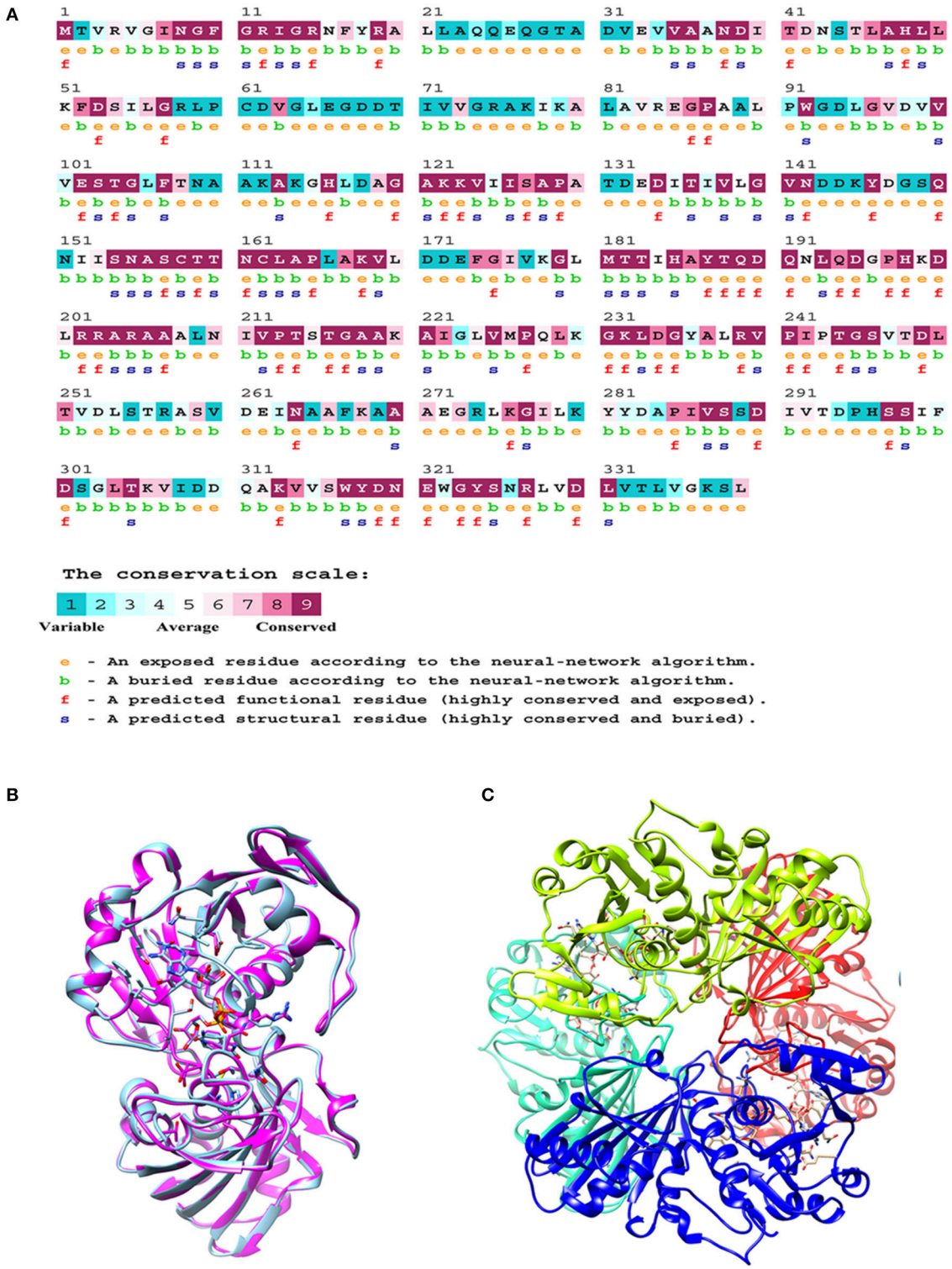

FIGURE 6 | *In silico* analysis of *M.tb* GAPDH: **(A)** Consurf analysis to determine functionally and structurally important residues. **(B)** Modeled structure of GAPDH monomer. **(C)** Homology model of tetrameric *M.tb* H37Rv GAPDH based on GAPDH template from *Bacillus stearothermophilus* (PDB ID: 1GD1).

specific surface receptors (Williams and Griffiths, 1992; Gray-Owen and Schyvers, 1996; Modun and Williams, 1999; Taylor and Heinrichs, 2002). Recently our group identified multiple cell surface receptors for human Tf on the surface of *M.tb*. These include evolutionarily conserved metabolic enzymes such as GAPDH and LDH (Boradia et al., 2014). GAPDH is a highly

TABLE 1 | Analysis of mutants by computational methods.

Mutations (predicted stability change ΔΔG)	mCSM	SDM	DUET	Conservation score
N142S	−1.216	−0.36	−1.223	Highly (8–9)
P295L	−0.994	0.67	−0.793	Lower (1–2)

ΔΔG in Kcal/mol, negative values indicate destabilization and positive values indicate stability of protein structure.
mCSM: Predicts the effect of mutations in proteins using graph-based signatures.
SDM: Site Directed Mutator is a statistical potential energy function method.
DUET: Protein Stability Change upon Mutation methods.

conserved glycolytic enzyme that is present in all organisms. In human macrophages GAPDH functions as a dual receptor for both Tf and Lf (Raje et al., 2007; Rawat et al., 2012), moreover *M.tb* and human GAPDH are ∼45% identical. Considering all these features we evaluated whether *M.tb* GAPDH can also function as a dual receptor for Lf. Preliminary studies using *M.tb* H37Ra cells revealed the specific binding of Lf to the bacterial surface. *In vitro* experiments confirmed that GAPDH is the receptor involved and overexpression of GAPDH in *M.tb* H37Ra cells resulted in a significant increase in binding and uptake of Lf as well as incorporation of associated iron. As reported by us in earlier studies involving GAPDH-Tf uptake (Boradia et al., 2014), Lf was internalized into the bacterium. At present the detailed mechanism of this process remains undefined.

Lf binding and uptake was also evident on the surface of virulent *M.tb* H37Rv and on the *M.tb* H37RvΔmbtB::hyg strain that is incapable of synthesizing siderophores. These findings are in agreement with previous reports demonstrating the intracellular survival and replication of siderophore negative strains within macrophages and in mice (De Voss et al., 2000; Tullius et al., 2008) indicative of the presence of alternate iron acquisition pathways.

To confirm whether this mechanism operates to deliver Lf to intraphagosomal bacilli, infected THP-1 cells were used as a model system. Confocal microscopy and live cell imaging studies clearly reveal the endocytosis and eventual co-localization of labeled Lf to the bacilli. Previous studies have evaluated the uptake of iron from endogenous and exogenous sources. In the endogenous model macrophages were preloaded with iron from Tf, Lf, or chelates and subsequently infected with *M.tb*. Iron uptake by the macrophages was comparable, but iron acquisition by *M.tb* was marginally more in cells preloaded with Lf-iron. In the case of experiments utilizing the exogenous model, cells were first infected with *M.tb* and then provided exogenous Tf, Lf, or Fe-citrate. When iron uptake by resident intracellular bacilli was evaluated, it was found that *M.tb* preferentially acquired Lf-iron as compared to Tf or Fe-citrate. Infected macrophages acquired 30-fold more iron from Lf and 3-fold more iron from citrate as compared to Tf. This suggests that if Lf and Tf are present in the external milieu, Lf is vastly more efficient at iron delivery to intra-phagosomal *M.tb* (Olakanmi et al., 2002, 2004). Our current study revealed that *M.tb* GAPDH possesses a 5-fold greater affinity for Lf as compared to Tf. Moreover, the Lf based iron uptake in the GAPDH mCh strain was evident within 1 h as opposed to 3 h in the case of Tf-iron (Boradia et al., 2014).

The crystal structure of *M.tb* GAPDH and structural details of the Lf/Tf-GAPDH interaction are at present unknown. In an effort to identify the key residues that may be involved in this interaction, analysis of two GAPDH mutants was carried out. Mutations of Asparagine at position 142 to Serine (N142S) and a Proline to Leucine alteration at position 295 (P295L) were assessed for their enzyme activity and ability to bind Lf. The N142S mutation demonstrated a drastic loss of enzyme activity as compared to wt GAPDH. The affinity of wild type protein and mutants for Lf were comparable (**Figure 5H**). This finding suggests that the two functions of GAPDH i.e., enzyme activity and Lf binding are independent of each other. Finally, the position of these residues within the GAPDH molecule was evaluated by *in silico* approaches. The sequence was evaluated for conserved, variable, exposed, or internal residues; a homology model was constructed for both the monomer and the tetrameric enzyme. It was found that N142 is a highly conserved, exposed residue that is present in a flexible loop region of GAPDH. Moreover, in *M.tb* GAPDH, the Glycine-Valine-Asparagine tripeptide sequence (at positions 140, 141, and 142 respectively) is highly conserved in several GAPDH homologs. Computational analysis suggested that this mutation may alter the stability of the molecule or its interaction with a helix that lies in close proximity (**Figures 7A,B**). Analysis also revealed that the interaction of N142 with conserved residues T136 and V138, hydrogen bonding with T136 was disrupted in the N142S mutant (**Figures 7C,D**), which may contribute to the observed loss of enzyme activity. However, detailed analysis by co-crystallization, molecular modeling, dynamic simulation, and mutagenesis would be necessary to ascertain the exact residues involved in the GAPDH-Lf/Tf interaction.

It is known that internalization of Tf into mammalian cells including macrophages can occur via the three identified receptors TfR1, TfR2 (absent on macrophages), and GAPDH (Jandl et al., 1959; Kawabata et al., 1999; Raje et al., 2007). Cell surface and soluble GAPDH are well-characterized routes for Lf uptake in macrophages (Rawat et al., 2012; Chauhan et al., 2015). Other known Lf receptors are Lipoprotein receptor-related protein (LRP) (Grey et al., 2004) and CD14 (Baveye et al., 2000). In the context of *M.tb* infection, further studies are essential to explore which of these pathways deliver iron to the phagosome and where the iron carrier molecules are transferred to the bacterial receptors. An alternate possibility is that unidentified, secreted bacterial proteins may intersect the endocytic pathway to capture and recruit Lf to the phagosome.

In conclusion, the current study reveals for the first time that *M.tb* can efficiently acquire iron from Lf utilizing GAPDH. These findings are relevant since lung fluids are rich in Lf and it is also an essential component of the innate immune response. The use of GAPDH as a single receptor that can acquire iron from both Tf and Lf indicates the ability of the bacilli to adapt to the external milieu. This study also brings into consideration the complex inter-relationship between the host and pathogen wherein GAPDH from both sources play parallel roles in iron acquisition. In siderophore mediated iron uptake, the host synthesizes siderocalins as a protective mechanism to inhibit iron uptake (Goetz et al., 2002; Flo et al., 2004; Berger

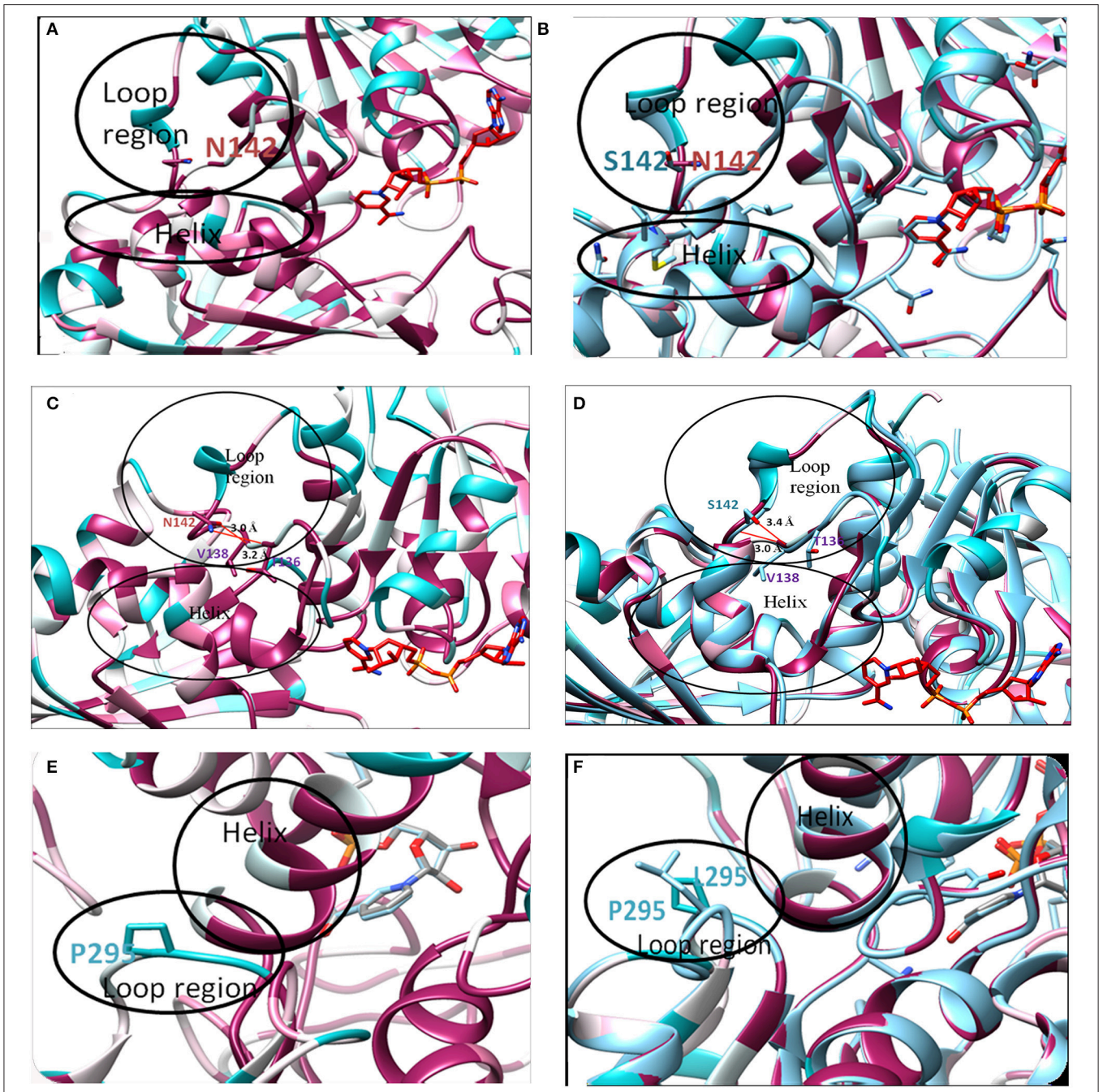

FIGURE 7 | *In silico* analysis of mutations: Location of original and mutant residues **(A)** Model of Asparagine at position 142 of GAPDH **(B)** Structure showing the replacement of Asparagine with serine **(C)** Hydrogen bond formation is observed (represented as red line) between O-atom of Threonine 136 and NH_2 group of Asparagine 142 (distance of interaction 3.2 Å). A second interaction occurs between the N-atom of Valine 138 and OH group of Asn 142 (distance of interaction 3.0 Å). **(D)** Formation of H-bond (represented as red line) is observed between O-atom of Valine 138 and N atom of Serine 142 (distance of interaction 3.0 Å) backbone interaction. A second interaction is observed between N-atom of Valine 138 and OH group of Serine 142 (distance of interaction 3.4 Å). As compared to the wild type Asparagine 142, the mutant Serine142 does not show any interaction with Threonine 136. **(E)** Model of Proline at position 295 of GAPDH **(F)** Structure showing the replacement of Proline with Leucine.

et al., 2006). Utilizing its GAPDH for hijacking host iron provides an ideal astute strategy that offers a means of camouflage allowing the bacterium to operate this critical pathway undetected by the host cell. Unraveling the contribution of host and bacterial components in this alternate pathway could offer an insight into iron acquisition by *M.tb* and perhaps other pathogens.

AVAILABILITY OF DATA AND SUPPORTING MATERIAL

The data supporting the research findings are available in the manuscript.

AUTHOR CONTRIBUTIONS

CR and MR initiated the project. HM, AP, VB, MR, and CR designed the experiments, analyzed the data, and prepared the manuscript. RKu, RN, and PG designed and analyzed the *in silico* component of this study. HM, AP, VB, AK, and ZG were involved with reagent preparation, data acquisition, and analysis. RKa, contributed to reagent preparation and standardization.

FUNDING

The financial assistance provided by Department of Science and Technology (DST) EMR/2016/001937, National Women Bioscientist Award (2014), Department of Biotechnology (DBT) SAN No.102/IFD/SAN/2599/2016-17, and Council of Scientific Research (CSIR), Govt. of India is sincerely acknowledged.

ACKNOWLEDGMENTS

We would like to thank Dr. CE. Barry, Tuberculosis Research Section, Laboratory of Host Defenses, National Institute of Allergy and Infectious Disease, Rockville, Maryland for generously providing us the *M.tb* H37Rv Δmbt::hyg siderophore knockout strain. Mr. Ranvir Singh is acknowledged for the skillful technical assistance provided for experiments. VB was a recipient of Research Associateship, from Council of Scientific and Industrial Research (CSIR), Government of India. RN, AK, and RKa were recipients of research fellowships provided by NIPER, SAS Nagar. RKu, HM, and AP were recipients of research fellowships from CSIR, University Grants Commission (UGC) and Department of Biotechnology (DBT) respectively. ZG was a recipient of research fellowship from Department of Biotechnology, Government of India.

SUPPLEMENTARY MATERIAL

The Supplementary Material for this article can be found online at: http://journal.frontiersin.org/article/10.3389/fcimb.2017.00245/full#supplementary-material

Movie 1 | Trafficking and co-localization of Lf-A647 with intraphagosomal M.tb H37Ra-GFP.

REFERENCES

Ashkenazy, H., Abadi, S., Martz, E., Chay, O., Mayrose, I., Pupko, T., et al. (2016). ConSurf 2016: an improved methodology to estimate and visualize evolutionary conservation in macromolecules. *Nucleic Acids Res.* 44, W344–W350. doi: 10.1093/nar/gkw408

Ashkenazy, H., Erez, E., Martz, E., Pupko, T., and Ben-Tal, N. (2010). ConSurf 2010: calculating evolutionary conservation in sequence and structure of proteins and nucleic acids. *Nucleic Acids Res.* 38, W529–W533. doi: 10.1093/nar/gkq399

Banerjee, S., Farhana, A., Ehtesham, N. Z., and Hasnain, S. E. (2011). Iron acquisition, assimilation and regulation in mycobacteria. *Infect. Genet. Evol.* 11, 825–838. doi: 10.1016/j.meegid.2011.02.016

Baveye, S., Elass, E., Fernig, D. G., Blanquart, C., Mazurier, J., and Legrand, D. (2000). Human lactoferrin interacts with soluble CD14 and inhibits expression of endothelial adhesion molecules, E-selectin and ICAM-1, induced by the CD14-lipopolysaccharide complex. *Infect. Immun.* 68, 6519–6525. doi: 10.1128/IAI.68.12.6519-6525.2000

Berger, T., Togawa, A., Duncan, G. S., Elia, A. J., You-Ten, A., Wakeham, A., et al. (2006). Lipocalin 2-deficient mice exhibit increased sensitivity to *Escherichia coli* infection but not to ischemia-reperfusion injury. *Proc. Natl. Acad. Sci. U.S.A.* 103, 1834–1839. doi: 10.1073/pnas.0510847103

Bermudez, L. E., Petrofsky, M., and Shelton, K. (1996). Epidermal growth factor-binding protein in *Mycobacterium avium* and *Mycobacterium tuberculosis*: a possible role in the mechanism of infection. *Infect. Immun.* 64, 2917–2922.

Boradia, V. M., Malhotra, H., Thakkar, J. S., Tillu, V. A., Vuppala, B., Patil, P., et al. (2014). *Mycobacterium tuberculosis* acquires iron by cell-surface sequestration and internalization of human holo-transferrin. *Nat. Commun.* 5:5730. doi: 10.1038/ncomms5730

Boradia, V. M., Patil, P., Agnihotri, A., Kumar, A., Rajwadi, K. K., Sahu, A., et al. (2016). *Mycobacterium tuberculosis* H37Ra: a surrogate for the expression of conserved, multimeric proteins of *M. tb* H37Rv. *Microb. Cell Fact.* 15:140. doi: 10.1186/s12934-016-0537-0

Carroll, M. V., Sim, R. B., Bigi, F., Jäkel, A., Antrobus, R., and Mitchell, D. A. (2010). Identification of four novel DC-SIGN ligands on *Mycobacterium bovis* BCG. *Protein Cell* 1, 859–870. doi: 10.1007/s13238-010-0101-3

Chauhan, A. S., Rawat, P., Malhotra, H., Sheokand, N., Kumar, M., Patidar, A., et al. (2015). Secreted multifunctional Glyceraldehyde-3-phosphate dehydrogenase sequesters lactoferrin and iron into cells via a non-canonical pathway. *Sci. Rep.* 5:18465. doi: 10.1038/srep18465

Cowley, S. C., and Av-Gay, Y. (2001). Monitoring promoter activity and protein localization in *Mycobacterium* spp. using green fluorescent protein. *Gene* 264, 225–231. doi: 10.1016/S0378-1119(01)00336-5

De Voss, J. J., Rutter, K., Schroeder, B. G., and Barry, C. E. (1999). Iron acquisition and metabolism by mycobacteria. *J. Bacteriol.* 181, 4443–4451.

De Voss, J. J., Rutter, K., Schroeder, B. G., Su, H., Zhu, Y., and Barry, C. E. (2000). The salicylate-derived mycobactin siderophores of *Mycobacterium tuberculosis* are essential for growth in macrophages. *Proc. Natl. Acad. Sci. U.S.A.* 97, 1252–1257. doi: 10.1073/pnas.97.3.1252

Flo, T. H., Smith, K. D., Sato, S., Rodriguez, D. J., Holmes, M. A., Strong, R. K., et al. (2004). Lipocalin 2 mediates an innate immune response to bacterial infection by sequestrating iron. *Nature* 432, 917–921. doi: 10.1038/nature03104

Goetz, D. H., Holmes, M. A., Borregaard, N., Bluhm, M. E., Raymond, K. N., and Strong, R. K. (2002). The neutrophil lipocalin NGAL is a bacteriostatic agent that interferes with siderophore-mediated iron acquisition. *Mol. Cell* 10, 1033–1043. doi: 10.1016/S1097-2765(02)00708-6

Gray-Owen, S. D., and Schyvers, A. B. (1996). Bacterial transferrin and lactoferrin receptors. *Trends Microbiol.* 4, 185–191. doi: 10.1016/0966-842X(96)10025-1

Grey, A., Banovic, T., Zhu, Q., Watson, M., Callon, K., Palmano, K., et al. (2004). The low-density lipoprotein receptor-related protein 1 is a mitogenic receptor for lactoferrin in osteoblastic cells. *Mol. Endocrinol.* 18, 2268–2278. doi: 10.1210/me.2003-0456

Jandl, J. H., Inman, J. K., Simmons, R. L., and Allen, D. W. (1959). Transfer of iron from serum iron-binding protein to human reticulocytes. *J. Clin. Invest.* 38:161. doi: 10.1172/JCI103786

Kawabata, H., Yang, R., Hirama, T., Vuong, P. T., Kawano, S., Gombart, A. F., et al. (1999). Molecular cloning of transferrin receptor 2 A new member of the transferrin receptor-like family. *J. Biol. Chem.* 274, 20826–20832. doi: 10.1074/jbc.274.30.20826

Kenworthy, A. K. (2001). Imaging protein-protein interactions using fluorescence resonance energy transfer microscopy. *Methods* 24, 289–296. doi: 10.1006/meth.2001.1189

Kulshreshtha, S., Chaudhary, V., Goswami, G. K., and Mathur, N. (2016). Computational approaches for predicting mutant protein stability. *J. Comput. Aided Mol. Des.* 30, 401–412. doi: 10.1007/s10822-016-9914-3

Meng, E. C., Pettersen, E. F., Couch, G. S., Huang, C. C., and Ferrin, T. E. (2006). Tools for integrated sequence-structure analysis with UCSF Chimera. *BMC Bioinformatics* 7:339. doi: 10.1186/1471-2105-7-339

Modun, B., and Williams, P. (1999). The staphylococcal transferrin-binding protein is a cell wall glyceraldehyde-3-phosphate dehydrogenase. *Infect. Immun.* 67, 1086–1092.

Olakanmi, O., Schlesinger, L. S., Ahmed, A., and Britigan, B. E. (2002). Intraphagosomal *Mycobacterium tuberculosis* acquires iron from both extracellular transferrin and intracellular iron pools impact of interferon-γ and hemochromatosis. *J. Biol. Chem.* 277, 49727–49734. doi: 10.1074/jbc.M209768200

Olakanmi, O., Schlesinger, L. S., Ahmed, A., and Britigan, B. E. (2004). The nature of extracellular iron influences iron acquisition by *Mycobacterium tuberculosis* residing within human macrophages. *Infect. Immun.* 72, 2022–2028. doi: 10.1128/IAI.72.4.2022-2028.2004

Pettersen, E. F., Goddard, T. D., Huang, C. C., Couch, G. S., Greenblatt, D. M., Meng, E. C., et al. (2004). UCSF Chimera-a visualization system for exploratory research and analysis. *J. Comput. Chem.* 25, 1605–1612. doi: 10.1002/jcc.20084

Pires, D. E. V., Ascher, D. B., and Blundell, T. L. (2014). DUET: a server for predicting effects of mutations on protein stability using an integrated computational approach. *Nucleic Acids Res.* 411, W314–W319. doi: 10.1093/nar/gku411

Raje, C. I., Kumar, S., Harle, A., Nanda, J. S., and Raje, M. (2007). The macrophage cell surface glyceraldehyde-3-phosphate dehydrogenase is a novel transferrin receptor. *J. Biol. Chem.* 282, 3252–3261. doi: 10.1074/jbc.M608328200

Ratledge, C. (2004). Iron, mycobacteria and tuberculosis. *Tuberculosis* 84, 110–130. doi: 10.1016/j.tube.2003.08.012

Rawat, P., Kumar, S., Sheokand, N., Raje, C. I., and Raje, M. (2012). The multifunctional glycolytic protein glyceraldehyde-3-phosphate dehydrogenase (GAPDH) is a novel macrophage lactoferrin receptor. *Biochem. Cell Biol.* 90, 329–338. doi: 10.1139/o11-058

Ryndak, M. B., Wang, S., Smith, I., and Rodriguez, G. M. (2010). The *Mycobacterium tuberculosis* high-affinity iron importer, IrtA, contains an FAD-binding domain. *J. Bacteriol.* 192, 861–869. doi: 10.1128/JB.00223-09

Siqueiros-Cendón, T., Arévalo-Gallegos, S., Iglesias-Figueroa, B. F., García-Montoya, I. A., Salazar-Martínez, J., and Rascón-Cruz, Q. (2014). Immunomodulatory effects of lactoferrin. *Acta Pharmacol. Sin.* 35, 557–566. doi: 10.1038/aps.2013.200

Sirover, M. A. (1999). New insights into an old protein: the functional diversity of mammalian glyceraldehyde-3-phosphate dehydrogenase. *Biochim. Biophys. Acta Protein Struct. Mol. Enzymol.* 1432, 159–184. doi: 10.1016/S0167-4838(99)00119-3

Taylor, J. M., and Heinrichs, D. E. (2002). Transferrin binding in *Staphylococcus aureus*: involvement of a cell wall - anchored protein. *Mol. Microbiol.* 43, 1603–1614. doi: 10.1046/j.1365-2958.2002.02850.x

Testa, U. (ed.). (2002). "Lactoferrin," in *Proteins of Iron Metabolism* (Boca Raton, FL: CRC Press), 71.

Tullius, M. V., Harmston, C. A., Owens, C. P., Chim, N., Morse, R. P., McMath, L. M., et al. (2011). Discovery and characterization of a unique mycobacterial heme acquisition system. *Proc. Natl. Acad. Sci. U.S.A.* 108, 5051–5056. doi: 10.1073/pnas.1009516108

Tullius, M. V., Harth, G., Masleša-Galić, S., Dillon, B. J., and Horwitz, M. A. (2008). A replication-limited recombinant *Mycobacterium bovis* BCG vaccine against tuberculosis designed for human immunodeficiency virus-positive persons is safer and more efficacious than BCG. *Infect. Immun.* 76, 5200–5214. doi: 10.1128/IAI.00434-08

Wards, B. J., and Collins, D. M. (1996). Electroporation at elevated temperatures substantially improves transformation efficiency of slow-growing mycobacteria. *FEMS Microbiol. Lett.* 145, 101–105. doi: 10.1111/j.1574-6968.1996.tb08563.x

Webb, B., and Sali, A. (2014). "Protein structure modeling with modeller," in *Protein Structure Prediction*, ed D. Kihara (New York, NY: Springer), 1–15.

Williams, P., and Griffiths, E. (1992). Bacterial transferrin receptors - structure, function and contribution to virulence. *Med. Microbiol. Immunol.* 181, 301–322. doi: 10.1007/BF00191543

Worth, C. L., Preissner, R., and Blundell, T. L. (2011). SDM-a server for predicting effects of mutations on protein stability and malfunction. *Nucleic Acids Res.* 39, W215–W222. doi: 10.1093/nar/gkr363

Conflict of Interest Statement: The authors declare that the research was conducted in the absence of any commercial or financial relationships that could be construed as a potential conflict of interest.

frontiers in Cellular and Infection Microbiology

PERSPECTIVE
published: 08 June 2017
doi: 10.3389/fcimb.2017.00240

Role of Bacterioferritin & Ferritin in *M. tuberculosis* Pathogenesis and Drug Resistance: A Future Perspective by Interactomic Approach

*Divakar Sharma * and Deepa Bisht*

Department of Biochemistry, National JALMA Institute for Leprosy and Other Mycobacterial Diseases, Agra, India

Tuberculosis is caused by *Mycobacterium tuberculosis*, one of the most successful and deadliest human pathogen. Aminoglycosides resistance leads to emergence of extremely drug resistant strains of *M. tuberculosis*. Iron is crucial for the biological functions of the cells. Iron assimilation, storage and their utilization is not only involved in pathogenesis but also in emergence of drug resistance strains. We previously reported that iron storing proteins (bacterioferritin and ferritin) were found to be overexpressed in aminoglycosides resistant isolates. In this study we performed the STRING analysis of bacterioferritin & ferritin proteins and predicted their interactive partners [ferrochelatase (hemH), Rv1877 (hypothetical protein/probable conserved integral membrane protein), uroporphyrinogen decarboxylase (hemE) trigger factor (tig), transcriptional regulatory protein (MT3948), hypothetical protein (MT1928), glnA3 (glutamine synthetase), molecular chaperone GroEL (groEL1 & hsp65), and hypothetical protein (MT3947)]. We suggested that interactive partners of bacterioferritin and ferritin are directly or indirectly involved in *M. tuberculosis* growth, homeostasis, iron assimilation, virulence, resistance, and stresses.

Keywords: bacterioferritin, ferritin, protein-protein interaction, aminoglycosides resistance, *M. tuberculosis*

OPEN ACCESS

Edited by:
Susu M. Zughaier,
Emory University, United States

Reviewed by:
Jiaoyu Deng,
Wuhan Institute of Virology (CAS), China
Anna Upton,
TB Alliance, United States

****Correspondence:***
Divakar Sharma
divakarsharma88@gmail.com

Received: *31 March 2017*
Accepted: *24 May 2017*
Published: *08 June 2017*

Citation:
Sharma D and Bisht D (2017) Role of Bacterioferritin & Ferritin in M. tuberculosis Pathogenesis and Drug Resistance: A Future Perspective by Interactomic Approach. Front. Cell. Infect. Microbiol. 7:240. doi: 10.3389/fcimb.2017.00240

INTRODUCTION

Mycobacterium tuberculosis is the causing factor of tuberculosis (TB) etiology and remains one of the top 10 causes of death worldwide in 2015. Recently WHO reported 10.4 million new TB cases and 1.8 million deaths worldwide (WHO Report, 2016). Due to disappointment of BCG vaccine in adults, chemotherapy through potent anti-TB drugs is the last option to reduce prevalence and mortality but unfortunately, emergence of drug resistant tuberculosis such as multi drug resistant tuberculosis (MDR-TB), extensively drug resistant tuberculosis (XDR-TB) and totally drug resistant tuberculosis (TDR-TB) have made chemotherapy complicated. Aminoglycosides are the second line drugs of choice used especially for the treatment of MDR-TB along with the fluoroquinolones. Aminoglycosides and fluoroquinolones are the only option for the treatment of MDR-TB (with some side effects as well as less efficacy as compared to first line drugs). When the usual treatments are not possible than recently approved drugs (bedaquiline and delamanid) have been used for the treatment of MDR TB, XDR-TB and TDR-TB (with more side effects as compared to first and second line drugs). In *M. tuberculosis*

they typically inhibit protein synthesis by interacting with protein translational machinery. Two dimensional gel electrophoresis coupled with mass spectrometry is the best accepted approach for expression proteomics (Lata et al., 2015a,b; Sharma et al., 2015b, 2016b; Sharma and Bisht, 2016). Since last decade a panel of proteomics and bioinformatics studies related to aminoglycosides resistance have been accumulated (Sharma et al., 2010, 2014, 2015b,a, 2016a,b; Kumar et al., 2013; Sharma and Bisht, 2017a,b). Here we emphasized on the *M. tuberculosis* iron storage proteins (bacterioferritin and ferritin) and their interactive protein partners which might be involved in pathogenesis, virulence and drug resistance.

Iron is an essential entity for metabolism of the biological cells and hence crucial for the chemistry of life. Iron assimilation, storage and their utilization play a crucial role not only in pathogenesis/pathobiology (growth, survival, virulence and latency) but also in emergence of aminoglycosides drug resistance strains of *M. tuberculosis* (Reddy et al., 2012; Kumar et al., 2013; Sharma et al., 2015b). Recently, Khare et al. (2017) reported that iron storage proteins are involved in maintaining iron homeostasis in *M. tuberculosis* (Khare et al., 2017). Bacterioferritin (Rv1876) and ferritin (Rv3841) are unique to maintain iron storage as well as homeostasis in *M. tuberculosis*. In mycobacteria, various genes products and their interactive partners required for high affinity iron acquisition have been identified such as siderophore production, uptake of ferric-siderophores, production of iron storage proteins and uptake of heme. Production, storage and function of iron uptake mechanisms are controlled by a regulatory protein IdeR (Gold et al., 2001). Heme is the preferable iron source for *M. tuberculosis* and its acquisition is done by a biosynthetic enzyme ferrochelatase (Rv1485). Rv1485 catalyzes the last step of heme biosynthesis in which iron is interleaved to protoporfhyrin IX to form protoheame (Dailey and Dailey, 2002). It is essential because it supplies the heme which is a preferred iron source for *M. tuberculosis* (Parish et al., 2005) and serves as a cofactor for various metabolic enzymes such as catalase-peroxidase and DosS/DosT two component system [active sites contains heme] (Svistunenko, 2005).

In pathogenic mycobacteria, usually high affinity systems are essential for maintenance of an infection, virulence and resistance. Greater definition of the functions of both the identified genes and their products, ferritin (*bfr*B) and bacterioferritin (*bfr*A) will refine our understanding of mycobacterial iron acquisition and the interplay between components of the iron systems have increased intensities under iron-rich and decreased intensities under iron deprived conditions (Pandey and Rodriguez, 2012). Under iron-rich conditions, *M. tuberculosis* represses iron acquisition and induces iron storage proteins suggesting the significant role of iron storage proteins in iron homeostasis. *M. tuberculosis* usually synthesizes two iron storage proteins: ferritin (*bfr*B) and bacterioferritin (*bfr*A). *Bfr*B is mandatory to overcome iron limitation and defense against oxidative stress, whereas *bfr*A is superfluous for victorious adaptation to those stresses. Studies of *M. tuberculosis* lacking *bfr*B gene (which encode the ferritin an iron storage protein) reported increased intracellular concentration of iron. They depicted that increasing iron concentration (absence of bacterioferritin and ferritin) decreased resistance to various anti-TB drugs including aminoglycosides as well as fluoroquinolones (Pandey and Rodriguez, 2012) and suggested that ferritin and bacterioferritin are not only mandatory to maintain iron homeostasis but also make *M. tuberculosis* resistant to aminoglycosides. Kurthkoti et al suggested that iron-dependent regulator IdeR induces ferritin (bfrB) expression by alleviating Lsr2 repression in *M. tuberculosis* (Kurthkoti et al., 2015). *Whi*B7 (Rv3197A) is Fe-S cluster-bound protein (transcriptional regulatory protein), which not only associates with aminoglycosides resistance but also predicted to be in the IdeR|Rv2711 regulon (Gold et al., 2001; Morris et al., 2005). Recently Kuberl et al. (2016) suggested that pupylation machinery maintains the iron homeostasis by targeting iron storage proteins (Kuberl et al., 2016).

In our previous studies of expression proteomics we have discovered, that bacterioferritin (Rv1876) and ferritin (Rv3841) were overexpressed in aminoglycosides (amikacin and kanamycin) resistant *M. tuberculosis* clinical isolates (Kumar et al., 2013; Sharma et al., 2015b). Molecular docking revealed that aminoglycosides drugs (AK and KM) bind to conserved bacterioferritin domain of Rv1876 and ferritin domain of Rv3841 and suggested that overexpression of these proteins might be to neutralize/modulate the drug effect and could be involved in aminoglycosides resistance mechanisms of *M. tuberculosis* (Kumar et al., 2013; Sharma et al., 2015b). Although the enzymes and their connected pathways involved in iron metabolism in *M. tuberculosis* are well recognized, still our information related to iron transportation, trafficking, iron dependent post-transcriptional & translational regulations and protein-protein interactions in mycobacteria is inadequate. Recently Sharma et al. (2016a) reported that inducible overexpression of recombinant ferritin in *E. coli* (BL21) leads to shift in MIC of AK & KM and suggested their probable roles in conferring aminoglycosides resistance (Sharma et al., 2016a). Consequently, proteins involved in iron storage, assimilation, regulation, uptake and their utilization can be a promising anti-mycobacterial targets against the drug resistant tuberculosis.

BACTERIOFERRITIN AND FERRITIN PROTEIN-PROTEIN INTERACTION: UNLOCK THE SECRETS OF IRON RELATED PATHWAYS IN AMINOGLYCOSIDES DRUG RESISTANCE

STRING-10 is an online server which is used to predict the interacting partners of the iron storage proteins [bacterioferritin (Rv1876) and ferritin (Rv3841)] (Sharma et al., 2016a,b; Sharma and Bisht, 2017a). "STRING uses a combination of prediction approaches and an integration of other information (neighborhood, transferred neighborhood, gene fusion, co-occurrence, co-expression, experiments, databases, text mining). Network was made at medium confidence level (0.400) allowing all active prediction methods, which corresponds to approximately 50% possibility of

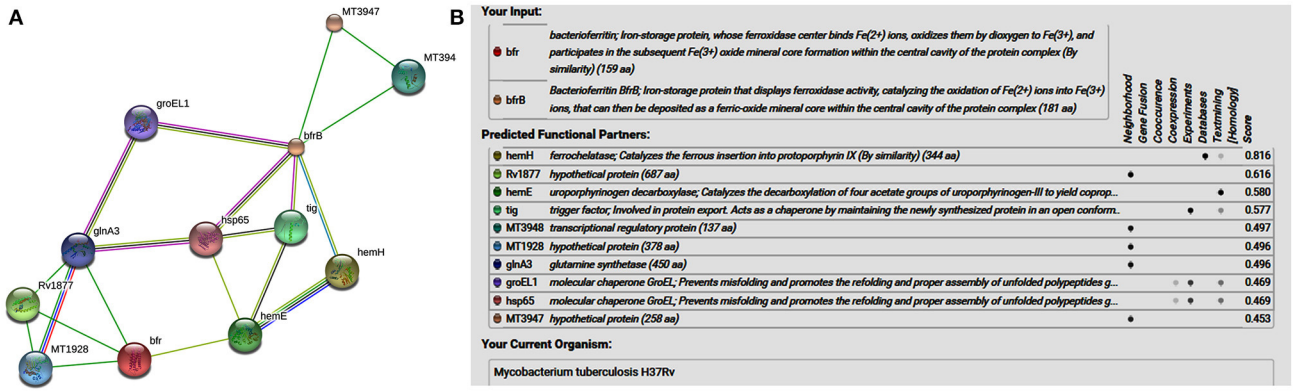

FIGURE 1 | (A) STRING analysis reveals the interaction partners of *M. tuberculosis* H37Rv bacterioferritin and ferritin protein. **(B)** The score for each interaction partner is assigned and shown in the table inbuilt in figure. The highest score for hemH association was found to be 0.816 followed by Rv1877, a probable transporter (its confidence score of association was 0.616). The confidence score for association for tig corresponds to 0.577, and for molecular cheprone (groEL1 & hsp65) was found to be 0.469.

association" (Sharma et al., 2016a,b). In the network display, each node represents a protein, and each edge represents an interaction.

STRING analysis predicted (**Figure 1**) that ferrochelatase (hemH), Rv1877 (hypothetical protein/probable conserved integral membrane protein), uroporphyrinogen decarboxylase (hemE) trigger factor (tig), transcriptional regulatory protein (MT3948), hypothetical protein (MT1928), glnA3 (glutamine synthetase), molecular chaperone GroEL (groEL1 & hsp65), and hypothetical protein (MT3947) were functional partners of the bacterioferritin and ferritin at medium confidence level (0.400) allowing all active prediction methods. Interactome analysis suggested that molecular chaperone GroEL (*gro*EL1 & *hsp*65) and trigger factor (tig) were co-expressed as well as experimentally reported. *In silico* analysis predicted trigger factor (tig) protein as a novel target for interaction with ferritin protein. Trigger factor (tig) is not only involved in eliciting the expression of proteins & their export but also helps in maintaining the open conformation of newly synthesized protein (chaperone activity).

PREDICTION OF PUPYLATION SITES

Using the default threshold (medium) with cutoff 2.452; GPS-PUP predicted pupylation sites in bacterioferritin and ferritin proteins which were tabulated in **Table 1**.

TABLE 1 | Predicted / identified pupylation sites in bacterioferritin and ferritin proteins.

ORF no.	Position of lysine residue undergoes pupylation	Peptides	Score	Cut-off
Rv1876	122	TSAVLLE**K**IVADEEE	2.819	2.452
Rv3841	10	EYEGPKT**K**FHALMQE	2.732	2.452

K-Lysine undergoes pupylation.

DISCUSSION

Emergence of extensively-drug resistant tuberculosis (XDR-TB) is the consequence of interrupted treatment of multi-drug resistant tuberculosis (MDR-TB) with second line anti-tubercular drugs (aminoglycosides and fluoroquinolones). Proteins engage in iron storage, assimilation, regulation, uptake and their utilization could not only be involved in *M. tuberculosis* pathobiology, growth, virulence and latency but also in aminoglycosides drug resistance and might be potential anti-mycobacterial drug target against the drug resistant tuberculosis (Reddy et al., 2012; Kumar et al., 2013; Sharma et al., 2015b, 2016a; Khare et al., 2017). Pandey and Rodriguez also suggested that ferritin is not only mandatory to maintain iron homeostasis in *M. tuberculosis* but also ferritin deficient bacilli are more susceptible to killing by antibiotics (Pandey and Rodriguez, 2012). Our previous studies reported that bacterioferritin (Rv1876) and ferritin (Rv3841) were overexpressed in aminoglycosides (amikacin and kanamycin) resistant *M. tuberculosis* clinical isolates and suggested their involvement in resistance (Kumar et al., 2013; Sharma et al., 2015b). Recently Sharma et al. (2016a) reported that inducible over expression of recombinant ferritin in *E. coli* (BL21) increased the MIC shift of AK & KM and make the bacteria more resistant against the aminoglycosides drugs (Sharma et al., 2016a). These findings suggested its probable roles in conferring resistance.

Interactome analysis of bacterioferritin (Rv1876) and ferritin (Rv3841) by STRING-10 also suggested that bacterioferritin and ferritin protein interacted with their partners such as ferrochelatase, hypothetical protein (Rv1877), uroporphyrinogen decarboxylase, trigger factor, transcriptional regulatory protein (MT3948), hypothetical protein (MT1928), glutamine synthetase, Molecular chaperones (groEL1 & Hsp65), and hypothetical protein MT3947 which were involved in intermediary metabolism and respiration, cell wall and cell processes, virulence, detoxification, adaptation, conserved

hypotheticals and regulatory proteins. Hypothetical protein (Rv1877), a Probable conserved integral membrane protein, ferrochelatase and trigger factor might be potential novel targets predicted by bacterioferritin and ferritin protein-protein interaction. Rv1877 having 14-transmembrane helixes (TMH), possibly involved in transport of drug across the membrane and could be a potential drug target against the aminoglycosides drug resistance. Rv1877 is the homologous of *lfr*A and deletion of this gene increased the susceptibility against various antibiotics including the aminoglycosides in mycobacteria (Li et al., 2004). Recently, Mehra et al. (2016) reported that Rv1877 is the part of ABC transporter and predicted its involvement in drug resistance (Mehra et al., 2016). Ferrochelatase involved in heme biosynthetic pathways is a preferred iron source for *M. tuberculosis*. Trigger factor which not only having chaperone activity but also involved in eliciting the protein expression and their export which could maintain the 3D conformation of newly synthesized proteins and prevents misfolding as well as promotes the refolding of unfolded polypeptides generated under stressed conditions. Bhuwan et al. (2016) reported and validated the STRING in the interaction of RipA with Chaperone MoxR1 (Bhuwan et al., 2016). Sharma et al. (2015b) reported that trigger factor, bacterioferritin and ferritin were overexpressed in aminoglycosides resistant *M. tuberculosis* clinical isolates (Sharma et al., 2015b) and suggested that trigger factor might trigger expression of bacterioferritin and ferritin and their interactive partners which could be involved in aminoglycosides drug resistance. We suggested that cumulative effect of iron storage proteins (bacterioferritin and ferritin) and their interactive partners {hypothetical protein (Rv1877), ferrochelatase, trigger factor and others} might be involved in various stress, and aminoglycosides drug resistance. Predicted pupylation sites in bacterioferritin and ferritin also suggested its involvement not only in iron homeostasis but also in aminoglycosides resistance (Kuberl et al., 2016; Sharma et al., 2016a). Further detailed and in-depth investigations of these interactome and pupylome could explore the aminoglycosides resistance and might be used as potential drug targets against this issue.

AUTHOR CONTRIBUTIONS

DS design the concept and wrote the manuscript. DS and DB finalized the manuscript.

ACKNOWLEDGMENTS

The authors are grateful to Director, NJIL, & OMD for the support. DS is ICMR-PDFs (ICMR, New Delhi).

REFERENCES

Bhuwan, M., Arora, N., Sharma, A., Khubaib, M., Pandey, S., Chaudhuri, T. K., et al. (2016). Interaction of *Mycobacterium tuberculosis* virulence factor RipA with chaperone MoxR1 is required for transport through the TAT secretion system. *MBio* 7:e02259. doi: 10.1128/mBio.02259-15

Dailey, T. A., and Dailey, H. A. (2002). Identification of [2Fe-2S] clusters in microbial ferrochelatases. *J. Bacteriol.* 184, 2460–2464. doi: 10.1128/JB.184.9.2460-2464.2002

Gold, B., Rodriguez, G. M., Marras, S. A., Pentecost, M., and Smith, I. (2001). The *Mycobacterium tuberculosis* IdeR is a dual functional regulator that controls transcription of genes involved in iron acquisition, iron storage and survival in macrophages. *Mol. Microbiol.* 42, 851–865. doi: 10.1046/j.1365-2958.2001.02684.x

Khare, G., Nangpal, P., and Tyagi, A. K. (2017). Differential roles of iron storage proteins in maintaining the iron homeostasis in *Mycobacterium tuberculosis*. *PLoS ONE* 12:e0169545. doi: 10.1371/journal.pone.0169545

Kuberl, A., Polen, T., and Bott, M. (2016). The pupylation machinery is involved in iron homeostasis by targeting the iron storage protein ferritin. *Proc. Natl. Acad. Sci. U.S.A.* 113, 4806–4811. doi: 10.1073/pnas.1514529113

Kumar, B., Sharma, D., Sharma, P., Katoch, V. M., Venkatesan, K., and Bisht, D. (2013). Proteomic analysis of *Mycobacterium tuberculosis* isolates resistant to kanamycin and amikacin. *J. Proteomics* 94, 68–77. doi: 10.1016/j.jprot.2013.08.025

Kurthkoti, K., Tare, P., Paitchowdhury, R., Gowthami, V. N., Garcia, M. J., Colangeli, R., et al. (2015). The mycobacterial iron-dependent regulator IdeR induces ferritin (bfrB) by alleviating Lsr2 repression. *Mol. Microbiol.* 98, 864–877. doi: 10.1111/mmi.13166

Lata, M., Sharma, D., Deo, N., Tiwari, P. K., Bisht, D., and Venkatesan, K. (2015b). Proteomic analysis of ofloxacin-mono resistant *Mycobacterium tuberculosis* isolates. *J. Proteomics* 127, 114–121. doi: 10.1016/j.jprot.2015.07.031

Lata, M., Sharma, D., Kumar, B., Deo, N., Tiwari, P. K., Bisht, D., et al. (2015a). Proteome analysis of ofloxacin and moxifloxacin induced *Mycobacterium tuberculosis* isolates by proteomic approach. *Protein Pept. Lett.* 22, 362–371. doi: 10.2174/0929866522666150209113708

Li, X. Z., Zhang, L., and Nikaido, H. (2004). Efflux pump-mediated intrinsic drug resistance in *Mycobacterium smegmatis*. *Antimicrob. Agents Chemother.* 48, 2415–2423. doi: 10.1128/AAC.48.7.2415-2423.2004

Mehra, V., Ghosh, T. S., and Mande, S. S. (2016). Insights into horizontal acquisition patterns of dormancy and reactivation regulon genes in mycobacterial species using a partitioning-based framework. *J. Biosci.* 41, 475–485. doi: 10.1007/s12038-016-9622-0

Morris, R. P., Nguyen, L., Gatfield, J., Visconti, K., Nguyen, K., Schnappinger, D., et al. (2005). Ancestral antibiotic resistance in *Mycobacterium tuberculosis*. *Proc. Natl. Acad. Sci. U.S.A.* 102, 12200–12205. doi: 10.1073/pnas.0505446102

Pandey, R., and Rodriguez, G. M. (2012). A ferritin mutant of *Mycobacterium tuberculosis* is highly susceptible to killing by antibiotics and is unable to establish a chronic infection in mice. *Infect. Immun.* 80, 3650–3659. doi: 10.1128/IAI.00229-12

Parish, T., Schaeffer, M., Roberts, G., and Duncan, K. (2005). HemZ is essential for heme biosynthesis in *Mycobacterium tuberculosis*. *Tuberculosis (Edinb).* 85, 197–204. doi: 10.1016/j.tube.2005.01.002

Reddy, P. V., Puri, R. V., Khera, A., and Tyagi, A. K. (2012). Iron storage proteins are essential for the survival and pathogenesis of *Mycobacterium tuberculosis* in THP-1 macrophages and the guinea pig model of infection. *J. Bacteriol.* 194, 567–575. doi: 10.1128/JB.05553-11

Sharma, D., and Bisht, D. (2016). An efficient and rapid lipophilic proteins extraction from *Mycobacterium tuberculosis* H37Rv for two dimensional gel electrophoresis. *Electrophoresis* 37, 1187–1190. doi: 10.1002/elps.201600025

Sharma, D., and Bisht, D. (2017a). Secretory proteome analysis of streptomycin resistant *Mycobacterium tuberculosis* clinical isolates. *SLAS Discov.* doi: 10.1177/2472555217698428. [Epub ahead of print].

Sharma, D., and Bisht, D. (2017b). *M. tuberculosis* hypothetical proteins and proteins of unknown function: hope for exploring novel resistance mechanisms as well as future target of drug resistance. *Front. Microbiol.* 8:465. doi: 10.3389/fmicb.2017.00465

Sharma, D., Kumar, B., Lata, M., Joshi, B., Venkatesan, K., Shukla, S., et al. (2015b). Comparative proteomic analysis of aminoglycosides resistant and susceptible *Mycobacterium tuberculosis* clinical isolates for exploring potential drug targets. *PLoS ONE* 10:e0139414. doi: 10.1371/journal.pone.0139414

Sharma, D., Lata, M., Faheem, M., Khan, A. U., Joshi, B., Venkatesan, K., et al. (2015a). Cloning, expression and correlation of Rv0148 to amikacin & kanamycin resistance. *Curr. Proteomics* 12, 96–100. doi: 10.2174/1570164612021509031130 53

Sharma, D., Lata, M., Faheem, M., Khan, A. U., Joshi, B., Venkatesan, K., et al. (2016a). *M. tuberculosis* ferritin (Rv3841): Potential involvement in Amikacin (AK) & Kanamycin (KM) resistance. *Biochem. Biophys. Res. Commun.* 478, 908–912. doi: 10.1016/j.bbrc.2016.08.049

Sharma, D., Lata, M., Singh, R., Deo, N., Venkatesan, K., and Bisht, D. (2016b). Cytosolic proteome profiling of aminoglycosides resistant *Mycobacterium tuberculosis* clinical isolates using MALDI-TOF/MS. *Front. Microbiol.* 7:1816. doi: 10.3389/fmicb.2016.01816

Sharma, D., Shankar, H., Lata, M., Joshi, B., Venkatesan, K., and Bisht, D. (2014). Culture filtrate proteome analysis of aminoglycoside resistant clinical isolates of *Mycobacterium tuberculosis*. *BMC Infect. Dis.* 14:P60. doi: 10.1186/1471-2334-14-S3-P60

Sharma, P., Kumar, B., Gupta, Y., Singhal, N., Katoch, V. M., Venkatesan, K., et al. (2010). Proteomic analysis of streptomycin resistant and sensitive clinical isolates of *Mycobacterium tuberculosis*. *Proteome Sci.* 8:59. doi: 10.1186/1477-5956-8-59

Svistunenko, D. A. (2005). Reaction of haem containing proteins and enzymes with hydroperoxides: the radical view. *Biochim. Biophys. Acta* 1707, 127–155. doi: 10.1016/j.bbabio.2005.01.004

WHO Report (2016). *Global Tuberculosis Control 2016*. Available online at: www.who.int/tb/publications/global_report/en/

Conflict of Interest Statement: The authors declare that the research was conducted in the absence of any commercial or financial relationships that could be construed as a potential conflict of interest.

Advantages of publishing in Frontiers

OPEN ACCESS
Articles are free to read for greatest visibility and readership

FAST PUBLICATION
Around 90 days from submission to decision

HIGH QUALITY PEER-REVIEW
Rigorous, collaborative, and constructive peer-review

TRANSPARENT PEER-REVIEW
Editors and reviewers acknowledged by name on published articles

Frontiers
Avenue du Tribunal-Fédéral 34
1005 Lausanne | Switzerland

Visit us: www.frontiersin.org
Contact us: info@frontiersin.org | +41 21 510 17 00

REPRODUCIBILITY OF RESEARCH
Support open data and methods to enhance research reproducibility

DIGITAL PUBLISHING
Articles designed for optimal readership across devices

FOLLOW US
@frontiersin

IMPACT METRICS
Advanced article metrics track visibility across digital media

EXTENSIVE PROMOTION
Marketing and promotion of impactful research

LOOP RESEARCH NETWORK
Our network increases your article's readership